AD-A014 229

TURBINE ENGINE CONTROL SYNTHESIS. VOLUME I. OPTIMAL CONTROLLER SYNTHESIS AND DEMONSTRATION

C. R. Stone, et al

Honeywell, Incorporated

Prepared for:

Air Force Aero Propulsion Laboratory

March 1975

DISTRIBUTED BY:

NTIS

National Technical Information Service
U. S. DEPARTMENT OF COMMERCE

NOTICE

When Government drawings, specifications, or other data are used for any purpose other than in connection with a definitely related Government procurement operation, the United States Government thereby incurs no responsibility nor any obligation whatsoever; and the fact that the Government may have formulated, furnished, or in any way supplied the said drawings, specifications, or other data, is not to be regarded by implication or otherwise as in any manner licensing the holder or any other person or corporation, or conveying any rights or permission to manufacture, use, or sell any patented invention that may in any way be related thereto.

This final report was submitted by Systems & Research Center, Honeywell Inc., under Contract F33615-72-C-2190. The effort was sponsored by the Air Force Aero-Propulsion Laboratory, Air Force Systems Command, Wright-Patterson AFB, Ohio under Project 3066, Task 306603, and Work Unit 30660363 with Charles E. Ryan, Jr, AFAPL/TBC as Project Engineer. Mr. C. R. Stone (Vol I & II) and Mr. R. B. Beale (Vol III) of Honeywell, Inc. were technically responsible for the work.

This report has been reviewed by the Information Office, (ASD/OIP) and is releasable to the National Technical Information Service (NTIS). At NTIS, it will be available to the general public, including foreign nations.

This technical report has been reviewed and is approved for publication.

C.E. Ryan

CHARLES E. RYAN, JR, GS-14
Project Engineer

FOR THE COMMANDER

Charles E. Bentz

CHARLES E. BENTZ
Technical Area Manager, Controls

ACCESSION for

NTIS White Section ☒
DDC Buff Section ☐
UNANNOUNCED ☐
JUSTIFICATION ....

BY ....
DISTRIBUTION/AVAILABILITY CODES

Dist.	AVAIL. and/or SPECIAL
A	

Copies of this report should not be returned unless return is required by security considerations, contractual obligations, or notice on a specific document.

Unclassified

SECURITY CLASSIFICATION OF THIS PAGE (When Data Entered)

REPORT DOCUMENTATION PAGE		READ INSTRUCTIONS BEFORE COMPLETING FORM
1. REPORT NUMBER: AFAPL-TR-75-14	2. GOVT ACCESSION NO.	3. RECIPIENT'S CATALOG NUMBER
4. TITLE (and Subtitle): TURBINE ENGINE CONTROL SYNTHESIS, Vol. I: Optimal Controller Synthesis and Demonstration		5. TYPE OF REPORT & PERIOD COVERED: Final Technical Report 30 June 1972 - 15 Mar 1975
		6. PERFORMING ORG. REPORT NUMBER: F0164-FR, Vol. I
7. AUTHOR(s): C. R. Stone, N. E. Miller, M. D. Ward, and R. D. Schmidt		8. CONTRACT OR GRANT NUMBER(s): F33615-72-C-2190
9. PERFORMING ORGANIZATION NAME AND ADDRESS: Honeywell Inc. Systems and Research Center Minneapolis, Minnesota 55413		10. PROGRAM ELEMENT, PROJECT, TASK AREA & WORK UNIT NUMBERS: Proj. 3066 Task 306603 W.U. 30660363
11. CONTROLLING OFFICE NAME AND ADDRESS: Air Force Aero-Propulsion Laboratory (TBC), Wright-Patterson Air Force Base OH 45433		12. REPORT DATE: March 1975
		13. NUMBER OF PAGES: 339
14. MONITORING AGENCY NAME & ADDRESS (if different from Controlling Office)		15. SECURITY CLASS. (of this report): Unclassified
		15a. DECLASSIFICATION/DOWNGRADING SCHEDULE: N/A

16. DISTRIBUTION STATEMENT (of this Report)

Approved for Public Release; distribution unlimited

17. DISTRIBUTION STATEMENT (of the abstract entered in Block 20, if different from Report)

18. SUPPLEMENTARY NOTES

19. KEY WORDS (Continue on reverse side if necessary and identify by block number)

Optimal control	Identification
J85 jet engine	Engine test
Synthesis	Frequency response
Digital control	Transfer functions

20. ABSTRACT (Continue on reverse side if necessary and identify by block number)

The objective was to determine whether optimal control synthesis methods provide superior means for designing jet engine controllers. The methods design controllers with more capability and/or can be exploited to provide less expensive hardware. For newer kinds of engines the cost to design should be less than for presently used methods. Volume I summarizes optimal control design methodology. A paper design of a command and disturbance controller shows that good power lever command response can be

DD FORM 1 JAN 73 1473 EDITION OF 1 NOV 65 IS OBSOLETE

Unclassified

SECURITY CLASSIFICATION OF THIS PAGE (When Data Entered)

20. Abstract (Continued)

achieved; the same controller is designed to be insensitive to inlet duct buzz. A command controller is synthesized and wind tunnel tested. This controller is a good approximation to time optimal with surge-stall, TT4, and flameout constraints. Small-amplitude control responses are precise. There is strong stability. Volume II contains three Appendices. Appendix A contains the details of engine math models. The software for the wind tunnel controller is presented in Appendix B. Appendix C contains a derivation of rate model following. Volume III presents results of frequency response tests of a J85-13 engine operating in the APL wind tunnel. The data are reduced and models identified.

FOREWORD

This final report was submitted by Systems and Research Center, Honeywell Inc., under Contract F33615-72-C-2190. The effort was sponsored by the Air Force Aero-Propulsion Laboratory, Air Force Systems Command, Wright-Patterson AFB, Ohio, under Project 3066, Task 306603, and Work Unit 30660363, with Charles E. Ryan, Jr., AFAPL/TBC, as Project Engineer. At Honeywell, Dr. E.E. Yore managed the effort. Mr. C.R. Stone (Vols. I and II) and Mr. R.B. Beale (Vol. III) were technically responsible for the work.

The report is presented in three volumes. Volume I contains the main part of the report for the optimization design and wind tunnel test evaluation. Volume II contains some very detailed computer programs and background material for the optimization effort. Volume III presents experimental identification and modeling of the General Electric J85 engine.

R.D. Schmidt, M.D. Ward, C.R. Stone, N.E. Miller, developed the results that are presented in Volume I. R.D. Schmidt provided the practical design experience to set the objectives for the program, and did most of the engine modeling at Honeywell. M.D. Ward set up engine simulations on Honeywell's computer facilities, and did the machine language programming for the digital controller for the test facility at Wright-Patterson Air Force Base. C.R. Stone finished the engine modeling, set up the control optimization problems, and worked with the optimization procedures. N.E. Miller did most of the control optimization work and revised models and procedures as the program continued. Stone, Ward, and Miller installed the optimal controller on the wind tunnel test facility at the Aero-Propulsion Laboratory.

Mr. Richard High, his APL wind tunnel test crew, and Mr. Sam Arnett of the Bendix Corporation provided expertise on the facility and invaluable assistance in getting the optimal controllers to run.

Messrs. Ed Milner and Clint Hart of the NASA Lewis Propulsion Laboratory provided very much appreciated consulting advice on the J85 engine model.

TABLE OF CONTENTS

Preceding page blank

LIST OF ILLUSTRATIONS

LIST OF ILLUSTRATIONS (CONTINUED)

LIST OF ILLUSTRATIONS (CONTINUED)

LIST OF ILLUSTRATIONS (CONTINUED)

LIST OF ILLUSTRATIONS (CONTINUED)

LIST OF ILLUSTRATIONS (CONTINUED)

LIST OF ILLUSTRATIONS (CONDLUDED)

LIST OF TABLES

LIST OF TABLES (CONTINUED)

LIST OF TABLES (CONTINUED)

LIST OF TABLES (CONCLUDED)

SECTION I
INTRODUCTION

Jet engine controllers have traditionally been designed by the application of good physics and/or for single-input, single-output control theory. In this report, "modern" multiple-input, multiple-output control theories were used to synthesize jet engine controllers. The objectives were to determine whether the resulting control systems would:

- Cost less to design
- Improve engine performance
- Be less complex to mechanize

As a part of the reported efforts, a controller was designed for a J85-13 jet engine by modern methods and wind-tunnel tested at the Aero Propulsion Laboratory. Test results were good.

Based on accomplishments, it can be said that the objectives were achieved. Modern methods are inexpensive to use, can improve engine performance, and can design less complex hardware.

Modern synthesis methods cost less to use because they provide easier means for achieving objectives; a priori goals are more readily attained. Less simulation, test, and a posteriori tailoring are required to obtain objectives. These attributes of modern methods result from the matching of vector control requirements with vector synthesis capabilities. Modern synthesis methods are particularly cost effective in new situations and/or for more-complex engines.

Improved engine performance is made available in two ways: by providing better quality in traditional control modes, and by providing new desirable control modes. In Section IV of this report, test results for TT4 (cf Table 1 for nomenclature)* control achieved wind tunnel operation are considered to be better than have been achieved before. Section III of this report demonstrates that engine controllers could be made tolerant of inlet buzz. This additional feature or mode would be a welcome additional capability.

Modern optimal synthesis methods are highly effective in developing less complex controls. The methods can do this because they so quickly and so inexpensively determine optimal compromises among component and system alternatives.

This volume of the report (Volume I) emphasizes the design and wind tunnel test aspects of optimal control. Volume II contains primarily data concerning the NASA component engine model and software for the wind tunnel test controller. The results of frequency response testing the wind tunnel J85 engine and of identifying its parameters are in Volume III.

Section II of this volume discusses engine models and the optimal control methodology used. The J85 math models and their evaluation are discussed to meet two sets of objectives. The discussion is sufficiently qualitative that the non-engine expert will get a feel for the physics, mathematics, and quality of the engine models. Rationale are provided for all. In optimal control there is some general philosophy to provide the big picture and there are the specifics to delineate exactly those parts of the optimal control methodology available that were actually used.

*To avoid interrupting the continuity of the text, all referenced figures and tables are gathered at the end of the section in which they are first mentioned.

Section III presents the paper design and evaluation of a command and disturbance controller for the J85 engine. The controller is synthesized not only to provide good throttle command response but also to make the engine insensitive to organ pipe-type inlet buzz to which many aircraft are so prone. The results of Section III strongly suggest that this desirable insensitivity can be achieved.

Section IV is the main part of this report. The detail synthesis of the wind tunnel test command controller is discussed and the wind tunnel results presented. The documentation is heavy and the discussions are candid. Optimal synthesis methods are a lot of work. Much computation must be done but the computations are more readily automated. There is a discussion of two problem areas. Finally, there are the results of wind tunnel tests that show good control was achieved.

Table 1. Nomenclature

Symbol	Description
A	Area, ft^2
BLD	Bleed valves
B_i	States associated with Bendix fuel valve (cf Tables 40-42)
C_n	Coefficient, $rpm^2/°R$
D	Matrix (cf Tables 11 and 12)
DHT	= HT4 - HT5
E	Expected value operator
F	Matrix (cf Tables 11 and 12)
G1	Matrix (cf Tables 11 and 12)
G2	Matrix (cf Tables 11 and 12)
H	Matrix (cf Tables 11 and 12)
$\bar{H}$	Total enthalpy, Btu/lbm
I	Moment of inertia, lbf-ft-sec^2
IGV	Inlet guide vane
J	Cost (cf Tables 11 and 12)
J	Mechanical equivalent of heat, 778.3 ft-lbf/Btu
K	Matrix (cf Tables 11 and 12)
K	Coefficient
K_A, K_B, K_C	Coefficients, $(lbf^2)(sec^2)/(lbm^2)(ft^4)(°R)$
K_D	Coefficient, $(lbm)(ft^2)(°R^{1/2})/(lbf)(sec)$
K_G	Coefficient, $(lbf)(sec)/(lbm)(ft^2)$
K_n	Coefficient, (rpm)(sec)/ft
K_R	Coefficient, $(lbf)(sec)/(lbm)(ft^2)$
K_8	Nozzle parameter, $(lbm)(ft^2)(°R^{1/2})/(lbf)(sec)$
L	Torque, N-m; ft-lbf

Table 1. Nomenclature (Continued)

Symbol	Description
M	Matrix (cf Table 12)
M	Mach number
N	Rotational speed, rpm
N′	Nonlinear rotational speed, rpm
P	Power lever
P	Pressure, N/m^2; lbf/ft^2
PLA	Power lever angle
PR = PT3/PT2	Pressure ratio
$\mathcal{P}$	Power, ft-lbf/sec
Q	Matrix (cf Table 30)
R	Universal gas constant, 53.3 (lbf)(ft)/(lbm)(°R)
RHT	= Integral {(HB*WT+HCD*WTC - DHT*WT - HT*WN)/1.53} ~ ρ5*TT5
RT	= Integral {(WT+WTC - WN)/1.53} ~ ρ5
T	Temperature, °R
ΔT′	Ideal total temperature drop across turbine, °R
TM	Temperature combustor can
TD_i	Time delay states
TWCD	≅ Integral {γ*TCD(WCD - WB - WTC)} = 0.504*PT3
U	Mean rotor speed, ft/sec
U_T	Tip rotor speed, ft/sec
V	Volume, ft^3
W	Weight, lbm
WDCD	= Integral (WCD - WB - WTC) ~ ρ3
$\dot{W}$	Weight flow, lbm/sec
a	Speed of sound, ft/sec

Table 1. Nomenclature (Continued)

Symbol	Description
c_p	Specific heat at constant pressure, Btu/(lbm)(°R)
c_v	Specific heat at constant volume, Btu/(lbm)(°R)
g	Gravitational constant, 32.17 (lbm)(ft)/(lbf)(sec^2)
h	Static enthalpy, Btu/lbm
Δh	Actual isentropic expansion value, Btu/lbm
$\Delta h'$	Ideal isentropic expansion value, Btu/lbm
h_c	Heat of combustion, Btu/lbm
k_b	Bleed flow coefficient, (kg)(K$^{1/2}$)/(N)(sec); (lbm)(°R$^{1/2}$)/(lbf)(sec)
ℓ	Length, ft
r	Response vector (cf Tables 11 and 12)
r	Mean radius, ft
r_T	Tip radius, ft
s	Laplace operator, sec^{-1}
t	Time, sec
u	Control vector (cf Tables 11 and 12)
u	Internal energy, Btu/lbm
v	Velocity, ft/sec
v_θ	Tangential velocity, ft/sec
v_z	Axial velocity, ft/sec
v_{zc}	Axial velocity associated with stage characteristics, ft/sec
x	State vector (cf Tables 11 and 12)
x	Distance, ft
y	Distance, ft
z	Distance, ft
z'	Distance, ft

Table 1. Nomenclature (Continued)

Symbol	Description
α	Coefficient, 30 sec/min
β	Rotor air inlet angle, deg
γ	Ratio of specific heats, 1.4
δ	Ratio of total pressure to standard atmospheric pressure
∂	Boundary
η	White noise (cf Tables 11 and 12)
η	Efficiency
θ	Ratio of total temperature to standard atmospheric temperature
λ	Work-speed parameter
ρ	Weight density, lbm/ft^3
σ	Delay time, sec
τ_A, τ_B	Time constant, sec
ϕ	Flow coefficient
ψ^P	Pressure coefficient
ψ^T	Temperature coefficient
ω	Angular velocity, sec^{-1}

Subscripts (suffix):

B	Burner
CD	Compressor discharge
G	Gas
N	Speed
N	Noise
R	Rotor
T	Total
TC	Thermocouple
TC	Turbine cooling
W	Whistle

Table 1. Nomenclature (Concluded)

Symbol	Description
WFD	Whistle filter digital
b	Variable associated with stage bleed
c	Variable associated with stage characteristics
f	Fuel
(i)	Denotes function, i = 1, 2, 3, ...
in	Inlet
n	Stage number designation
out	Outlet
p	Variable associated with particle
s	Static condition
sc	Static condition variable associated with stage characteristics
stg 1	First stage
stg 2	Second stage
sv	Static condition variable associated with stage volume
t	Total condition
tc	Total condition variable associated with stage characteristics
tr	Total condition reference state
tv	Total condition variable associated with stage volume
v	Variable associated with stage volume
0	Free-stream condition (cf Figure 2)
2	Compressor inlet
3	Compressor discharge
4	Combustor
5	Turbine
5.1	Turbine discharge
8	Nozzle

SECTION II
MODELS AND CONTROL

Brief descriptions and summaries of the engine system and control synthesis are presented in this section.

MODELS

The J85 engine, its actuators, disturbances, and the system sensors are discussed.

J85 Engine

Figure 1 presents a cutaway drawing of the J85 engine; an equivalent functional schematic is shown in Figure 2. The engine for which the controls were designed has an afterburner, but for this contract, afterburner controls were not designed. An increase in the tailpipe volume was the only effect the afterburner presence had on this effort.

The math model of the J85 engine used for control synthesis was developed by the Lewis Research Center of the National Aeronautics and Space Administration. The model was originally developed for analog simulation (Reference 1) and later modified into an all-digital simulation. The reference presents a rationale and develops the equations for the math model of the J85 engine. With the reference and the computer listings for the digital version (presented in Appendix A of Volume II), it is a straightforward task to set up a simulation for the J85 engine. In this section of the report, a brief summary of the engine, the digital simulation, and Honeywell's use is presented.

The engine model uses:

- Experimentally determined steady-state compressor stage data
- Experimentally determined steady-state lumped turbine data
- Real gas combustion model
- Formal one-dimensional inviscid continuity, momentum, and energy approximations to unsteady intracompressor stage, combustor can, and tailpipe dynamics

The model judiciously combines experimental and theoretical results. Experimental data provide accurate low-frequency results while the theory provides means for extending the dynamics into the high-frequency range.

Discussion of the engine is separated into three major parts: the compressor, the turbine, and the burner-nozzle rotor. The compressor discussion is further broken down into the steady-state, dynamics, and problem areas. Considerable attention is devoted to the compressor because it is a source of major control problems. The burner-nozzle-rotor discussion describes the fuel addition in the burner, the real gas combustion model, and combustion efficiency in the burner. Flow in the tail pipe, the effects of the nozzle, and the effect of the exhaust area are presented under nozzle. The burner and nozzle discussions present dynamic models for the gas flows in these parts of the engine. The rotor discussion presents the model for showing how the unbalanced torques (of the compressor and turbine) accelerate the spool.

The compressor is built up by the stage-stacking technique. The overall characteristics of the compressor are obtained by cascading the results from each of the eight stages; dynamic and static. Experimental data are used to determine the static characteristics of a stage; continuum mechanics are used to determine the dynamic characteristics.

The steady-state characteristics of a compressor stage are described by the pressure gain and efficiency. The pressure gain across a stage or, equivalently, the isentropic enthalpy change, is required. In addition, the efficiency

of the compressor stage or the actual enthalpy change are needed. The major assumptions in developing the experimental data are that the flow is one-dimensional, steady, the in-flow angle to a stage in invariant, and that the usual correction coefficients for compressors are applicable to stage characteristics. In Reference 1, there is a discussion that justifies the invariant in-flow assumption.

The steady-state characteristics of a compressor stage are given in terms of the two dependent variables, ψ^P and ψ^T, which are functions of the independent flow coefficient, ϕ:

- Pressure coefficient:

$$\psi^P = 2gJ \frac{\Delta h'}{U_T^2} \tag{1}$$

- Temperature coefficient:

$$\psi^T = 2gJ \frac{\Delta h}{U_T^2} \tag{2}$$

- Flow coefficient:

$$\phi = \frac{(v_z / \sqrt{\theta})}{(U / \sqrt{\theta})} \tag{3}$$

where

$\Delta h'$ = Ideal (isentropic) change in enthalpy

Δh = Actual change in enthalpy

U_T = Rotor tip speed

U = Mean rotor speed

v_z = Axial flow velocity

The relationships across a typical compressor stage are shown in Figure 3. The engine operates on that portion of the flow coefficient where the derivative of the ψ^P with respect to ϕ is negative. In fact, there is a rough rule (Hartog) for stability of compressors which indicates that this is the range for which the flow is stable (Reference 2). This condition is intuitively obvious: If $d\psi^P/d\phi < 0$, the flow is self-equilibrating. If $d\psi^P/d\phi > 0$, the flow is divergent.

The velocity, v_z, appearing in the flow coefficient expression is the implicit function:

$$v_{zc,\ n} = \frac{\left(\dot{W}_{c,n}\right)\left(R\ T_{sv,n-1}\right)}{\left(A_{c,n}\right)\left(P_{sv,n-1}\right)} \tag{4}$$

where

$$\frac{\dot{W}_{c,\ n}\sqrt{\theta_{v,\ n-1}}}{\delta_{v,n-1}\ A_{c,n}} = \frac{v_{zc,\ n}}{\sqrt{\theta_{v,\ n-1}}}\left[1 - \left(\frac{v_{zc,\ n}}{\sqrt{\theta_{v,\ n-1}}}\right)^2 \frac{1}{2gJc_pT_{tr}\cos^2\beta n}\right]^{1/(\gamma-1)} \rho_{tr} \tag{5}$$

where

βn = Flow angle

T_{tr} = $\theta\ T_t$; i.e., total wrt to standard

To simplify the computation, NASA approximates the implicit function by the terms of a powers series:

$$\frac{v_{zc}}{\sqrt{\theta_{v,\ n-1}}} \approx (KA)_n + (KA)_{n+10} * FPn + (KA)_{n+20} * FPn * FPn \tag{6}$$

where

$$FPn \triangleq \frac{\dot{W}_{c,\ n}\sqrt{\theta_{v,\ n-1}}}{A_{c,n}\ \delta_{v,\ n-1}} \tag{7}$$

This explicit computation is quite accurate as is indicated by the results of Figure 4.

The pressure gain characteristics of the first compressor stage are affected by the inlet guide vane position so that for this stage the ψ^P curves are a function of the inlet guide position. These data are as indicated in Figure 5. Therefore, the ψ^P curves for the first stage are a family of curves rather than a single curve.

The two sets of experimentally determining curves, ψ^P and ψ^T, provide the steady-state characteristics for a compressor stage. It is assumed that all the dynamics of a compressor stage are associated with the interstage volume shown in Figure 6. In the nth stage equivalent volume the flow is considered to be compressible, one-dimensional, and isentropic. The output of the stage volume then drives the (n+1)th compressor stage. Lumped approximations to the conservation laws are used to compute flows through the stage volume.

The conservation equations for quasi one-dimensional inviscid flow are:

- Mass:

$$\frac{\partial}{\partial t}(\rho A) + \frac{\partial}{\partial x}(\rho A v) = 0 \tag{8}$$

- Momentum:

$$\frac{\partial}{\partial t}(\rho A v) + \frac{\partial}{\partial x}(\rho A v^2) = -Ag\frac{\partial P}{\partial x} \tag{9}$$

- Energy:

$$\frac{\partial}{\partial t}(\rho A u_t) + \frac{\partial}{\partial x}(\rho A v H) = 0 \tag{10}$$

While it would be desirable to use the conservation laws directly, the computational requirements would be excessive. Therefore, lumped parameter approximations are made.

The lumped mass approximation is made first:

$$1. \quad \frac{\partial}{\partial t}(\rho A) = -\frac{\partial}{\partial x}(\rho A v) \tag{11}$$

$$2. \quad \frac{\partial}{\partial t}(\rho A) = -\frac{\partial}{\partial x}(\dot{W}) \tag{12}$$

$$3. \quad \frac{\partial}{\partial t}(\rho) = -\frac{1}{A}\frac{\partial}{\partial x}\dot{W} \tag{13}$$

$$4. \quad \frac{d}{dt}\rho = +\frac{1}{V}(\dot{W}_1 - \dot{W}_2) \tag{14}$$

$$5. \quad \frac{d}{dt}(V\rho)_n \triangleq \frac{d}{dt}(WV)_n = (\dot{W}_n - \dot{W}_{n+1}) \tag{15}$$

Line one is simply a rewriting of the conservation law, line two is a symbolic change, in line three the approximation is made that the cross-sectional area is constant, and in line 4 the major approximation is made; the partial derivatives are replaced with ordinary derivatives. It is seen that the increase in density within the volume is inversely proportional to the volume and the differences in flow rates in and out of the volume. As written, the density should be at the center of the volume, but in the use that follows, the density change is taken either at the left or the right end as required. Line 5 is simply a symbolic change.

Lumping of the momentum equation proceeds similarly:

$$1. \quad \frac{\partial}{\partial t}(\rho A v) = -\frac{\partial}{\partial x}(\rho A v^2) - Ag\frac{\partial p}{\partial x} \tag{16}$$

$$2. \quad \frac{\partial}{\partial t}(\rho A v) \approx -Ag\frac{\partial P}{\partial x} \tag{17}$$

3. $\frac{d}{dt}\dot{W} \approx \frac{Ag}{\ell}(P_1 - P_2)$ (18)

4. $\frac{d}{dt}\dot{W}_n \approx \frac{Ag}{\ell}(P_{T1} - P_{T2})\left(1 + \frac{\gamma - 1}{2} M^2\right)^{\frac{-\gamma}{(\gamma-1)}}$ If $M_1 = M_2$ (19)

5. $\frac{d}{dt}\dot{W}_n \triangleq \frac{d}{dt} WD_n \approx KGAL_n + 10\left(P_{T_n} - P_{V_n}\right)$ (20)

Lumping of the energy equations follows:

1. $\frac{\partial}{\partial t}(\rho A u_t) = -\frac{\partial}{\partial x}(\rho A v H)$ (21)

2. $\frac{\partial}{\partial t}(\rho c_v T_t) = -\frac{1}{A}\frac{\partial}{\partial x}(\dot{W} c_p T_t)$ (22)

3. $\frac{d}{dt}(\rho T_t) \approx \frac{\gamma}{v}(W_1 T_{t,1} - W_2 T_{t,2})$ (23)

4. $\frac{d}{dt}(V\rho T_t)_n \triangleq \frac{d}{dt}(TWV)_n = \gamma(\dot{W}_n T_{t,n} - \dot{W}_{n+1} T_{t,\ n+1})$ (24)

The lumping of the momentum and energy conservation equations is thus quite similar to that for mass conservation equations, although less conservative assumptions are required to get to the lumped models.

Reference 1 shows that the steady-state results of lumping the conservation equations are exact. It is thus to be expected these lumped parameter approximations are exact in the steady state, and reasonably good over a low-frequency range. The approximation would be poor at extremely high frequencies.

Table 2 presents a Fortran listing for the seventh compressor stage. The listing is presented at the top of the page and then embellishments are provided at the bottom. Amplification is shown on five computer lines where the nature of the computation and of approximations are indicated. The assembling of the experimental steady-state characteristics and the dynamics

through the interstage volume do provide a plausible dynamic simulation for the compressor stage. Results presented in Reference 1 compare test and model data.

One of the things that should be noted in the compressor model is that for each stage of the compressor there are three orders of differential equations. The roots of the typical stage will consist of a complex pair and of a single damped root. The lightly damped complex pair can be associated with organ pipe-type resonance.

The other stages of the compressor are modeled quite similarly to that for the seventh stage. There are some differences, however, as indicated in Table 3. Special considerations must be made, for instance, at stage 1 to provide for flow matching with inlet. Also, since the inlet guide vanes affect the characteristics of the first stage, the first stage ψ^P is a function not only of flow but of the inlet guide vane position. From stages 3, 4, and 5, there can be bleed flow if the bleed valves are open. The equation for the bleed flow is indicated in Table 3. This equation assumes that the airflow through the bleed valves is choked. Bleed increases the flow through the early compressor stages and therefore increases the stability of operation. There must be special considerations made at the outlet of the last stage to match the characteristics with the combustion can.

Compressor control problems include stall, surge, and flutter.

Compressor stall is much like wing stall in that the blade sections of the compressor may enter into the stall region. For the compressor, the problem is serious because it reduces the efficiency of the compressor and will ultimately lead to higher temperatures and more deleterious conditions throughout the engine. The stall may be steady or unsteady and it could be one-, two-, or three-dimensional. Since one-dimensional assumptions have been used here, the two- and three-dimensional types of stall are not modeled.

Surge produces oscillations in the compressor outlet pressure, PT3. The magnitude of this oscillation may build up to such a large value that the airflow through the compressor is reversed. Surge may occur if the sign of $d\psi^P/d\phi$ is positive. Decreasing pressure ratio or increasing airflow inhibits tendencies toward surge.

Compressor blade flutter can be a problem, though it is not one on the J85-13 engine. The presence of blade flutter could require special restrictions on compressor pressure ratio and airflow; these restrictions would be similar to stall-surge limitations.

Surprisingly, both the steady-state and dynamic characteristics of the turbine are modeled differently than for the compressor stages. There is much more cross coupling in the steady-state characteristics, and it is considered feasible to neglect the gas dynamics within the turbine stage. The latter is feasible because of the higher frequencies of the gas dynamics and because the gas turbine is operating in a more favorable stability range than is the compressor. It will be shown later that the Hartog stability condition for the turbine is inherently favorable; this is one of the reasons that the interstage turbine dynamics can be neglected.

Figure 7 presents a stage map across two stages of the turbine. These data could be approximated with digital techniques but not very easily. The math model was originally developed by NASA for analog simulation. Analog simulation of the data in Figure 7 would be practically impossible. NASA developed a simplification of the data in Figure 7, and the results are shown in Figure 8. The latter shows that the steady-state turbines characteristics can be approximated with two two-dimensional functions.

The simplification that was necessary for analog simulation also makes it considerably easier for digital simulation.

Figure 8 shows that the Hartog stability criterion is inherently satisfied by the turbine. The partial derivative of $\partial PT5/\partial \dot{W}5$ with respect to the flow through the turbine is negative over the entire operating range.

The exhaust nozzle is modeled with steady-flow equations. The nozzle may run choked or unchoked, so both of these conditions need to be provided for. For mathematical reasons, it is necessary to set up the equations so that gas flow in the tailpipe cannot be reversed. The nozzle simulation is presented in Table 4.

The rotor acceleration is simply the sum of the unbalanced torques across the rotor, i.e., the sum of the torques on the compressor and on the turbine:

$$I\dot{W} = \Sigma L \tag{25}$$

$$\mathcal{P} = \omega(\Sigma L) = J * \Sigma (\dot{W} * \Delta H) \tag{26}$$

$$\dot{N} = \left[\left(\frac{30}{\pi}\right)^2 \frac{J}{1}\right] * (1/N) \Sigma \dot{W} \Delta H \tag{27}$$

$$= [KSPEED] * (1/N) * [DLWHT - DLWHC] \tag{28}$$

where

$$DLWHT = HB * WT + HCD * WTC - HT * WN \tag{29}$$

$$DLWHC = HCD * WCD + 0.24 (WBLTBL - TVO * WDO) \tag{30}$$

The simulation has other "goodies" as listed in Table 5. The functions TFNH and PROCOM model real gas effects at high temperature and are used in the high-temperature sections of the engine. The subroutine (function) EFFB models the heat release from the fuel as a function of operating conditions within the burner can. Heat storage capacity in the combustion can and turbine introduce another state, TM, which is referred to as thermal

capacitance. This effect is a single addition that Honeywell added to the NASA model. It is a first-approximation to long-time thermal constants which are known to be present in the engine. Volume III of this report indicates that the thermal capacitances modeled are not very accurate. Their inclusion in the model is considered to be desirable in that the very-low-frequency effects help in designing integral controls to provide setpoint accuracy.

Now we can turn to the section of the program that provides a digital simulation for the burner, turbine, nozzle, and rotor. This is shown in Table 6. The table has been embellished with comments to the right of the Fortran statements. With the previous comments and with these embellishments, the reader should be able to ascertain the gist of the simulation. In getting from line 279 to 281, the following will be helpful:

$$\frac{\partial}{\partial t}(\rho A U_t) = -\frac{\partial}{\partial x}(\rho A v H) \text{ (Energy equation w/o heat addition)} \quad (31)$$

$$\frac{d}{dt}(\rho C_v T_t) \approx -\frac{1}{V}(\dot{W}_{CD} H_{CD} - \dot{W}_B H_B) \quad (32)$$

$$\frac{d}{dt}(\rho H) = \frac{\gamma}{V}(\dot{W}_{CD} H_{CD} - \dot{W}_B H_B) \quad (33)$$

$$\frac{dH_B}{dt} = \frac{\gamma}{V\rho_B}(\dot{W}_{CD} H_{CD} - \dot{W}_B H_B) - \frac{H_B}{V\rho_B}(\dot{W}_{CD} - \dot{W}_B) \text{ (Uses continuity)} \quad (34)$$

$$\frac{dH_B}{dt} = \frac{\gamma}{V\rho_B}(\dot{W}_{CD} H_{CD} + \dot{W}_F * 18650 * \eta_B - \dot{W}_B H_B) - \frac{H_B}{V\rho_B}(\dot{W}_{CD} + \dot{W}_F - \dot{W}_B) \text{ (Heat and mass addition)} \quad (35)$$

but

$$\frac{\gamma}{V\rho_B} = \frac{\gamma}{V}\ \frac{RT}{P} \approx \frac{\gamma}{V} R \frac{T_B}{P_B} = \frac{J(\gamma-1)\ C_P T_B}{V\ P_B} = \frac{J(\gamma-1)}{V}\ \frac{H_B}{P_B}$$

$$= \frac{J(\gamma-1)}{144\ \tilde{V}}\ \frac{H_B}{P_B} = (KVOLB)\ \frac{H_B}{P_B} \tag{36}$$

Therefore,

$$\frac{dH_B}{dt} = (KVOLB)\ \frac{H_B}{P_B}\left[\dot{W}_{CD}H_{CD} + \dot{W}_F * 18650 * \eta_B - \dot{W}H_B - \frac{H_B}{\gamma}(\dot{W}_{CD} + \dot{W}_F - \dot{W}_B)\right] \tag{37}$$

Now use Line 279 in Equation (37) and get Line 281:

$$\frac{dH_B}{dt} = \frac{H_B}{P_B}\left[\dot{P}_B - KVOLB\left(\frac{H_B}{\gamma}\right)(\dot{W}_{CD} + \dot{W}_F - \dot{W}_B)\right] \tag{38}$$

Table 6 for burner, turbine, nozzle, and rotor contains six orders of differential equation. It includes the dominant dynamics for the spool, for the tailpipe, and for the combustion can. For the listing, the thermal capacitance effects had not yet been added. The details of those can be seen in the computer listings as provided in Appendix A of Volume II.

Actuators

Models of the actuators are presented in Table 7.

Two models of the fuel valve dynamics were used. The first uses a first-order lag. The second model was developed by personnel of the Energy Controls Division of Bendix.

First-order representations were used for the IGV and bleed.

The exhaust nozzle is operated through a clutch brake system. The second-approximation shown is quite accurate, although it does neglect clutch dynamics and slippage. For control synthesis, the linearized first-approximation was used.

Disturbances

Controls were designed for two kinds of disturbances: command (pilot) and inlet buzz.

For control synthesis and analysis, there is a component of the state (P) called power lever. Power lever position is taken to range between 0 and 1 and vary linearly with commanded spool speed; e.g., 1 corresponds to a command of 100 percent spool speed. Where perturbation control only is being considered, a value of P corresponds to a perturbation from trim. For synthesis purposes, the power lever position is modeled by

$$\dot{P} = -4.0\,P + 0.028241\,\eta \tag{39}$$

The engine inlet duct is an organ pipe. It may resonate to yield nearly sinusoidal pressure variations at the compressor face.

Duct buzz is modeled with the following:

$$\begin{Bmatrix} \dot{\widetilde{PT}}\ 2 \\ \dot{DUM} \end{Bmatrix} = \begin{bmatrix} 0 & +1.0 \\ -900.0 & -6.0 \end{bmatrix} \begin{Bmatrix} \widetilde{PT}\ 2 \\ DUM \end{Bmatrix} + \begin{Bmatrix} 0 \\ 432.09 \end{Bmatrix} \eta \tag{40}$$

With this model, $\widetilde{PT}$ is nearly sinusoidal with a frequency of 30 radians per second, an amplitude of 0.4 x 14.7 = 5.88, and an rms value of 4.16 pounds per square inch.

Sensors

Spool speed, pressure, and burner temperature sensor dynamics were considered.

The spool speed sensor on the APL wind tunnel test J85 has flat dynamics to beyond 100 Hz. Transfer dynamics were therefore taken to be 1.

Dynamic representations for the pressure sensors (P3 and PT5) should include the effects of both the transducers and the transmission lines. Natural frequencies of the transducers (used in the APL wind tunnel tests) are greater than 10,000 Hz. APL estimates of transmission line dynamics show very small effects at frequencies below 100 Hz. Since the design passband for the wind tunnel controller was to be below 5 Hz, the dynamics for the pressure sensors were neglected; i.e., the transfer functions were taken to unity.

In the final math models used to design the controllers for wind tunnel test, there appear to be dynamics associated with the P3 and PT5 pressure sensors: first-order lags with time constants of 0.020 and 0.025 second, respectively. Filtered white noise is also added. These dynamics are crude attempts at trying to compensate for the final drastic approximations made to the engine math model. The 0.020- and 0.025-second time constants are associated with the combustion can and tailpipe fill dynamics. The added noise simulated pressure fluctuations due to combustion and aerodynamics.

The sensor for burner temperature is fluidic (a sonic whistle). Its response is given by

$$TT4W = \left\{ \frac{k}{1 + \tau_1 s} + \frac{(1 - k)}{1 + \tau_2 s} \right\} * TT4 \qquad (41)$$

where k, τ_1, and τ_2 are functions of burner pressure PT4. TT4 sensor (whistle) characteristics are listed below:

TT4 Sensor (Whistle) Characteristics

N%	PT4~psi	k	τ_1 ~ sec	τ_2 ~sec
50	24.5	0.50	0.020	30.0
70	39.0	0.53	0.020	17.0
85	58.5	0.56	0.020	10.0
100	100.0	0.60	0.020	8.0

The functional dependence is on PT4; the values of N shown correspond to the values of PT4 when the engine is operating near its temperature limit.

Combustion temperature contains a highly fluctuating component (Reference 3). This component was arbitrarily taken to be a part of the sensor system. The sensor representation then becomes

$$\begin{vmatrix} \dot{TT4W} \\ \dot{WDUM} \\ \dot{X13} \end{vmatrix} = \begin{vmatrix} 0 & 1.0 & 1.0 \\ -\frac{1}{(\tau_1)(\tau_2)} & -\left(\frac{1}{\tau_1}+\frac{1}{\tau_2}\right) & 0 \\ 0 & 0 & (-0.20E+5) \end{vmatrix} \begin{vmatrix} TT4W \\ WDUM \\ X13 \end{vmatrix} + \begin{vmatrix} \frac{k}{\tau_1}+\frac{(1-k)}{\tau_2} \\ \frac{-k\left(\tau_2^2-\tau_1^2\right)-\tau_1^2}{(\tau_1\ \tau_2)^2} \\ 0 \end{vmatrix} TT4 + \begin{vmatrix} 0 \\ 0 \\ G2(13,4) \end{vmatrix} \eta 4 \qquad (42)$$

The root at (-0.20E+5) is an eyeball estimate for the bandwidth of the combustion noise. The coefficient G2(13, 4) is adjusted during design work so that the rms value of TT4W is on the order of tens of degrees.

It is clear from Equ... (41) that TT4W is a poor dynamic approximation to TT4. A lead-lag filter of TT4W will yield an approximation to TT4 that corresponds to lagging TT4 by 0.02 second; i.e., take:

$$M10 = \frac{\tau 2*s+1}{k*\tau 2*s+1}\ TT4W \qquad (43)$$

Then

$$M10 = \frac{1}{\tau 1 * s + 1} \left\{ \frac{\tau 1 * s * (1 - k) + (k * \tau 2 * s + 1)}{\tau 2 * s + 1} \right\} \left\{ \frac{\tau 2 * s + 1}{k * \tau 2 * s + 1} \right\} TT4$$

$$\approx \frac{TT4}{\tau 1 * s + 1} \tag{44}$$

This filtering is realized with

$$\dot{X}10 = -\left(\frac{1}{k * \tau 2}\right) X10 + \left(\frac{1}{k * \tau 2}\right) TT4W \tag{45}$$

$$M10 = \left(\frac{1}{k}\right) TT4W + \left(1 - \frac{1}{k}\right) X10 \tag{46}$$

For the linearized design, the coefficients in Equations (45) and (46) are taken to be the constant values shown in the tabulation of TT4 sensor (whistle) characteristics. For wind tunnel test, the coefficients were scheduled with P3 (taken to be an acceptable approximation to PT4).

The above whistle filter was "designed" by a classical technique. It may be wondered why optimal methods were not used, since this is a contract for optimal control design. The answer is that there is a subsequent optimization and simplification. It was considered to be unlikely that an extra optimization step would have yielded significantly superior dynamic performance.

CONTROL

We now have an engine model and we know the objectives for jet engine control. Tables 8 and 9 summarize the characteristics of the model. From the summary data, Table 8, it is seen that the model order is very high, there is a very wide frequency spread, and there are significant nonlinearities, including bounded phase constraints. There are multiple controls. These

things make it appear that the control design job is a rather formidable one. The formidability is more apparent than real. The control synthesis job is tractable because the design is dominated by one significant nonlinearity of first order and the remainder of the dynamics can be considered secondary.

The comments in Table 8 on the accuracy of the model are engineering judgments based in part on the design synthesis and wind tunnel tests at APL. For more detail one should refer to Volume III of this report and to Reference 1.

The rough control passband requirements indicated in Table 8 start to give a clue as to why the engine control synthesis task is tractable. It is seen that the command requirements are only over a passband from zero to 15 radians per second. The engine dynamics over the 15-radian-per-second passband (cf Table 9) are of relatively low order.

If disturbance control or dynamic surge recovery control are necessary, passband requirements are raised to at least 200 radians per second. The order of the model containing all frequencies below 200 radians per second is high.

At this time, we had an engine model and a plan for use of the model in control synthesis. Control synthesis went in broad outline as planned; there were traumatic changes in detail due to model problems.

Those experienced in building and using models will recognize the gore of a typical engineering application. A few words of explanation will be offered for the neophytes. The situation started as it usually does. The analog model had been designed, built, tested, and favorably compared with engine test results. What could possibly go wrong? Two kinds of model problems emerged: usage and conversion.

This model was designed with particular user applications in mind. This permitted particular exploitations for simplicity. An example: The NASA model essentially assumes the exhaust nozzle will be driven on the Bill of Material (BOM) schedule. Engine perturbation response with this built-in hypothesis is different than when the exhaust nozzle is taken as an independent variable.

Honeywell acquired the digital version of the model while it was being converted from analog to CSMP language; Honeywell converted this to Fortran. Typical of the exasperating little problems: Honeywell initially left the integration statements for Fortran where they appear in CSMP. Until the integration statements were moved, the Fortran version had markedly less high-frequency stability. More serious was compressor model instability at the normal 60-percent operating point. This anomaly was not resolved during the contract period.

Honeywell used four models during the contract period:

- The complete model
- The disturbance model
- The wind tunnel design model
- The steady-state model

The steady-state (trim) is a part of all models and is a user option (cf Appendix A). "Trim" data were obtained at steady state and under accelerated conditions by artificially loading the compressor shaft. This permits trim near the surge-stall boundary.

The complete model (by staying away from 60 percent) was used for qualitative studies and for sensitivity studies to inlet disturbances. Frequency response tests, for example, showed mild resonance peaks near 40 radians per second (tailpipe resonance).

It was the intention to use the complete model to determine the surge-stall boundary. Because of the unresolved anomaly at 60 percent, the Hartog criterion for the steady state was used instead. It was also the intent to design controllers for lower-order representations, but to test them using the complete model. This had to be abandoned.

The disturbance model is the complete model with the compressor dynamics truncated. It contains gas dynamics of the combustion can and tailpipe. It was used for the disturbance control results of Section III.

The design of the controllers for wind tunnel test was initiated with the disturbance model. We ran into the exhaust nozzle problem previously discussed.

With help from NASA personnel, we got a fix on the exhaust nozzle. This was late in the contract period. To minimize the probability of unnecessary problems due to modeling, we truncated all gas dynamics to obtain the wind tunnel design model. This was permissible because the wind tunnel could only test command controllers, and command passband requirements are low.

Synthesis

The control synthesis is divided into three tasks:

- Setpoint (steady-state optimization)
- Trajectory optimization
- Perturbation control optimization:
  - State control over commands and disturbances
  - Control for wind tunnel test

To separate the control optimization problem into the three parts of trim, trajectory, and perturbation requires an underlying set of simplifying assumptions. The overall assumption is that the optimization problems can be separated by speed of response. For trim optimization this is certainly valid; the engine operates for long periods in steady state. Trajectory optimization considers those frequencies or transient times which are comparable to the transient times of the dominant dynamics of the engine. For a single-spool engine (with matched actuators, such as the J85), this characteristic response time is that for the spool. For the J85, and other single-spool engines, the single significant nonlinearity of the engine can be associated with the spool.

Of the three optimization tasks that generally need to be accomplished for optimal control design, only the third was accomplished under this contract effort. For setpoints, the General Electric trim data were used with a revised exhaust actuator schedule determined under a previous Honeywell program. The trajectory optimization was accomplished under simplified assumptions. The assumptions were permissible because of the simplicity of the J85 engine and because some of its ancillary equipment (IGV, bleeds, and exhaust actuator) have been matched by General Electric to the response characteristics of the engine. Extensive perturbation control optimization was performed.

A consequence of the trim optimization was the determination of the steady-state and ancillary actuator schedules. These schedules are presented in Figure 9.

Figure 10 clearly shows why trajectory optimization is not a difficult problem for the J85. For example, assume that on a standard day it is desired to accelerate the engine from 95-percent operating speed to 100-percent operating speed in minimum time. In Figure 10, the engine would initially be at point A with $\dot{N}$ and a fuel flow of 2000 pounds per hour. The fuel flow

should be increased as quickly as possible to about 3000 pounds per hour which will put the engine in point B where it is run into the TT4 temperature limit. At this point, $\dot{N}$ is at the maximum positive value and spool speed will accelerate at 5000 rpm per second. The trajectory will then follow from point B to point C, with the fuel flow being increased slightly during this period of time, and at point C, the engine is operating at 100 percent. The fuel flow will then be decreased to 3000 pounds per hour to again reach the equilibrium now at 100-percent operating speed. By doing it in this manner, it is clear from the figure that the engine speed will have been changed in minimum time subject to the constraint that the TT4 will not be exceeded.

With different operating temperatures or a different TT4 operating limit, the TT4 could be so far to the right it would not be a limiting condition. Taking the same problem as previously, instead of moving from point A to point B, we move from point A to point B′, which would be near the surge-stall boundary of the engine. The fuel flow would then be increased to follow along the surge boundary to get to point C′, at which point engine speed would be 100 percent and then fuel flow would be decreased to 3000 pounds per hour to bring the engine back into equilibrium.

Similar conditions hold for maximum deceleration as limited by the flameout boundary.

Figure 11 shows an engine map. Here the trajectories can be plotted and viewed in more detail. The points (A, B, B′, C, C′, and D) of the previously discussed trajectory are labeled.

Trajectory optimization for the J85 engine has just been discussed. The trajectory optimization is both modern and classical. The answers obtained are the same that would be obtained by the classical control designer and are the same that would result from the use of modern trajectory optimization techniques. Under the assumptions made here, no fancy mathmetics are required.

Perturbation design might be effected in one of two ways: time-varying or time-invariant. Each offers advantages. Both are tractable. From the theoretical point of view, one should chose the time-varying method in that there are no major assumptions necessary in developing the controller. One could be assured that with the techniques currently available, good control would be achieved. The disadvantages in using the time-varying synthesis for perturbation controls are twofold. First, perturbation design costs are much higher because controls must be synthesized for a linear time-varying system. Second, implementation costs would be considerably more in that families of time-varying trajectories would have to be stored within the computer to provide the closed-loop control function.

Perturbation design for constant coefficient representations is both simply synthesized and easily implemented. Speed, surge-stall (PT3/PT2), and temperature (TT4) perturbation feedbacks are determined at four different operating speeds (50, 70, 85, and 100 percent) along the equilibrium, surge-stall, or maximum temperature lines. Nonlinear control is realized by gain scheduling with speed, adding trim fuel flows, and by selecting which of the three controllers is in command by using the one for minimum fuel flow. To prevent flameouts, a minimum fuel flow (open-loop in the present case) limit is added. Table 10 and Figure 12 present equations and schematics.

Perturbation control synthesis was by "quadratics": computer programs developed from quadratic control theory. Two programs were used: state and simple. State control has a gain matrix that feeds back every component of the state. Simple control permits only sensor feedbacks. State control is unique and is used for initial studies. Simple control is generally not unique but is made so in our applications, starting the simplification from a unique state control. Simple control is practical: mechanizable.

State optimization determines what performance can be obtained from the system under idealized conditions. The simple optimization then determines a simple control structure that both achieves the performance necessary and the simplification desired.

The state control optimization problem is presented in Table 11. The linear model is obtained by using the linearizer (Appendix A) on the nonlinear model to obtain the J85 engine states and responses. Actuator, sensor, and disturbance are added to these by the designer. The response vector permits evaluating components not in the state (such as PT3) and makes it easy to enforce design requirements (such as the PT3 response will be first-order with a 0.1-second time constant). The control designer picks a Q matrix. The optimization procedure calculates the gain matrix K and presents results for evaluation. If performance is faulty in some respect, a new weighting matrix Q is chosen and the procedure repeated.

Simple optimization (Reference 4) is presented in Table 12. In this optimization problem, forms for filters and the feedbacks are specified. The optimization procedure then determines the feedback matrix gain K^*. Appendix D presents a derivation of the algorithm.

Most of the components (PT3, TT4, N, WFV) in the response vector are naturally arrived at. To add a component that will make achieving a 0.1-second PT3 response to power lever and stable integral control requires a little effort. Table 13 summarizes how to augment the state to get integral control and how to augment the response vector to get the desired response. This is an abridgement of Appendix C.

Frequency Response

In Section IV, three sets of frequency response plots are presented: closed-loop, conventional actuator open-loop, and gain-breaking open-loop. In Figure 13, these correspond to:

- Closed-loop: $\hat{u}/r$ with all loops closed
- Actuator open-loop: $\tilde{u}/\hat{u}$ with the loop broken at α and $r = 0$
- Gain-breaking open-loop: $\tilde{u}_\xi/\hat{u}_\xi$ with the loop broken at β and $r = 0$

Their formulas are given by:

$$\hat{u}/r = K^*M\left[s - (F + gK^*M)\right]^{-1} g \tag{47}$$

$$\tilde{u}/\hat{u} = K^*M\,(s - F)^{-1}\, g \tag{48}$$

$$\tilde{u}_\xi/\hat{u}_\xi = K_\xi^* \sum_j M_{\xi j}\left[\left(s - F - g \sum_{k \neq \xi} K_k^* M_{kj}\right)^{-1} g\right]_j \tag{49}$$

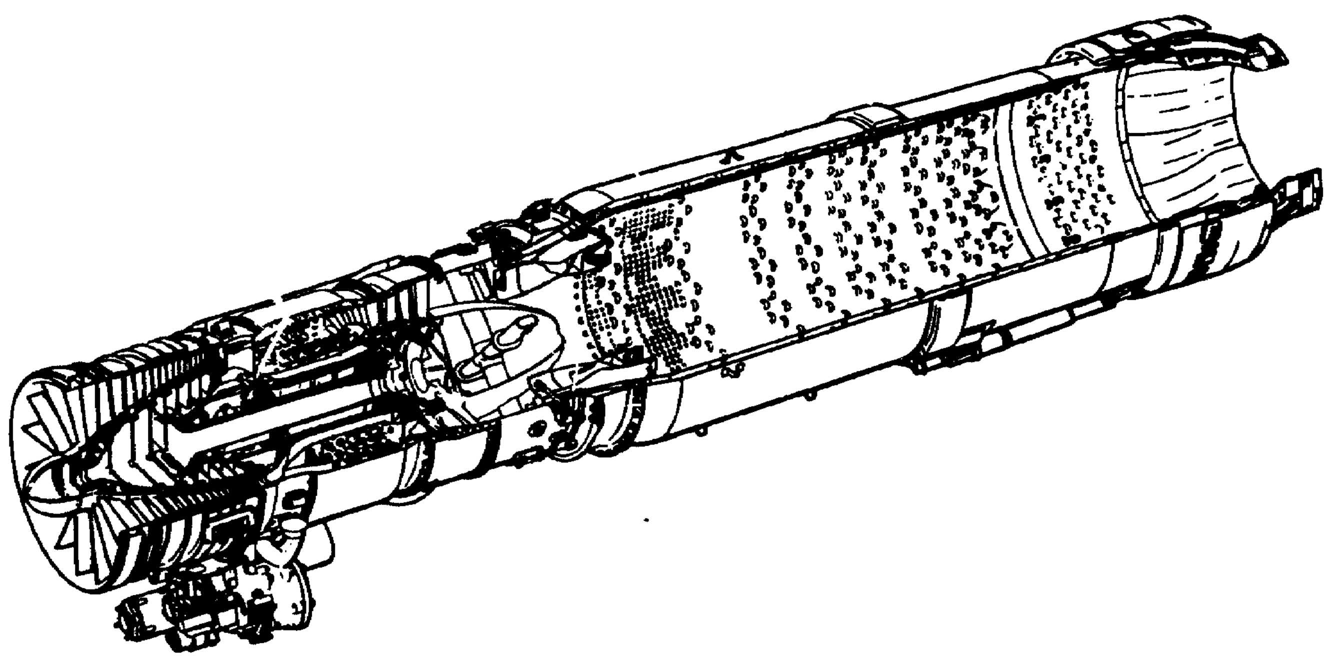

Figure 1. Cutaway Section of J85-13 Turbojet Engine and Afterburner

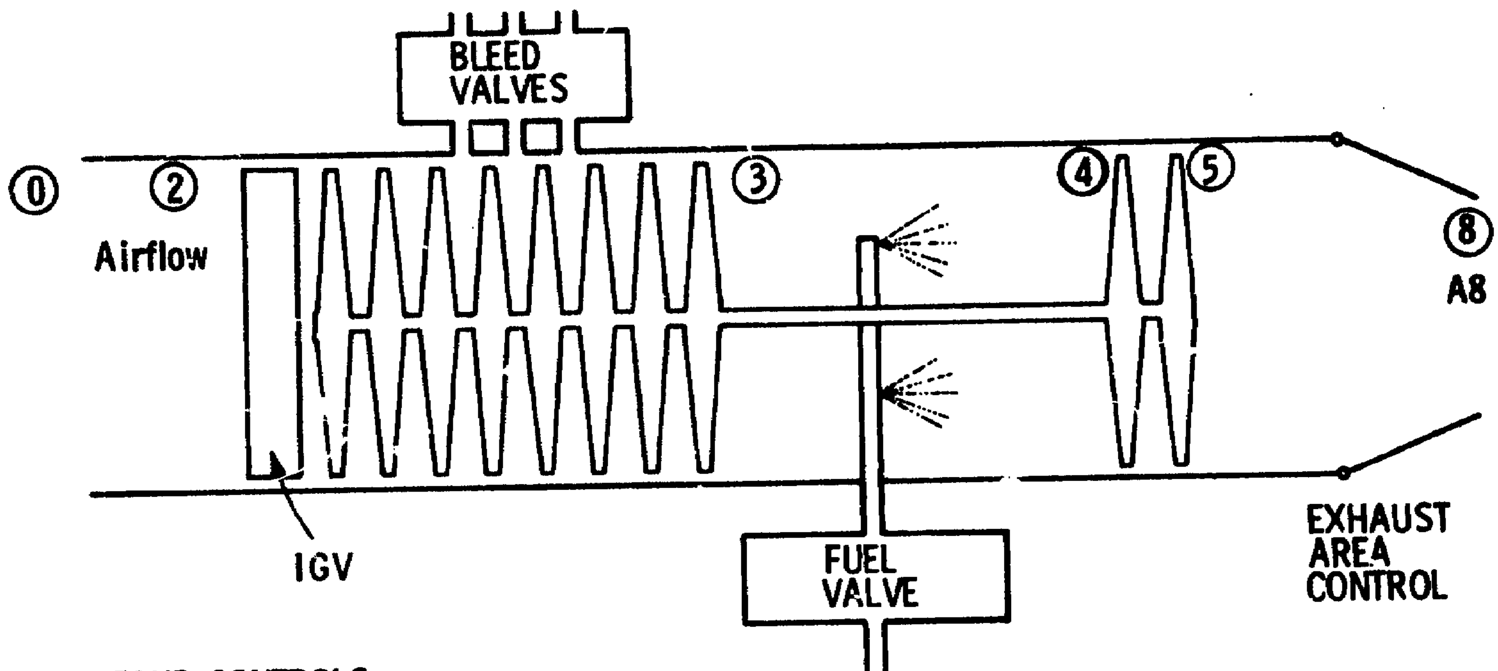

FOUR CONTROLS

- ▶ IGV (Inlet Guide Vane)
- ▶ BLEED (Bld)
- ▶ FUEL (WF)
- ▶ EXHAUST AREA (A8)

Figure 2. A Simple Jet Engine (J85-13, 3000-Pound Class)

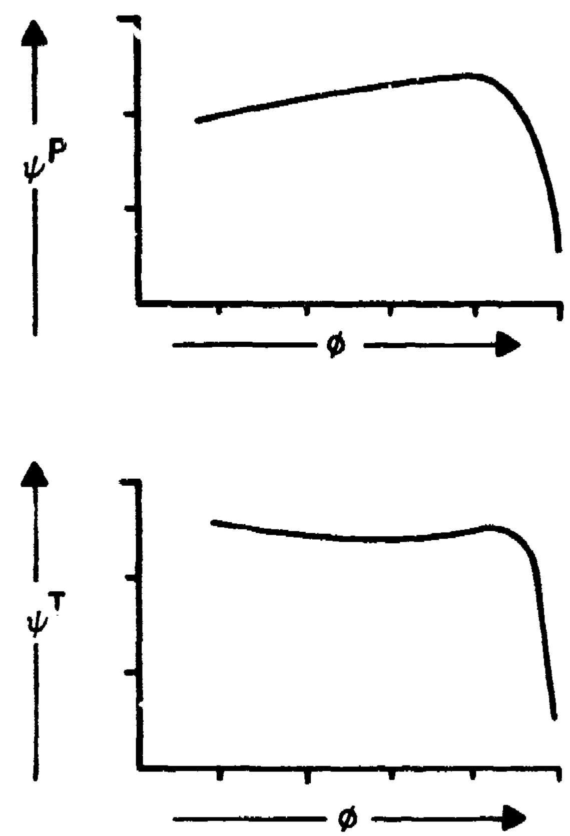

Figure 3. Typical Compressor
ψ^P and ψ^T

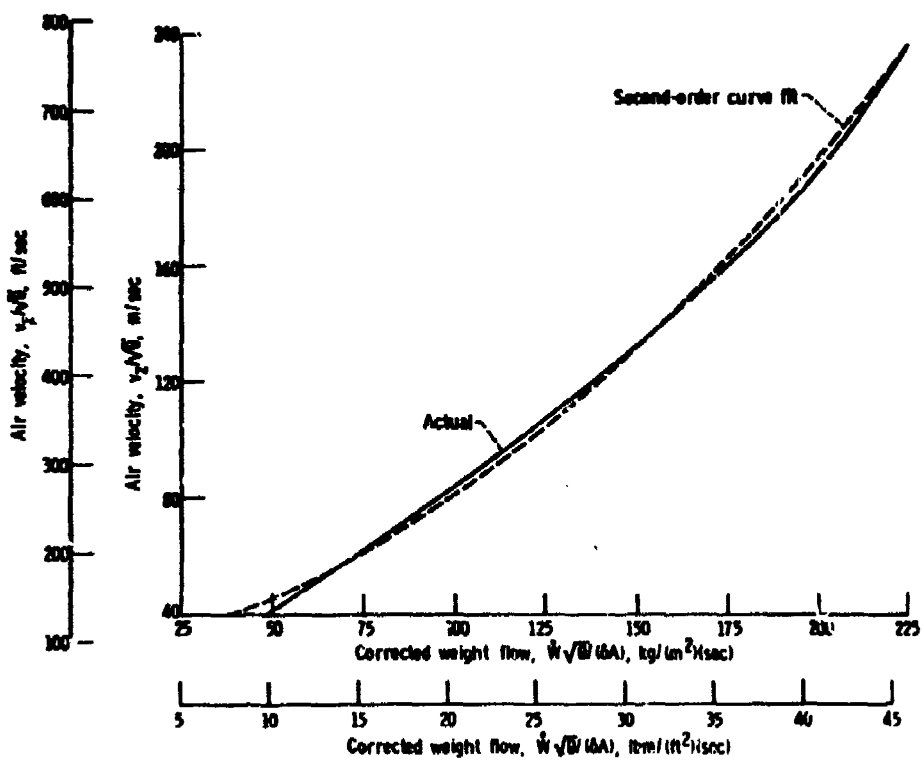

Figure 4. Compressor Axial Flow Velocity Goodness of Approximation--Typical Air Velocity Computation

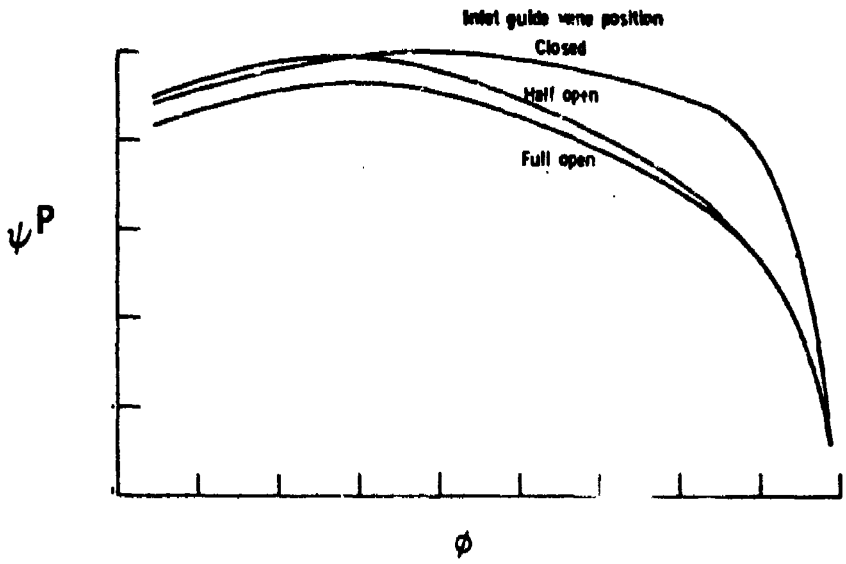

Figure 5. Effect of IGV on First-Stage ψ^P

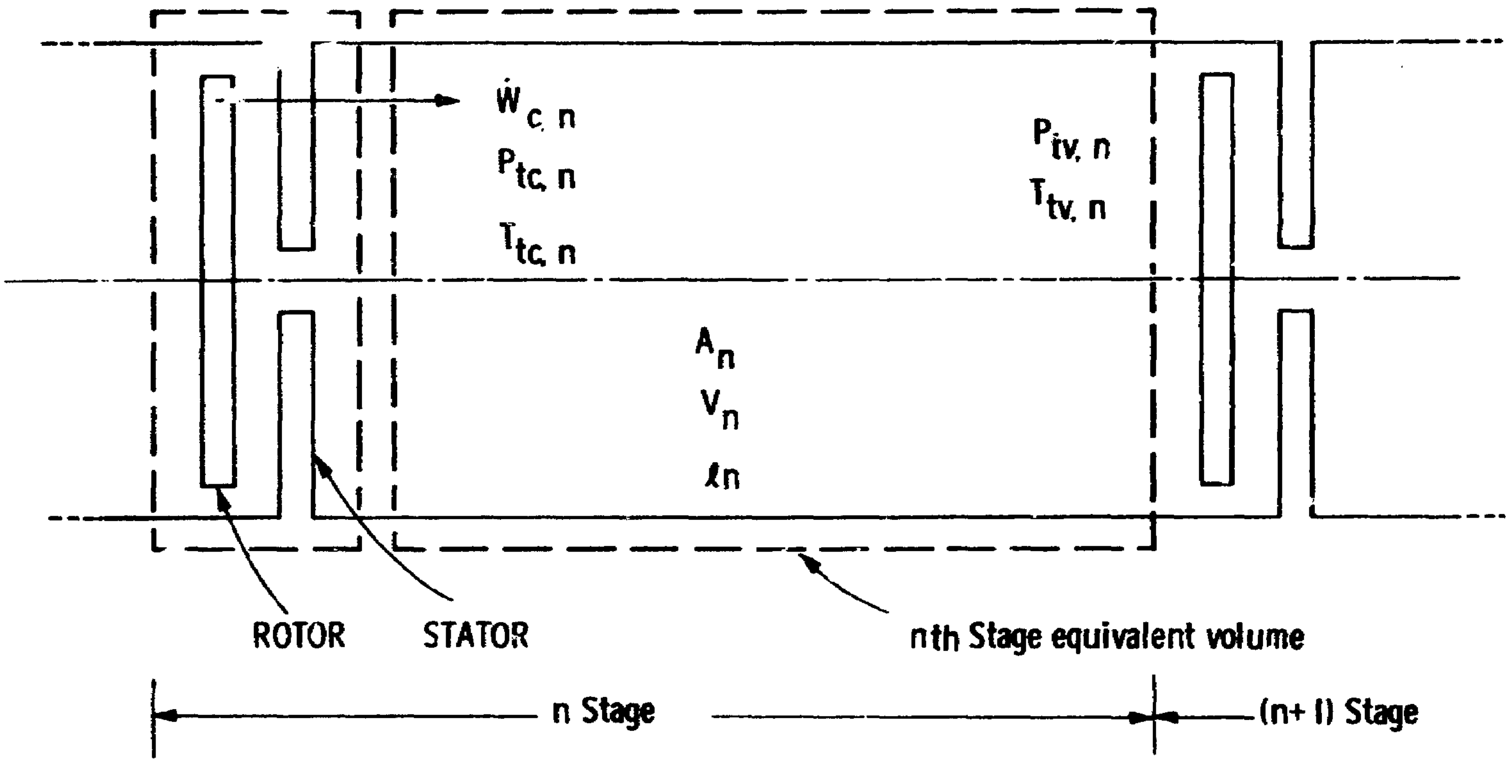

Figure 6. Nth Compressor Stage

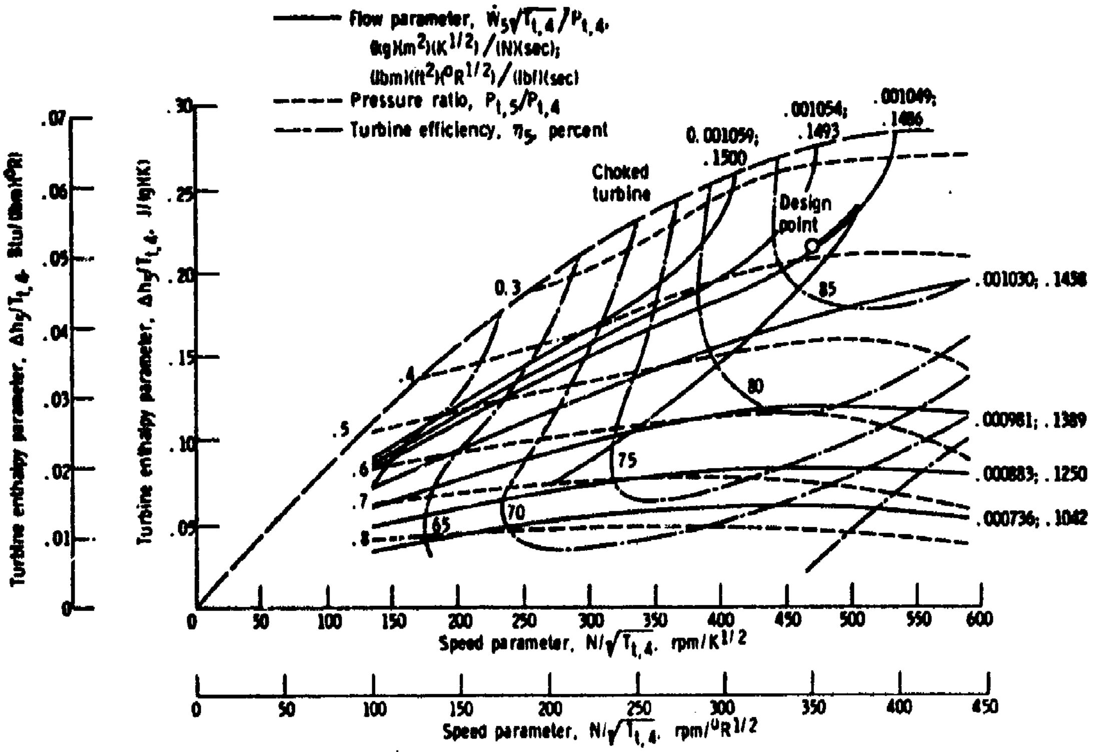

Figure 7. Overall Turbine Performance Map

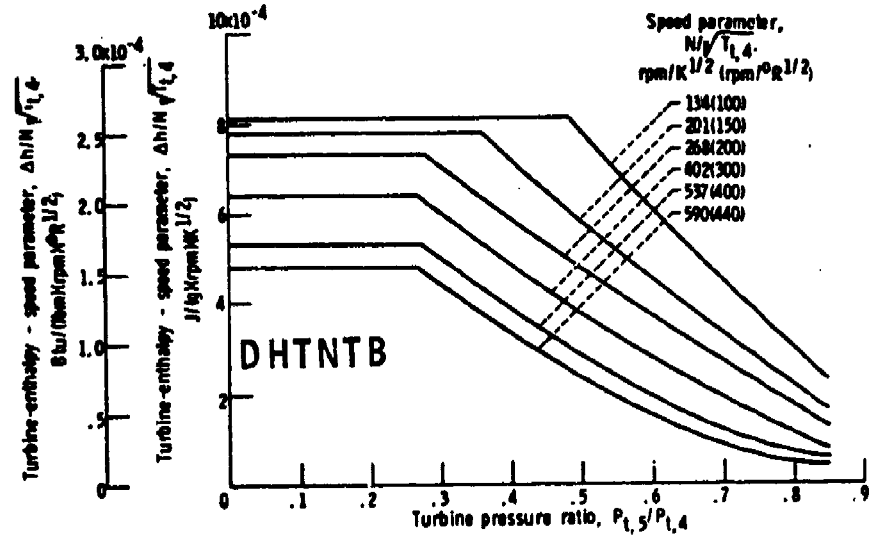

a. Turbine Torque Characteristics

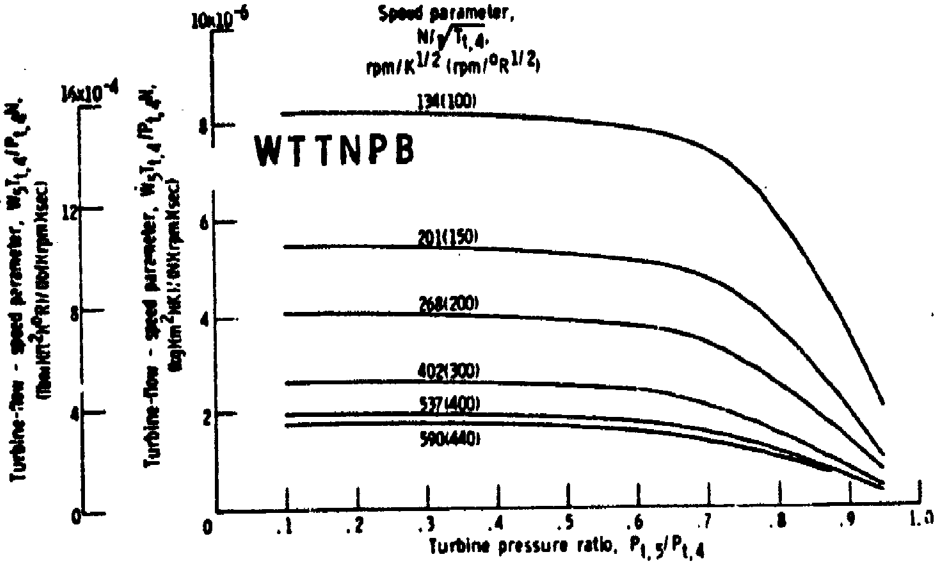

b. Turbine Normalized Flow Characteristics

Figure 8. Two-D Turbine Functions

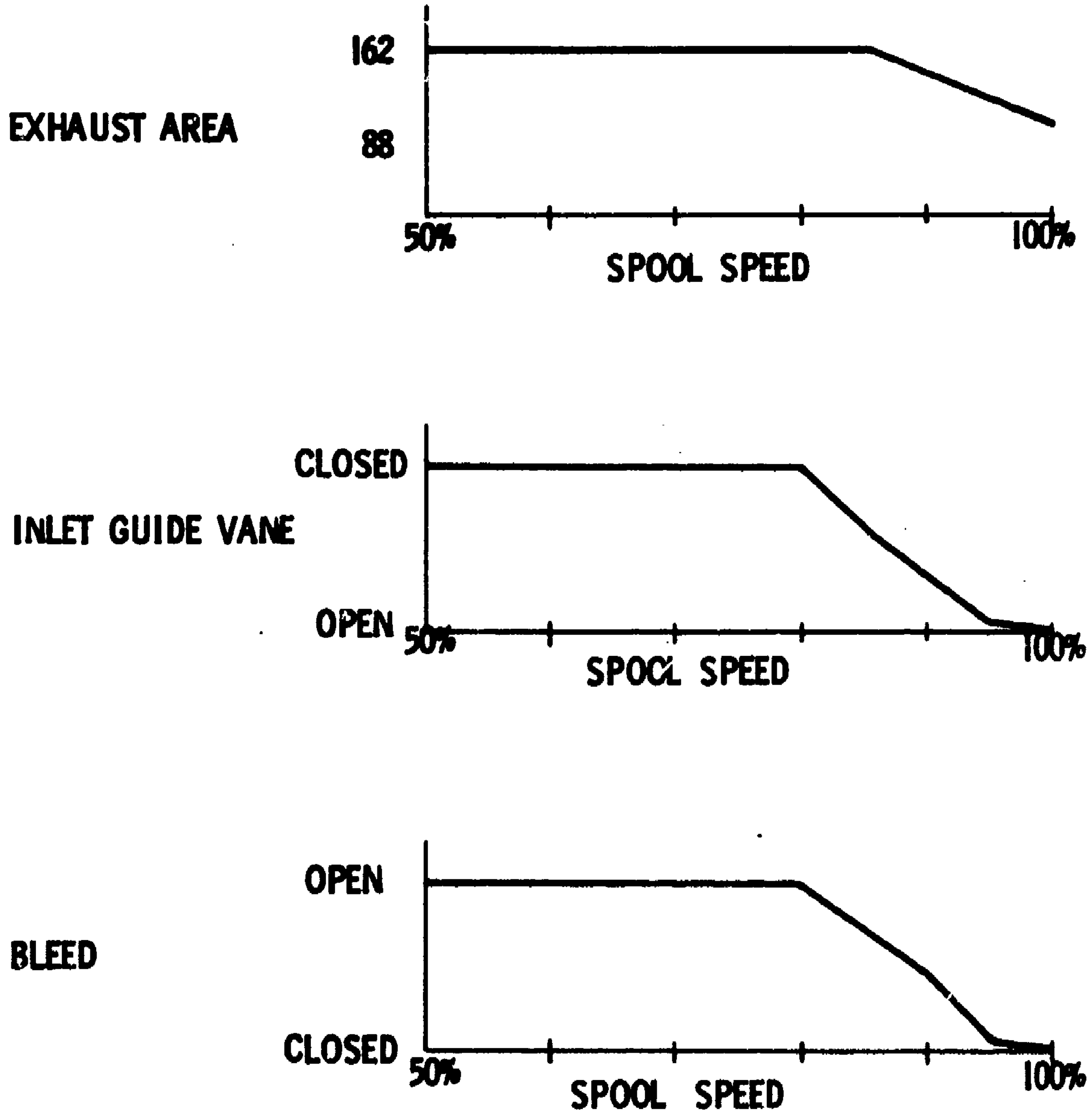

Figure 9. Steady-State Actuator Schedules

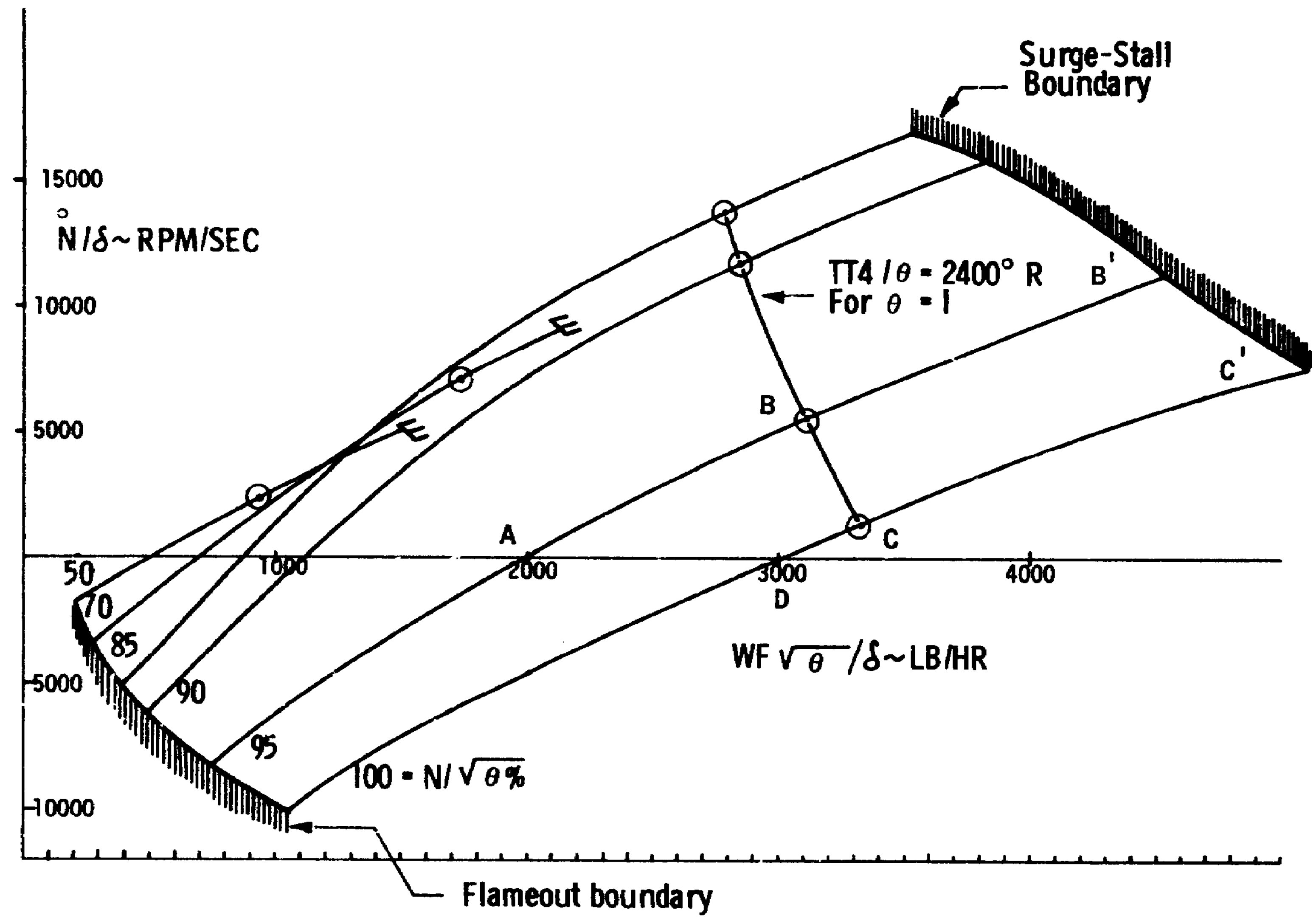

Figure 10. J85 Trajectory Optimization (Nominal IGV, Bleed, and A8)

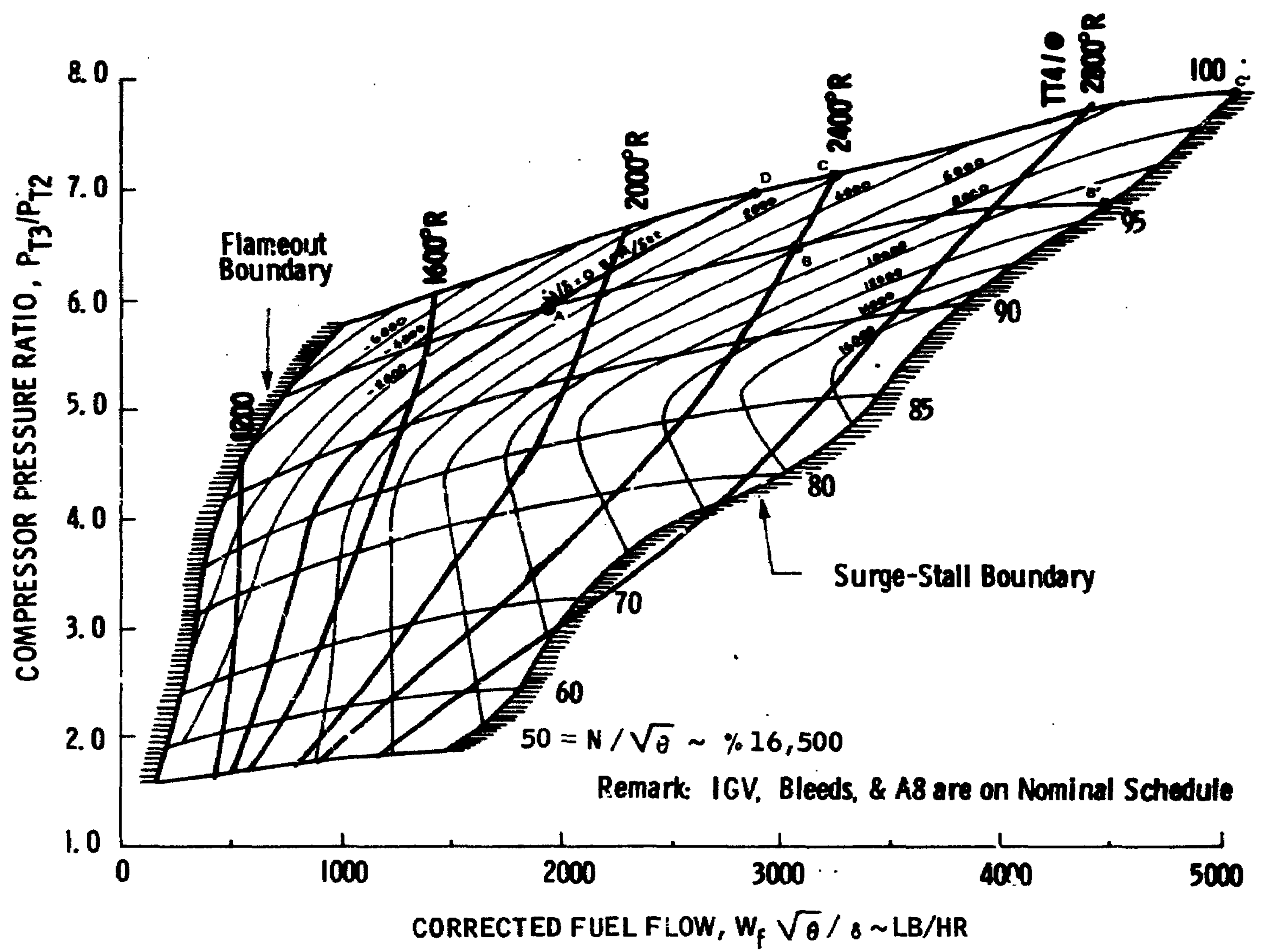

Figure 11. Engine Map

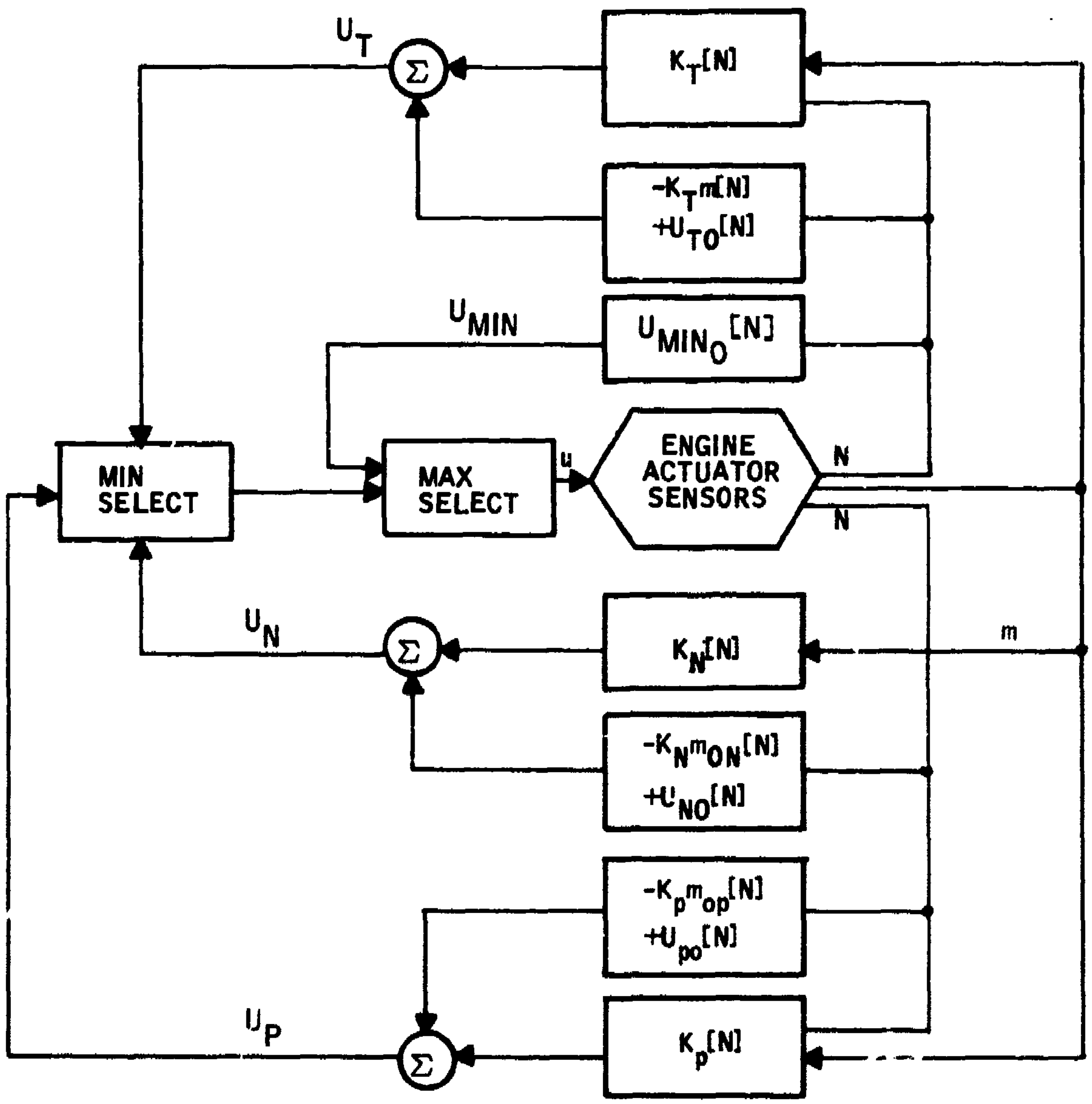

Figure 12. Mode Switching Principle (Fuel Flow Only)

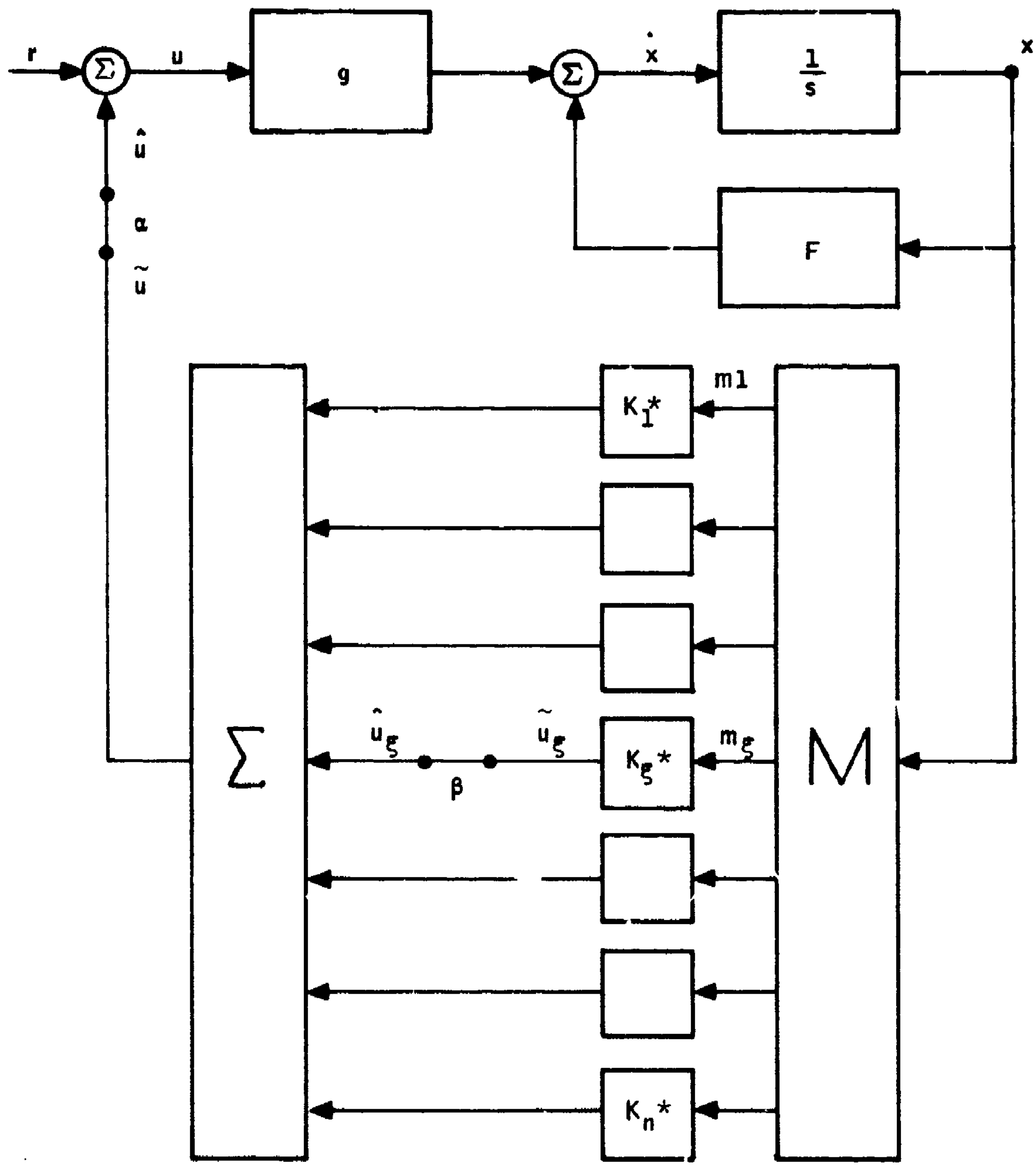

Figure 13. Loop Breaking

Table 2. Seventh Compressor Stage (Typical)

Line	Description
198	PV7 = KVOL(17) * TWV7
199	RTH6 = SQRT(TV6/518.7)
200	NC7 = N/RTH6
201	DEL6 = PV6/14.7
202	FP7 = WD7 * RTH6/(DEL6 * A(17))
203	VZT7 = KA(7) + KA(17) * FP7 + KA(27) * FP7 * FP7
204	PHI7 = VZT7/(KRAD(7) * NC7)
205	PSIP7 = FUN1(15, PHI7, 27)
206	PD7 = PV6 * (1.+ PSIP7 * KNR(7)/TV6) ** 3.5
207	WD7DT = KGAL(17) * (PD7 - PV7)
208	WD7 = INTGRL(ICWD7, WD7DT)
209	WV7DT = WD7 - WD8
210	WV7 = INTGRL(ICWV7, WV7DT)
211	TV7 = TWV7/WV7
212	PSIT7 = FUN1(16, PHI7, 29)
213	TD7 = TV6 + KNR(7) * PSIT7
214	TWV7DT = 1.4 * (TD7 * WD7 - TV7 * WD8)
215	TWV7 = INTGRL(ICTWV7, TWV7DT)
198	$P_t(V7) = R * \rho_t T_t \approx R * \rho * T_t = (R/V) * (V\rho T_t) = KVOL * (TWV7)$
202	$FP7 = \dot{W} * \sqrt{\theta} / (A * \delta) \approx \dot{W} * \sqrt{\theta_t} / (A * \delta_t)$
204	$\phi 7 = (VZ/\sqrt{\theta}) / (U/\sqrt{\theta}) = (VZ/\sqrt{\theta}) / (K * N/\sqrt{\theta})$
206	$PD7 = PV6 \left[1 + \frac{\Delta h'}{C_P(TV6)}\right]^{\gamma/(\gamma-1)}$
	$= PV6 \left[1 + \frac{\psi^P U_T 2}{2\, gJC_P(TV6)}\right]^{\gamma/(\gamma-1)}$
	$= PV6 \left[1 + \frac{\psi^P \left(\frac{r}{12}\right)^2 \left(\frac{2\pi N}{60}\right)^2}{2\, gJC_P(TV6)}\right]^{\gamma/(\gamma-1)}$
	$= PV6 \left\{1 + \frac{\psi^P}{TV6} \left[\frac{r^2 N^2 \pi^2}{g\left(2 \frac{\gamma}{\gamma-1} R\right)(360)^2}\right]\right\}^{\gamma/(\gamma-1)}$
213	$T_{tc,\,7} = T_{tv,\,6} + \Delta h/C_P$
	$= T_{tv,\,6} + \frac{\psi^T U_T 2}{C_P 2 gJ}$

Table 3. Typical Compressor Stages

Stage	Function
1	Flow matching with aircraft inlet Inlet guide vane
3, 4, and 5	Bleed controls: $\dot{W}_{b,j} = K_b A_{b,j} \dfrac{P_{tv,j}}{\sqrt{T_{tv,j}}}$ $J = 3, 4, 5$
8	Flow matching with combustion chamber

Table 4. Nozzle Flow.* Based on 1-D Isentropic Nozzle Flow With a Contraction Coefficient. Stagnation Pressure and Temperature are Taken as PT5 and TT5. Nozzle Static Pressure is Ambient.

Line	Description	Comments
1	FUNCTION HOKEY (POPT)	
2	IF (POPT.GE.1.) GOTO 1	(No gas up the tailpipe)
3	IF (POPT.GE..53) HOKEY = POPT**(1./1.4)*SQRT(1. = POPT**(.4/1.4))	
4	IF (POPT.GE.0..AND.POPT.LE..53) HOKEY = .2588	(Choked)
5	RETURN	
6	1 HOKEY = 0.	
7	RETURN	
8	END	

*cf Burner lines 283-285

Table 5. Additional Features

Feature	Description
1	Function TFNH computes T[F/A, H].
2	Subroutine PROCOM computes H[F/A, T].
3	EFFB calculates heat release as a function of the product of PT4 and temperature across the burner.
4	Heat storage in the combustion can and turbine introduce another state TM with a long time constant.

Table 6. Burner, Turbine, Nozzle, and Rotor Simulations

Line	Description	Comments
263	FAB = WF/WB	Fuel-air
264	TB = TFNH(2, FAB, HB, TV)	Real gases
265	DELPB = KWB * WB ** 2/PCD * (.771 * TCD - .083 * TB)	Friction + combustion loss
266	WBDT = KGALB * (PCD - PB - DELPB)	Momentum
267	WB = INTGRL(ICWB, WBDT)	
268	NRTTB = N/SQRT(TB)	
269	HT = RHT/RT	Turbine (outlet) enthalpy
270	FAT = WF/(WB + WF + WTC)	Fuel-air
271	TT = TFNH(3, FAT, HT, TV)	Real gas
272	PT = K4 * RT * TT	
273	PTPB = PT/PB	
274	WTTNPB = FUN2(3, PTPB, NRTTB, 6)	Turbine FN
275	WT = WTTNPB * N * PB/TB	
276	PBDLTB = PB * (TB - TCD)	
277	ETAB = FUN1(19, PBDLTB, 35)	Combustion efficiency
278	CALL PROCOM (0, TCD, CPCD, GMCD, CMCDX, HCD, IFA)	Real-gas enthalpy
279	PBDT = KVOLB* (HCD * WB + 18650. * ETAB * WF - WT * HB)	Energy equation (slightly modified)
280	PB = INTGRL(ICPB, PBDT)	
281	HBDT = HB/PB * (PBDT - KVOLB/1.4 * HB * (WB + WF - WT))	Energy + continuity (cf HBDT)
282	HB = INTGRL(ICHB, HBDT)	
283	P0PT = P8/PT	Nozzle static to turbine total nozzle flow
284	WNTKNP = HOKEY (P0PT)	
285	WN = WNTKNP * A8 * KNA8 * PT/SQRT(TT)	
286	DHTNTB = FUN2(4, PTPB, NRTTB, 8)	Turbine FN
287	DHT = N/1000. * DHTNTB * SQRT(TB)	
288	RHTDT = (HB * WT + HCD * WTC - DHT * WT-HT * WN)/1.53	Energy equation
289	RHT = INTGRL(ICRHT, RHTDT)	
290	RTDT = (WT + WTC - WN)/1.53	Continuity
291	RT = INTGRL(ICRT, RTDT)	
292	WBLTBL = WBL3 * TV3 + WBL4 * TV4 + WBL5 * TV5	Proportional to wasted bleed power
293	DLWHC = HCD * WCD + .24 * (WBLTBL - TV0 * WD0)	
294	DLWHT = HB * WT + HCD * WTC - HT * WN	Rotor acceleration cf Rotor speed explanation
295	NDT = KSPEED/N * (DLWHT - DLWHC)	
296	N = INTGRL(ICN, NDT)	
297	RETURN	
298	END	

Table 7. Actuator Equations

Actuator	Equation
Fuel valve	• First approximation: $\dot{W}_f = -62.5\ W_f + 62.5\ u_f$ • Second approximation: $\dot{y}_4 = -3546.2\ y_3 - 301\ y_4 - 5.9127\ u_f$ $\dot{y}_3 = +10\ y_4$ $\dot{y}_2 = +3.1333\ W_f - 50.384\ y_2 + 1880\ y_3$ $\dot{W}_f = -5040\ y_2$ Roots $(\omega, \xi) = (126,\ 0.2),\ (188.3,\ 0.8)$
Inlet guide vane	• $\dot{IGV} = -5.0\ IGV + 5.0\ u_{IGV}$
Bleed position	• $\dot{BLD} = -2.0\ BLD + 2.0\ u_{BLD}$
Exhaust position, A_8	• First approximation: $\dot{A}_8 = -3.0\ A_8 + 3.0\ u_{A_8}$ • Second approximation: $\dot{A}_8 = \begin{cases} +KN & \text{if } (u_{A_8} - A_8) \geq 4\ in^2 \\ 0 & \text{if } -4 < (u_{A_8} - A_8) < 4\ in^2 \\ -KN & \text{if } (u_{A_8} - A_8) \leq -4\ in^2 \end{cases}$ where $K = \dfrac{0.00325\ in^2/sec}{rpm}$

Table 8. J85 Jet Engine Summary

Parameter	Description
Order of model	70th-order
Root spread	• 0.000001 to 30 sec • 50 to 5000 rad/sec
Special features	• One significant nonlinearity associated with spool dynamics • One minor nonlinearity associated with A8 • Three bounded-phase constraints (PT?MAX, TT4MAX, TT4MIN) • Four controls (WF, A8, IGV, BLD)
Accuracy of model	• Poor below 1 rad/sec because of thermal capacitance • Good between 1 and 20 rad/sec • Poor above 20 rad/sec because of gas dynamics
Control passband requirements	• Command 0 to 15 rad/sec • Disturbance 0 to 200 rad/sec • Surge recovery 0 to 200 rad/sec

Table 9. J85 Bandpass Characteristics

Component	Nominal Time Constant (sec)
Spool	1.0
Thermal capacitance	2.0
Fuel	0.02
A8	0.3
Bleed	0.2
IGV	0.5
Thermocouple	1.0
Whistle	0.02 3.0
Tailpipe	0.03
Inlet	0.03
Combustion can	0.01
Combustion	0.003
Compressor	0.000001 to 0.01
Turbine	0.000001

Table 10. Mode Switching Principle (Fuel Flow Only)

Step	Description
1	Four fuel flows are calculated: $U_N = K_N[N]\, m - K_N[N]\, m_{ON}[N] + U_{NO}[N]$ $U_P = K_P[N]\, m - K_P[N]\, m_{OP}[N] + U_{PO}[N]$ $U_T = K_T[N]\, m - K_T[N]\, m_{OT}[N] + U_{TO}[N]$ $U_{MIN} = U_{MINO}[N]$
2	One is used: $U = \mathrm{Max}\begin{cases} U_{MIN} \\ U_L \end{cases}$ where $U_L = \mathrm{Min}\begin{cases} U_N \\ U_P \\ U_T \end{cases}$

Table 11. Optimal Quadratic State Control

Function	Description
Linear model	$\dot{x} = Fx + G_1 u + G_2 \eta$ $r = Hx + Du$
Performance index	$J[u] = E\{r' Q r\}$
Optimal control law	$u = Kx$
Performance measures	Eigenvalues RMS responses Transient responses

Table 12. Control Simplification

Control	Description	
State	• $\begin{Bmatrix} \dot{x}_I \\ \dot{x}_{II} \end{Bmatrix} = \begin{bmatrix} F_{I,I} & 0 \\ F_{II,I} & F_{II,II} \end{bmatrix} \begin{Bmatrix} x_I \\ x_{II} \end{Bmatrix} + \begin{Bmatrix} G1_I \\ 0 \end{Bmatrix} u + \begin{Bmatrix} G2_I \\ G2_{II} \end{Bmatrix} \eta$ where x_I includes engine and actuator dynamics x_{II} are the sensor dynamics	(1)
	• $r = H x_I + D u$	(2)
	• $J[U] = E\{r' Q r\}$	(3)
	• $\underset{u}{\text{Min}}\ J[u]$	(5)
	• $u_o = K_o x_I$	(6)
Simplified	• Equations 1, 2, and 3. above	(1-3A)
	• $\tilde{m} = Mx \quad m \in \tilde{m}$, where M is invertible	(4A)
	• Equation 5 is subject to $u = L\{m\}$	(5A)
	• $u = K^* m$	(6A)

Table 13. Command Response Synthesis (Rate Model-Following With Integral Control and a Noisy Pilot)

Step	Description
1	Ideal Command Response Model: $\dot{x}_m = a\,x_m + b\,\dot{e} + ce \qquad (1)$ $\dot{e} = d\,x_m + fP \qquad (2)$ Choose f and τ. Then calculate a, b, c, d (cf Appendix C) so that $\frac{x_m}{P} \cong \frac{f}{s + (1/\tau)} \qquad (3)$
2	Construct a Response Component: $r_k = \dot{x}_n - \dot{x}_m; \qquad (4)$ where: $\dot{x}_n = \sum_j F_{nj} x_j + \sum_j (G1)_{nj} u_j \qquad (5)$ $r_k \cong \sum_j \left[F_{nj} x_j + (G1)_{nj} u_j\right] - ax_n - b(dx_n + fP) - ce \qquad (6)$
3	Consider PLA = P to be driven by a noisy pilot: $\dot{P} = -4.0P + .028241\eta_p \qquad (7)$

SECTION III
COMMAND AND DISTURBANCE CONTROL

The response characteristics of the J85 engine with controls synthesized to yield both good command response and insensitivity to inlet buzz disturbances and shock swallowing are presented. The results show that engine controllers could be designed to be more tolerant of installation and operating anomalies than is current practice.

Command and disturbance control results presented in this section are of a preliminary nature. Assumptions, modeling, and testing of results are idealized. It is believed that based on the results presented here, and on the extension of comparable results in other applications that the command and disturbance control quality indicated here can be obtained in practice.

MOTIVATION

Engine controls are usually designed to enforce throttle command control: steady-state spool speed as a function of PLA (power level angle) and good transient spool speed response due to PLA commands. Because the controls are designed only against command requirements, whatever disturbance response characteristics are achieved must be accepted. The results are engines that are unnecessarily sensitive to disturbances.

Synthesis of engine controls to provide both good command and disturbance response characteristics would increase the operating flexibility of the aircraft, alleviate the problems of engine and aircraft integration, and reduce the time required to introduce a new aircraft into service. The latter would be made possible by eliminating a susceptibility (to inlet buzz) that often occurs with new aircraft.

In this section, idealized controls are synthesized to provide good command control and to be insensitive to inlet buzz and shock swallowing.

Inlet buzz manifests itself as a nearly sinusoidal pressure variation (PT2) at the compressor face. Buzz is generated by the inlet duct which is much like an organ pipe. The fundamental buzz frequency is inversely proportional to the length of the inlet duct, and it may well be equal to that of maximum engine susceptability. Herein, it is taken to be at 30 radians per second which corresponds to a resonance peak for the open-loop engine (tailpipe resonance). The value of 30 radians per second could occur in the inlet ducts of lengths used on fighter aircraft. The amplitude of the buzz is taken at 0.4 times the steady-state value of PT2. An amplitude of this magnitude can occur.

For shock swallowing, the disturbance is taken as a step input in the change in PT2 at the compressor face. Results to be presented will show that step changes in PT2 equal to the steady-state value can be accommodated.

In this section, it is desired to show that controls can be designed to be effective for both commands and disturbances. The demonstration is not complete in two respects: (1) the controls were not tested on an engine, and (2) both the design and the controls are highly idealized. The reader might legitimately object that it is an excessive extrapolation from results presented here to successful realization in engine hardware. However, it has been shown in a large number of studies and in several hardware applications at Honeywell that successful control synthesis at the level demonstrated here implies comparable results will be obtained in more complete designs and in hardware. That is, a successful idealized design implies that comparable performance can be effected with simple, cost-competitive hardware. There is a demonstration of this in the next section of the report; an idealized design is first executed and then reduced to practical hardware without losing performance.

In the results to be presented, two pecularities may be noted: (1) disturbance control achieved is vastly better than required, and (2) high (but achievable) performance actuators are used. Why wasn't the disturbance control performance degraded towards minimum objectives to permit using cheaper actuators? The answer is that the results presented here were generated in four computer runs (one for each operating condition) during the final writing period after it was discovered the original disturbance control specification had been incorrectly set. The criterion was incorrectly set on PT3 rather than PT3/PT2. By making one computer run for each condition on PT3/PT2, the results presented were generated. The results aptly demonstrated the main objective "that inlet buzz" need not unduly affect the engine.

MODELS

The J85 engine has significant nonlinearities, particularly with respect to spool speed but also with respect to PT3 and other variables. In the next section, it is shown that a good, nonlinear command control system can be designed by first designing good linear controls at four different speed points along the equilibrium line and the same four speed points near the surge-stall pressure boundary. The nonlinear control is then simply affected by linearly interpolating feedback gains as a function of speed for equilibrium or for surge-stall pressure boundary control.

In this section, it is assumed that if good linear command and disturbance control can be demonstrated at four points along the equilibrium line, good nonlinear control can again be effected by gain scheduling with speed. Therefore, in this section, controls are synthesized at four points along the equilibrium line (50, 70, 85, and 100 percent of maximum spool speed). Hence, linear models are required at these four operating points.

The linear models are generated in state vector form:

$$\dot{x} = Fx + (G1)u + (G2)\eta \tag{50}$$

$$r = Hx + Du \tag{51}$$

Nomenclature are presented in Table 1. Table 14 defines the components, the F matrices are presented in Tables 15 through 18, G1 matrices in Table 19, G2 matrices in Table 20, H matrices in Tables 21 through 24, and D matrices in Table 25.

Data for the first 10 components of the state vector (x) were generated by linearizing the nonlinear component model (with truncated compressor-stage dynamics) for reasons discussed in Section II and accomplished in the manner described in Appendix A. Compressor-stage dynamics were truncated because of an anomaly in the model. Without the compressor-stage dynamics, the pressure ratio, PT3/PT2, across the compressor is an instantaneous function of spool speed. An approximate correction for this deficiency is presented later.

The 11th component (EN) of the state vector provides for integral control on spool speed; cf Table 13 and Appendix C. Computation of numerical values for F 11, 10 and F 11, 21 is presented under the discussion of the response vector.

First-order control-actuator representations are used for states 12 to 15. Time constants are presented in Table 26 (and also in Tables 15 through 18). Maximum slew rates are listed in Table 27.

Duct buzz is generated by states 19 and 20:

$$\begin{Bmatrix} \dot{\widetilde{PT2}} \\ \dot{DUM} \end{Bmatrix} = \begin{Bmatrix} \dot{x}19 \\ \dot{x}20 \end{Bmatrix} = \begin{bmatrix} 0 & +1.0 \\ -900.0 & -6.0 \end{bmatrix} \begin{Bmatrix} x19 \\ x20 \end{Bmatrix} + \begin{Bmatrix} 0 \\ 432.09 \end{Bmatrix} \eta 2 \tag{52}$$

With this model, x19 = $\tilde{PT2}$ is nearly sinusoidal with a frequency of 30 radians per second, an amplitude of 0.4 x 14.7 = 5.88, and an rms value of 4.16 lb/in^2.

To compensate for the truncated compressor dynamics, $\tilde{PT2}$ should be delayed about 0.002 second. This delay is approximated by a zero/second Pade approximate:

$$\begin{Bmatrix} \dot{x}16 \\ \dot{x}17 \end{Bmatrix} = \begin{bmatrix} 0 & 1 \\ -500,000 & -1000 \end{bmatrix} \begin{Bmatrix} x16 \\ x17 \end{Bmatrix} + \begin{Bmatrix} 0 \\ 500,000 \end{Bmatrix} x19 \tag{53}$$

or

$$\frac{x16}{x19} = \frac{500,000}{s^2 + 1000s + 500,000} \tag{54}$$

State x16 drives the bare engine model (cf F matrices, column 16, rows 1, 2, 5, 10, and 18).

The 18th state $(\dot{N} - \dot{N}M)L$ is introduced to inhibit the synthesis procedure from developing controllers with too large a passband. This will be made clear during the discussion of the response components.

The 21st component (P) of the state is the power lever. In this report, power lever position is taken to range between 0 and 1 and vary linearly with command spool speed (e.g., 1 corresponds to a command of 100 percent spool speed). In this section, where perturbation control only is being considered, a value of P corresponds to a perturbation from trim. For synthesis purposes the power lever position is modeled by

$$\dot{P} = -4.0P + 0.028241\,\eta_p \tag{55}$$

This yields an rms value for P = 0.01. The model tacitly assumes the power lever is being driven by the pilot in a nervous situation.

The response vector (r) is constructed to permit the synthesis procedure to enforce desirable response characteristics. It is desired that the response characteristics of components 1, 2, 9, 10, 15, and 16 (N, EN, TT4, PT3, PR, and PRΔ) be "nice" without excessive values for components 3, 4, 5, and 6 ($\dot{\text{W}}$FV, $\dot{\text{A}}$8, $\dot{\text{I}}$GV, and B$\dot{\text{L}}$D). Components 7, 8, 11, 12, 13, and 14 [$(\dot{N} - \dot{N}M)$, $(\dot{N} - \dot{N}M)_L$, UWF, UA8, UIGV, and UBLD)] assist in the task. The purpose and determination of all components except 7, 8, 15, and 16 should be clear.

If the response component 7 $(\dot{N} - \dot{N}M)$ can be held to small values, the engine spool speed will respond to throttle commands like a zero-over-first-order plant with a time constant of 0.25 second. This is the rate model-following scheme of Reference 5 as generalized to integral control in Reference 6. Construction of r7 is outlined in Table 28. First, an ideal response model is constructed. In the present case, x_m corresponds to the ideal spool speed (N) response; because of the approximation made in rate model-following, x_m is not added to the state vector. The integral term e does appear in the state as EN (the 11th component). As noted on Table 28, computation of the constants a, b, c, d, and f to achieve the desired first-order response characteristics is presented in Appendix C. The response component is then constructed by assuming that $x_m \cong x1 = N$; this does not imply that $\dot{x}_m \cong \dot{x}1 = \dot{N}$. In the present case, k = 7 and n = 1. Equation (6) of Table 28 provides the explicit computation for r7.

In most applications, use of $r7 = \dot{N} - \dot{N}M$ in the control synthesis would be sufficient to obtain good command transient characteristics without undesirable side effects. The engine model contains very high-frequency dynamics (open-loop roots near -10^6). Use of r7 results in a controller with an excessively large bandpass. To eliminate this, $\dot{N} - \dot{N}M$ is lagged with an 0.02-second time constant as state component x18 and response component r8.

The pressure ratio (PR) across the compressor is PT3/PT2. The linearized perturbation pressure ratio is

$$\partial PR = \frac{\partial PT3}{PT20} - \frac{PT30}{PT20}\frac{\partial PT2}{PT20} = \left(\frac{1}{PT20}\right)\partial PT3 - \left(\frac{PRO}{PT20}\right)\partial PT2 \qquad (56)$$

Dropping the perturbation symbols,

$$PR = \left(\frac{1}{PT20}\right) PT3 - \left(\frac{PRO}{PT20}\right) PT2 \qquad (57)$$

For sea level static, PT20 = 14.7 pounds per square inch. From the engine map (Figure 11), PRO = 6.950, 3.978, 2.678, and 1.669 for N = 100, 85, 70, and 50 percent, respectively. PT3 = 1.981 TWCD = (1.981)X1.

Two pressure ratios are computed:

$$r15 = PR1 = \left(\frac{1.981}{PT20}\right)X1 - \left(\frac{PRO}{PT20}\right)X19 \qquad (58)$$

$$r16 = PR2 = \left(\frac{1.981}{PT20}\right)X1 - \left(\frac{PRO}{PT20}\right)X16 \qquad (59)$$

The latter is considered to be the best indicator and is used in the summary results to be presented.

DESIGN OBJECTIVES

The control design objectives are to effect good steady-state and transient command control and to make the engine insensitive to inlet buzz and shock-swallowing disturbances. It is desired that these objectives be met within the capabilities of the BOM (Bill of Materials) actuator capabilities. Table 29 lists the objectives more specifically.

Good command control can be effected with the BOM actuators. To achieve both good command and disturbance control it was necessary to modestly decrease the bleed time constant and increase its slew rate. The increased bleed actuator performance is easily achievable.

CONTROL SYNTHESIS

Control synthesis is by application of optimal quadratic control theory as discussed in Section II and outlined in Table 11. The final Q matrices used are presented in Table 30.

RESULTS

Gains, roots, rms responses, and transient responses are presented and discussed.

Gains

Table 30 presents the final feedback (Q) matrices. The numerical values appear to be reasonable. The controller should not be overly sensitive to parameter variations and should be physically realizable.

A rough guide for judging feedback matrices is that the components should have magnitudes small relative to 1. With the usual system representations, if the gain components are small relative to 1, two naturally desired results are achieved: 1) The closed-loop actuator roots are near their open-loop values. 2) The system gain level is sufficiently low that saturation seldom occurs.

The first-order approximation of the closed-loop bleed actuator root is

$$\begin{aligned} \text{root } 15 &\cong F_{15,15} + (G1_{15,4})*(K_{4,15}) \\ &= -2.0 + 2.0(-19.153) = -40.306 \end{aligned} \quad (60)$$

where the numerical values are for the 100-percent case. It will be shown later that this first-order approximation is reasonably close to the actual closed-loop value. It was found to be necessary to increase the size of the bleed root to meet disturbance control requirements.

$K_{2,12}$, $K_{3,12}$, and $K_{4,12}$ are large relative to 1. These simply imply that the IGV, A8, and BLD tend to follow the fuel valve. This is an example where the rough guide is never valid.

$K_{3,3}$ = 314.5 (for 100 percent). This appears to be very large but is an allusion perpetrated by the mixing dimensions used in engine. The closed-loop rms value of x3 for the disturbance input is 0.00982. $\Delta \dot{A}8 \cong 314.5 \times 0.00982 = 3.09$. Table 27 shows this is less than 10 percent of that available.

By similarly considering each gain component, it will be concluded that the gain matrices of Table 30 are satisfactory. This was not the case when $Q_{7,7}$ rather than $Q_{8,8}$ was nonzero.

Roots

The open- and closed-loop roots are presented in Tables 32 and 33. They show that:

1) Control has little effect above 100 radians per second.

2) Fuel valve, IGV, and A8 actuator roots have nearly the same open- and closed-loop values.

3) The closed-loop bleed valve root is near 100 radians per second.

4) Closed-loop N and EN roots are near -4.0.

These results satisfy the design objectives for the roots.

RMS Responses

Open-loop, closed-loop, and summary rms response data are presented in Tables 34, 35, and 36. These data indicate that the closed-loop command response will be as prescribed. The open-loop engine would surge-stall due to inlet buzz. The controlled engine is not dangerously affected by inlet buzz disturbances. The controlled engine results presented use actuator deflections and rates beyond BOM capabilities but yet readily realizable. Engineering judgments suggest that buzz control could be maintained with BOM actuators.

Table 35 presents the r8 responses for command disturbances. Simulation results (to be subsequently presented) establish that the rms values for r8 are relatively small. This implies that the command step response will be similar to that of a first-order lag with a time constant of 0.25 second.

Table 36 summarizes the major buzz response results of Tables 34 and 36. At both the 100 percent and the 50 percent operating conditions the open-loop PR2 exceeds the margin available. At 70 percent and 85 percent, the open-loop pressure ratios are barely acceptable. The closed-loop rms pressure ratios are very small. This shows that control can reduce the surge-stall susceptability. In this case, however, excessive margin has been achieved which implies that more is required of the actuators than is necessary.

Table 35 shows rms buzz values at 100 percent for A8, IGV, and BLD are 1.179, 0.2220, and 1.48 inches squared. The BLD value is in excess of the

BOM allowable (1.0). Table 35 also presents rms buzz values for A8, IGV, and BLD of 39.10, 6.859, and 45.90 inches squared per second. Relative to BOM values in Table 27, the exhaust actuator rate is marginally acceptable, but both the IGV and BLD rate capabilities would have to be increased markedly to achieve the summary results shown in Table 35.

The results presented here show that by modestly increasing the BOM actuator capability, both good command control and surge-stall buzz margin requirements can be bettered by wide margins. It is our opinion, based on the results presented here and upon some preliminary results presented previously, that the BOM actuators provide sufficient capability to meet both command and inlet buzz control requirements.

Transient Response

Command response plots are presented in Figures 14, 17, 20, and 23. Open-loop responses to PT2 are presented in Figures 15, 18, 21, and 24. Closed-loop responses to PT2 are presented in Figures 16, 19, 22, and 25. Table 37 summarizes the PT2 step response data. The data show the command responses are as prescribed. Control effectively reduces the PR2 rise to PT2 steps.

Figures 14a, 17a, 20a, and 23a show that both N and FN closely approximate the step responses of a first-order lag with a time constant of 0.25 second. Control movements and responses (TB, PT3, PR1 and PR2) are smooth and mild.

Figure 16d shows PR2 decreasing by -0.0814 for the first 0.02 second, followed by recovery to approximately -0.04. The bleed, IGV, and A8 (Figure 16c) act immediately to reduce PR2. The engine speeds up by 204 revolutions per minute (Figure 16a) during the first 0.04 second and then

returns toward zero perturbation error with a time constant of about 0.25 second. All responses are smooth.

Table 37 summarizes the PT2 step response data. The uncontrolled engine could tolerate a 2.0-pound-per-square-inch step change in PT2. The controlled engine is much more tolerant of the step disturbance to PT2.

CONCLUSIONS

It is shown that under highly idealized conditions using moderate response control actuators that overly severe inlet disturbances could be tolerated. Engineering judgments based on these results and extrapolations of comparable studies in other situations suggest the J85 engine could be made buzz-tolerant and shock-resistant.

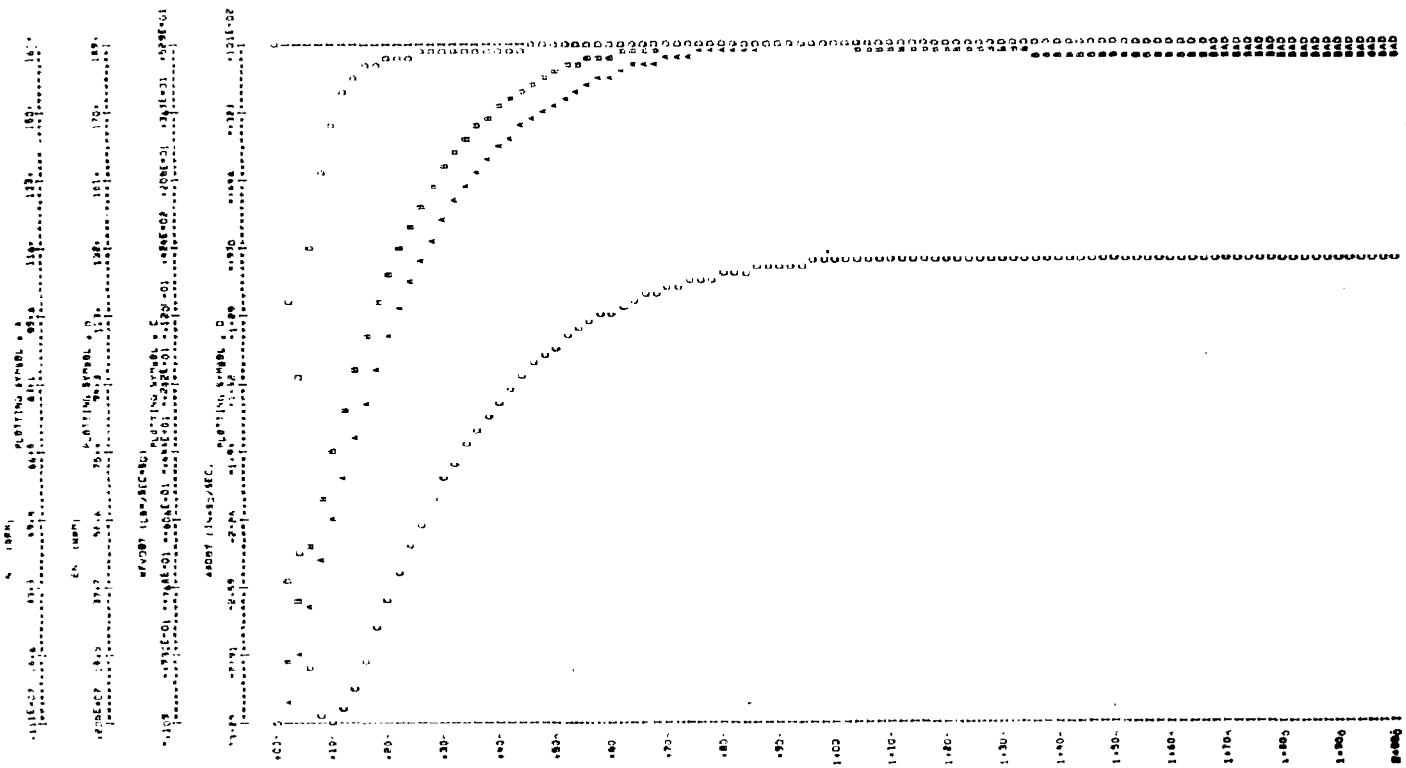

Figure 14a. Disturbance Controller at 100 Percent, Δ Pilot = 0.01

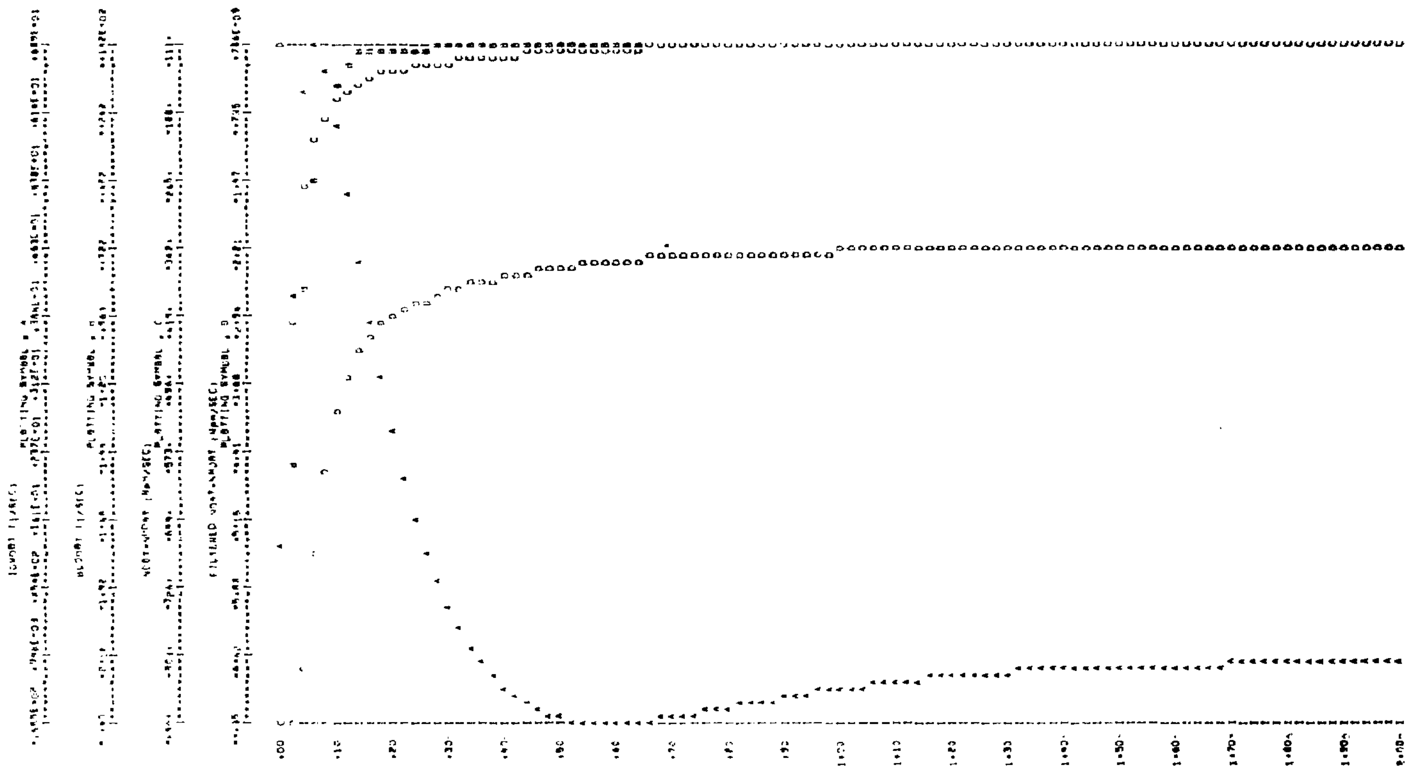

Figure 14b. Disturbance Controller at 100 Percent, Δ Pilot = 0.01

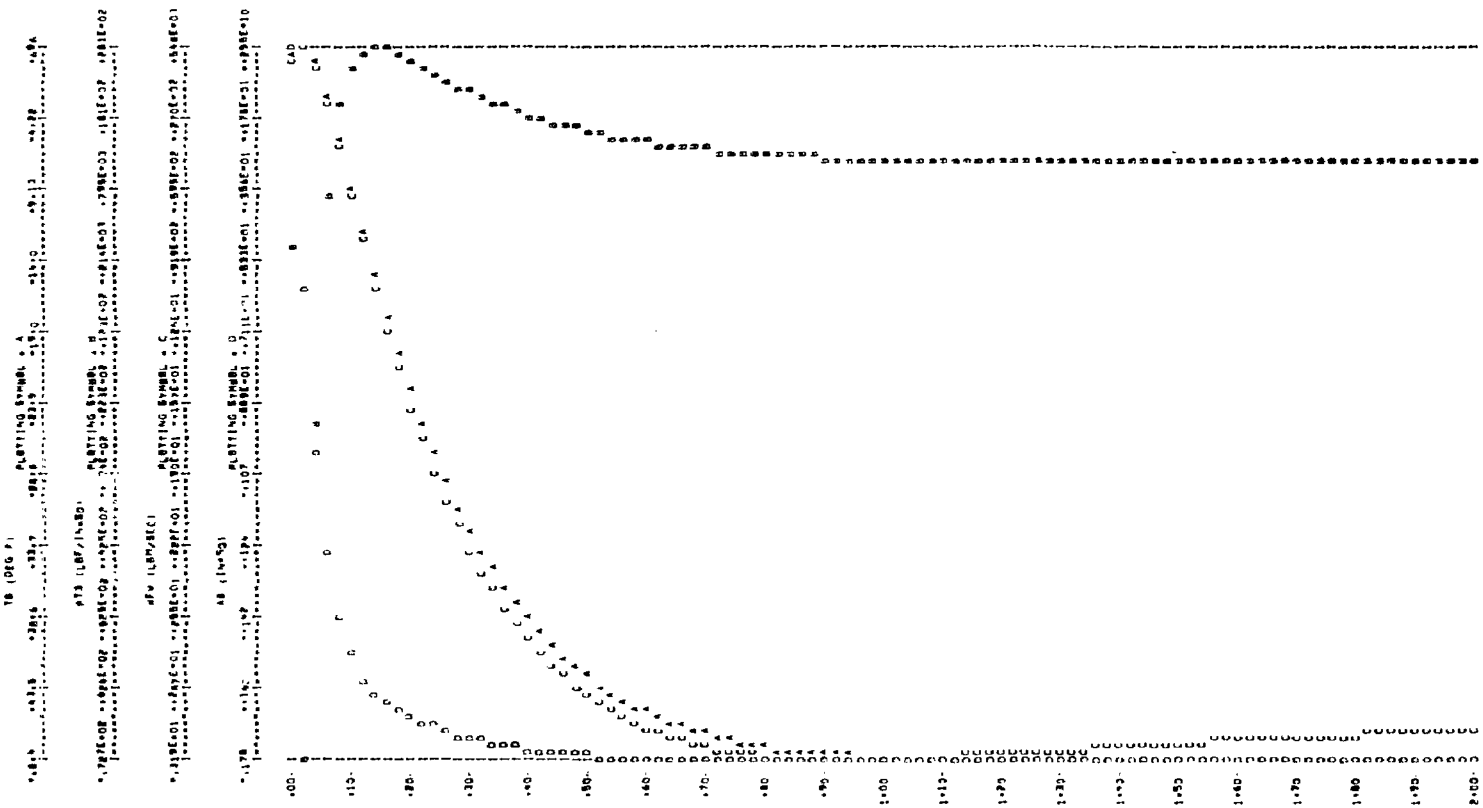

Figure 14c. Disturbance Controller at 100 Percent, Δ Pilot = 0.01

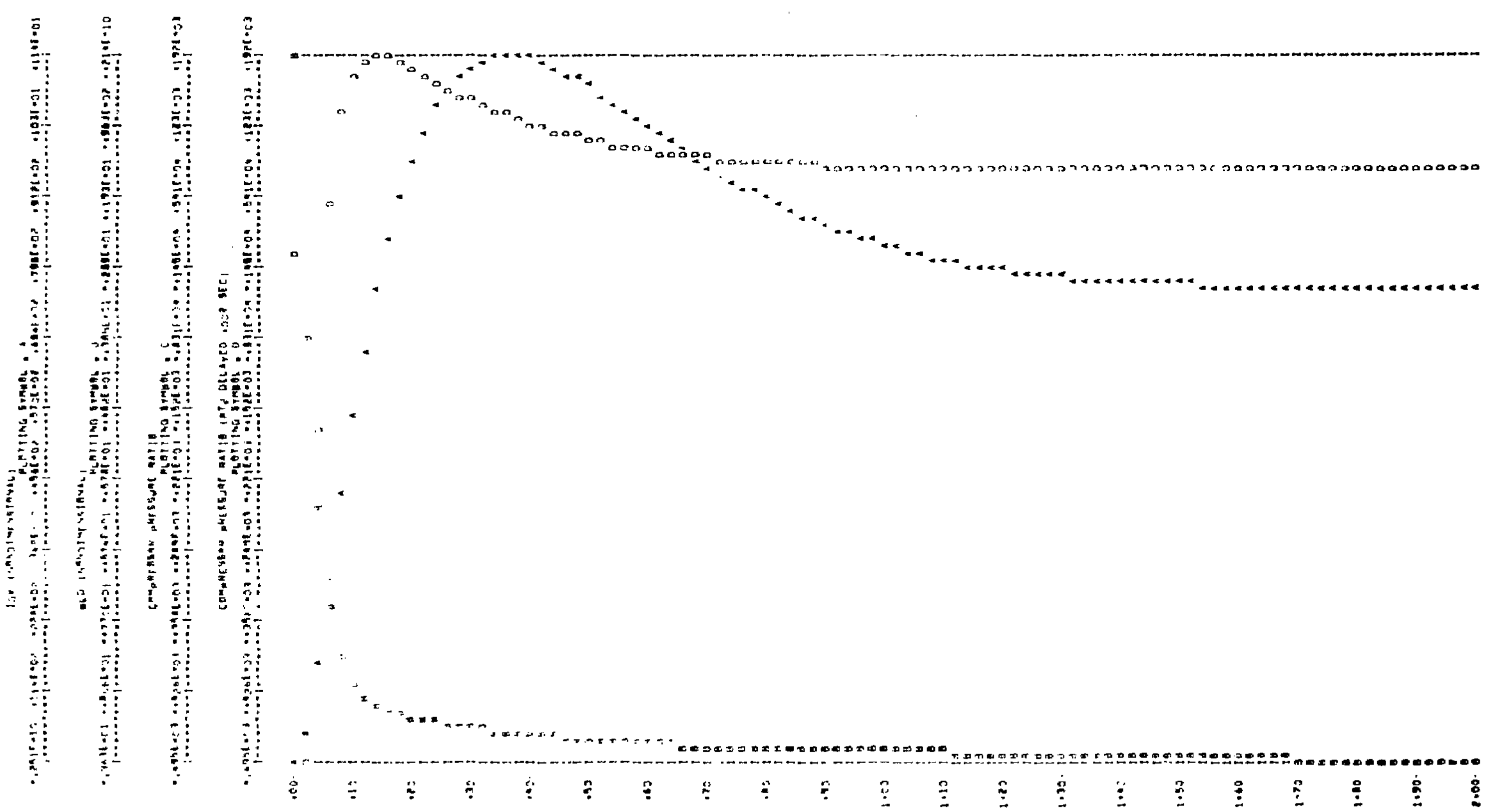

Figure 14d. Disturbance Controller at 100 Percent, Δ Pilot = 0.01

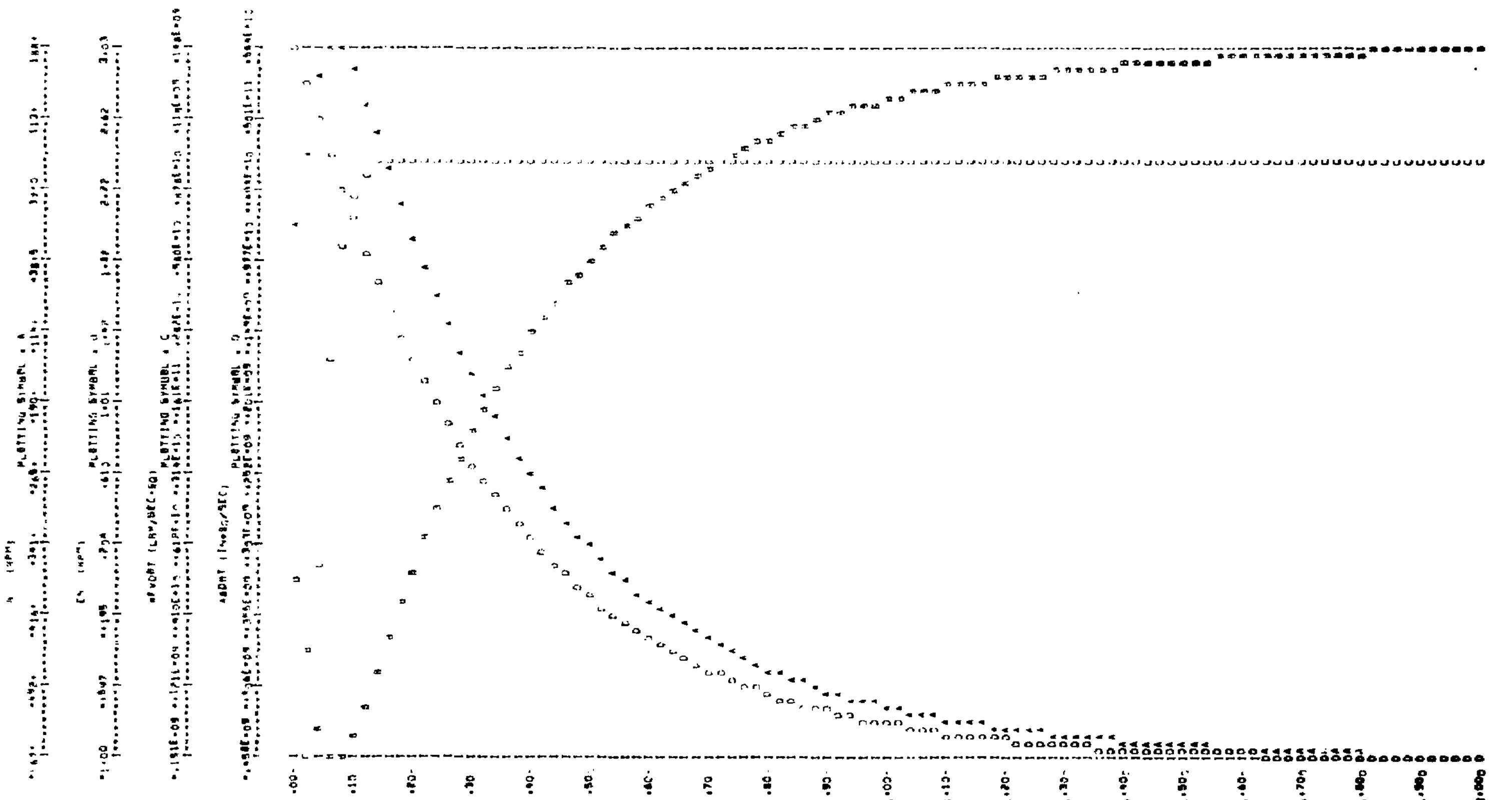

Figure 15a. Open-Loop Disturbance Response at 100 Percent
$\Delta PT2 = 2.0$ psi

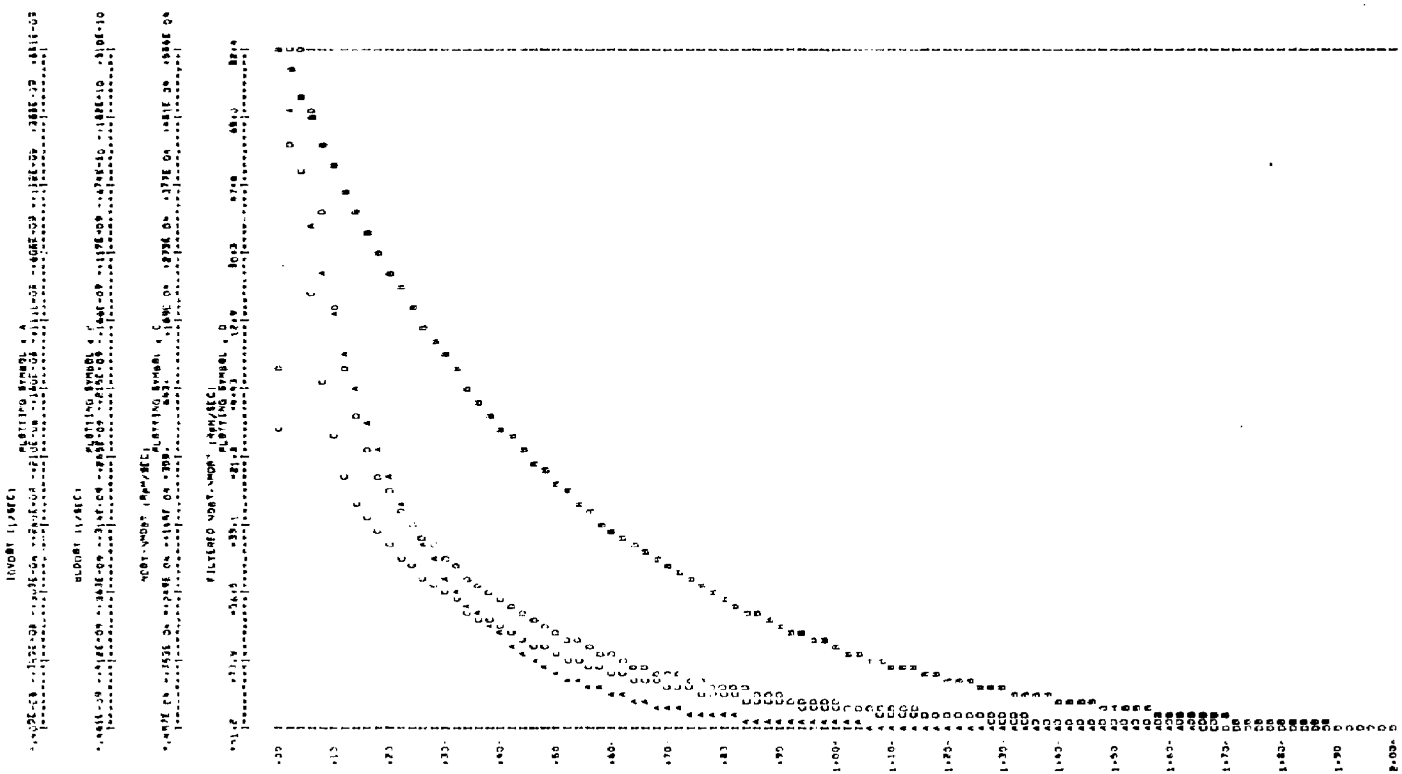

Figure 15b. Open-Loop Disturbance Response at 100 Percent
$\Delta PT2 = 2.0$ psi

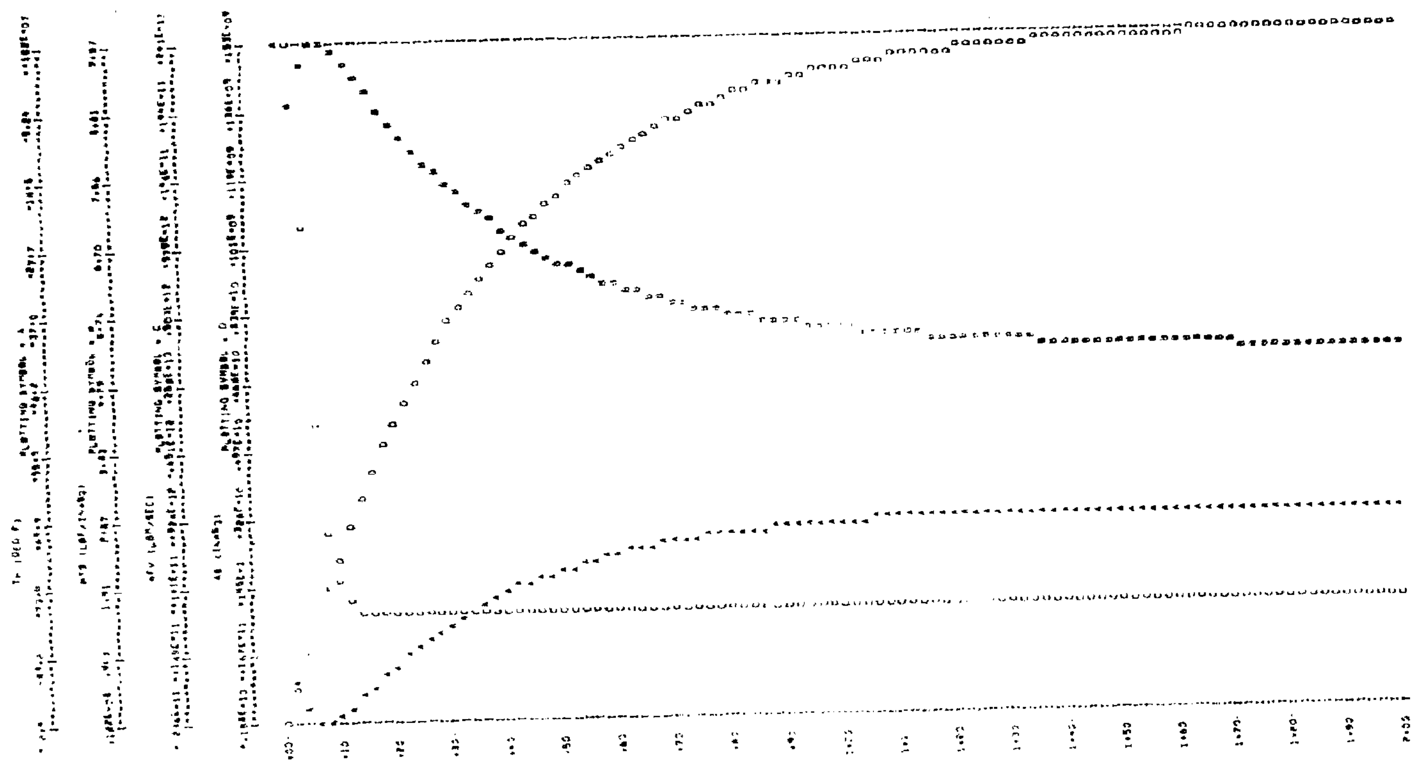

Figure 15c. Open-Loop Disturbance Response at 100 Percent
ΔPT2 = 2.0 psi

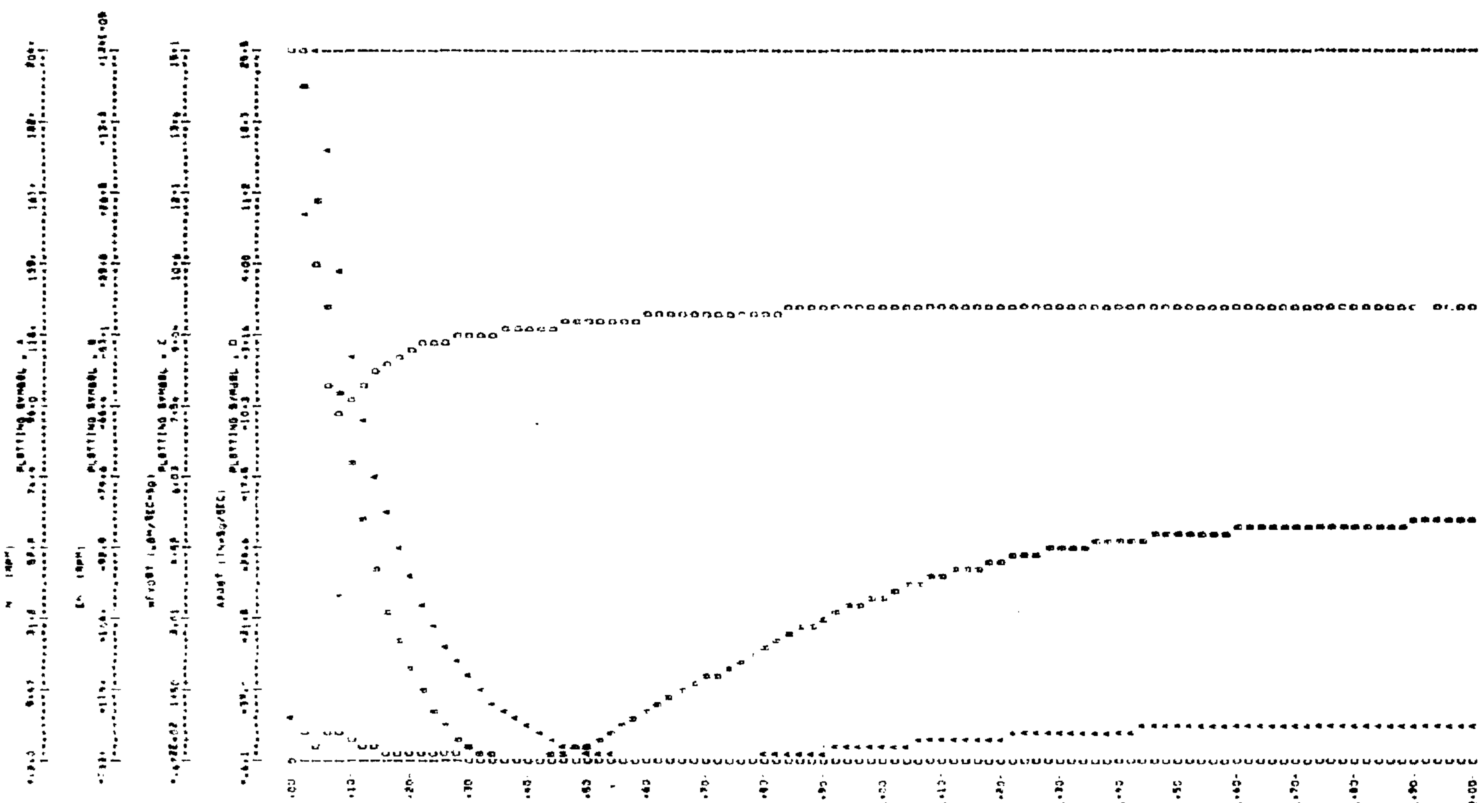

Figure 16a. Disturbance Controller at 100 Percent, $\Delta PT2 = 2.0$ psi

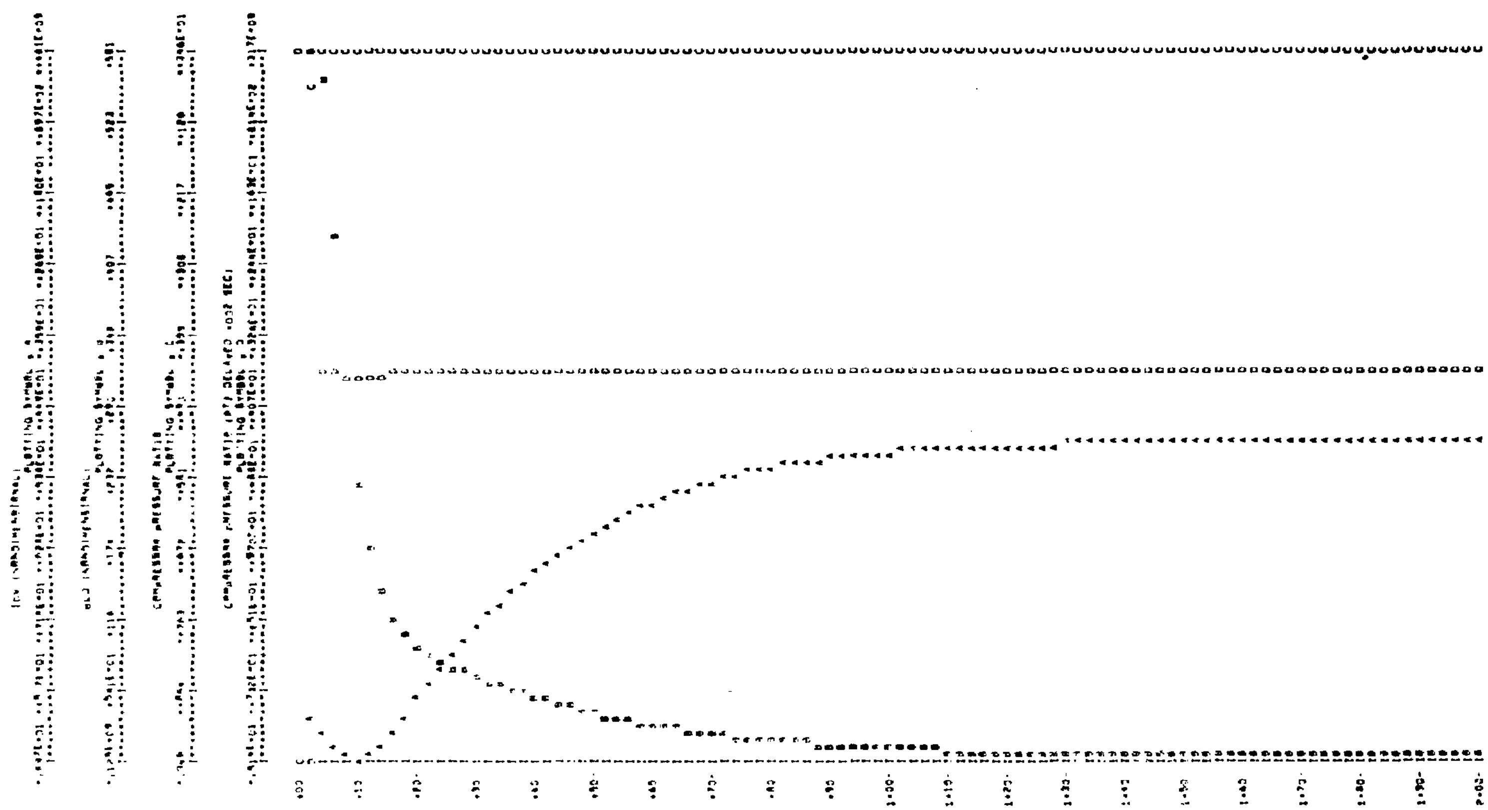

Figure 16d. Disturbance Controller at 100 Percent, $\Delta PT2 = 2.0$ psi

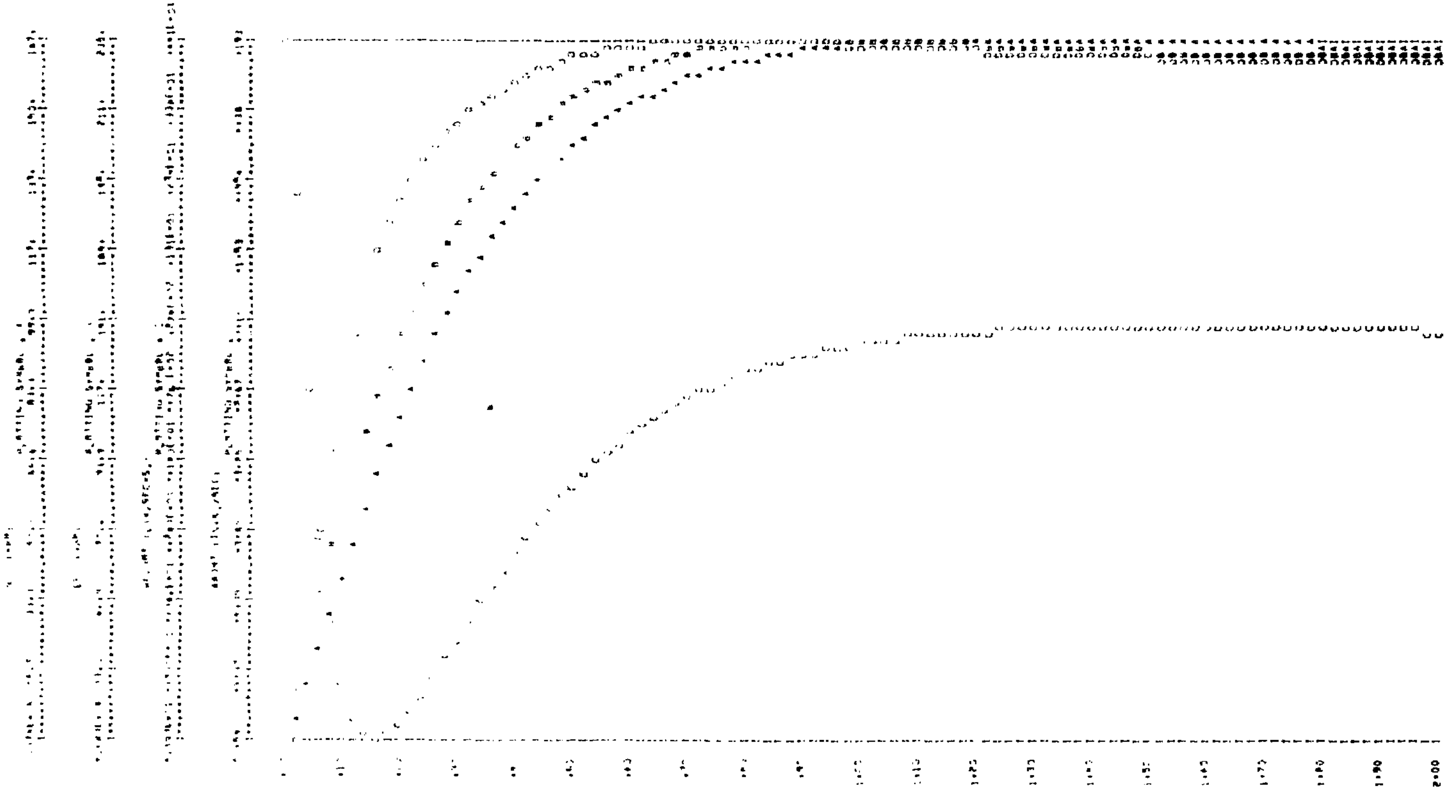

Figure 17a. Disturbance Controller at 85 Percent, Δ Pilot = 0.01

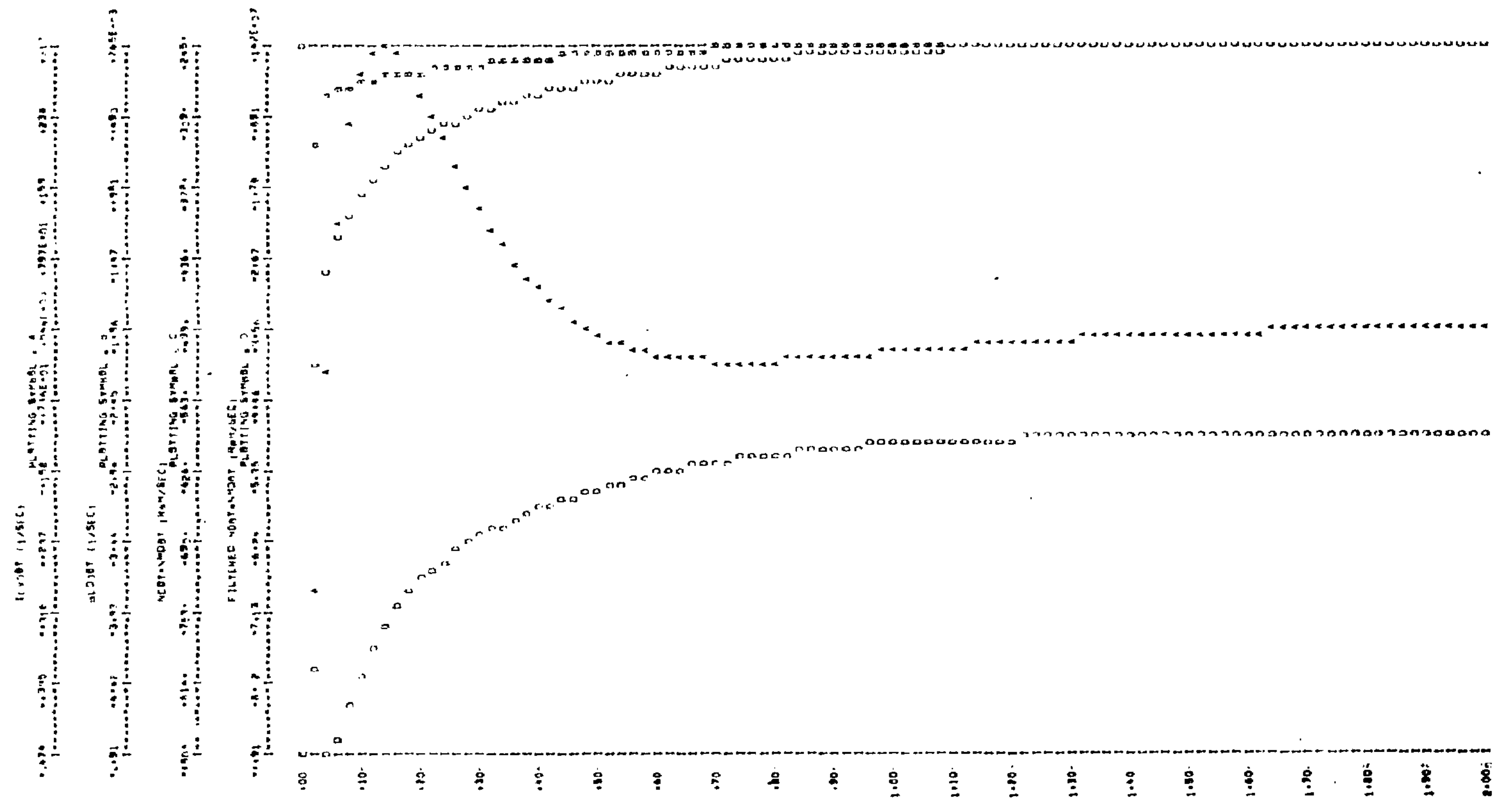

Figure 17b. Disturbance Controller at 85 Percent, Δ Pilot = 0.01

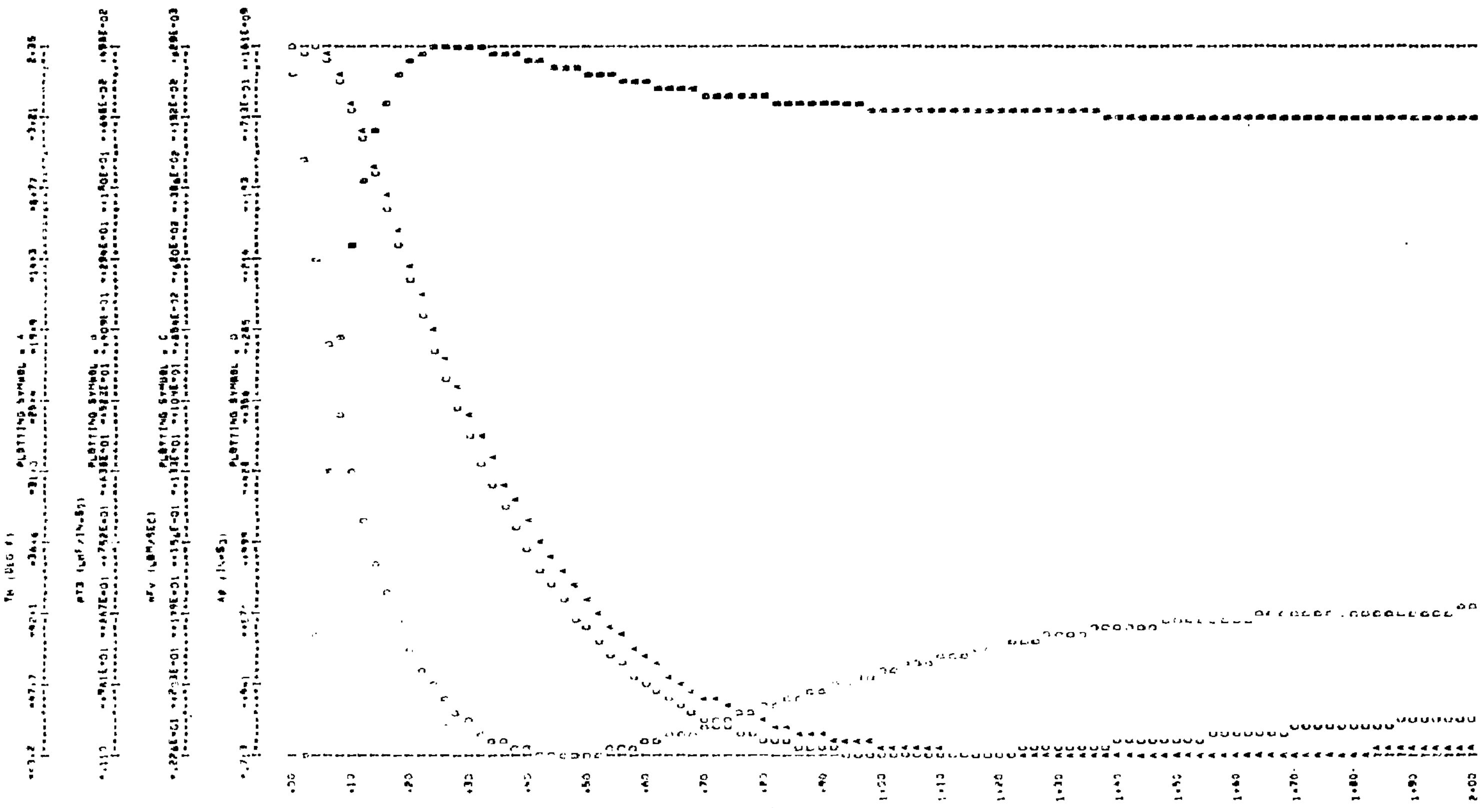

Figure 17c. Disturbance Controller at 85 Percent, Δ Pilot = 0.01

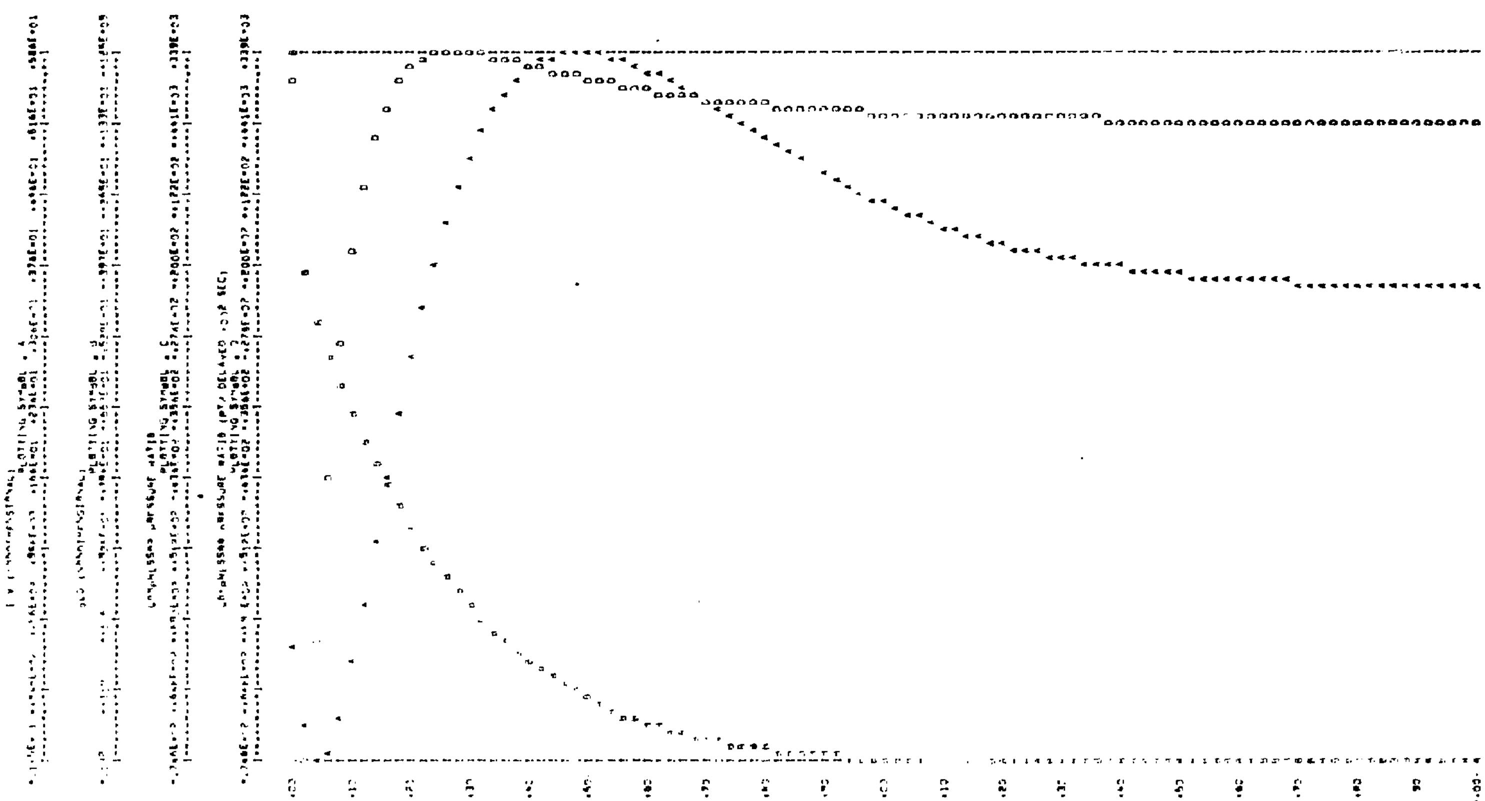

Figure 17d. Disturbance Controller at 85 Percent, Δ Pilot = 0.01

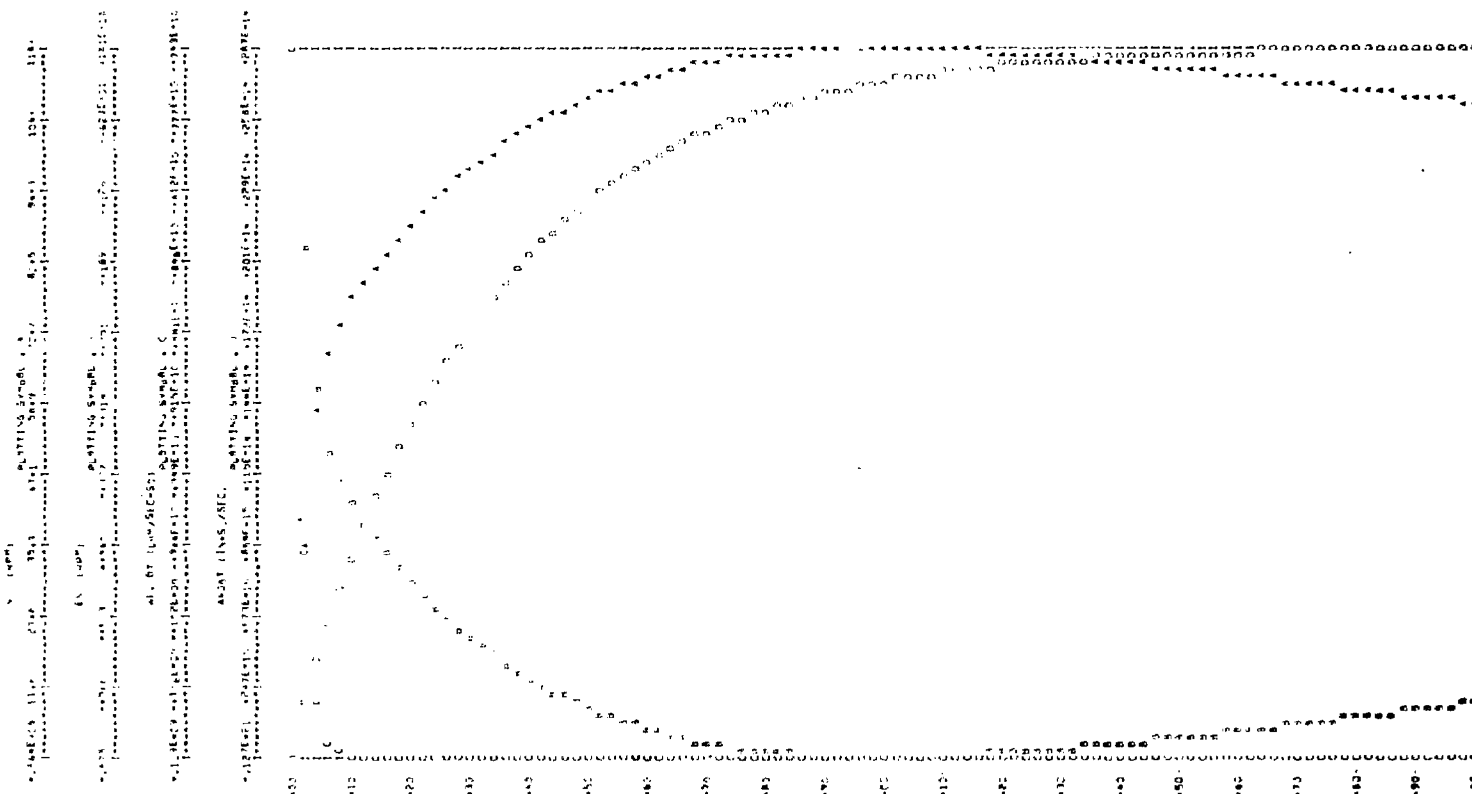

Figure 18a. Open-Loop Disturbance Response at 85 Percent, $\Delta PT2 = 2.0$ psi

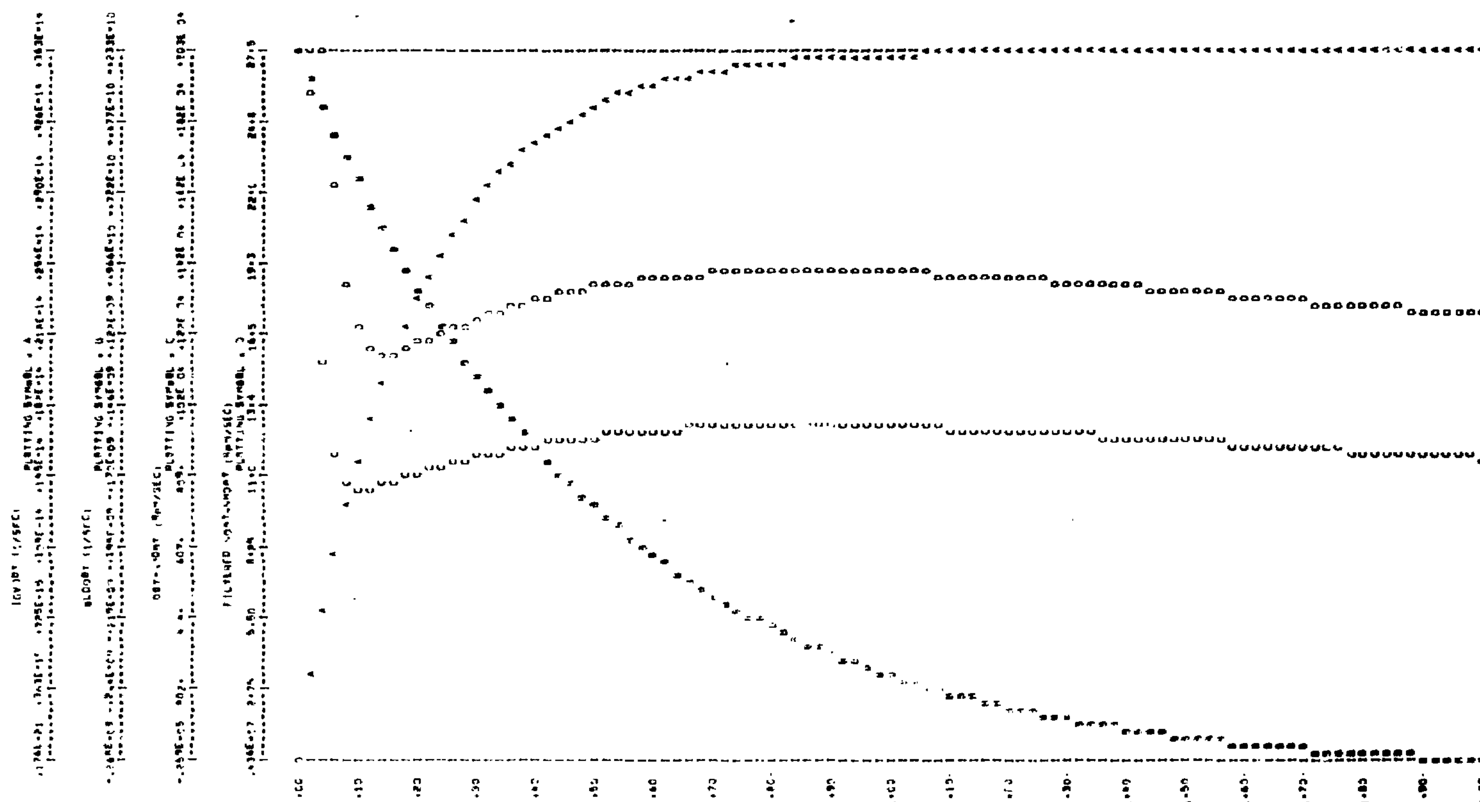

Figure 18b. Open-Loop Disturbance Response at 85 Percent, $\Delta PT2 = 2.0$ psi

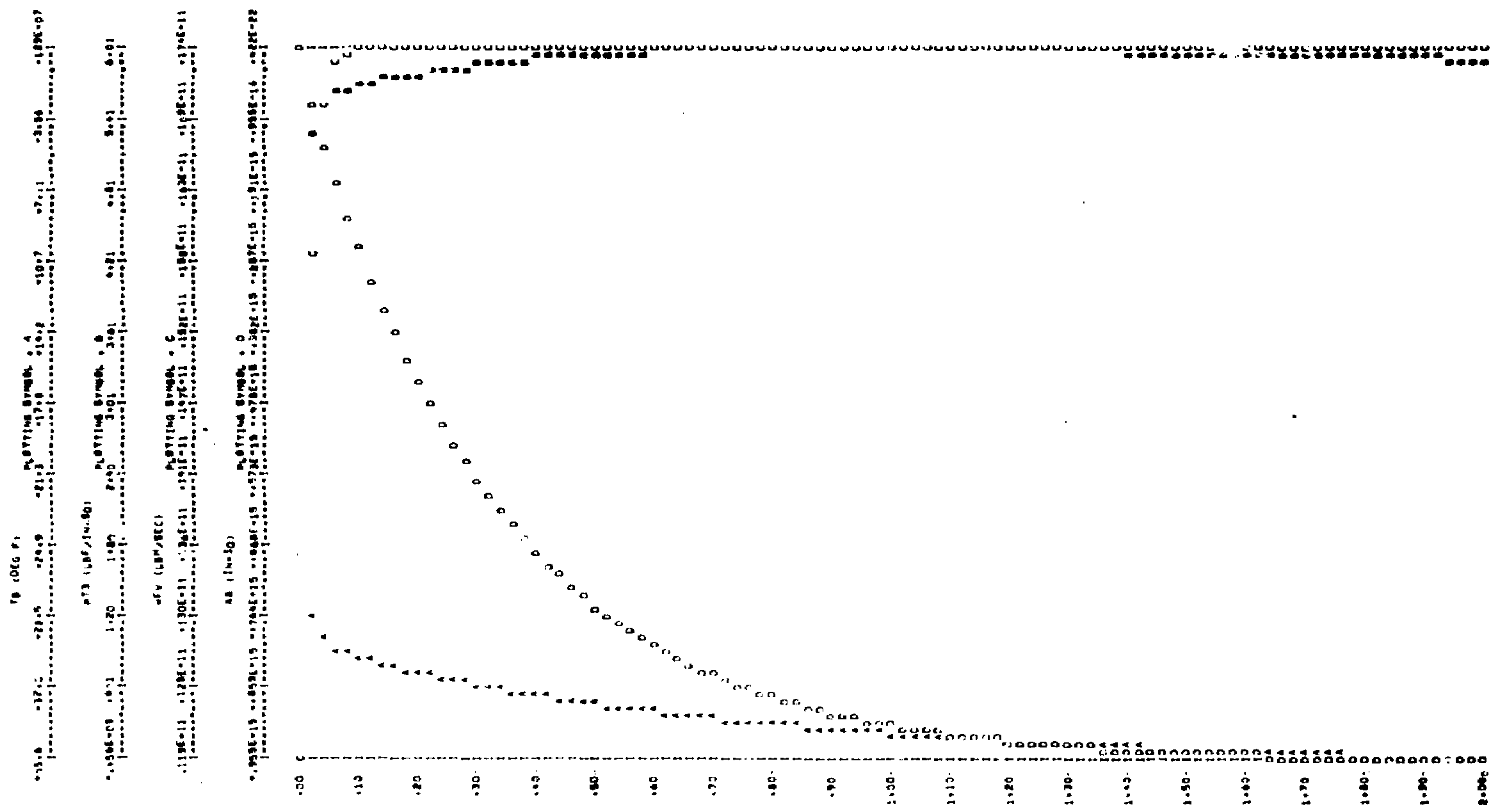

Figure 18c. Open-Loop Disturbance Response at 85 Percent, $\Delta PT2 = 2.0$ psi

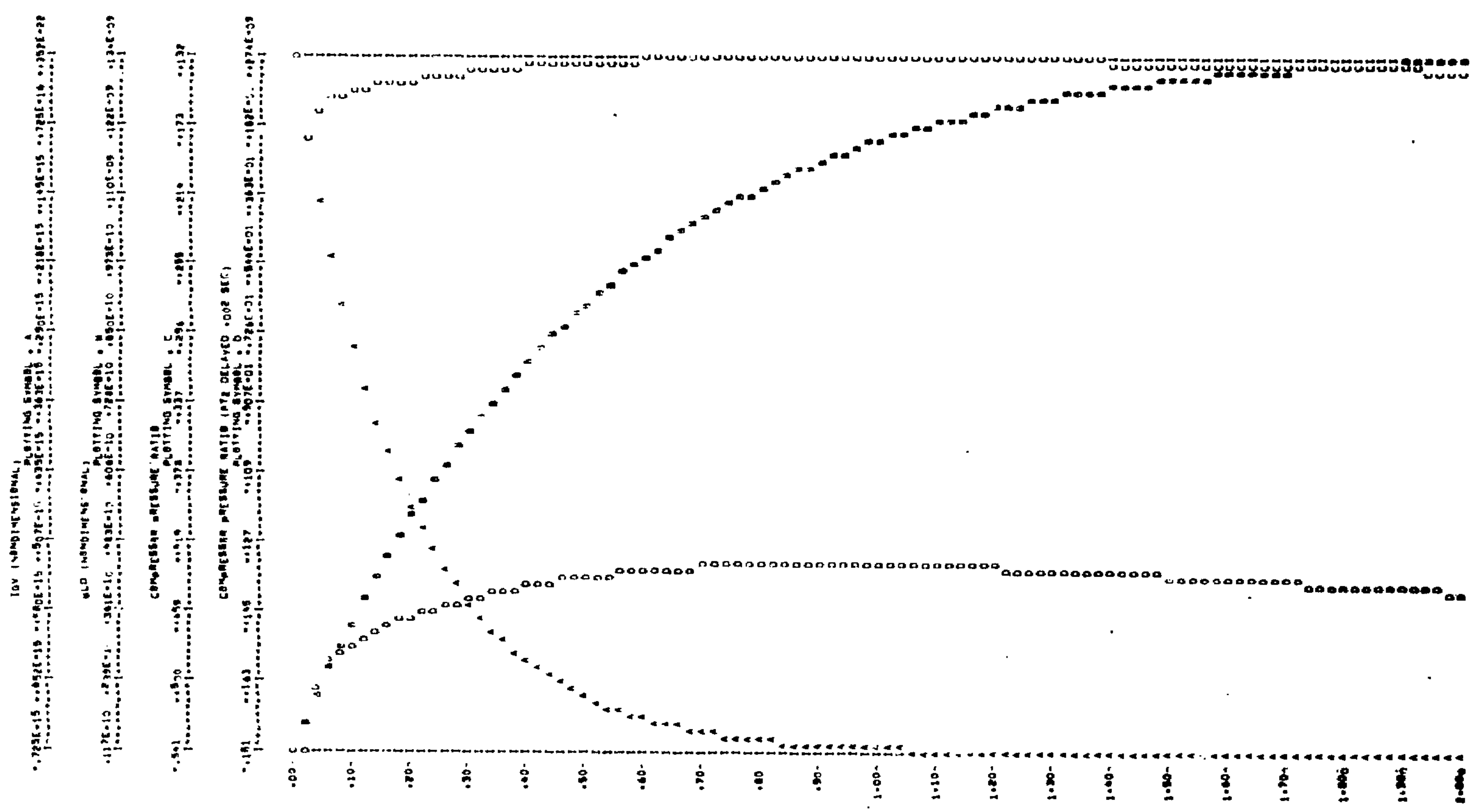

Figure 18d. Open-Loop Disturbance Response at 85 Percent, $\Delta PT2 = 2.0$ psi

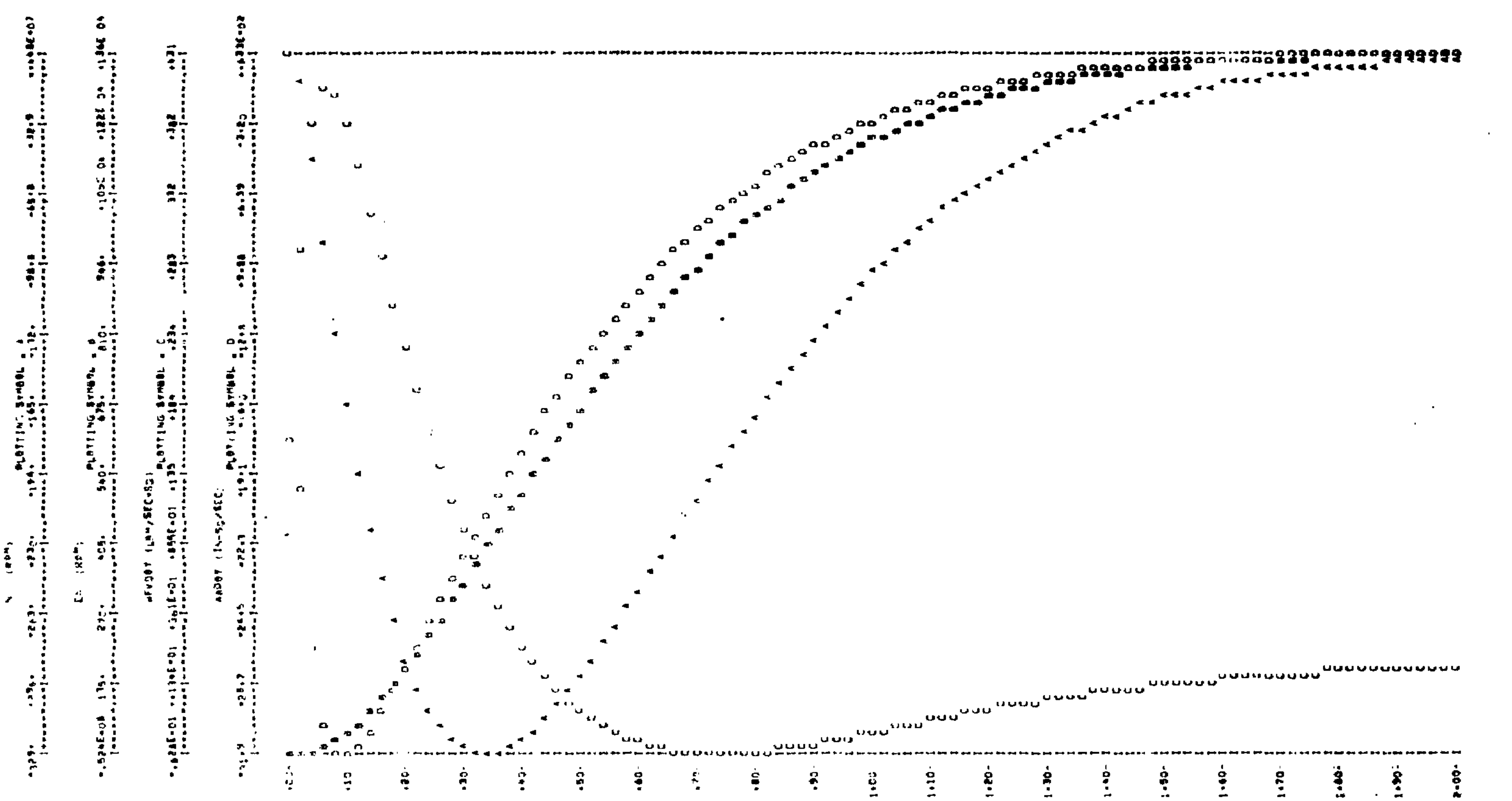

Figure 19a. Disturbance Controller at 85 Percent, $\Delta PT2 = 2.0$ psi

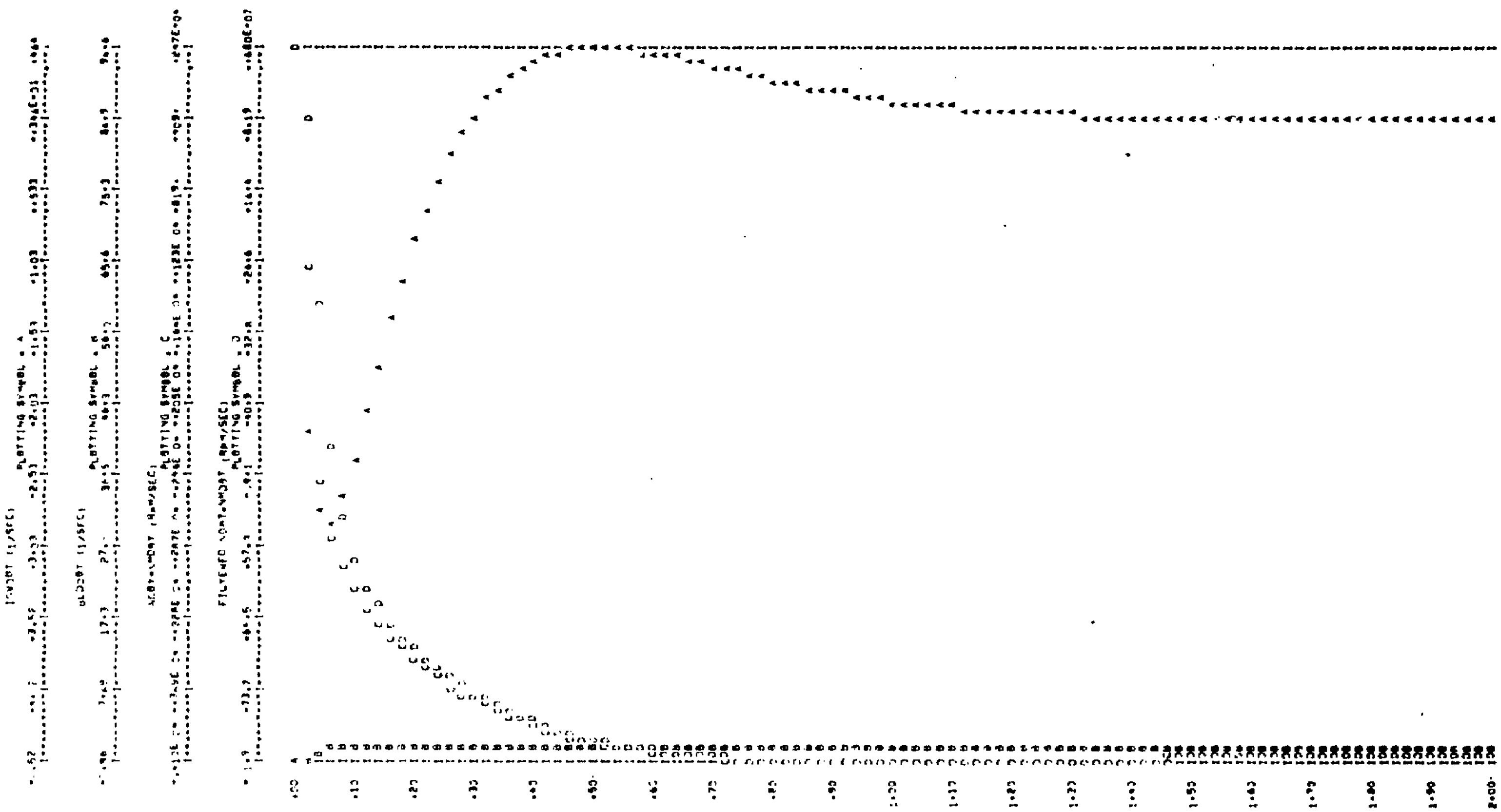

Figure 19b. Disturbance Controller at 85 Percent, $\Delta PT2 = 2.0$ psi

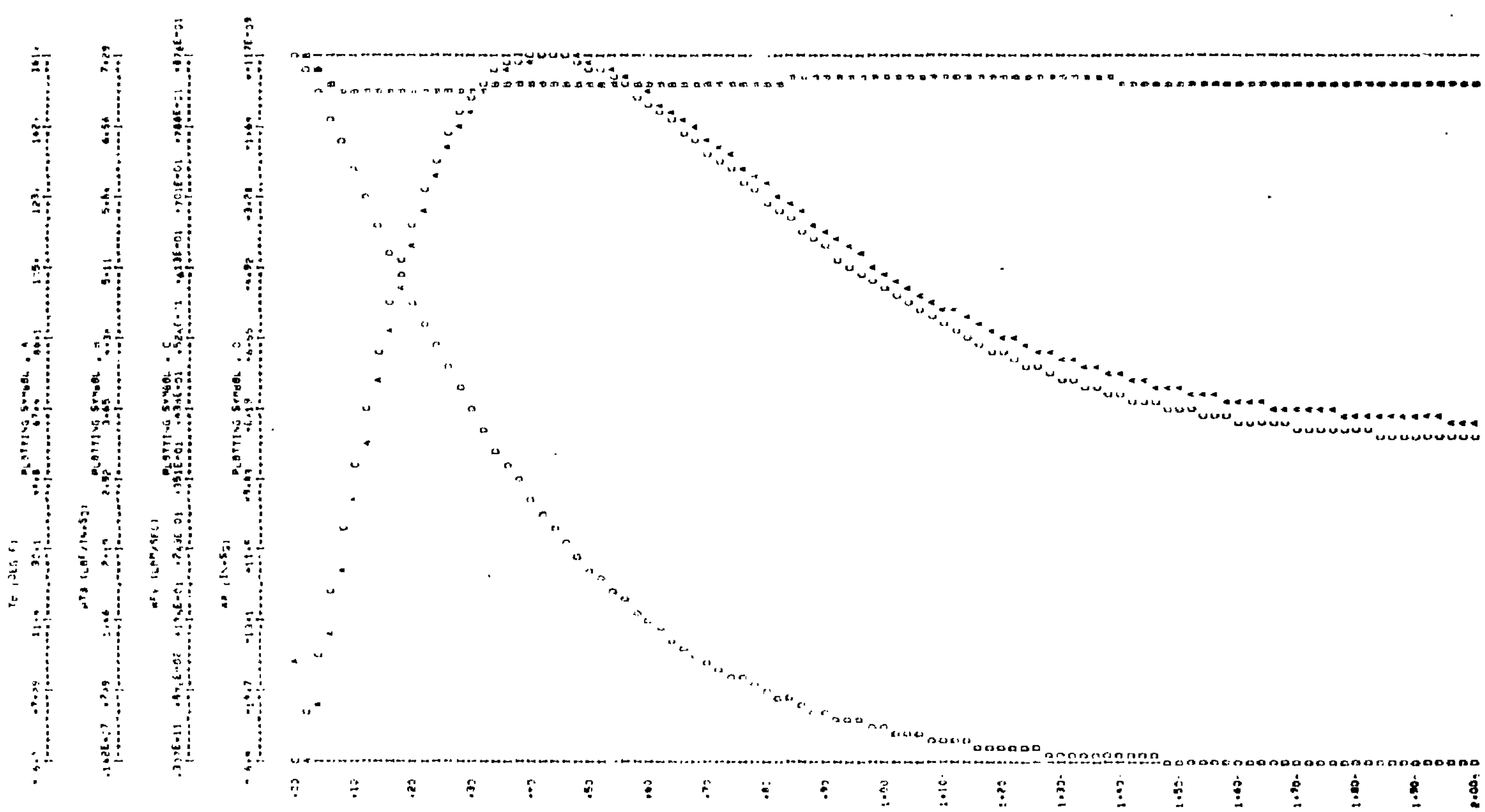

Figure 19c. Disturbance Controller at 85 Percent, ΔPT2 = 2.0 psi

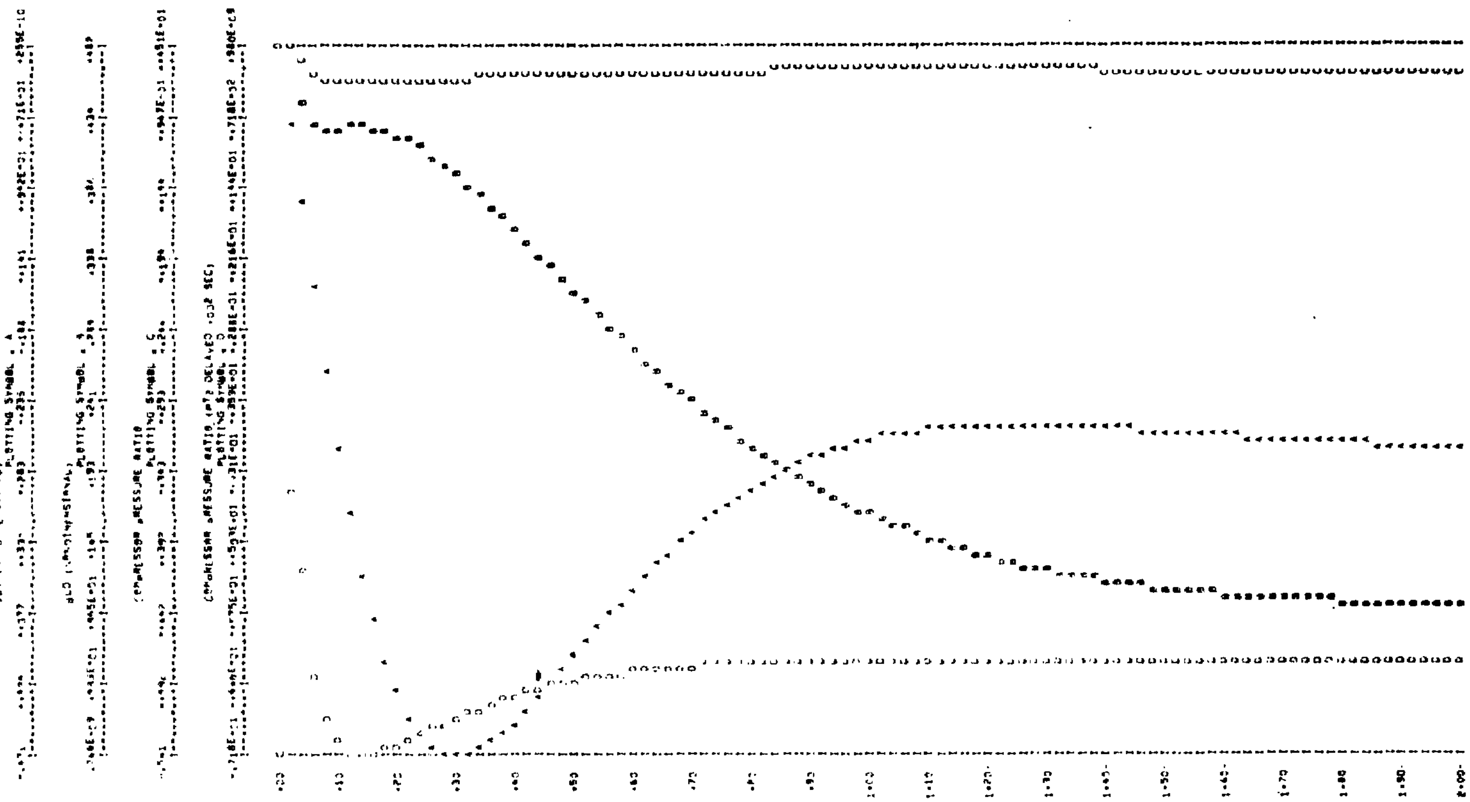

Figure 19d. Disturbance Controller at 85 Percent, ΔPT2 = 2.0 psi

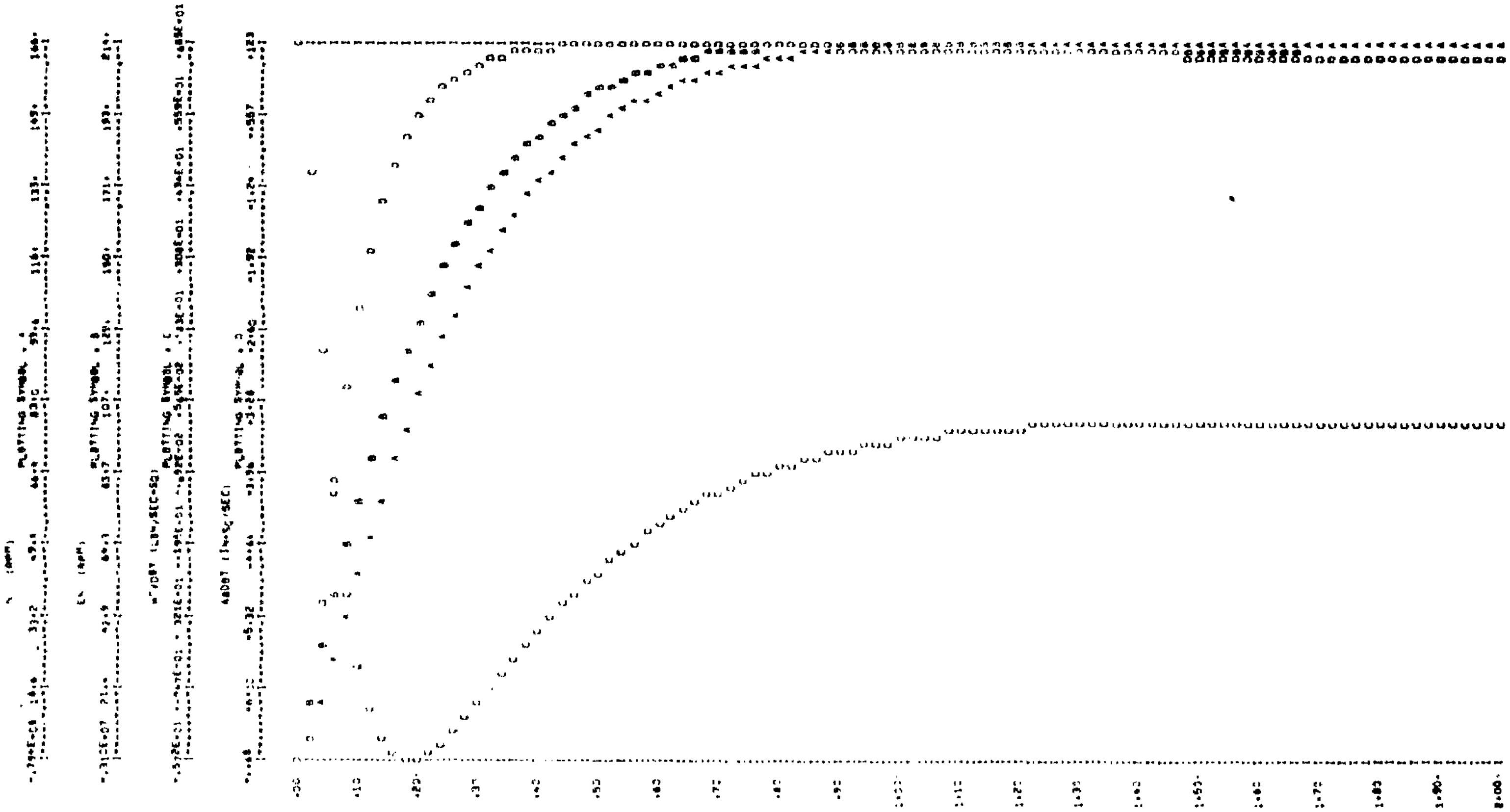

Figure 20a. Disturbance Controller at 70 Percent, Δ Pilot = 0.01

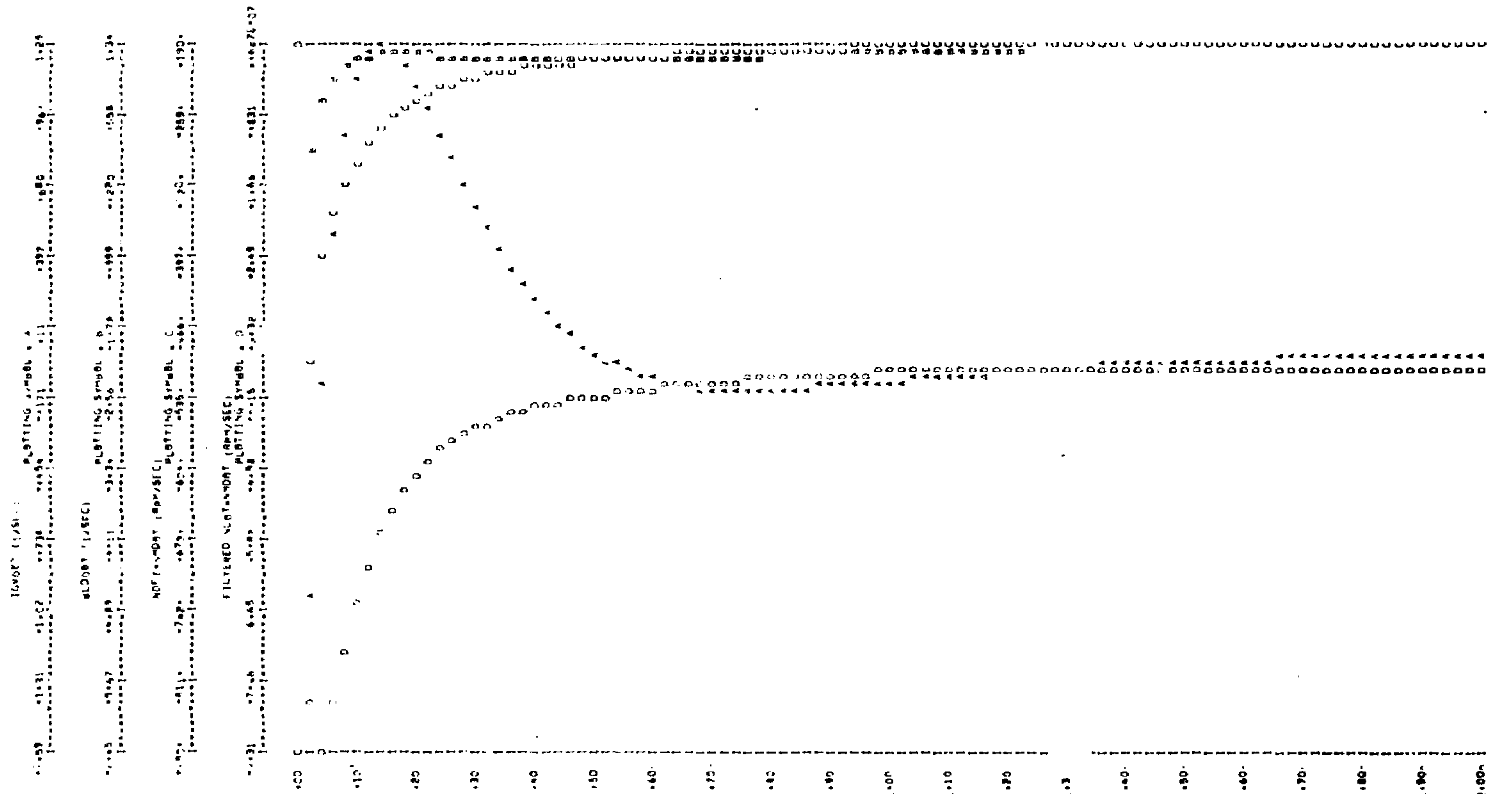

Figure 20b. Disturbance Controller at 70 Percent, Δ Pilot = 0.01

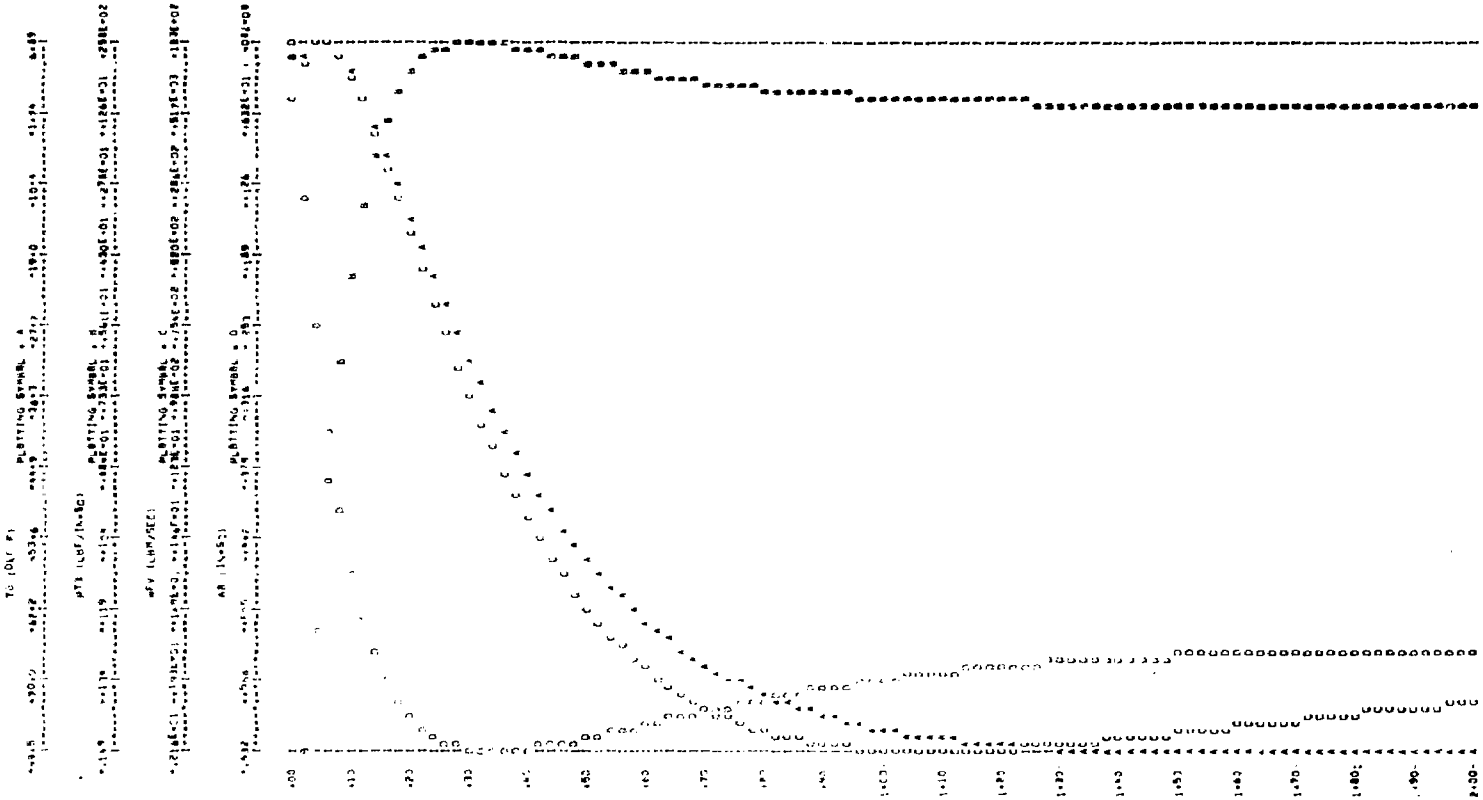

Figure 20c. Disturbance Controller at 70 Percent, ΔPilot = 0.01

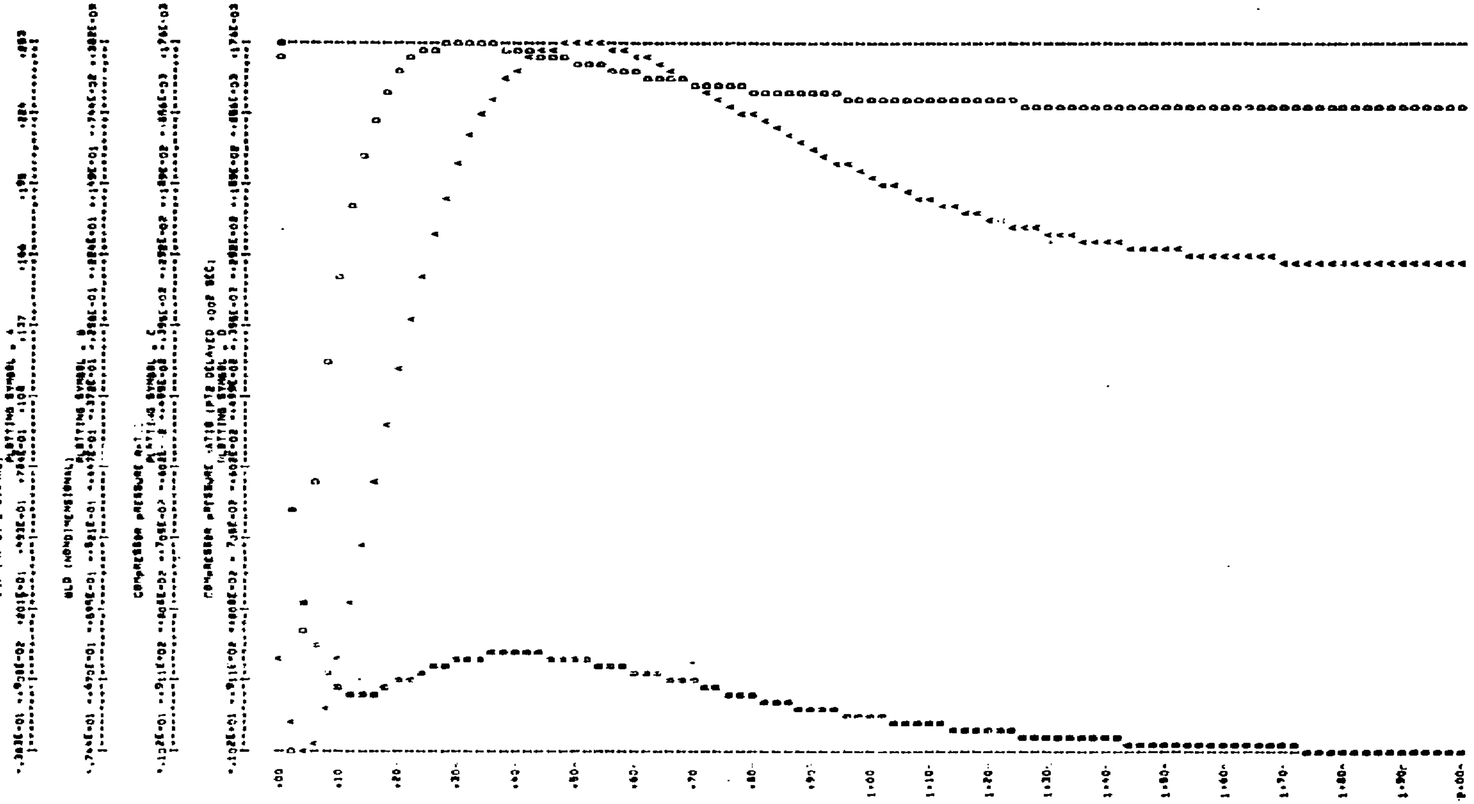

Figure 20d. Disturbance Controller at 70 Percent, Δ Pilot = 0.01

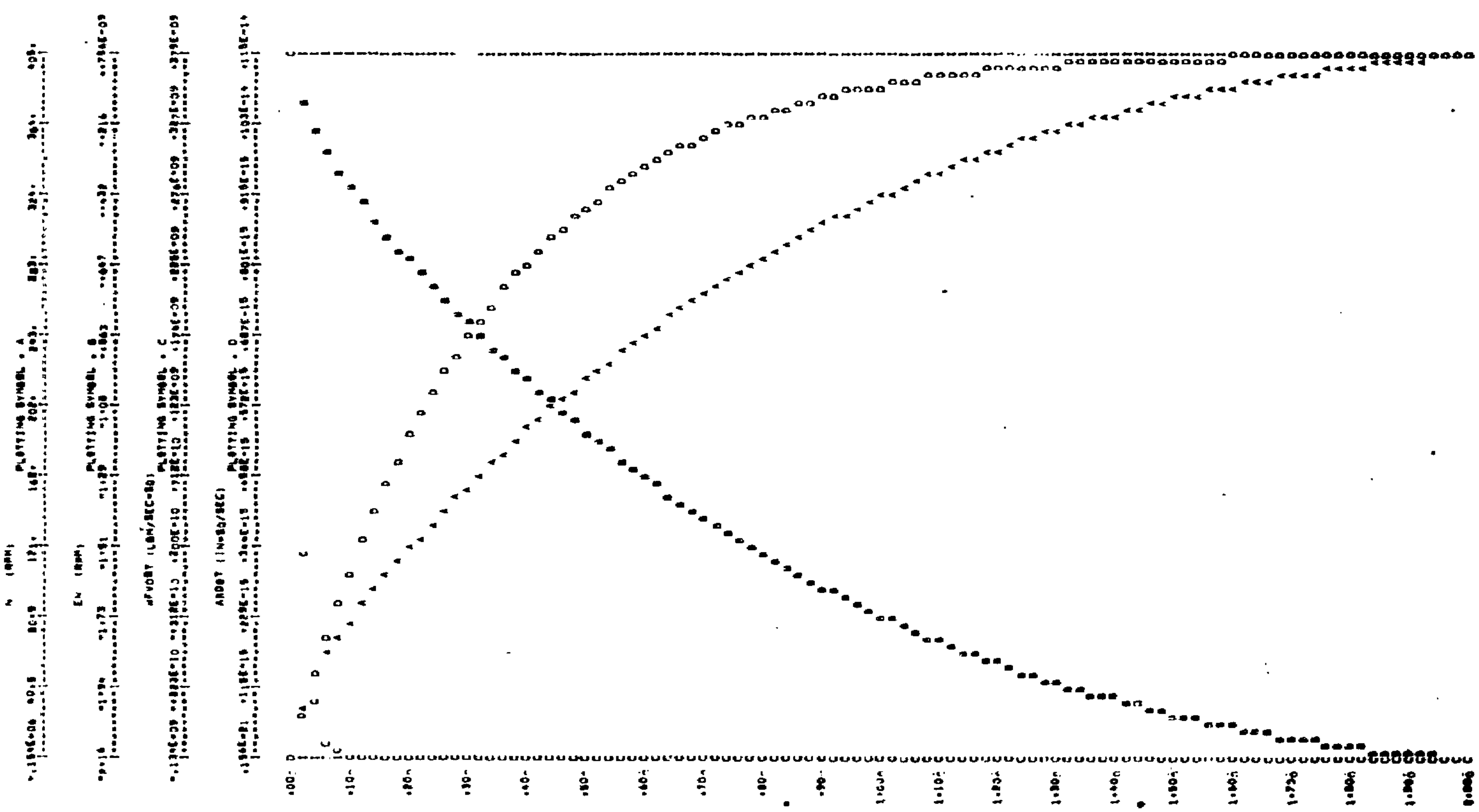

Figure 21a. Open-Loop Disturbance Response at 70 Percent, ΔPT2 = 2.0 psi

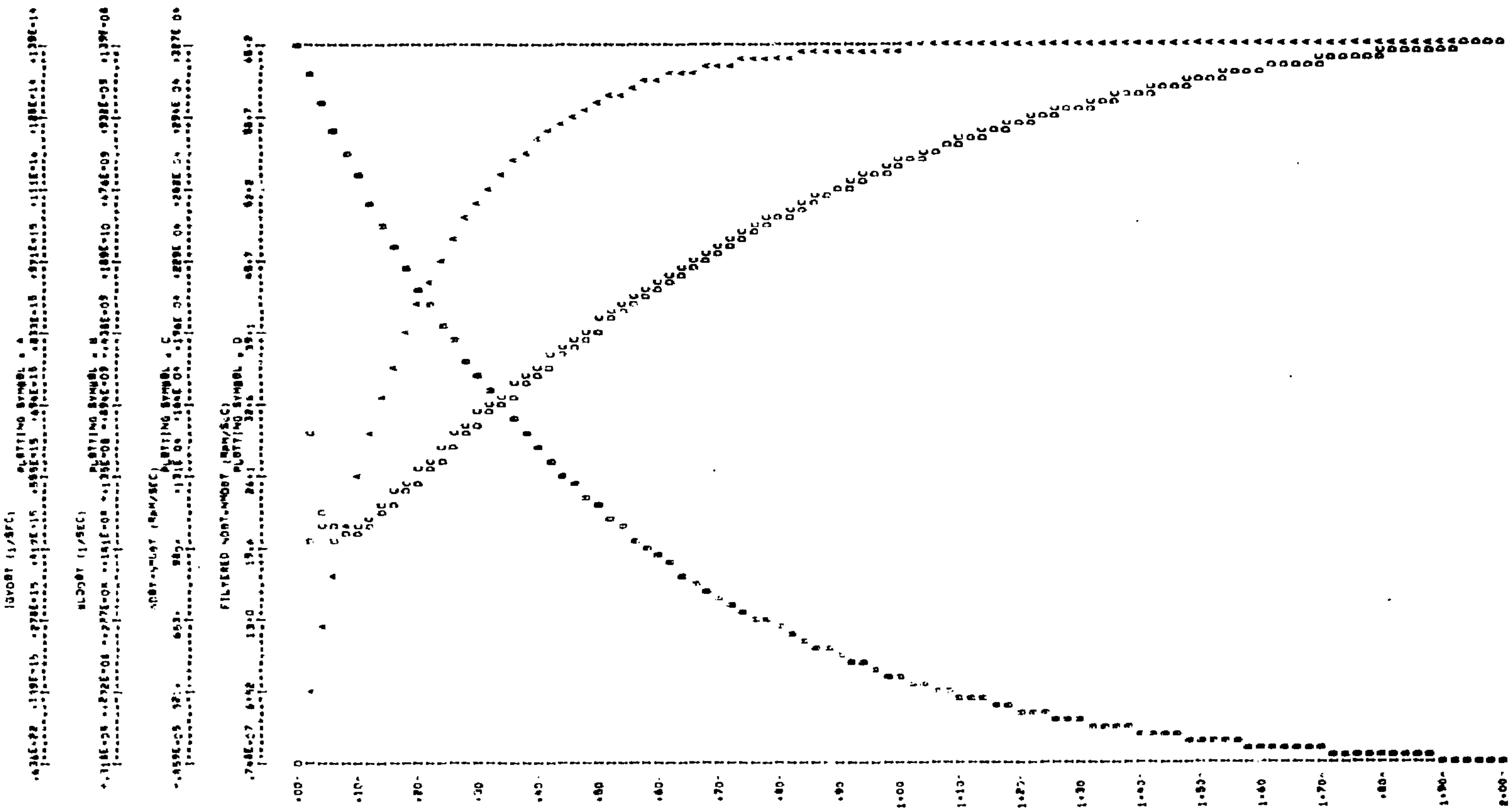

Figure 21b. Open-Loop Disturbance Response at [illegible] Percent,
$\Delta PT2 = 2.0$ psi

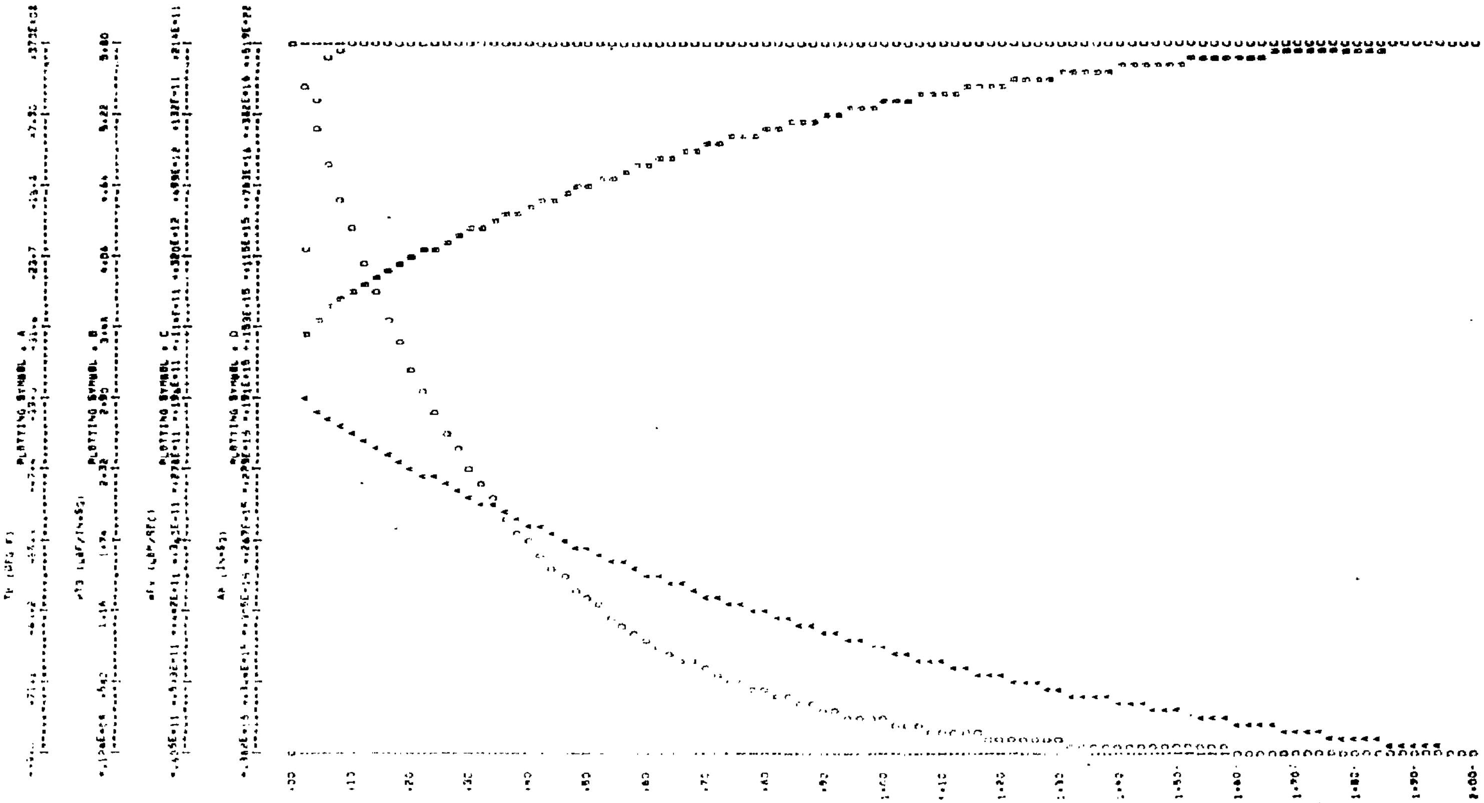

Figure 21c. Open-Loop Disturbance Response at 70 Percent, $\Delta PT2 = 2.0$ psi

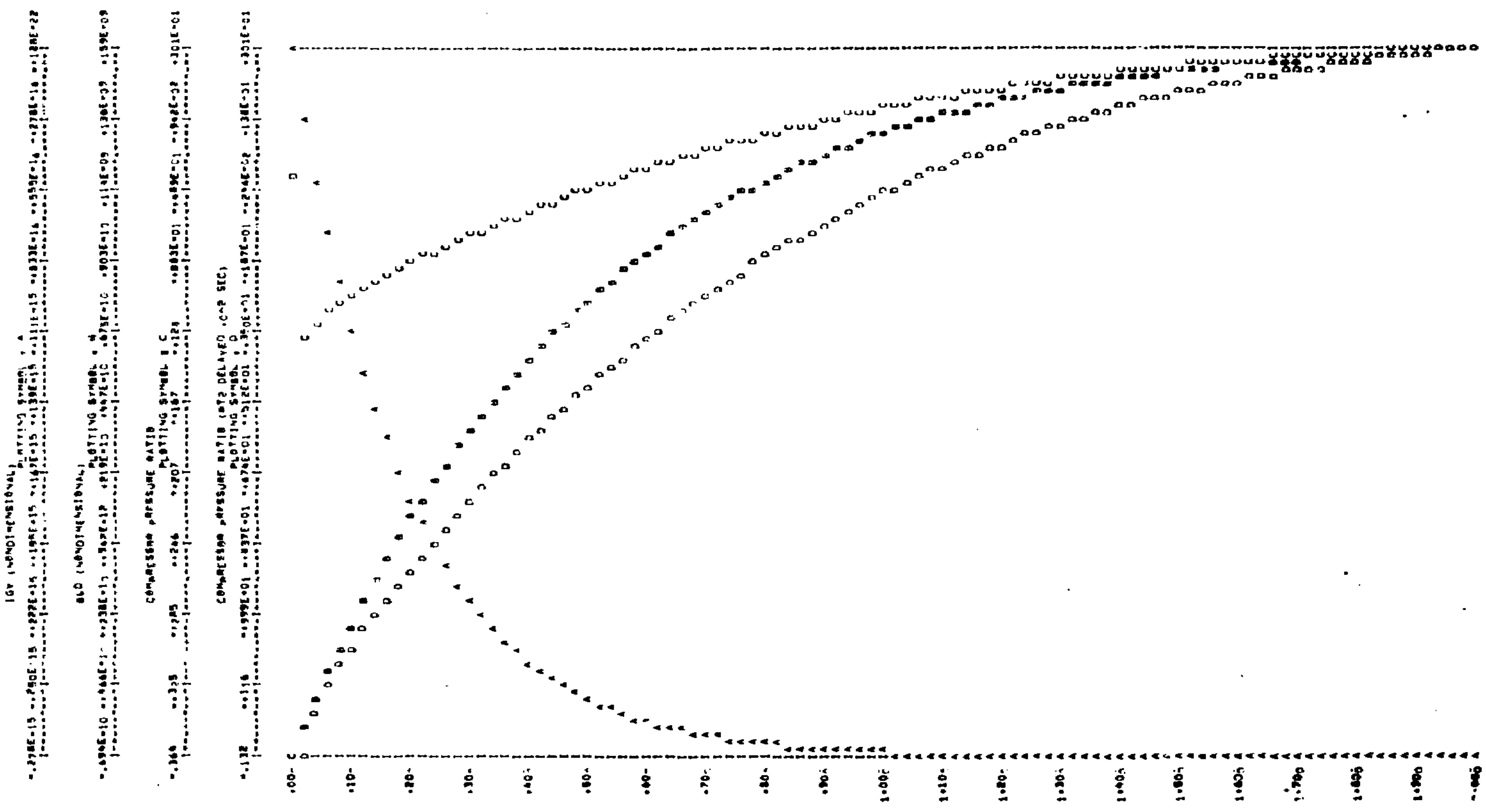

Figure 21d. Open-Loop Disturbance Response at 70 Percent, $\Delta PT2 = 2.0$ psi

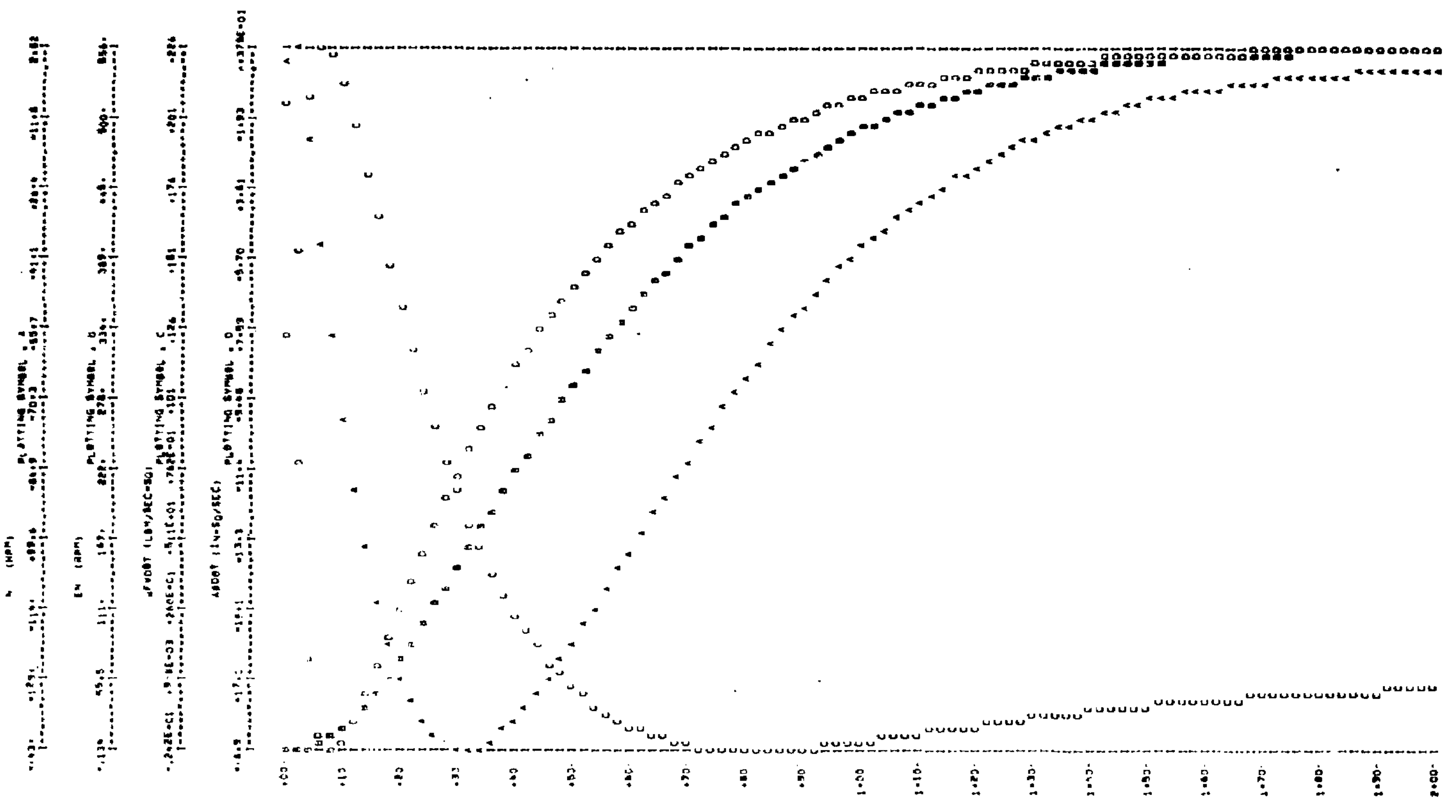

Figure 22a. Disturbance Controller at 7̆ Percent, ΔPT2 = 2.0 psi

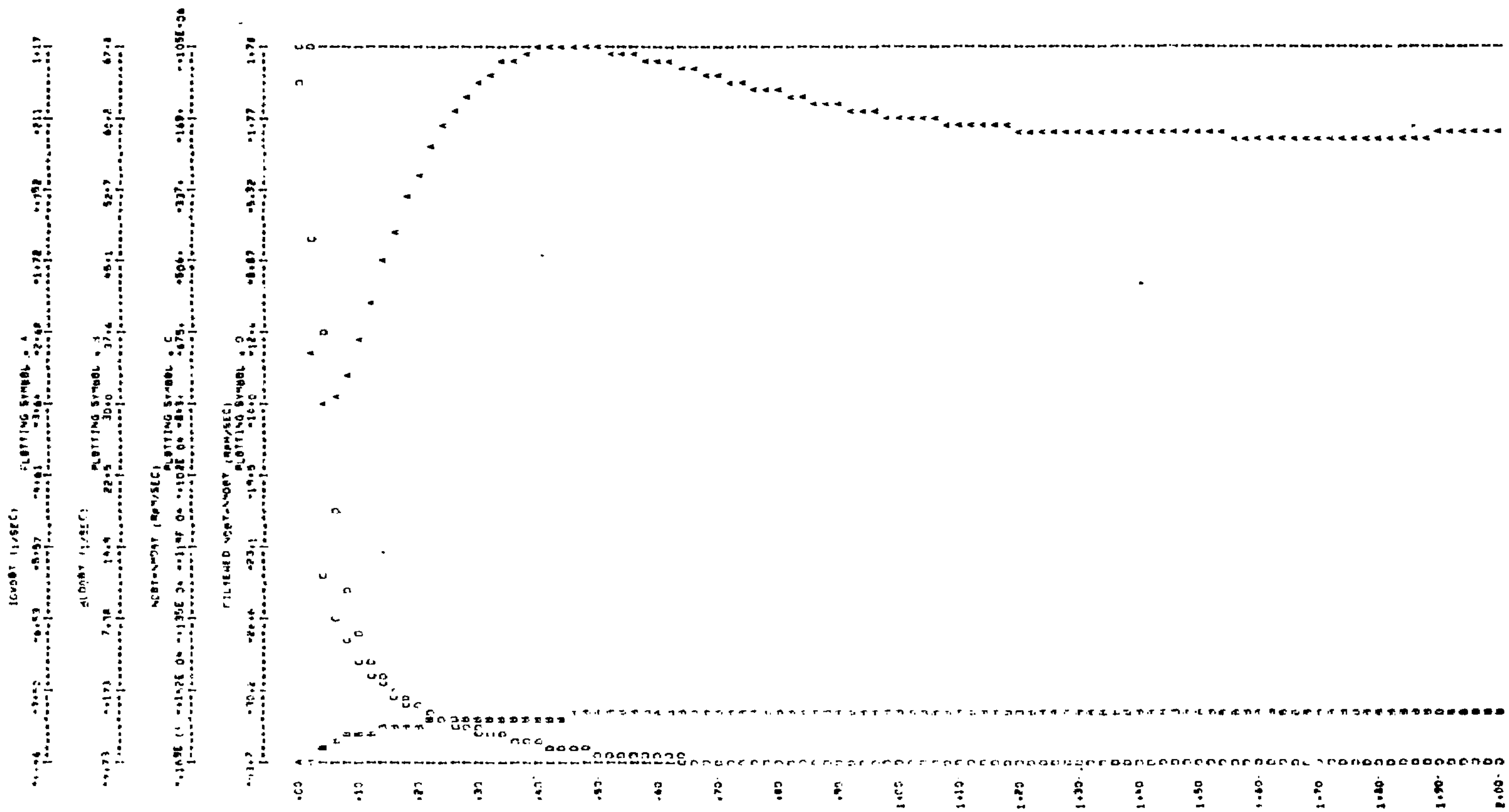

Figure 22b. Disturbance Controller at 70 Percent, $\Delta PT2 = 2.0$ psi

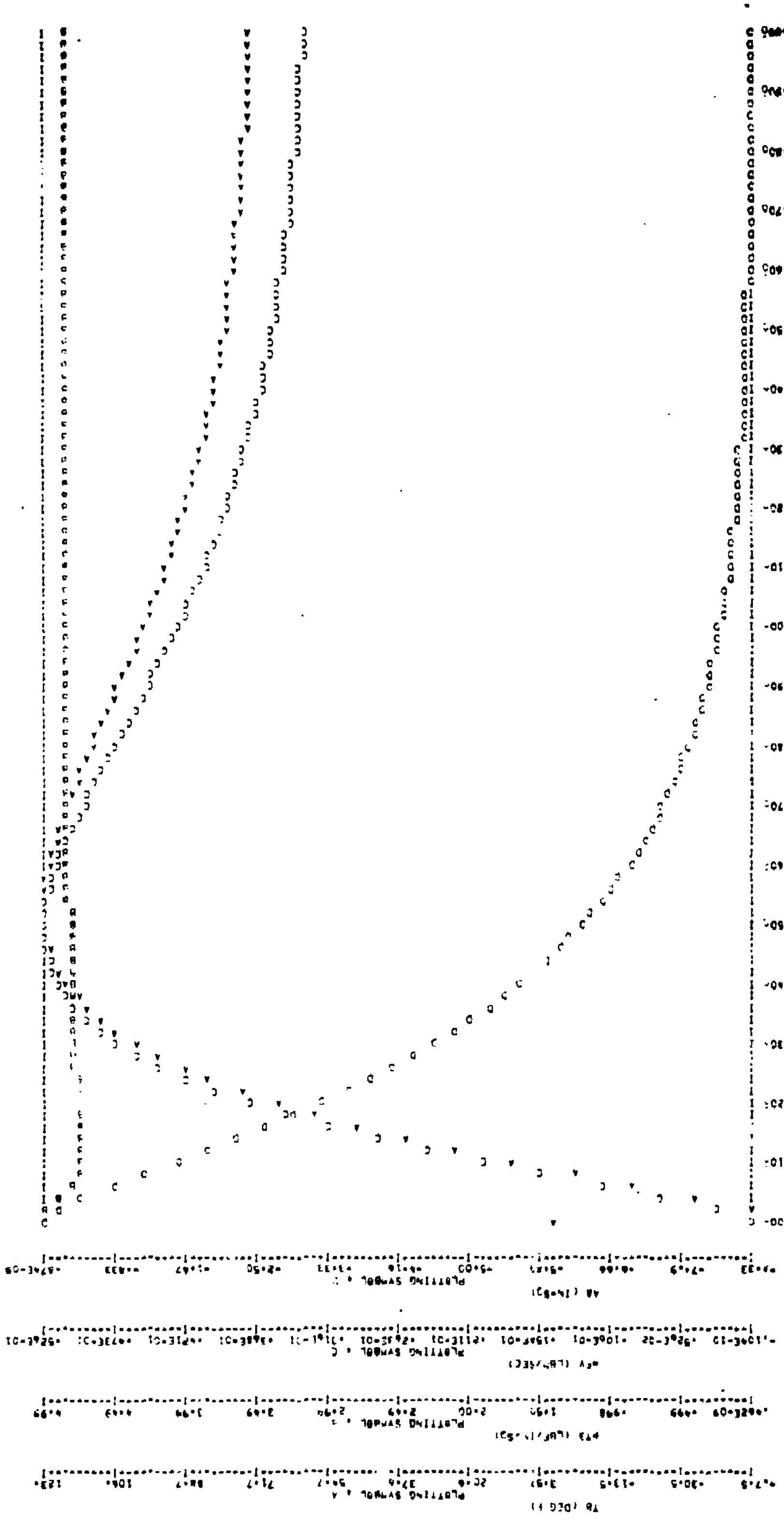

Figure 22c. Disturbance Controller at 70 Percent, $\Delta PT2 = 2.0$ psi

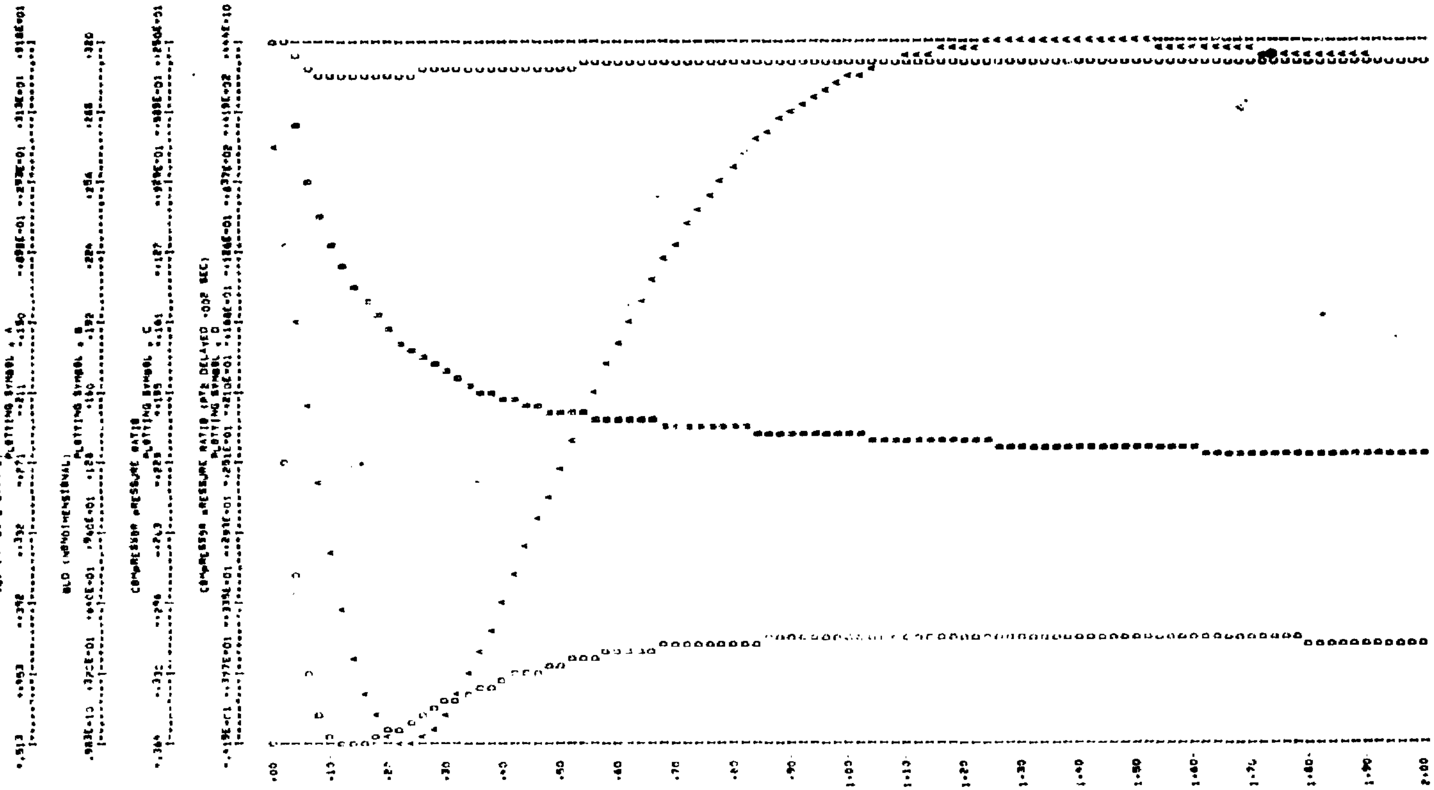

Figure 22d. Disturbance Controller at 70 Percent, ΔPT2 = 2.0 psi

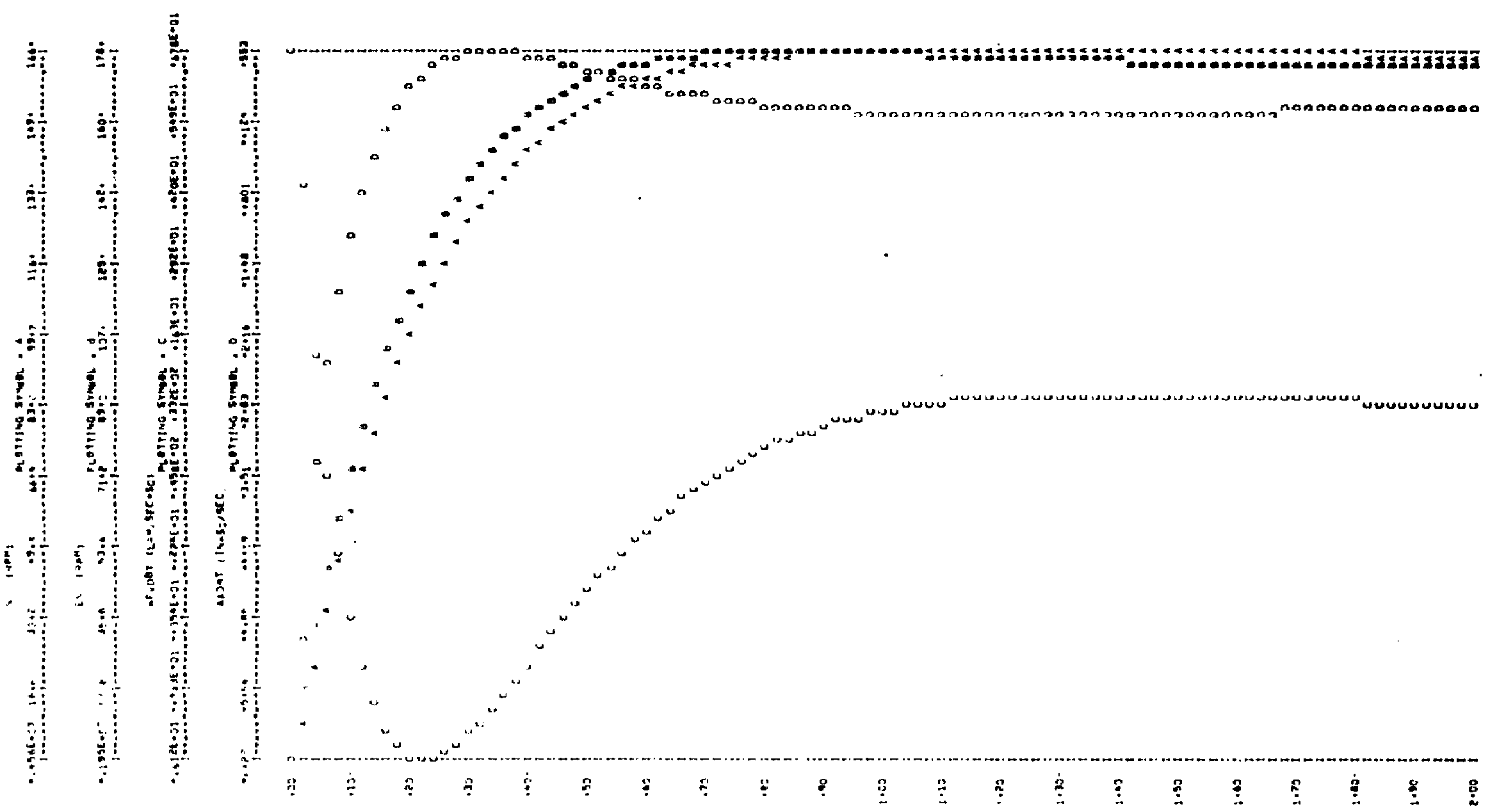

Figure 23a. Disturbance Controller at 50 Percent, Δ Pilot = 0.01

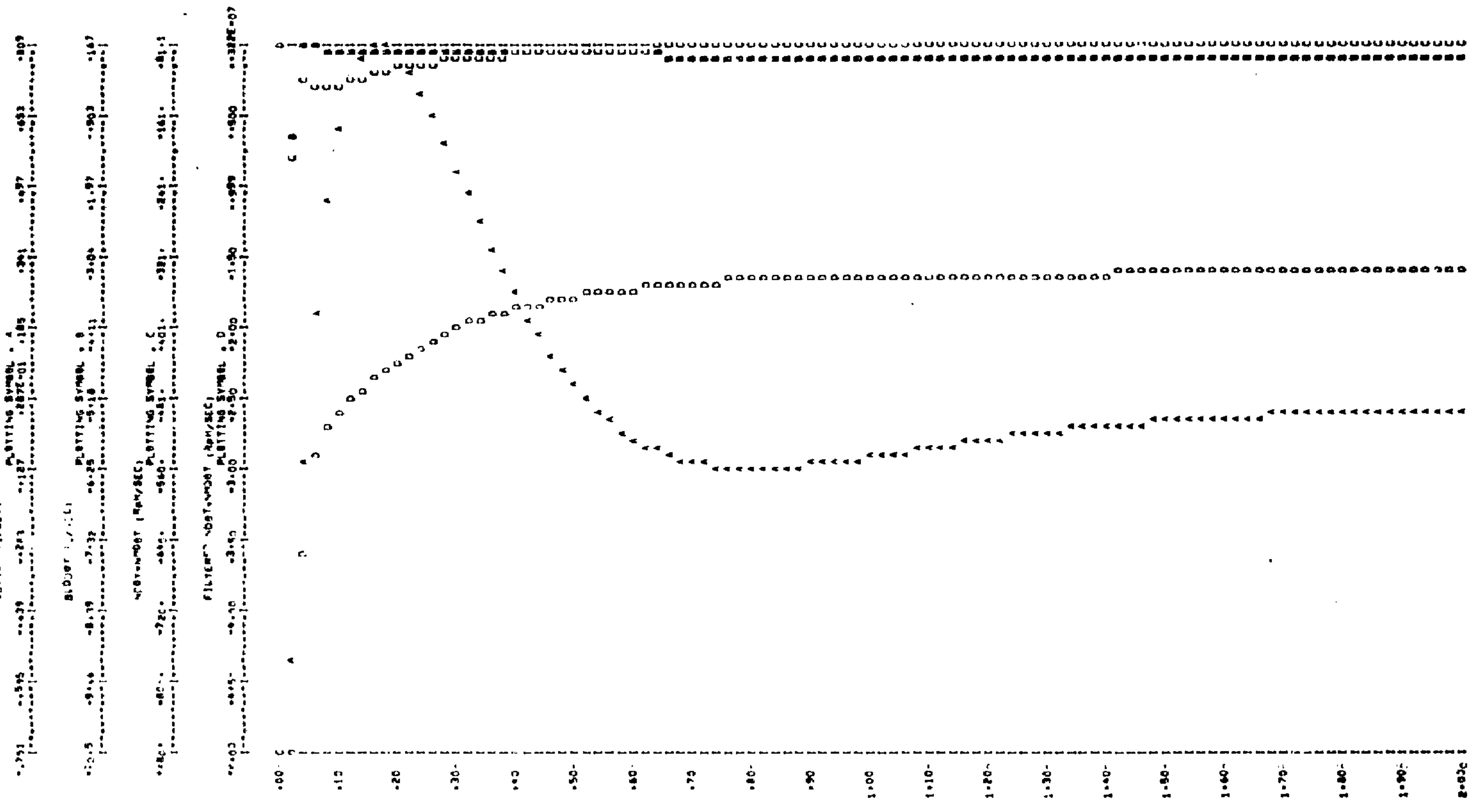

Figure 23b. Disturbance Controller at 50 Percent, ΔPilot = 0.01

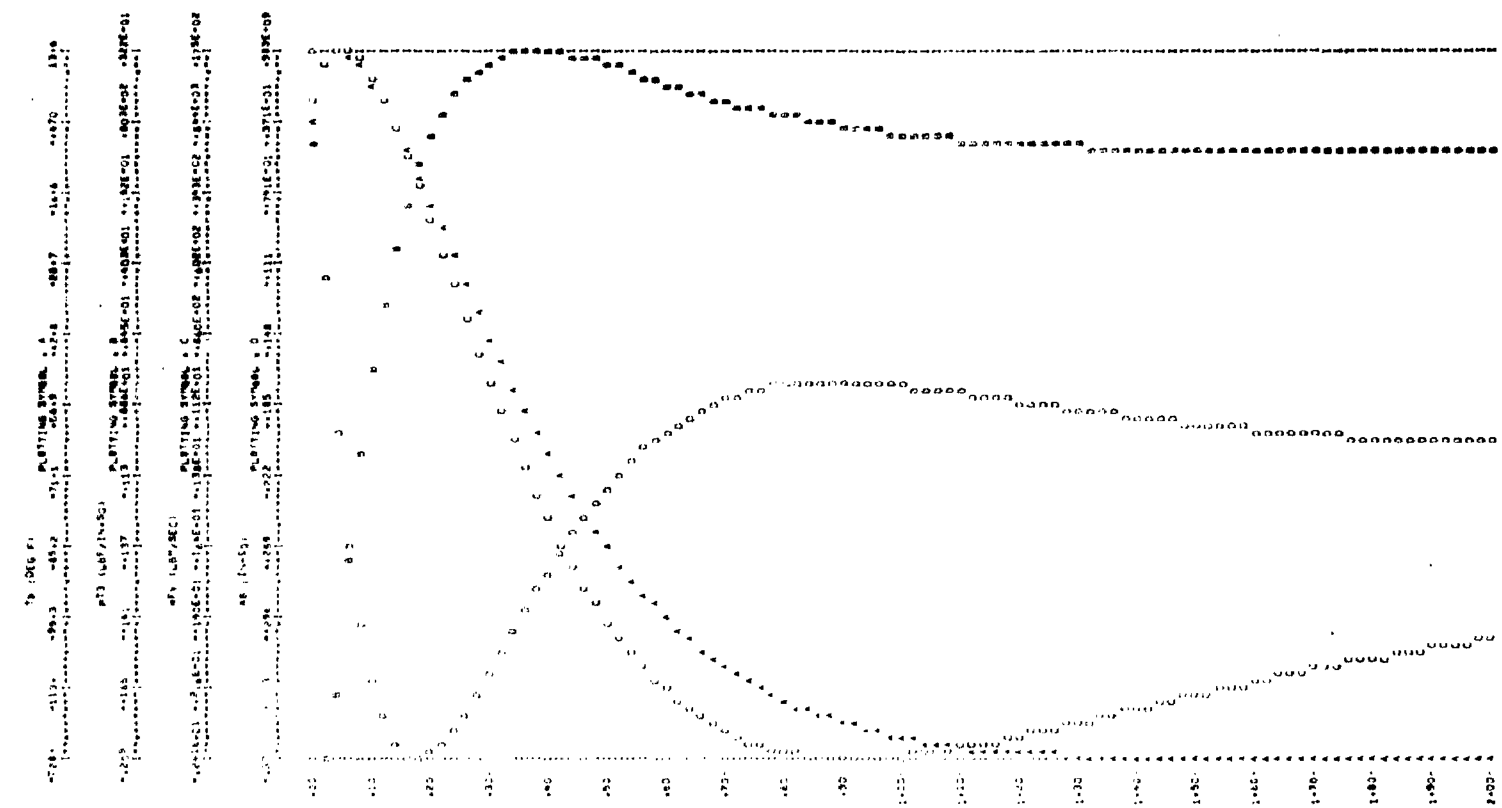

Figure 23c. Disturbance Controller at 5) Percent, ΔPilot = 0.01

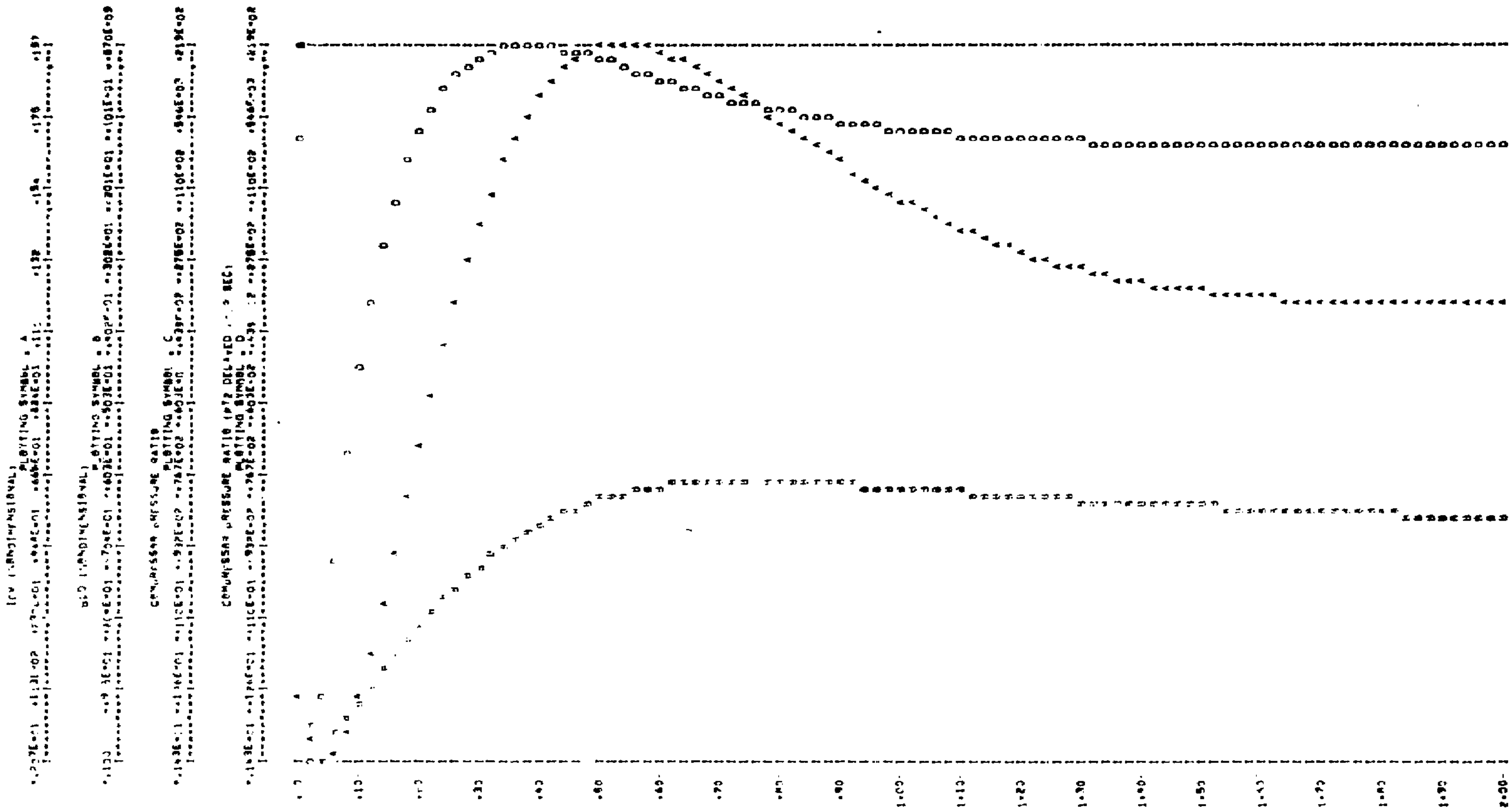

Figure 23d. Disturbance Controller at 50 Percent, ΔPilot = 0.01

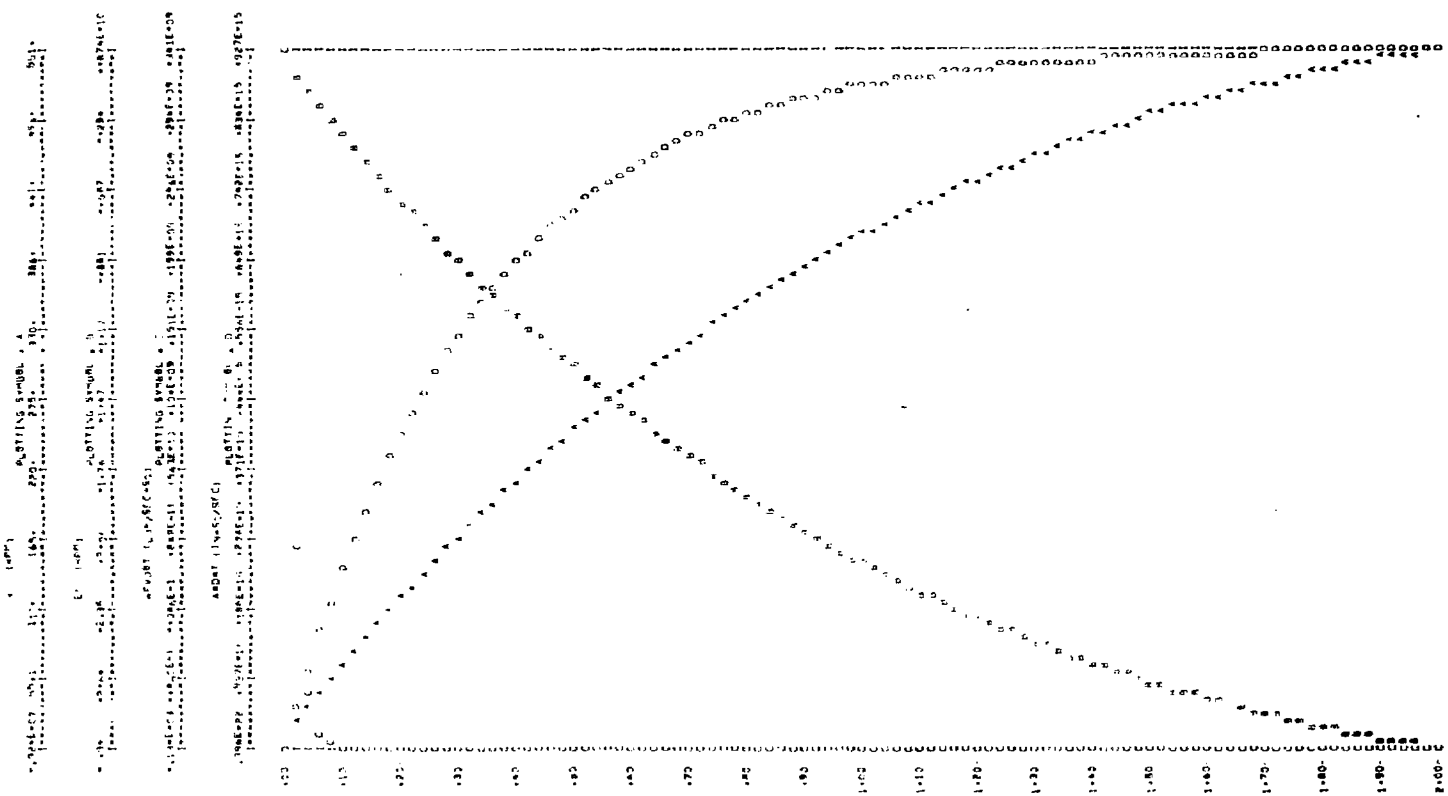

Figure 24a. Open-Loop Disturbance Response at 50 Percent, $\Delta PT2 = 2.0$ psi

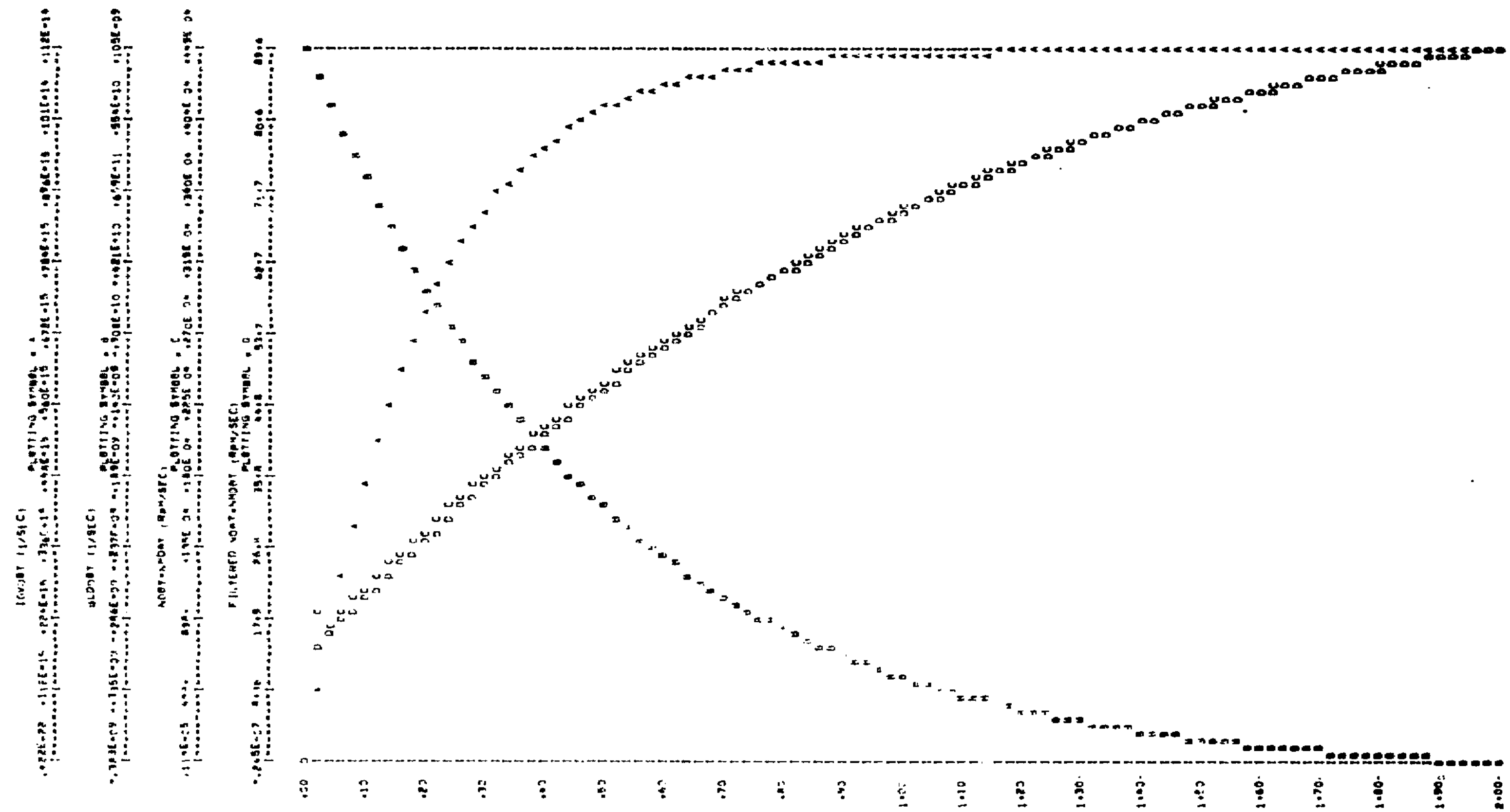

Figure 24b. Open-Loop Disturbance Response at 50 Percent, $\Delta PT2 = 2.0$ psi

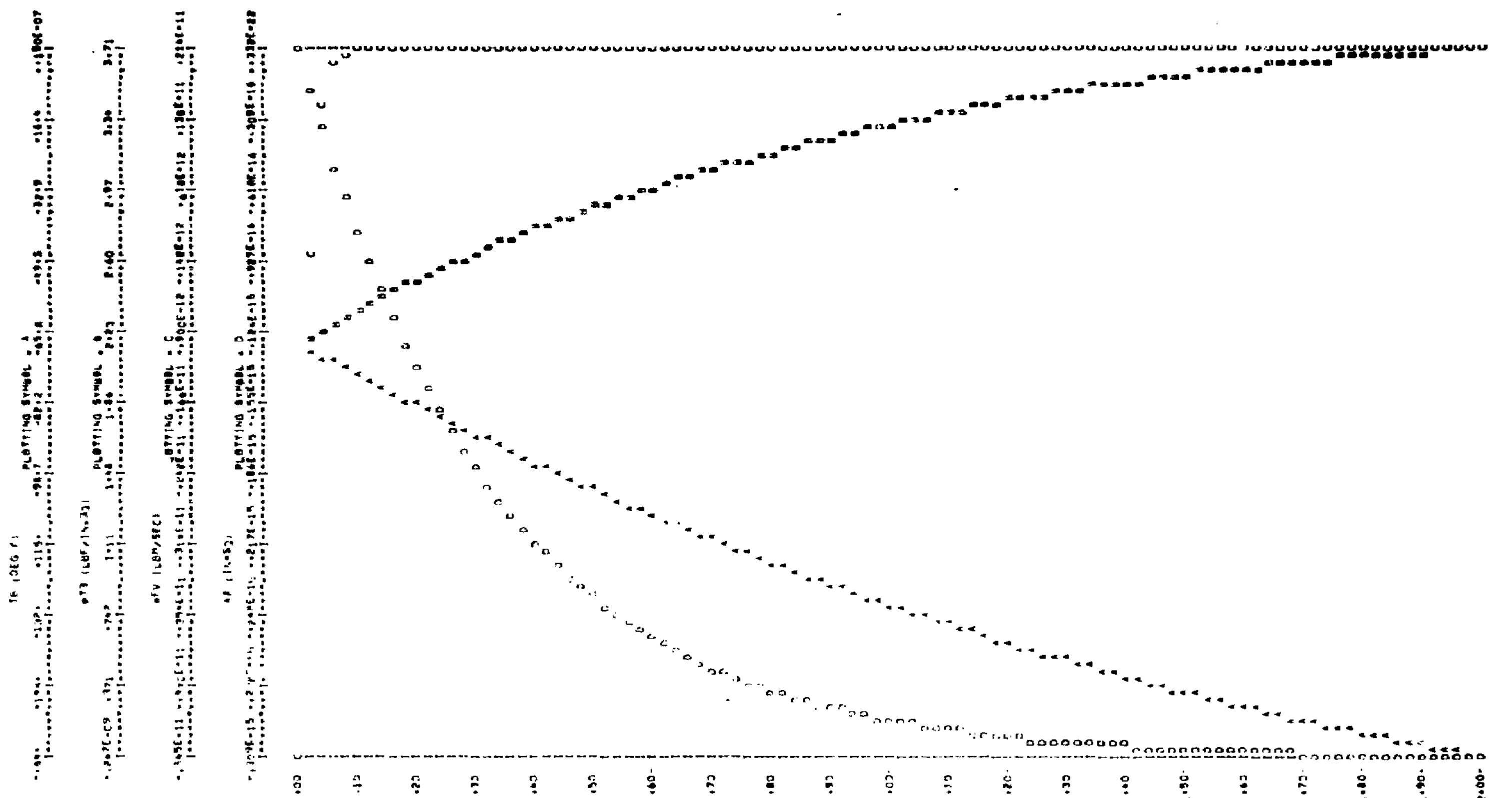

Figure 24c. Open-Loop Disturbance Response at 50 Percent,
$\Delta PT2 = 2.0$ psi

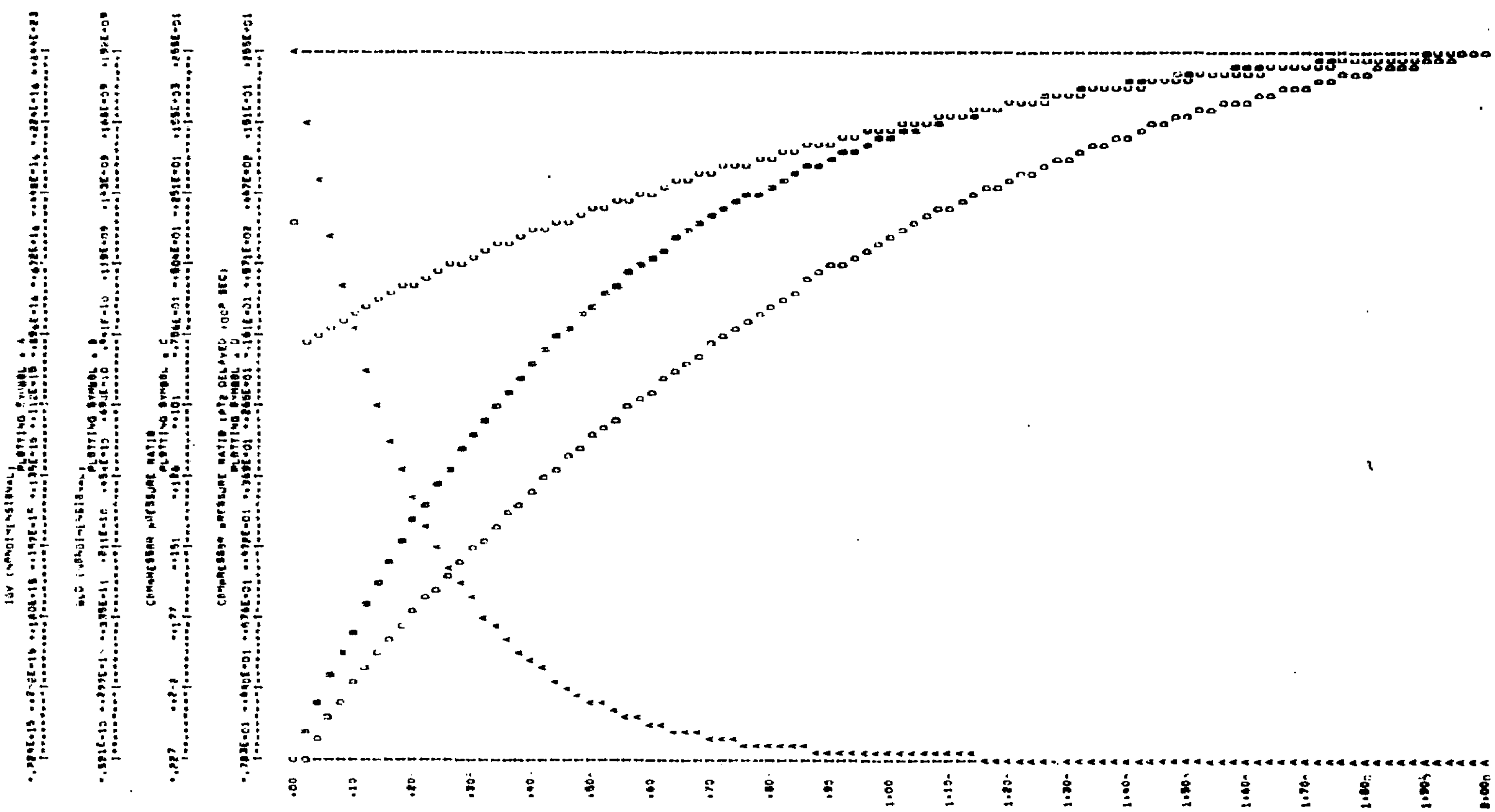

Figure 24d. Open-Loop Disturbance Response at 50 Percent, ΔPT2 = 2.0 psi

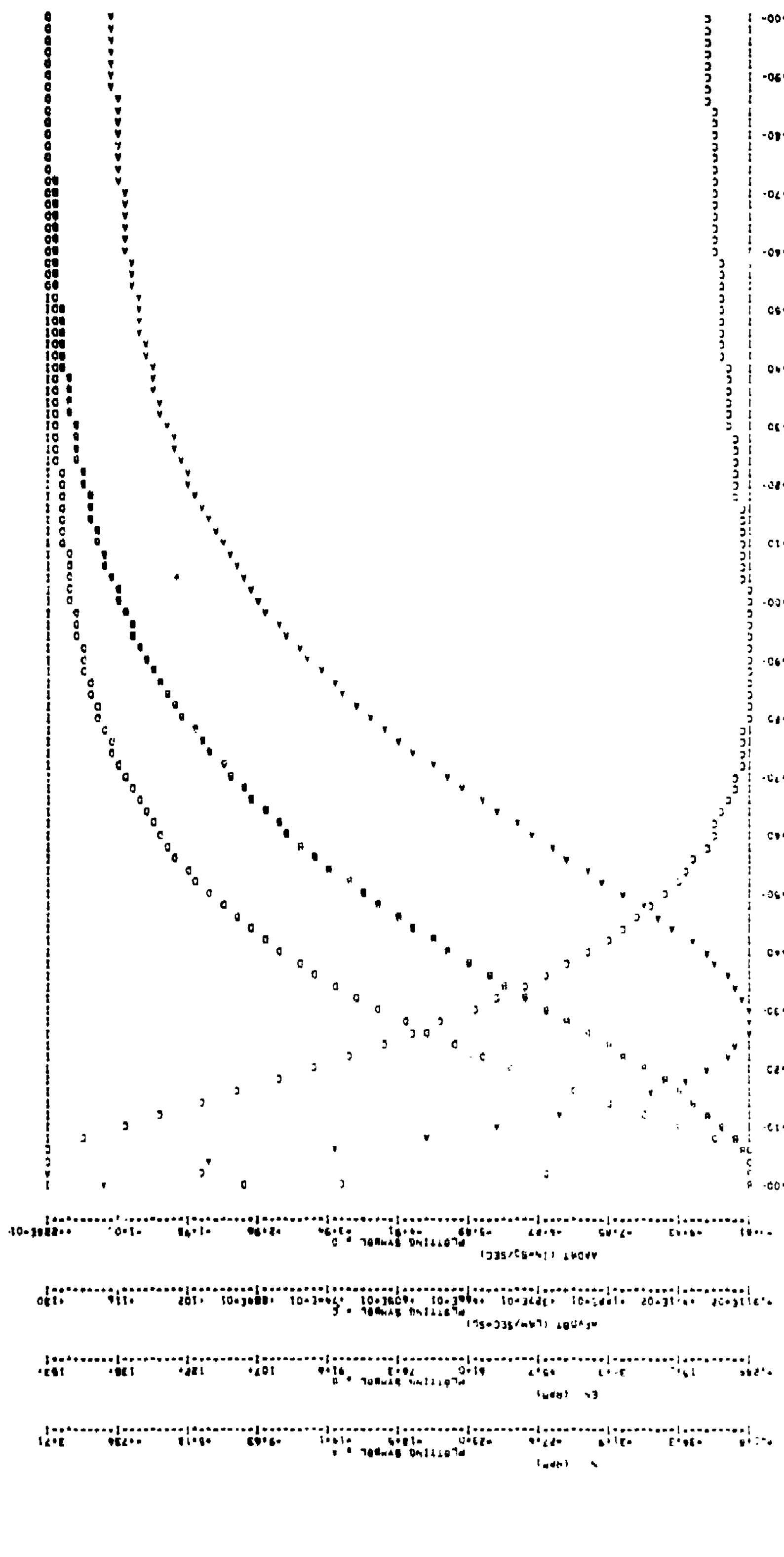

Figure 25a. Disturbance Controller at 50 Percent, $\Delta PT2$ = 2.0 psi

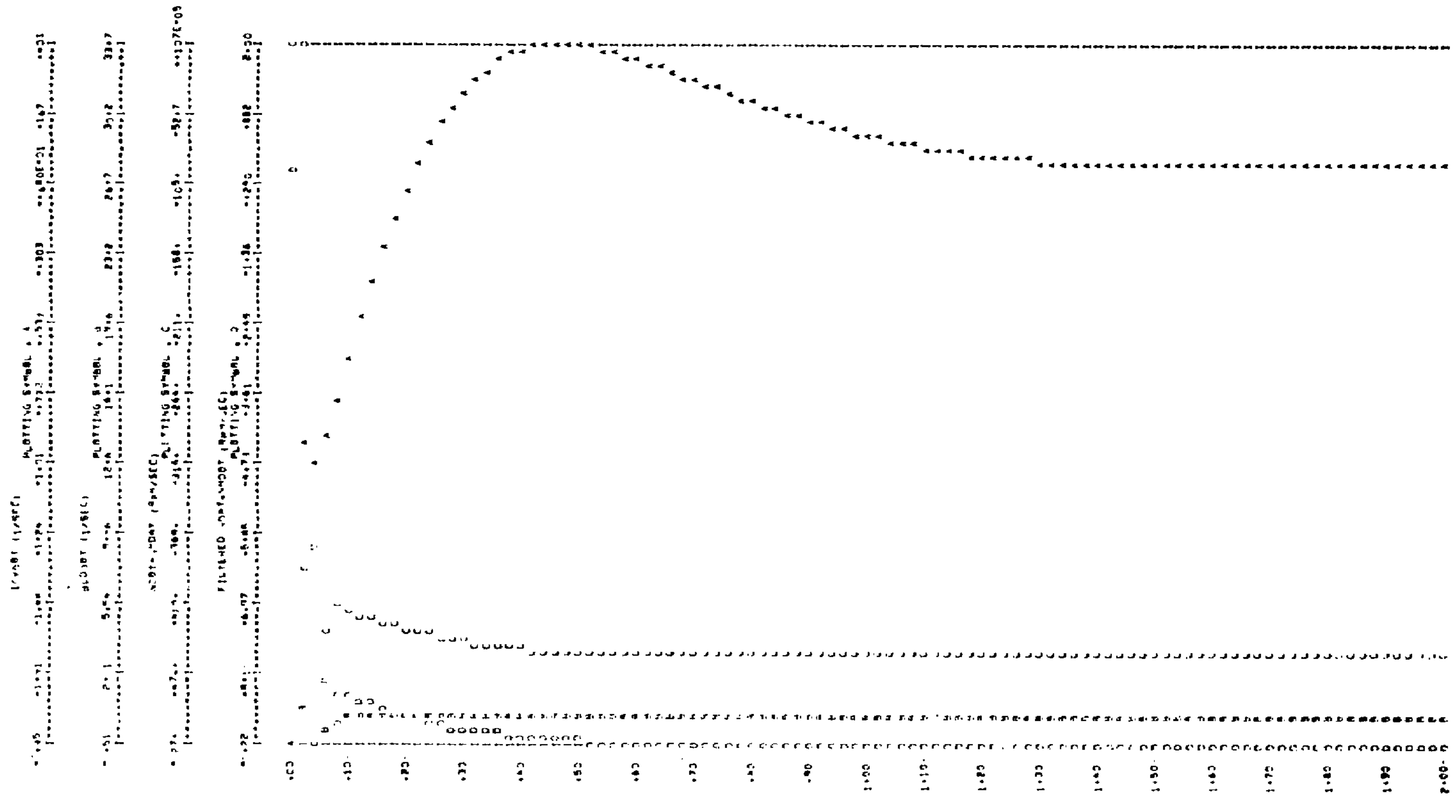

Figure 25b. Disturbance Controller at 50 Percent, $\Delta PT2 = 2.0$ psi

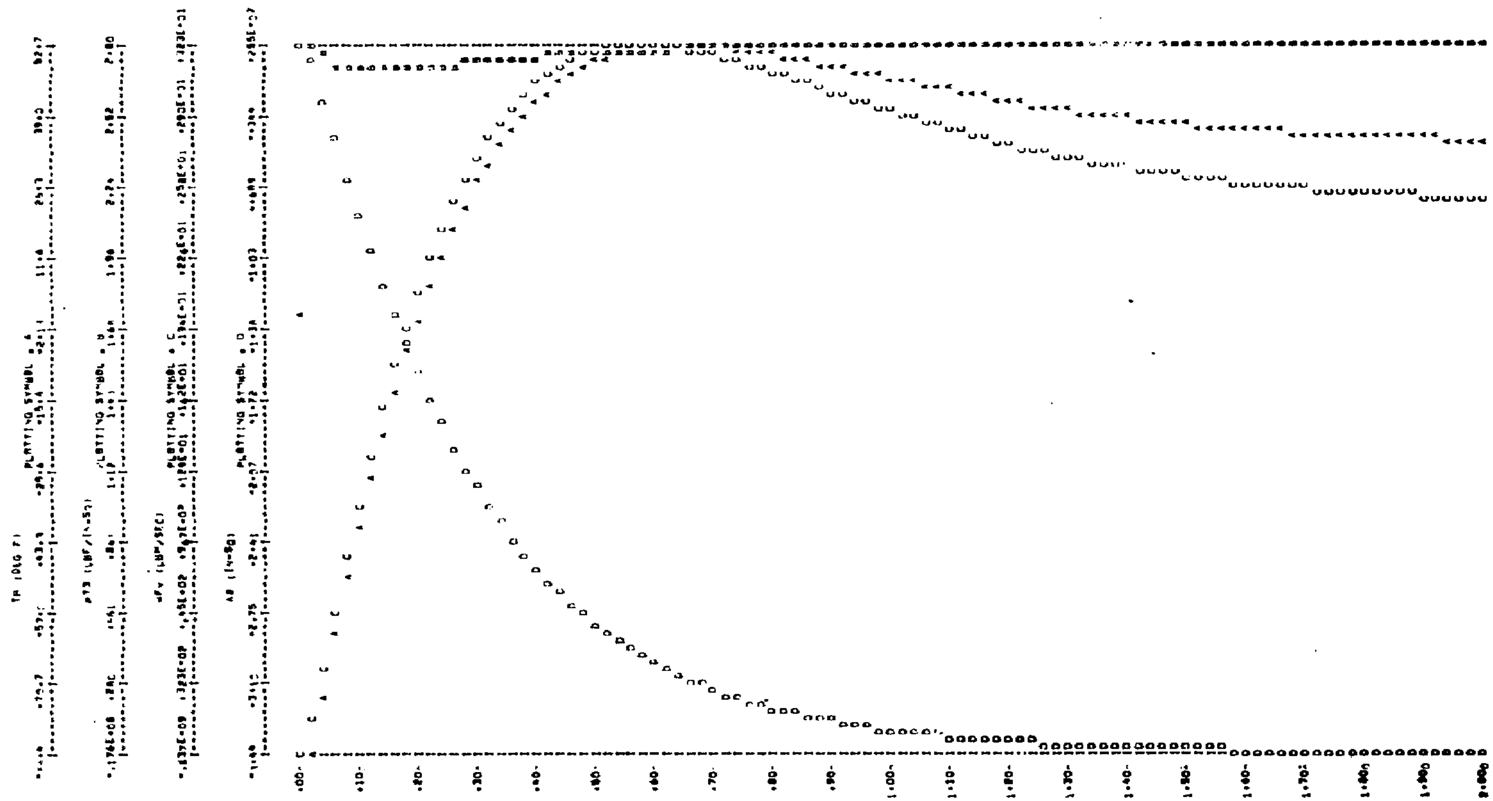

Figure 25c. Disturbance Controller at 50 Percent, ΔPT 2 = 2.0 psi

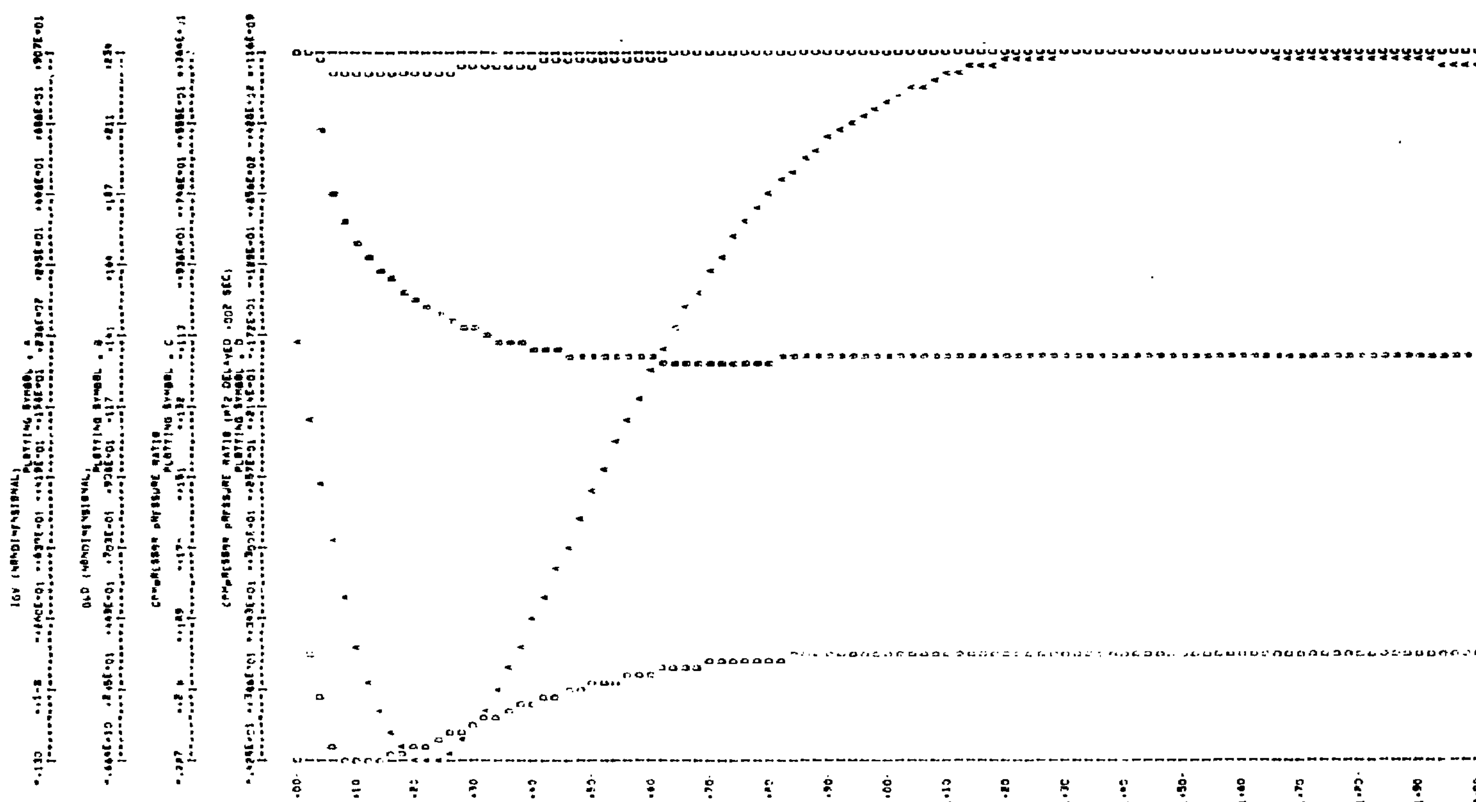

Figure 25d. Disturbance Controller at 50 Percent, $\Delta PT\ 2 = 2.0$ psi

Table 14. Models for Linear Command and Disturbance State Control Synthesis

Parameter	1	2	3	4	5	6	7	8	9	10
States (x')	TWCD	$\dot{W}3$	WDCD	TM	$\dot{W}4$	PT4	HT4	RHT	RT	N
	EN	WFV	A8	IGV	BLD	Z1	Z2	$(N - \dot{N}M)L$	$\tilde{PT}2$	DUM
	P									
Controls (u')	u_{WF}	u_{IGV}	u_{A8}	u_{BLD}						
Noises (η')	$\tilde{PT}2$	P								
Responses (r')	N	EN	$\dot{WFV}$	$\dot{A8}$	$\dot{IGV}$	$\dot{BLD}$	$(\dot{N} - \dot{NM})$	$(\dot{N} - \dot{NM})L$	TT4	PT3
	u_{WF}	u_{A8}	u_{IGV}	u_{BLD}	PR1	PR2				

Note:

TWCD = 0.504 PT3   WDCD ~ $\rho 3$ RHT ~ ρ (TT5)   RT ~ $\rho 5$.

$\tilde{PT}2$ and DUM generate duct buzz, and Z1 and Z2 delay the PT3 change.

Table 15. F Matrix--100-Percent Disturbance Control

1 1	-.11591E 04	1 2	-.16511E 05	1 3	.11378E 07	1 5	-.13743E 04	110	.49303E 02
114	-.32663E 05	115	.10727E 05	116	.38524E 05	117	.38524E 05	119	.38527E 05
2 1	-.17294E 05	2 2	-.94885E 06	210	.25874E 04	214	-.17184E 07	215	.84616E 06
216	.20537E 07	217	.20537E 07	219	.20537E 07	3 2	.96700E 00	3 5	-.10000E 01
314	.14552E-07	315	.14552E-07	4 4	-.62000E 00	4 5	.71966E 00	4 7	.21163E 01
412	-.36231E 02	414	.18477E-04	415	.18477E-04	5 1	.10577E 05	5 3	.10071E 07
5 4	.62326E 00	5 5	-.18746E 04	5 6	-.54700E 04	5 7	.18153E 02	5 9	-.28425E-03
512	-.31087E 03	514	.63679E-03	515	.31840E-03	6 1	.53417E 03	6 3	-.52435E 06
6 4	.14703E 01	6 5	.64416E 03	6 6	-.73237E 03	6 7	-.71239E 02	6 6	.71501E 01
6 9	.33514E 03	610	.16973E 00	612	.47887E 05	614	.12679E-02	615	.98093E-03
7 1	.33100E 04	7 3	-.32492E 07	7 4	.24692E 01	7 5	-.30019E 04	7 6	-.13137E 04
7 7	-.63494E 03	7 8	.12659E 02	7 9	.59336E 03	710	.30050E 00	712	.29333E 06
714	.78568E-02	715	.75046E-02	8 1	.44347E 01	8 2	.50597E 01	8 3	-.43532E 04
8 4	-.43570E 00	8 5	-.60537E 01	8 6	.11083E 03	8 7	.15347E 02	8 8	-.68583E 02
8 9	.11435E 05	810	-.60981E-01	812	.30477E 03	813	-.15924E 03	814	-.31166E-03
815	-.15583E-03	9 2	.21569E-01	9 4	-.62697E-03	9 5	-.12915E-01	9 6	.30440E 00
9 7	-.18266E-01	9 8	-.53413E-01	9 9	-.28375E 02	910	-.70917E-04	912	.65022E 00
913	-.34094E 00	914	-.15218E-06	915	.15218E-06	10 1	-.16677E 04	10 2	-.87360E 03
10 3	.16371E 07	10 4	-.47335E 01	10 5	-.87663E 02	10 6	.22981E 04	10 7	.22195E 03
10 8	-.98885E 03	10 9	.13985E 06	1010	-.53481E 00	1012	.44133E 04	1013	-.20436E 04
1014	-.44997E-02	1015	-.91598E 04	1016	.88288E 03	1017	.88288E 03	1019	.88288E 03
1110	-.53330E 01	1121	.88000E 05	1212	-.62500E 02	1313	-.30000E 01	1414	-.50000E 01
1515	-.20000E 01	1616	.10000E 01	1617	.10000E 01	1716	-.50000E 06	1717	-.10000E 04
1719	.50000E 06	18 1	-.16677E 04	18 2	-.87360E 03	18 3	.16371E 07	18 4	-.47335E 01
18 5	-.87663E 02	18 6	.22981E 04	18 7	.22195E 03	18 8	-.98885E 03	18 9	.13985E 06
1810	.74652E 01	1811	-.30000E 01	1812	.44133E 04	1813	-.20436E 04	1814	-.44997E-02
1815	-.91598E 04	1816	.88288E 03	1817	.88288E 03	1818	-.50000E 02	1819	.88288E 03
1821	-.88000E 05	1920	.10000E 01	2019	-.90000E 03	2020	-.60000E 01	2121	-.40000E 01

Table 16. F Matrix--85-Percent Disturbance Control

1 1	-.12179E 04	1 2	-.44076E 04	1 3	.99604E 06	1 5	-.11449E 04	110	.25498E 02
114	-.82186E 03	115	.14538E 05	116	.84220E 04	117	.84220E 04	119	.84220E 04
2 1	-.17294E 05	2 2	-.26747E 06	210	.12253E 04	214	-.39974E 05	215	.70096E 06
216	.41119E 06	217	.41119E 06	219	.41119E 06	3 2	.96700E 00	3 5	-.10000E 01
4 4	-.62000E 00	4 5	.25017E 00	4 7	.23424E 01	412	-.31009E 02	5 1	.10601E 05
5 3	.10320E 07	5 4	.73782E 00	5 5	-.20022E 04	5 6	-.54704E 04	5 7	.16184E 02
512	-.21424E 03	6 1	.51567E 03	6 3	-.42172E 06	6 4	.14840E 01	6 5	.52487E 03
6 6	-.51721E 03	6 7	-.48540E 02	6 8	.26441E 01	6 9	.28401E 02	610	.19189E 00
612	.48195E 05	7 1	.33208E 04	7 3	-.27158E 07	7 4	.34521E 01	7 5	-.80373E 03
7 6	-.89937E 03	7 7	-.44649E 03	7 8	.48651E 01	7 9	.52257E 02	710	.35307E 00
712	.30800E 06	8 1	.50814E 01	8 2	.42288E 01	8 3	-.41556E 04	8 4	-.40809E 00
8 5	-.27229E 01	8 6	.75226E 02	8 7	.10891E 02	8 8	-.11740E 03	8 9	.48992E 04
810	-.49436E-01	812	.33838E 03	813	-.33150E 02	9 2	.21569E-01	9 4	-.95695E-03
9 5	-.10023E-01	9 6	.38116E 00	9 7	-.20991E-01	9 8	-.32272E 00	9 9	-.28379E 02
910	-.13838E-03	912	.12424E 01	913	-.12767E 00	10 1	-.20235E 04	10 2	-.36216E 03
10 3	.16549E 07	10 4	-.49250E 01	10 5	-.42098E 02	10 6	.19617E 04	10 7	.19291E 03
10 8	-.19291E 04	10 9	.72286E 05	1010	-.25337E 01	1012	.52181E 04	1013	-.80050E 03
1014	.76893E 02	1015	-.83257E 04	1016	.67254E 02	1017	.67254E 02	1019	.67254E 02
1110	-.53330E 01	1121	.88000E 05	1212	-.62500E 02	1313	-.30000E 01	1414	-.50000E 01
1515	-.20000E 01	1617	.10000E 01	1716	-.50000E 06	1717	-.10000E 04	1719	.50000E 06
18 1	-.20235E 04	18 2	-.36216E 03	18 3	.16549E 07	18 4	-.49250E 01	18 5	-.42098E 02
18 6	.19617E 04	18 7	.19291E 03	18 8	-.19291E 04	18 9	.72286E 05	1810	.84603E 01
1811	-.30000E 01	1812	.52181E 04	1813	-.80050E 03	1814	.76893E 02	1815	-.83257E 04
1816	.67254E 02	1817	.67254E 02	1818	-.50000E 02	1819	.67254E 02	1821	-.88000E 05
1920	.10000E 01	2019	-.90000E 03	2020	-.60000E 01	2121	-.40000E 01		

Table 17. F Matrix--70-Percent Disturbance Control

1 1	-.10788E 04	1 2	-.21654E 03	1 3	.77826E 06	1 5	-.10100E 04	110	.58641E 01
114	-.76888E 03	115	.46535E 04	116	.14907E 04	117	.14907E 04	119	.14907E 04
2 1	-.17294E 05	2 2	-.41877E 05	210	.22638E 03	214	-.29894E 05	215	.17424E 06
216	.58849E 05	217	.58849E 05	219	.58849E 05	3 2	.96700E 00	3 5	-.10000E 01
314	-.72670E-08	315	-.72760E-08	4 4	-.62000E 00	4 5	.37100E 00	4 7	.23468E 01
412	-.39630E 02	414	-.92387E-05	415	-.92387E-05	5 1	.10596E 05	5 3	.82584E 06
5 4	.75487E 00	5 5	-.17610E 04	5 6	-.54700E 04	5 7	.10298E 02	512	-.17390E 03
514	-.15920E-03	515	-.15920E-03	6 1	.43580E 03	6 3	-.31440E 06	6 4	.16554E 01
6 5	.46366E 03	6 6	-.57511E 03	6 7	-.32167E 02	6 8	.25058E 02	6 9	.32167E 03
610	.68844E-01	612	.47552E 05	614	-.15775E 02	615	-.15775E 02	7 1	.40909E 04
7 3	-.29514E 07	7 4	.61159E 01	7 5	-.17130E 04	7 6	-.14035E 04	7 7	-.43052E 03
7 8	.67206E 02	7 9	.86274E 03	710	.18464E 00	712	.44335E 06	714	-.42311E 02
715	-.42311E 02	8 1	.47246E 01	8 2	.37226E 01	8 3	-.34086E 04	8 4	-.37864E 00
8 5	-.60369E 01	8 6	.97856E 02	8 7	.82923E 01	8 8	-.14742E 03	8 9	.33855E 04
810	-.45197E-01	812	.64485E 03	813	-.24098E 02	814	.70996E 02	815	.70996E 02
9 2	.21569E-01	9 4	-.10202E-02	9 5	-.22150E-01	9 6	.43251E 00	9 7	-.13981E-01
9 8	-.43096E 00	9 9	-.22855E 02	910	-.49973E-04	912	.23660E 01	913	-.86373E-01
914	.27131E 00	915	.27131E 00	10 1	-.21522E 04	10 2	-.49991E 03	10 3	.15527E 07
10 4	-.63338E 01	10 5	-.11662E 03	10 6	.26851E 04	10 7	.16032E 03	10 8	-.28595E 04
10 9	.60055E 05	1010	-.12618E 01	1012	.12457E 05	1013	-.44180E 03	1014	.16321E 04
1015	-.56074E 04	1016	.28029E 03	1017	.28029E 03	1019	.28029E 03	1110	-.53333E 01
1121	.88000E 05	1212	-.62500E 02	1313	-.30000E 01	1414	-.50000E 01	1515	-.20000E 01
1617	.10000E 01	1716	-.50000E 04	1717	-.10000E 04	1719	.50000E 06	18 1	-.21552E 04
18 2	-.49991E 03	18 3	.15527E 07	18 4	-.63338E 01	18 5	-.11662E 03	18 6	.26851E 04
18 7	.16032E 03	18 8	-.28595E 04	18 9	.60055E 05	1810	.67382E 01	1811	-.30000E 01
1812	.12457E 05	1813	-.44180E 03	1814	.16321E 04	1815	-.56074E 04	1816	.28029E 03
1817	.28029E 03	1818	-.50000E 02	1819	.28029E 03	1821	-.88000E 05	1920	.10000E 01
2019	-.90000E 03	2020	-.60000E 01	2121	-.40000E 01						

Table 18. F Matrix--50-Percent Disturbance Control

1 1	-.83138E 03	1 2	.41376E 03	1 3	.51761E 06	1 5	-.87163E 03	110	.14175E 01
114	-.12036E 03	115	.11961E 04	116	.45085E 03	117	.45085E 03	119	.45085E 03
2 1	-.17294E 05	2 2	-.14943E 05	210	.60266E 02	214	-.51719E 04	215	.57612E 05
216	.22423E 05	217	.22423E 05	219	.22423E 05	3 2	.96700E 00	3 5	-.10000E 01
314	-.36380E-08	315	-.36380E-08	4 4	-.62000E 00	4 5	.10020E 01	4 7	.23071E 01
412	-.79234E 02	414	-.46194E-05	415	-.46194E-05	5 1	.10624E 05	5 3	.50161E 06
5 4	.68712E 00	5 5	-.12966E 04	5 6	-.54700E 04	5 7	.40164E 01	512	-.13794E 03
514	-.11940E-03	515	-.11940E-03	6 1	.33603E 03	6 3	-.20921E 06	6 4	.15611E 01
6 5	.40586E 03	6 6	-.81133E 03	6 7	-.21382E 02	6 8	.70331E 02	6 9	.16614E 04
610	.12372E 00	612	.46658E 05	614	-.19811E-03	615	-.19811E-03	7 1	.53609E 04
7 3	-.33377E 07	7 4	.95751E 01	7 5	-.48443E 04	7 6	-.34633E 04	7 7	-.43072E 03
7 8	.32058E 03	7 9	.75728E 04	710	.56396E 00	712	.74202E 06	713	-.20133E-05
714	-.31606E-02	715	-.25083E-02	8 1	.37930E 01	8 2	.32080E 01	8 3	-.23615E 04
8 4	-.35357E 00	8 5	-.18311E 02	8 6	.16661E 03	8 7	.54319E 01	8 8	-.21571E 03
8 9	-.44062E 03	810	-.35727E-01	812	.14480E 04	813	-.16060E 02	814	.77915E-04
815	.38957E-04	9 2	.21569E-01	9 4	-.89400E-03	9 5	-.55677E-01	9 6	.55288E 00
9 7	-.52256E-02	9 8	-.58649E 00	9 9	-.26096E 02	910	-.82223E-04	912	.44026E 01
913	-.48227E-01	914	.11413E-06	915	.76088E-07	10 1	-.22961E 04	10 2	-.33647E 03
10 3	.14295E 07	10 4	-.84871E 01	10 5	-.48206E 03	10 6	.52487E 04	10 7	.14286E 03
10 8	-.56854E 04	10 9	-.14824E 05	1010	-.13876E 01	1012	.38118E 05	1013	-.41220E 03
1014	.11931E 03	1015	-.65793E 04	1016	.14104E 03	1017	.14104E 03	1019	.14104E 03
1110	-.53330E 01	1121	.88000E 05	1212	-.62500E 02	1313	-.30000E 01	1414	-.50000E 01
1515	-.20000E 01	1617	.10000E 01	1716	-.50000E 06	1717	-.10000E 04	1719	.50000E 06
18 1	-.22961E 04	18 2	-.33647E 03	18 3	.14295E 07	18 4	-.84871E 01	18 5	-.48206E 03
18 6	.52487E 04	18 7	.14286E 03	18 8	-.56854E 04	18 9	-.14824E 05	1810	.66124E 01
1811	-.30000E 01	1812	.38118E 05	1813	-.41220E 03	1814	.11931E 03	1815	-.65793E 04
1816	.14104E 03	1817	.14104E 03	1818	-.50000E 02	1819	.14104E 03	1821	-.88000E 05
1920	.10000E 01	2019	-.90000E 03	2020	-.60000E 01	2121	-.40000E 01		

Table 19. G1 Matrices--(All Conditions) Disturbance Control

12 1	.62500E 02	13 3	.30000E 01	14 2	.50000E 01	15 4	.20000E 01

Table 20. G2 Matrices--(All Conditions) Disturbance Control

20 2	-.43209E 03	21 1	.28284E-01

Table 21. H Matrix--100-Percent Disturbance Control

110	.10000E 01	211	.10000E 01	312	-.62500E 02	413	-.30000E 01	514	-.50000E 01
615	-.20000E 01	7 1	-.16677E 04	7 2	-.87360E 03	7 3	.16371E 07	7 4	-.47335E 01
7 5	-.87663E 02	7 6	.22981E 04	7 7	.22195E 03	7 8	-.98885E 03	7 9	.13985E 06
710	.74652E 01	711	-.30000E 01	712	.44133E 04	713	-.20436E 04	714	-.44997E-02
715	-.91598E 04	716	.88288E 03	717	.88288E 03	719	.88288E 03	721	-.8[illegible]000E 05
818	.10000E 01	9 4	.10488E 00	9 5	.10390E 01	9 7	.30554E 01	912	-.[illegible]2308E 02
914	.26676E-04	915	.26676E-04	10 1	.19810E 01	15 1	.13476E 00	1519	-.47279E 00
16 1	.13476E 00	1616	-.47279E 00	1617	-.47279E 00	1619	-.47279E 00		

Table 22. H Matrix--85-Percent Disturbance Control

110	.10000E 01	211	.10000E 01	312	-.62500E 02	413	-.30000E 01	514	-.50000E 01
615	-.20000E 01	7 1	-.20235E 04	7 2	-.36216E 03	7 3	.16[illegible]49E 07	7 4	-.49250E 01
7 5	-.42098E 02	7 6	.19617E 04	7 7	.19291E 03	7 8	-.19291E 04	7 9	.72286E 05
710	.54663E 01	711	-.30000E 01	712	.52181E 04	713	-.50050E 03	714	.76893E 02
715	-.83257E 04	716	.67254E 02	717	.67254E 02	719	.67254E 02	721	-.88000E 05
818	.10000E 01	9 4	.14694E 00	9 5	.34421E 00	9 7	.32291E 01	912	-.42665E 02
10 1	.19810E 01	15 1	.13476E 00	1519	-.27061E 00	16 1	.13476E 00	1616	-.27061E 00

Table 23. H Matrix--70-Percent Disturbance Control

1 10	.10000E 01	2 11	.10000E 01	3 12	-.62500E 02	4 13	-.30000E 01	5 14	-.50000E 01
6 15	-.20000E 02	7 1	-.21552E 04	7 2	-.49991E 03	7 3	.15527E 07	7 4	-.63338E 01
7 5	-.11662E 03	7 6	.26851E 04	7 7	.16032E 03	7 8	-.28595E 04	7 9	.60055E 05
7 10	.67382E 01	7 11	-.30000E 01	7 12	.12457E 05	7 13	-.44180E 03	7 14	.14321E 04
7 15	-.56074E 04	7 16	.28029E 03	7 17	.28029E 03	7 19	.23029E 03	7 21	-.88000E 05
8 18	.10000E 01	9 4	.21717E 00	9 5	.46844E 00	9 7	.29631E 01	9 12	-.90038E 02
9 14	-.11665E-04	9 15	-.11665E-04	10 1	.19810E 01	15 1	.13476E 00	15 19	-.18218E 00
16 1	.13476E 00	16 16	-.18218E 00						

Table 24. H Matrix--50-Percent Disturbance Control

1 10	.10000E 01	2 11	.10000E 01	3 12	-.62500E 02	4 13	-.30000E 01	5 14	-.50000E 01
6 15	-.20000E 01	7 1	-.22961E 04	7 2	-.33647E 03	7 3	.14295E 07	7 4	-.84871E 01
7 5	-.48206E 03	7 6	.52487E 04	7 7	.14286E 03	7 8	-.56854E 04	7 9	-.14824E 05
7 10	.66124E 01	7 11	-.30000E 01	7 12	.3811[illegible]E 05	7 13	-.4122[illegible]E 03	7 14	.11931E 03
7 15	-.65793E 04	7 16	.14104E 03	7 17	.14104E 03	7 19	.14104E 03	7 21	-.88000E 05
8 18	.10000E 01	9 4	.38902E 00	9 5	.90742E [illegible]	9 7	.22735E 01	9 12	-.78081E 02
9 14	-.45582E-05	9 15	-.45522E-05	10 1	.19810E 01	15 1	.13476E 00	15 19	-.11354E 00
16 1	.1[illegible]476E 00	16 16	-.11[illegible]34E 00						

Table 25. D Matrices--(All Conditions) Disturbance Control

3 1	.62500E 02	4 3	.30000E 01	5 2	.50000E 01	6 4	.20000E 01	11 1	.10000E 01
12 3	.10000E 01	13 2	.10000E 01	14 4	.10000E 01				

Table 26. Nominal Actuator Time Constants

Actuator	Time Constant (sec)
Fuel valve	1/62.5
Exhaust actuator	1/3
Bleed	1/2
IGV	1/5

Table 27. Maximum Slew Rates

Actuator	Maximum at 50% Spool Speed	Maximum at 100% Spool Speed
Exhaust area	27 in^2/sec	54 in^2/sec
Bleed*	0.77/sec	1.67/sec
IGV*	0.315/sec	0.63/sec

*Bleeds and IGV are operated from the same hydraulic supply. Individual slew rates are reduced by simultaneous demands.

Table 28. Command Response Synthesis (Rate Model-Following With Integral Control and a Noisy Pilot)

Step	Description
1	Use ideal command response model: $\dot{x}_m = a x_m + b \dot{e} + ce$ (1) $\dot{e} = d x_m + fP$ (2) Choose f and τ. Then calculate a, b, c, d (cf Appendix C), so that $\frac{x_m}{P} \cong \frac{f}{s + (1/\tau)}$ (3)
2	Construct a response component: $r_k = \dot{x}_n - \dot{x}_m$ (4) where $\dot{x}_n = \sum_j F_{nj} x_j + \sum (G1)_{nj} u_j$ (5) $r_k \cong \sum_j [F_{nj} x_j + (G1)_{nj} u_j] - ax_n - b(dx_n + fP) - ce$ (6)
3	Consider PLA = P to be driven by a noisy pilot: $\dot{P} = -4P + 0.2824\, \eta_p$ (7)

Table 29. Design Objectives

Objective	Description
1	Complete state feedback permitted
2	PLA response first-order with a 0.25-sec time constant
3	Integral control on PLA commands
4	Intensitivity to inlet buzz of amplitude 0.4*PT20
5	Insensitivity to step PT2 disturbances of 2 lb/in^2
6	Closed-loop actuator time constants near open-loop values
7	Maintenance of actuator rate and displacement limits

Table 30. Q Matrices Disturbance Control (Off-Diagonal Elements are Zero)

Response	Units	Response Component	Quadratic Weight			
			100%	85%	70%	50%
N	rpm	1				
EN	rpm/sec	2	.30000-4	.30000-4	.30000-4	.30000-4
$W\dot{F}V$	(lbm/sec)/sec	3	.30000+3	.10000+5	.10000+5	.10000+5
$\dot{A}8$	(in-sq)/sec	4	.10000-4	.10000-8	.10000-8	.10000-8
$I\dot{G}V$	1/sec	5	.10000-5	.10000-4	.10000-4	.10000-4
$B\dot{L}D$	1/sec	6	.10000-4	.10000-4	.10000-4	.10000-4
$(\dot{N} - \dot{N}M)$	rpm/sec	7				
$(\dot{N} - \dot{N}M)L$	rpm/sec	8	.10000+0	.50000+0	.10000+1	.30000+1
TT4	deg F	9				
PT3	lbf/(in-sq)	10				
UWF		11	.10000+1	.10000+1	.10000+1	.10000+1
UA8		12	.10000+1	.10000+1	.10000+1	.10000+1
UIGV		13	.10000+4	.10000+3	.10000+3	.10000+3
UBLD		14	.10000+2	.10000+2	.10000+2	.10000+2
PR1	Nondimensional	15				
PR2	Nondimensional	16	.55065+6	.55065+6	.55065+6	.55065+6

Table 31. K Matrices

100 PERCENT

```
ROW   1
-.96360E-04 -.22393E-05 -.40730E 01 -.71523E-04 -.79513E-05 -.47929E-02  .55505E-03  .16379E-02 -.1 371E 00 -.22197E-03
 .31304E-05 -.40384E 00  .39593E-02  .12738E 00 -.16265E-01  .10688E-01  .19651E-04 -.32694E-04  .12063E 00  .12367E-02
 .84520E-01
ROW   2
 .14739E-02  .87007E-05  .36004E 02  .66820E-03 -.33166E-02  .37965E-01 -.42339E-02 -.85481E-02  .14798E 01  .20826E-02
 .71500E-05  .11942E 02 -.25767E-01 -.12707E 01  .33782E 00 -.57632E-01 -.99571E-04 -.20039E-03 -.11987E 01 -.13743E-01
 .26552E 00
ROW   3
-.98452E-01  .19593E-02  .31450E 03  .71051E-02  .77915E-03  .19977E 00 -.20347E-01 -.86540E 00  .68159E 02  .34445E-01
-.30112E-02  .22269E 03 -.20970E 01 -.15459E 02 -.54476E 01  .59460E 00  .61396E-03  .42860E-01 -.76879E 01 -.21374E 00
-.10787E 03
ROW   4
-.89740E-01  .11041E-02 -.44790E 03 -.42649E-02  .57614E-01 -.55990E 00  .62262E-01 -.38792E 00 -.10557E 02 -.10056E-01
-.44331E-02 -.60994E 02 -.36320E 00  .13513E 02 -.19153E 02  .12606E 01  .19838E-02  .19977E-01  .16796E 02  .11824E 00
-.12022E 03
```

85 PERCENT

```
ROW   1
 .86501E-04 -.24046E-05 -.30068E 00 -.24621E-04 -.19380E-05 -.35892E-03  .39095E-04  .99605E-03 -.43886E-02 -.58872E-04
 .26159E-05  .59346E 00  .11926E-03 -.12291E-02 -.81925E-03 -.54513E-05  .25607E-06 -.94074E-05  .34495E-02  .12330E-03
 .70502E-01
ROW   2
-.70583E-02  .22742E-03  .33966E 02  .23890E-02 -.1 382E-02  .41847E-01 -.44529E-02 -.94856E-01  .33021E 00  .63722E-02
-.36473E-03  .38410E 02 -.11461E-01 -.13576E 00  .37600E 00 -.77543E-02 -.24362E-04  .29429E-03 -.45207E 00 -.14133E-01
-.94309E 01
ROW   3
-.13573E 00  .31243E-02  .28297E 03  .92109E-02  .27917E-02  .22094E 00 -.24282E-01 -.13015E 01  .17228E 02  .39224E-01
-.66173E-02  .22361E 03 -.29605E 00 -.68763E 00 -.97999E 00  .28080E 00  .23865E-03  .46451E-01 -.29439E 01 -.86519E-01
-.14471E 03
ROW   4
-.32063E 00  .18873E-02 -.94920E 03  .57551E-03  .14349E 00 -.20382E 01  .21417E 00 -.10819E 01 -.16077E 02 -.17893E-01
-.93299E-02 -.10241E 03 -.65332E-01  .15040E 01 -.58453E 02  .16941E 01  .27672E-02  .41844E-01  .23642E 02  .34618E-01
-.24541E 03
```

Table 31. K Matrices (Concluded)

70 PERCENT

```
ROW   1
 .13138E-03 -.55439E-05 -.24976E 00 -.17025E-04 -.73857E-05 -.24151E-03  .18453E-04  .12009E-02 -.62525E-02 -.47429E-04
 .39654E-05  .70517E 00  .12728E-02  .26306E-02 -.79298E-03  .19909E-04  .16811E-06 -.19958E-04  .1655+E-02  .57394E-04
 .10953E 00
ROW   2
-.23036E-01  .17301E-02  .76947E 02  .54143E-02 -.49763E-02  .95570E-01 -.70253E-02 -.23896E 00  .15210E 00  .16087E-01
-.12229E-02  .82208E 02 -.19742E-01 -.11000E 01  .17826E 01 -.51907E-01 -.87850E-04 -.18612E-02 -.84585E 00 -.22846E-01
-.31789E 02
ROW   3
-.22070E 00  .69730E-02  .31506E 03  .84435E-02  .87495E-02  .18695E 00 -.13840E-01 -.19487E 01  .18689E 02  .39965E-01
-.79069E-02  .23865E 03 -.27468E 00 -.11845E 01 -.17447E 01  .21204E 00  .17985E-03  .67535E-01 -.13072E 01 -.44262E-01
-.22280E 03
ROW   4
-.32762E 00 -.15689E-01 -.72386E 03 -.37864E-02  .15407E 00 -.18071E 01  .12317E 00 -.18419E 01 -.12429E 02 -.62213E-02
-.11668E-01 -.99122E 02 -.11632E 00  .71304E 01 -.67077E 02  .17264E 01  .24832E-02  .59522E-01  .16949E 02  .42996E-01
-.32257E 03
```

50 PERCENT

```
ROW   1
 .23501E-03 -.81922E-05 -.26195E 00 -.10613E-04 -.12622E-04 -.14712E-03  .58276E-05  .20055E-02  .16779E-02 -.30507E-04
 .38134E-05  .75705E 00  .14026E-03  .93305E-03  .24895E-02 -.34783E-04  .22357E-07 -.51243E-04  .56969E-03  .30619E-04
 .10845E 00
ROW   2
-.19959E-01  .11509E-02  .27948E 02  .19435E-02 -.11787E-02  .21291E-01 -.10486E-02 -.14571E 00  .14128E 00  .59266E-02
-.58495E-03  .29158E 02 -.94792E-02 -.22820E 00  .42188E 00 -.59497E-02 -.13625E-04  .14117E-04 -.19457E 00 -.60195E-02
-.15031E 02
ROW   3
-.38329E 00  .11376E-01  .40067E 03  .50227E-02  .16094E-01  .18255E 00 -.43031E-02 -.34130E 01 -.39049E 01  .28055E-01
-.72494E-02  .26299E 03 -.25154E 00 -.56875E 00 -.54554E 01  .19973E 00  .17838E-03  .11508E 00 -.45475E 00 -.25393E-01
-.20727E 03
ROW   4
-.57665E 00 -.11732E-01  .20017E 03  .30686E-02  .10211E 00 -.56275E 00  .28245E-01 -.60380E 01 -.20805E 02  .36937E-01
-.18577E-01  .31119E 03 -.36369E 00  .16875E 01 -.51780E 02  .76044E 00  .10536E-02  .18317E 00  .84321E 01  .33137E-01
-.52663E 03
```

Table 32. Open-Loop Roots Disturbance Control

Root Association	100%		85%		70%		50%	
	Frequency	Damping	Frequency	Damping	Frequency	Damping	Frequency	Damping
TWCD	+4397.	.2316**	+4046.	.2710	+3835.	.2692	+3660.	.2730
$\dot{W}3$	-949149.		-267754.		-41973.		-14486.	
WDCD								
TM	-.6548		-.6610		+.7887	.9181	+.6847	.8642
$\dot{W}4$	+872.8	.9997	-872.1		-850.9		-973.4	
PT4			-567.5		+430.0	.9882	+463.8	.9512
HT4	-325.1		-276.2					
RHT	-49.75		-88.19		-120.8		-190.6	
RT	-36.89		-45.30		-34.61		-25.03	
N	-3.255		-2.073					
EN*	-1000.		-1000.		-1000.		-1000.	
WFV	-62.5		-62.5		-62.5		-62.5	
A8	-3.000		-3.000		-3.000		-3.000	
IGV	-5.000		-5.000		-5.000		-5.000	
BLD	-2.000		-2.000		-2.000		-2.000	
Z1	+706.4	.7071	+707.1	.7071	+707.1	.7071	+707.1	.7071
Z2								
$(\dot{N} - \dot{N}M)L$	-50.00		-50.00		-50.00		-50.00	
$\tilde{P}T2$	+30.00	.1000	+30.00	.1000	+30.00	.1000	+30.00	.1000
DUM								
Pilot	-4.000		-4.000		-4.000		-4.000	

*F11, 11 set to -.1E+04 for open-loop root and covariance determination.

**Arrow indicates two states coupled into complex pair.

Table 33. Closed-Loop Roots Disturbance Control

Root Association	100%		85%		70%		50%	
	Frequency	Damping	Frequency	Damping	Frequency	Damping	Frequency	Damping
TWCD	+4397.	.232	+4047.	.2711	+3835.	.2693	+3660.	.2731
$\dot{W}3$	-949149.		-267754.		-41973.		-14486.	
WDCD								
TM	-.6910		-.7342		-.8100		-1.044	
$\dot{W}4$	+868.8	.9995	-564.5		+407.8	.9957	-972.5	
PT4			-872.2		-849.7		+459.3	.9515
HT4	-340.9		-231.7					
RHT	-59.48		-77.76		+142.4	.9940	-193.7	
RT	+30.67	.9183	-42.03		-33.07		-25.60	
N	+3.748	.9576	+3.339	.9186	+3.275	.9528	+3.479	.9703
EN								
WFV	+89.00	.4183	-82.24		-67.60		+93.94	.8718
A8	-2.953		-2.986		-2.995		-3.007	
IGV	-4.904		-4.986		-4.723		-4.620	
BLD			-153.1					
Z1	+706.4	.7071	+707.1	.7071	+707.1	.7071	+707.1	.7071
Z2								
$(\dot{N} - \dot{N}M)L$			-16.86		-14.81		-7.775	
$\tilde{PT}2$	+30.00	.1000	+30.00	.1000	+30.00	.1000	+30.00	.1000
DUM								
Pilot	-4.000		-4.000		-4.000		-4.000	

Table 34. Open-Loop RMS Responses Due to Inlet Buzz (PT2 = 4.16 Lb/In^2 RMS)

Response	Response Component	100%	85%	70%	50%
TWCD	x1	.9835+1	.5707+1	.3828+1	.2291+1
$\dot{W}3$	x2	.9843+1	.6470+1	.4699+1	.3743+1
WDCD	x3	.7337-2	.5144-2	.3774-2	.3055-2
TM	x4	.1068+2	.3111+1	.1057+2	.2362+2
$\dot{W}4$	x5	.9504+1	.6244+1	.4536+1	.3214+1
PT4	x6	.1701+2	.9699+1	.6099+1	.3832+1
HT4	x7	.6530+2	.1940+1	.2865+2	.6509+2
RHT	x8	.3262+2	.6712+1	.3338+1	.9956+0
RT	x9	.1333+0	.6142-1	.4981-1	.4722-1
WFV	x12	.0000	.0000	.0000	.0000
A8	x13	.0000	.0000	.0000	.0000
IGV	x14	.0000	.0000	.0000	.0000
BLD	x15	.0000	.0000	.0000	.0000
Z1	x16	.4166+1	.4158+1	.4158+1	.4158+1
Z2	x17	.1247+3	.1244+3	.1244+3	.1244+3
$P\dot{T}2$	x19	.4157+1	.4158+1	.4158+1	.4158+1
DUM	x20	.1247+3	.1247+3	.1247+3	.1247+3
P	x21	.0000	.0000	.0000	.0000
N	r1	.5175+3	.1235+3	.1186+3	.1197+3
EN	r2	.2759+1	.6583+0	.6324+0	.6384+0
$W\dot{F}V$	r3	.0000	.0000	.0000	.0000
$\dot{A}8$	r4	.0000	.0000	.0000	.0000
$I\dot{G}V$	r5	.0000	.0000	.0000	.0000
$B\dot{L}D$	r6	.0000	.0000	.0000	.0000
$(\dot{N} - \dot{N}M)$	r7	.1422+5	.3547+4	.2635+4	.1887+4
$(\dot{N} - \dot{N}M)L$	r8	.2444+3	.6026+2	.4539+2	.3350+2
TT4	r9	.1897+3	.6055+2	.8304+2	.1456+3
PT3	r10	.1958+2	.1131+2	.7187+1	.4539+1
UWF	r11	.0000	.0000	.0000	.0000
UA8	r12	.0000	.0000	.0000	.0000
UIGV	r13	.0000	.0000	.0000	.0000
UBLD	r14	.0000	.0000	.0000	.0000
PR1	r15	.7523+0	.4027+0	.2974+0	.1759+0
PR2	r16	.7119+0	.3804+0	.2847+0	.1695+0

Table 35. Closed-Loop RMS Responses Due to Inlet Buzz and Throttle Commands (PT2 = 4.16 Lb/In^2 RMS; P = 0.01 RMS)

Response	Response Component	100%		85%		70%		50%	
		ETA 1	ETA 2	ETA 1	ETA 2	ETA 1	ETA 2	ETA 1	ETA 2
TWCD	x1	.2113-2	.1415+2	.3065-1	.7854+1	.4234-1	.5278+1	.6788-1	.2949+1
$\dot{W}3$	x2	.2839+0	.1133+2	.3037+0	.8600+0	.3556+0	.6643+1	.3276+0	.4701+1
WDCD	x3	.4502-4	.9812-2	.2799-4	.6934-2	.7146-4	.5276-2	.1065-3	.3890-2
TM	x4	.1455+2	.1870+2	.1998+2	.1716+2	.3089+2	.1525+2	.5445+2	.1087+2
$\dot{W}4$	x5	.2746+0	.1094+2	.2937+0	.8295+1	.3439+0	.6409+1	.3167+0	.4535+1
PT4	x6	.1393+0	.2547+2	.1374+0	.1348+2	.1318+0	.8920+1	.1153+0	.4968+1
HT4	x7	.1187+2	.2808+2	.1142+2	.3043+2	.1795+2	.4036+2	.3536+2	.7550+2
RHT	x8	.1264+1	.6057+2	.4728+0	.1075+2	.5608+0	.5801+1	.1101+1	.1951+1
RT	x9	.9346-2	.1220+0	.1461-1	.6043-1	.2083-1	.6995-1	.2766-1	.5607-1
WFV	x12	.2399-1	.2118+0	.1639-1	.4136-1	.1597-1	.2349-1	.1825-1	.1532-1
A8	x13	.1589+0	.1179+1	.5988+0	.4520+1	.5551+0	.2464+1	.3196+0	.1215+1
IGV	x14	.9624-2	.2220+0	.5169-1	.2750+0	.2183+0	.4409+0	.1660+0	.1797+0
BLD	x15	.6589-1	.1480+1	.9797-1	.8900+0	.6468-1	.6052+0	.8394-1	.4719+0
Z1	x16	.0000	.4166+1	.0000	.4158+1	.0000	.4158+1	.0000	.4158+1
Z2	x17	.0000	.1247+3	.0000	.1244+3	.0000	.1244+3	.0000	.1244+3
$P\tilde{T}2$	x19	.0000	.4157+1	.0000	.4158+1	.0000	.4158+1	.0000	.4158+1
DUM	x20	.0000	.1247+3	.0000	.1247+3	.0000	.1247+3	.0000	.1247+3
P	x21	.9997-2	.0000	.1000-1	.0000	.1000-1	.0000	.1000-1	.0000
N	r1	.1238+3	.5359+3	.1174+3	.2531+3	.1203+3	.1214+3	.1242+3	.4267+2
EN	r2	.1455+3	.1218+3	.1737+3	.3137+3	.1616+3	.1324+3	.1374+3	.3735+2
$W\dot{F}V$	r3	.9559-1	.6402+1	.5859-1	.5872+0	.6348-1	.3237+0	.6876-1	.2716+0
$\dot{A}8$	r4	.1467+1	.3910+2	.3636+1	.4013+2	.4043+1	.2604+2	.3166+1	.1860+2
$\dot{I}GV$	r5	.5499-1	.6859+1	.3514+0	.5456+1	.1340+1	.1044+2	.8796+0	.4739+1
$B\dot{L}D$	r6	.8964+0	.4590+2	.9405+0	.2687+2	.1650+1	.2155+2	.2179+1	.1462+2
$(\dot{N} - \dot{N}M)$	r7	.2882+3	.1655+5	.4009+3	.5509+4	.3524+3	.2789+4	.2030+3	.1001+4
$(\dot{N} - \dot{N}M)L$	r8	.4476+1	.2760+3	.7186+1	.9653+2	.6090+1	.4853+2	.2875+1	.1863+2
TT4	r9	.3564+2	.8428+2	.3756+2	.9597+2	.5565+2	.1171+3	.8971+2	.1677+3
PT3	r10	.4186-2	.2803+2	.6072-1	.1556+2	.8387-1	.1046+2	.1344+0	.5842+1
UWF	r11	.2404-1	.2353+0	.1642-1	.4241-1	.1600-1	.2405-1	.1828-1	.1593-1
UA8	r12	.5143+0	.1309+2	.1352+1	.1412+2	.1457+1	.9021+1	.1103+1	.6317+1
UIGV	r13	.1462-1	.1390+1	.8724-1	.1125+1	.3456+0	.2134+1	.2419+0	.9647+0
UBLD	r14	.4563+0	.2300+2	.4804+0	.1346+2	.5883+0	.9317+1	.1003+1	.7328+1
PR1	r15	.2848-3	.1528+0	.4130-2	.1088+0	.5705-2	.6762-1	.9145-2	.8100-1
PR2	r16	.2848+1	.6842-1	.4130-2	.7630-1	.5705-2	.4951-1	.9145-2	.7516-1

Table 36. Buzz Response Summary

Response	100%	85%	70%	50%
PT3/PT2 margin	0.800	1.08	0.475	0.150
PT3/PT2 rms margin	0.566	0.764	0.336	0.106
PT2 rms (lbf/in^2)	4.16	4.16	4.16	4.16
PT3/PT2 = PR2 rms open loop	0.7119	0.3804	0.2847	0.1635
PT3/PT2 = PR2 rms closed loop	0.06842	0.07630	0.04951	0.07516

Table 37. PT2 Step Response Summary

Response	100%	85%	70%	50%
PT2 psi	2.0	2.0	2.0	2.0
PT3/PT2 margin	0.7993	1.0782	0.4748	0.1497
PT3/PT2 = PR2 max open loop	0.602	0.181	0.132	0.0783
PT3/PT2 = PR2 max closed loop	0.0495	0.0718	0.0419	0.0428

SECTION IV
WIND TUNNEL TEST CONTROLLER

The design and wind tunnel testing of a controller are described. The controller was synthesized to be a good approximation to spool-speed time-optimal control with constraints for surge-stall (PT3/PT2 maximums), burner temperature (TT4 maximum), and flameout. Control design was effected by synthesizing three controllers whose spool speed, PT3, or TT4 perturbation response characteristics were those of a first-order lag with a small time constant. A select logic chooses the perturbation controller whose trajectory is closest to that for time-optimal control. Table 38 presents specific design objectives.

The wind tunnel test results show that design objectives are achieved. The controller achieves precise trim stability, good perturbation response, and a reasonable approximation to time-optimal control with bounded-phase constraints. Simulation results are much better than wind tunnel test results. These differences are ascribed to the differences between the model and the engine used in the wind tunnel test.

Perturbation synthesis methodology is used to design the controller. Setpoint and trajectory optimization are used to establish steady-state and gross response characteristics for large-amplitude commands. Perturbation design approximates gross characteristics and provides the perturbation response characteristics.

Setpoint and trajectory optimization are described in Section II. Only the perturbation design is considered here.

CONTROL SYNTHESIS

Design of the controllers consists primarily of determining the perturbation gains that will enforce good transient response, good rms response, and will have satisfactory stability margins through the operating envelope. Once this task has been accomplished, that is, the perturbation controller gains have been determined and it has been ascertained that the responses and stability characteristics are satisfactory, the main job is done. It is then simply a matter of determining the open-loop fuel flows, of making reasonable estimates as to the integration limits on the mode-switching controller, and of using these data in the mode-switching controller to affect the nonlinear control design.

The perturbation controller design is first affected by designing a full-state-feedback controller using a simplified model of the engine (that is, one without instrumentation dynamics, with simplified characteristics for the fuel actuator, in particular, and neglecting the computational delays in the digital computer). A controller is designed under these simplified conditions because experience has shown that if this task can be satisfactorily accomplished, then compensation for the additional complexity is reasonably straightforward and does not cause an excessive loss in performance. The results to be presented show that the procedure applies at least to the J85 engine.

First, speed control synthesis and, subsequently, pressure and temperature control synthesis are presented.

Speed Control

Table 39 presents the forms for the models used for linear state control synthesis. The F, G1, G2, H, and D matrices at equilibrium are presented in Tables 43 through 47. Table 48 presents the quadratic weights used to design both the state speed control and the simplified speed control.

Table 49 presents the state control gain matrices. The state control gain matrices are presented primarily for completeness. Rough-order-of-magnitude checks indicate the feedback gains are reasonably low. This is primarily a qualitative judgment.

The open-loop roots for the state models are presented in Table 50 and the closed-loop roots are presented in Table 51. The primary observation to be made is that the closed-loop roots associated with spool speed and the integral of spool speed are very close to the prescribed values of -4.0. Closed-loop actuator poles are near the open-loop values.

The rms response values for the speed state controllers are presented in Table 52. Values are tabulated for response due to 1 percent of power level setting (η_1) and due to 4.0 square inches of exhaust area movement (η_2). The best measure of the goodness of the control that will result from power level response is that due to the model-following (response component 13). It is primarily of use in comparison with the other controllers during the iterative process of control design. By comparing the relative values of r13, the quality of the speed response to power level movements can be inferred.

The response due to exhaust area perturbation of 4 square inches is indicated as the rms value of the first response variable. Again, the primary merit of the rms value is on a comparative basis. Detailed comparisons of a few controllers obtained during the design iteration provide a basis for estimating whether the current iteration controller will be sufficiently insensitive to exhaust nozzle position.

Figures 26 through 29 present the throttle command perturbation transient responses for the state speed controllers. This set of plots for the four operating conditions for 100, 85, 70, and 50 percent is presented primarily to show spool-speed response. Later, the corresponding spool speed and sensor and actuator responses will be presented with the simplified controls.

At all four operating conditions, the "A" transients representing spool speed on the figures are a very close approximation to a 0.25-second time response. The results for these four operating conditions show that the synthesis procedure is enforcing design objectives. This also implies that the engine can be controlled in the manner desired. If there is a subsequent degradation due to control simplification, this is not due to a lack of engine capability.

The synthesis of the simplified speed control proceeds in a manner very similar to that for the state control. First, the state model previously discussed is augmented for completeness. The results are a model of the form indicated in Table 40. States 9, 12, and 13 shape the noise on A_8, the PT3, and PT5 sensors, respectively. States 14 and 15 are the Pade approximates to the 0.015-second computational delay. The fuel valve is modeled by states 3, 16, 17, and 18. State 20 is a rolloff filter in front of the fuel actuator. State 19 is used only during quadratic optimization; not for transient response, frequency response, or control. By doing this, controllers with more phase margin are developed.

The F, G1, G2, H, D, and M matrices are presented in Tables 53 through 58. The quadratic weights tabulated in Table 48 and the restriction to particular feedback gains (as indicated in Table 40) lead to the simplified speed-controller perturbation gains as tabulated in Table 94. Table 12 shows what the simplication algorithm does; Appendix D shows how the algorithm works.

The closed-loop roots for the simplified speed control are tabulated in Table 59. The roots for the simplified control are not nearly as good barometers as they were for the state control. In part, this is due to the extra complexity. The 20th-order system has considerable coupling. For example, at the 100 percent condition, the root that is associated with spool speed is part of a complex pair at11.18 radians per second, with a damping ratio of 0.5161; this is coupled with the state x19 which is part of the filter system. The closest association to a 0.25-second response time is that for E_N, for which there is indicated a root of 3.356. The association of closed-loop roots in the manner being done here is not precise. The indication is only one of association. The association can be used as a guide.

Table 60 presents the rms response values for the simplified speed controllers. Again, the primary value of the rms responses are on a comparative basis. For example, it might be expected by comparing spool speed rate model-following errors [$\dot{N}$ - $\dot{N}M$ due to power lever (η_1)] between Tables 60 and 52, that the speed response for the simplified controller is much worse than that for the state controller. The value of $\dot{N}$ - $\dot{N}M$ for the simplified controller is more than three times the value for the state controller. The transient responses will subsequently show there is only a small degradation; similarly, for the frequency responses, control performance for the simplified speed controller is well in excess of requirements for perturbation jet engine control. This again points out that the rms values have to be judiciously used to design a good controller. They are most useful in comparative analyses.

Similarly, for the response due to the exhaust actuator (associated with η_2), it is seen that at 100 percent, the spool perturbation due to the exhaust actuator for the simplified controller is more than 10 times that for the state controller. The perturbation amplitude is still relatively small for the size of the disturbance being put on the system. Again, on a comparative basis during the design, it was found to be very helpful to be able to obtain a very quick assessment from the rms responses.

Simplified speed-control responses for a step speed command of 1 percent change in operating speed are presented; the commands are for a change in operating speed of 165 rpm.

Figures 30 through 33 present the perturbation responses for the simplified speed controllers at 100, 85, 70, and 50 percent operating speed. At all operating conditions, perturbation responses meet all objectives. While response characteristics for the simplified controls are very good, there has been some degradation from that with the state control. The degradations are due to two things: model simplification and control simplification. With the state control results presented previously, there was an over-simplification

in the models in neglecting the computational time delay; this is of significance. The limited number of sensor feedbacks for the simplified controller is the other source of the somewhat degraded performance.

The "A" plots of Figures 30 through 33 present spool-speed responses. The spool-speed responses look quite similar to those of a first-order lag with a time constant of 0.25 second. Common to each of the four transient responses of spool speed is the transport-type delay near the initial time. This transport delay due to the digital control is unavoidable. The magnitude is on the order of 0.02 second and is so small that it would not affect the pilot's appreciation of the control system. The second main noticeable difference between the simplified control results and those of the state control are at times larger than about 0.3 second. At the 100-percent and at the 85-percent conditions, the simplified speed-control results are more lethargic than those for the state control. The opposite is true for those perturbation control results at 70 percent and 50 percent operating speed. The 70-percent and 50-percent results are somewhat more responsive but they also display some overshoot. More as an academic exercise than because of necessity, an attempt was made to determi[illegible] what it is in the control simplification that cuased somewhat degraded [illegible]ool-speed response for times larger than 0.3 second. Experiments made [illegible]ablished that the somewhat degraded performance is due to not taking into [illegible]count the thermal capacitance term in the simplified controller feedbacks.

There is an interesting set of trend results that is quite noticeable in comparing the four sets of figures. The amount of TT4 overshoot decreases from 100-percent to the 50-percent operating speed conditions (Figures 30a through 33a). Consistent with these responses are the responses for fuel flow shown in Figures 30b through 33b.

The "C" plots of Figures 30 through 33 show that the thermal capacitance response for the engine is qualitatively the same for the 85-percent and 100-percent conditions and also qualitatively the same for the 50-percent and

70-percent operating conditions, but that the former and latter groups have markedly different response characteristics. This lends credence to the argument for the association of the differences in spool-speed response to thermal capacitance.

Quantitatively, the transient response plots presented in Figures 30 through 33 show that the primary design objective of obtaining the 0.25-second response at a spool speed with a large amount of integral control has been achieved, and that transient responses are "nice;" there appears to be no tendency toward instability of any kind nor are there wild excursions in any of the variables that would raise the spectre of violation of any of the assumptions.

Figures 34 through 37 present frequency response plots for the simplified speed controllers.

The closed-loop frequency response plots are almost identical for each of the four operating conditions. Therefore, only the one for the 100-percent condition in Figure 34d is presented. For frequencies below 10 radians per second, the closed-loop frequency response for the engine is much like that for a 0.25-second lag. The closed-loop response does meet those objectives that were initially set up.

In Section II, there is a description of how the frequency response plots were to be made. Provisions were for breaking the loops at a number of points. The "A" plots are the actuator open-loop plots; the loop is broken at the actuator. The "B" plots are with the loop broken at the speed sensor. The "C" plots are with the loop broken on the integral control.

The actuator open-loop frequency response "A" plots of Figures 34 through 37 for the four operating conditions are both qualitatively and quantitatively very similar. The system is gain stable for all frequencies above 20 radians per second. Gain margins are about 15 decibels and phase margins are a minimum of 60 degrees.

Qualitatively and quantitatively, the open-loop integral "C" plots of Figures 34 through 37 are also similar. They are all gain stable for frequencies above 5 radians per second. They each have at least 15 decibels of gain margin. Phase margins are well in access of 60 degrees. This verifies that the design technique yields adequate stability margins in respect to the integral gain.

The open-loop frequency response with respect to speed sensor feedback are not qualitatively similar. They break into two groups. The frequency responses with respect to speed gain are similar at the 85-percent and 100-percent operating conditions, and they are also similar at the 50-percent and 70-percent operating conditions. But, qualitatively, the responses between the high-speed and low-speed conditions are markedly quite different. At the 85-percent and 100-percent operating conditions, the system with respect to the speed gain can always be gain stabilized. At the lower-speed operating condition, that is, at 50-percent and 70-percent operating conditions, the system is conditionally stable.

It is noted in Figures 34b and 35b for the 100-percent and 85-percent operating conditions that at very low frequencies, say at 1 radian per second, the phase is near -270 degrees. As frequency increases toward 4 radians per second, the phase changes through -360 degrees (or zero degrees) as it swings through the first quadrant. It continues its swing through the first and fourth quadrants as the frequency increases to about 8 radians per second. At 8 radians per second it enters the third quadrant and finally crosses the -180-degree line near 30 radians per second. The gain margins at both the 85-percent and 100-percent operating conditions are about 15 decibels and phase margins are again near 70 degrees.

At the 50-percent and 100-percent conditions (Figures 36b and 37b), the phase at low frequencies, say below 1 radian per second, is again at -270 degrees. The phase shift is from -270 degrees through -180 degrees up toward -90 degrees as the frequency increases from 1 radian to 4 radians per second.

During this same frequency change, the gain level rises from negative to positive decibels. As the frequency then increases from 4 radians per second to 30 radians per second, the phase again regresses toward -180 degrees, and in the same frequency band the gain drops below the zero-decibel line. On a Nyquist plot, these would show as an encirclement of the -1 point; i.e., conditional stability. If the gain level were lowered by 15 decibels at 50-percent operating condition, the system would be unstable at about 2 radians per second. Similarly, a lowering of the speed gain by about 30 radians per second by about 30 decibels would cause the system to be unstable at about 2 radians per second for the 70-percent case. If the gain were raised about 15 decibels, the system would be unstable near 30 radians a second at the higher frequency crossover point. At both the 50-percent and 70-percent operating conditions, the system is conditionally stable. However, both gain and phase margins for these conditions are entirely adequate to prevent undue sensitivity toward engine modeling. On the other hand, the common practice of reducing gains when stability troubles are incurred would not always be safe.

Our conclusions, then, are that the quadratic design procedure has designed a controller with adequate stability margins with respect to reasonable variations in system characteristics. The systems are gain stable at reasonably large frequencies, gain margins are in excess of 6 decibels, and phase margins are in excess of 60 degrees. The only special care required for this multiple-loop system is to note the fact that at low engine operating speeds the system with respect to the speed gain is conditionally stable. Therefore, the usual crutch of reducing gain to stay out of trouble (stability problems) is not valid at the low engine operating speed with respect to speed gain. Gain stabilization can, however, be used for the system at the actuator level, for the integral control, and for the speed control at the higher operating speeds.

Pressure Control

The pressure (surge-stall) controller design procedure is the same as for the speed controller; first, the state controller is designed and then the simplified controller is designed.

Table 39 identifies the vector components for state control. Table 61 presents the F matrix; the G1 matrix and G2 matrices are presented in Tables 44 and 45, the H matrix is presented in Table 62, and the D matrix is presented in Table 63.

Quadratic weights for the pressure control are presented in Table 64. There are different quadratic weights for the state and for the simple control. The gain matrices for the pressure control are presented in Table 65. Table 66 presents the open-loop roots for both the pressure and temperature controllers, since they are both taken up along the stall boundary. The closed-loop roots of the state pressure control are presented in Table 67. There is close association between the PT3 root and the response that we specified. At 100 percent, there is a complex pair at 10 radians per second with a damping ratio of 0.999 (essentially, two real pair at -10). At the 85-percent condition, there is a root at -9.9 and another one at -10.1: a good approximation to the pair at -10. At the 70-percent and 50-percent conditions, where 0.25-second time constants are specified, there is a complex pair at 4 radians per second with a damping ratio slightly less than 1 (again corresponding almost exactly to two real roots at -4).

Table 68 presents the rms responses for the pressure state controllers. Again, on an absolute basis, the values presented in the table are not subject to precise interpretation. As for speed control, the rms responses are primarily of value on a comparative basis.

State pressure control transient response is presented in Figures 38 through 41. The "C" traces for PT3 are very close to first-order response. Those for the two higher operating speeds of 85 percent and 100 percent have a time constant of 0.1 second. At the lower engine operating speed, they are 0.25 second.

Control simplification for the pressure controller proceeds similarly to that for the speed controller. Table 41 identifies components. The F, G1, G2, H, D, and M matrices for the simplified pressure control are presented in Tables 69 through 74. The quadratic weights are presented in Table 64. It is again pointed out that it was necessary to change the quadratic weights between the design of the state controllers and the design of the simple controllers. The primary reason for this was because of the extra dynamics that were added to the system (the Pade approximate for the computation dynamics of the digital computer and the extra sophistication in the control valve were the primary contributors). It is believed, for instance, that if the same design models had been used for both the state and the simple controller, no change in quadratic weights would have been necessary, or at most, a very small change perhaps in one of them, but nothing of the order of magnitude indicated here.

The perturbation gain matrices are presented in Table 94. The closed-loop roots for the simplified controller are presented in Table 75. Here, in contrast to the speed control, there is better association between the closed-loop roots and the prescription for response. At the 100-percent condition, there is a complex pair near 5 radians per second and a damping ratio of 0.86. This is about half the closed-loop frequency specified. From the root inspection alone, it might be expected that the response would be lethargic it is not. At the 85-percent condition, however, there is a root at 11.9 which is relatively close to the 0.1 second prescribed. On the other hand, the damping ratio appears very low. But again, looking at denominators of transfer functions can be very misleading in estimating transient response characteristics because of the importance of numerator dynamics.

The rms responses for the simplified pressure control are presented in Table 76. Again, there is a vast quantity of data here that superficially appear to be without great value. Again, during the design iteration process, using the comparative value between iterations of the various rms quantities provided considerable insight as to what was happening, what was significant, what provided insensitivity, and what provided good response characteristics. The primary value of tabulating them here is for reference purposes. For example, by comparing these data with those for the state controller, some of the little difficulties we had in getting controllers would be easily resolved in another design.

Perturbation time responses for the simplified pressure controllers are presented in Figures 42 through 45 for the 100-percent, 85-percent, 75-percent, and 50-percent operating conditions. For the 85- percent and 100-percent operating conditions, the design condition for PT3 response is 0.1-second; for 50-percent and 75-percent operating speeds, the time response is to be 0.25 second.

Figures 42a through 45a demonstrate that the PT3 response is qualitatively that specified. For the two higher operating speeds, the initial response is not that of a first-order lag due to the computational delays in the digital computer. In the range between 0.02 second and 0.15 second, the transient responses closely approximate that of a 0.1-second lag. For larger times, the actual responses from the engine display some overshoot: less than 10 percent. This is a satisfactory approximation to the prescribed 0.1-second response.

Figures 44a and 45a show that the PT3 response for the 70-percent and 50-percent operating conditions is very close to 0.25 second, with the major deviation being that of the initial transport lag due to the computational delay within the digital computer.

The fuel flow responses for the four operating conditions are much like those for the speed controllers. At the lower operating speeds, the fuel is used to accelerate the engine, with very little fuel being used to achieve the increase in state. At the higher operating conditions, the percentage increase in fuel to increase the steady-state operating speed is the higher percentage of the peak fuel used.

As for the speed controllers, the collective responses shown on the ABC plots for each operating condition display no undesirable characteristics. There is no tendency toward lightly damped oscillations. There are no wild transients that would cause saturation difficulties. The qualitative and quantitative response characteristics for each of the variables are very desirable.

The frequency responses for the PT3 perturbation controllers are satisfactory for all four design conditions. The closed-loop frequency response is as would be expected of an approximation to a 0.1-second or 0.25-second lag. The open-loop gain and phase margins are all satisfactory; all generally exceed 6 decibels gain margin and 60 degrees phase margin. Two things were not entirely anticipated. One of these was noted with the speed controllers, namely, that under some situations, there is conditional stability. Probably the most surprising result displayed by the frequency response plots for the pressure perturbation control is the apparent lack of effectiveness of the PT5 feedback gain. In no case does the gain level reach zero decibels, and, particularly for the two lower operating speed conditions, it is below -5 decibels over the entire frequency range. This might make it appear as though the PT5 gain were very ineffective (it certainly is from a frequency response standpoint). When this was noted, the simplification procedure was used to eliminate the PT5 feedback gain. Without the PT5 feedback, the perturbation control could be affected, but both transient responses and rms responses suffered. It is for this reason that the gain was retained in the results that are reported here.

First, we will dispense with the closed-loop frequency responses. Figures 46e through 49e present the closed-loop frequency responses for the 100-percent and 50-percent conditions. The 100-percent plot shows that to a good approximation over 10 radians per second bandwidth, the closed-loop response is close to that for a first-order lag with a 0.1-second time constant. This also applies to the 50-percent operating condition with a 0.25-second time constant.

Figures 46a through 49a present the frequency response plots with the loop broken at the actuator. They are generally quite similar. The gain margins for each are at least 10 decibels and phase margins exceed 60 degrees. The qualitative characteristics at 100 percent and 85 percent (Figures 46a and 47a) are pleasing; high gain and relatively small phase shift for low frequencies, with a gradual attenuation of gain and phase shift as the frequency increases toward the crossover point. There is a consistent trend between the results for 85, 70, and 50 percent as shown by Figures 47a, 48a, and 49a. There is a marked increase in phase change at low frequency from the higher-speed to the lower-speed operating condition. At 85 percent, the phase shift is small; at 70 percent, there is considerable phase shift (in fact, an increase in phase lag around the 1-radian-per-second point). For the 50-percent operating condition, there is a very large phase shift of nearly 180 degrees at a frequency of 0.18 radian per second. It might be suspected that this behavior would lead to conditional stability. A visualization of how a Nyquist plot would look will reveal that this is not the case. The 50-percent condition is unconditionally stable. An assessment of why there is such marked phase shift at the 50-percent condition was not made.

Figures 46b through 49b present the open-loop frequency response for the system broken at the PT3 feedback sensor. Gain and phase margins are adequate, but there is some rather surprising behavior. The system is unconditionally stable at both 50 and 85 percent, but at 70 and 100 percent, the system is conditionally stable. Gain and phase margins at the higher

frequency rolloff are adequate. Gain margins are in excess of 6 decibels, and phase margins are usually in excess of 60 degrees; at the 85-percent operating condition, the phase margin is only 55 degrees. At the 50-percent and 85-percent conditions, there is conditional stability near 2 radians per second; it would require a gain change on the order of 50 decibels for stability problems to be encountered. This should provide satisfactory control.

Figures 46c through 49c present the PT5 open-loop frequency response results. In no case does the gain get to as high a value as zero decibels. Gain margins are generally adequate, although at the 100-percent condition, at a frequency near 40 radians per second, there is barely 6 decibels of gain margin. It would probably be desirable to put an additional rolloff filter in the PT5 loop to eliminate this characteristic. All of the plots show the increase with frequency for the PT5 feedback, so the rolloff filter would be desirable in this feedback loop.

Figures 46d through 49d present the frequency response for the pressure integration term. The qualitative and quantitative characteristics for this feedback gain are consistent. Gain and phase margins are adequate.

Results presented for the pressure perturbation controllers indicate that stability and response characteristics should be adequate over the desired passband and operating condition range of the engine.

Temperature Control

Synthesis of the temperature control proceeds in a manner almost identical to that for speed and pressure controls.

Table 39 identifies the components. The F, G1, G2, H, and D matrices for the state temperature synthesis are presented in Tables 77 through 81. The quadratic weights for the state and simple temperature controls are presented

in Table 82. The quadratic weight changes between state and simple controls are quite marked. The open-loop roots for the temperature control are presented in Table 66. The state control gain matrices are presented in Table 83. The temperature state controller closed-loop roots are presented in Table 84. Here again, there is good association between the prescription of 0.1-second response time and a root in the system of 9.99 with a damping ratio of greater than 0.9. Table 85 presents the rms responses for the temperature state controller.

Transient responses of temperature state controllers are presented in Figures 50 through 53. The request is for a 0.1-second response on TT4. The "D" traces of the figures show that the responses closely correspond to those of a 0.1-second, first-order lag. There is a little overshoot, on the order of 2 to 3 percent, but, certainly, this is an excellent approximation to that which has been requested.

Table 42 presents the components for the simple temperature control. Tables 86 through 91 present the F, G1, G2, H, D, and M matrices required for synthesis for the simplified temperature controllers. The quadratic weights are presented in Table 82, and the feedback matrices for the simplified controller are presented in Table 94. Table 92 presents the simplified temperature controller closed-loops roots: comments relative to these roots are the same as they were for the other simplified controls. Table 93 presents the rms responses for the simplified temperature controllers.

Transient responses for the perturbation temperature controllers are presented in Figures 54 through 57. Transient responses are close to those prescribed; the TT4 responses are very close to those of a first-order lag with a 0.1-second time constant. As for the speed and pressure controllers, transient controllers are smooth, there is no indication of any lightly damped terminal oscillations, and there are no initial wild transient overshoots to cause concern.

The "B" traces of Figures 54a through 57a show the TT4 perturbation response. Qualitatively they are very close to corresponding to those of a 0.1-second lag. Quality is slightly better for the higher operating speeds than for the lower operating speeds. At the 100-percent operating speed, the TT4 response is almost exactly as prescribed. At 85 percent a very good approximation to a 0.1-second response is achieved. At 70 percent, the response up to about 92 percent of the 100 degrees commanded is about as desired. For the 50-percent operating condition, the initial 85 percent of the response comes in as prescribed and then there is little hang up for about 0.1-second. The quality for each is well in excess of that required.

The second feature should be noted on Figures 54a through 57a: the closeness of correspondence of the TT4 and filtered TT4 whistle which is the approximation to TT4. The correspondence of the B and D traces is an indication of the quality of the TT4 sensor in measuring the actual TT4.

In Figures 54b through 57b, of most interest again is the fuel flow response. Qualitatively, the transient response is relatively smooth without wild overshoots or tendency toward residual oscillations. Collectively, Figures 54a, b, c through 57 a, b, c again display qualitatively "nice" control.

The frequency response for the perturbation temperature controllers demonstrates that system stability in terms of gain and phase margins is adequate. The closed-loop response over the low passband range where criteria are set, again meets objectives. Again, there are some funny little things of the type that are now not unexpected, in that the speed and pressure controllers have demonstrated some of the same pecularities. The frequency response plots for the perturbation controllers are presented in Figures 58 through 61.

The closed-loop responses are presented on "F" plots of Figures 58 through 61. This frequency response substantiation of a first-order lag specification is again a source of satisfaction in using the quadratic design procedure.

The actuator open-loop frequency responses for the four conditions (Figures 58a through 61a) are remarkably consistent. There is relatively high gain and small phase shift for frequencies below 20 radians per second; cross-overs are near 50 radians per second. Gain margins are at least 7.5 decibels (with a minimum gain for the 50-percent condition), with much larger gain margins at the other three operating conditions. Phase margins are in excess of 80 degrees.

The TT4 open-loop frequency response plots have two peculiar features. At very low frequencies, the TT4 feedbacks provide very little control; gain levels are at -40 decibels and below. For 100-percent condition, in particular, but also for the 85-percent operating speed condition, the gain level never gets as high as zero decibels, and even for the 70-percent and 50-percent conditions it barely gets to zero decibels. This is at first somewhat surprising, but it simply indicates that the TT4 feedback is not the primary sensor for TT4 control; it will subsequently be shown that the primary feedback is that of the integral feedback. The TT4 feedback gain is small because of the noise estimate used on the TT4 sensor. That is, the feedback gain has been attenuated by the noise level the TT4 sensor produces. The TT4 feedback loop is unconditionally stable. The phase breaks near 5 radians per second at the 50-percent and 70-percent conditions are in a direction so that the system would be gain stable with respect to the TT4 feedback.

Figures 58c, d through 61c, d indicate that the PT3 and PT5 feedbacks are not very effective, in that gain levels remain well below zero decibels. Again, for these sensors, synthesis was performed without the PT3 and PT5. Stable feedback control was achievable but the quality of performance was degraded, much more so than would be estimated by looking at the gain levels on the PT3 and PT5 plots.

Figures 58e through 61e again show a rather remarkable consistency among the four operating conditions. For frequencies below 10 radians per second,

the phase shift is remarkably constant and the gain attenuation is slight. Gain and phase margins are again adequate; gain margins are on the order of 20 decibels, and phase margins are near 80 degrees.

So again, based on the assumed model characteristics that the quadratic design procedure has yielded, perturbation controllers have been attained with good rms response, good transient response, and good frequency response, indicating that all design objectives have been met.

WIND TUNNEL TEST RESULTS

The wind tunnel tests verified that optimal control techniques could design good engine controllers. Good steady-state, perturbation, and dynamic response characteristics were achieved. The test uncovered one anomaly in the model and also pointed out a small error that was made in the design.

The technical objective for this contract was to show that optimal control methodology could be used to design good engine controls. The verification that the design procedures are effective is in the wind tunnel test results. There are three sets of test objectives:

- Steady-state stability
- Small-amplitude perturbation command response
- Large-amplitude transient response

Setting up tests to substantiate the first two objectives was easy. The tests were run, the results measured, and these results were checked against objectives. In the case of the first two objectives, the objectives and the control results were satisfactory. Setting up tests for large amplitude commands involved some artificial restrictions. It was desired to be able to test the engine to the extremes of its operating limits so as to substantiate

(without doubt) that the large-amplitude control objectives were met. It was not possible to do this. The test engine at APL was being used for a number of programs other than the optimal control effort. It was therefore mandatory that the engine life not be jeopardized. For this reason it was necessary to set up tests that would substantiate the objectives of the large-amplitude command response but that would not jeopardize the engine. The tests that were performed demonstrated that the large-amplitude command objectives could be met, although the test did not exercise the engine fully throughout its envelope. The objectives were met by setting up boundaries or operating limits well below those that could actually be achieved by the engine. Then the controller was set up to control to these bounds. The objectives then were measured in terms of how well operating limits could be maintained within these bounds. For example a measure of the goodness of the controller was the accuracy to which it could maintain the PT3 below a prescribed operating limit. It will subsequently be shown that the controller tested in the wind tunnel actually controlled to within 3.5 pounds per square inch (psi) of a priori prescribed values of PT3. For reasons which will be discussed later, it is believed that it is quite a straightforward matter to reduce these bound error bounds by at least a factor of 2 if not 3. That is, the a priori controller limits should actually control the engine to within 0.5 pound per square inch.

The control policy was developed so as to control speed, pressure, and temperature. For expediency in getting the controllers on the APL test facility, it was decided to split the control functions and test the speed-pressure and the speed-temperature control separately. This made it somewhat easier to install the controllers on the APL test facility and also helped greatly in the presentation of the test results to show what kind of results were achieved.

Speed-Pressure Controller

The speed-pressure controller results were satisfactory but less desirable than could have been achieved for two reasons. First, there is a difference between the engine math model and the engine as installed in the APL tunnel. Second, a minor mistake was made in implementing the speed-pressure controller that caused some excessive overshoot for large-amplitude commands.

Table 95 presents speed-controller gains, both for the early test where we have the anomaly that we are about to discuss and for the controller for which we present our final results. It is seen that the controller with which we had a stability problem had gain magnitudes of from 2 to 10 times as large as those that we finally used.

Figures 62 and 63 present P3-N and time history plots of equilibrium, a very slow acceleration, and then deceleration at speeds from about 58 to 64 percent. Figure 63 shows that at equilibrium and during acceleration, there is an incipient oscillation of slightly greater than 2 Hz. This is manifested in the oscillatory character of the fuel flow trace (where it is very clear), and it also appears on the P3 trace of the time history plot of Figure 63. Figure 62 clearly shows that the engine is nearly neutrally stable at this particular operating condition. These results were not anticipated, although, at the time this test was run, frequency response plots had not been made.

Figures 64, 65, and 66 present the open-loop actuator, speed sensor, and integral speed open-loop response plots for the controller on the design math model of the J85 engine. Figure 64, for the actuator open-loop condition, shows that the gain crossover occurs at about 1.2 Hz where there is about 60 degrees of gain margin. The gain margin at 8 Hz is in excess of 15 decibels. Breaking the loop at the speed sensor shows comparable

stability. The phase margin at about 1.2 Hz is about 70 degrees, and the gain margin at 8 Hz is again about 15 decibels. On the integral gain, the phase margin is about 170 degrees and at about 0.5 Hz, while the gain margin is about 55 decibels at 24 Hz. These results show that the controller should not have exhibited the nearly neutral stability as the wind tunnel test results displayed.

Considerable effort was spent trying to resolve the anomaly between the wind tunnel test results and the stability results based on the math model just discussed. It was suspected that the extra 60 degrees of phase shift in the engine during this initial test was due to one of the six following probabilities:

- The speed sensor
- The analog-to-digital speed converter
- The link lines
- The equilibrium calculations in the IBM 1800
- The digital-to-analog fuel conversion
- All of the above

The Air Force Propulsion Laboratory made a frequency response test that seemed to clear the converters and the link lines. The speed sensor was not a likely candidate. We isolated the anomaly by considering what it might be caused by:

- Differences between the APL engine and the simplified NASA model of the engine that we were using.

- Inadequate stability margins due to neglect during design synthesis.

- Inadequate stability margins due to digitization effects.

The first of these was ruled out by some early frequency response work at APL and which is further discussed in Volume III of this report.

It was just shown that the stability margins based on the math model were adequate.

Assessments of magnitude and time quantization effects of the digital computation were shown not to be the cause of the anomaly.

During this early test period, open-loop runs were made. Fuel flow and engine responses were smooth. These results established that open-loop fuel magnitude quantization was not the source of the difficulty. The closed-loop part of the control achieved comparable resolution. It was therefore concluded that the magnitude quantization was satisfactory.

To better assess the time quantization, the Pade approximate for the computational delay was deleted and the Tustin transform was used for the computational delay in the integration (EN) being accomplished in the IBM 1800. With 0.015-second sample time, the closed-loop roots were computed at 0.5, 1.0, 2.0, and 3.0 times nominal gains. This system was stable at the first three sets of gains but had a root at 0.722 ±0.756 i at 3.0 times nominal. This was outside the unit circle and corresponded in the continuous domain to an unstable pair at 9.1 Hz. The continuous representation indicated the frequency of instability would be 8.4 Hz; good agreement.

The sensitivity to different magnitudes of computational delays was also assessed. Roots were computed for the closed-loop system with nominal gains, with sample times of 0.0001, 0.0005, 0.0075, 0.0300, 0.0450, and 0.0600 second. Only with the last sample time was this system unstable. This provided another indication of the tolerance that shouls have been expected from the controllers that demonstrated during the wind tunnel test at near-neutral stability.

The apparent 50 degrees of phase shift in the engine system near 2 Hz was never resolved. To get on with the testing of the optimal controllers, new controllers were designed with:

- Lower bandwidth
- Increased gain margins
- Increased phase margins

These are the controllers the detailed data of which are presented earlier in this section of the report. These controllers generally exhibited somewhat less desirable perturbation transient response than did the earlier controllers based on the math model of the engine, but the deterioration was not overly marked.

On the speed-pressure controllers, the limits that were set on the integral terms were the only provisions that were made to inhibit pressure integration when on speed control and vice versa. A preferable arrangement was to reset the pressure integrator to zero when on speed control and vice versa. During the nonlinear simulation tests on the computer at the contractor's facility in Minneapolis, the controllers were tested and it was found that the overshoot was not excessive by simply using the integrators in the matter described. However, it was clear that by using a reset on the integrators, overshoot could be reduced. And, in fact, on the speed-temperature controllers whose results are subsequently presented, the reset mechanism was used.

Figure 67 presents P3-N plots for a series of slow engine accelerations. Their associated time histories are presented in Figures 68 through 71. The strong speed stability expected from the use of controls with large amounts of integral control feedback is demonstrated. Speed repeatability is smaller than the resolutions of the plots; i.e., well within 0.1 percent of engine rpm. The second thing to note is the small-amplitude perturbation

command response of the P3-N plot of Figure 67. The P3-N transient response plots generally demonstrate some overshoot. These overshoots on the time history are somewhat more difficult to detect because of the scale resolution. This was not expected from the linearized results presented earlier in this section. The linearized speed response of the math model showed little or no overshoot in speed. But, on the actual engine there is overshoot. This difference is ascribed to the difference between the math model and the engine. It perhaps should have been expected from the 50 degrees phase shift anomaly at 2 Hz.

One of the things that needs to be pointed out on the time history plots on the fuel flow, and in particular on Figure 68, is the oscillatory behavior displayed in the fuel flow response. This oscillatory behavior is not a real oscillation but is a characteristic of the particular instrument, particularly at very low fuel flows. It will be seen again during some of the maximum decelerations.

Figure 72 presents the P3-N large-amplitude speed-pressure response, and the associated time histories are presented in Figures 73 and 74. The "prescribed" surge-stall limit has been dubbed in on Figure 72. For fast accelerations there is overshoot. The maximum excess is about 3.5 pounds per square inch. This excess is ascribed to the two causes previously discussed: the differences between the math model used for design, and the characteristics of the actual engine. Half of it could be eliminated; that is, overshoot could be reduced to about 1.5 pounds per square inch simply by using a reset mechanism on the integrators rather than using the integral limits.

Figure 75 presents P3-N results for Bode-type slams, and Figures 76 through 78 present the corresponding time histories. The P3-N figure shows that the Bode slams are highly repeatable; the differences in equilibrium value at high speed at the ends were set in to separate the figures. The time

histories show smooth acceleration and deceleration for the slams. There is markedly different timing in the three slams but that the time histories for each are quite similar. Again, the erratic behavior of fuel flow of low rpm is an instrumentation problem; it is not something that happens on the actual engine, as can be seen from the TT4 trace. If fuel flow were actually wiggling as badly as is indicated on the figures, there would have been undesirable side effects.

Speed-Temperature Controller

The kinds of results presented for the speed-temperature controller are quite similar to those for speed-pressure except that the boundary-following is more clearly displayed as an error term, TT4WD-TT4∂.

Figure 79 presents the boundary error term versus speed, N, for some moderate accelerations, and the time histories are shown in Figure 80. The boundary speed plot during "equilibrium" indicates considerable noise on the temperature sensor. Even under the quietest equilibrium conditions there is considerable burner noise that is manifested in variations in TT4 as shown. This appears on both the XY and time history plots. The boundary-speed plots for the accelerations of Figure 79 show what appear to be reasonably good accelerations, although the overshoot of 80 degrees might be deleterious. However, the corresponding time history (the second strip of Figure 80) shows the time that the boundary was exceeded was about 0.25 second. It is not likely that the 80 degrees overshoot for 0.25 second would have serious deleterious effects on the engine.

Figure 81 presents larger-amplitude TT4∂-N large-acceleration response, and the associated time history is shown in Figure 82. The results are quite comparable to those for the lower-amplitude results.

Figure 83 presents the boundary error-speed for a Bode slam. Its time history plot is shown in Figure 84. The time that the temperature is in access of the boundary value is on the order of 0.25 second.

Summary

Table 96 summarizes the results from the wind tunnel tests achieved at APL. Good results were achieved, but improvements can be made. The results show that optimal control methodology can successfully be used to design an engine controller.

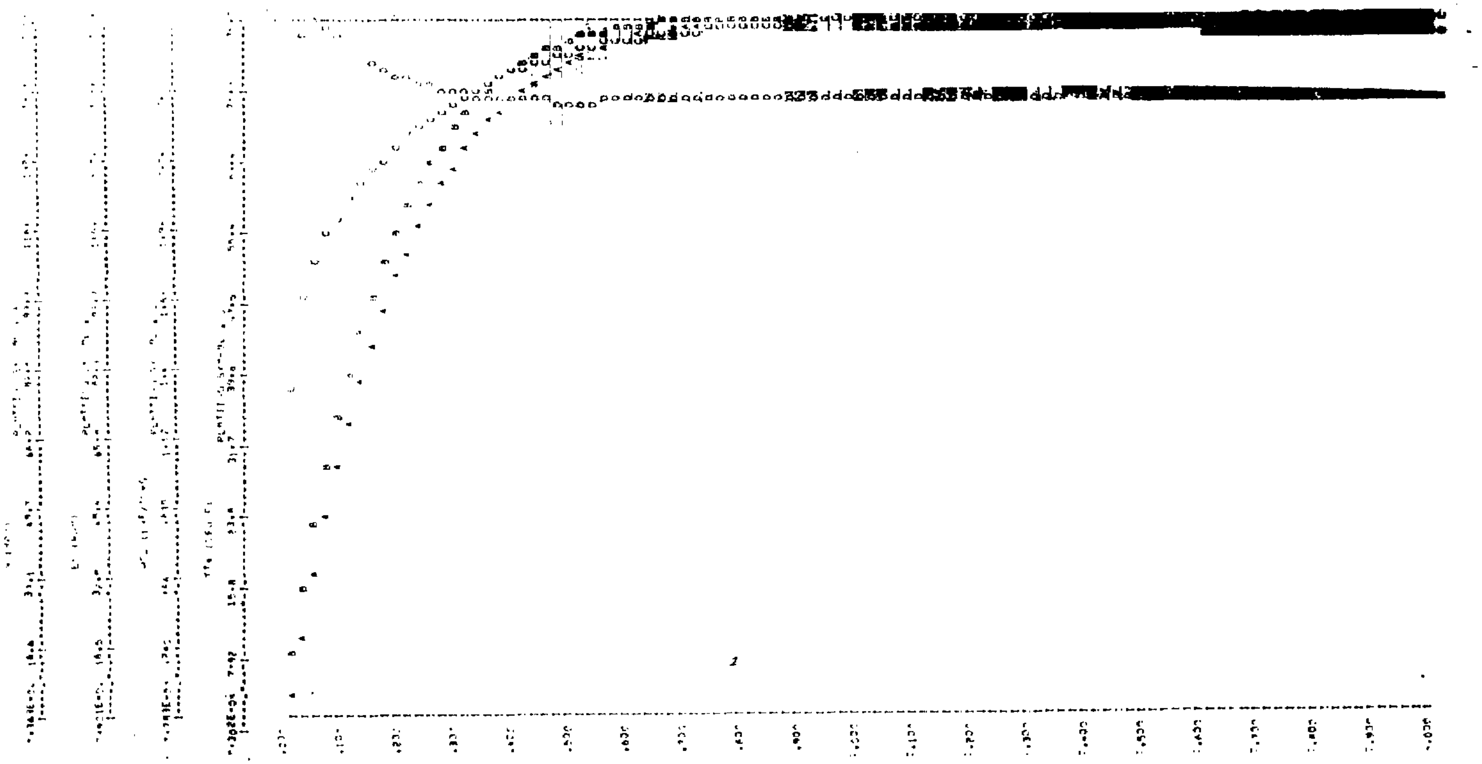

Figure 26. State Control--100-Percent Operating Condition--Equilibrium

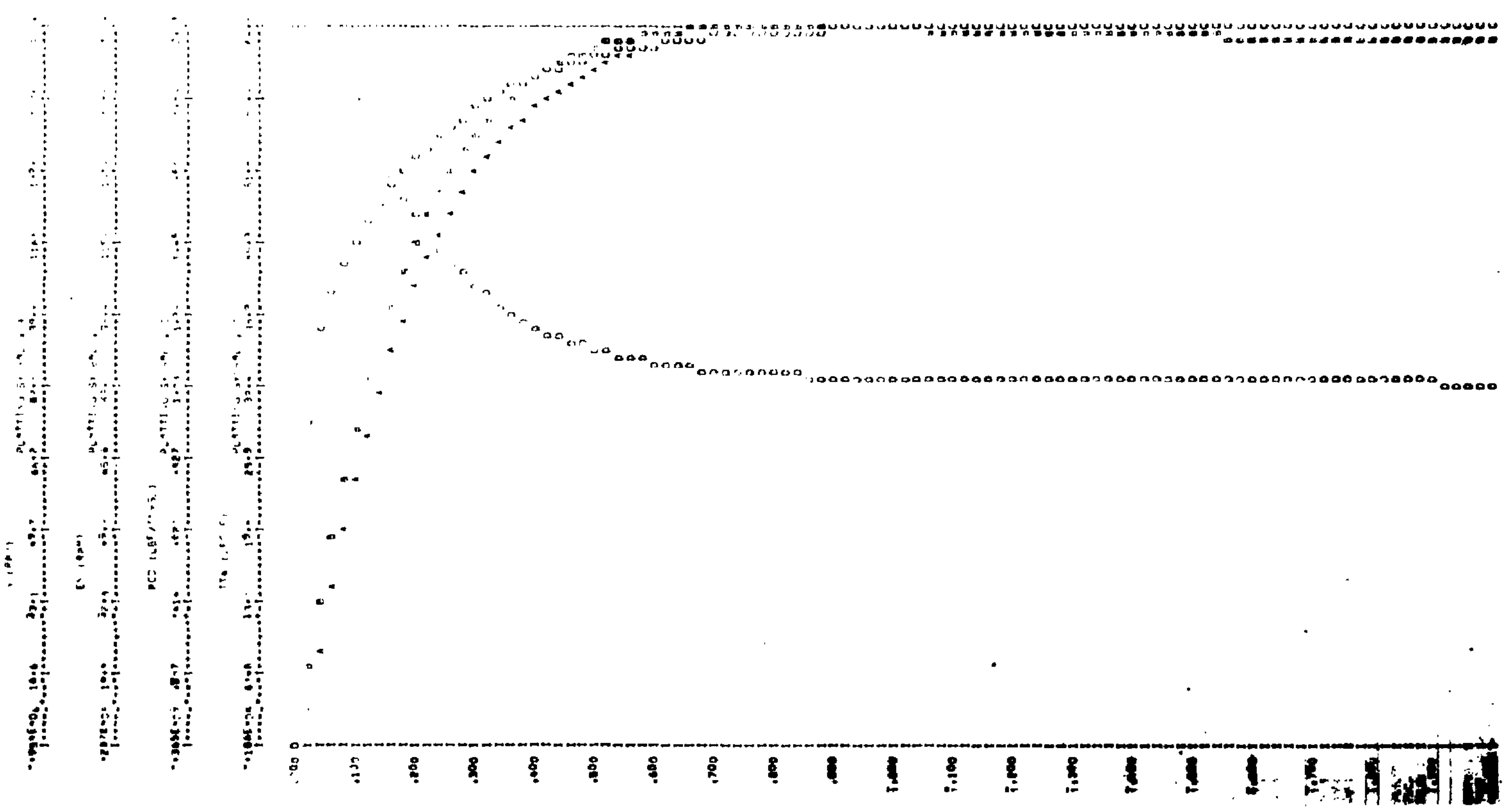

Figure 27. State Control--85-Percent Operating Condition--Equilibrium

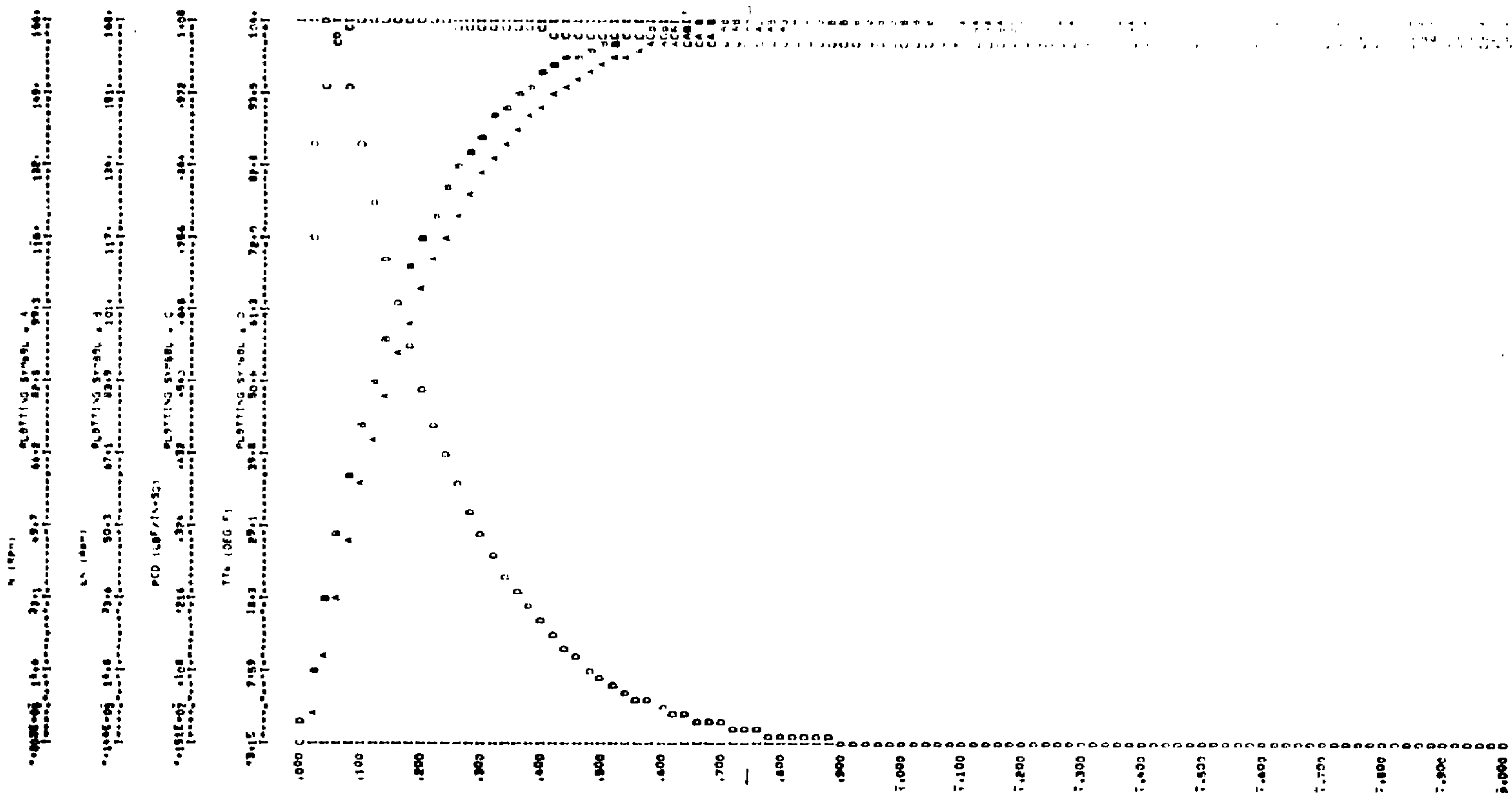

Figure 28. State Control--70-Percent Operating Condition--Equilibrium

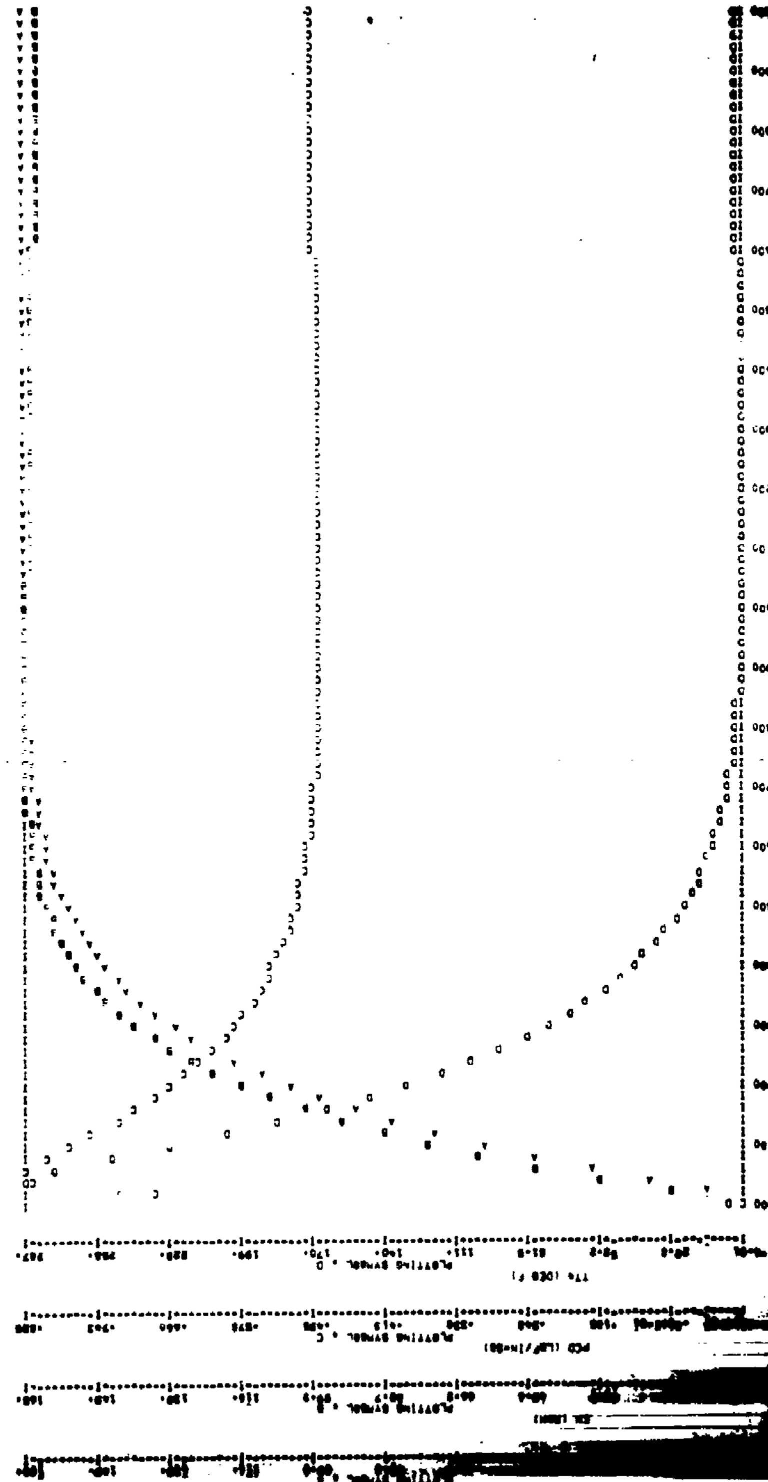

Figure 29. State Control--50-Percent Operating Condition--Equilibrium

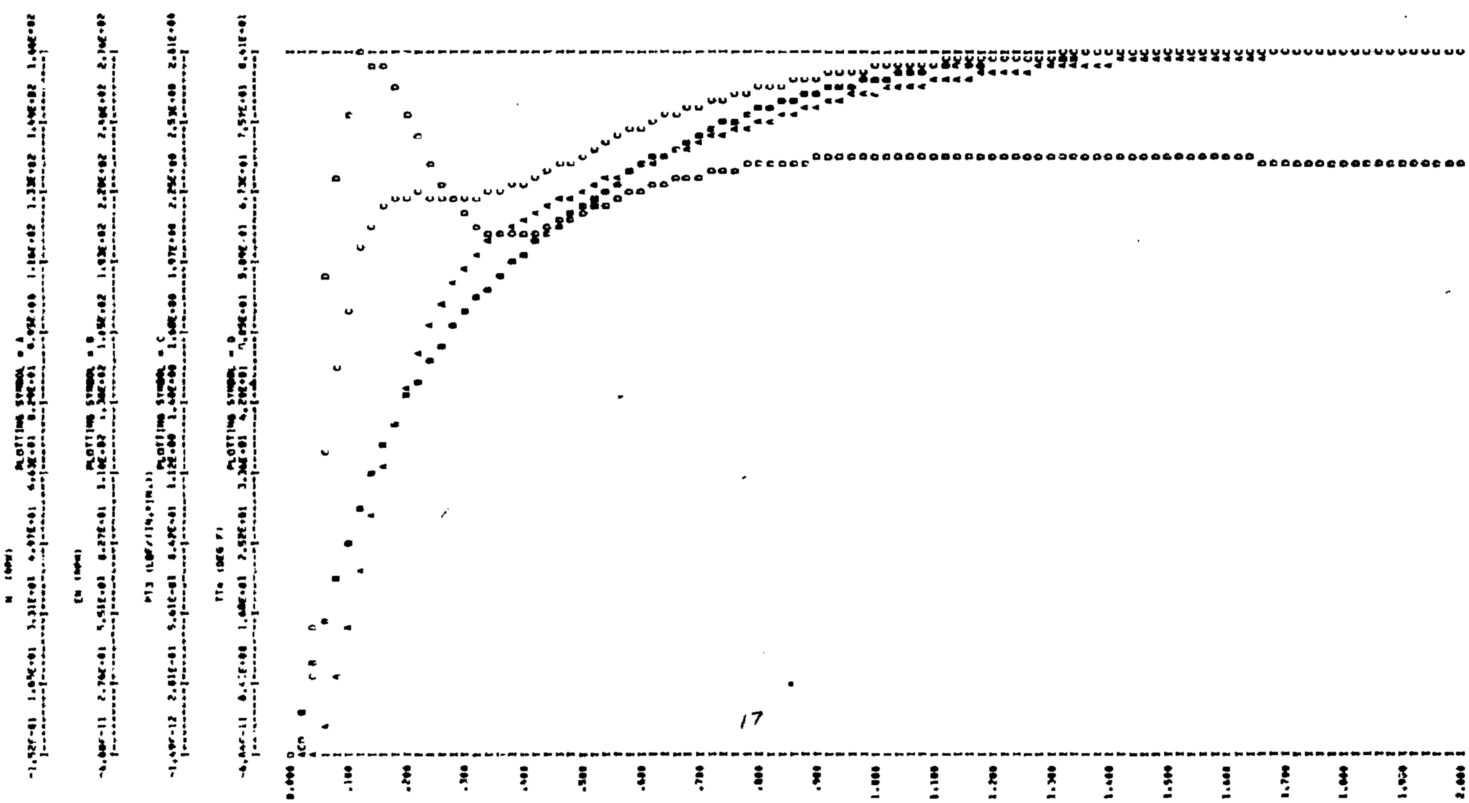

Figure 30a. Simplified Control--100-Percent Operating Condition--Equilibrium

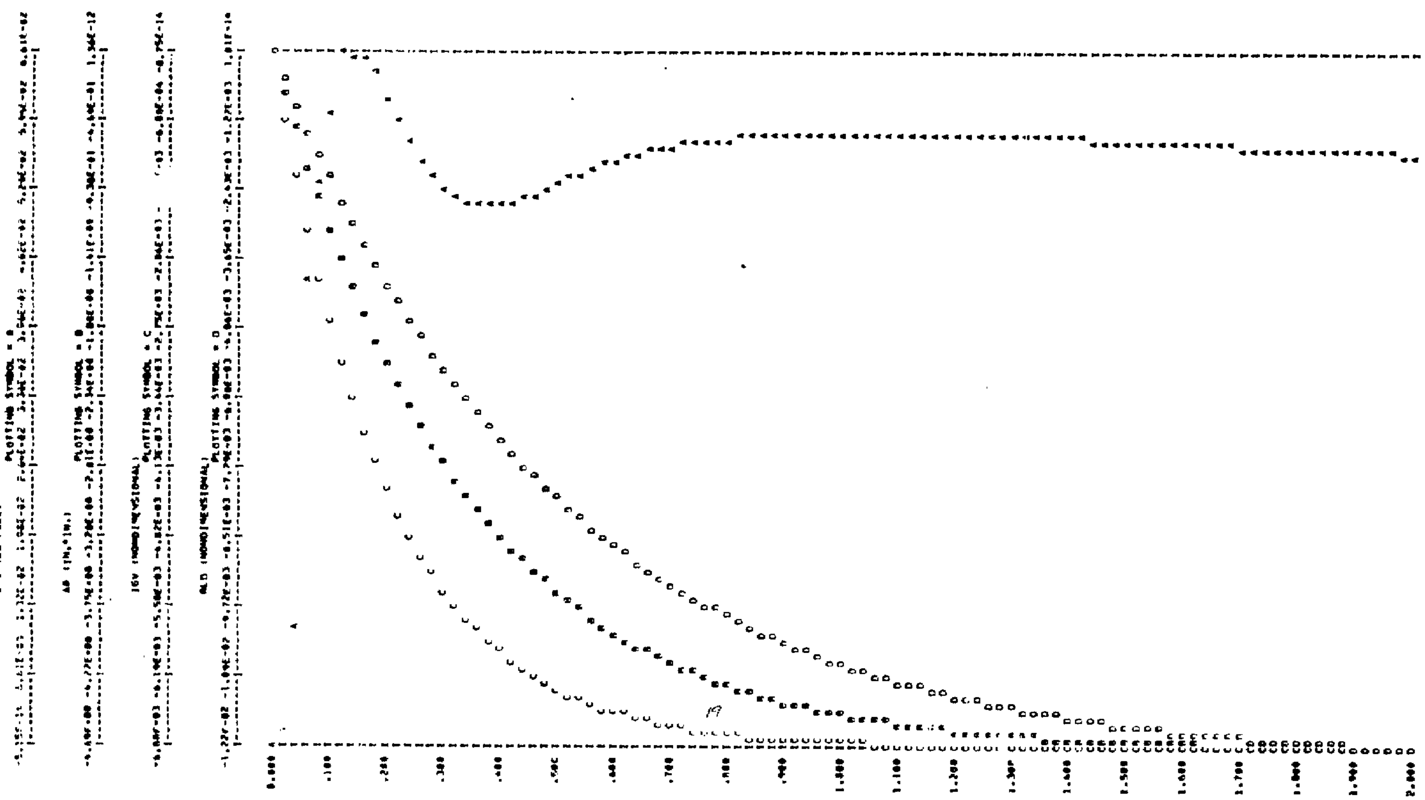

Figure 30b. Simplified Control--100-Percent Operating Condition--Equilibrium (Continued)

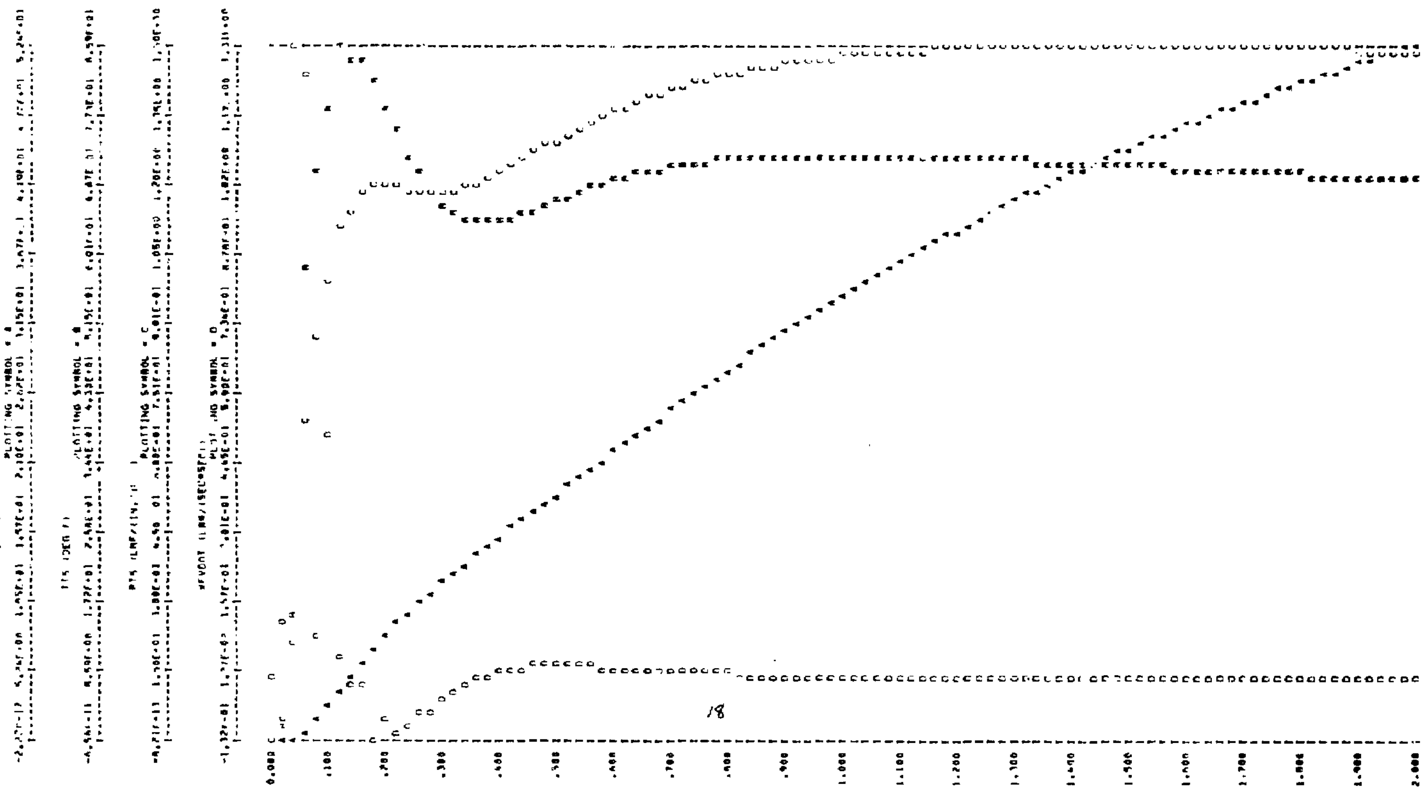

Figure 30c. Simplified Control--100-Percent Operating Condition--Equilibrium (Concluded)

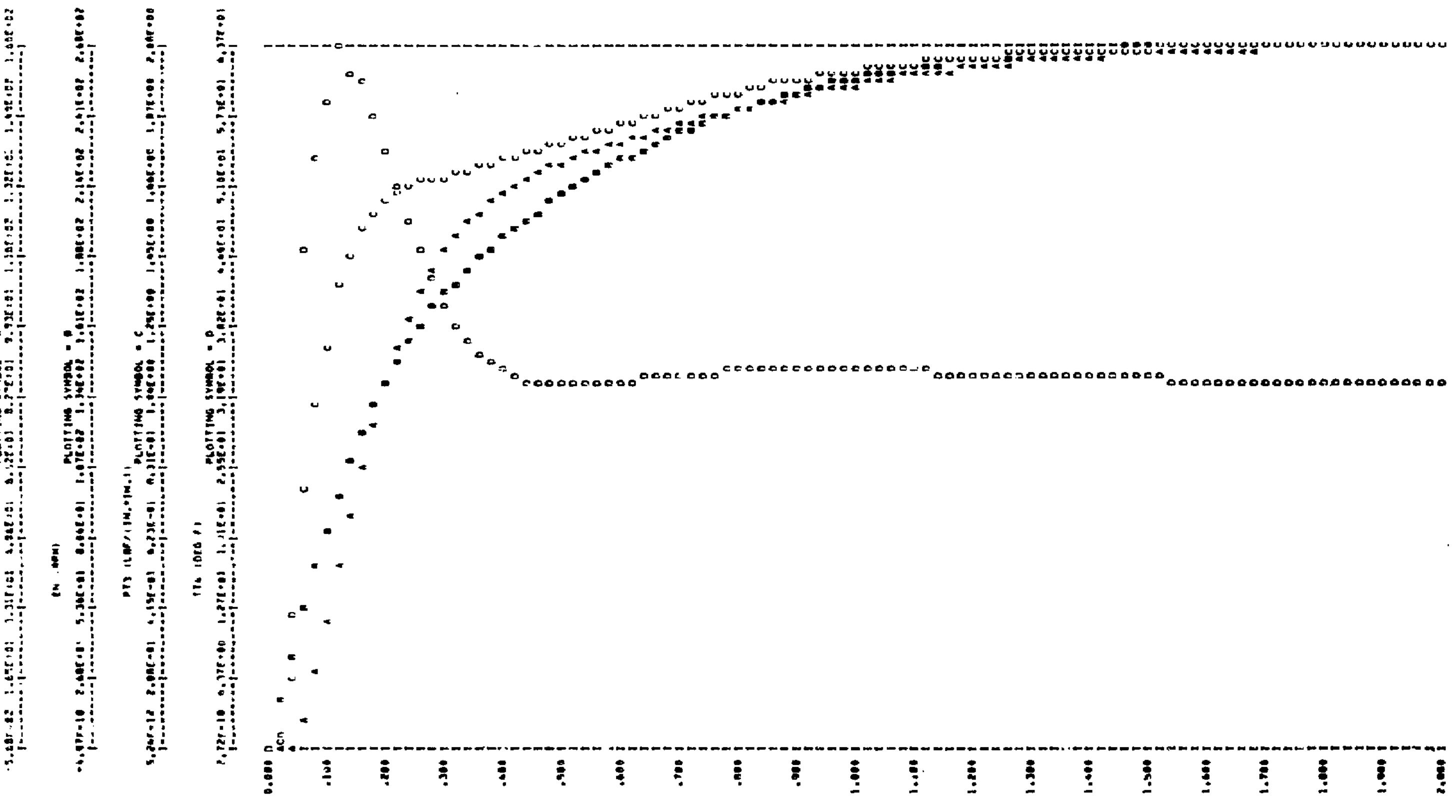

Figure 21a. Simplified Control--85-Percent Operating Condition--Equilibrium

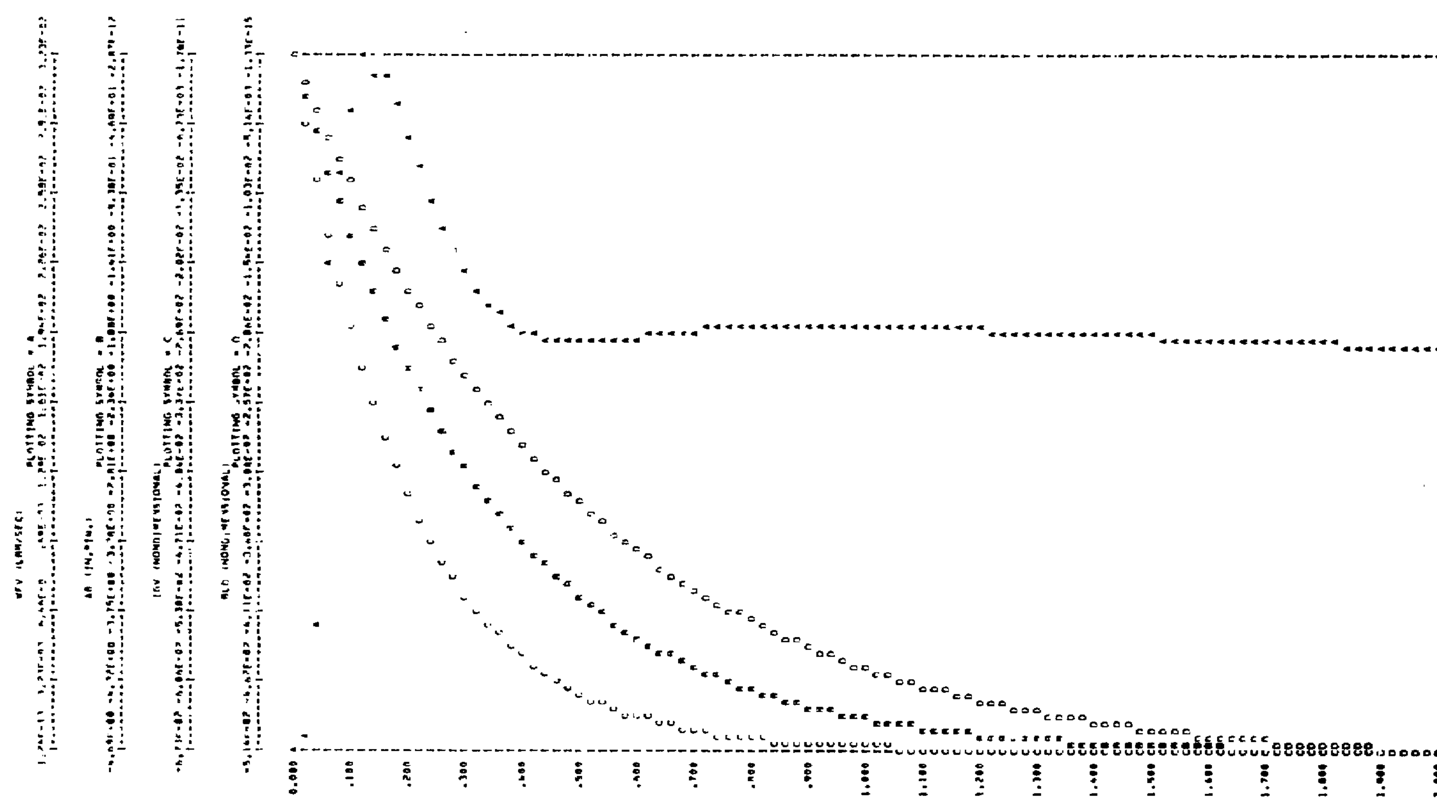

Figure 31b. Simplified Control--85-Percent Operating Condition--Equilibrium (Continued)

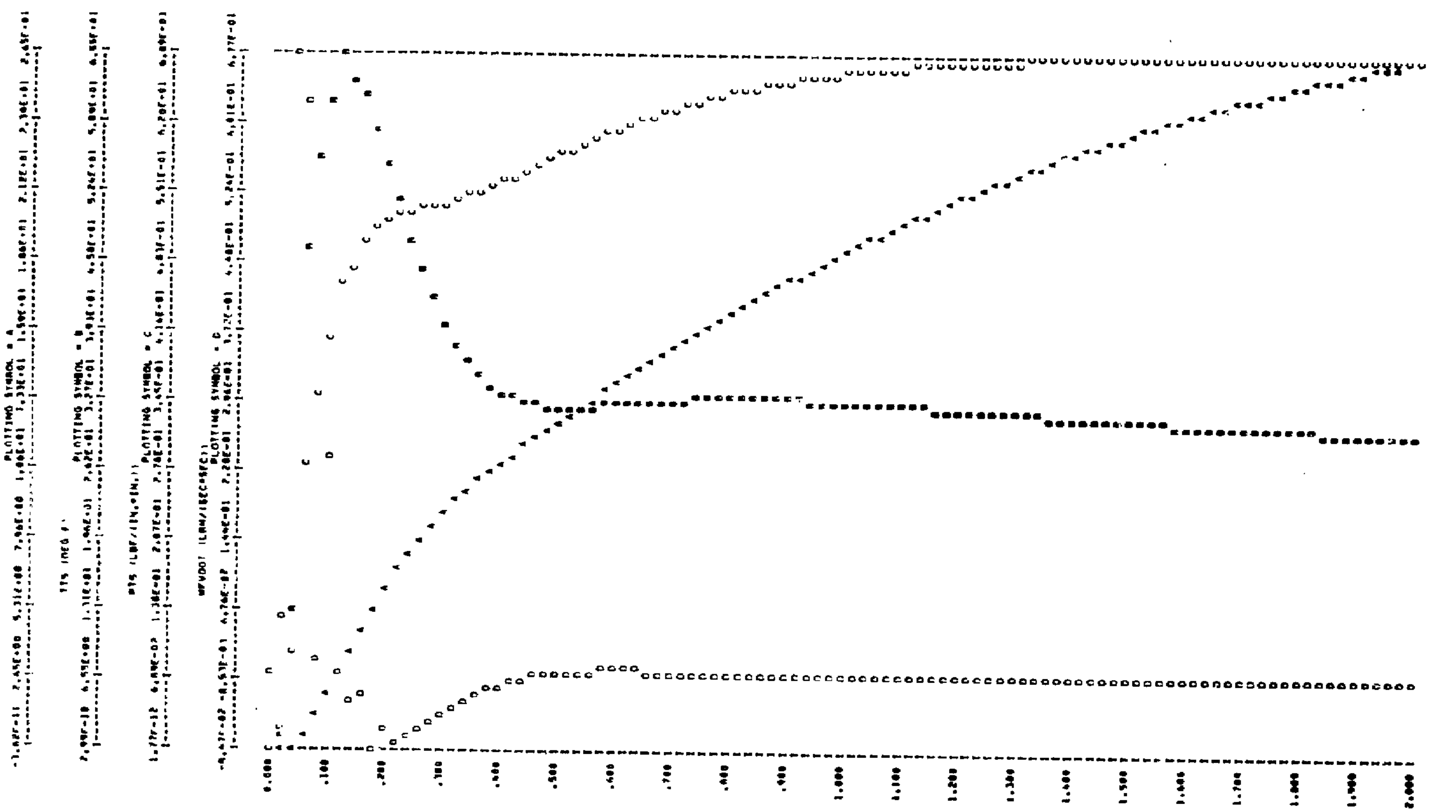

Figure 31c. Simplified Control--85-Percent Operating Condition--Equilibrium (Concluded)

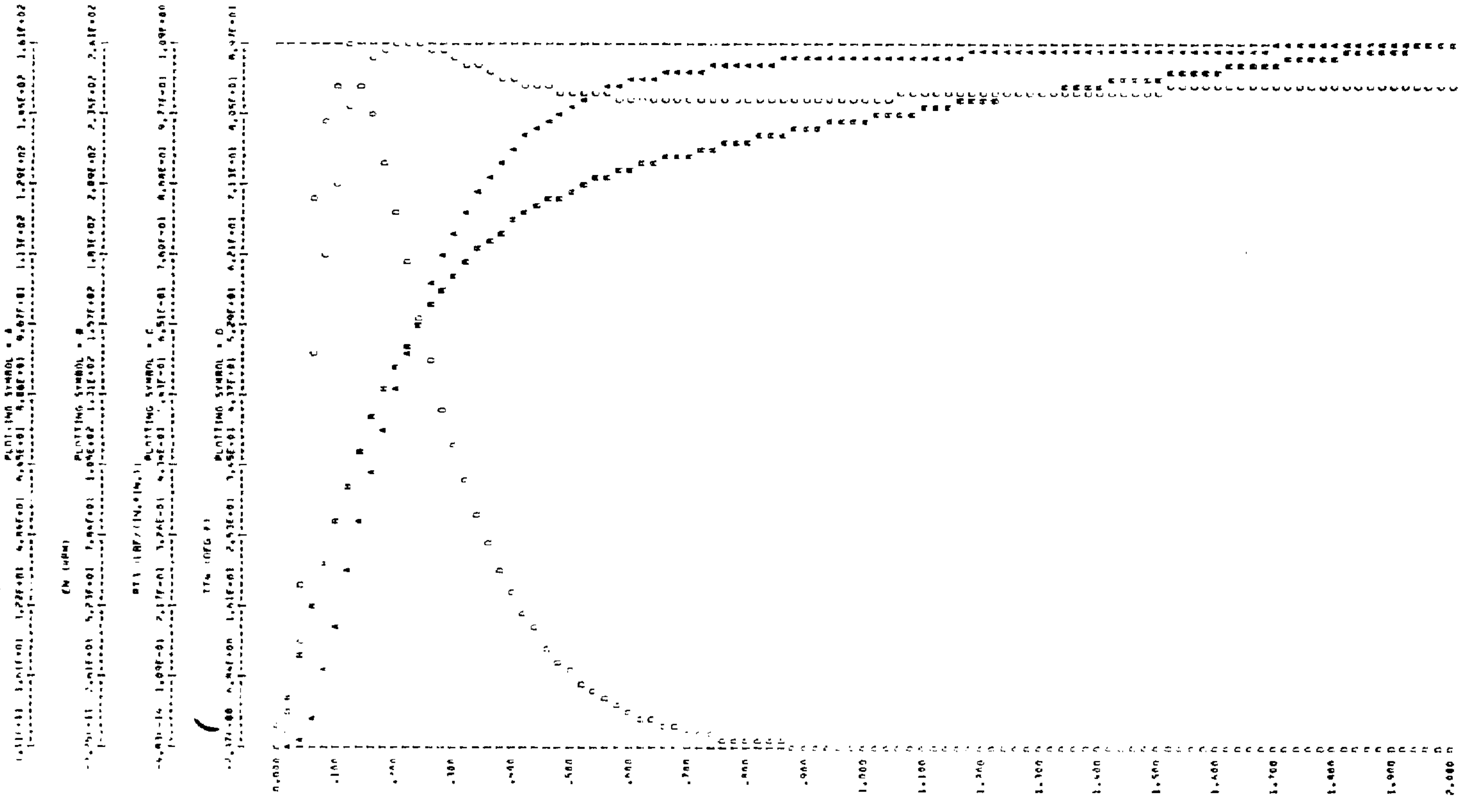

Figure 32a. Simplified Control--70-Percent Operating Condition--Equilibrium

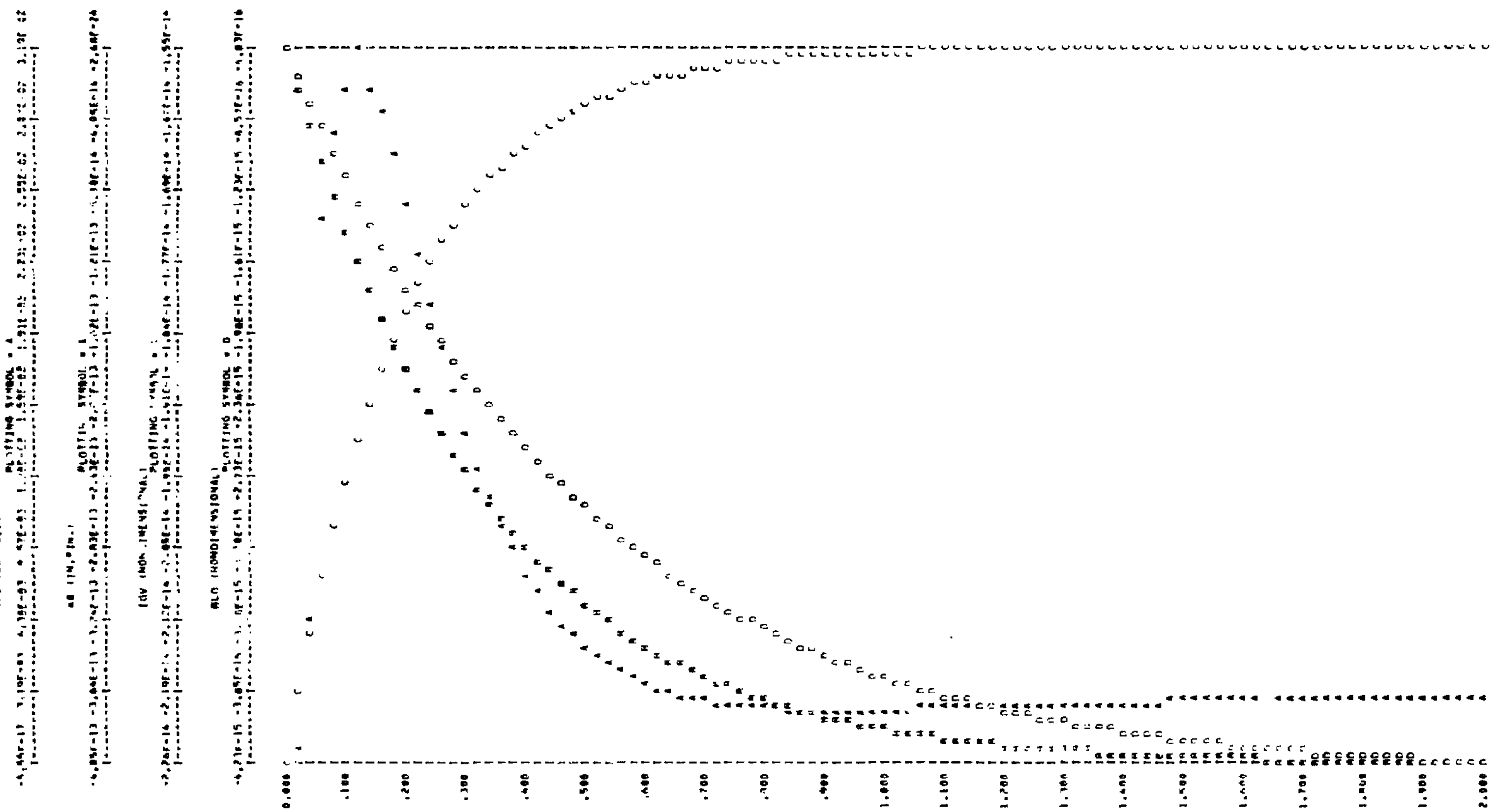

Figure 32b. Simplified Control--70-Percent Operating Condition--Equilibrium (Continued)

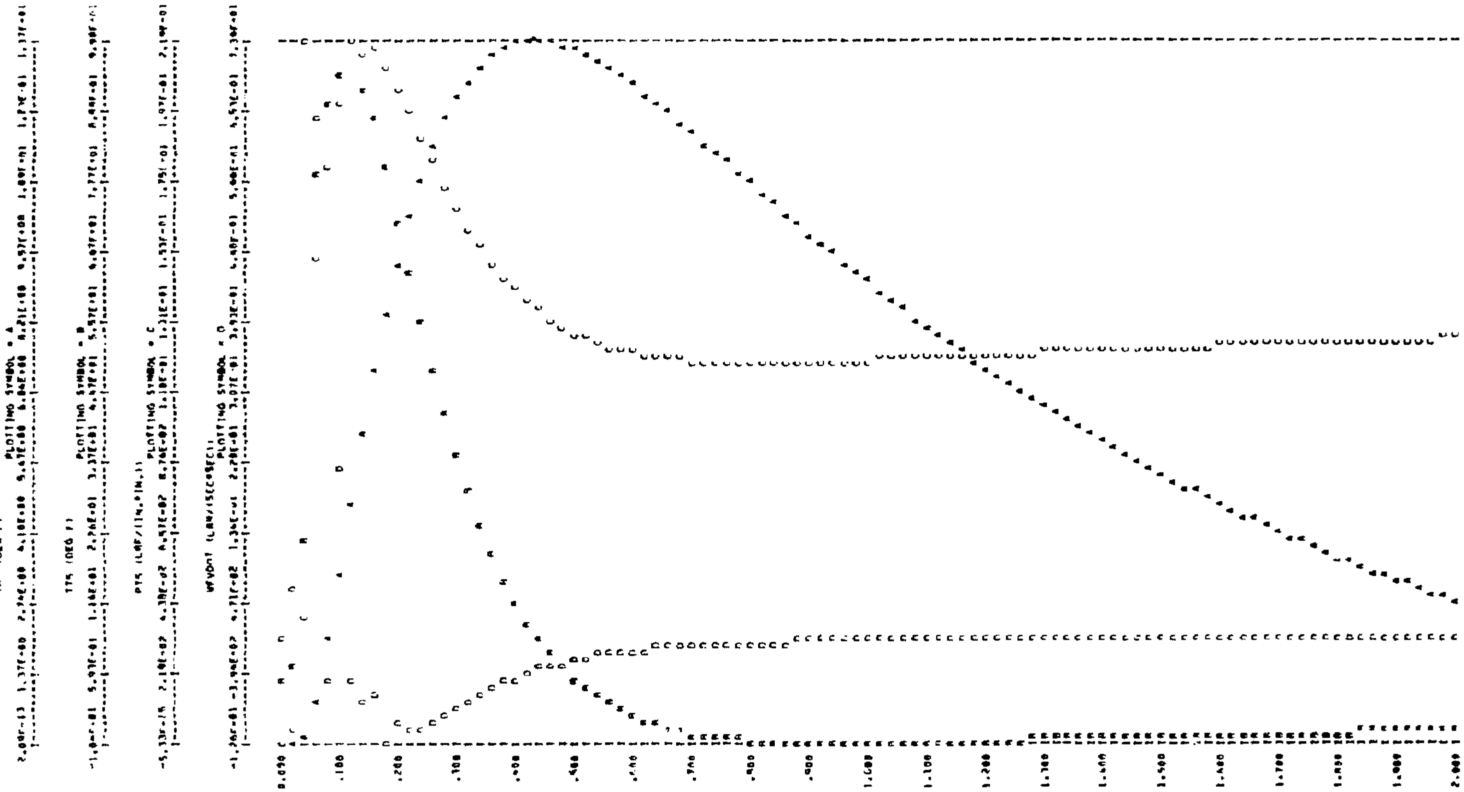

Figure 32c. Simplified Control--70-Percent Operating Condition--Equilibrium (Concluded)

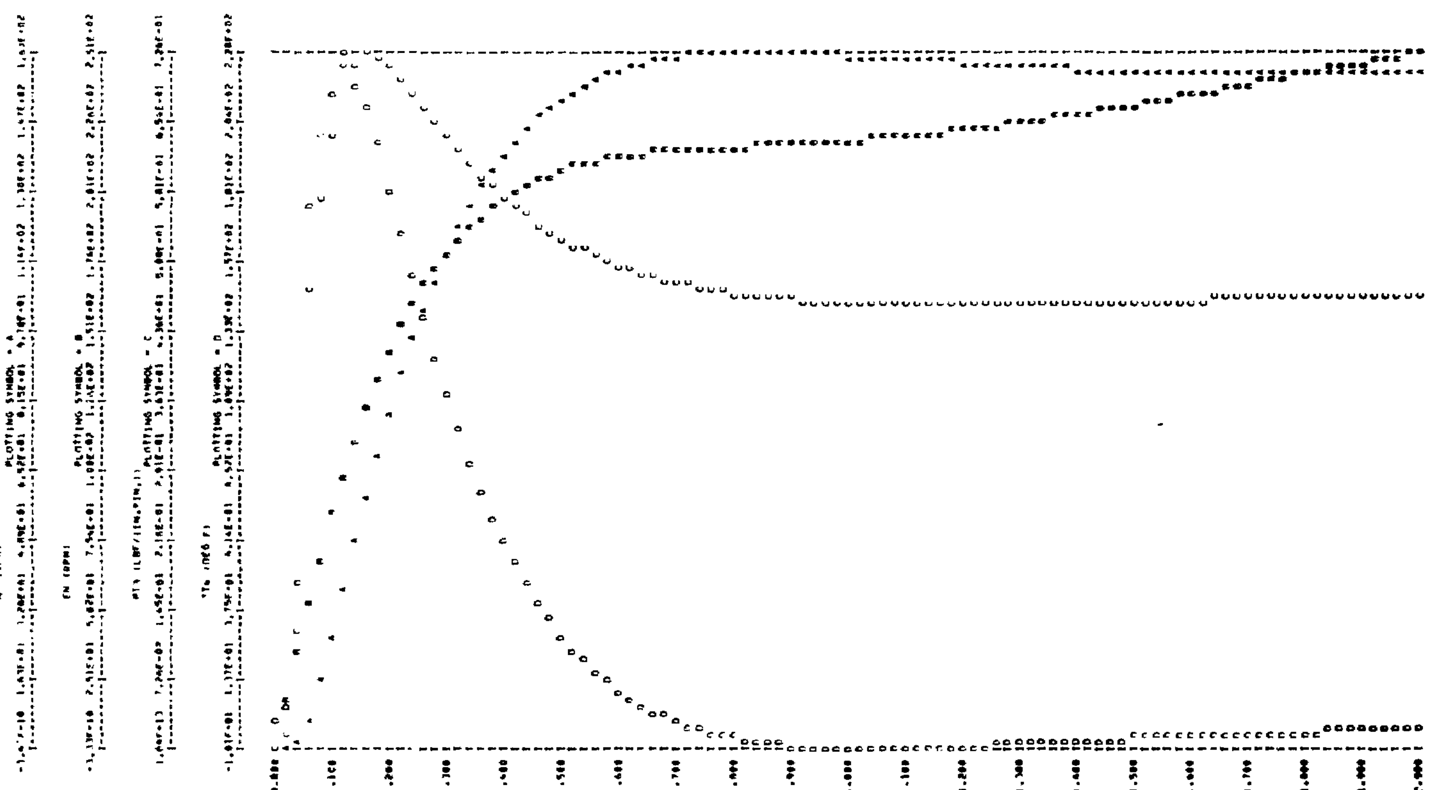

Figure 33a. Simplified Control--50-Percent Operating Condition--Equilibrium

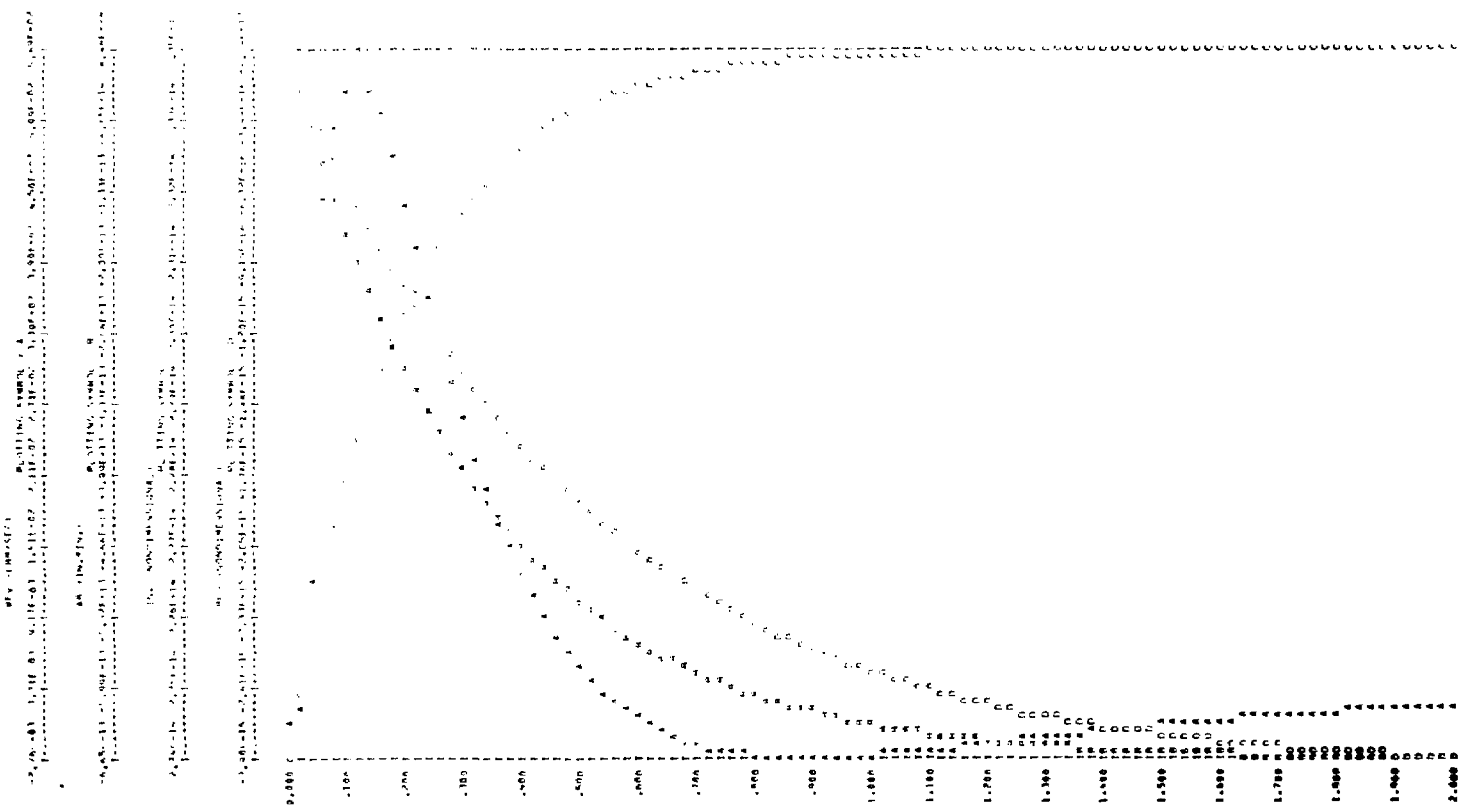

Figure 33b. Simplified Control--50-Percent Operating Condition--Equilibrium (Continued)

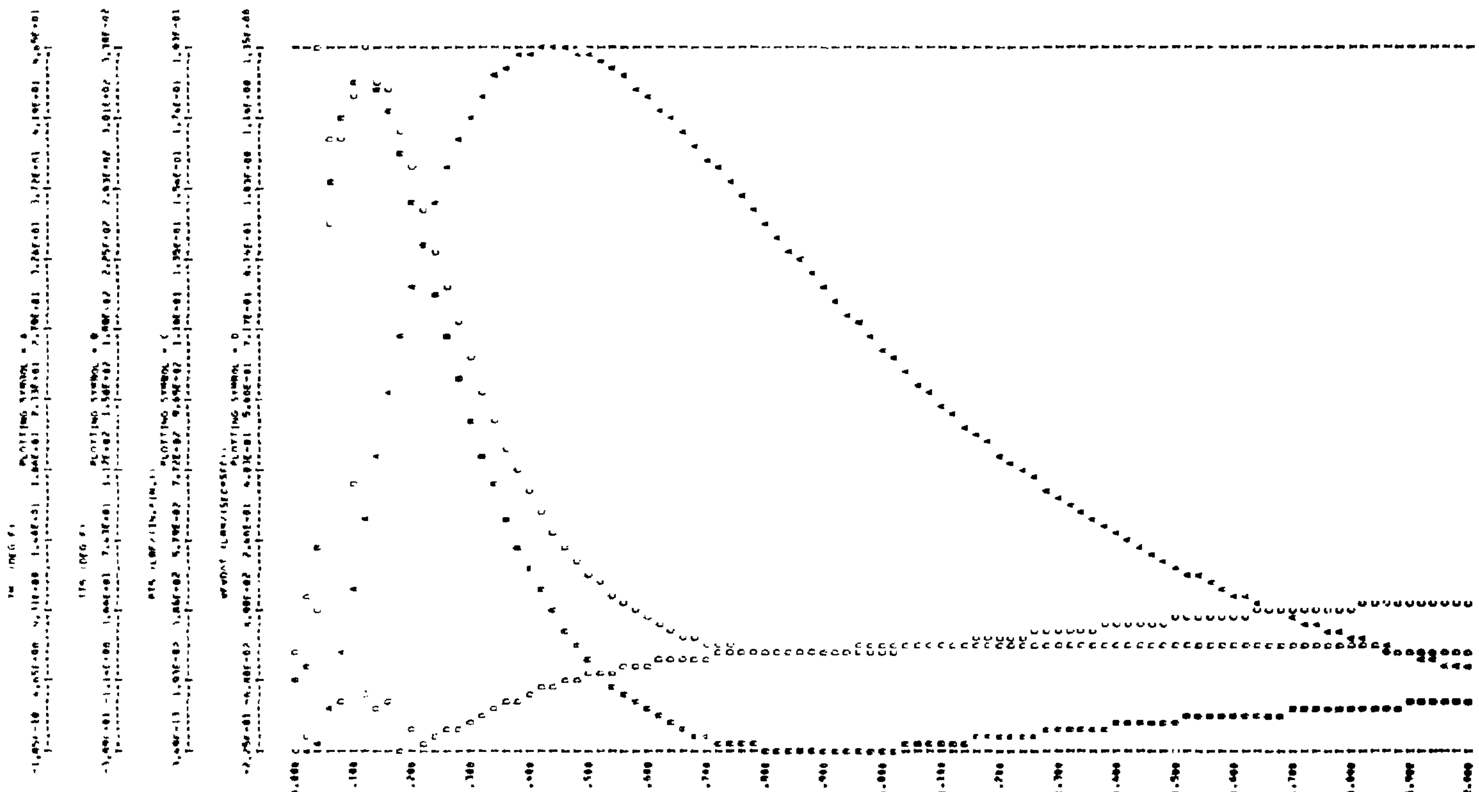

Figure 33c. Simplified Control--50-Percent Operating Condition--Equilibrium (Concluded)

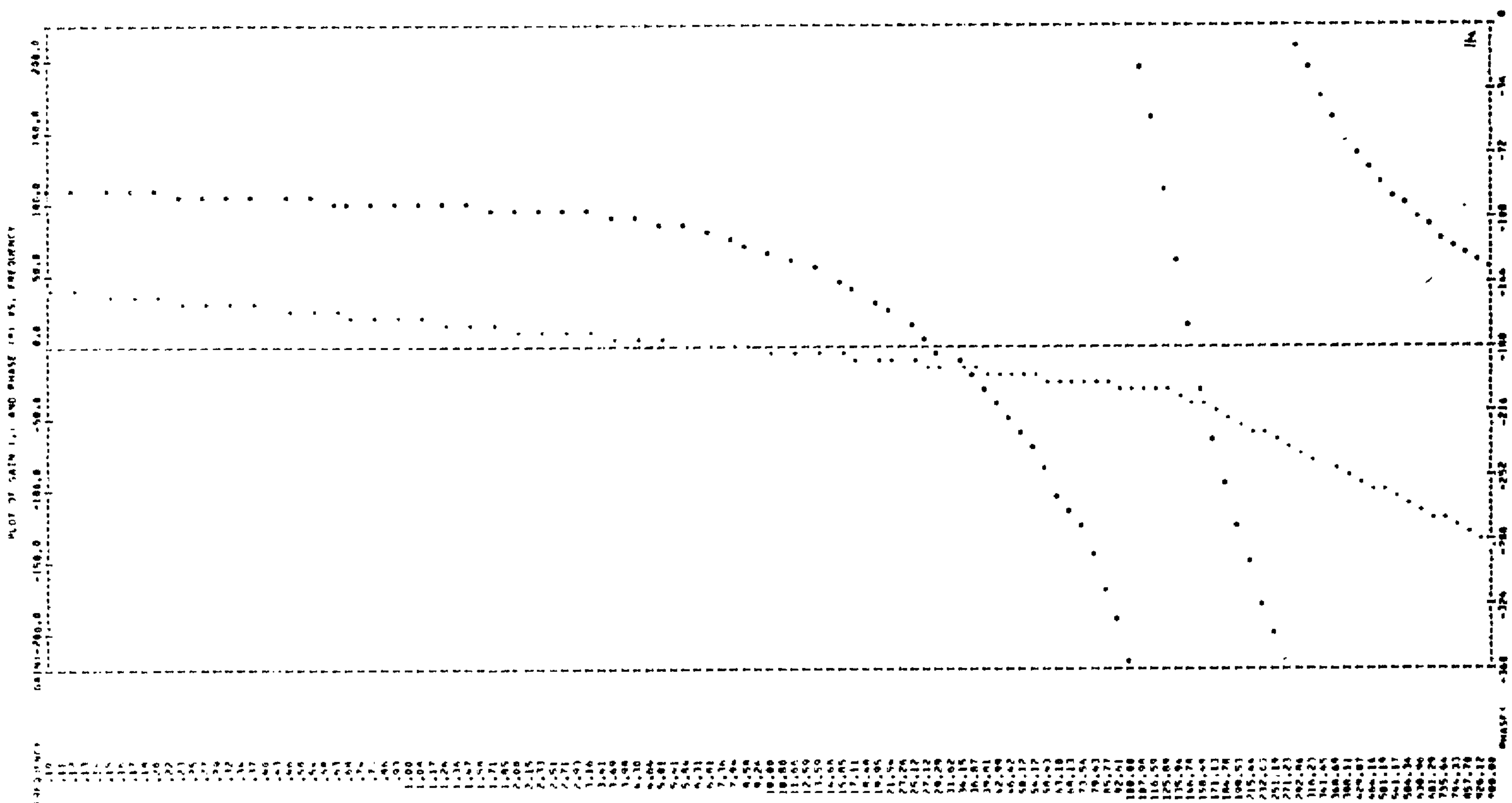

Figure 34a. Actuator Open Loop--100-Percent Operating Condition--Equilibrium

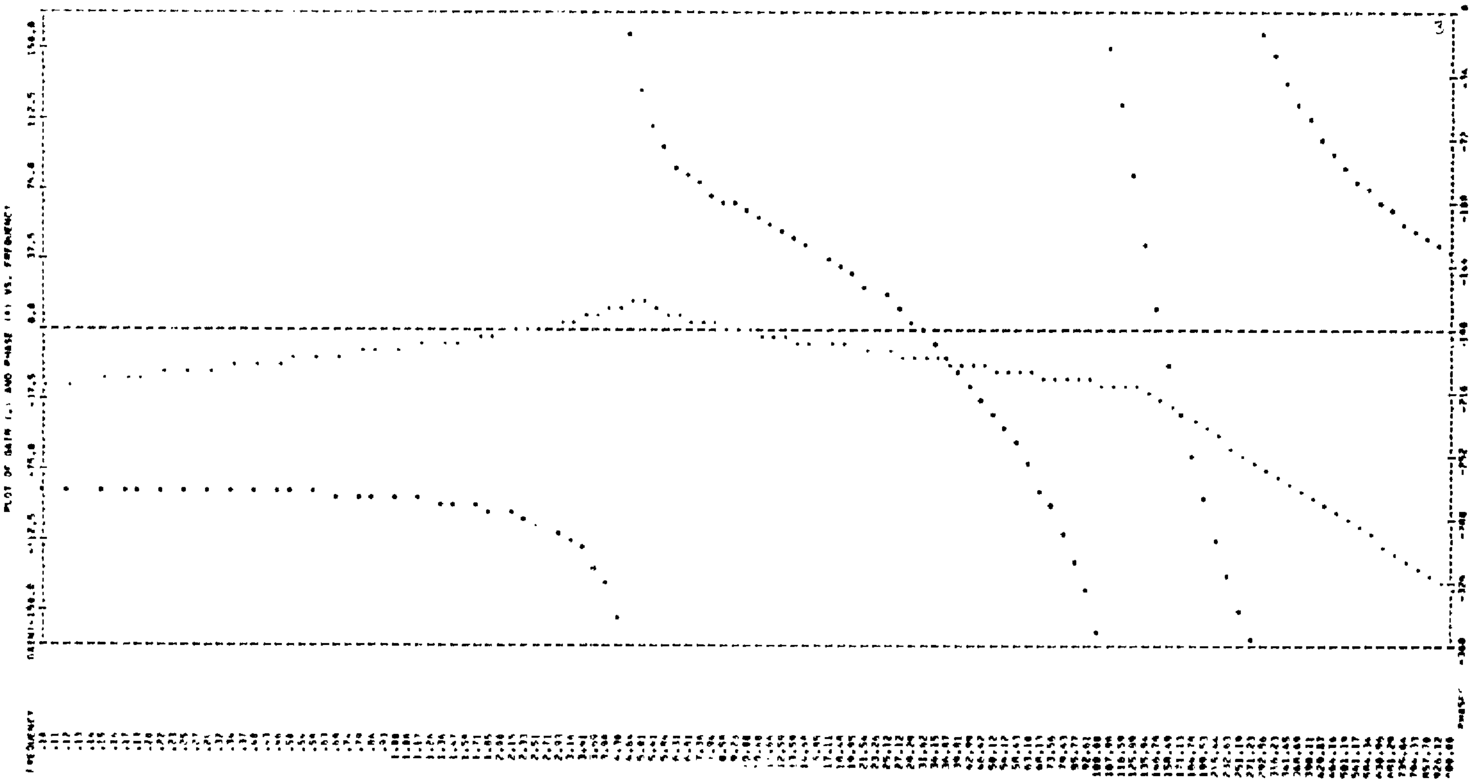

Figure 34b. N Open Loop--100-Percent Operating Condition--Equilibrium

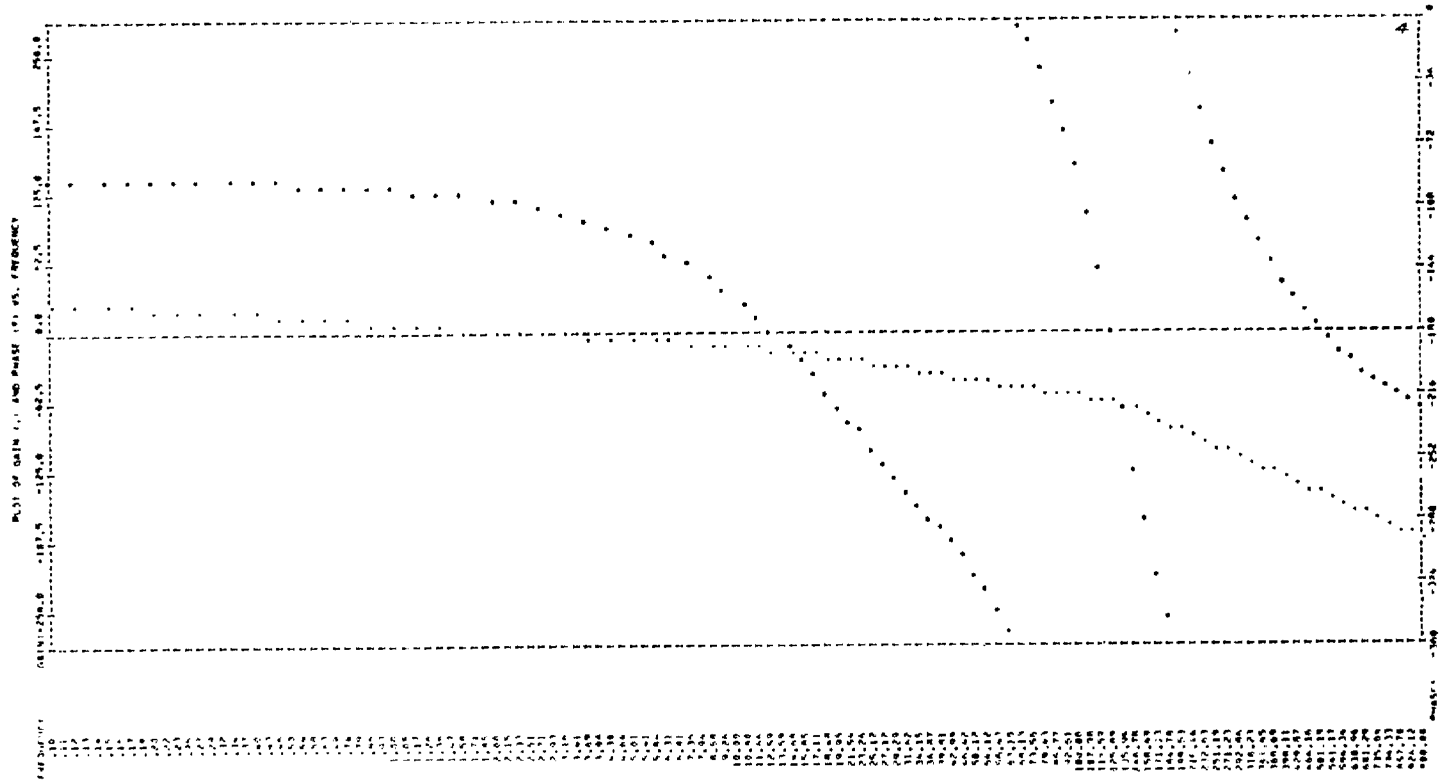

Figure 34c. EN Open Loop--100-Percent Operating Condition--Equilibrium

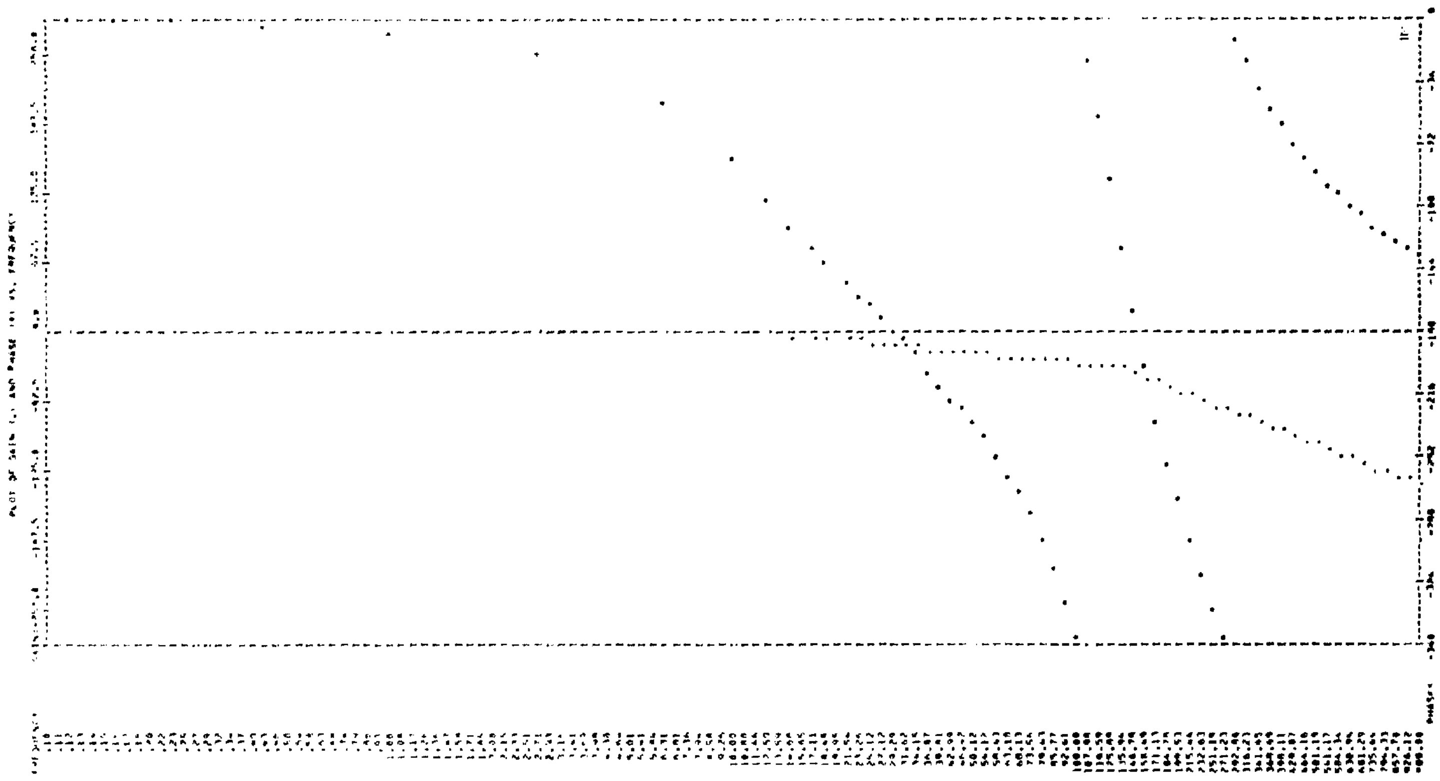

Figure 34d. Closed-Loop--100-Percent Operating Condition--Equilibrium

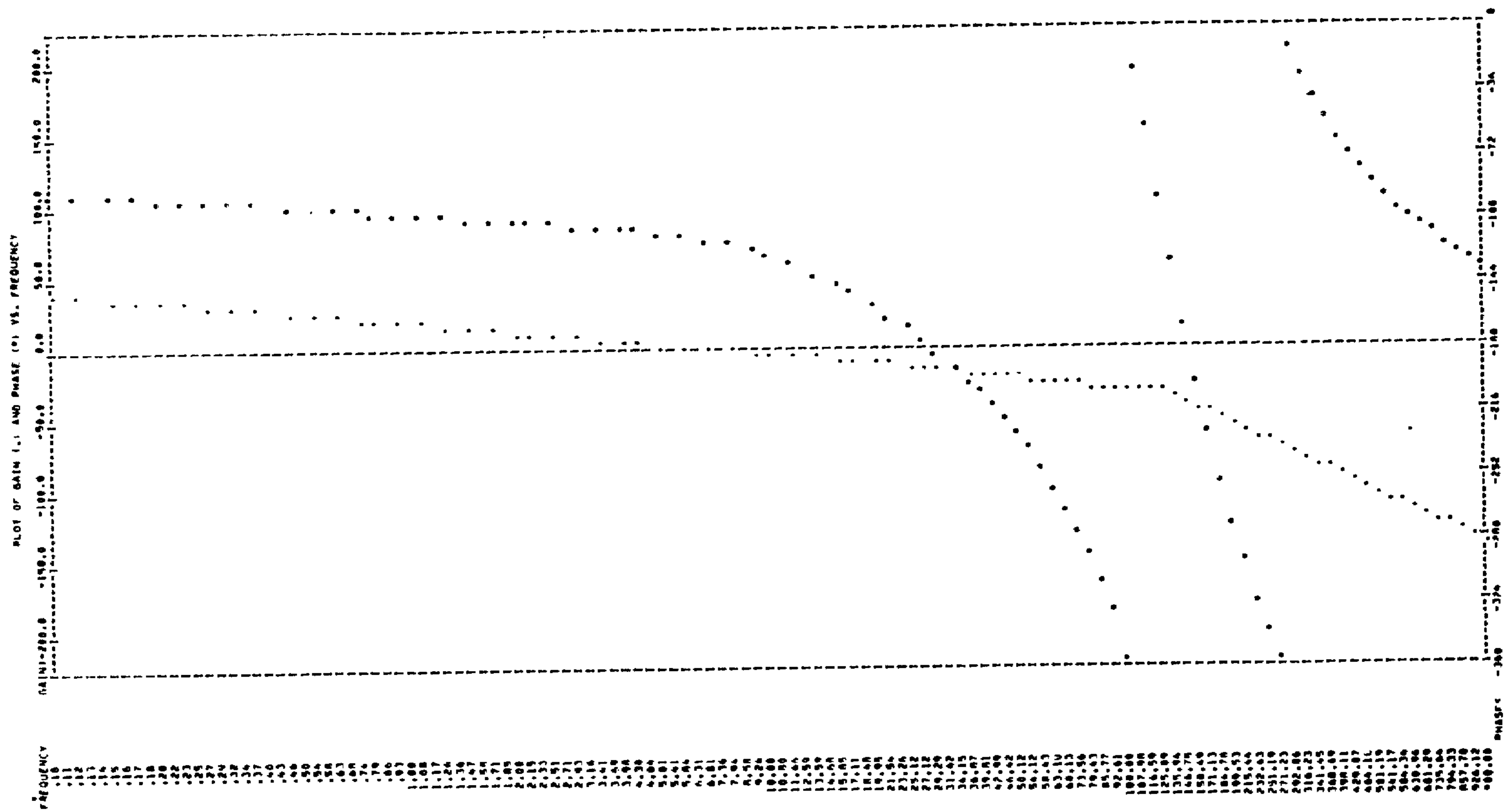

Figure 35a. Actuator Open Loop--85-Percent Operating Condition--Equilibrium

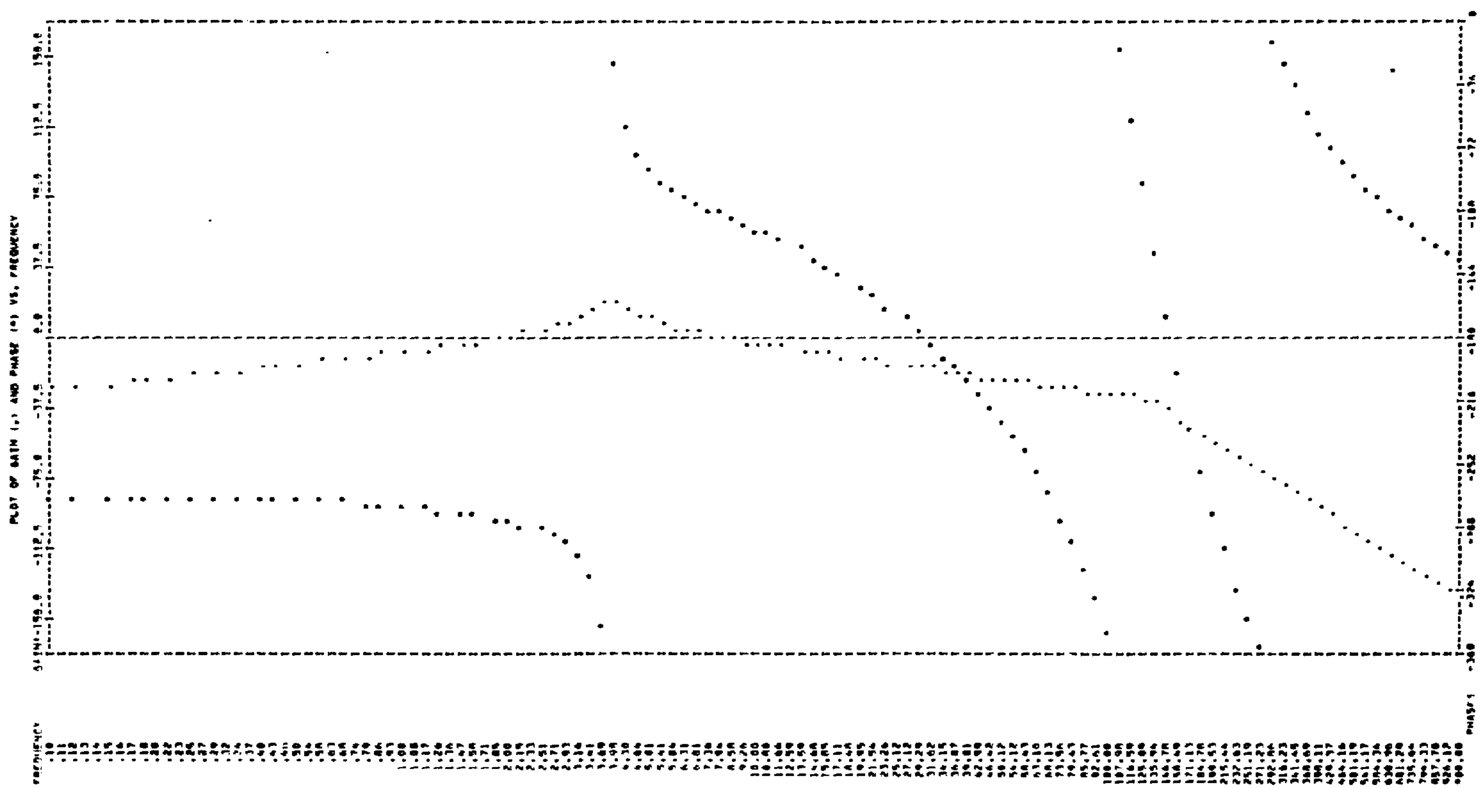

Figure 35b. N Open Loop--85-Percent Operating Condition--Equilibrium

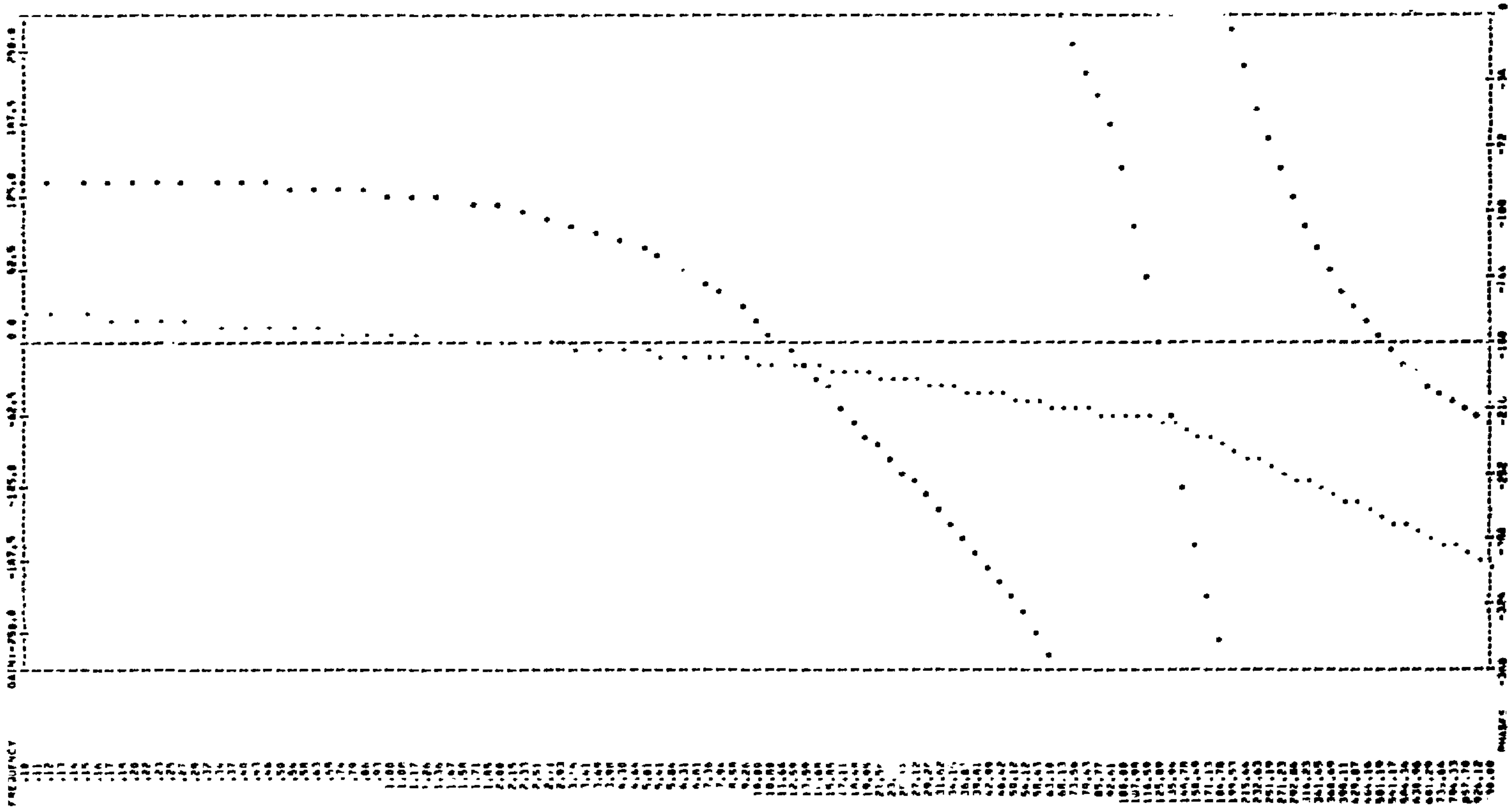

Figure 35c. EN Open Loop--85-Percent Operating Condition--Equilibrium

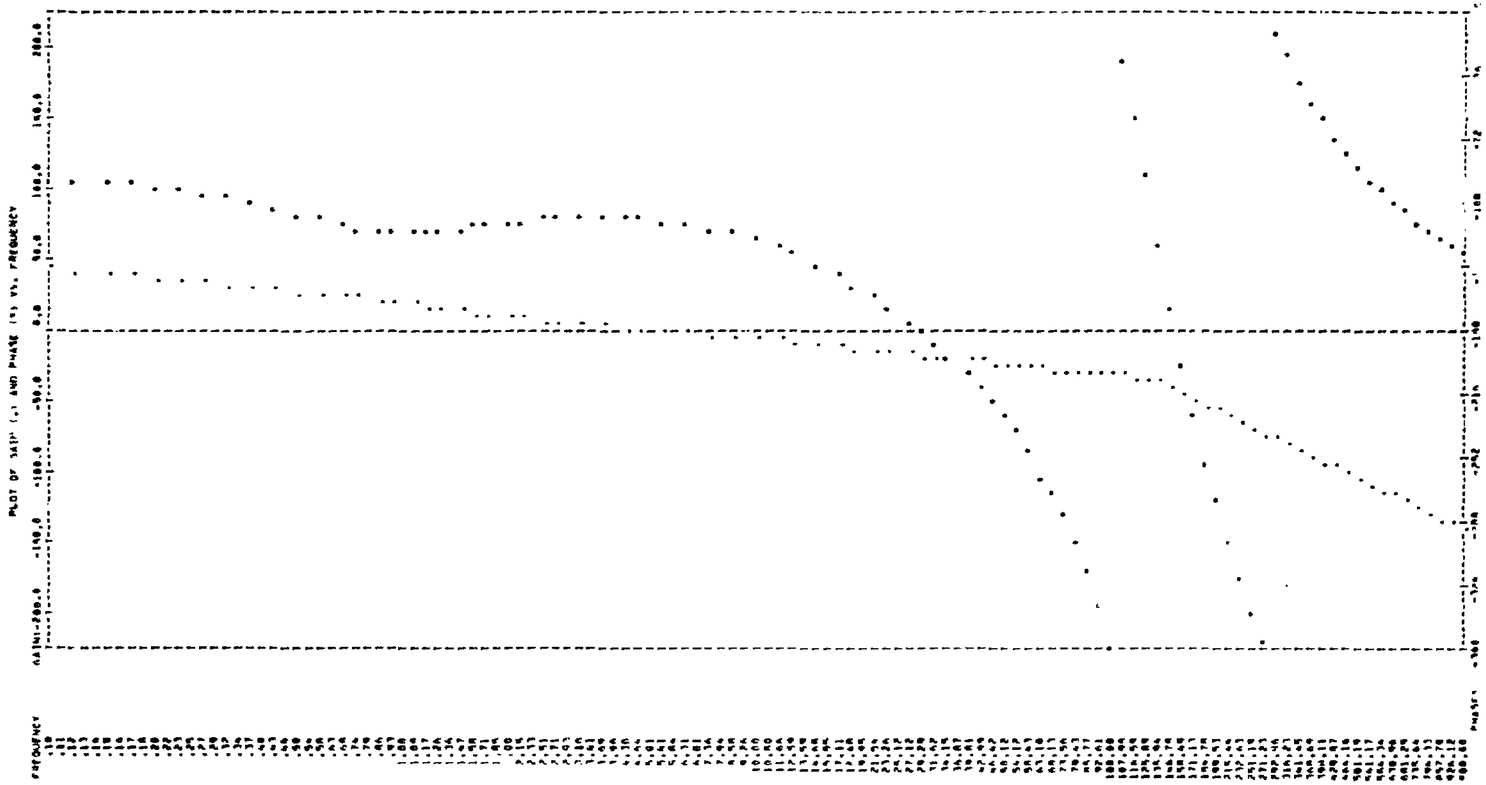

Figure 36a. Actuator Open Loop--70-Percent Operating Condition--Equilibrium

Figure 36b. N Open Loop--70-Percent Operating Condition--Equilibrium

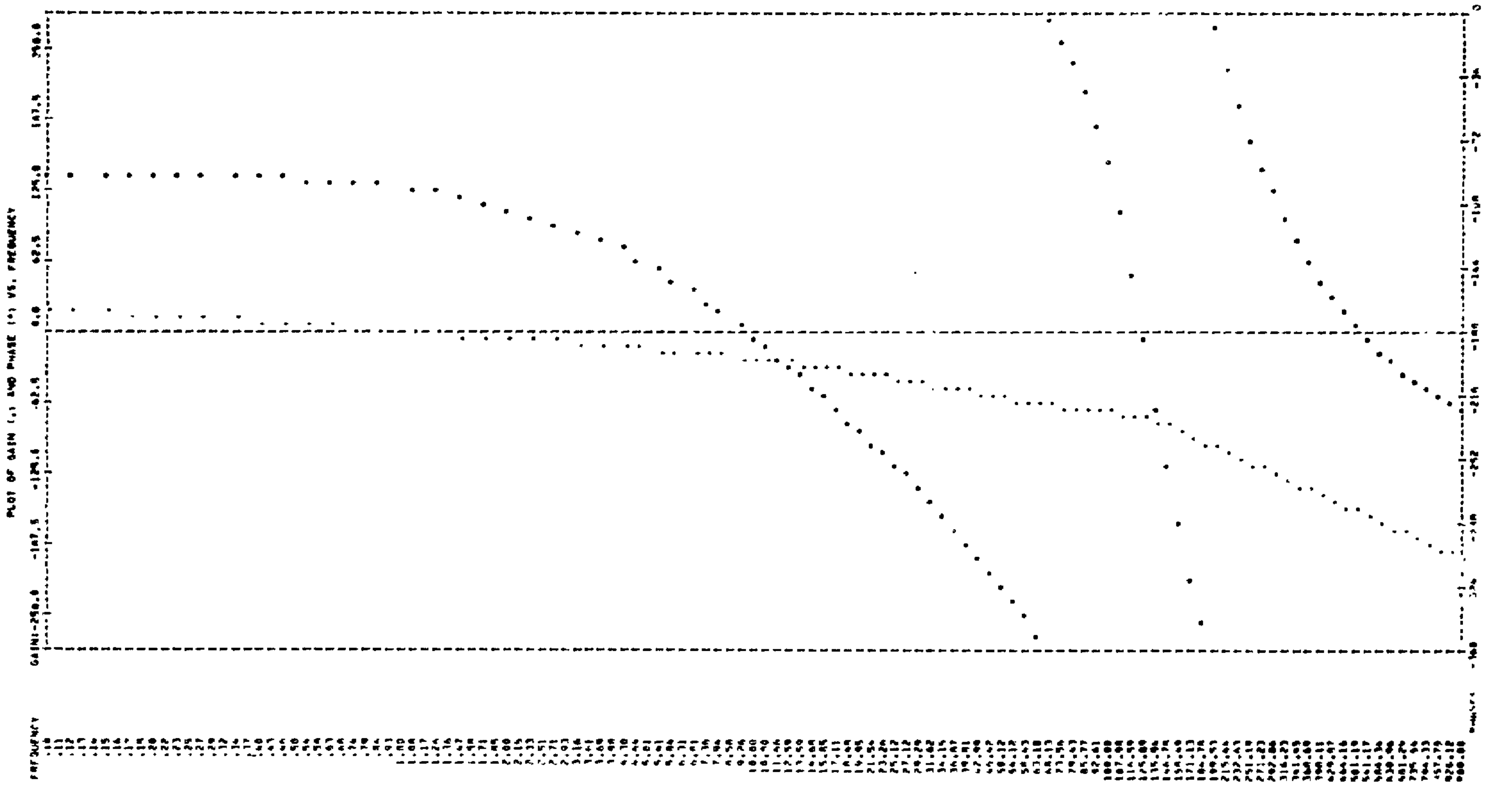

Figure 36c. EN Open Loop--70-Percent Operating Condition--Equilibrium

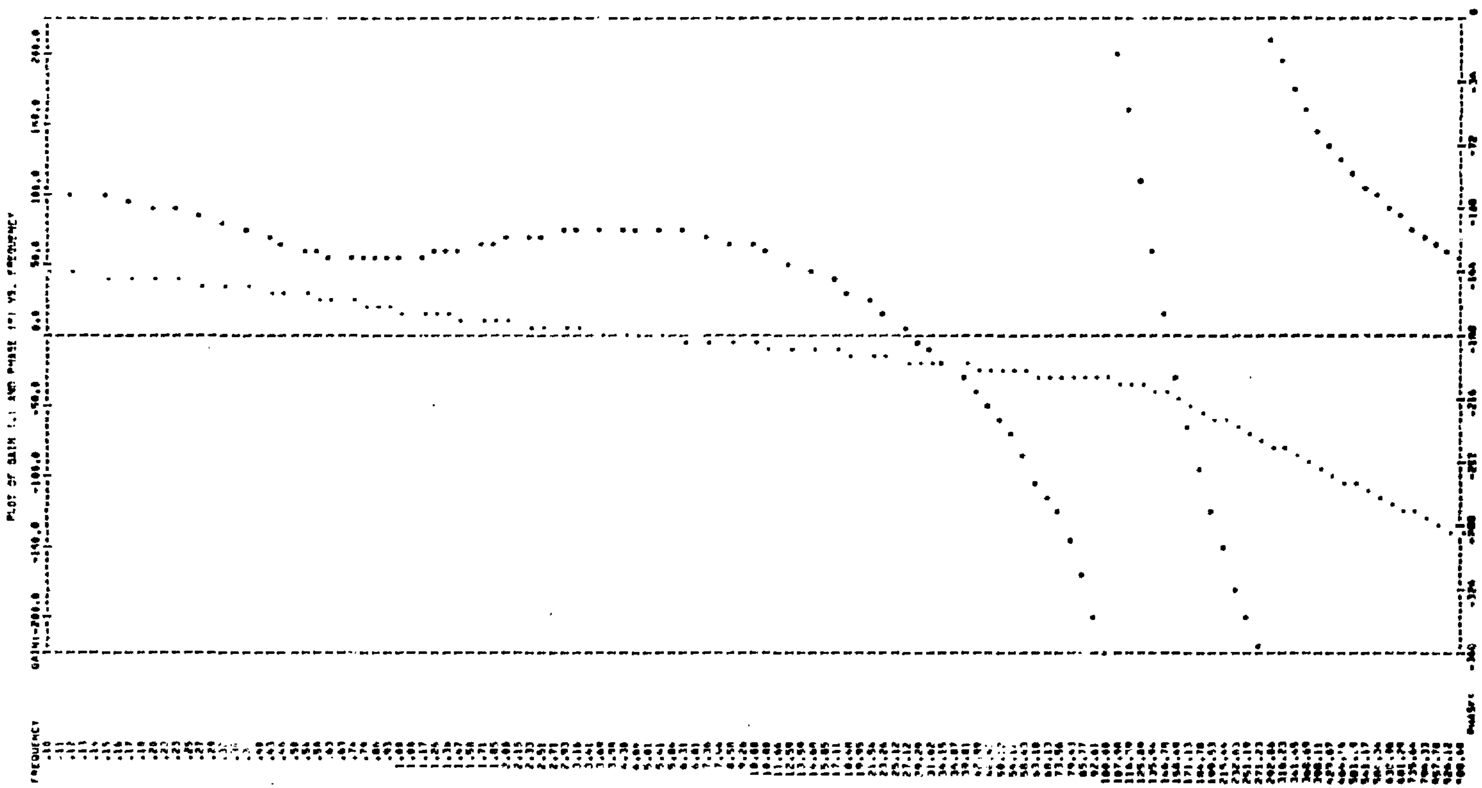

Figure 37a. Actuator Open Loop--50-Percent Operating Condition--Equilibrium

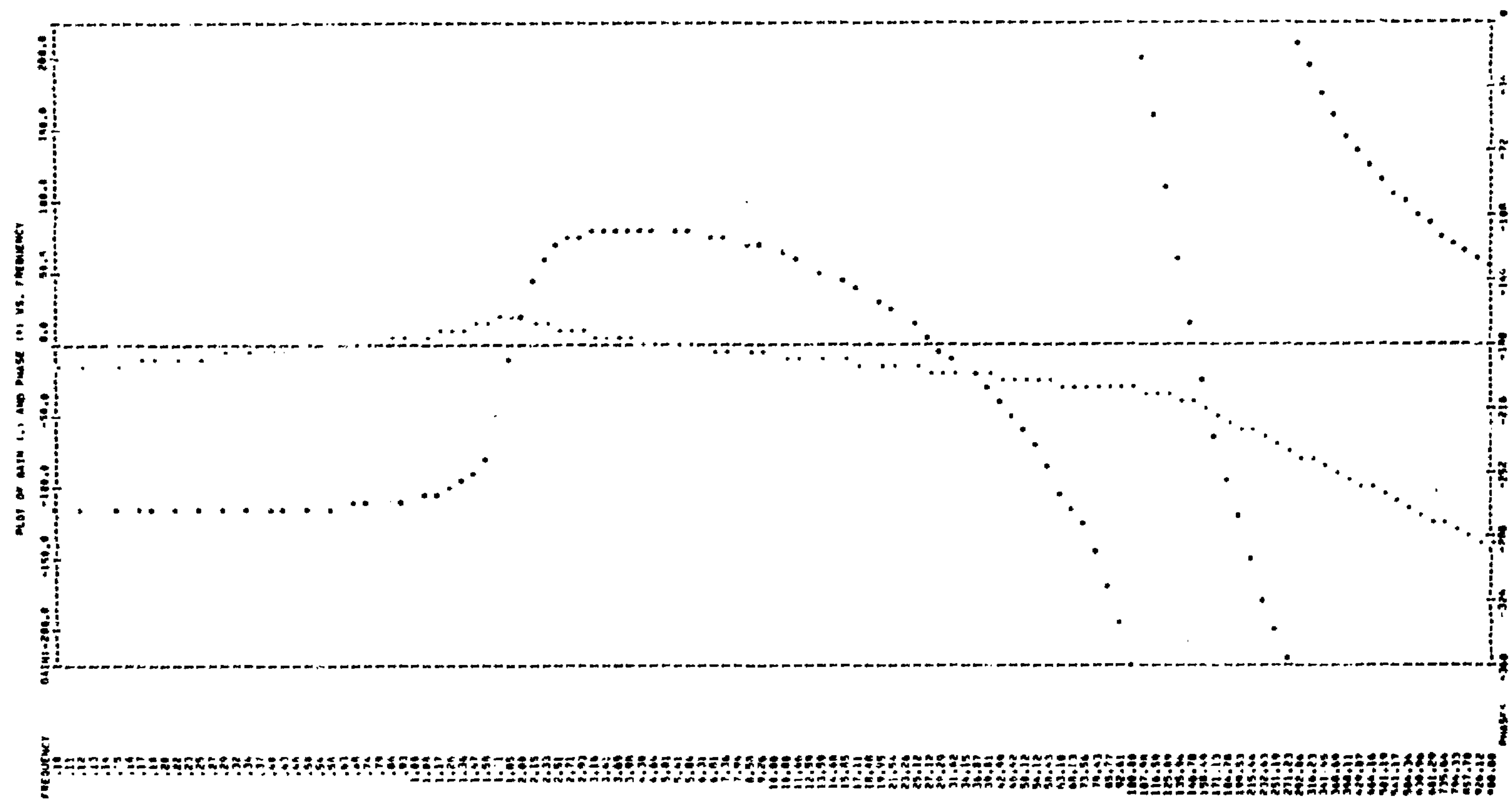

Figure 37b. N Open Loop--50-Percent Operating Condition--Equilibrium

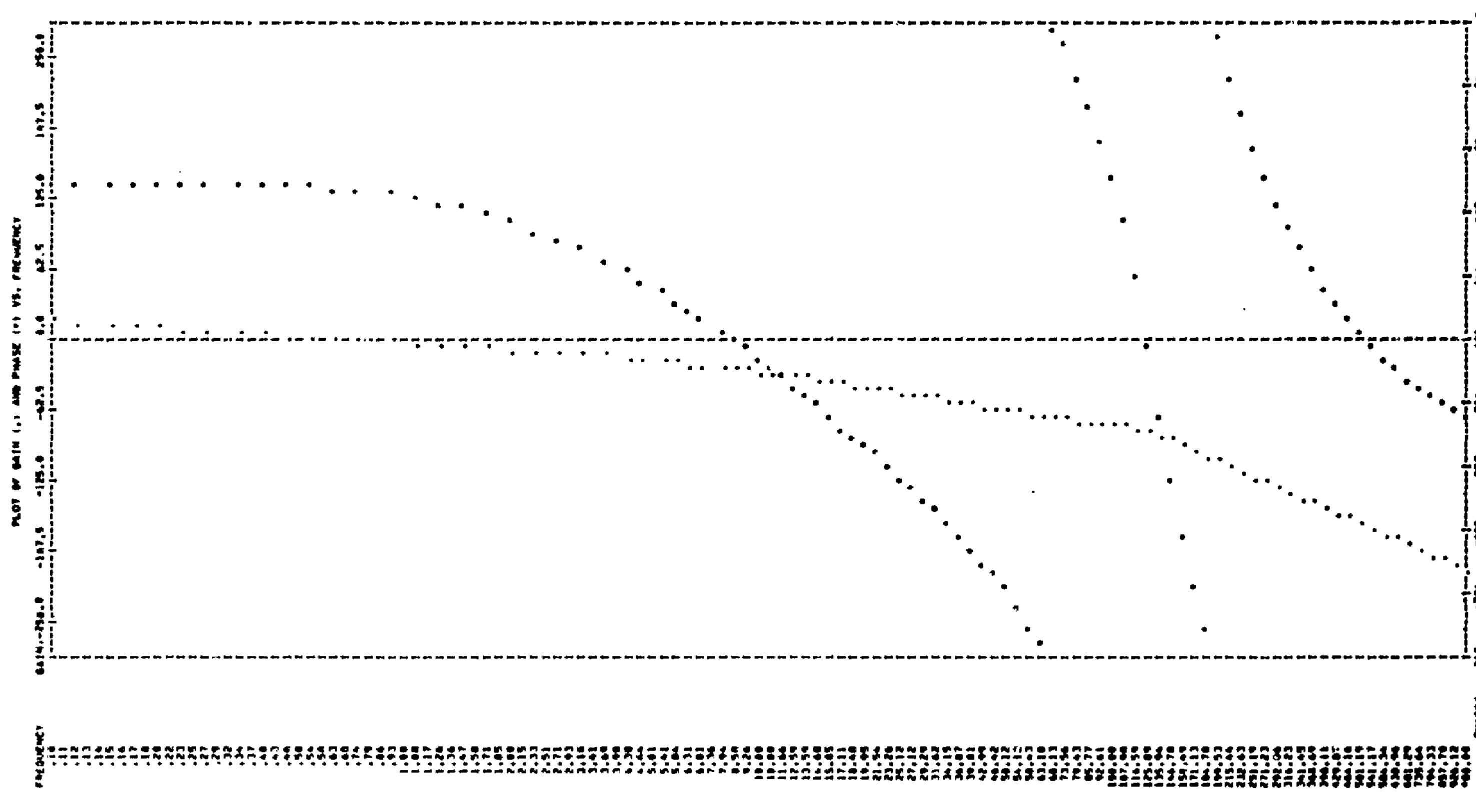

Figure 37c. EN Open Loop--50-Percent Operating Condition--Equilibrium

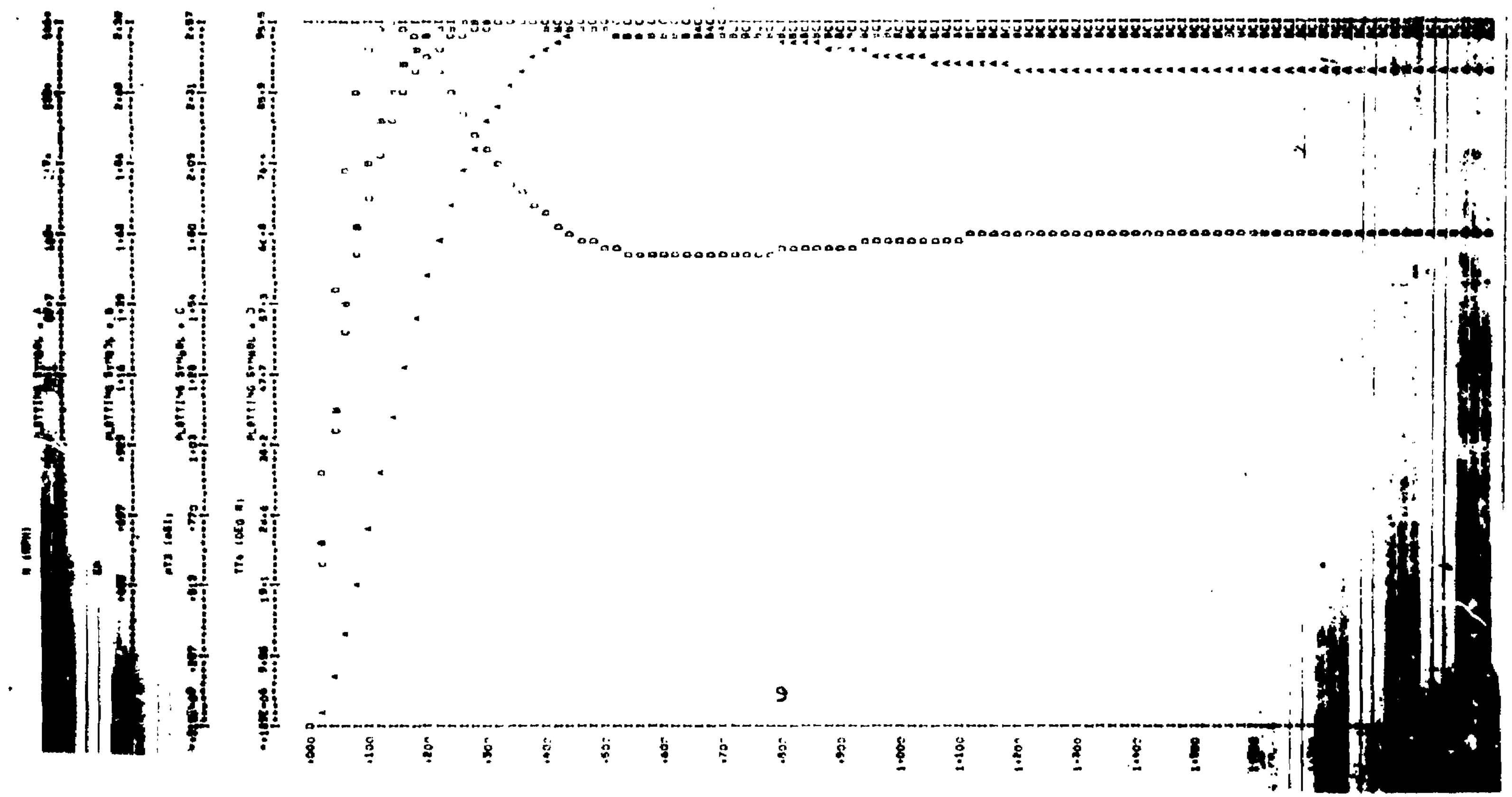

Figure 38. State Control--100-Percent Operating Condition--Pressure

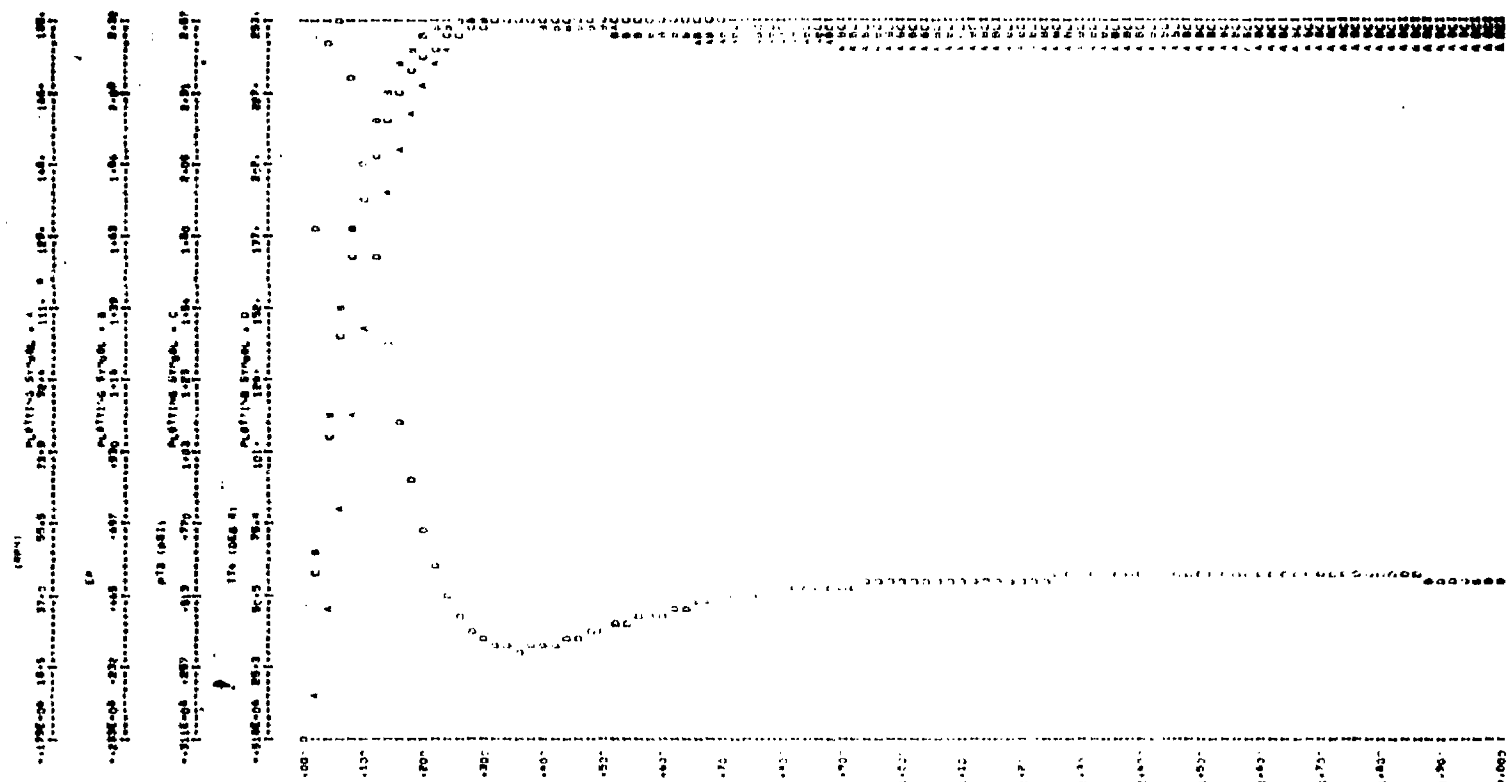

Figure 39. State Control--85-Percent Operating Condition--Pressure

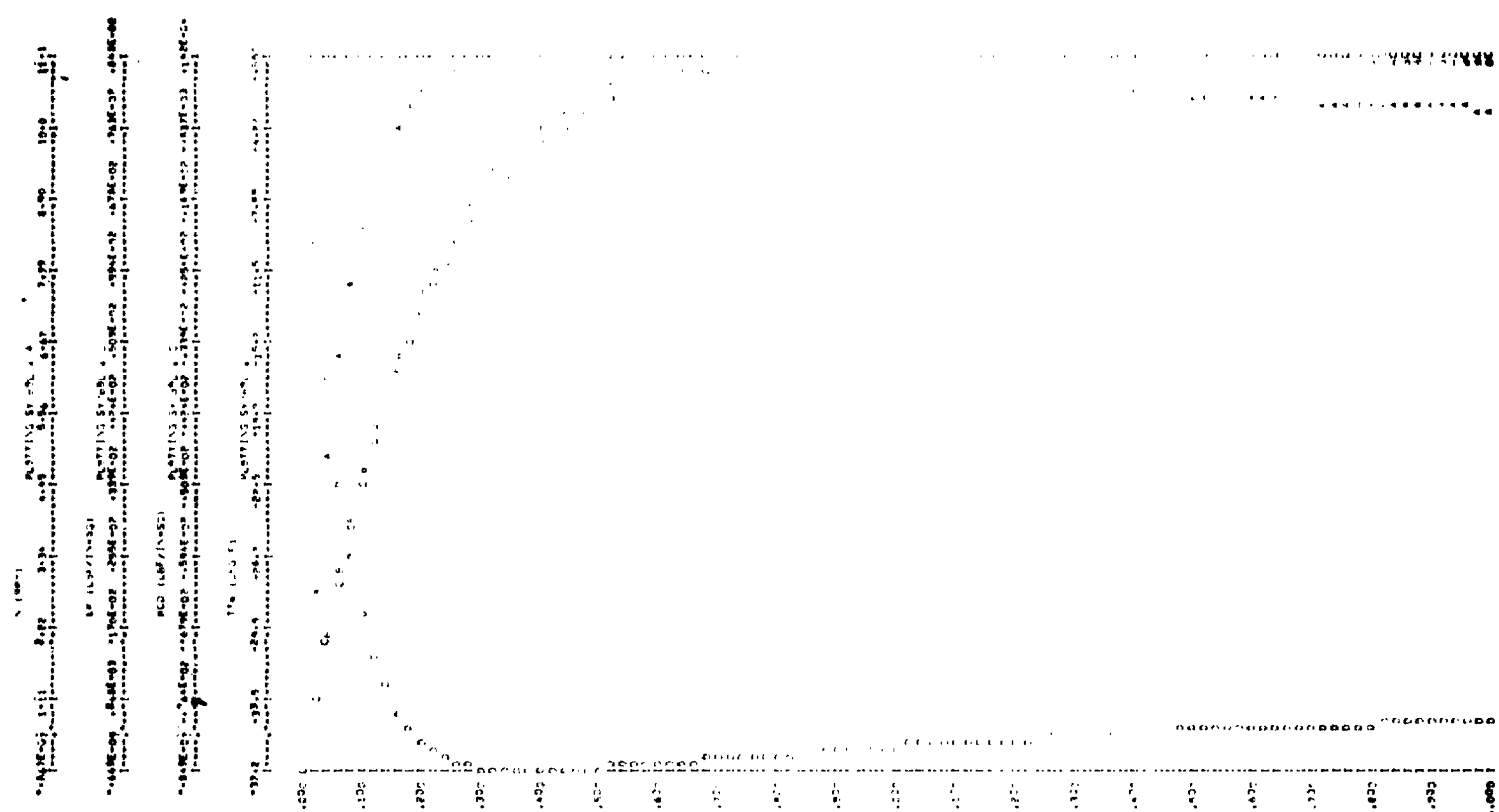

Figure 40. State Control--70-Percent Operating Condition--Pressure

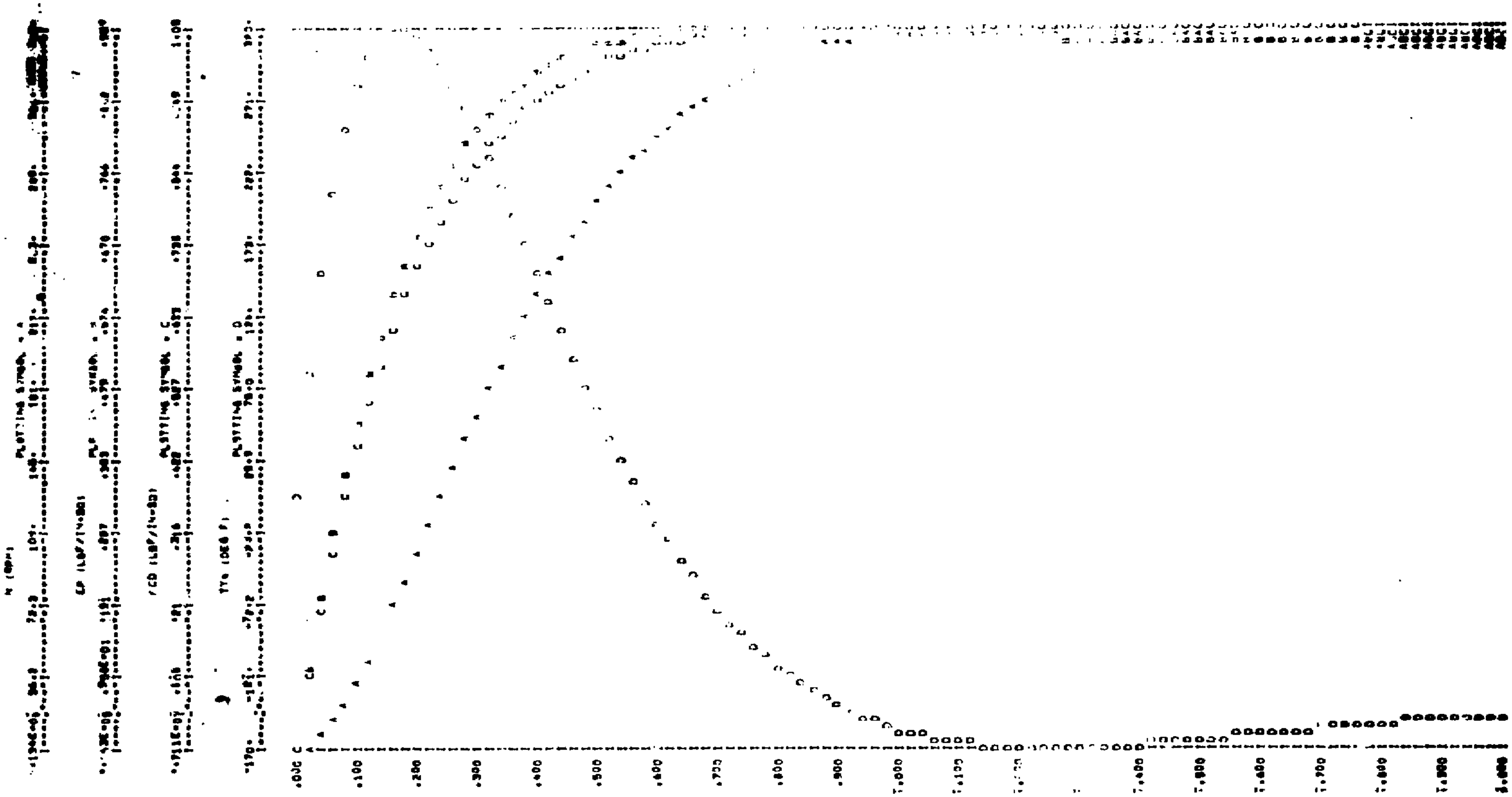

Figure 41. State Control--50-Percent Operating Condition--Pressure

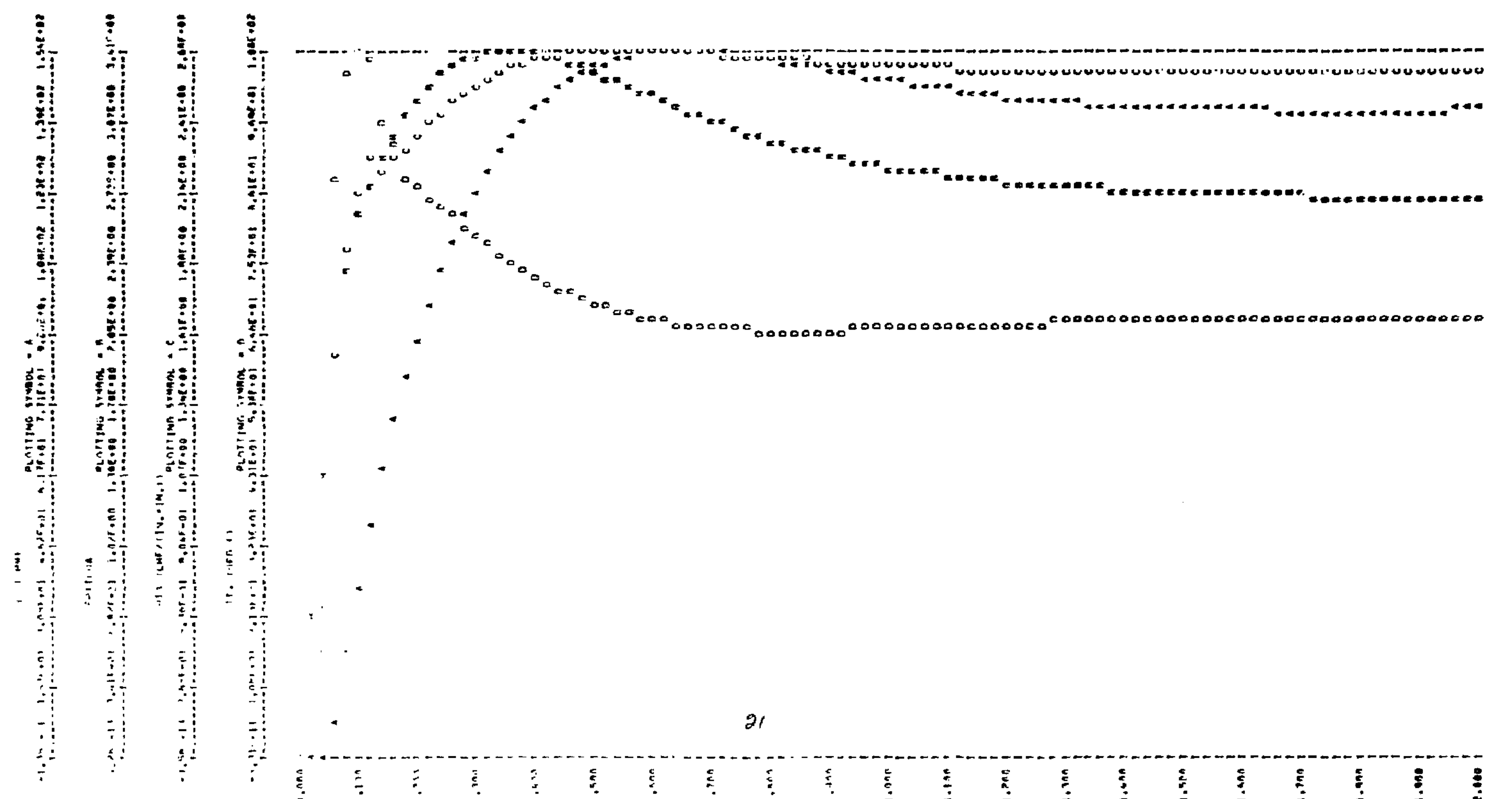

Figure 42a. Simplified Control--100-Percent Operating Condition--Pressure

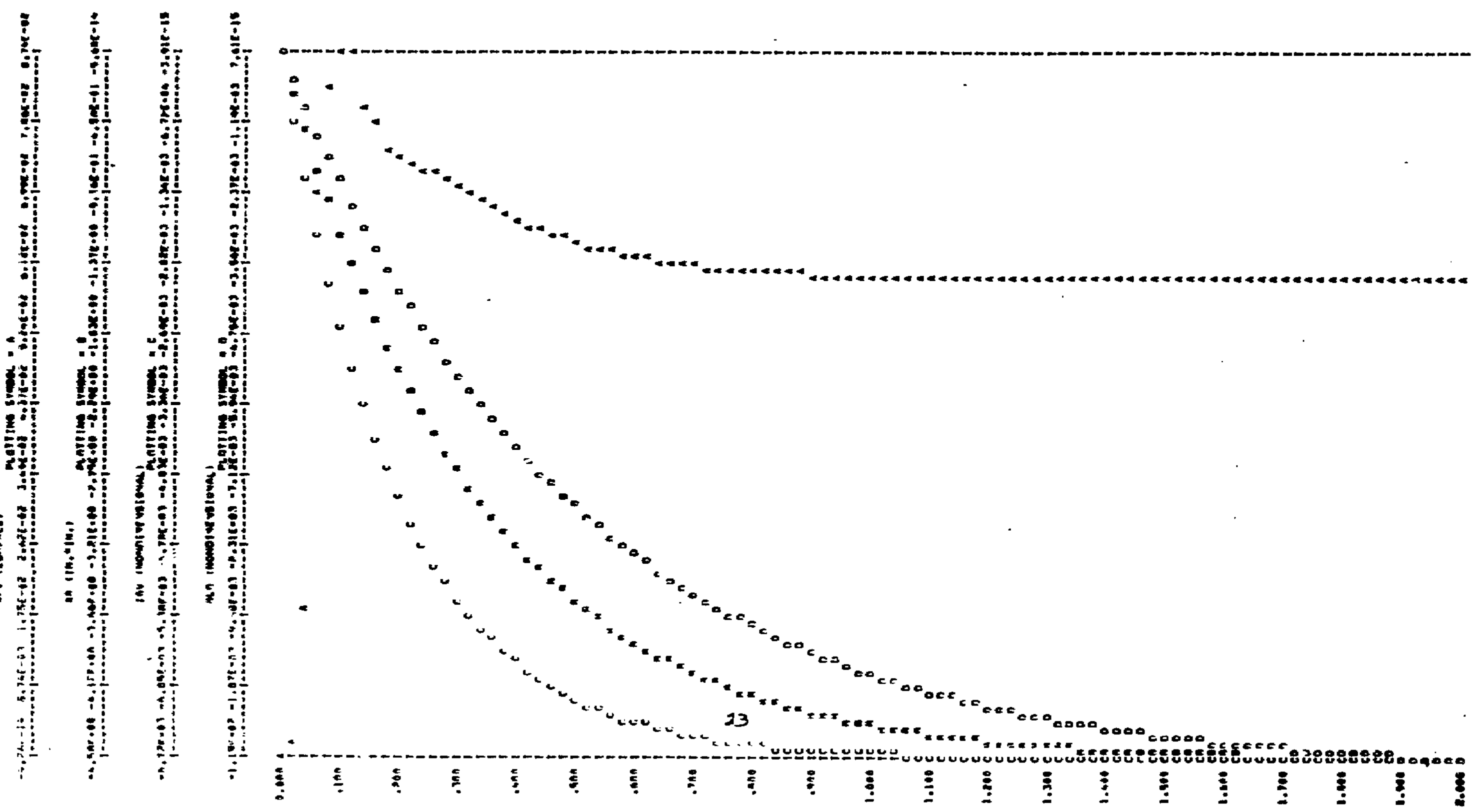

Figure 42b. Simplified Control--100-Percent Operating Condition--Pressure (Continued)

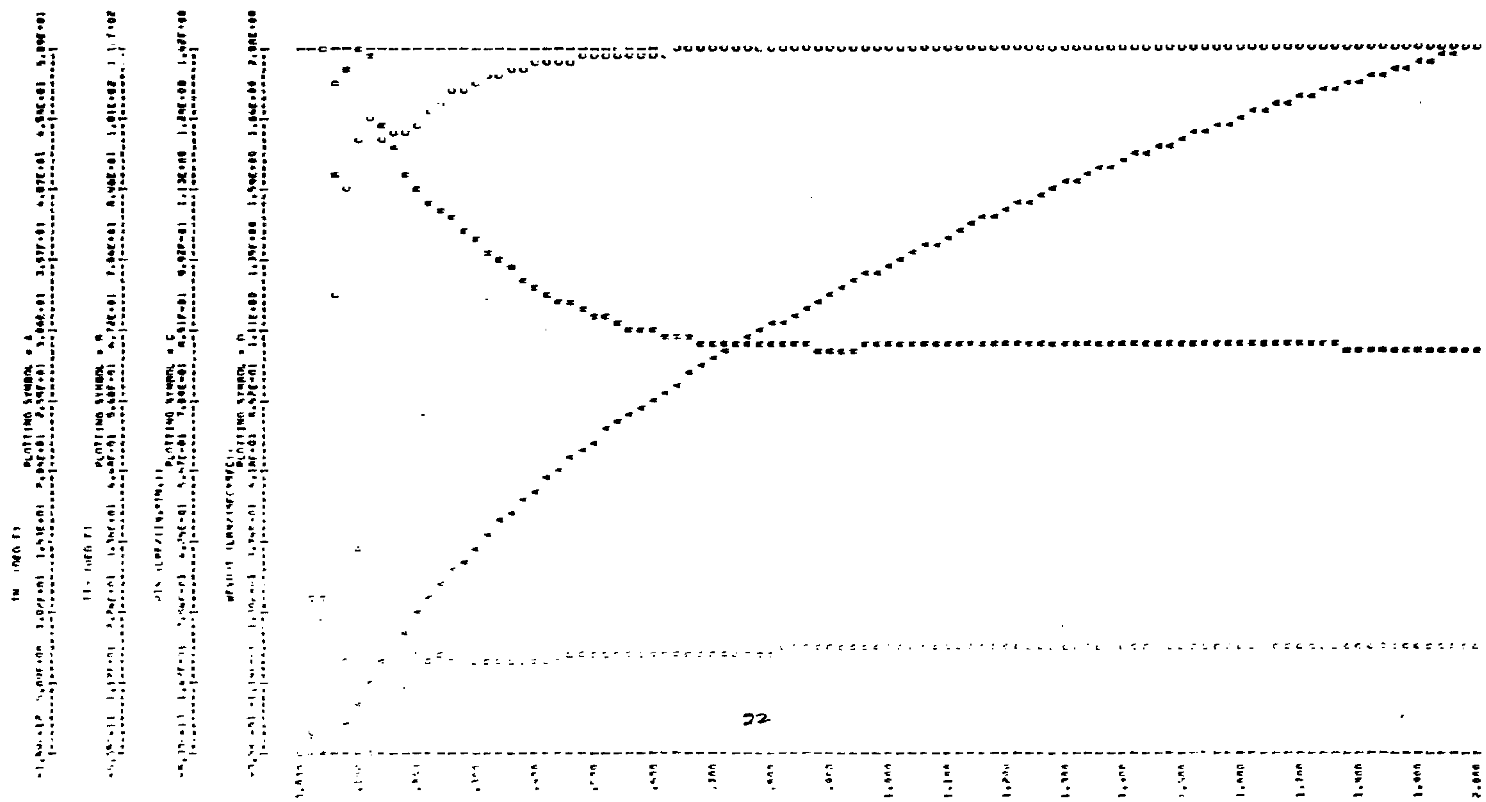

Figure 42c. Simplified Control--100-Percent Operating Condition--Pressure (Concluded)

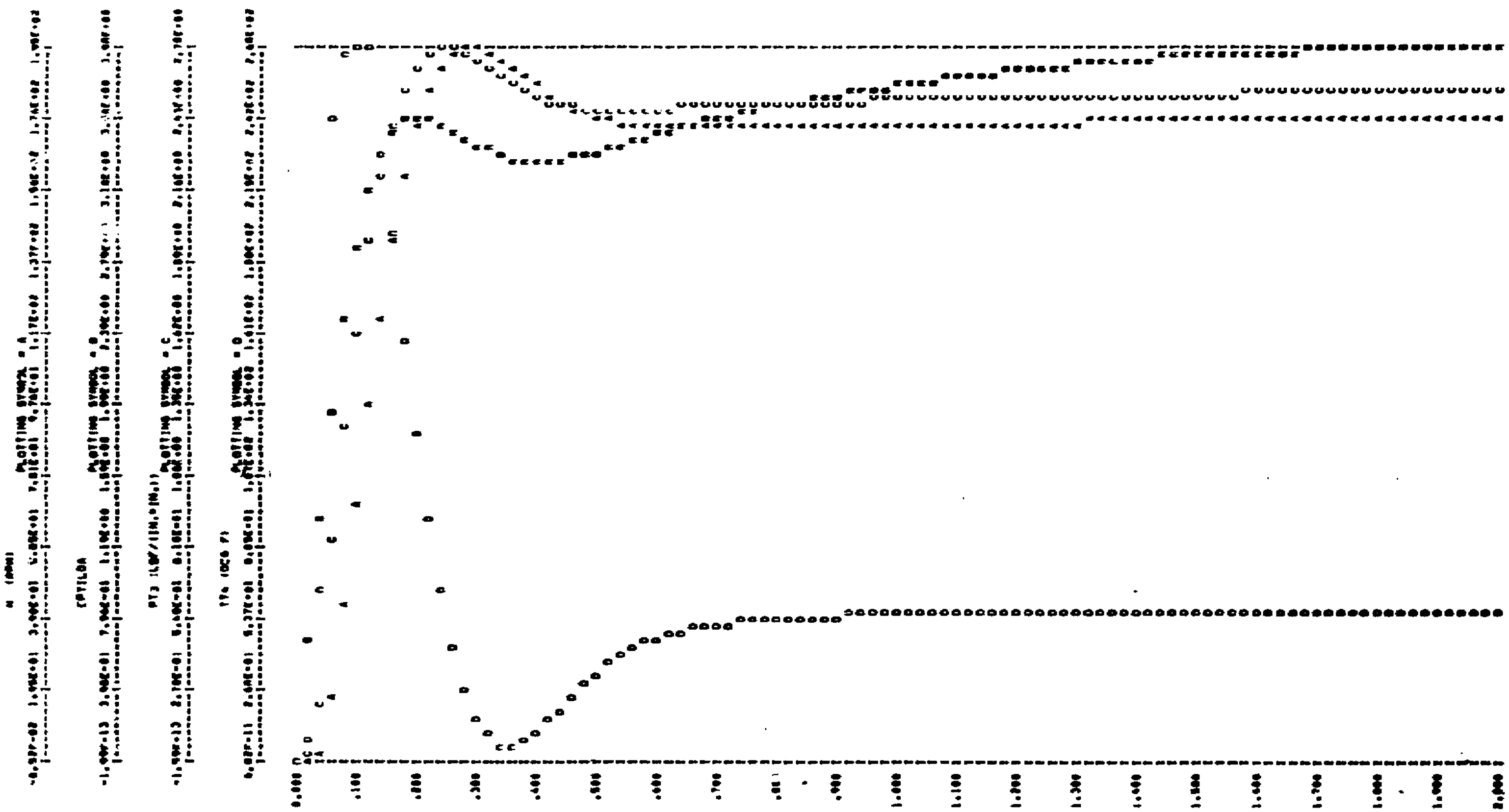

Figure 43a. Simplified Control--85-Percent Operating Condition--Pressure

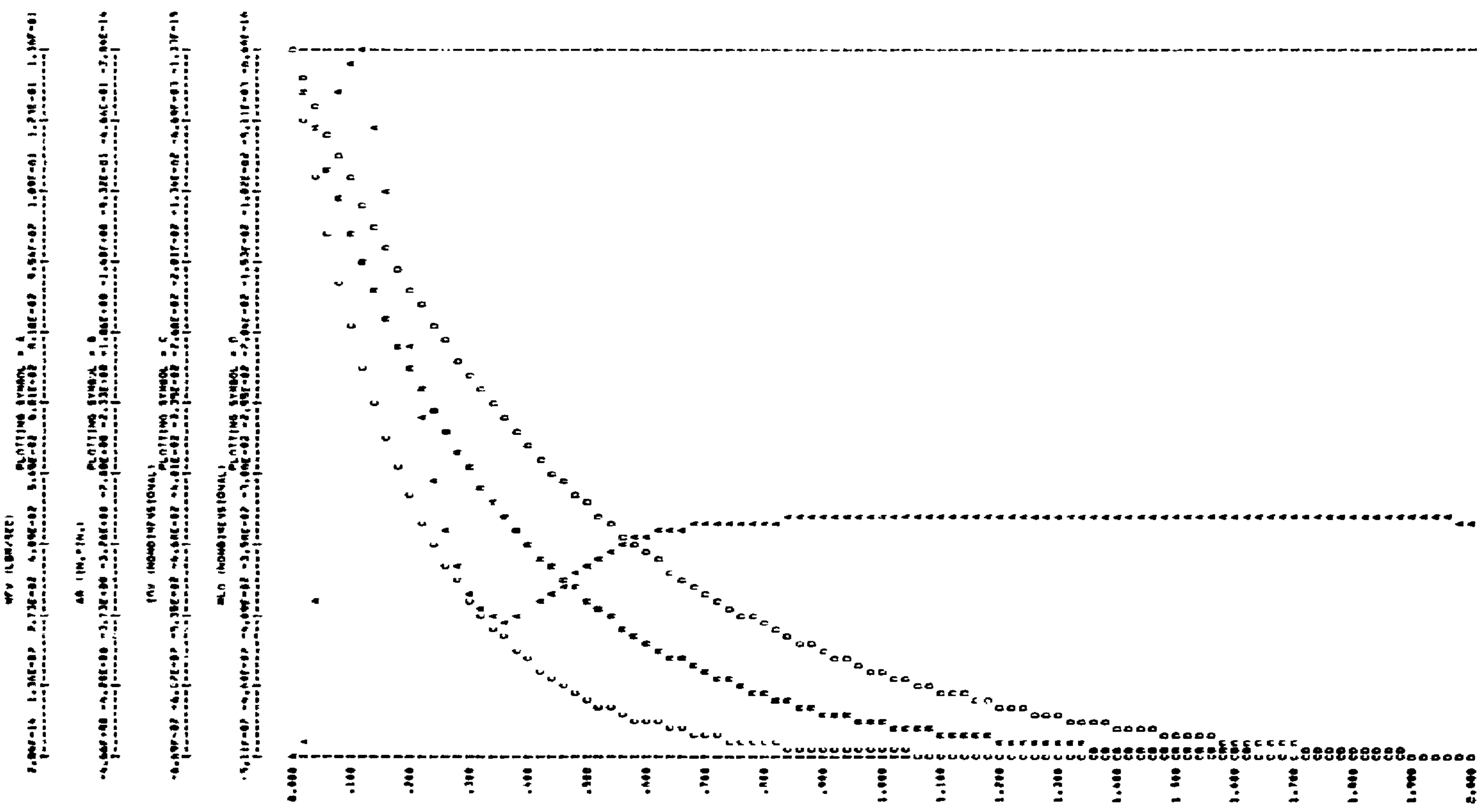

Figure 43b. Simplified Control--35-Percent Operating Condition--Pressure (Continued)

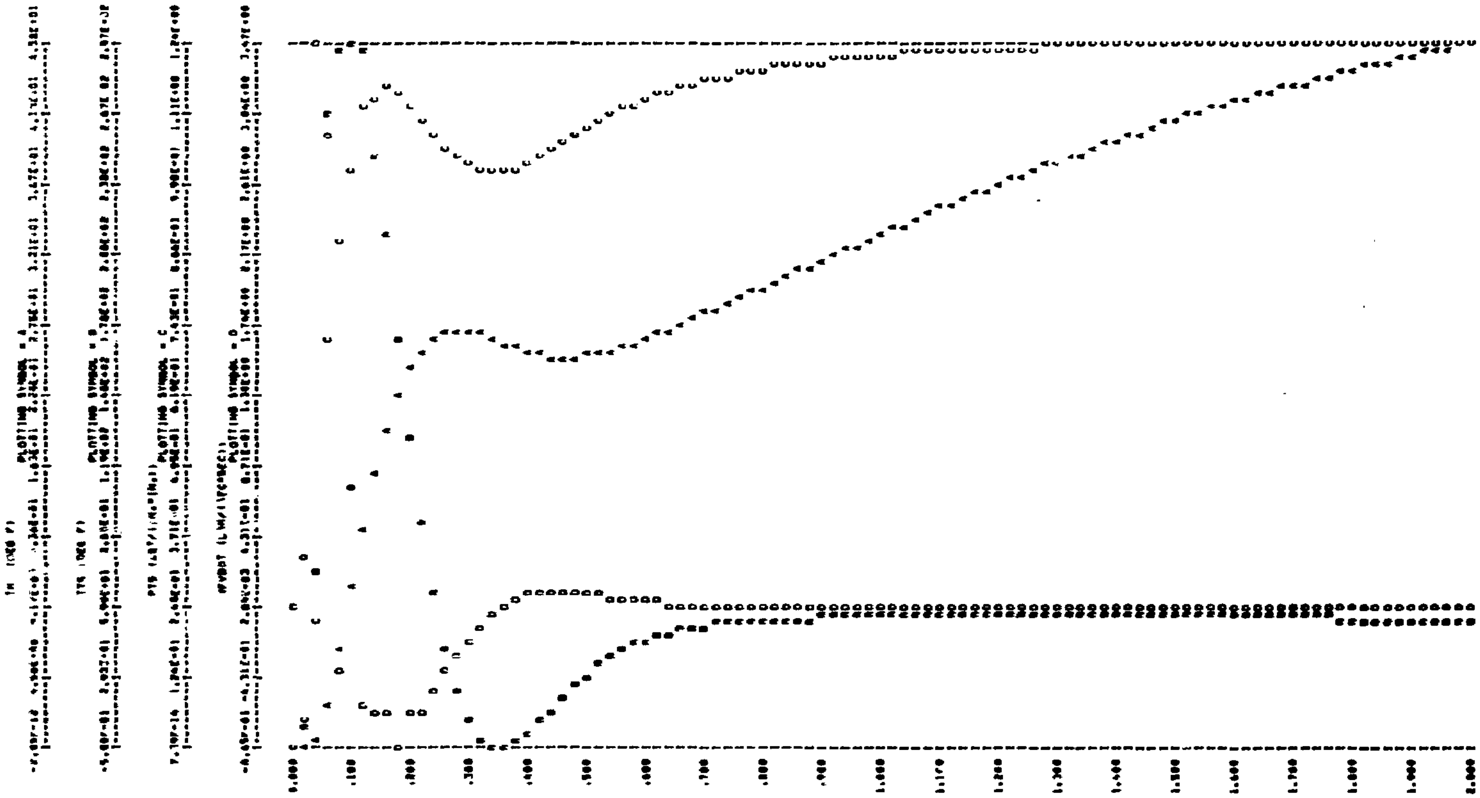

Figure 43c. Simplified Control--85-Percent Operating Condition--Pressure (Concluded)

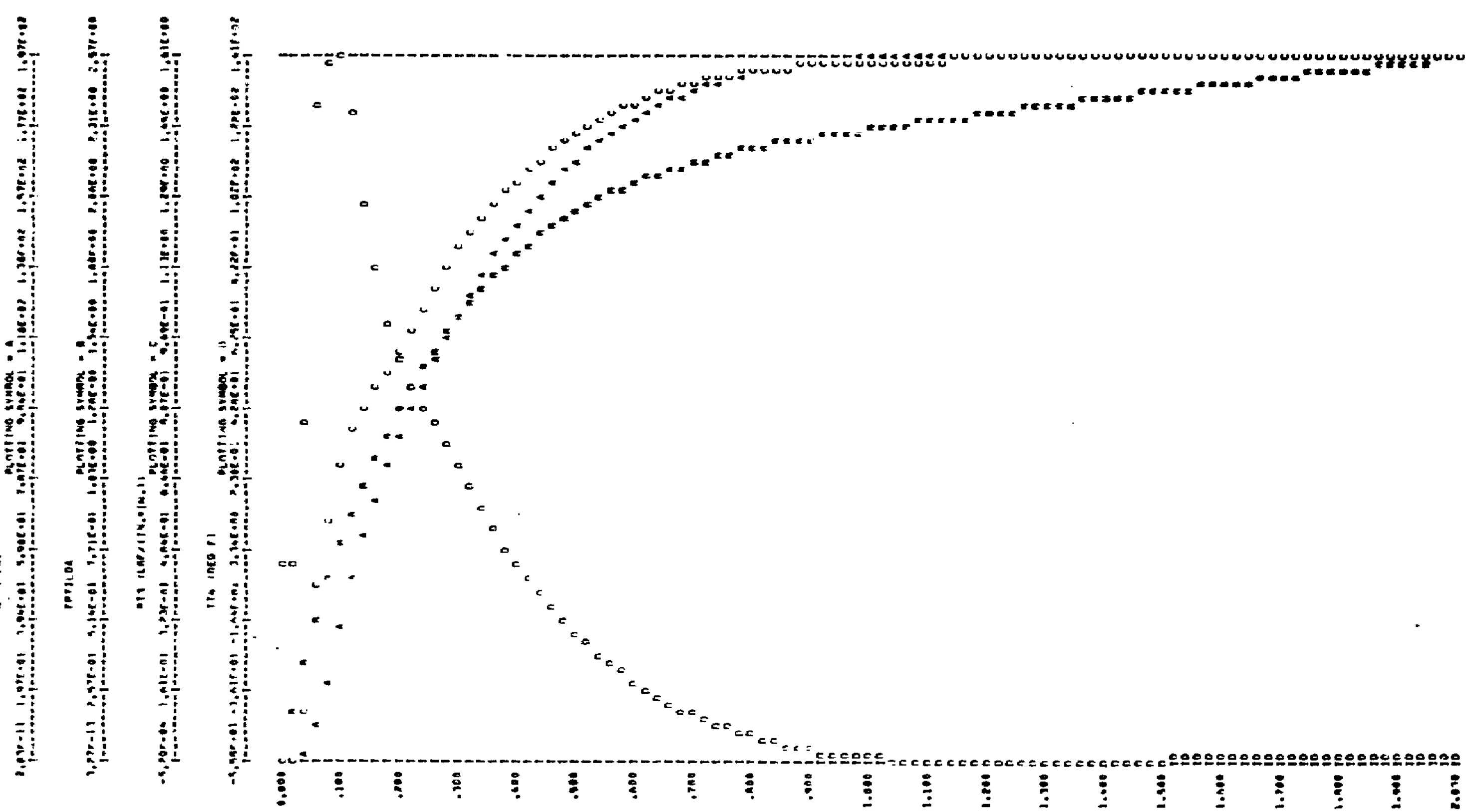

Figure 44a. Simplified Control--70-Percent Operating Condition--Pressure

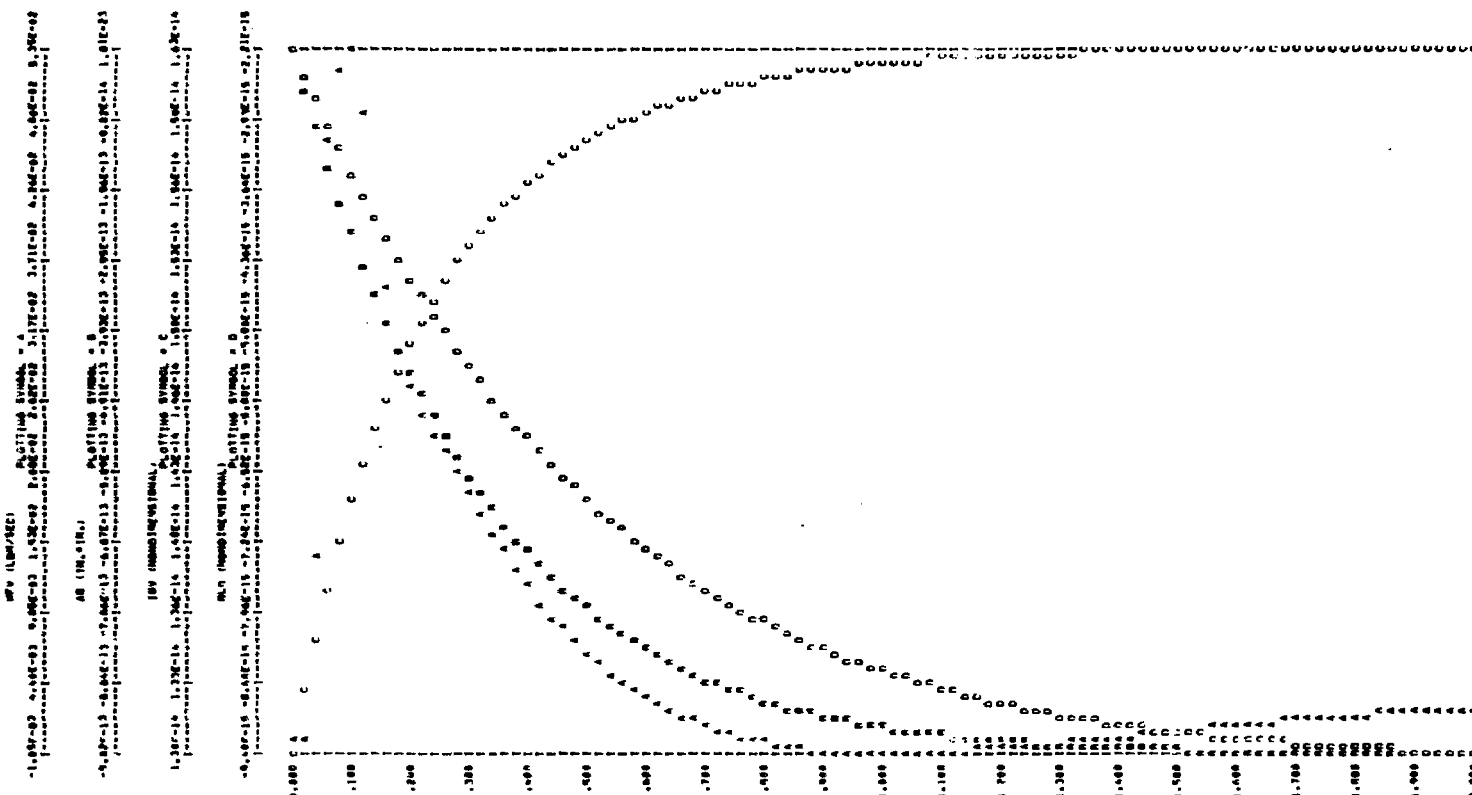

Figure 44b. Simplified Control--70-Percent Operating Condition--Pressure (Continued)

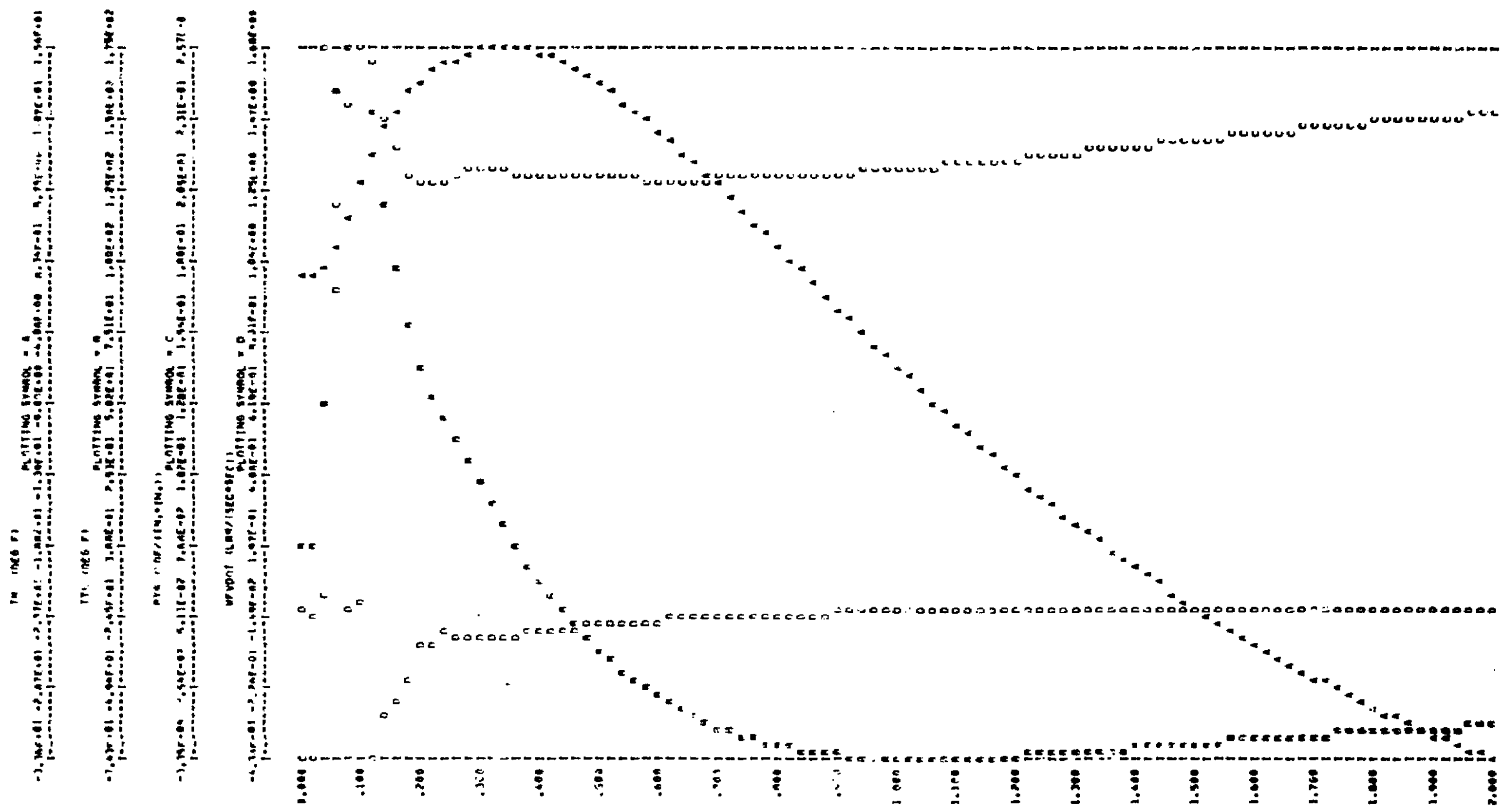

Figure 44c. Simplified Control--70-Percent Operating Condition--Pressure (Concluded)

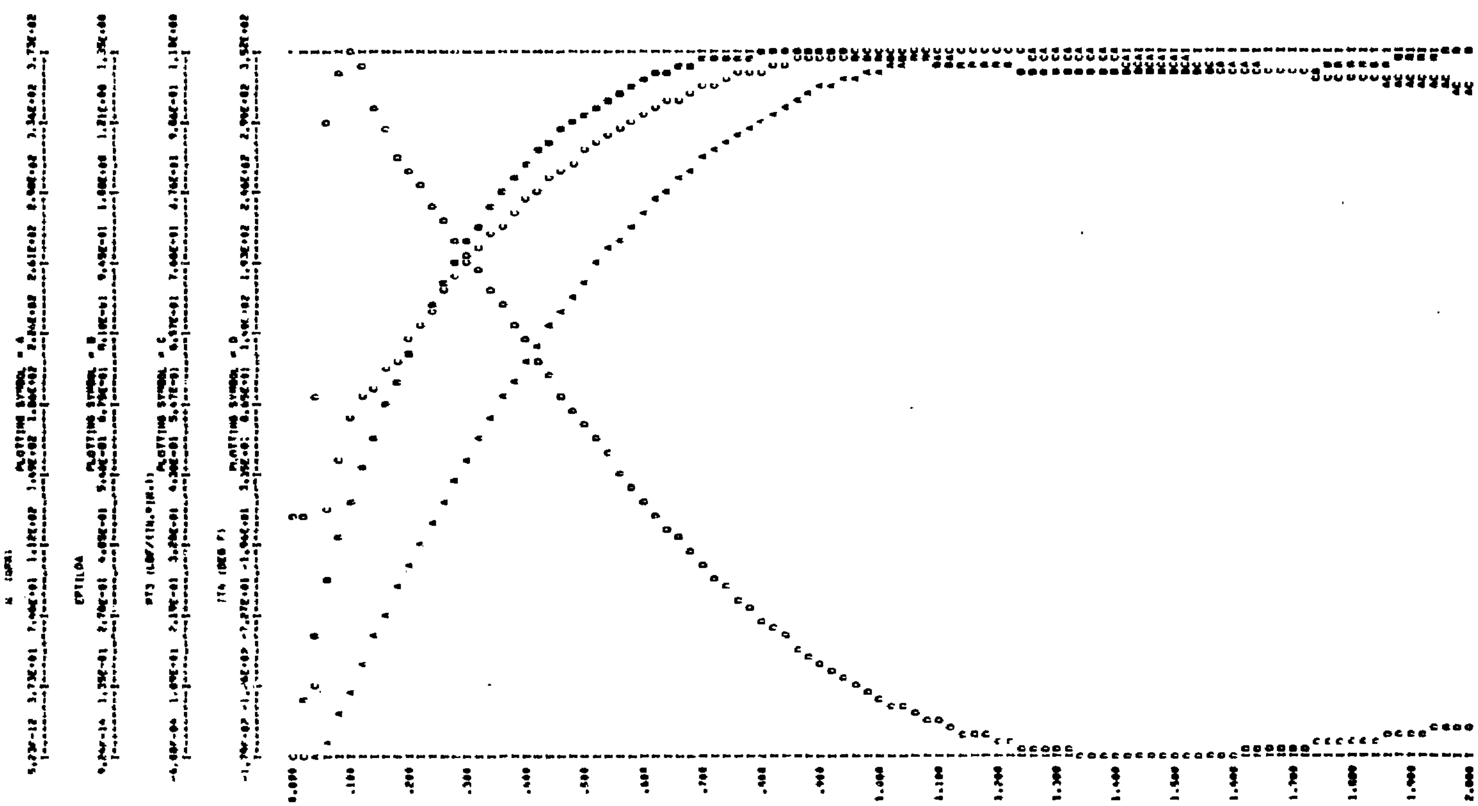

Figure 45a. Simplified Control--50-Percent Operating Condition--Pressure

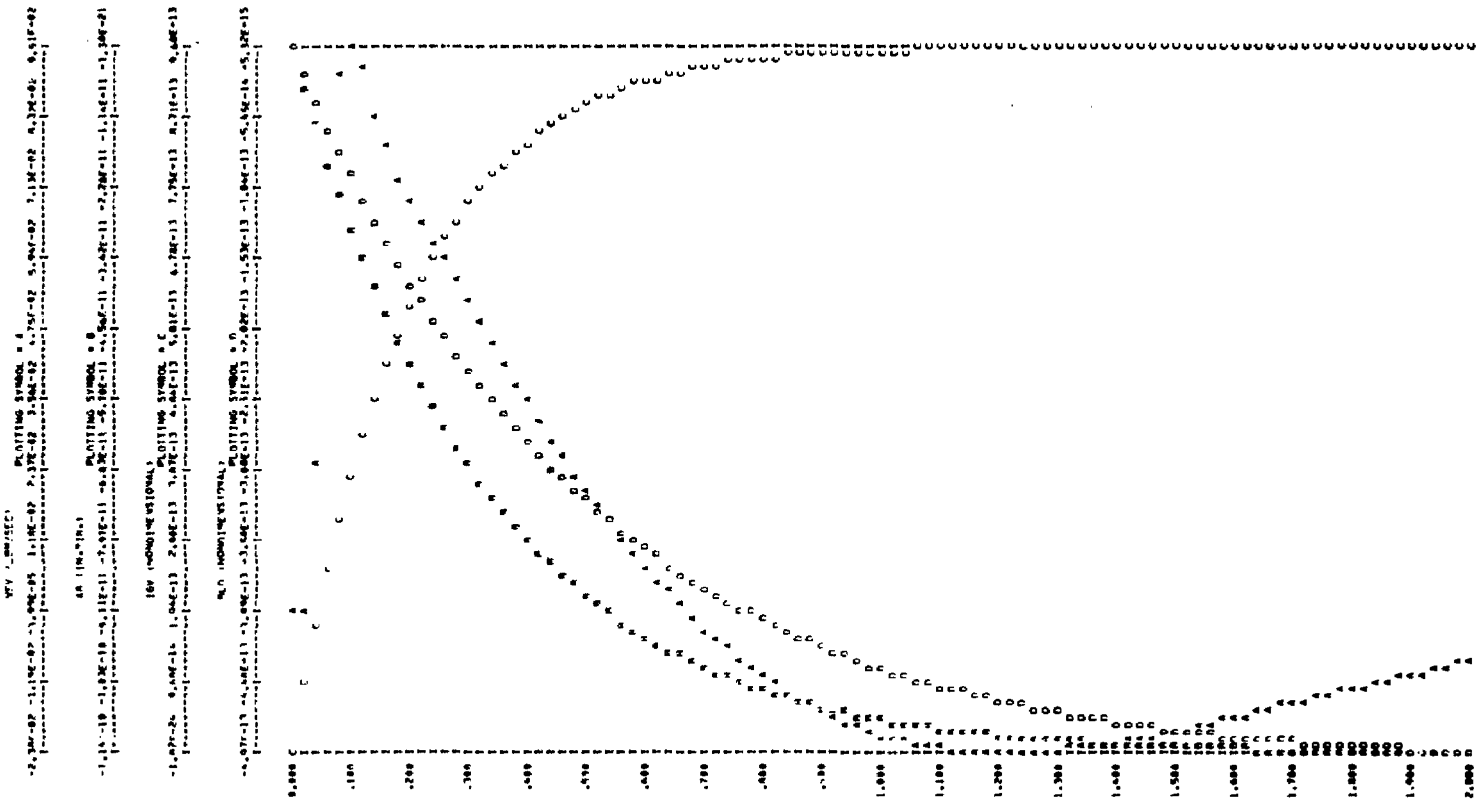

Figure 45b. Simplified Control--50-Percent Operating Condition--Pressure (Continued)

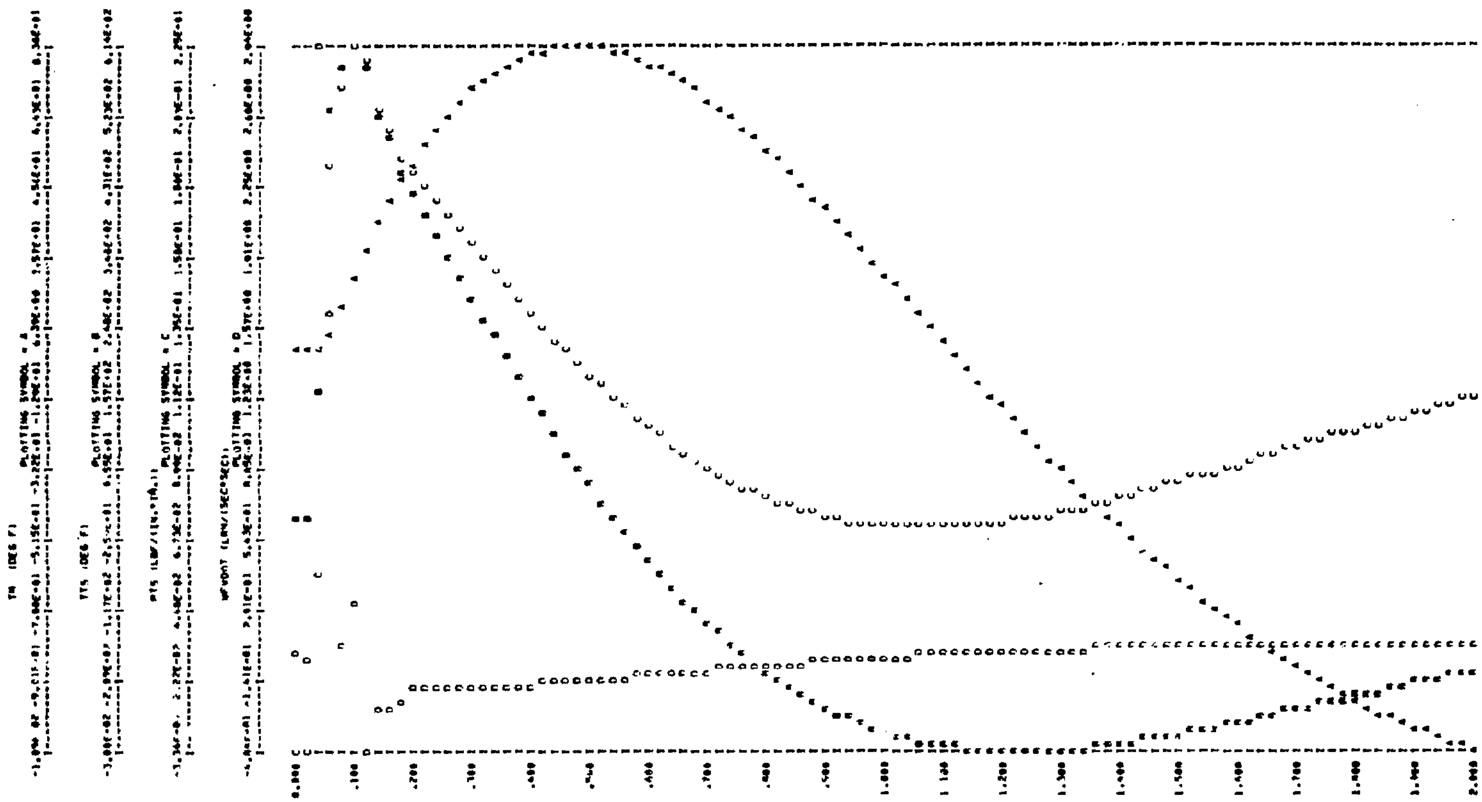

Figure 45c. Simplified Control--50-Percent Operating Condition--Pressure (Concluded)

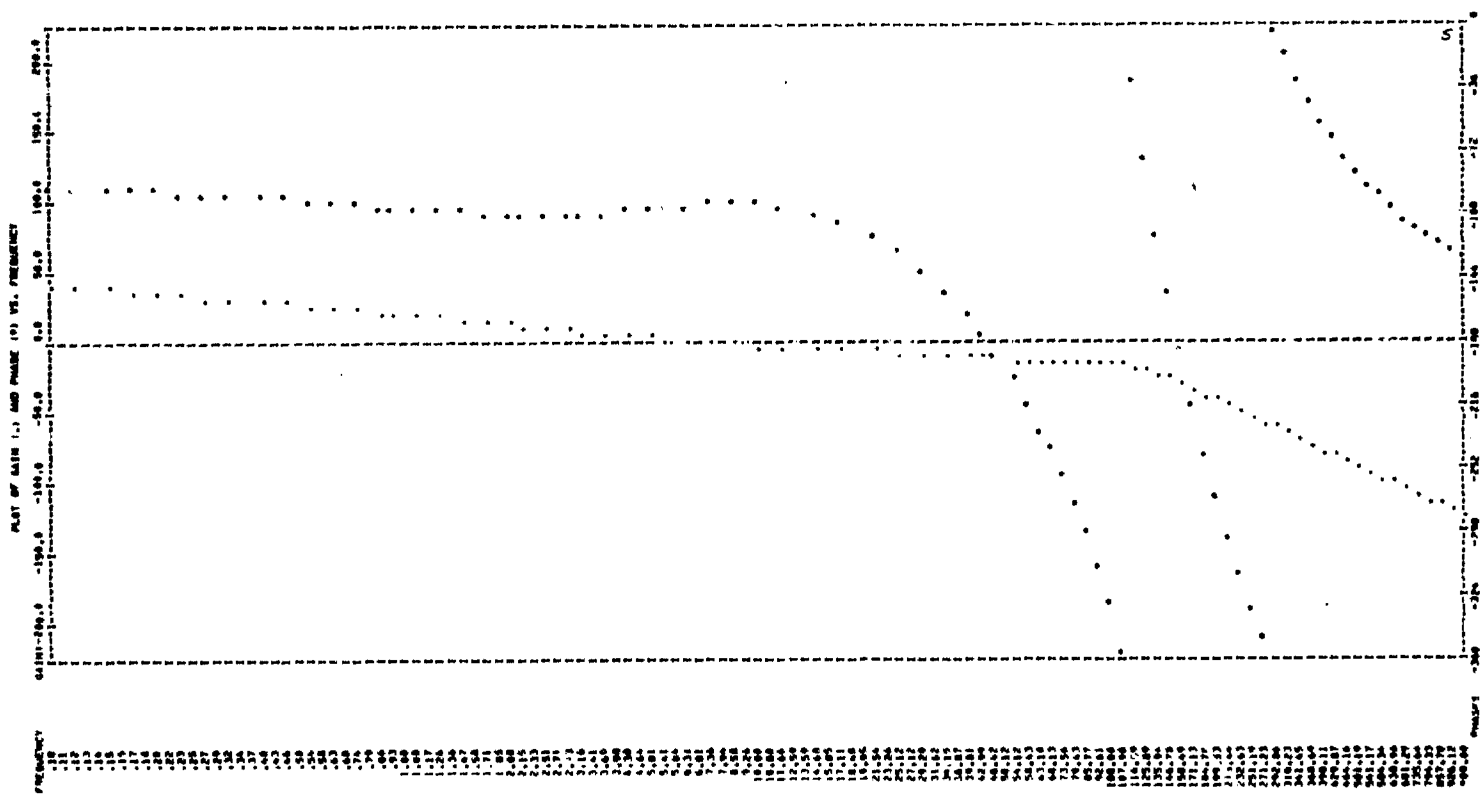

Figure 46a. Actuator Open Loop--100-Percent Operating Condition--Pressure

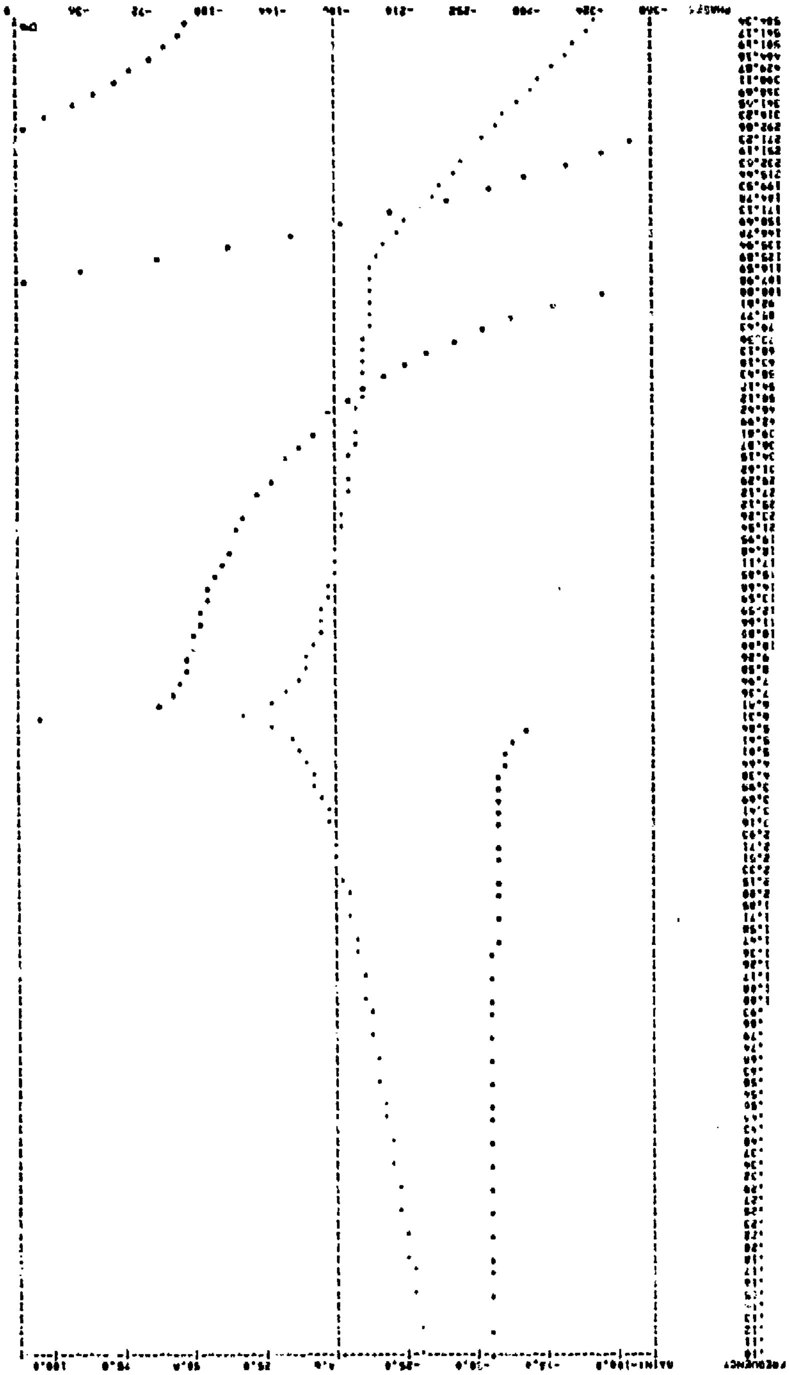

Figure 46b. PT3 Open Loop--100-Percent Operating Condition--Pressure

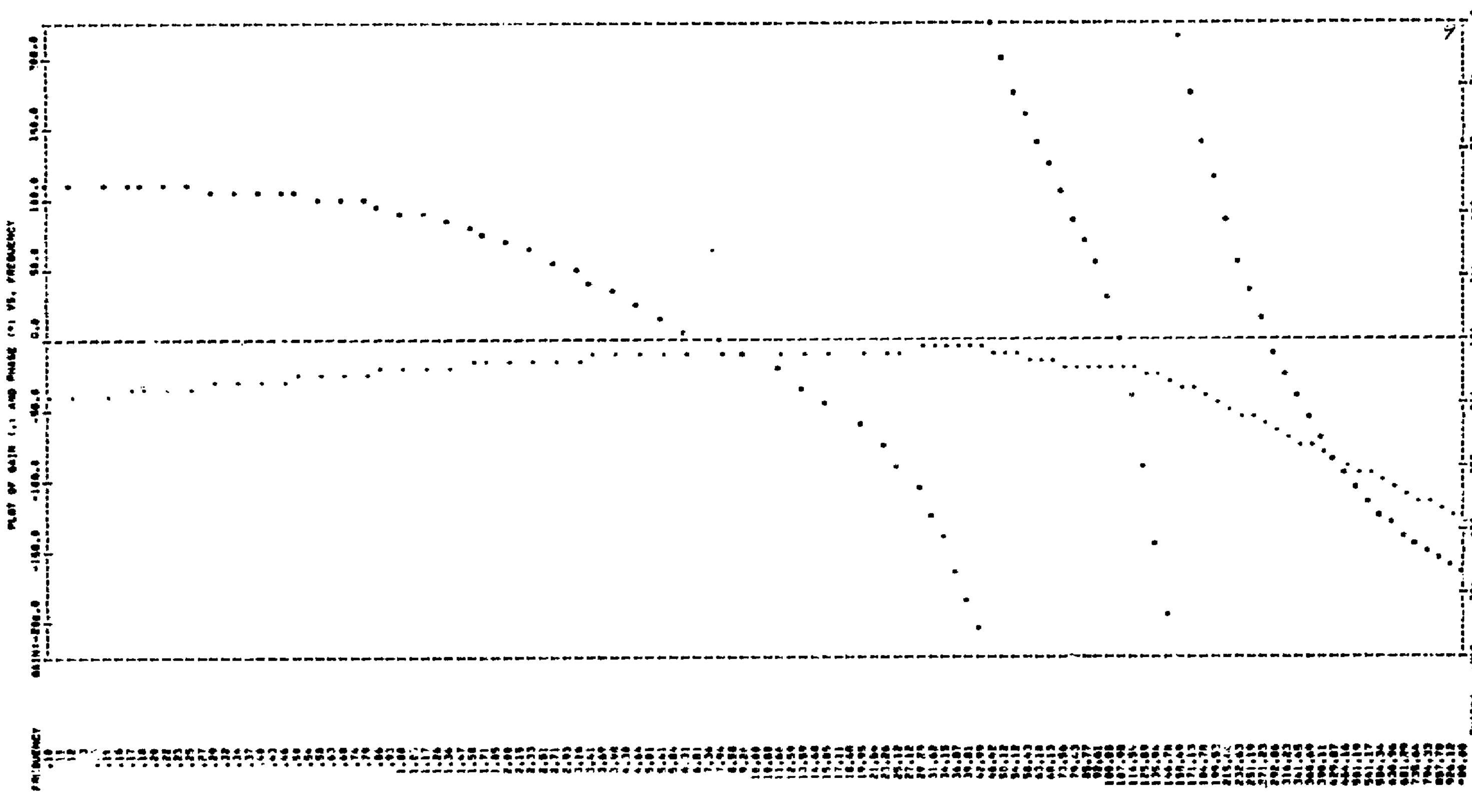

Figure 46c. PT5 Open Loop--100-Percent Operating Condition--Pressure

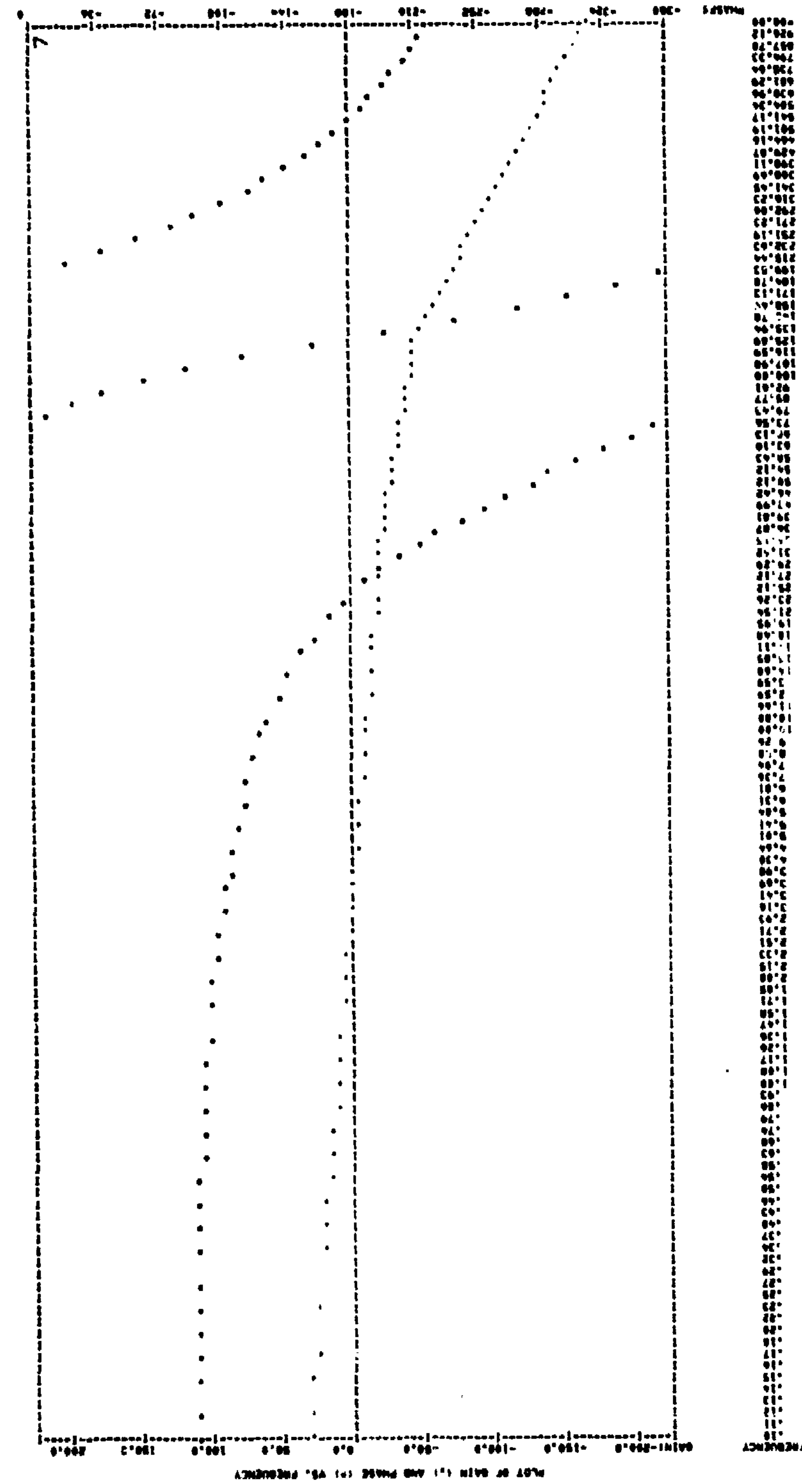

Figure 46d. EP Open Loop--100-Percent Operating Condition--Pressure

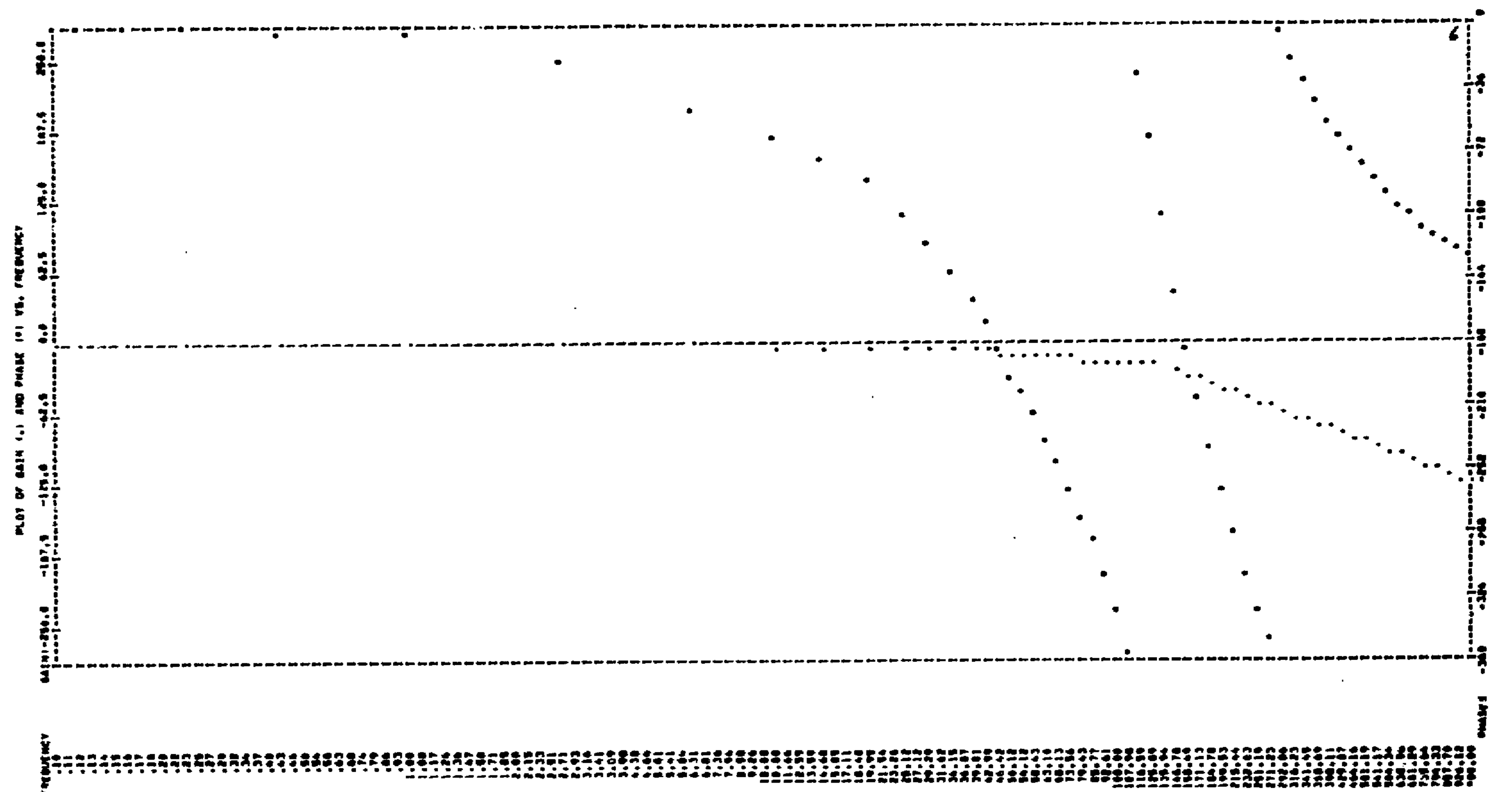

Figure 46e. Closed-Loop--100-Percent Operating Condition--Pressure

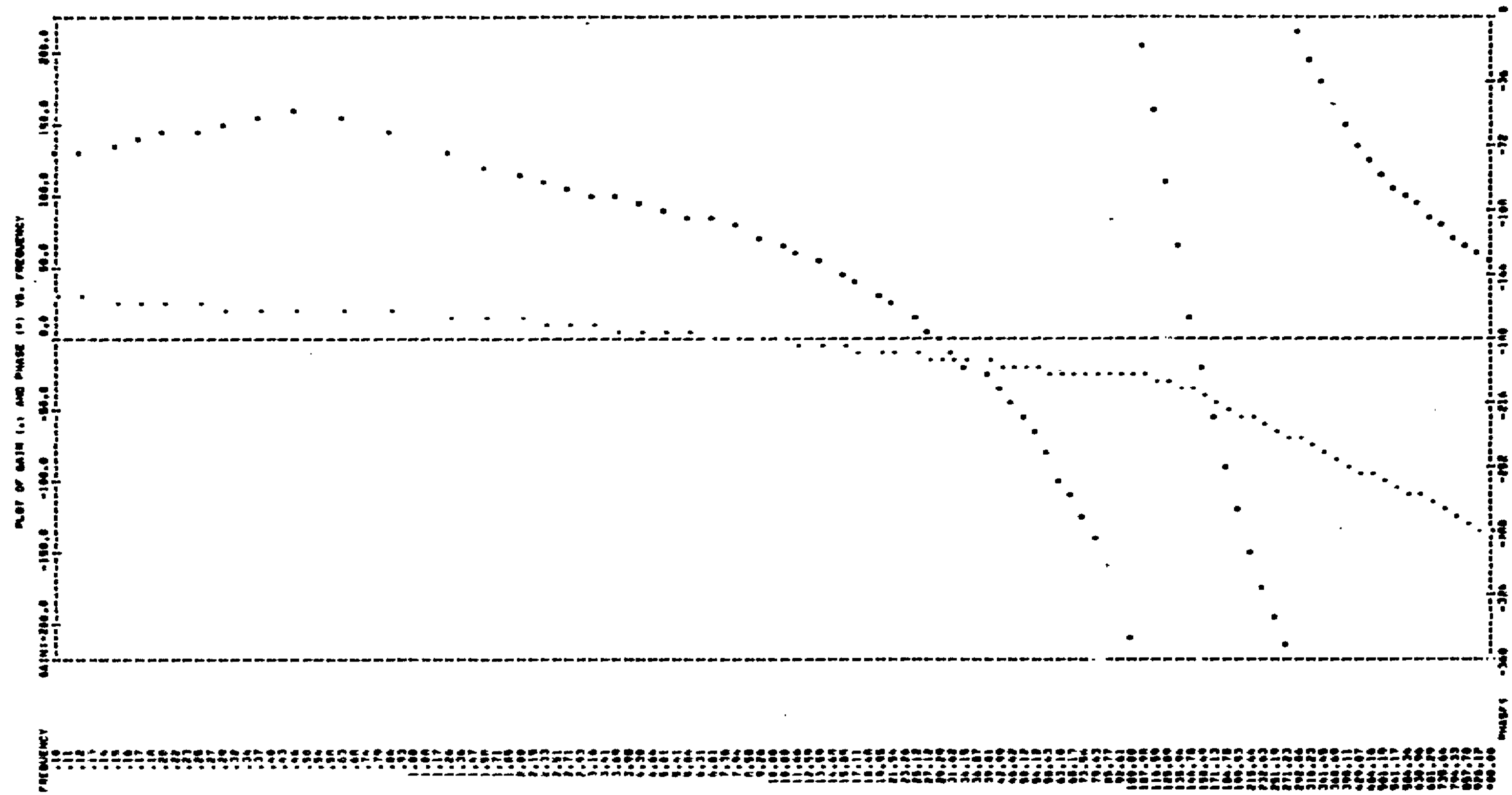

Figure 47a. Actuator Open Loop--85-Percent Operating Condition--Pressure

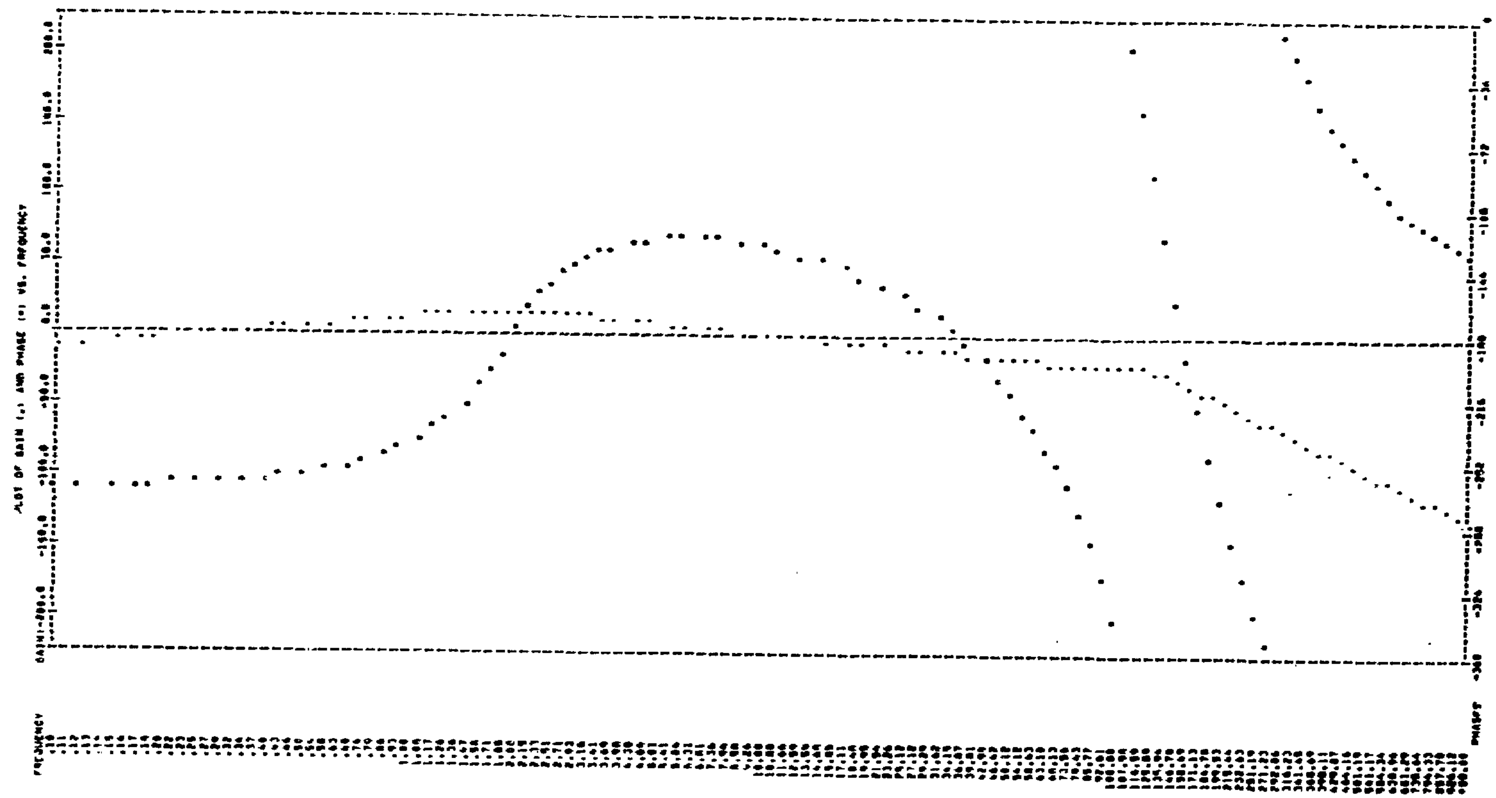

Figure 47b. PT3 Open Loop--85-Percent Operating Condition--Pressure

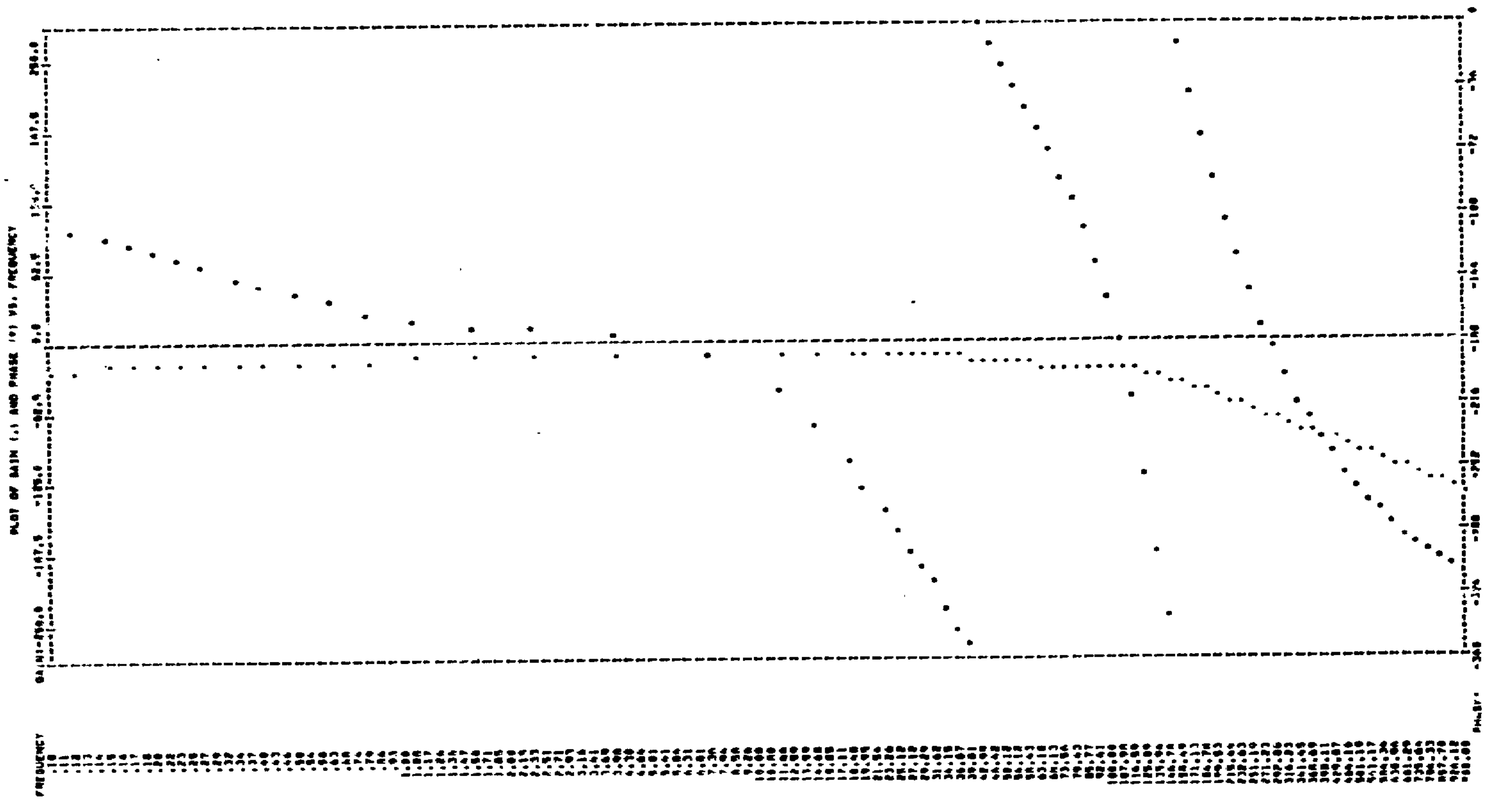

Figure 47c. PT5 Open Loop--85-Percent Operating Condition--Pressure

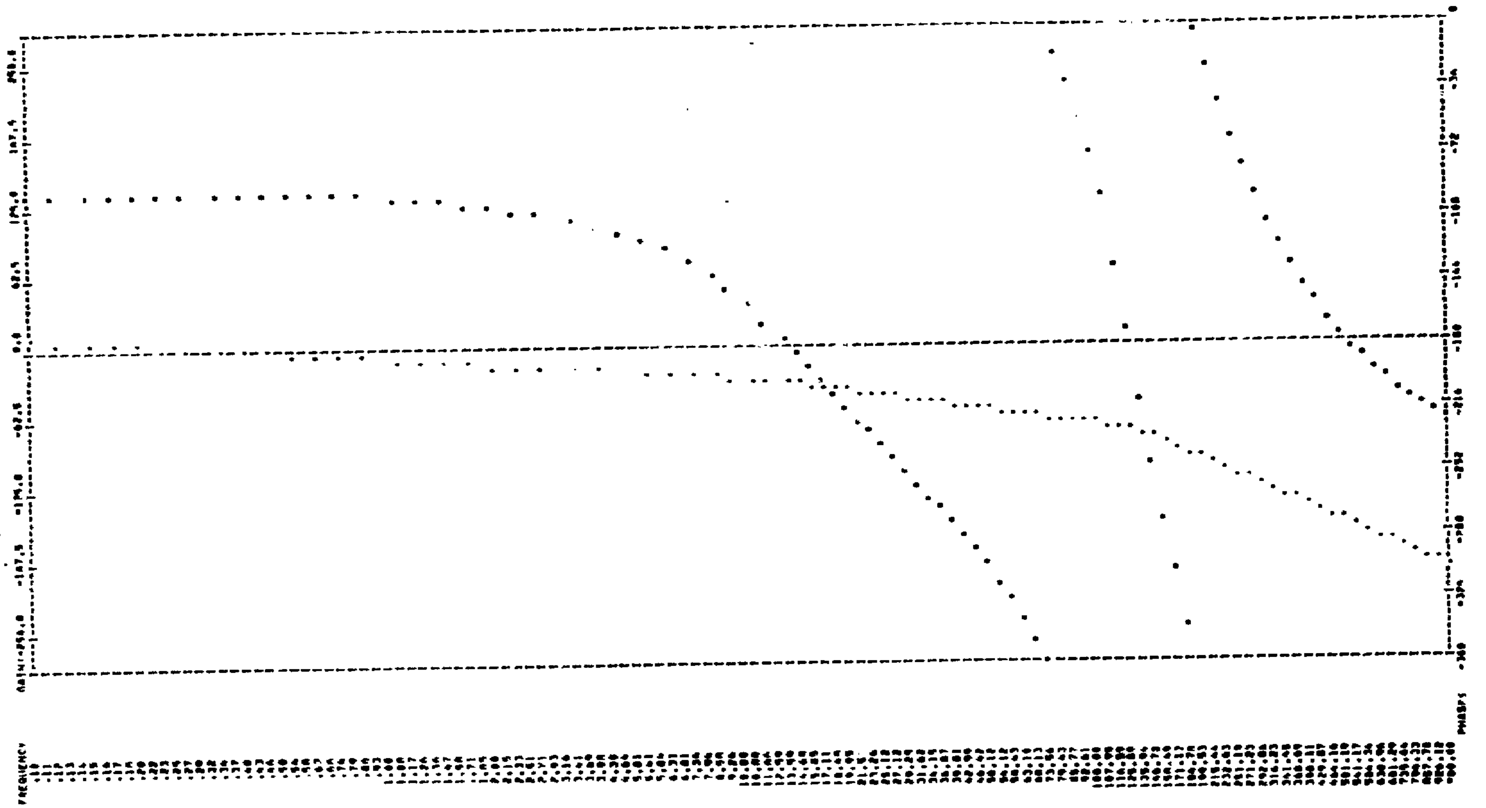

Figure 47d. EP Open Loop--85-Percent Operating Condition--Pressure

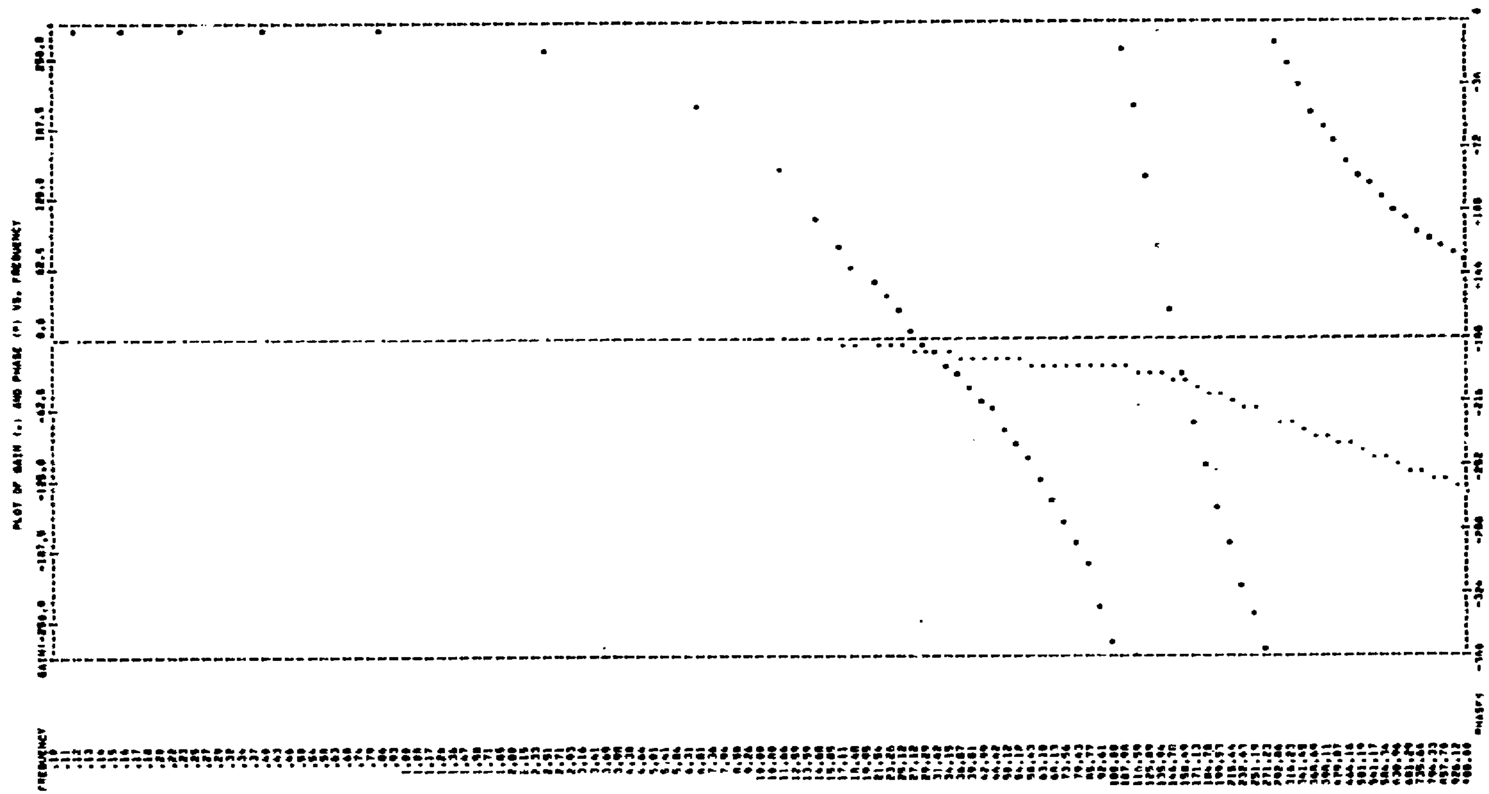

Figure 47e. Closed-Loop--85-Percent Operating Condition--Pressure

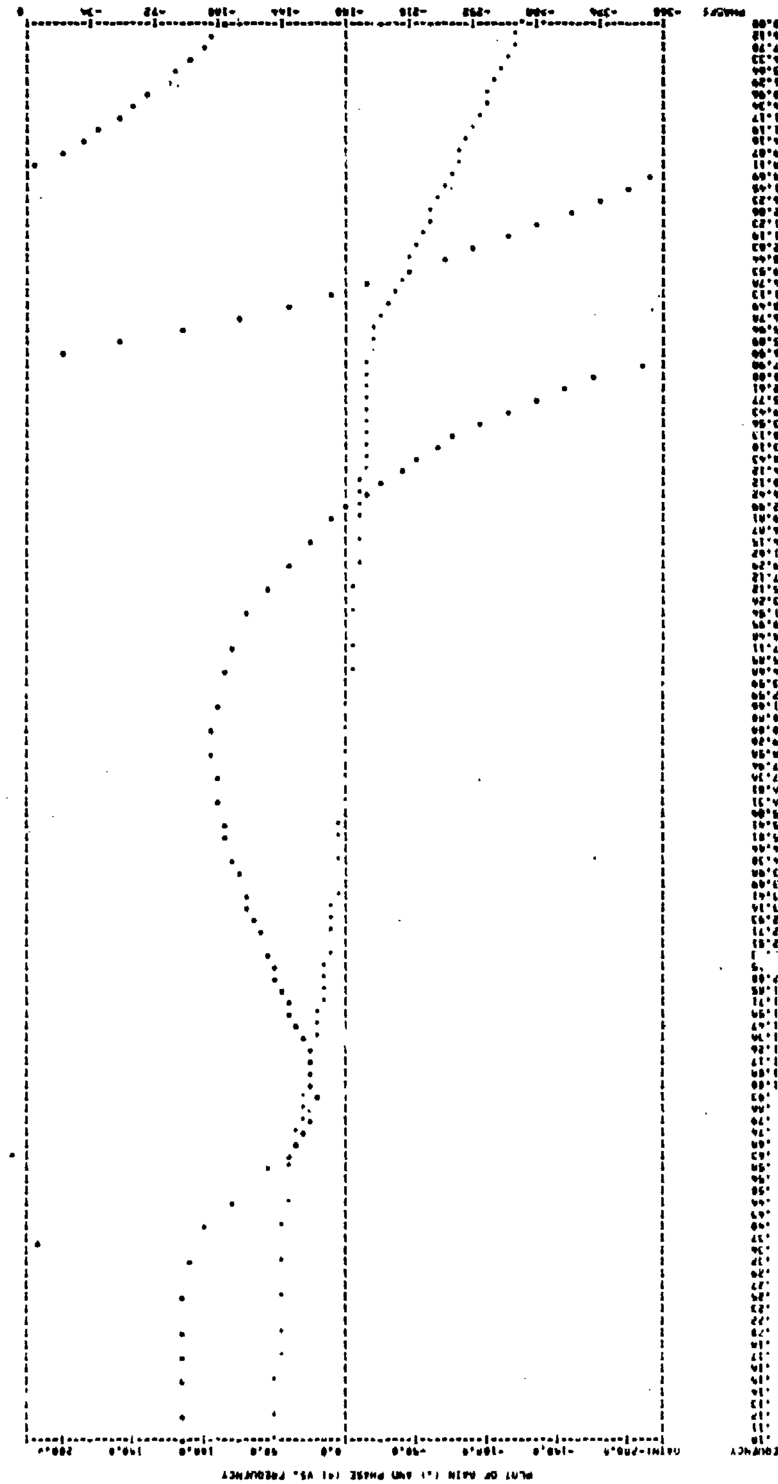

Figure 13a. Actuator Open Loop--70-Percent Operating Condition--Pressure

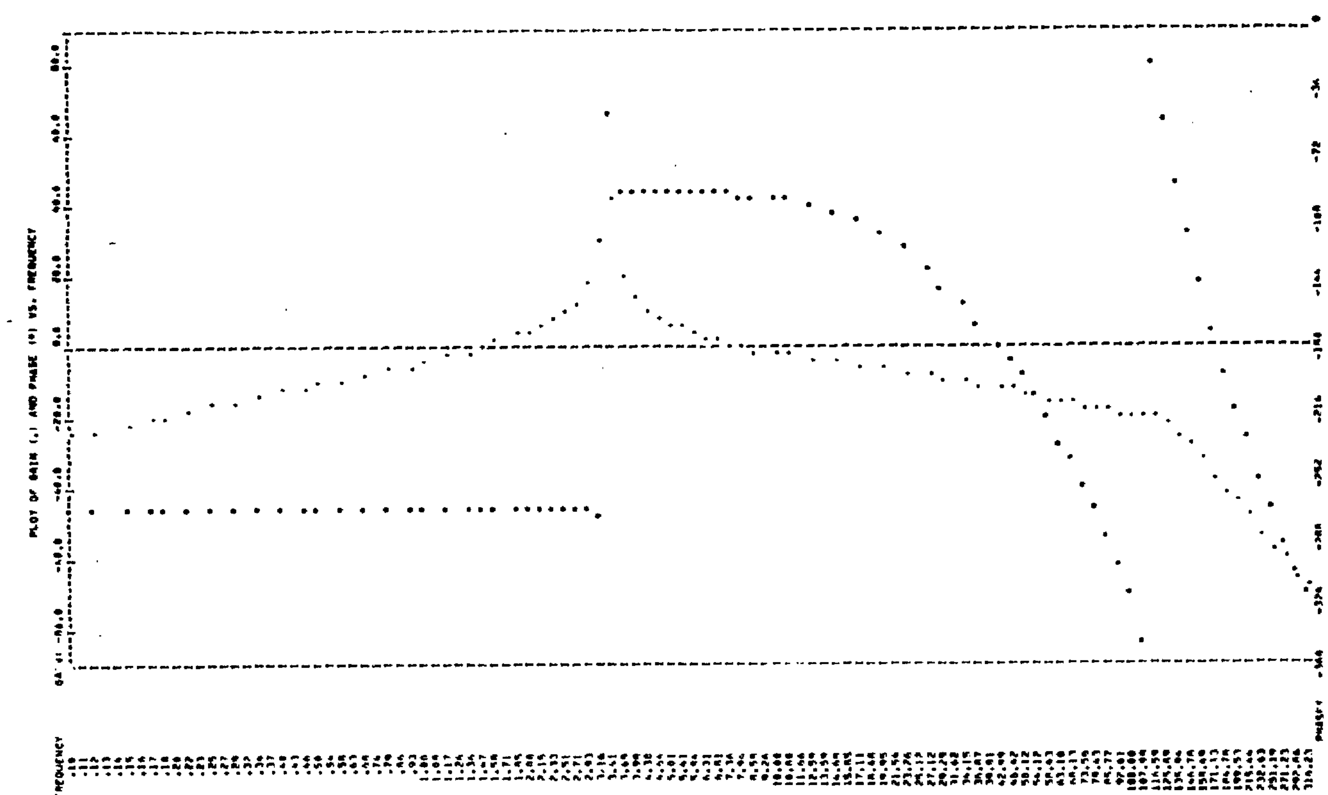

Figure 48b. PT3 Open Loop--70-Percent Operating Condition--Pressure

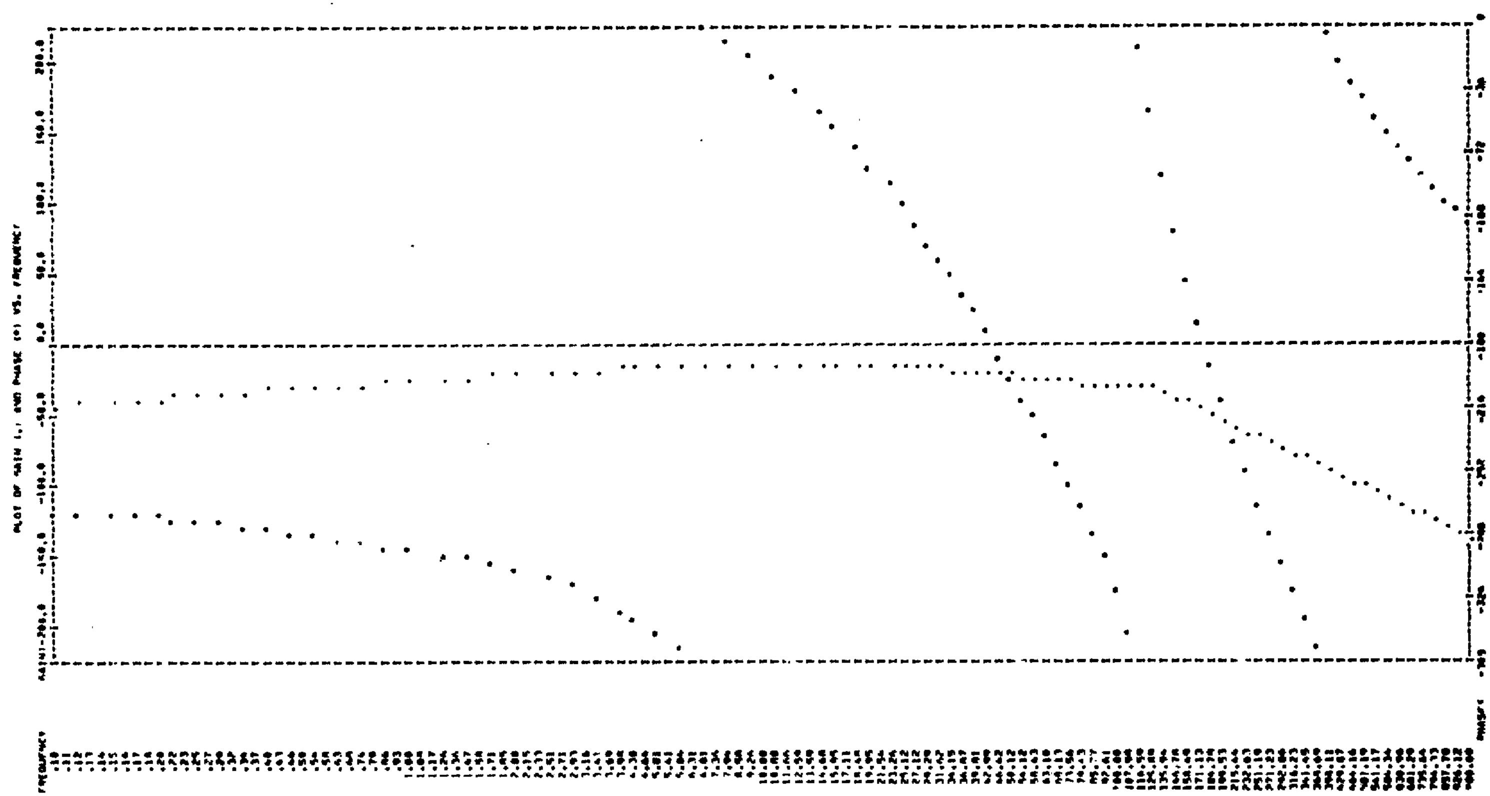

Figure 48c. PT5 Open Loop--70-Percent Operating Condition--Pressure

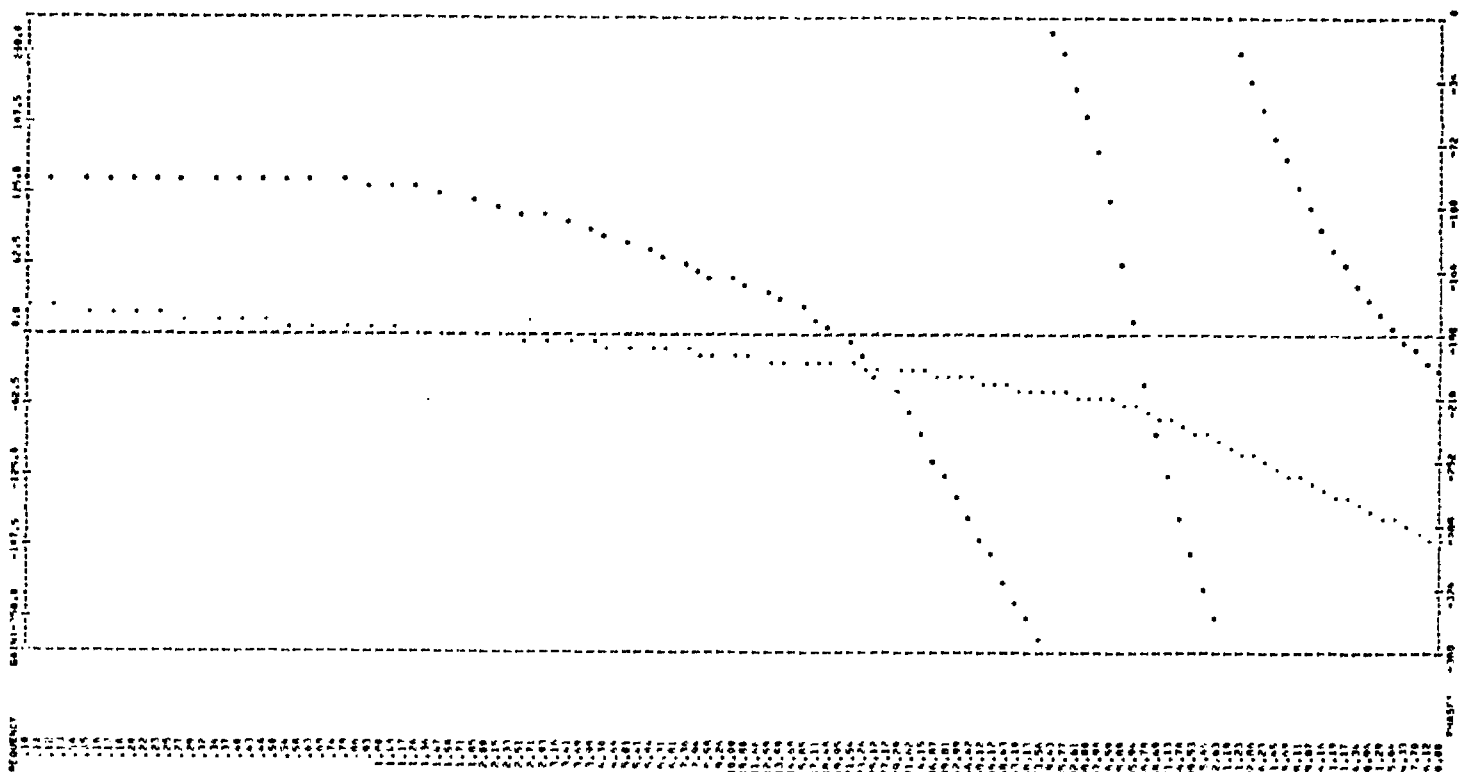

Figure 48d. EP Open Loop--70-Percent Operating Condition--Pressure

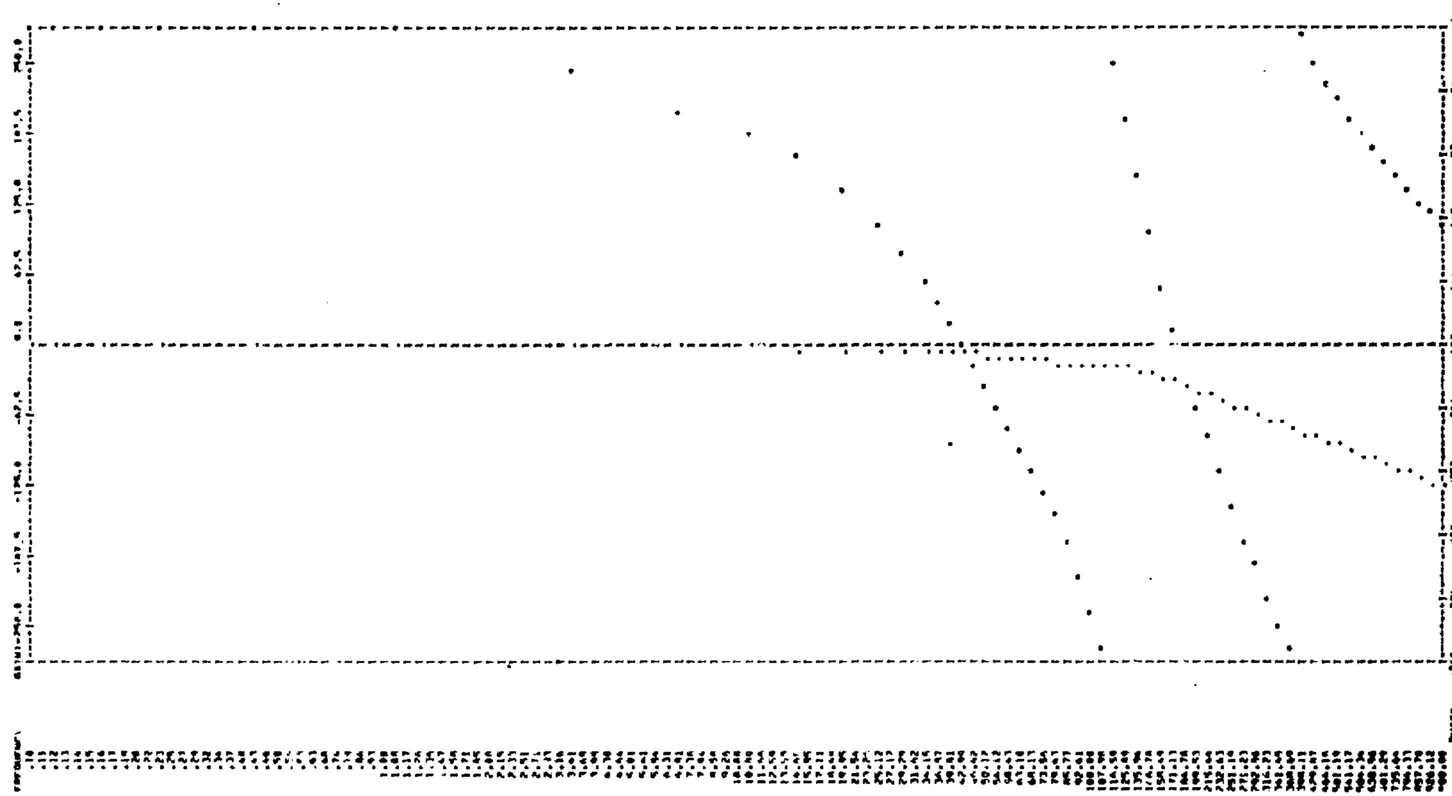

Figure 48e. Closed-Loop--70-Percent Operating Condition--Pressure

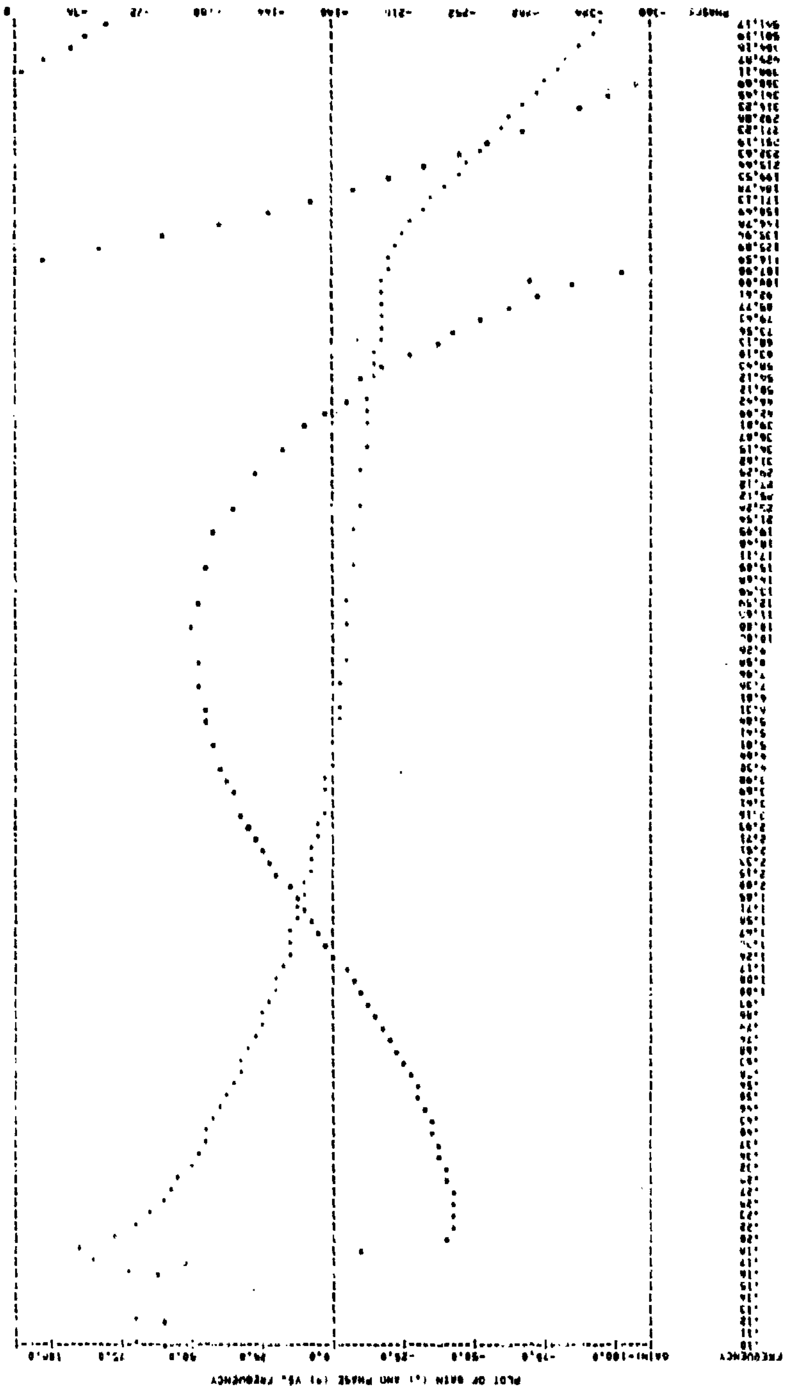

Figure 49a. Actuator Open Loop--50-Percent Operating Condition--Pressure

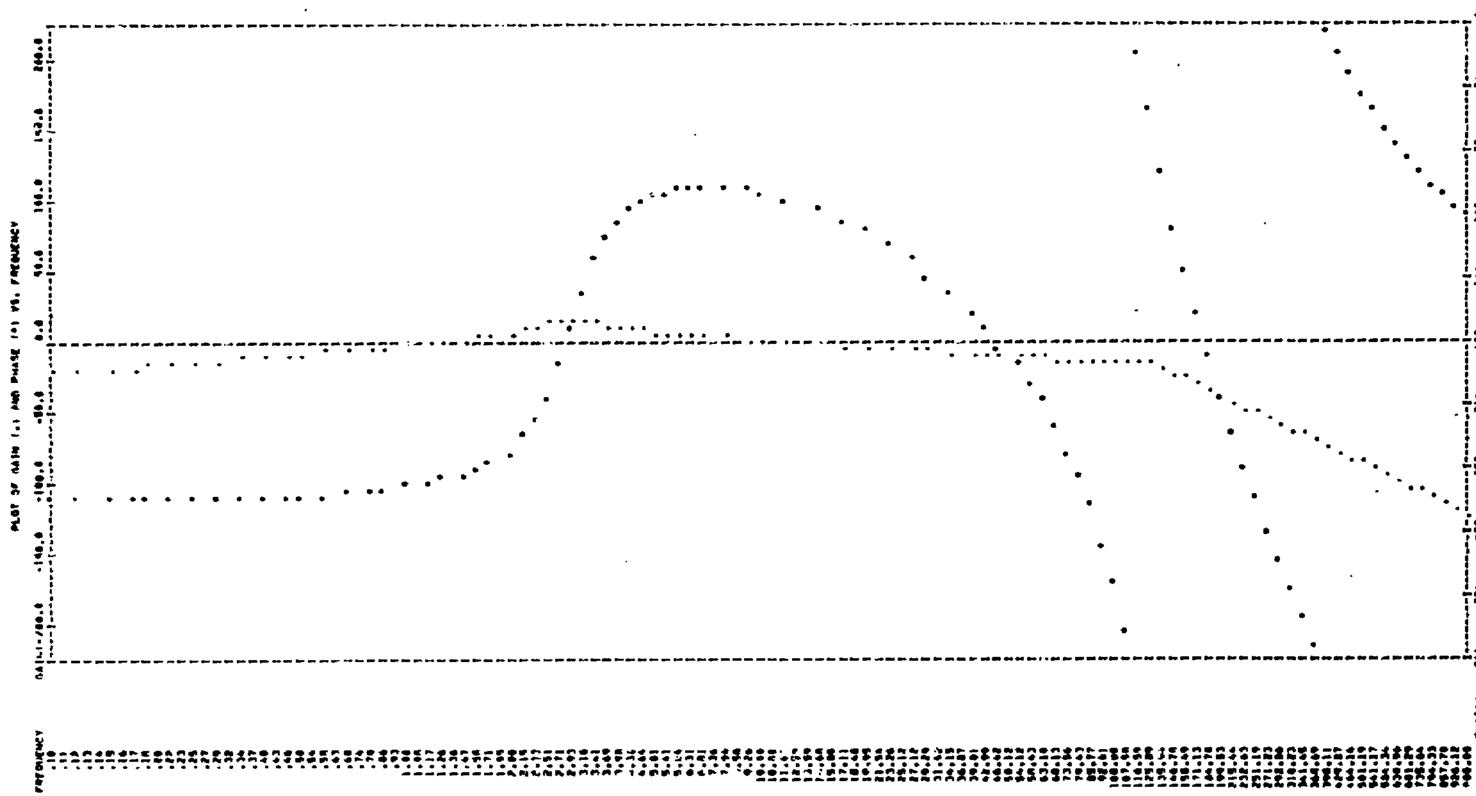

Figure 48b. PT3 Open Loop--50-Percent Operating Condition--Pressure

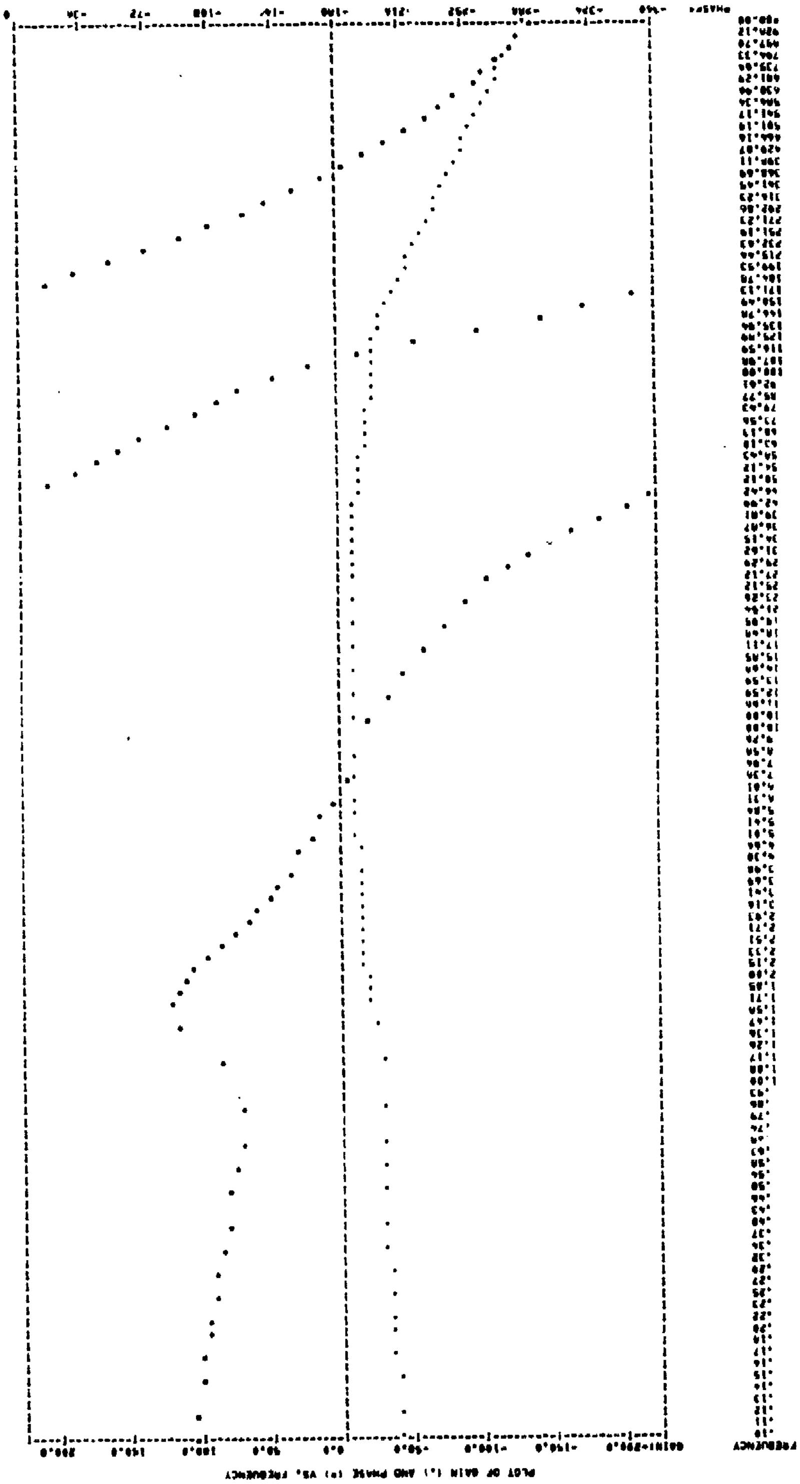

Figure 49c. PT5 Open Loop--50-Percent Operating Condition--Pressure

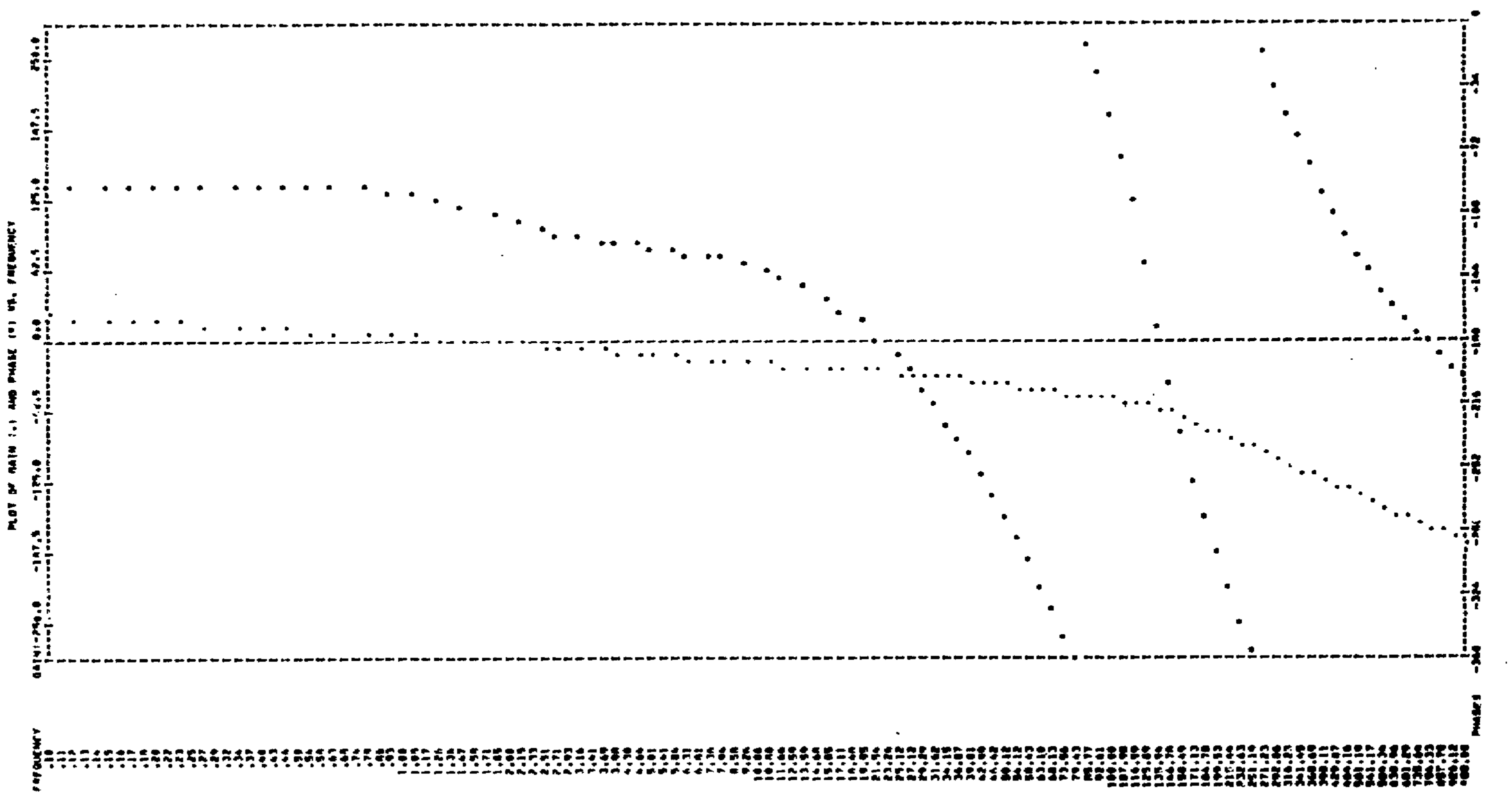

Figure 49d. EP Open Loop--50-Percent Operating Point-Pressure

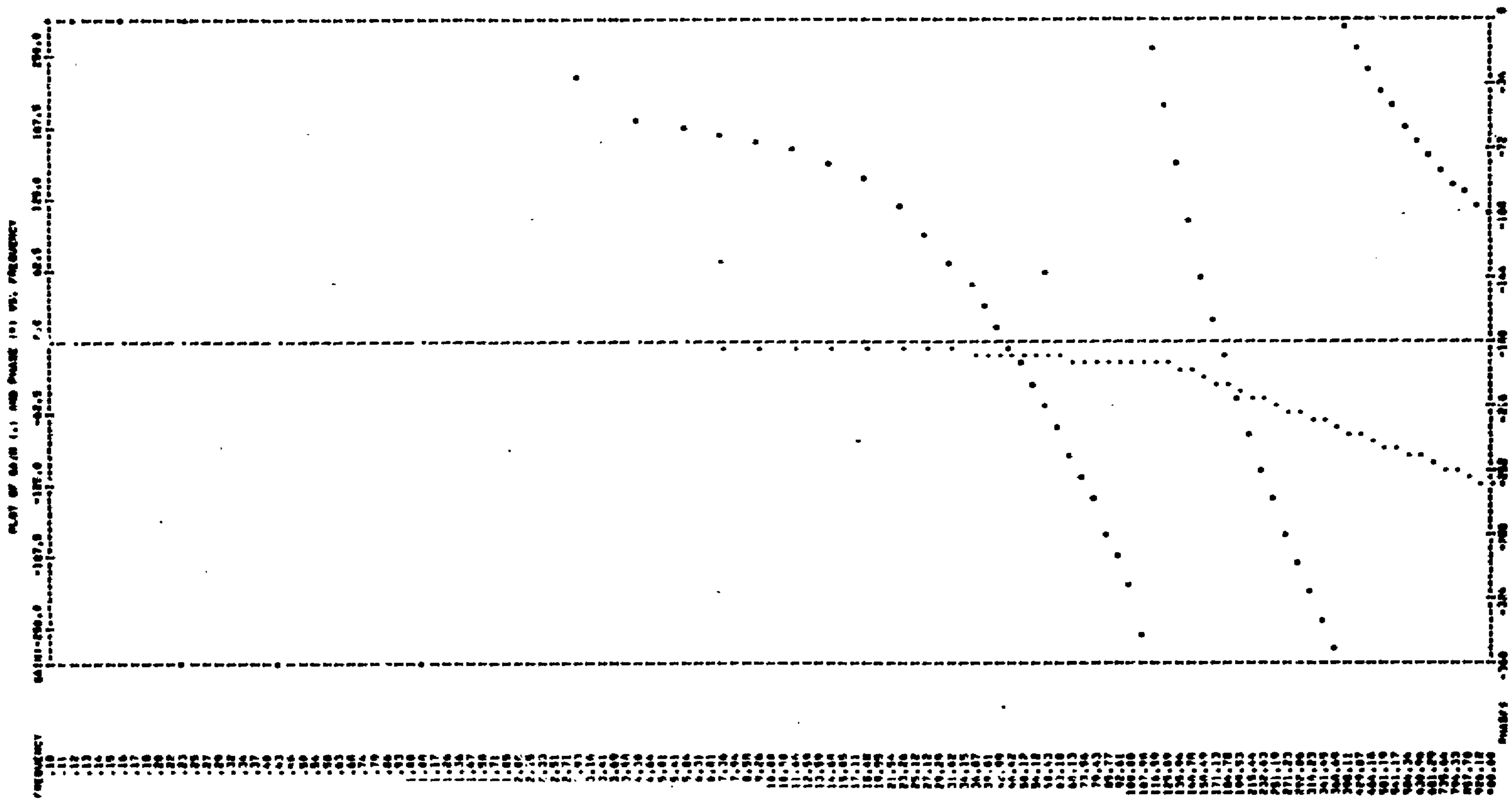

Figure 49e. Closed Loop--50-Percent Operating Condition--Pressure

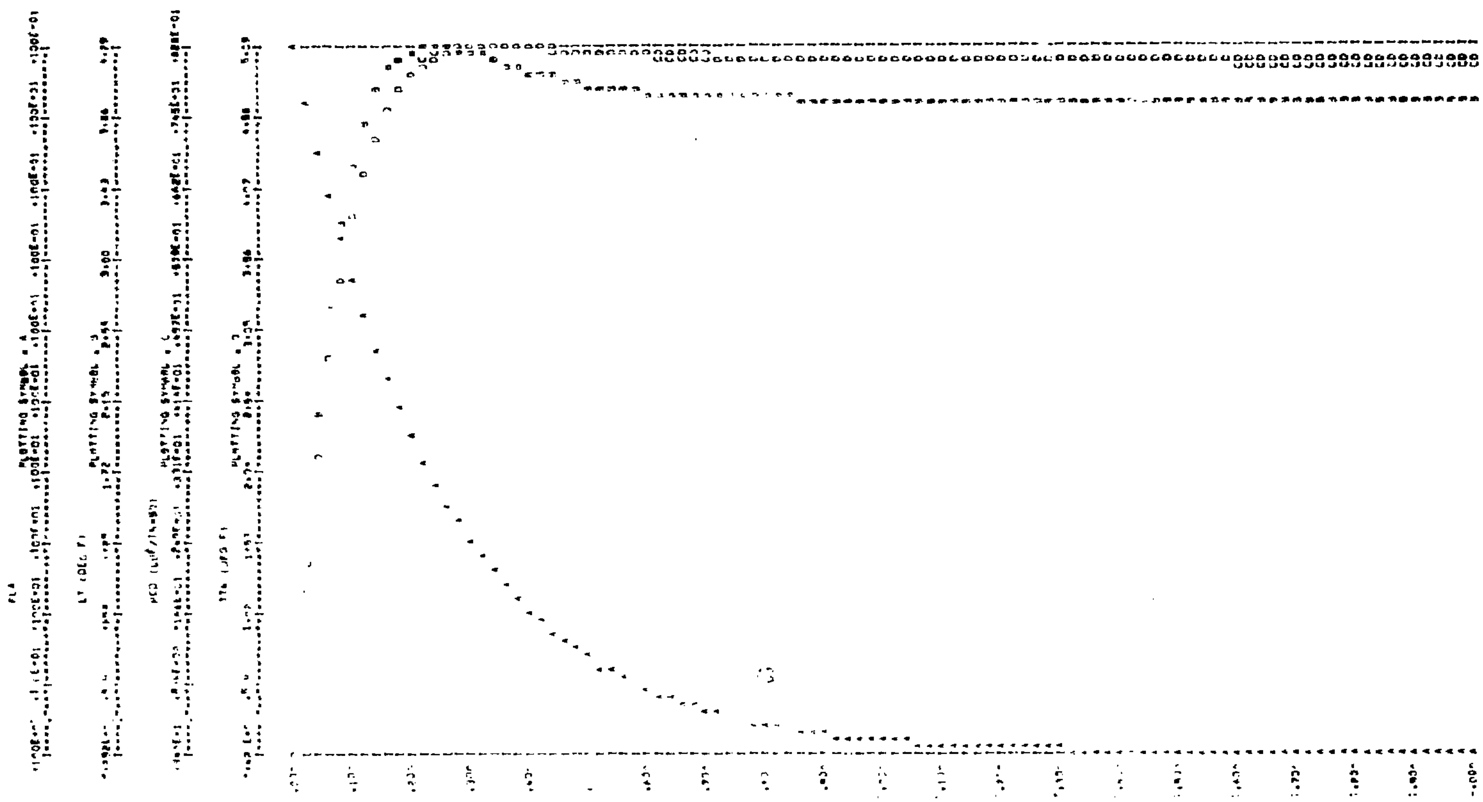

Figure 50. State Control--100-Percent Operating Condition--Temperature

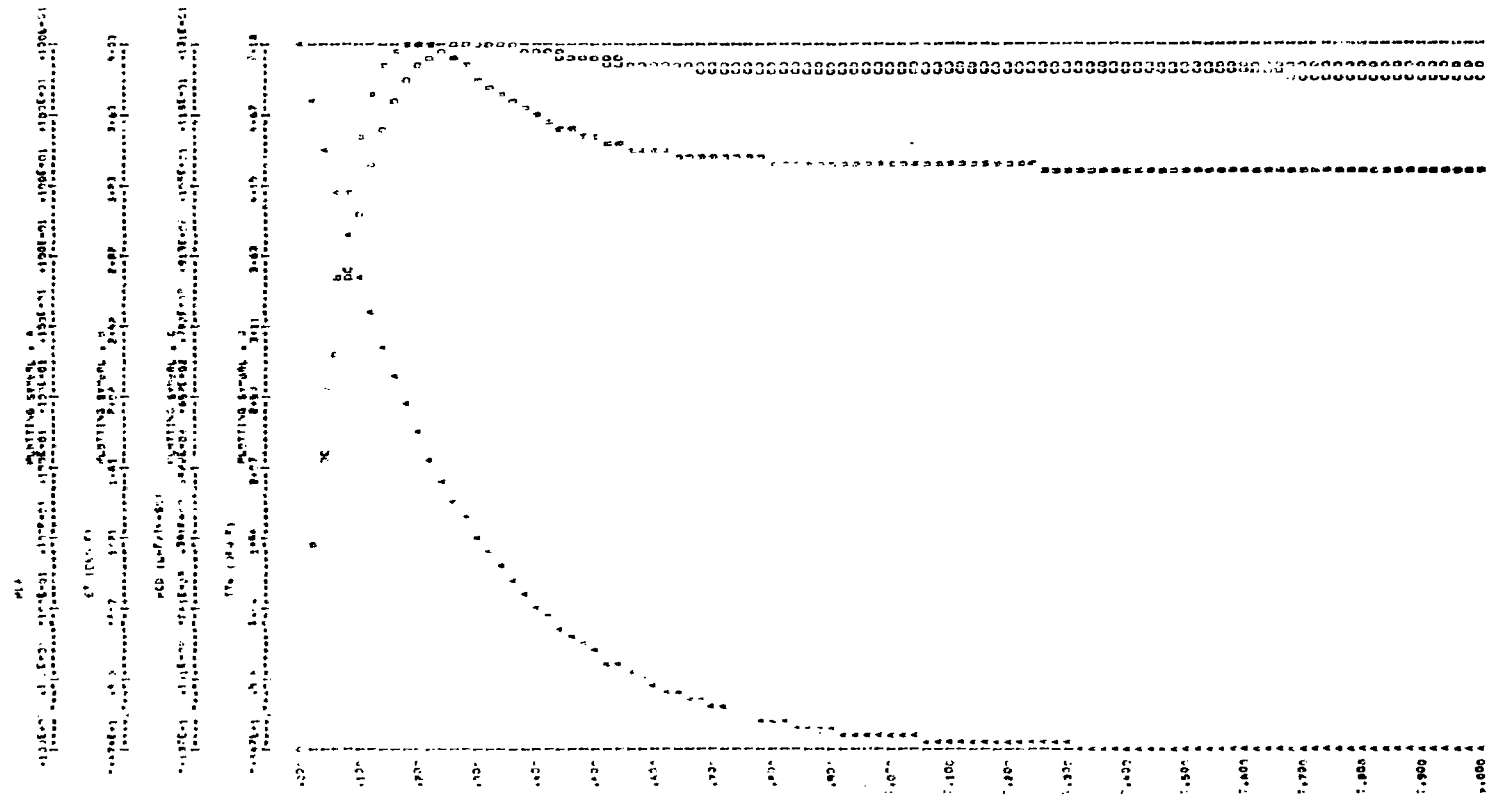

Figure 51. State Control--85-Percent Operating Condition--Temperature

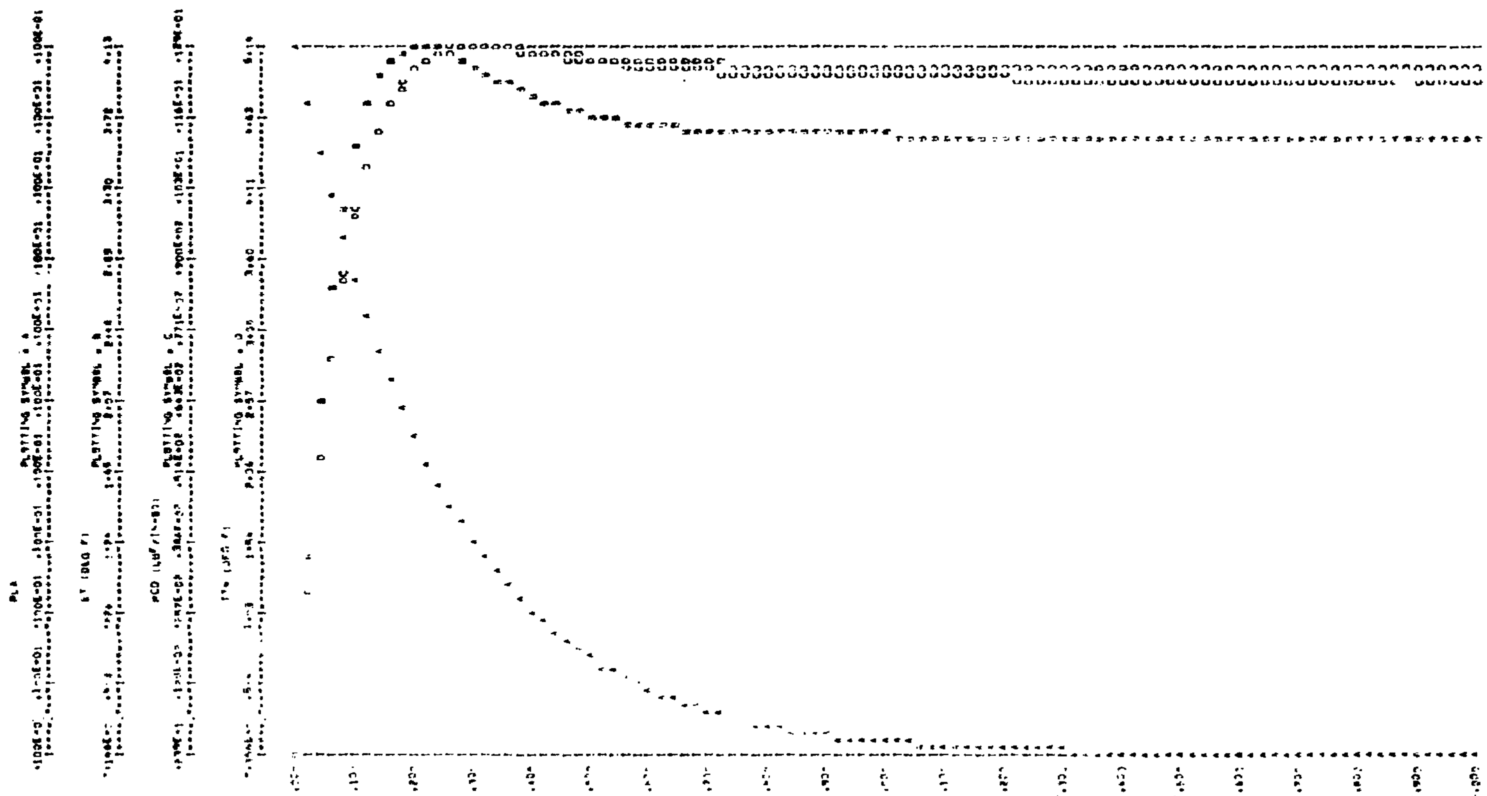

Figure 52. State Control--70-Percent Operating Condition--Temperature

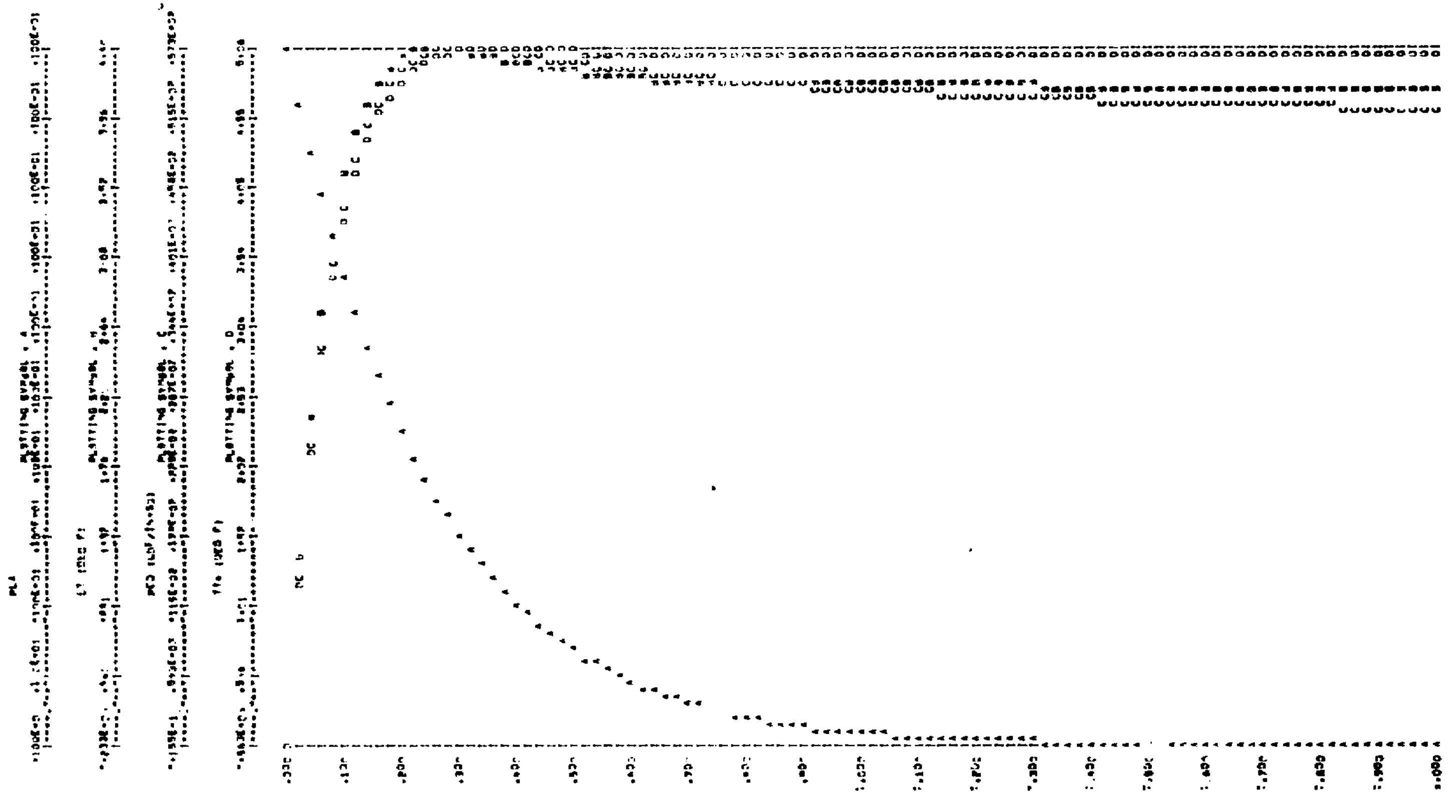

Figure 53. State Control--50-Percent Operating Condition--Temperature

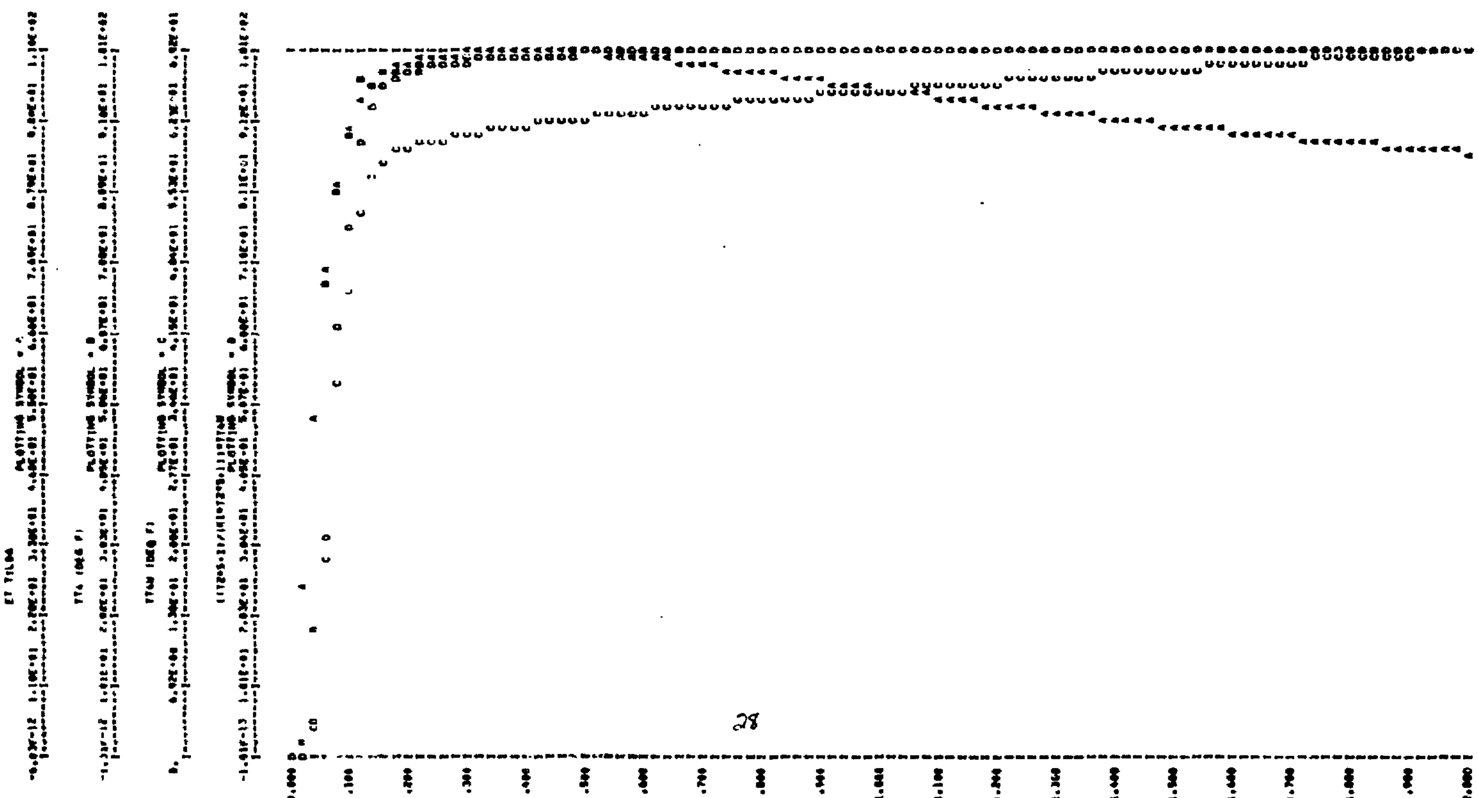

Figure 54a. Simplified Control--100-Percent Operating Conditions--Temperature

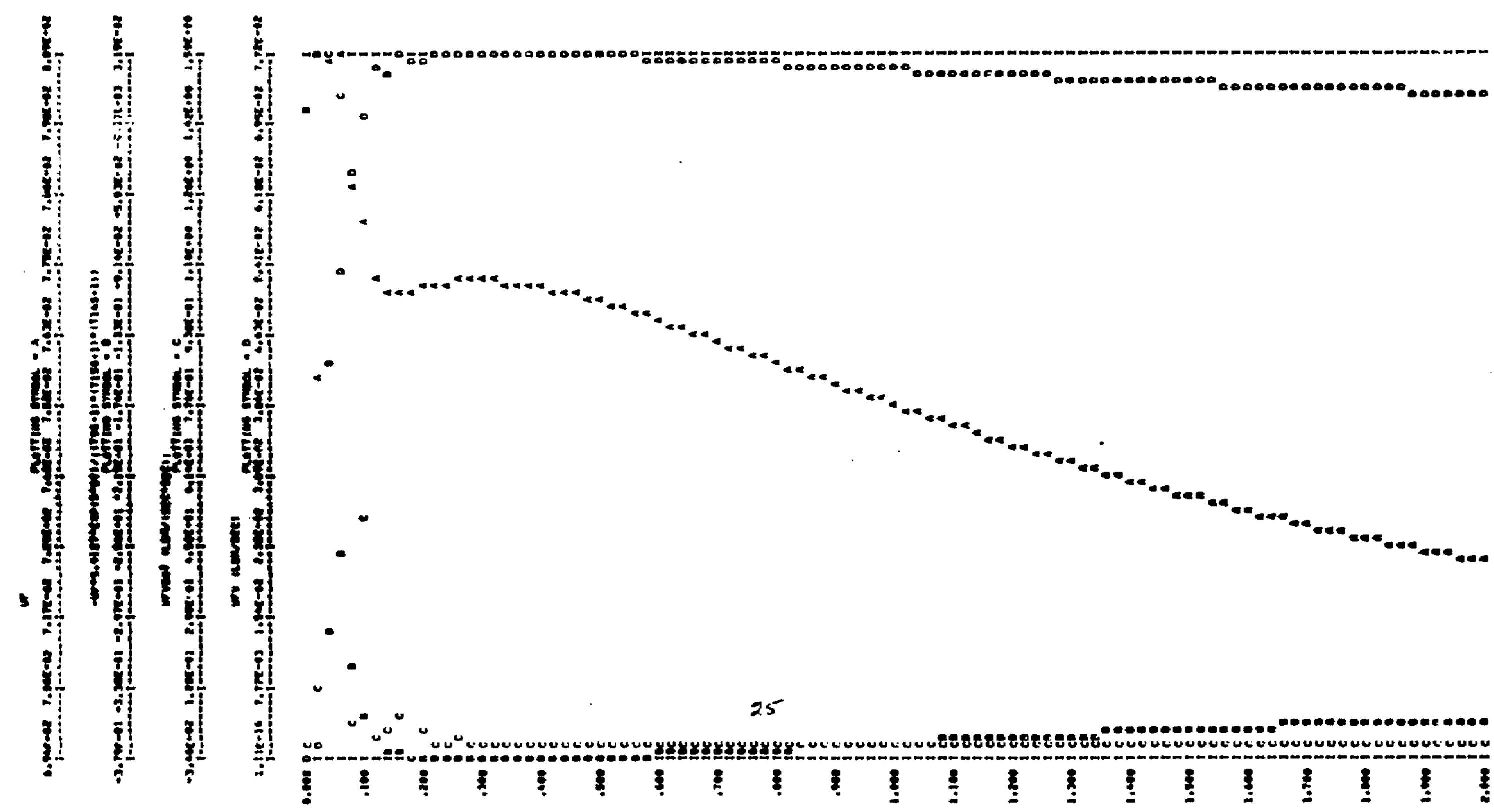

Figure 54b. Simplified Control--100-Percent Operating Conditions--Temperature (Continued)

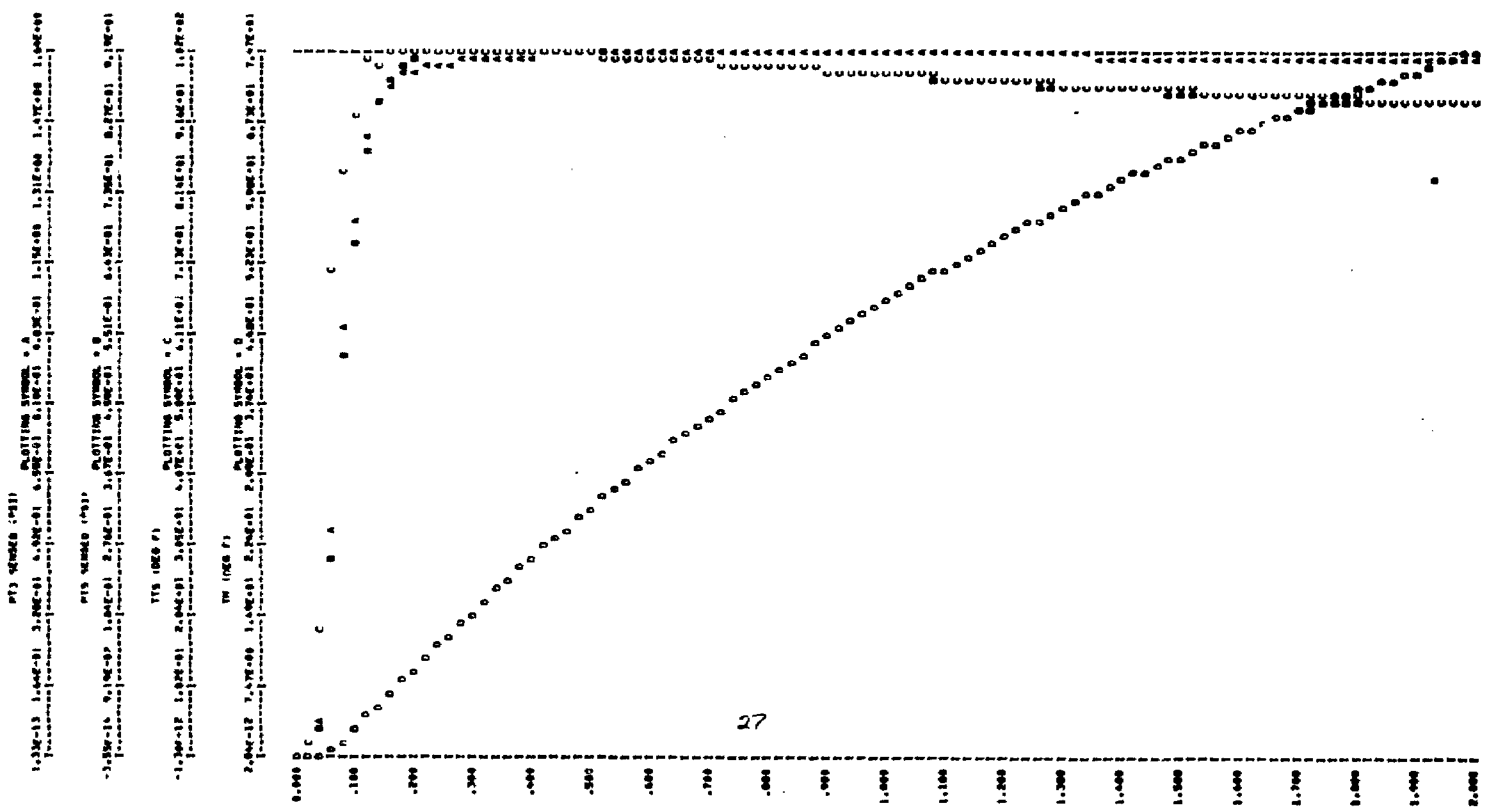

Figure 54c. Simplified Control--100-Percent Operating Conditions--Temperature (Concluded)

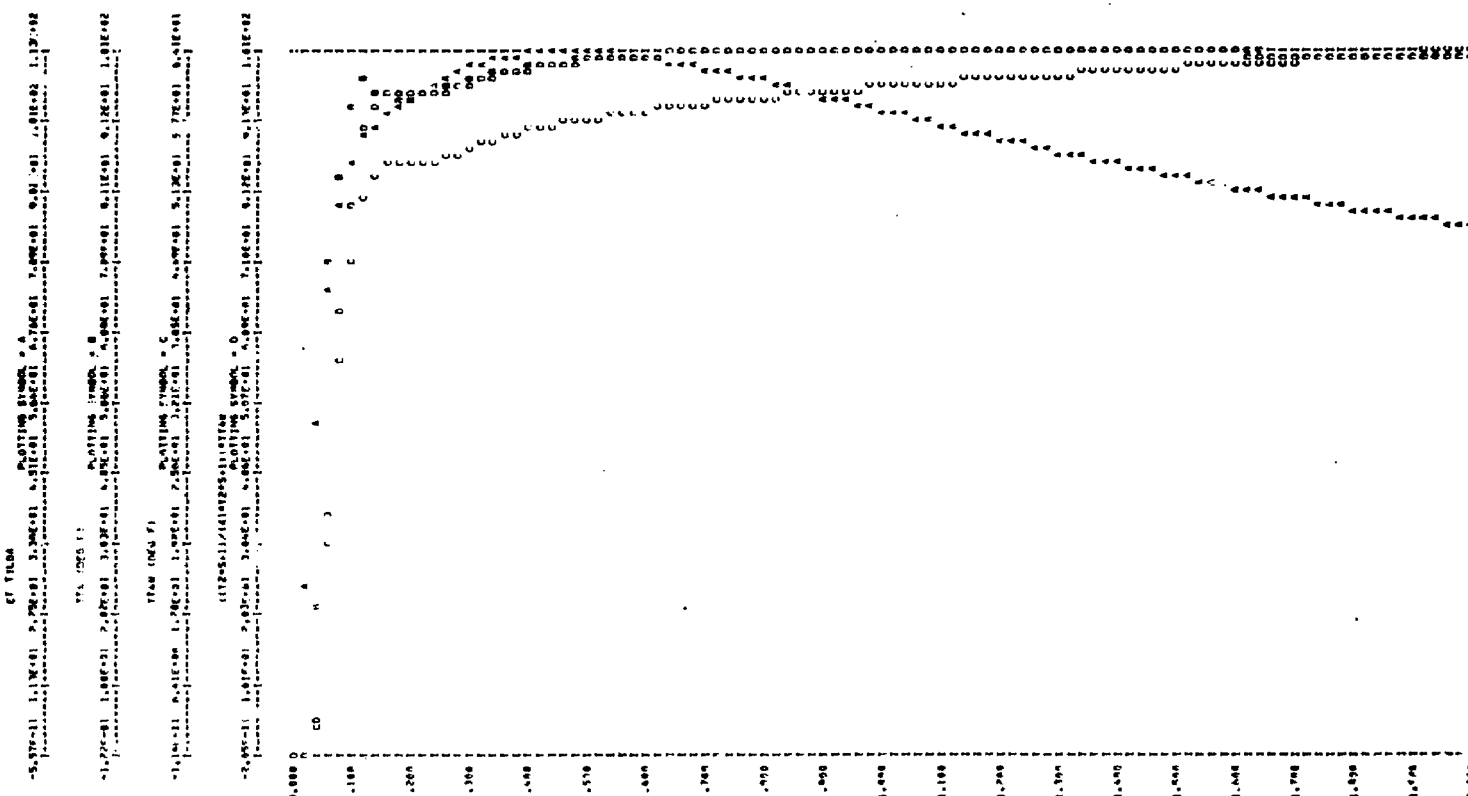

Figure 55a. Simplified Control--85-Percent Operating Condition--Temperature

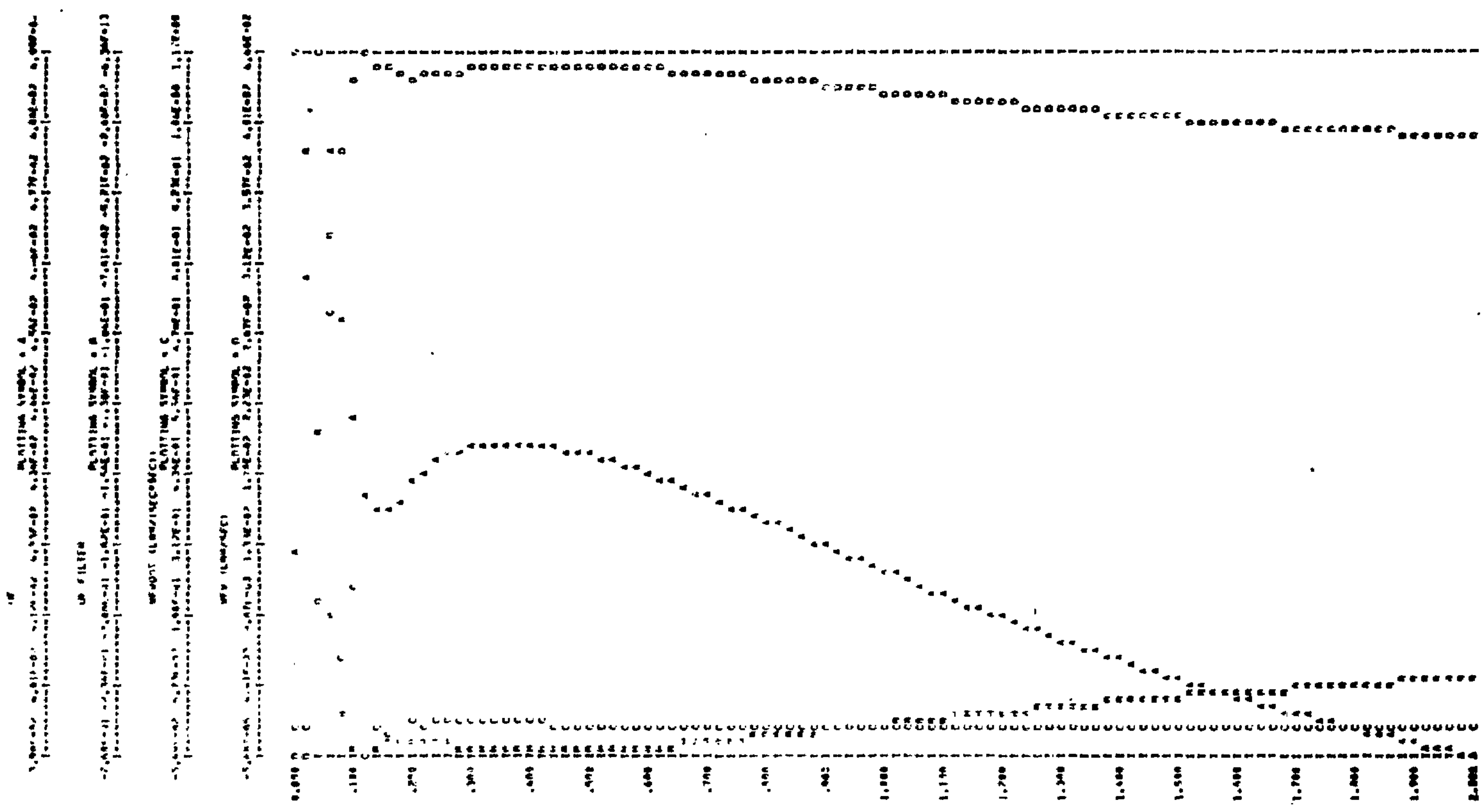

Figure 55b. Simplified Control--85-Percent Operating Condition--Temperature (Continued)

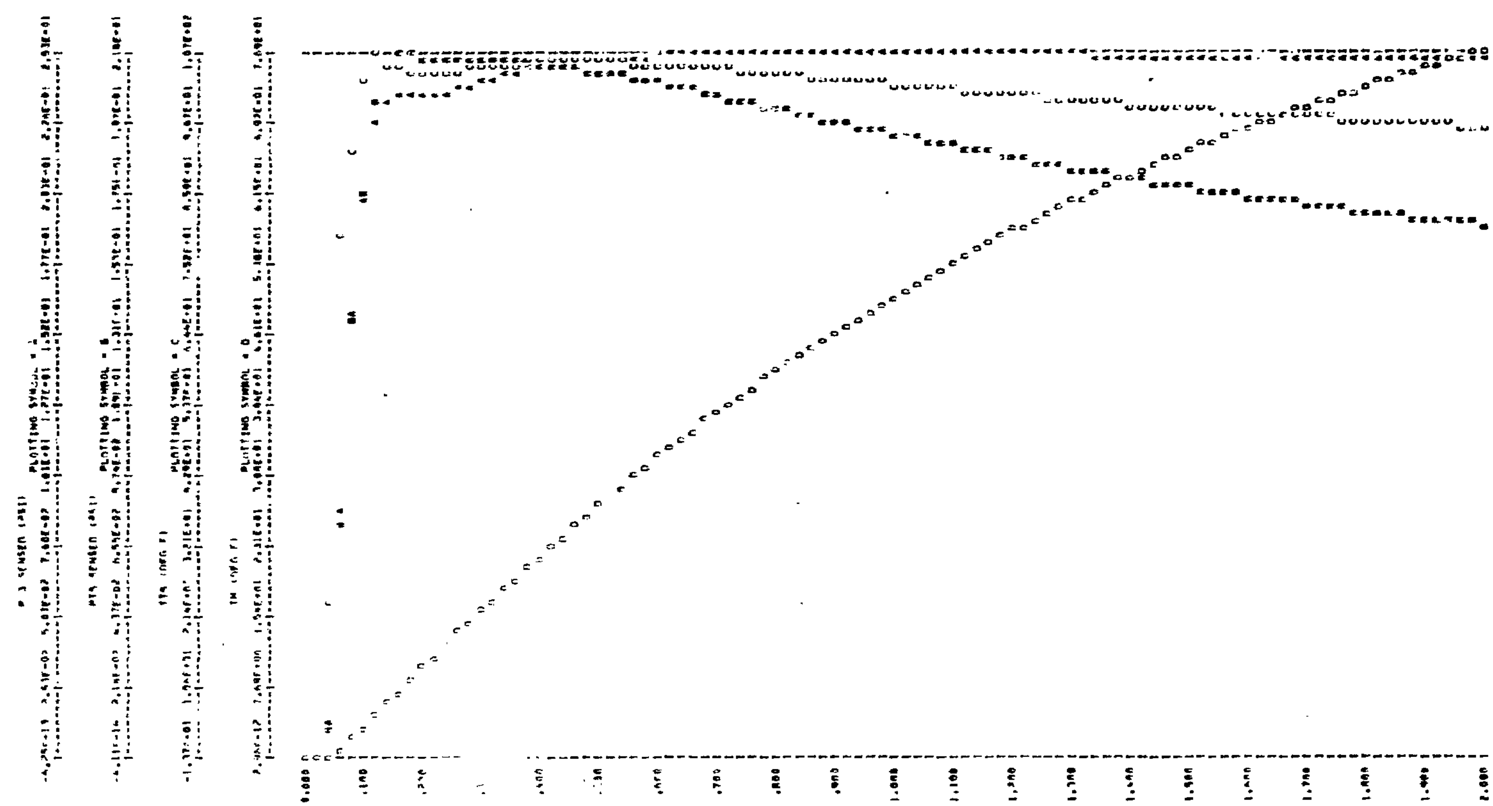

Figure 55c. Simplified Control--35-Percent Operating Condition--Temperature (Concluded)

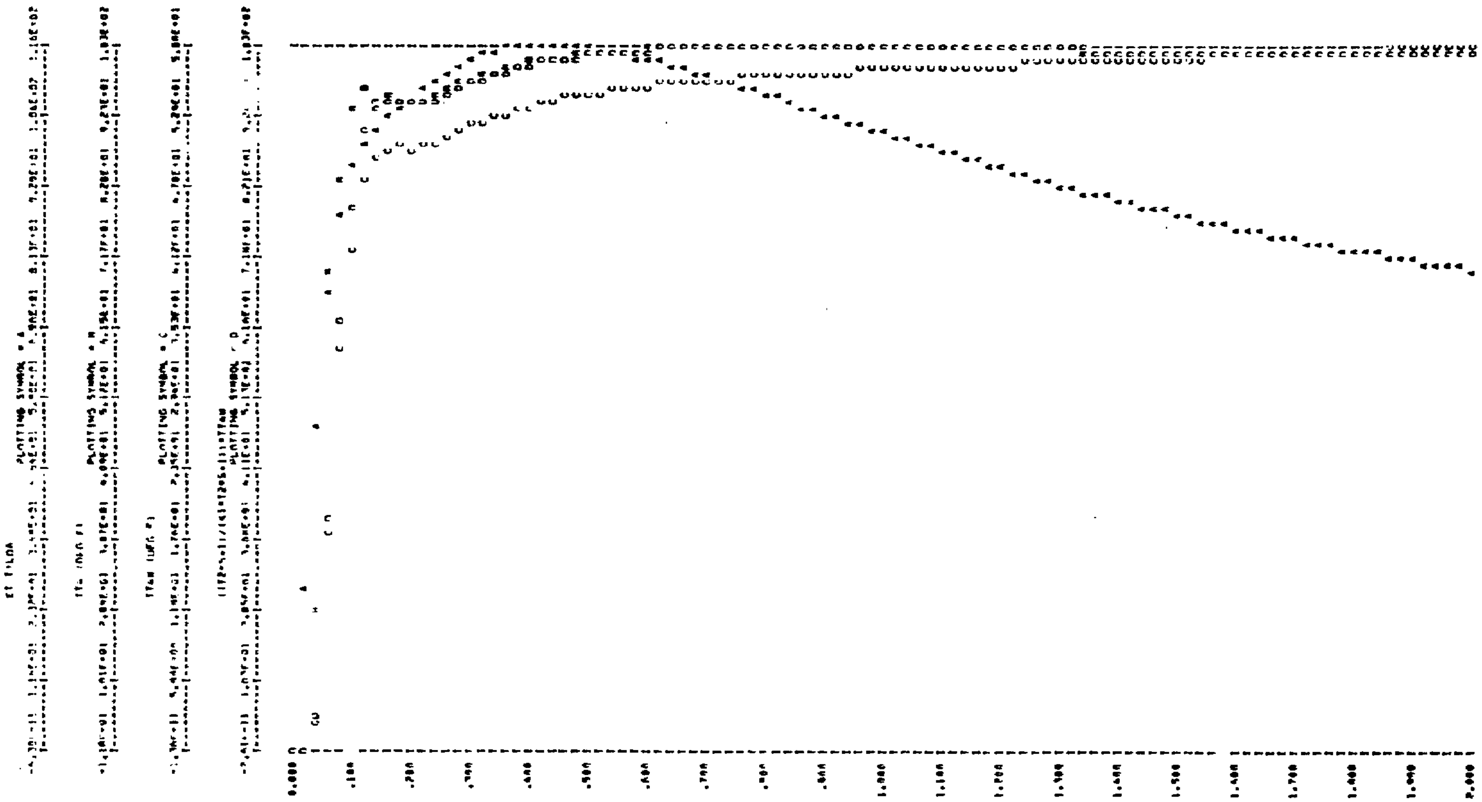

Figure 56a. Simplified Control--70-Percent Operating Condition--Temperature

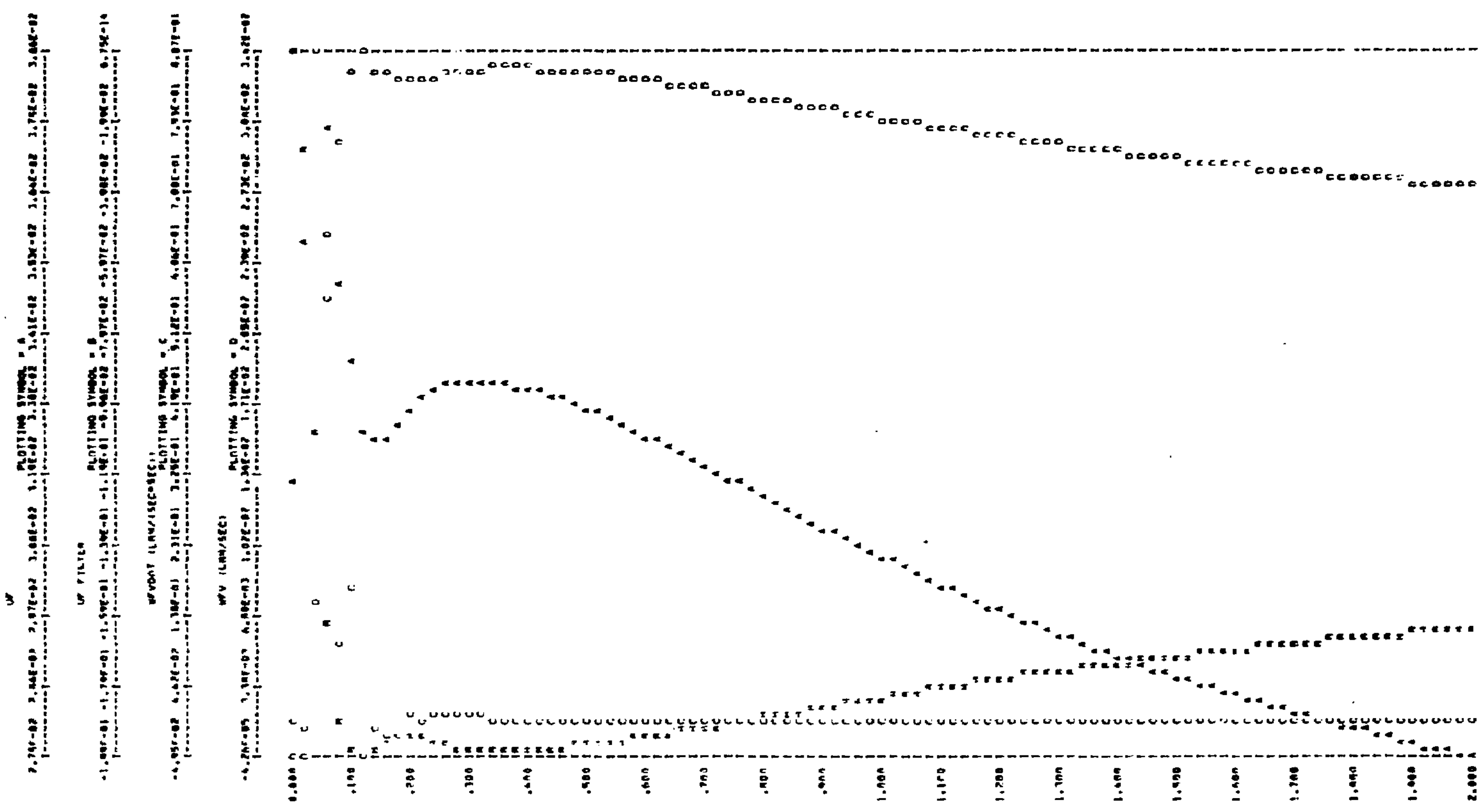

Figure 56b. Simplified Control--70-Percent Operating Condition--Temperature (Continued)

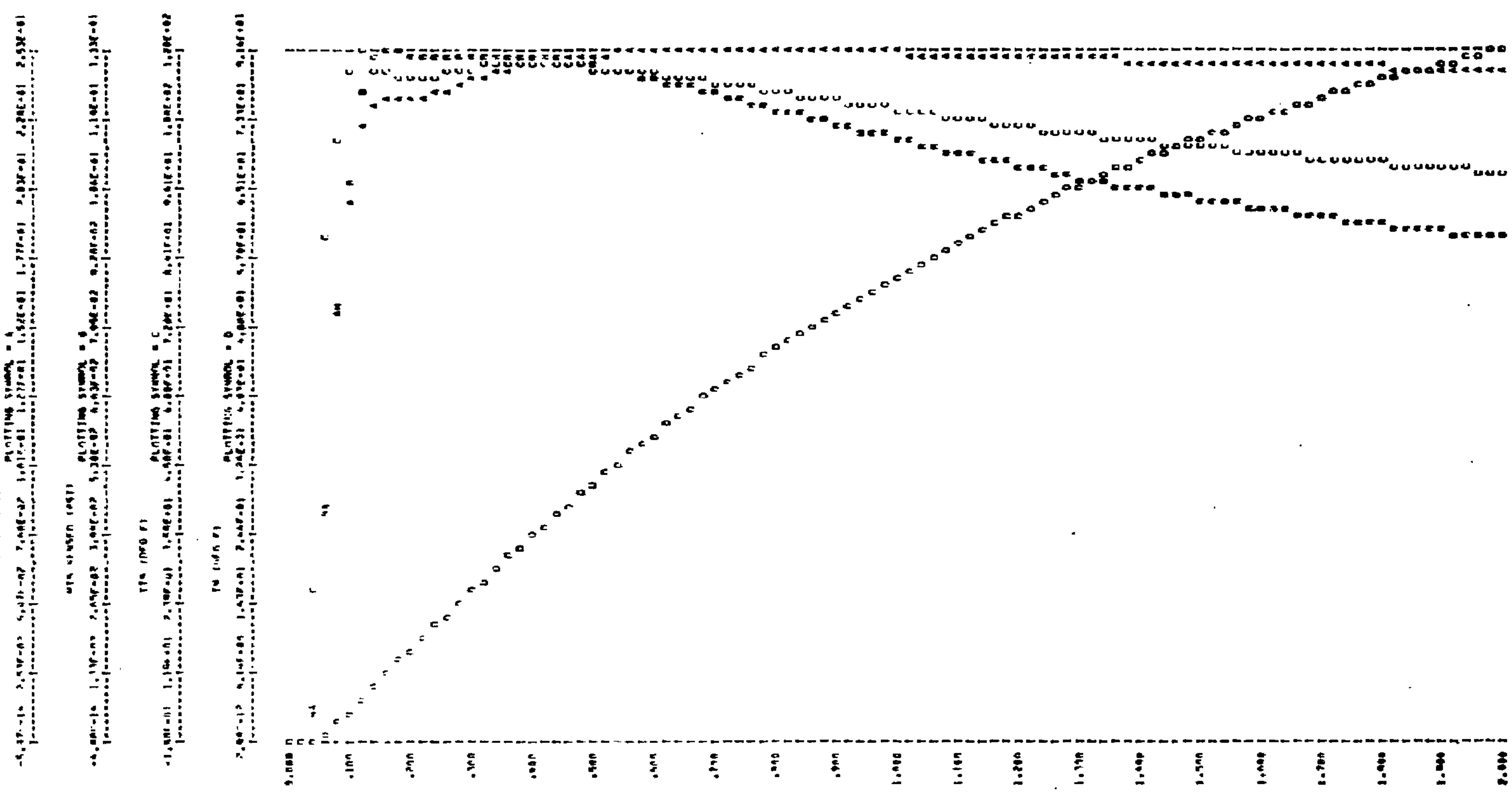

Figure 56c. Simplified Control--70-Percent Operating Condition--Temperature (Concluded)

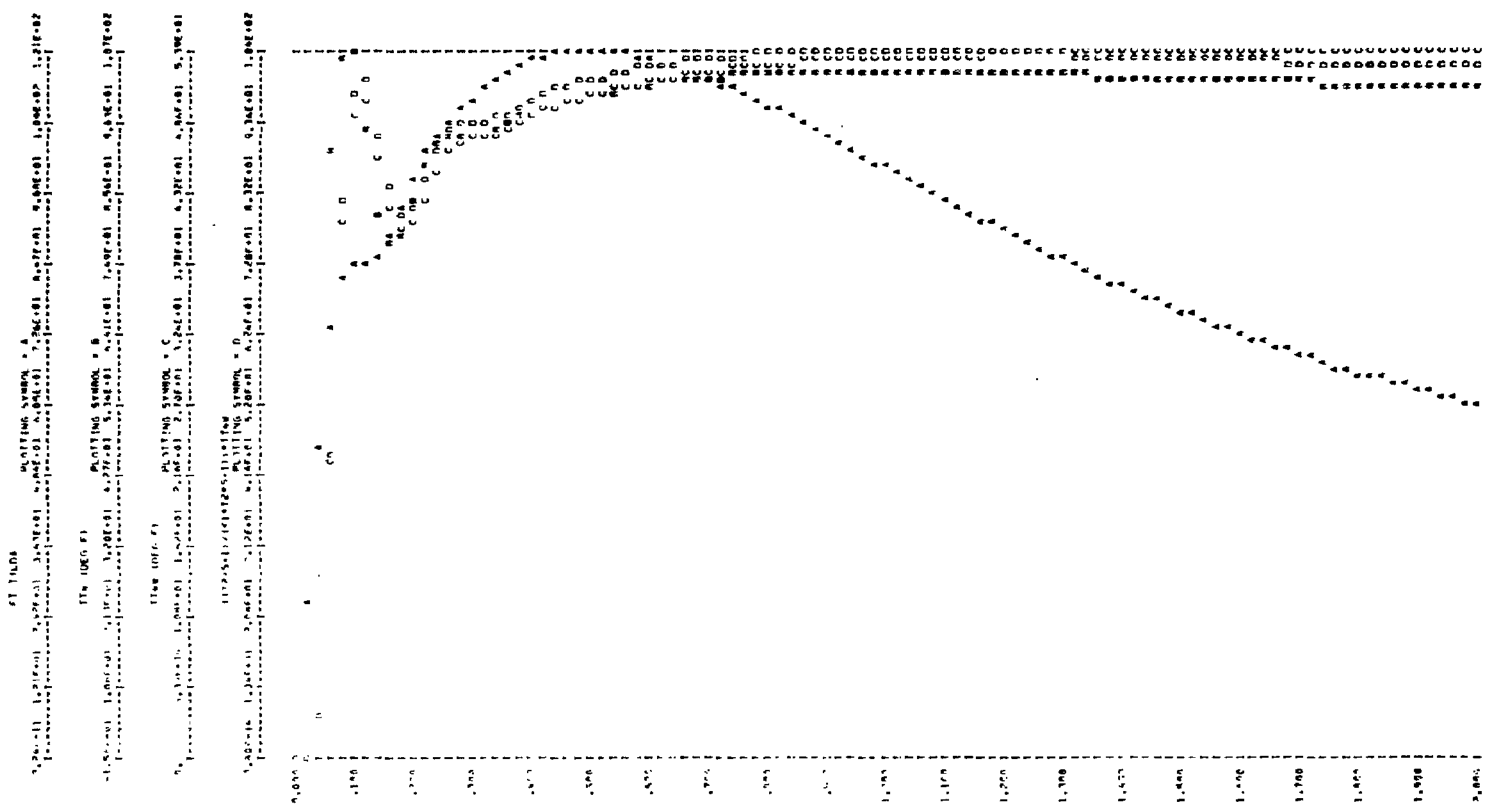

Figure 57a. Simplified Control--50-Percent Operating Condition--Temperature

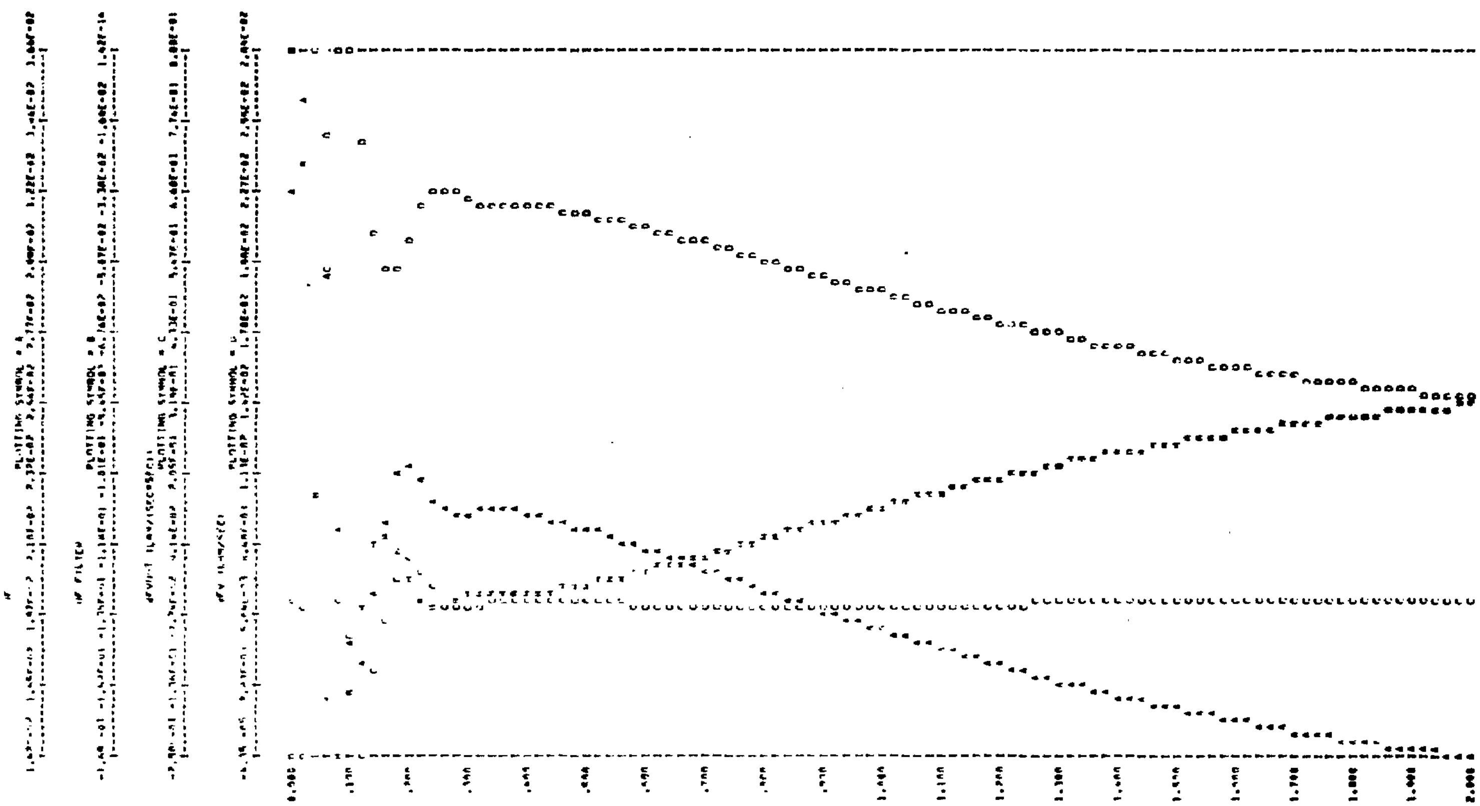

Figure 57b. Simplified Control--50-Percent Operating Condition--Temperature (Continued)

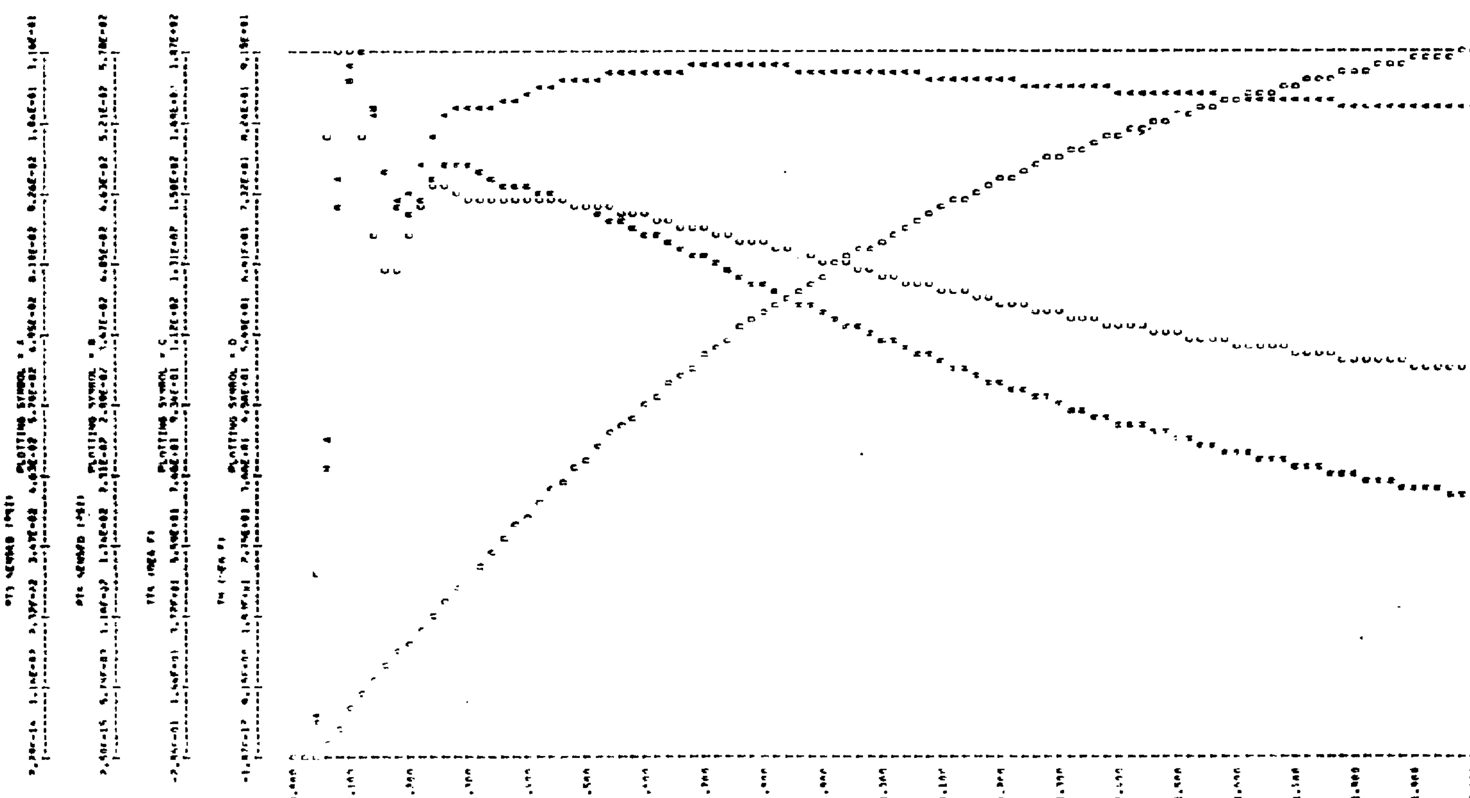

Figure 57c. Simplified Control--50-Percent Operating Condition--Temperature (Concluded)

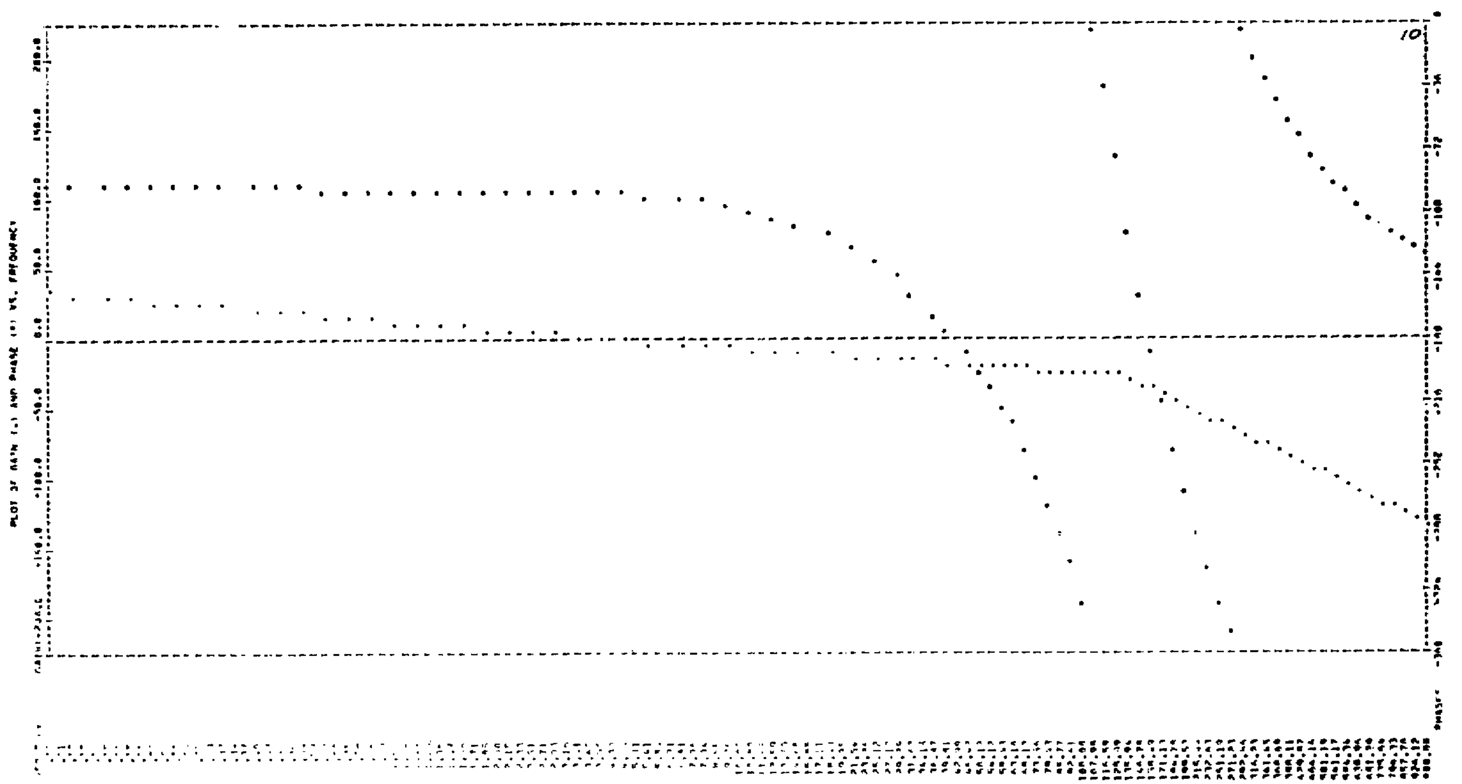

Figure 58a. Actuator Open Loop--100-Percent Operating Condition--Temperature

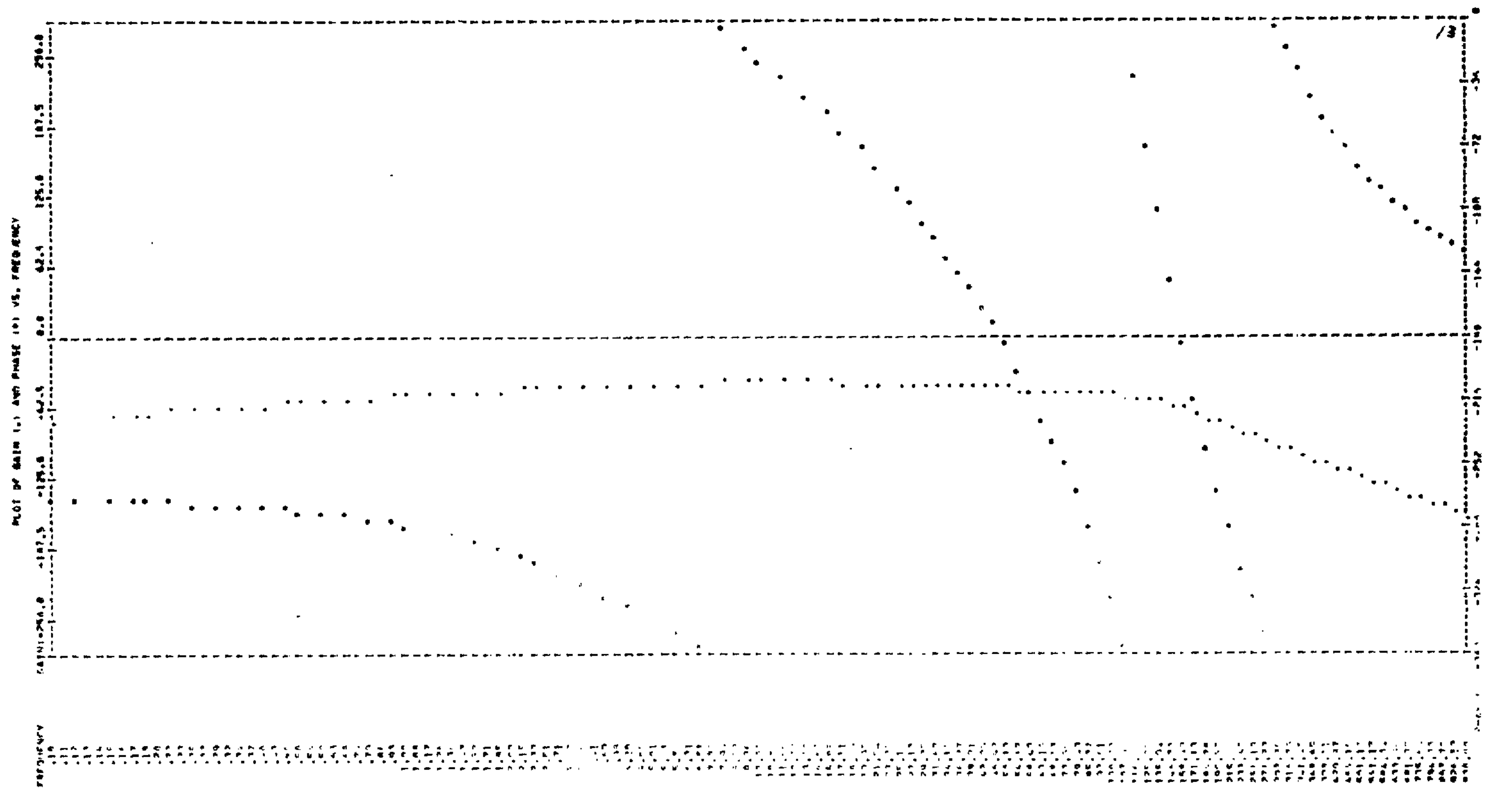

Figure 58b. TT4 Open Loop--100-Percent Operating Condition--Temperature

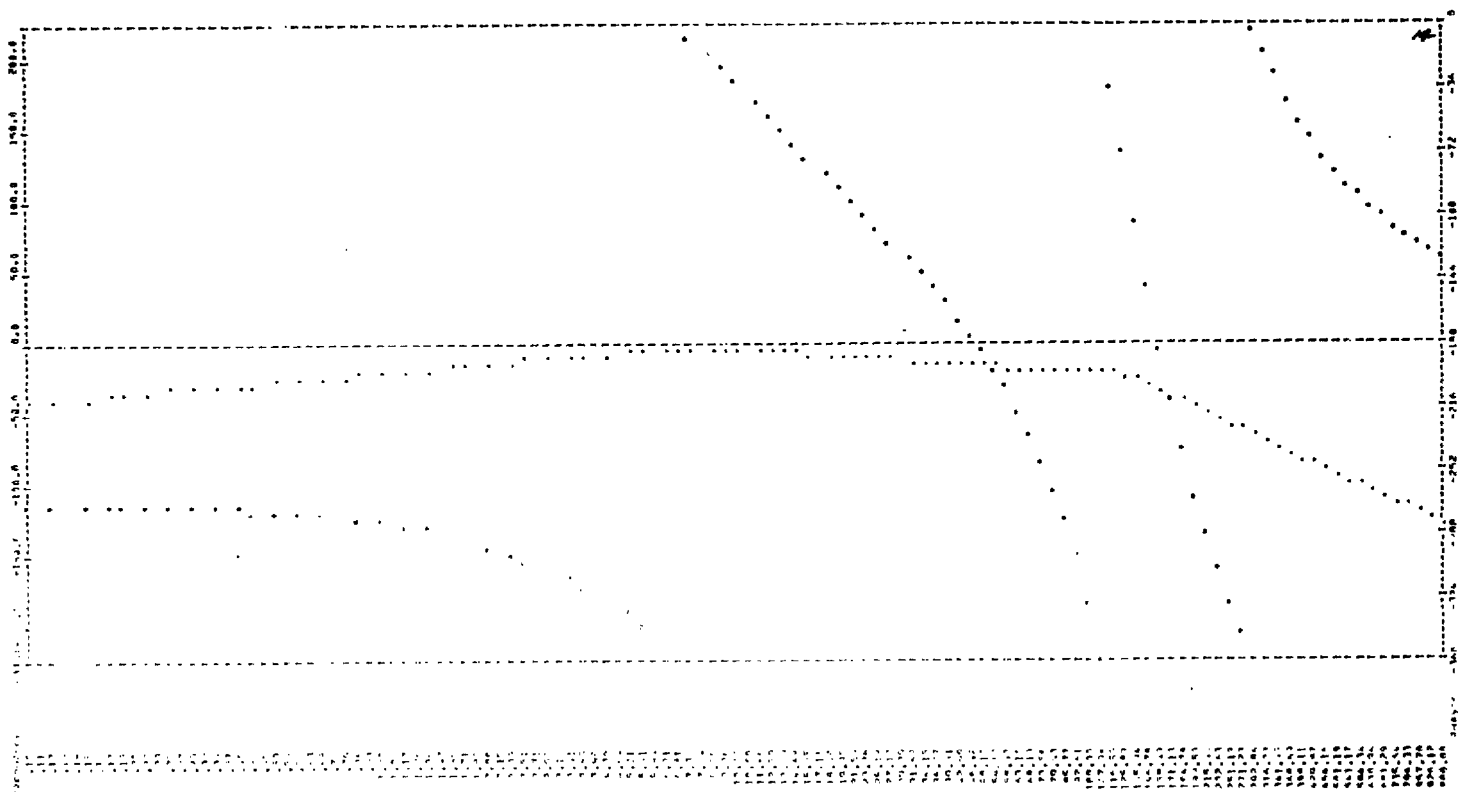

Figure 58c. PT3 Open Loop--100-Percent Operating Condition--Temperature

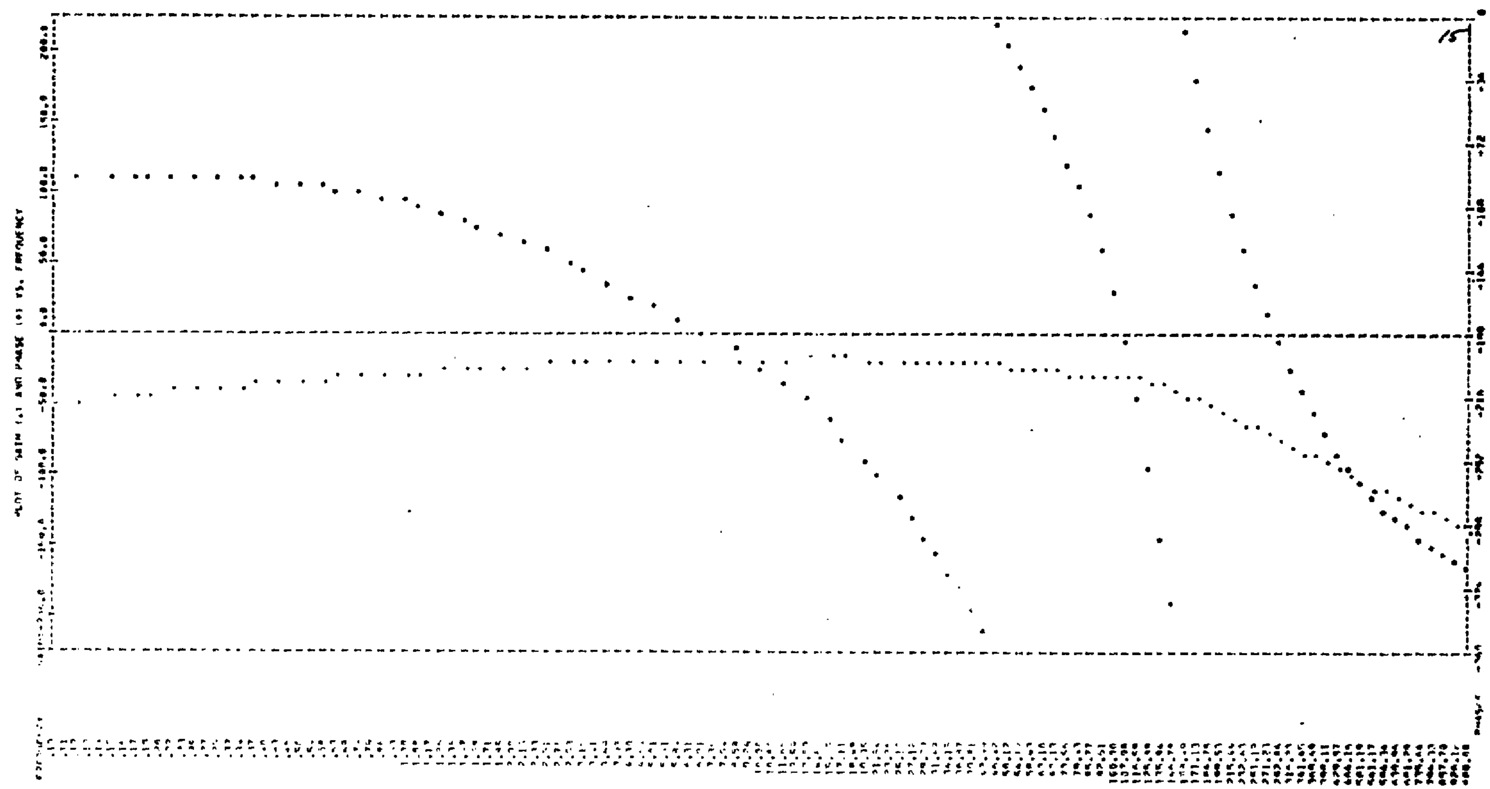

Figure 58d. PT5 Open Loop--100-Percent Operating Condition--Temperature

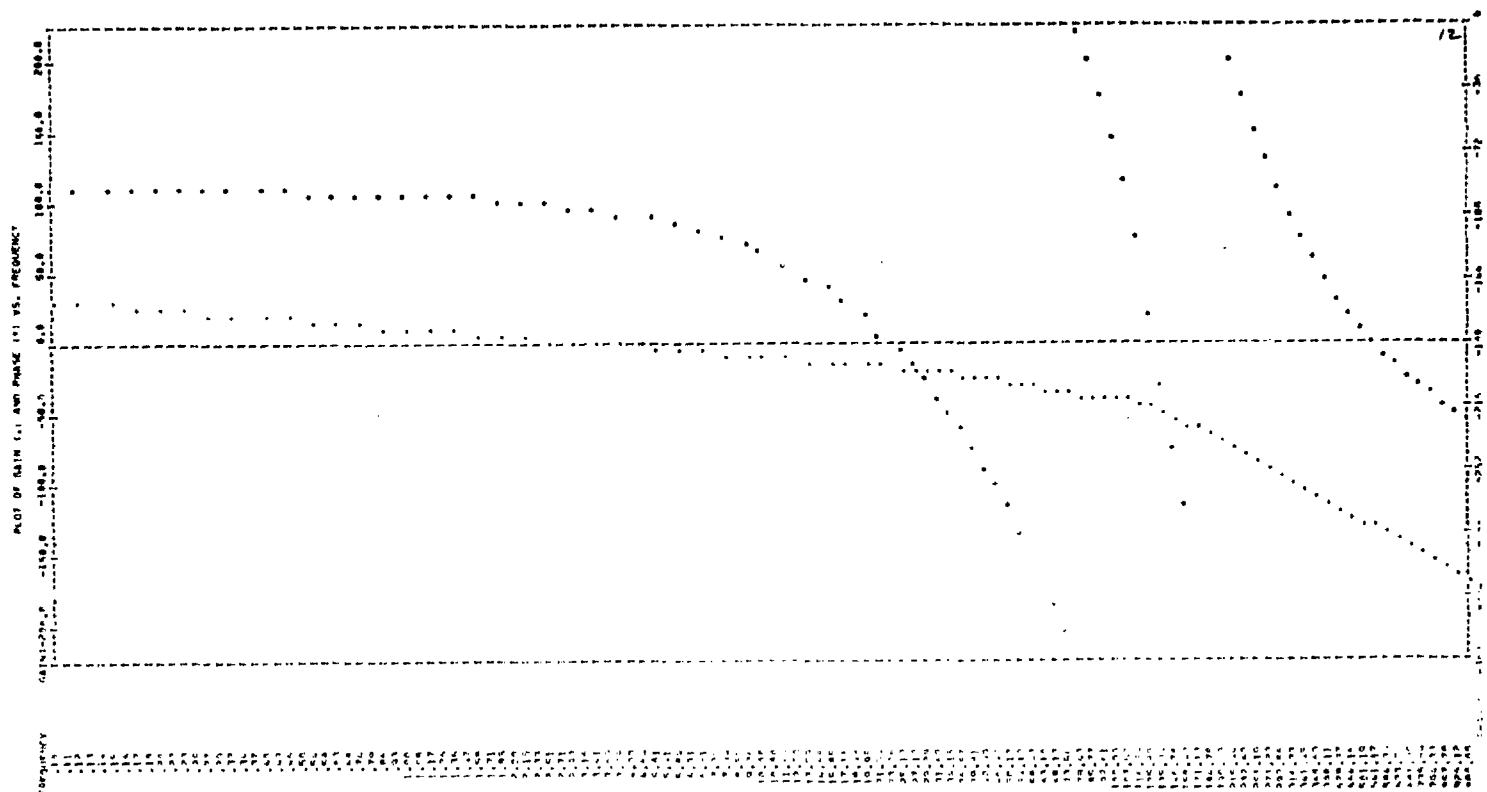

Figure 58e. ET Open Loop--100-Percent Operating Condition--Temperature

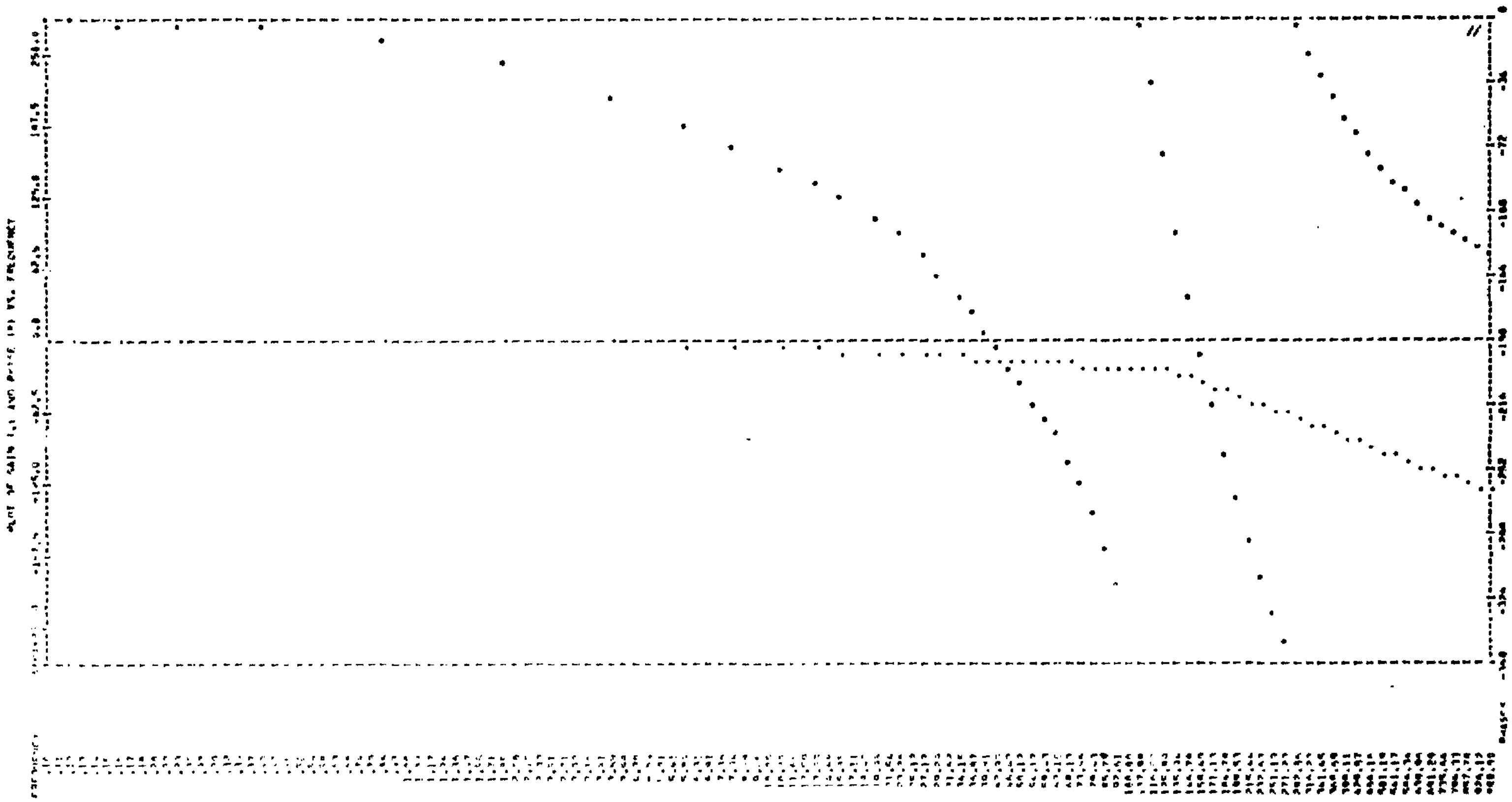

Figure 58f. Closed-Loop--100-Percent Operating Condition--Temperature

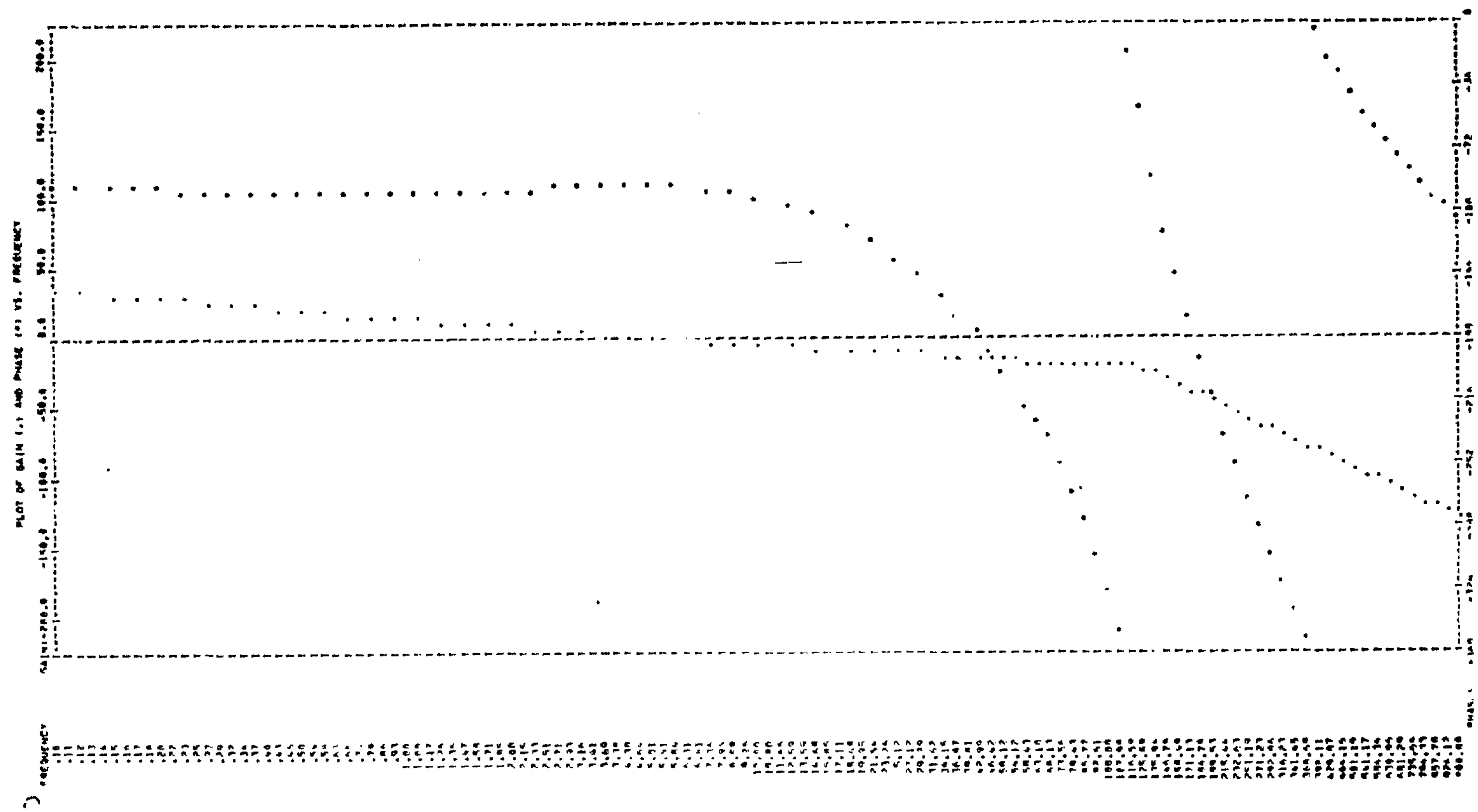

Figure 59a. Actuator Open Loop--85-Percent Operating Condition--Temperature

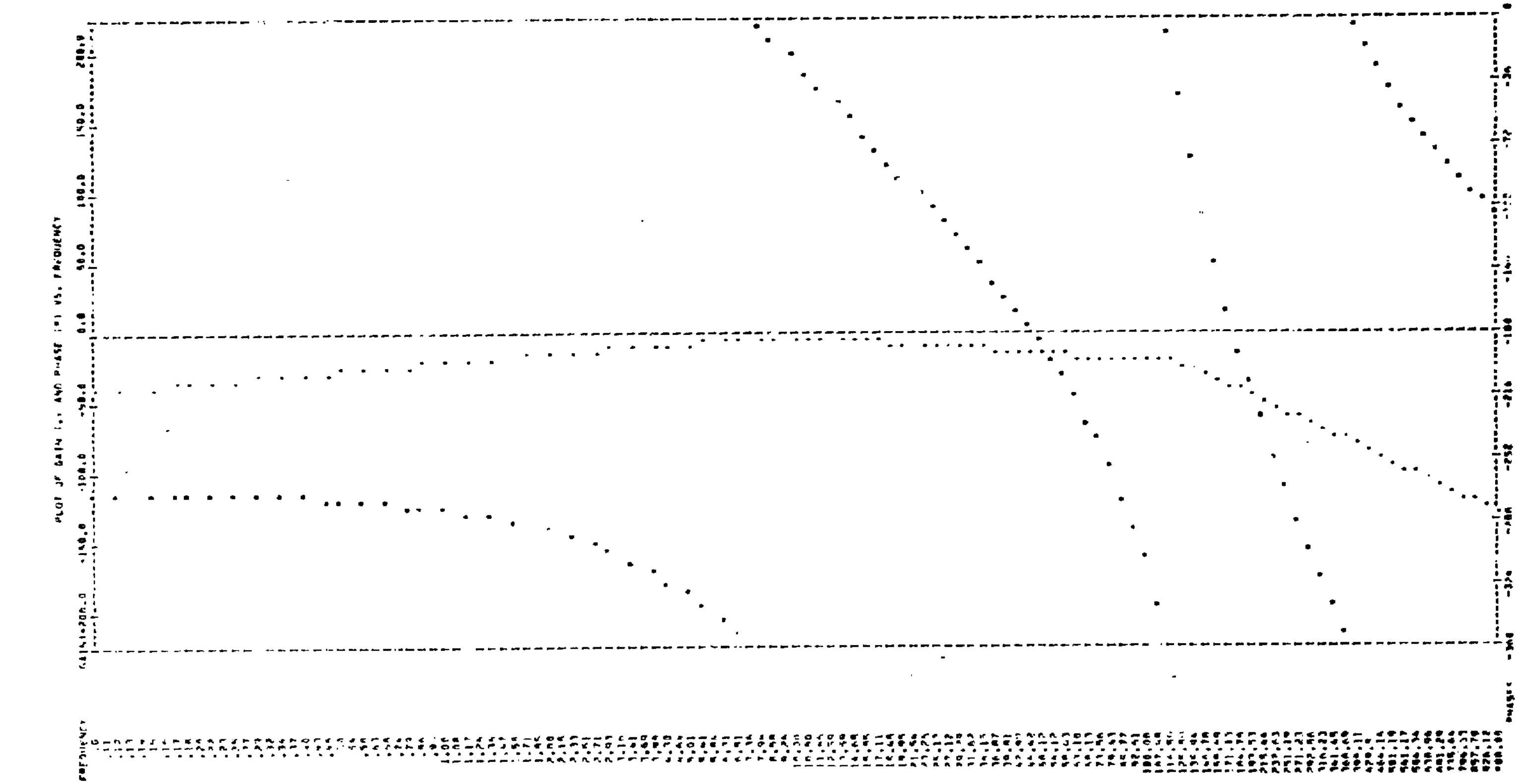

Figure 59b. TT4 Open Loop--85-Percent Operating Condition--Temperature

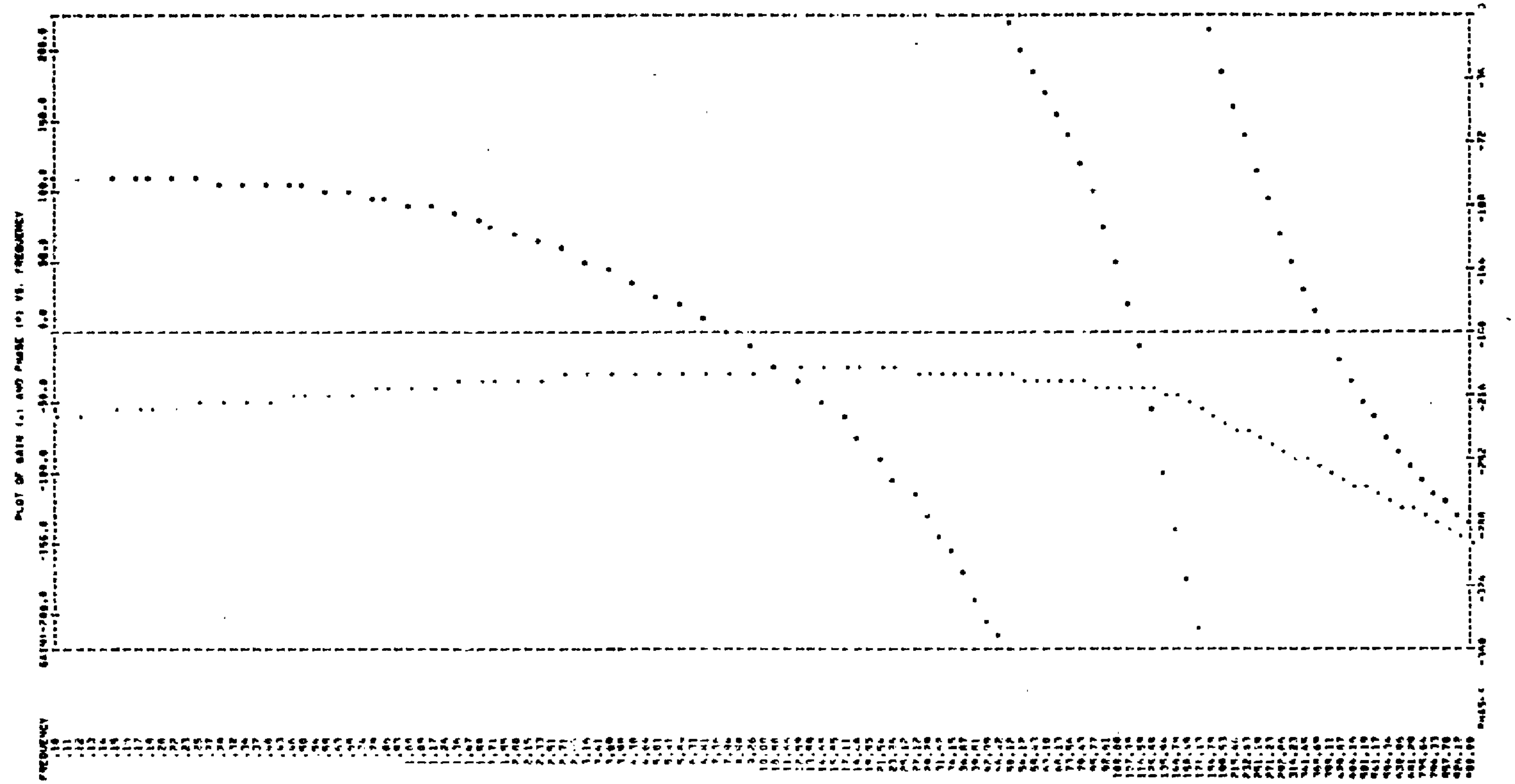

Figure 59c. PT3 Open Loop--85-Percent Operating Condition--Temperature

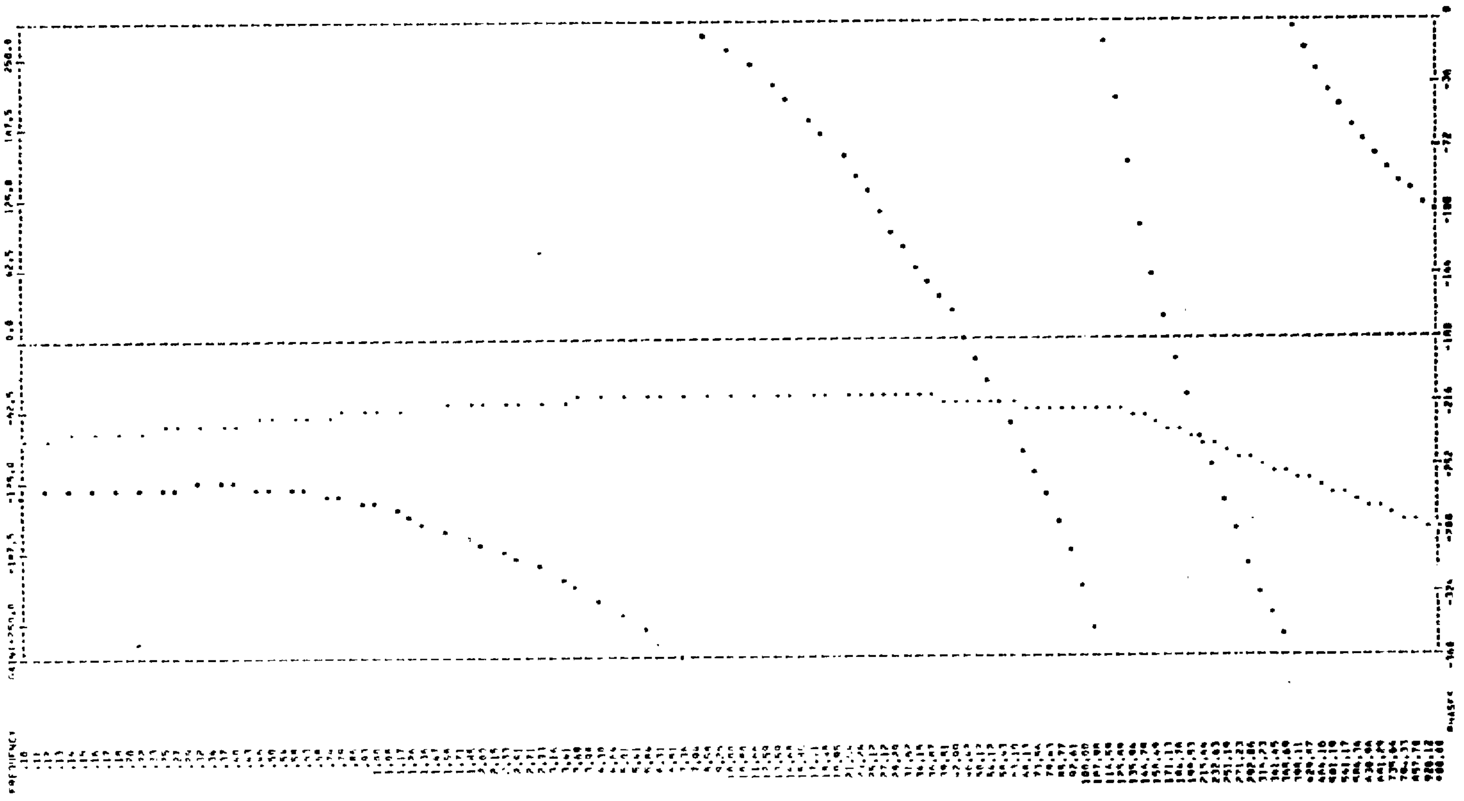

Figure 59d. PT5 Open Loop--85-Percent Operating Condition--Temperature

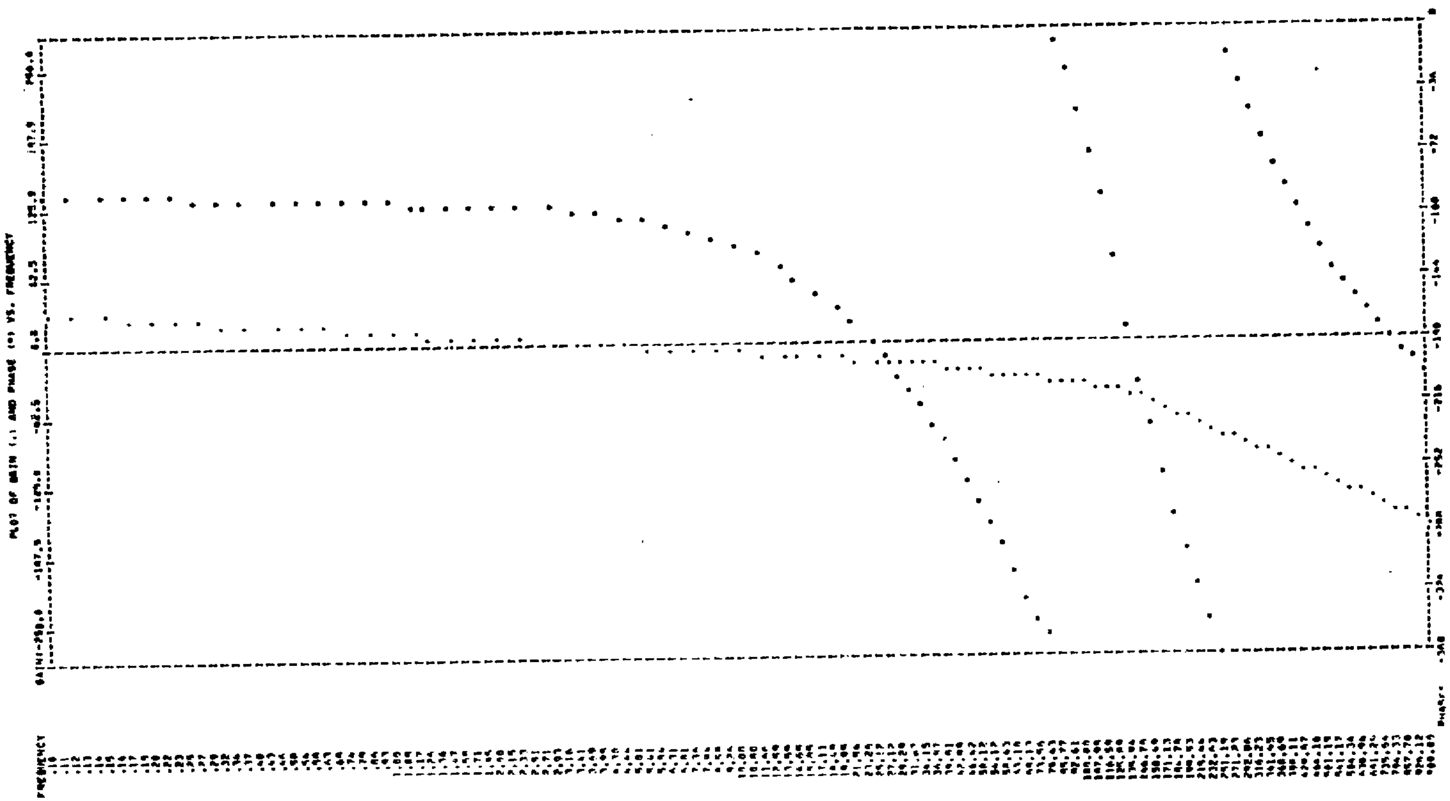

Figure 59e. ET Open Loop--85-Percent Operating Condition--Temperature

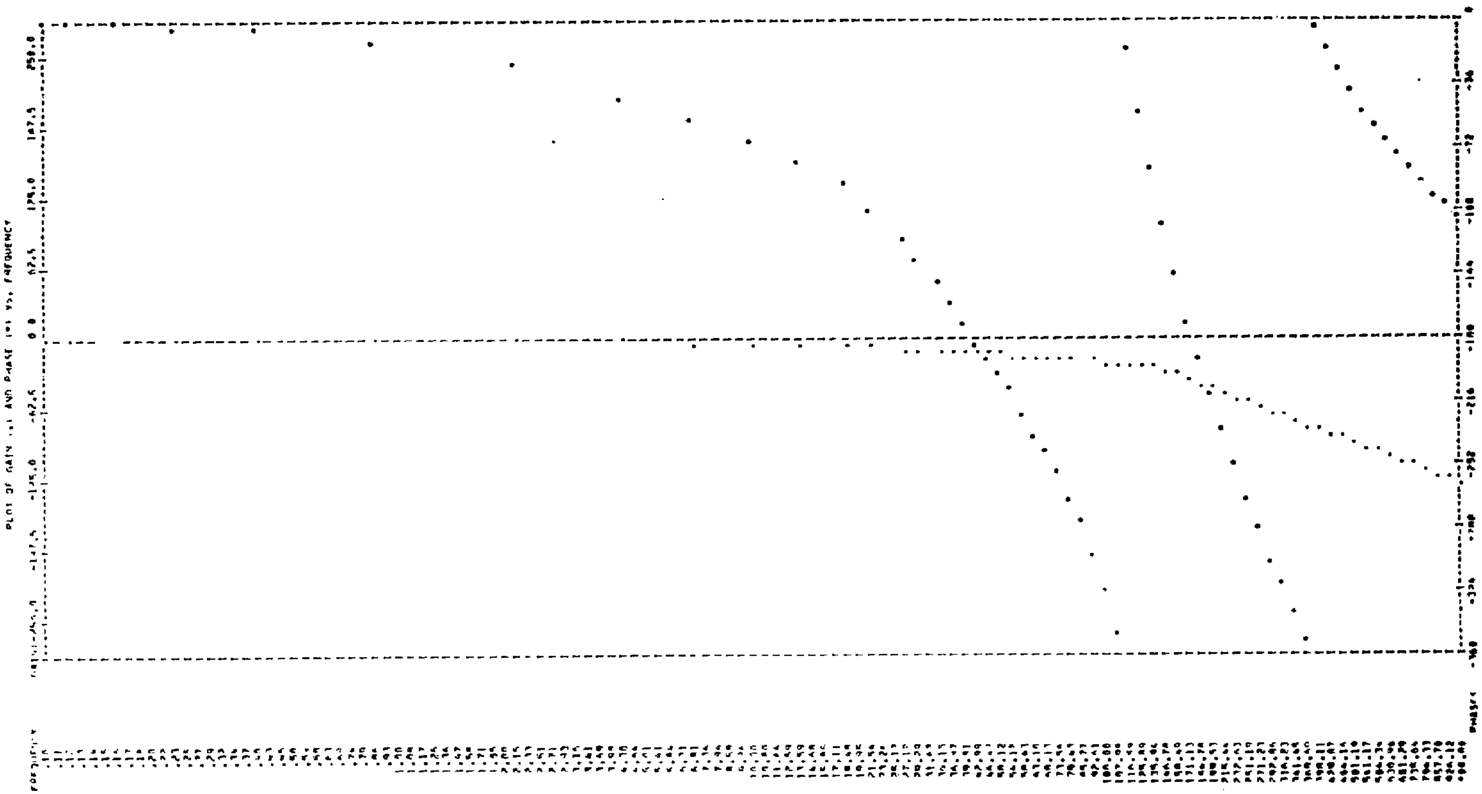

Figure 59f. Closed Loop--85-Percent Operating Condition--Temperature

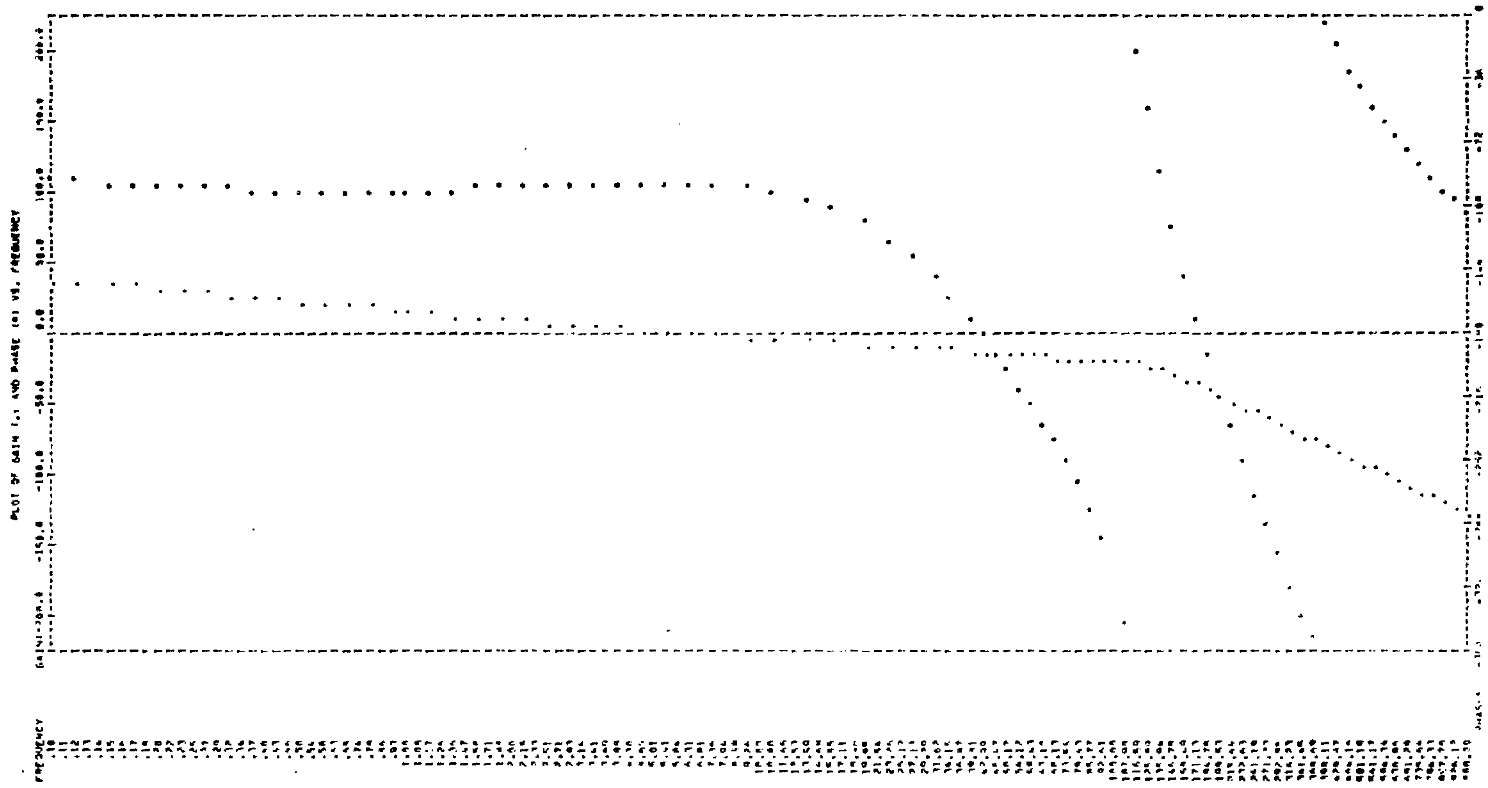

Figure 60a. Actuator Open Loop--70-Percent Operating Condition--Temperature

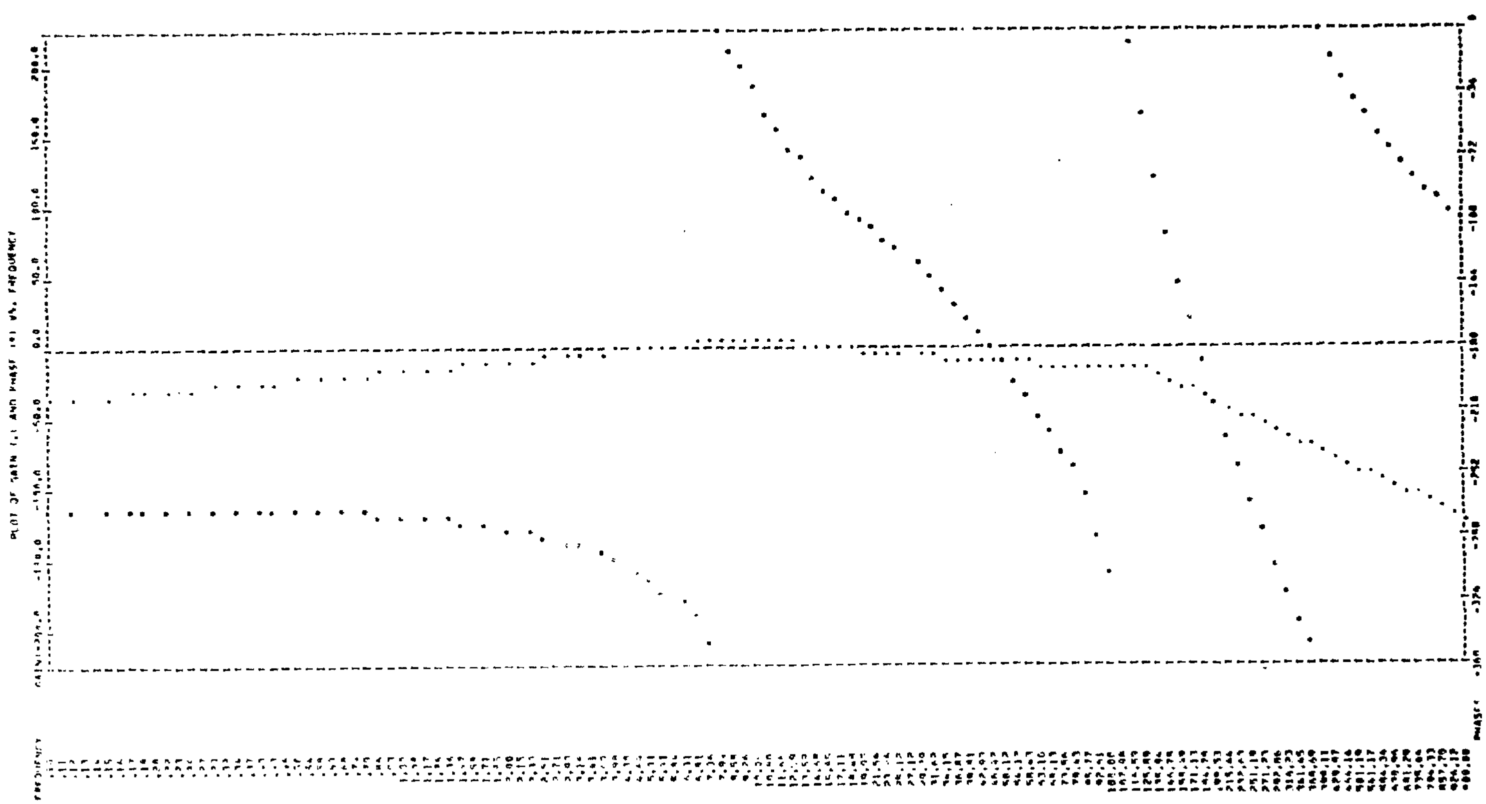

Figure 60b. TT4 Open Loop--70-Percent Operating Condition--Temperature

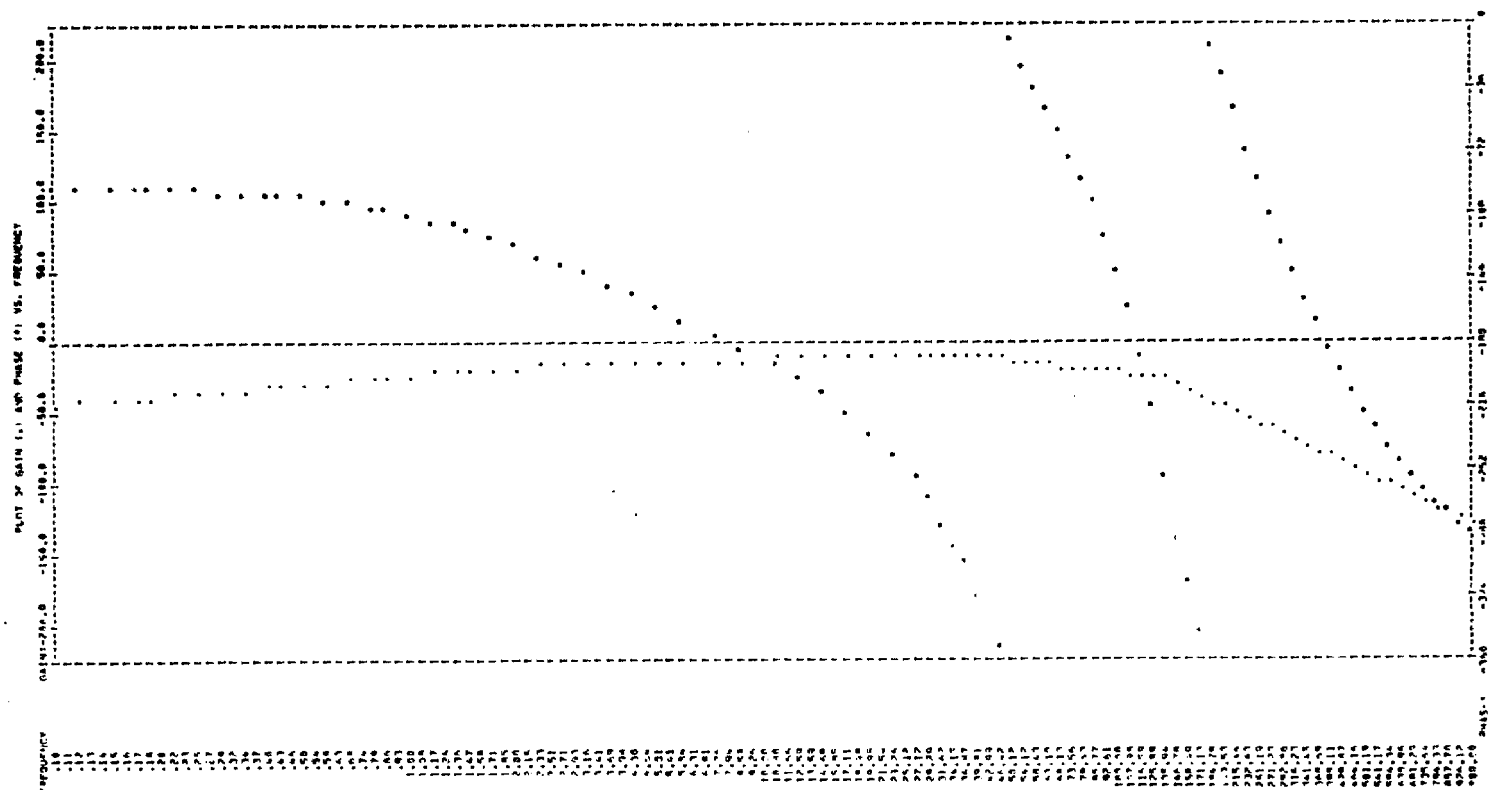

Figure 60c. PT3 Open Loop--70-Percent Operating Condition--Temperature

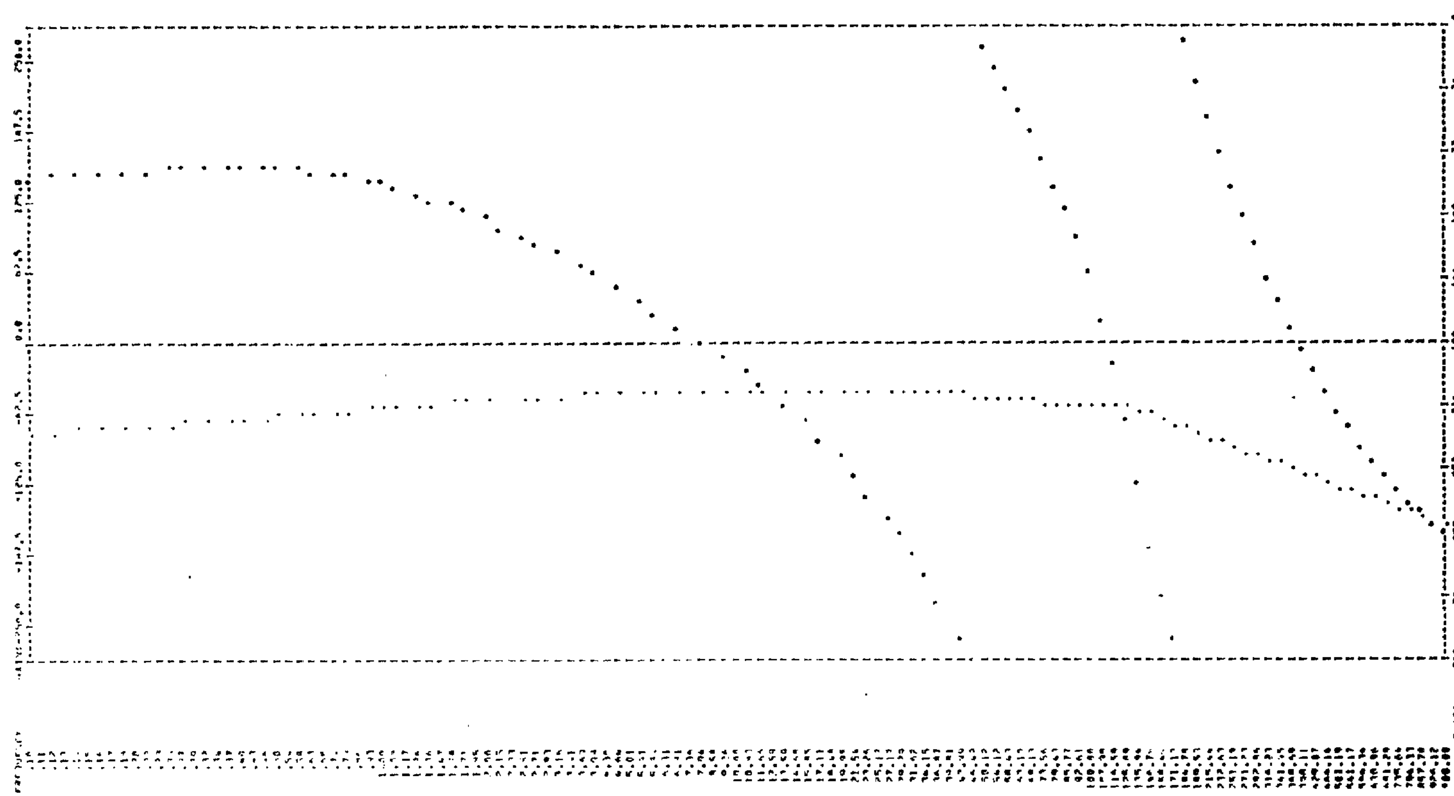

Figure 60d. PT5 Open Loop--70-Percent Operating Condition--Temperature

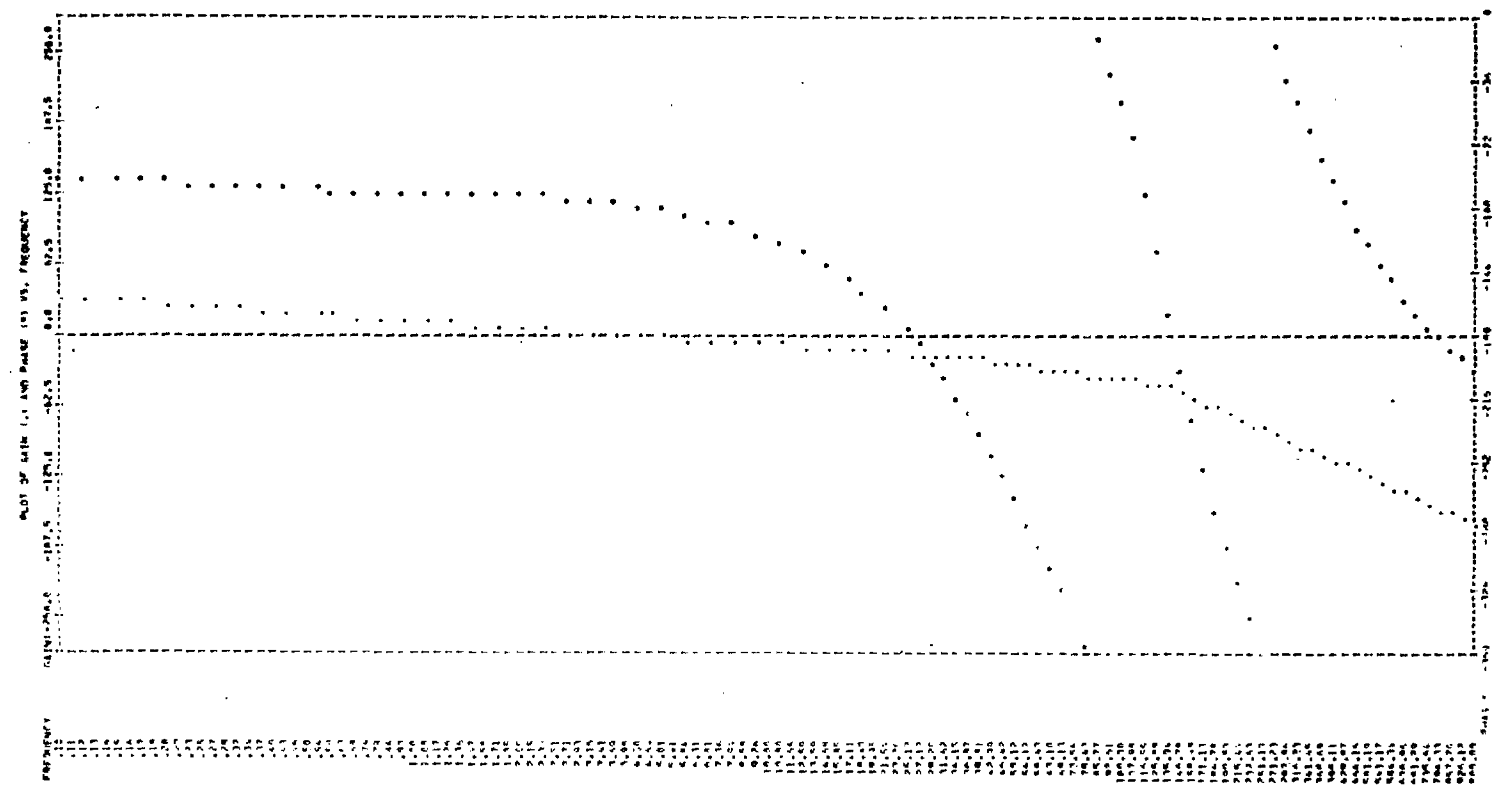

Figure 60e. ET Open Loop--70-Percent Operating Condition--Temperature

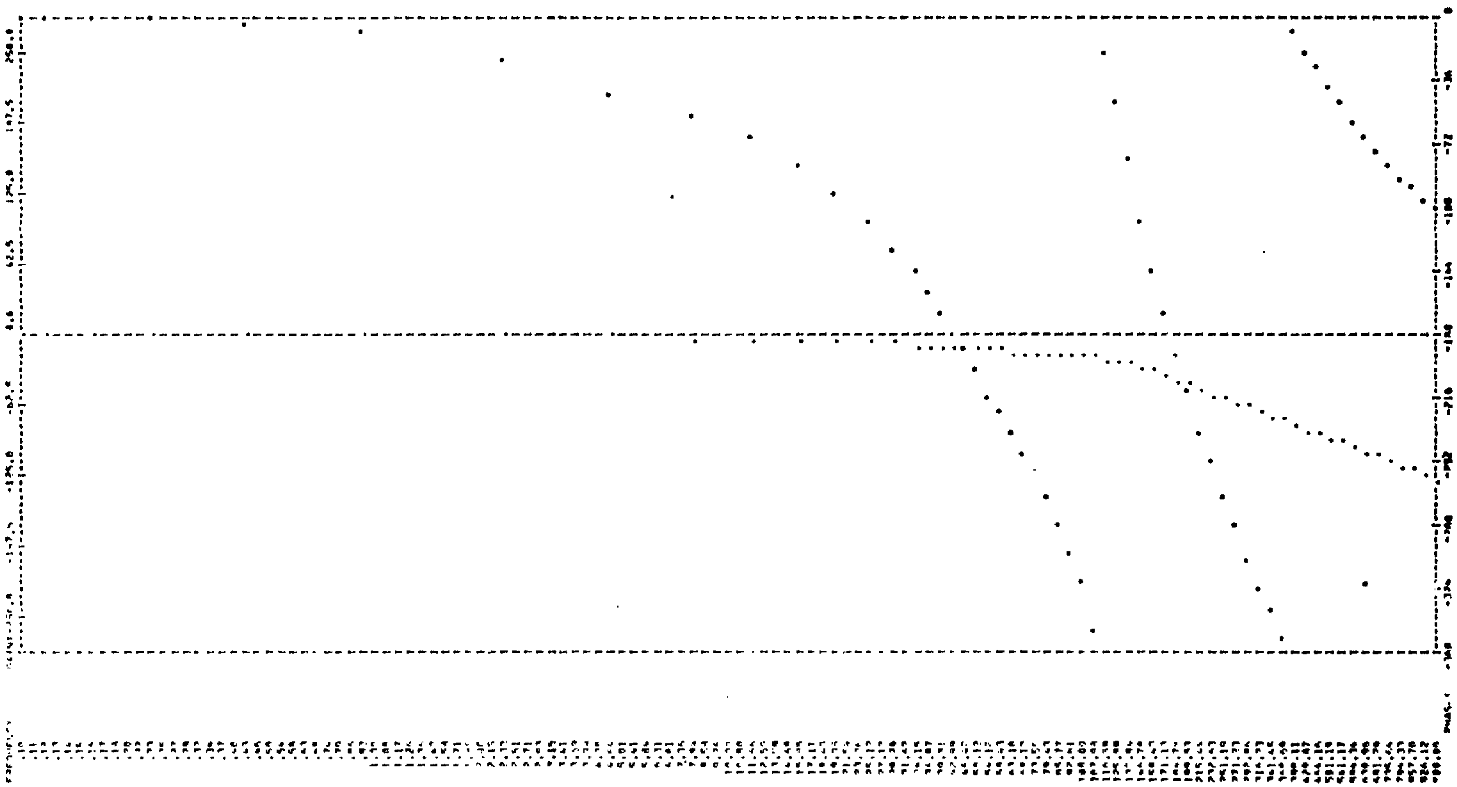

Figure 60f. Closed Loop--70-Percent Operating Condition--Temperature

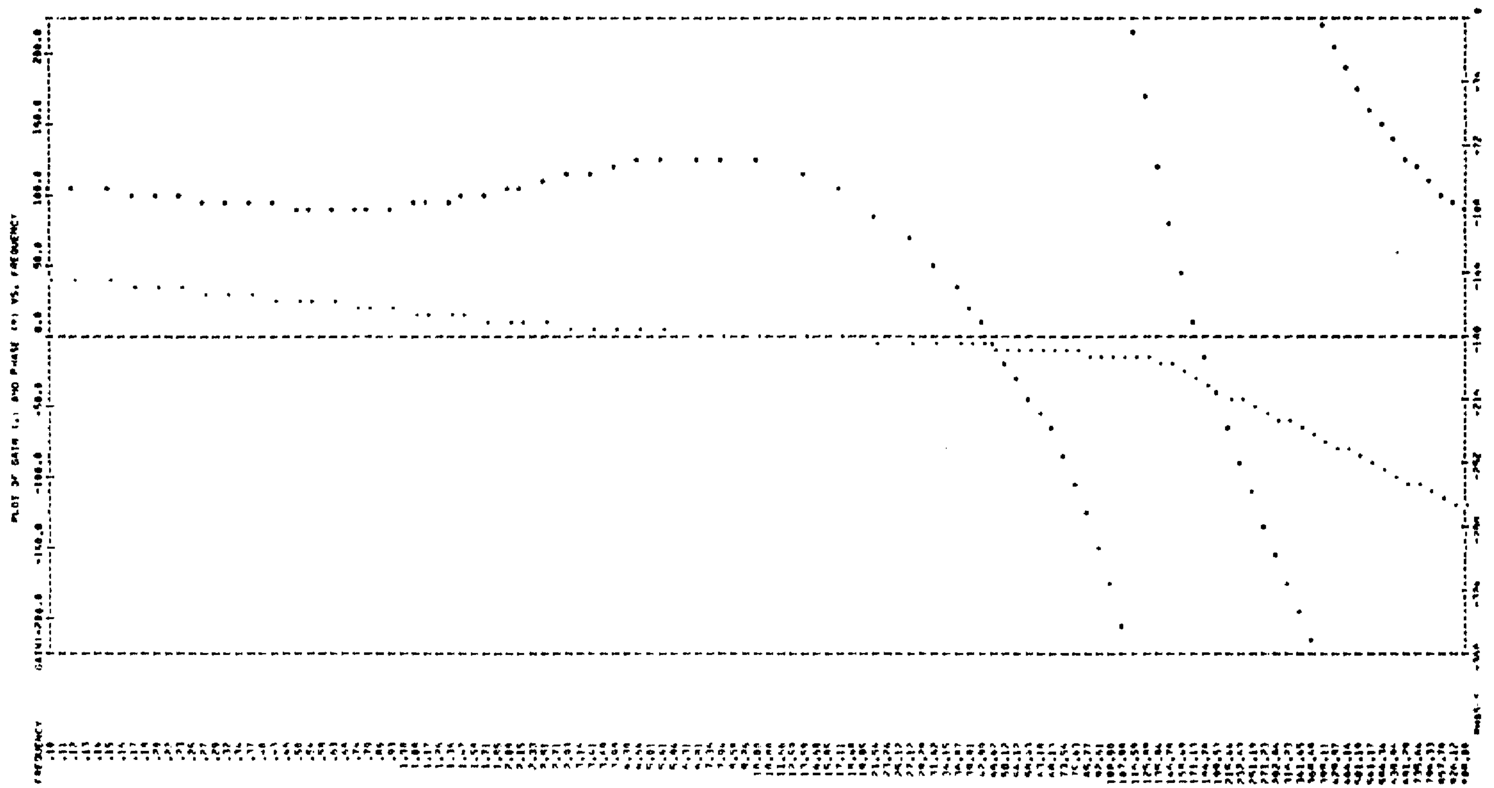

Figure 61a. Actuator Open Loop--50 Percent Operating Condition--Temperature

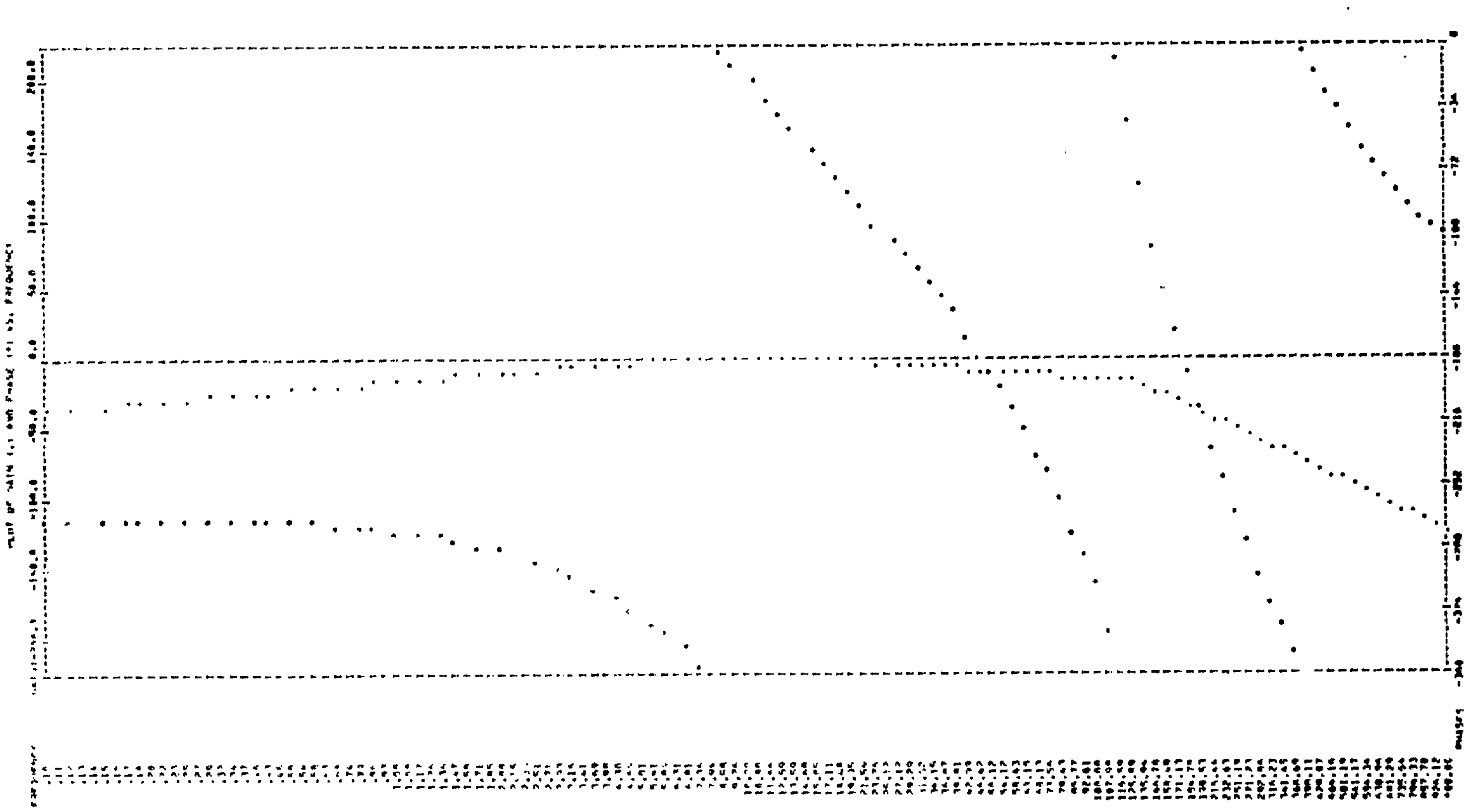

Figure 61b. TT4 Open Loop--50-Percent Operating Condition--Temperature

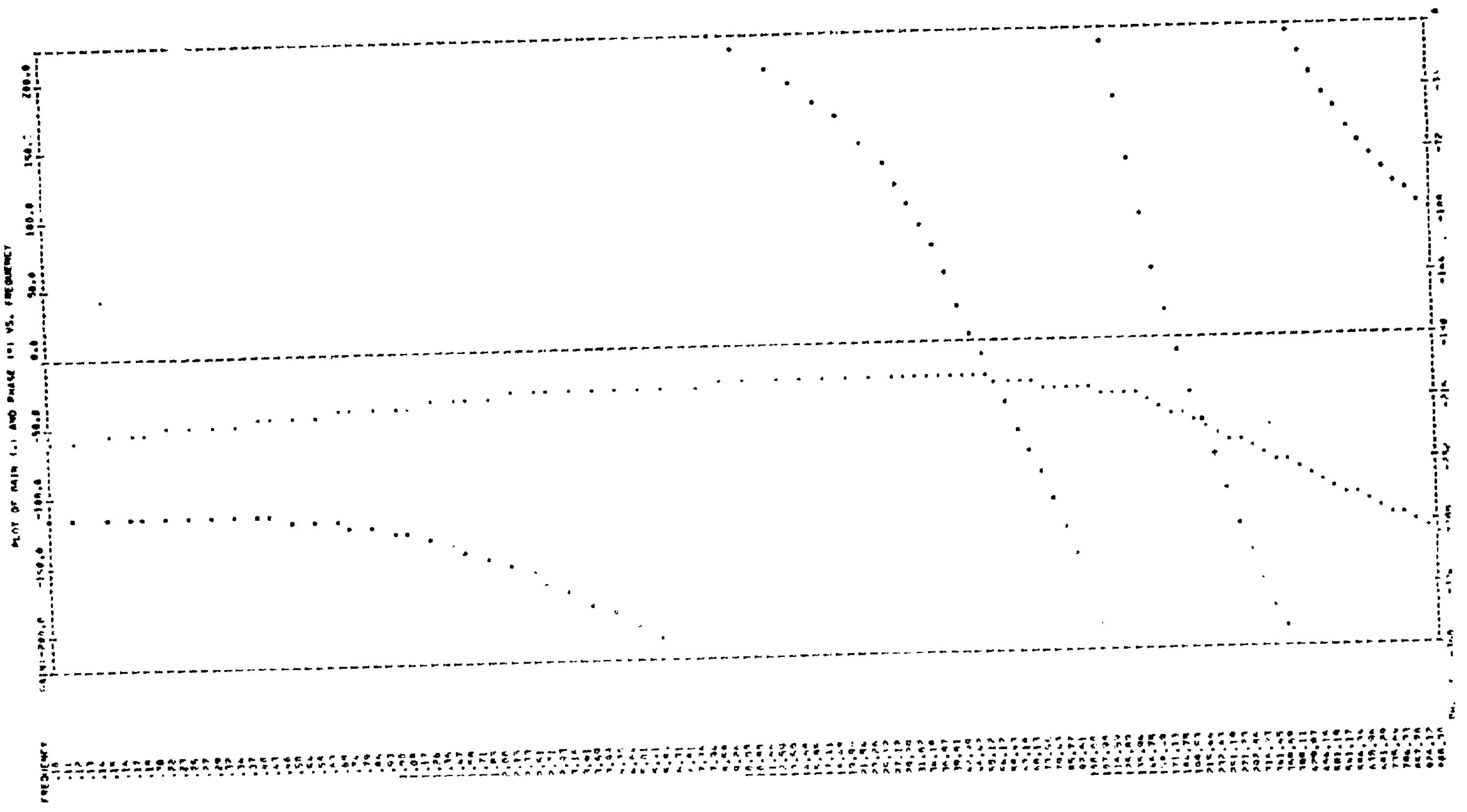

Figure 61c. PT3 Open Loop--50-Percent Operating Condition--Temperature

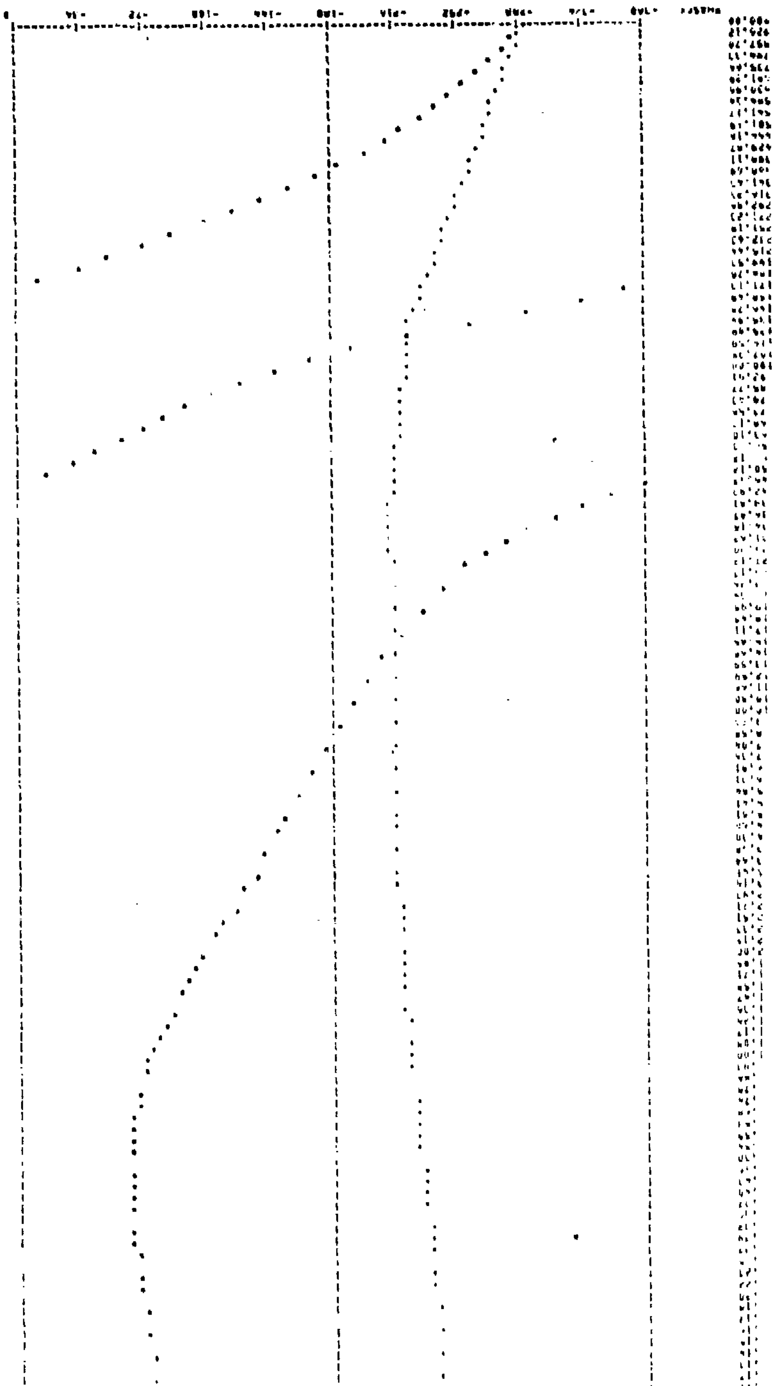

Figure 61d. PT5 Open Loop--50-Percent Operating Condition--Temperature

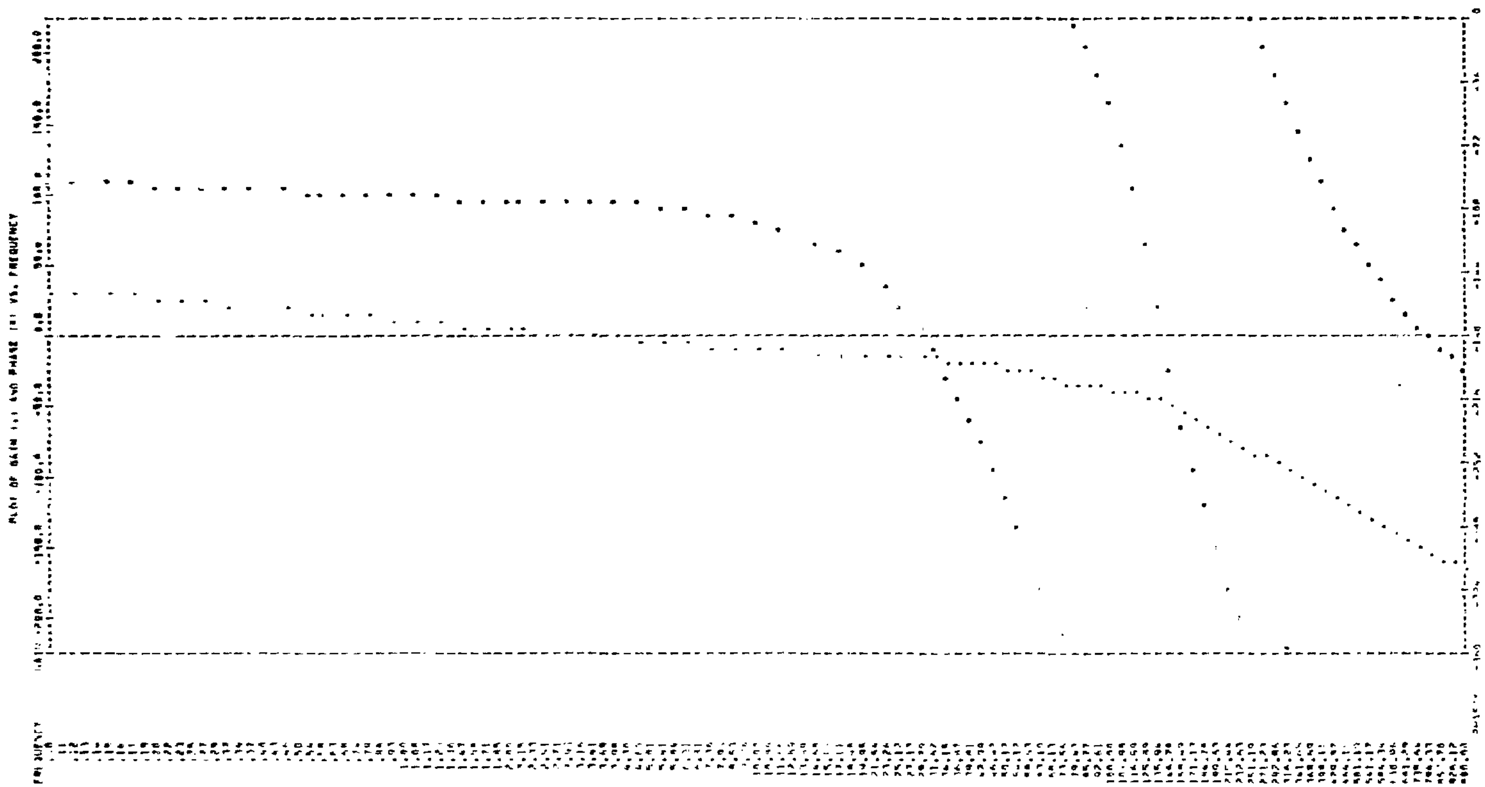

Figure 61e. ET Open Loop--50-Percent Operating Condition--Temperature

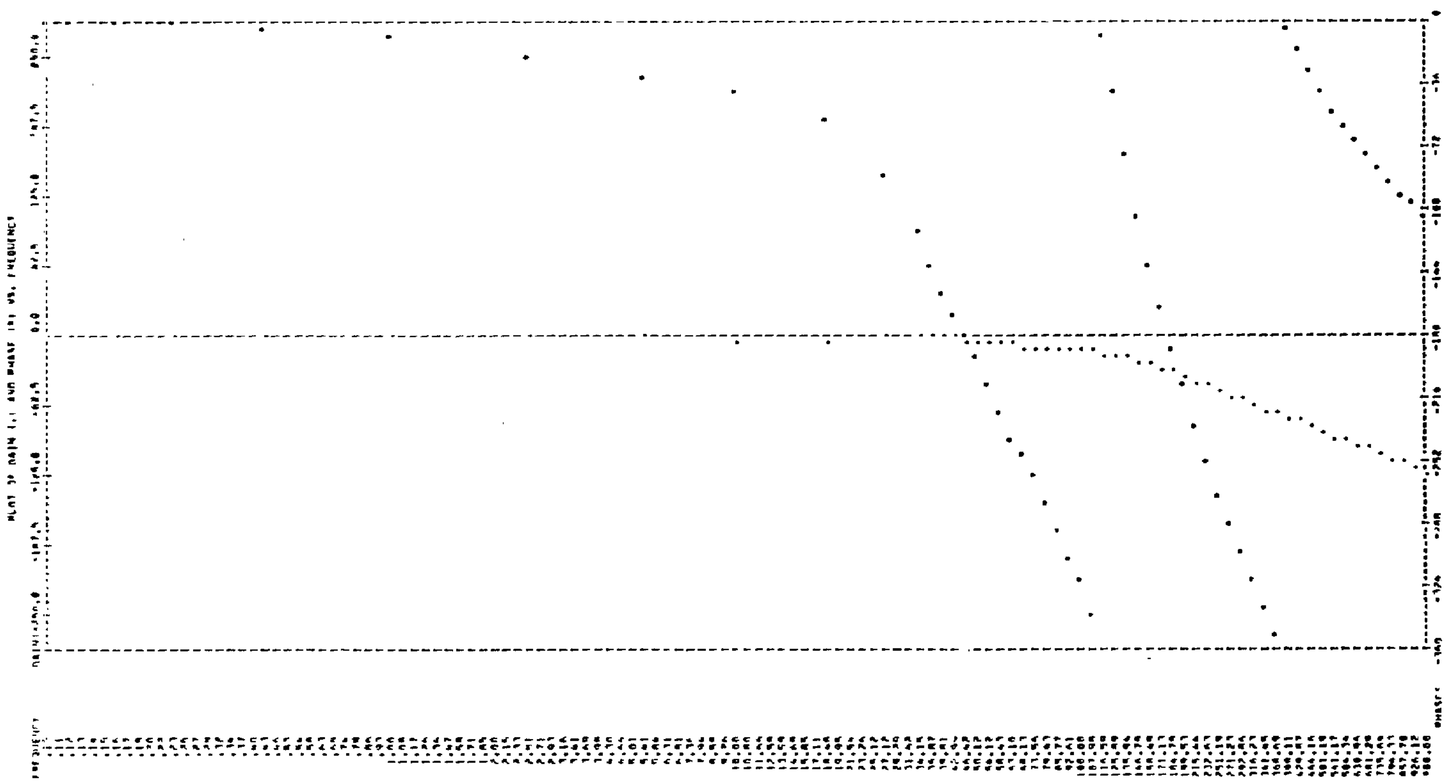

Figure 61f. Closed Loop--50-Percent Operating Condition--Temperature

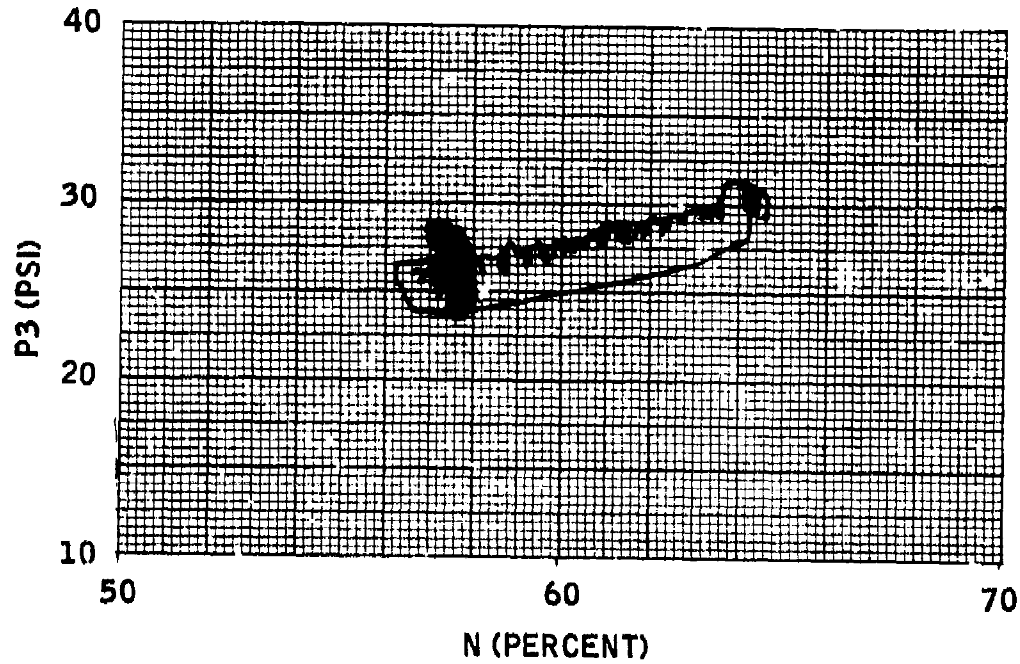

Figure 62. Anomalous Speed Behavior

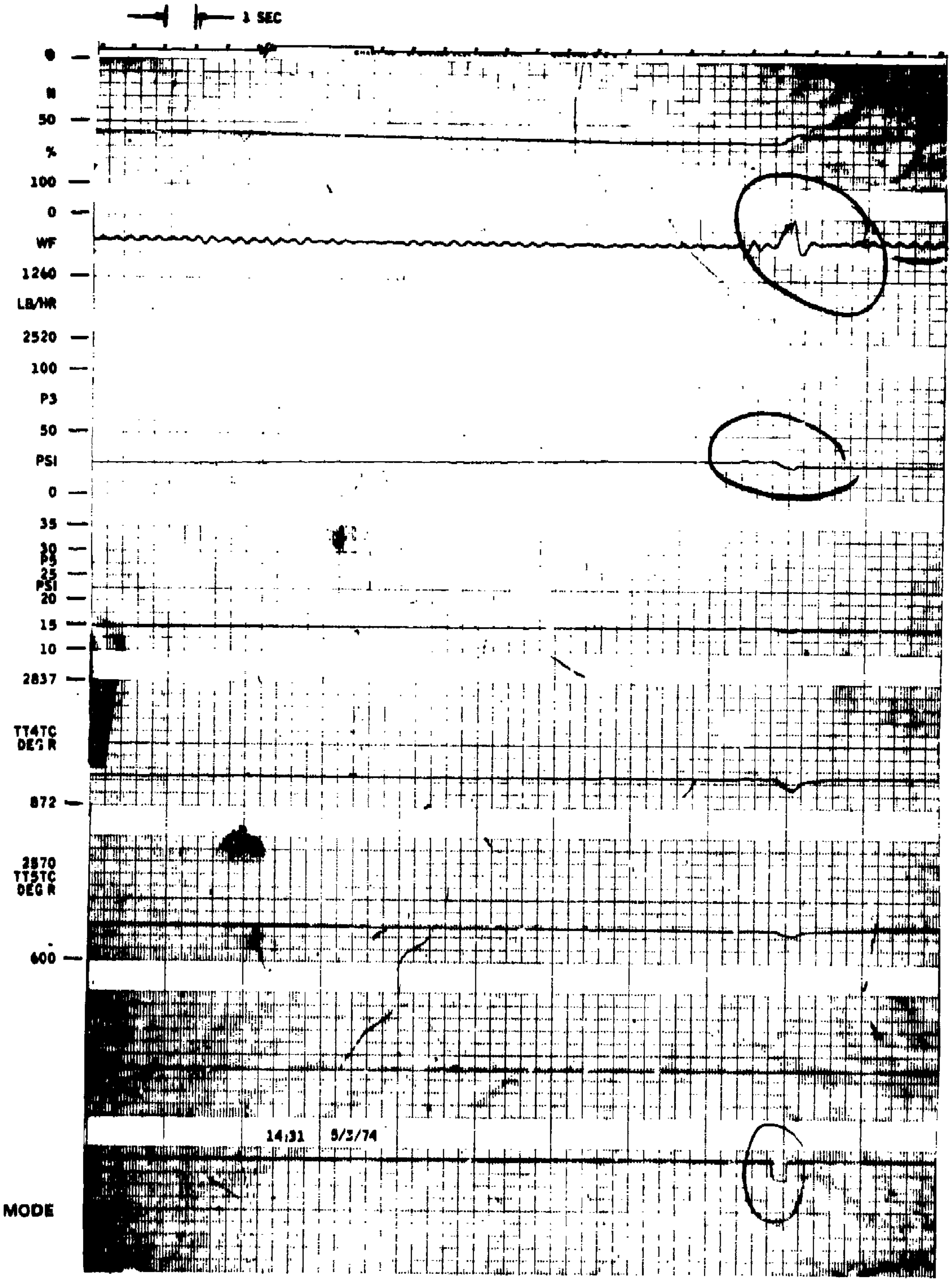

Figure 63. Anomalous Time Behavior

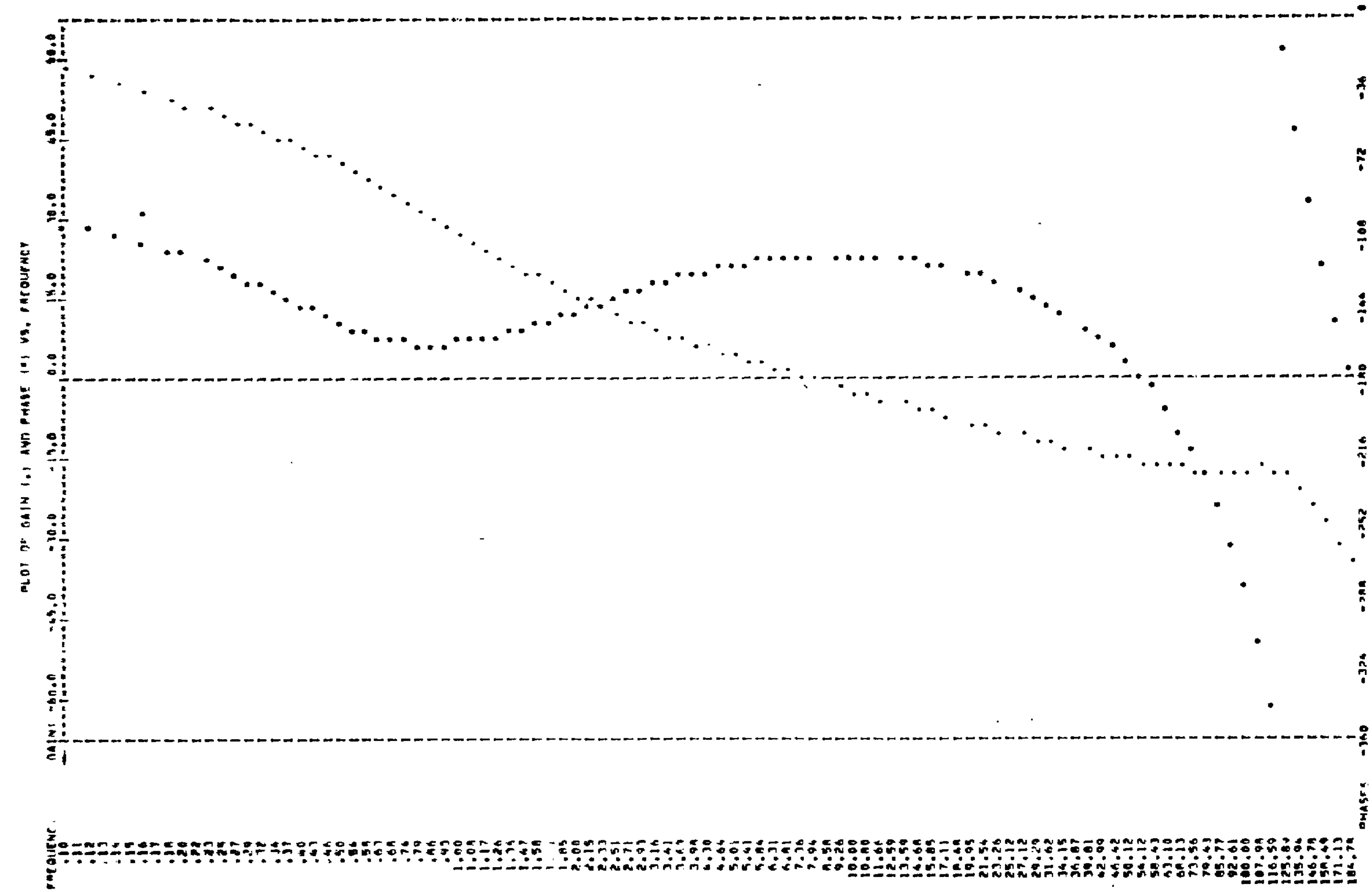

Figure 64. Simplified Control -- High Gain -- 50-Percent Operating Condition -- Equilibrium -- Actuator Open Loop

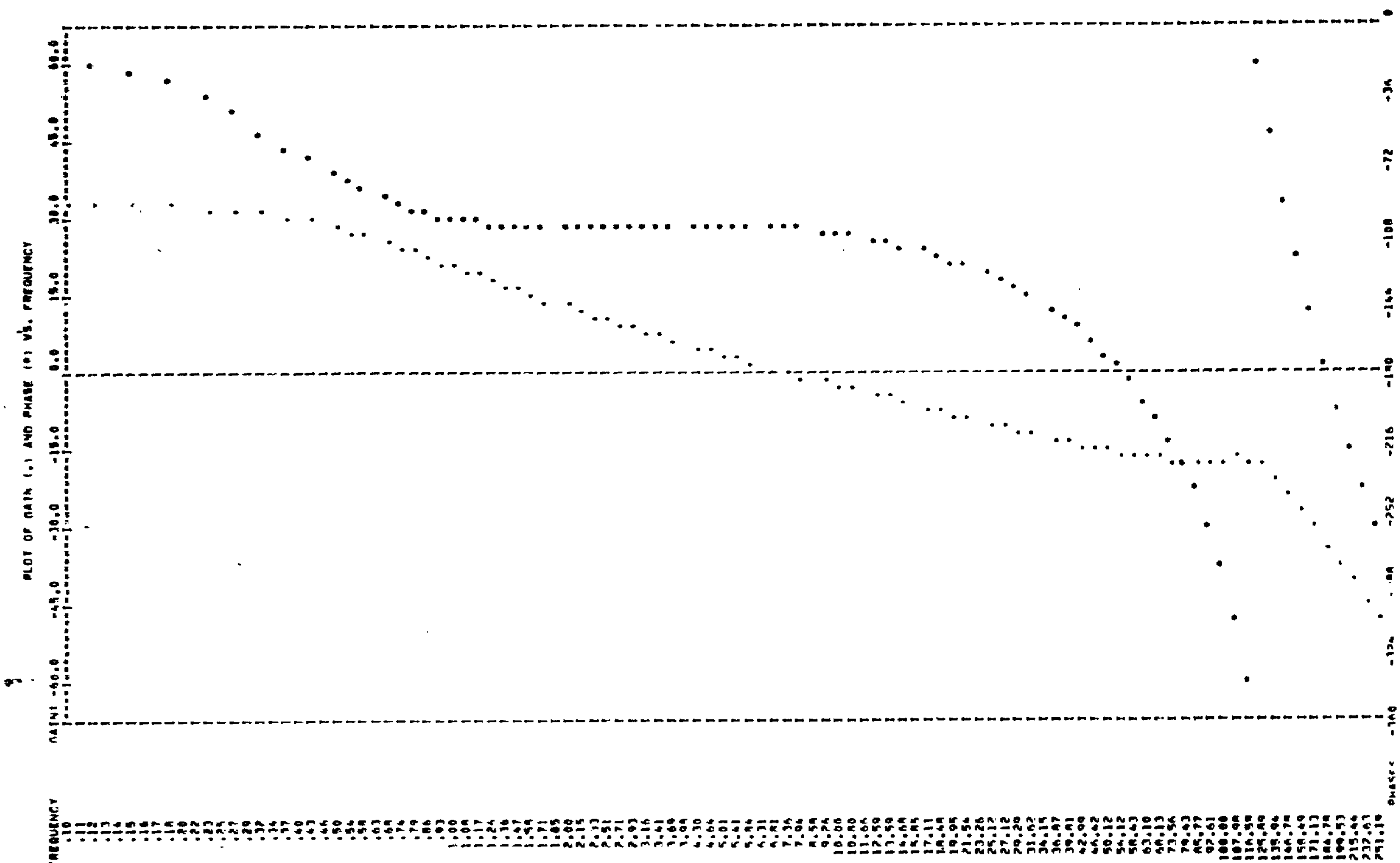

Figure 65. Simplified Control -- High Gain -- 50-Percent Operating Condition -- Equilibrium -- N Open Loop

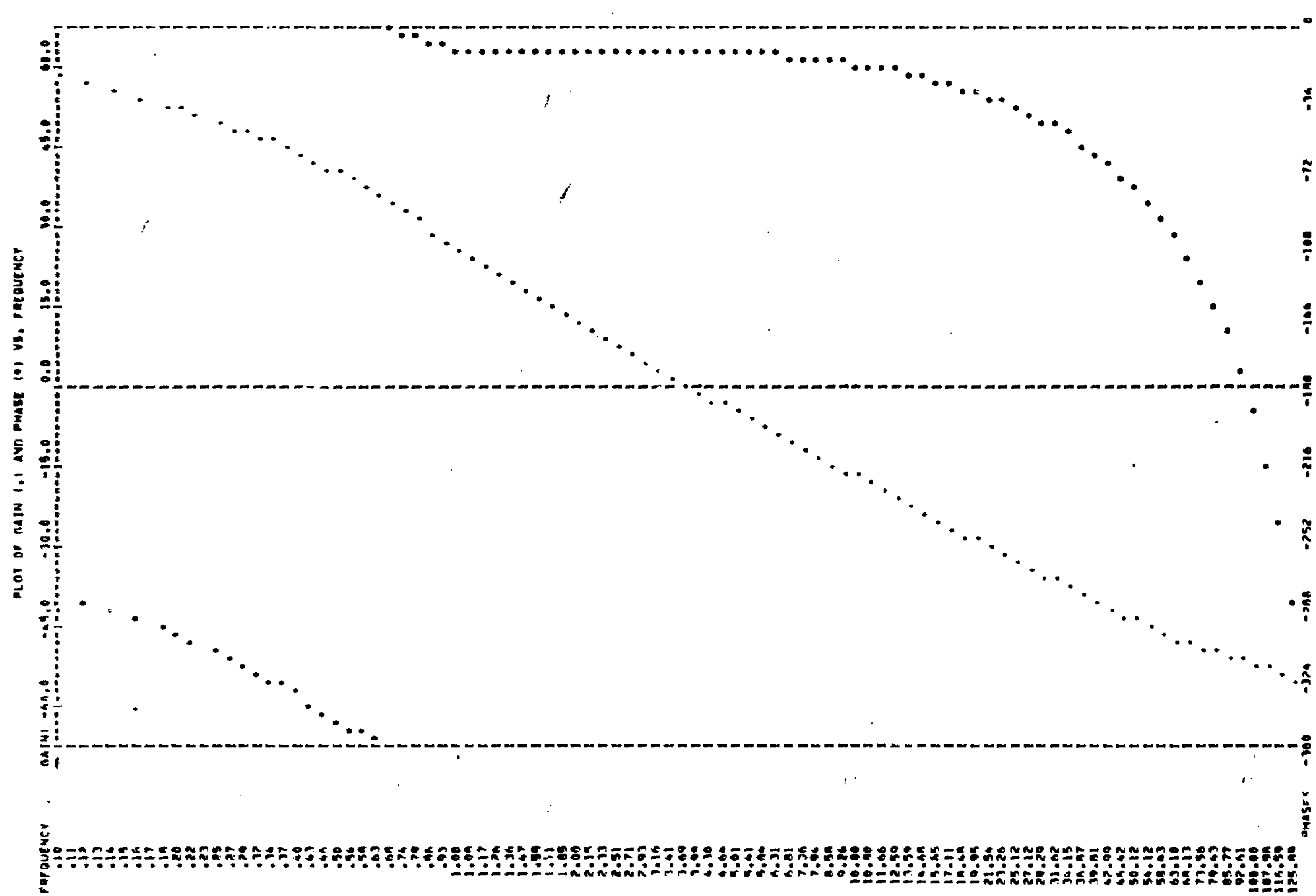

Figure 66. Simplified Control--High Gain--50-Percent Operating Condition--Equilibrium--EN Open Loop

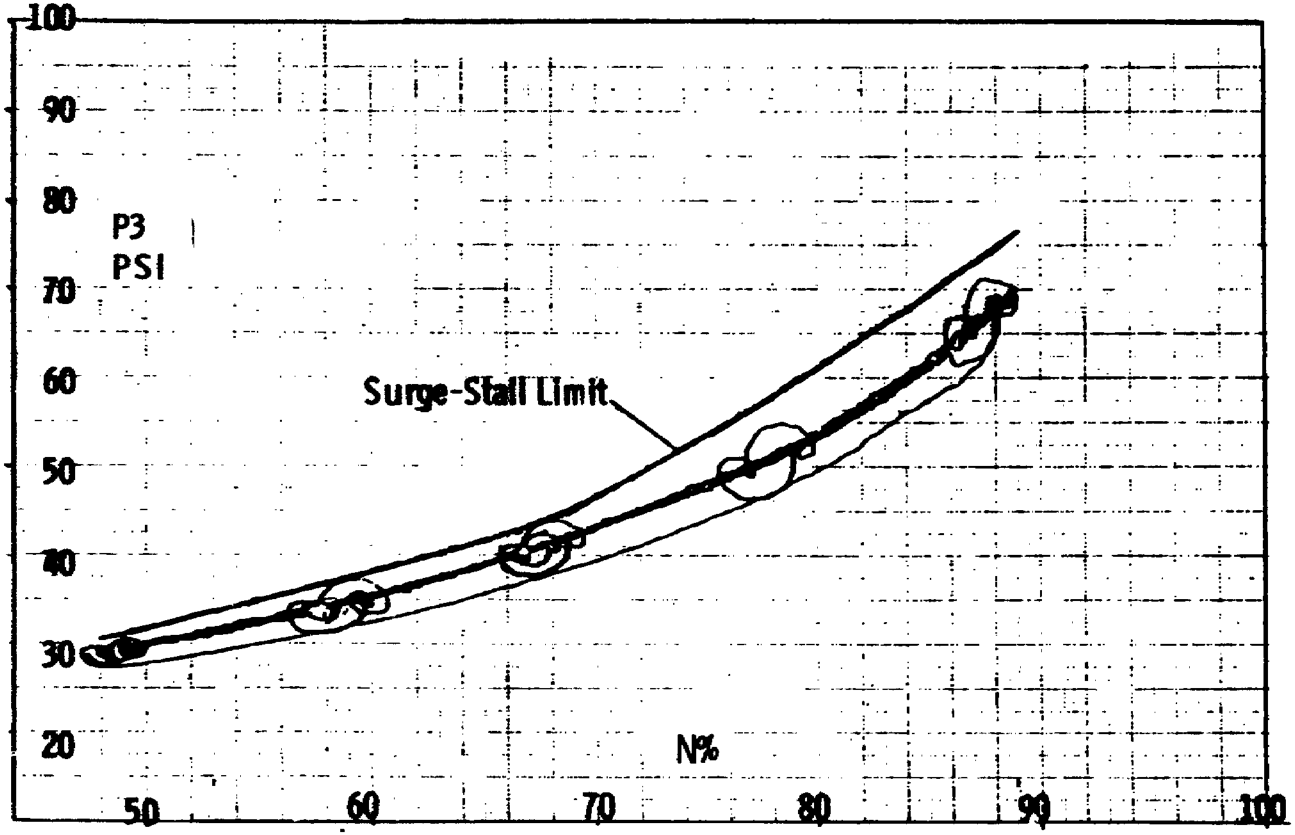

Figure 67. Speed-Pressure Slow Acceleration

Mode Legend: B = Bendix, E = Equilibrium

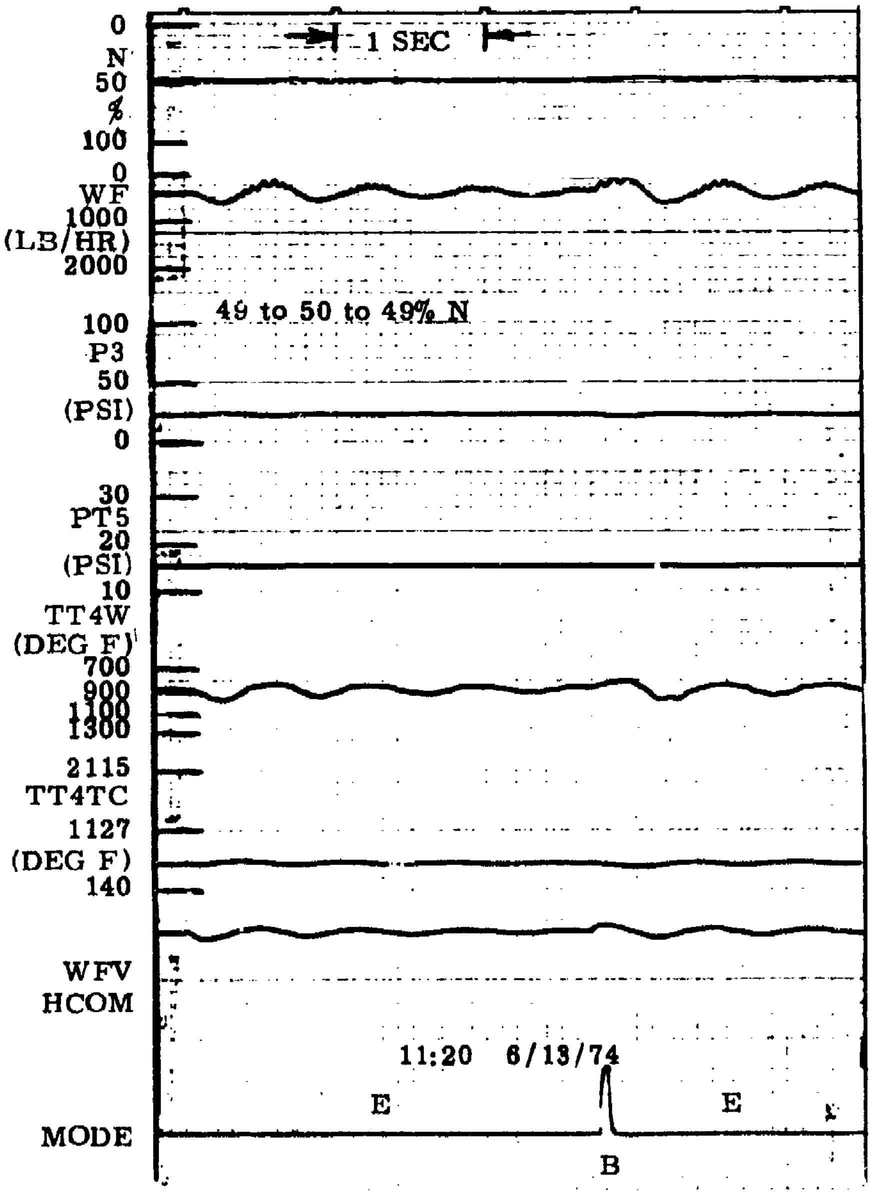

Figure 68. Speed-Pressure Slow Acceleration

Mode Legend: D = Deceleration, E = Equilibrium

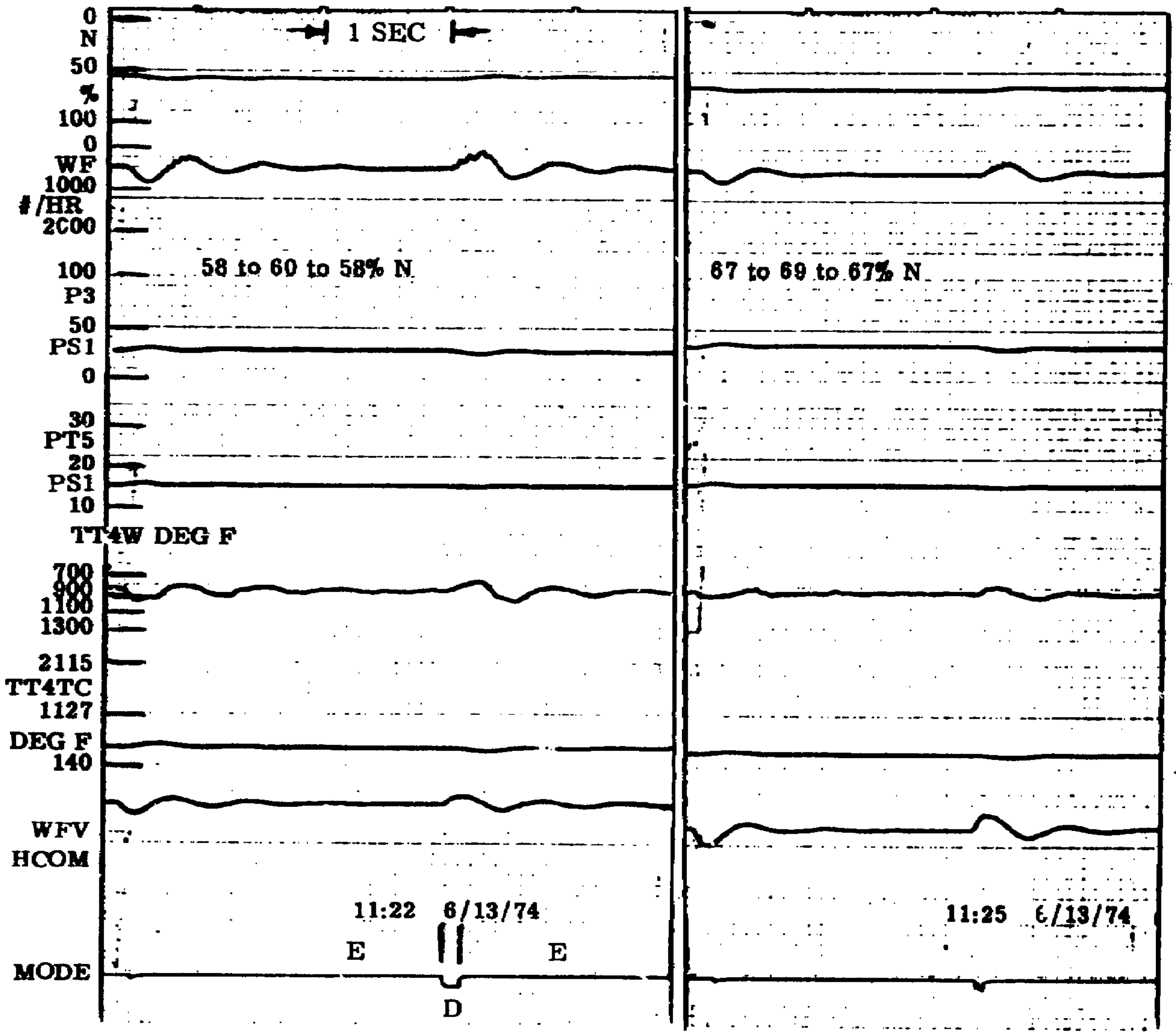

Figure 69. Speed-Pressure Slow Acceleration

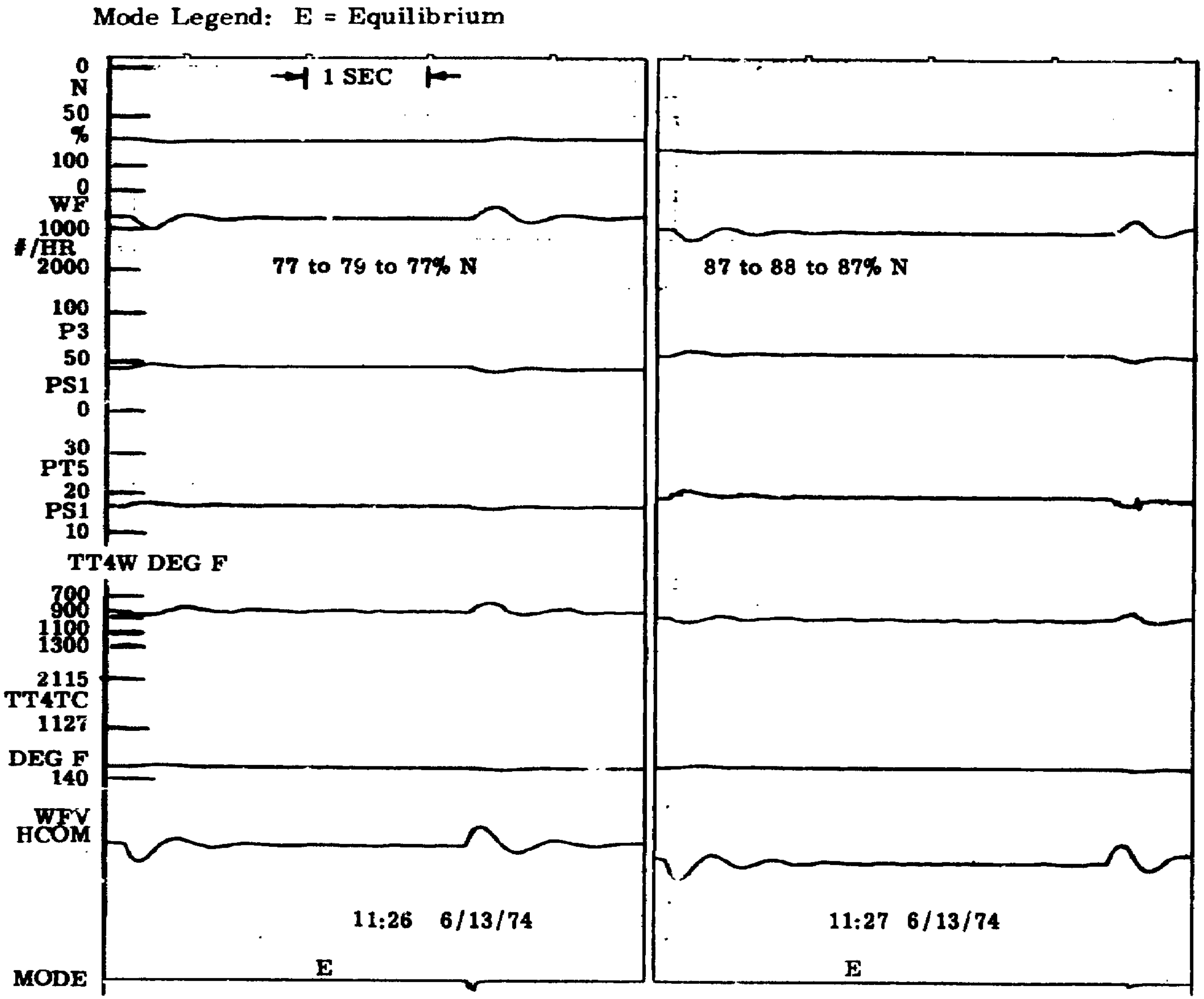

Figure 70. Speed-Pressure Slow Acceleration

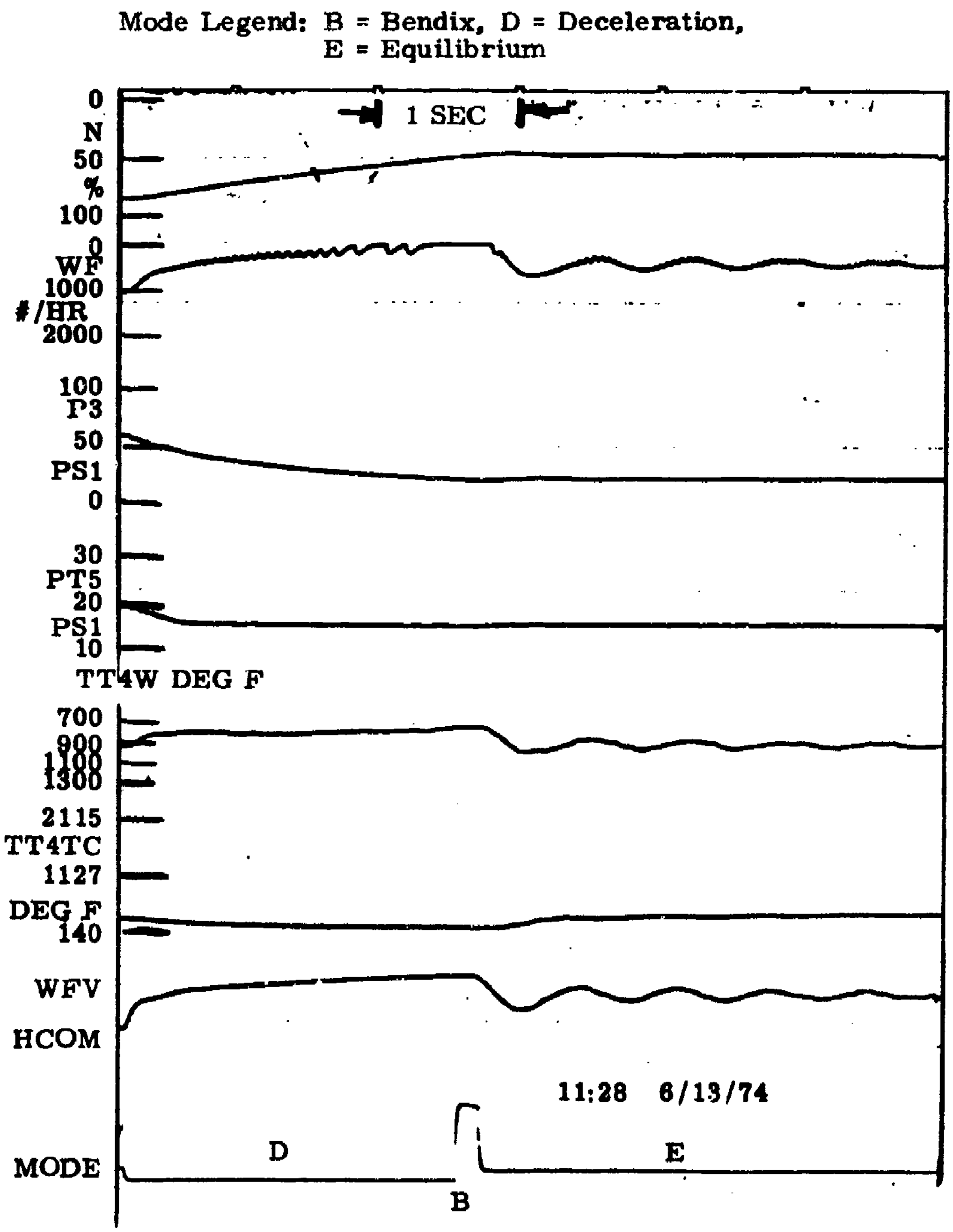

Figure 71. Speed-Pressure Maximum Deceleration

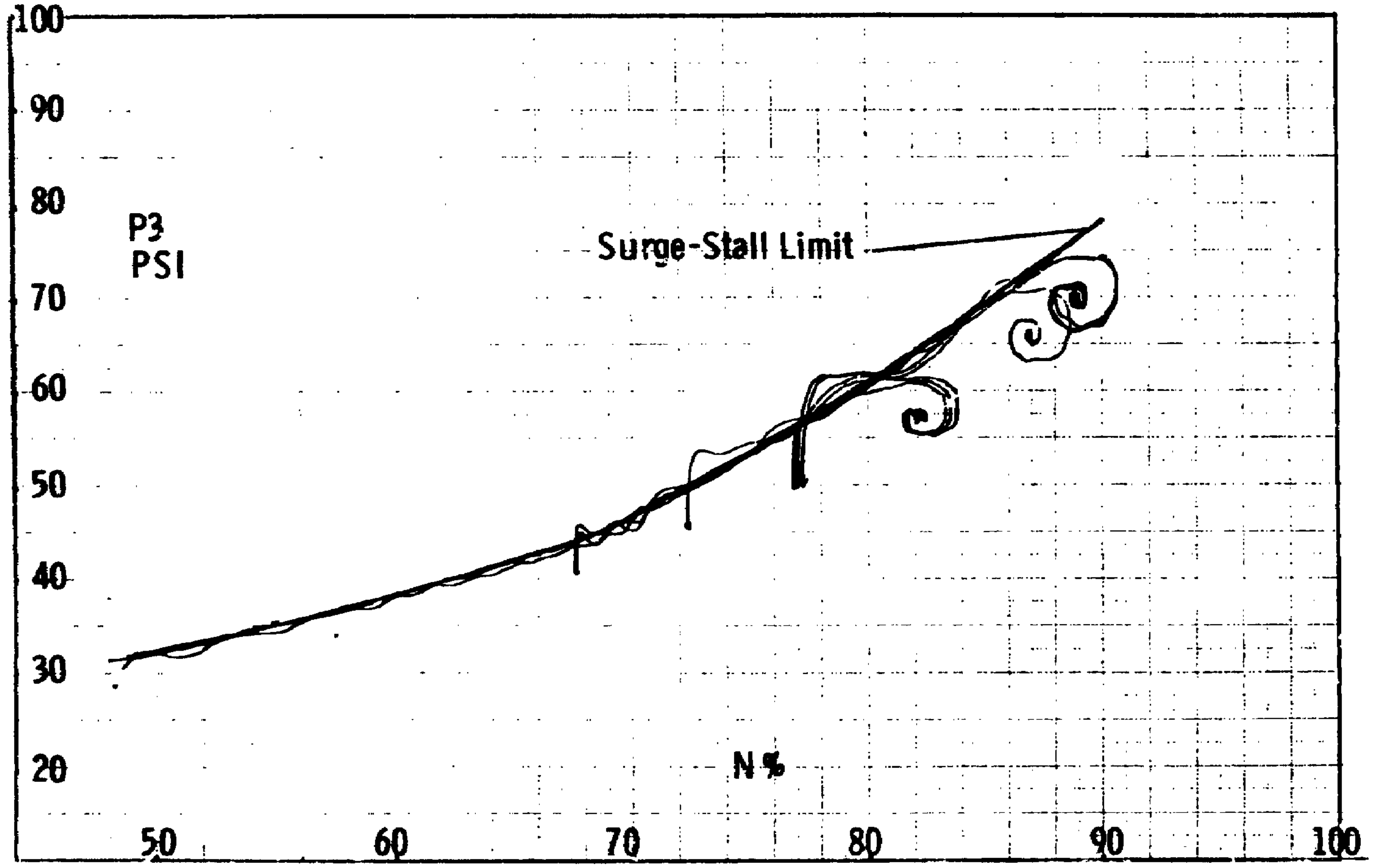

Figure 72. Speed-Pressure Fast Acceleration

Mode Legend: B = Bendix, F = Equilibrium, P = Pressure

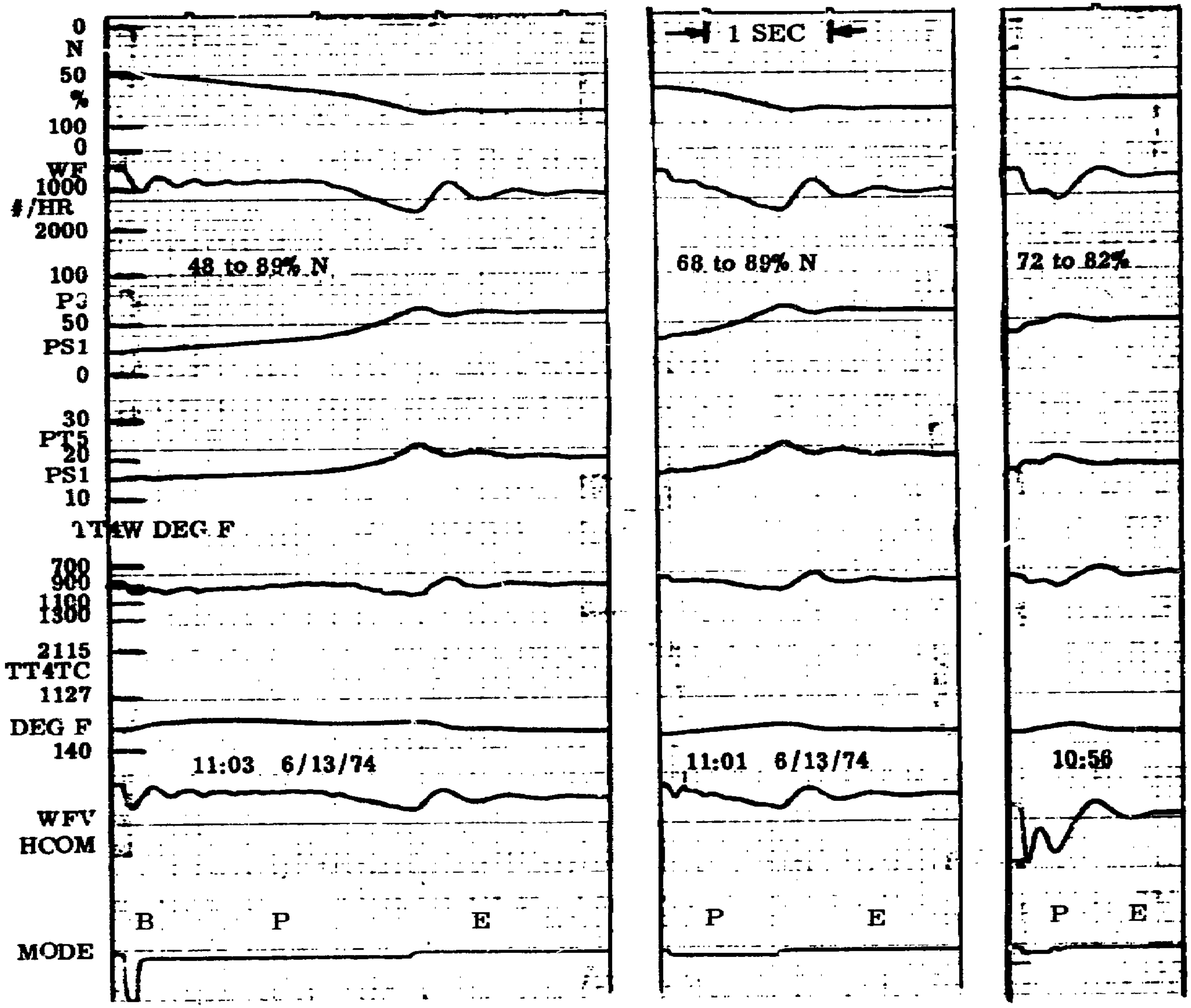

Figure 73. Speed-Pressure Maximum Acceleration

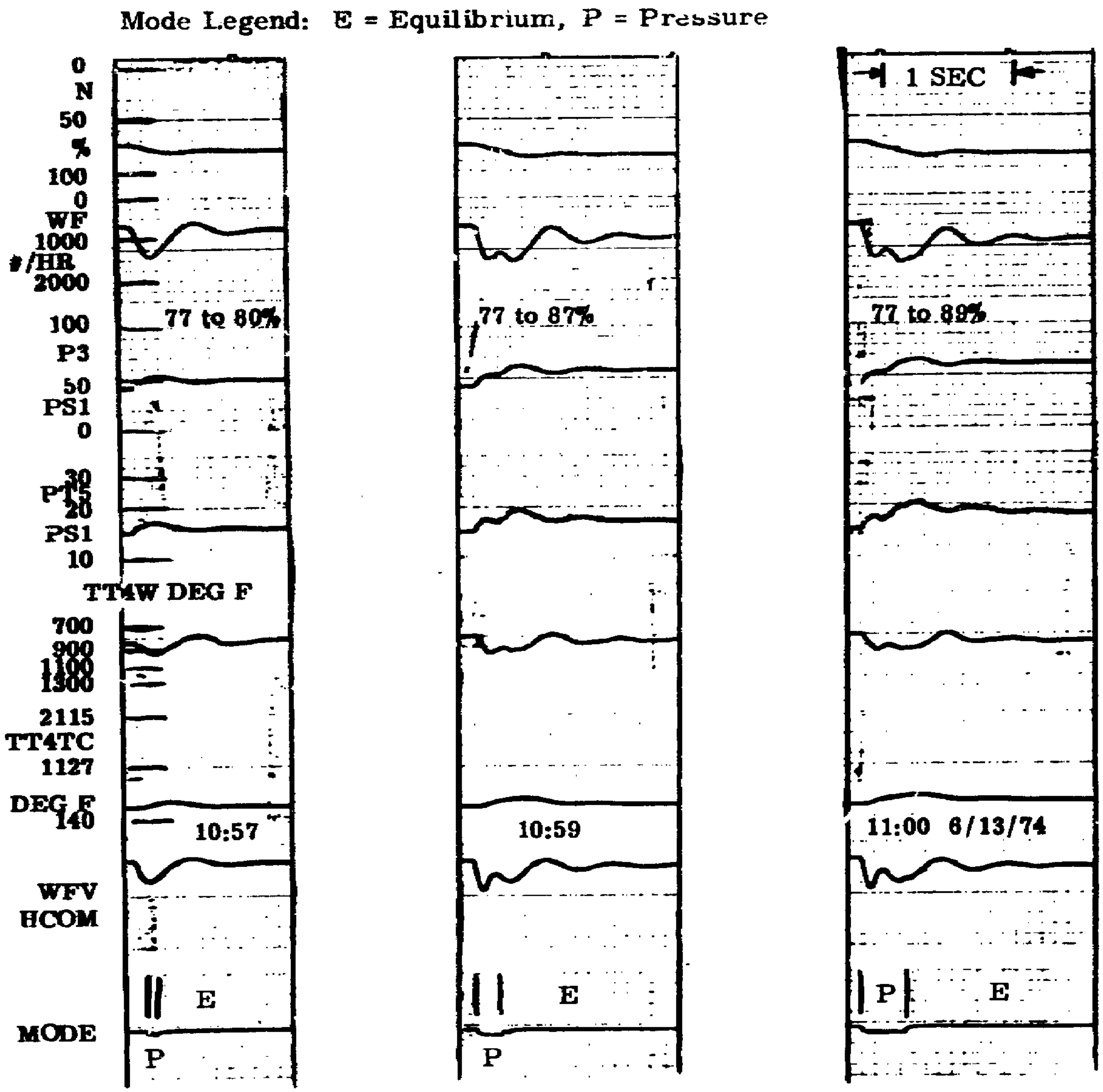

Figure 74. Speed-Pressure Maximum Acceleration

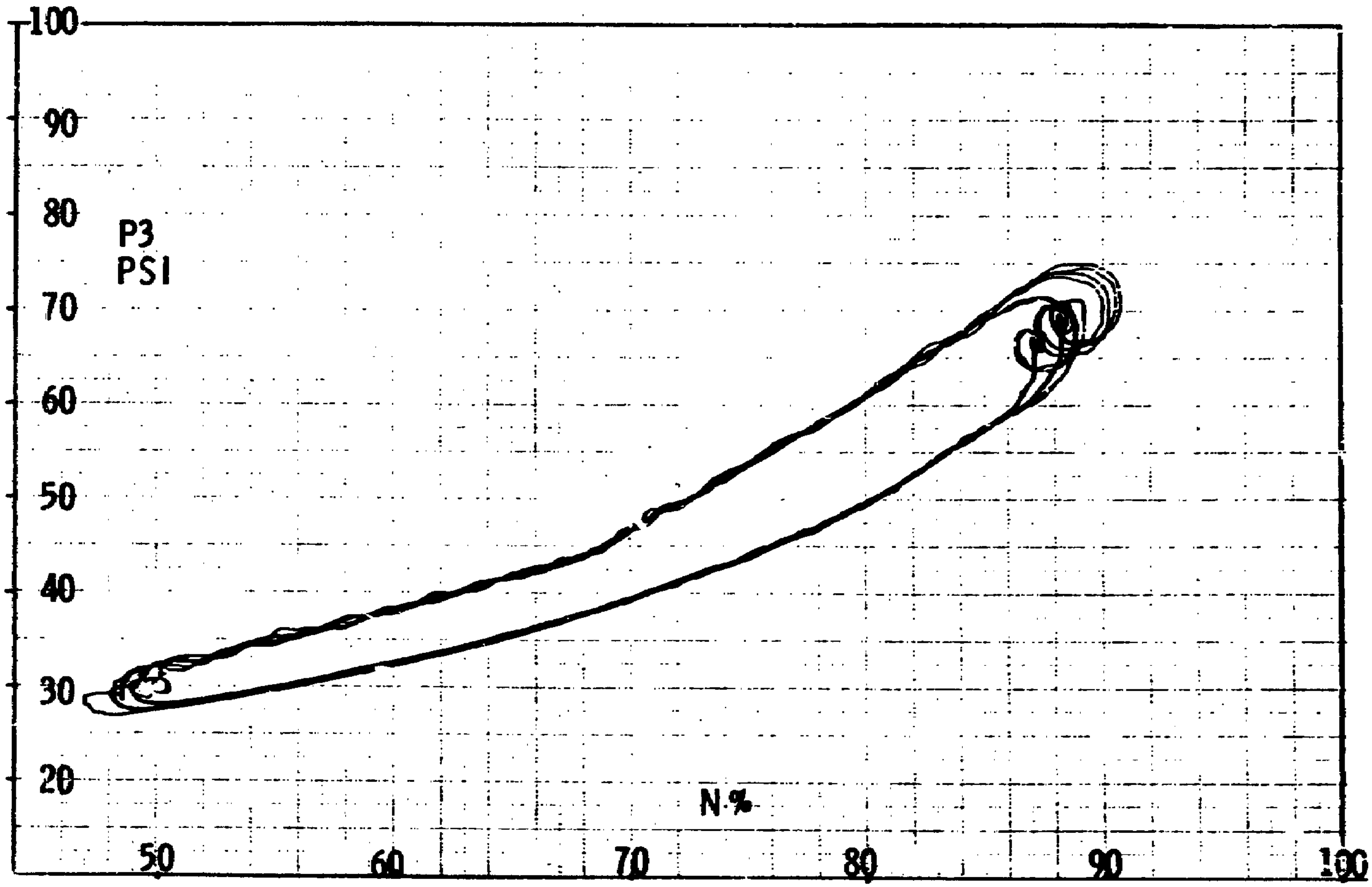

Figure 75. Speed-Pressure Bode Slams

Mode Legend: B = Bendix, D = Deceleration, E = Equilibrium, P = Pressure

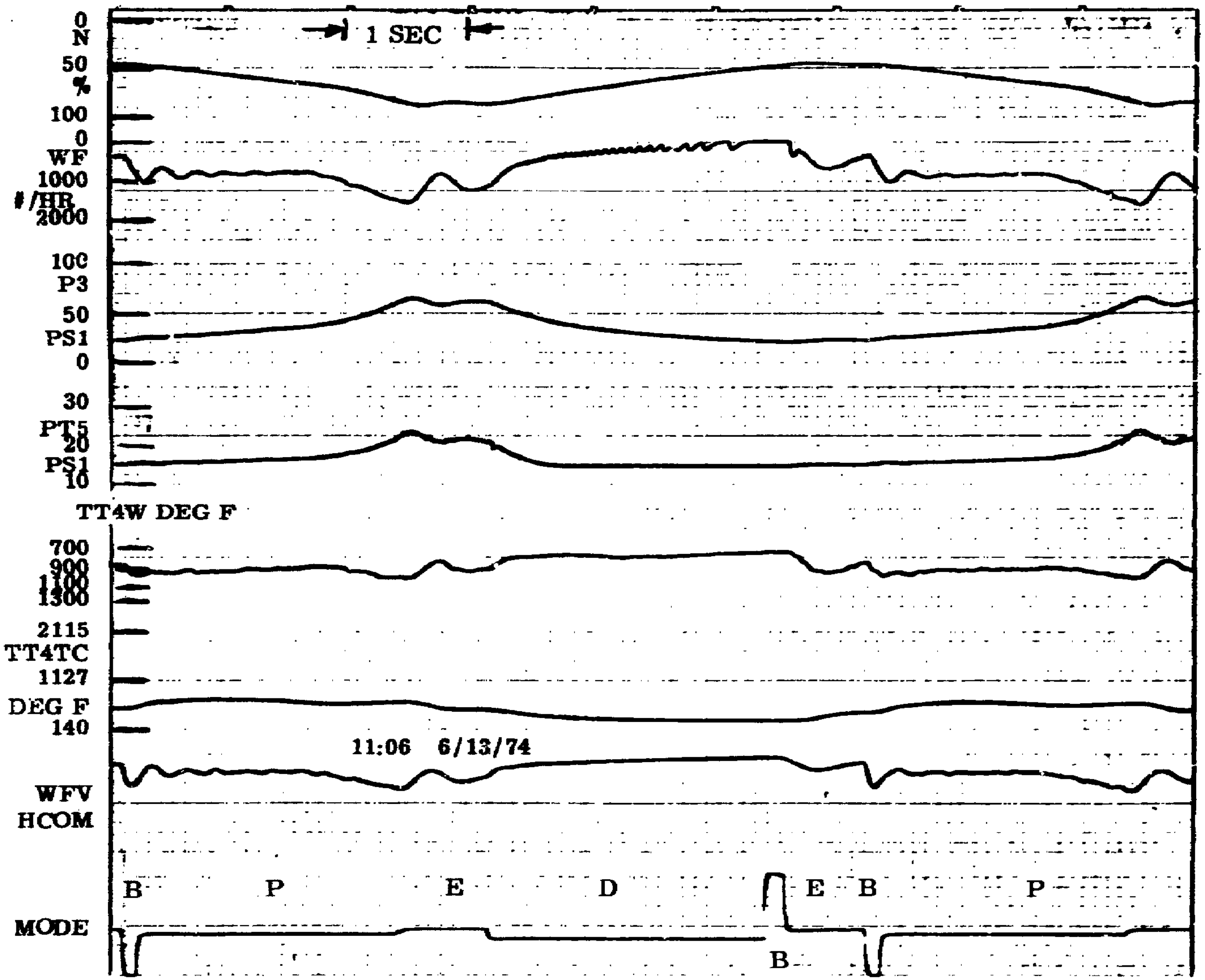

Figure 76. Speed-Pressure Bode Slam No. 1

Mode Legend: B = Bendix, D = Deceleration, E = Equilibrium, P = Pressure

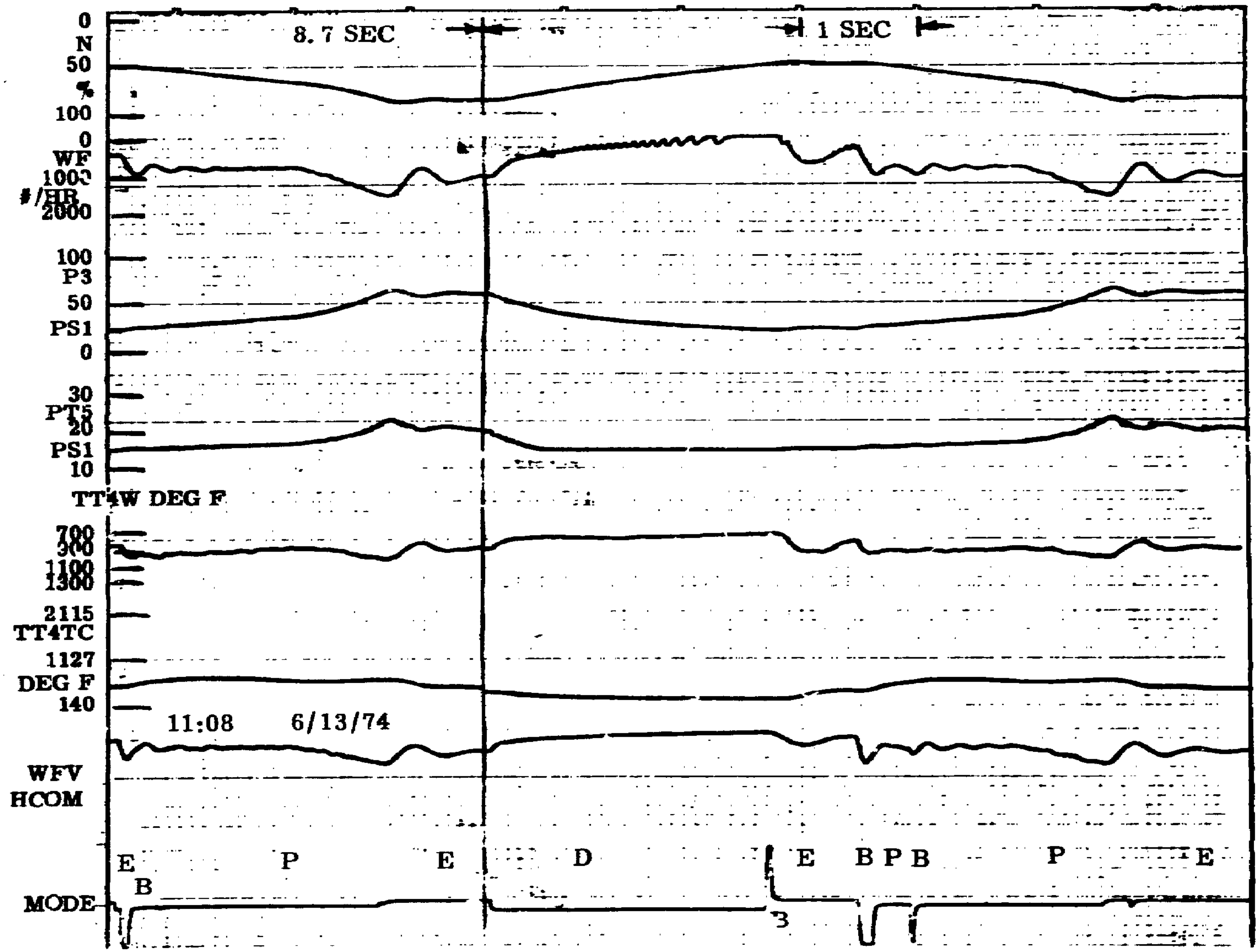

Figure 77. Speed-Pressure Bode Slam No. 2

Mode Legend: B = Bendix, D = Deceleration, E = Equilibrium, P = Pressure

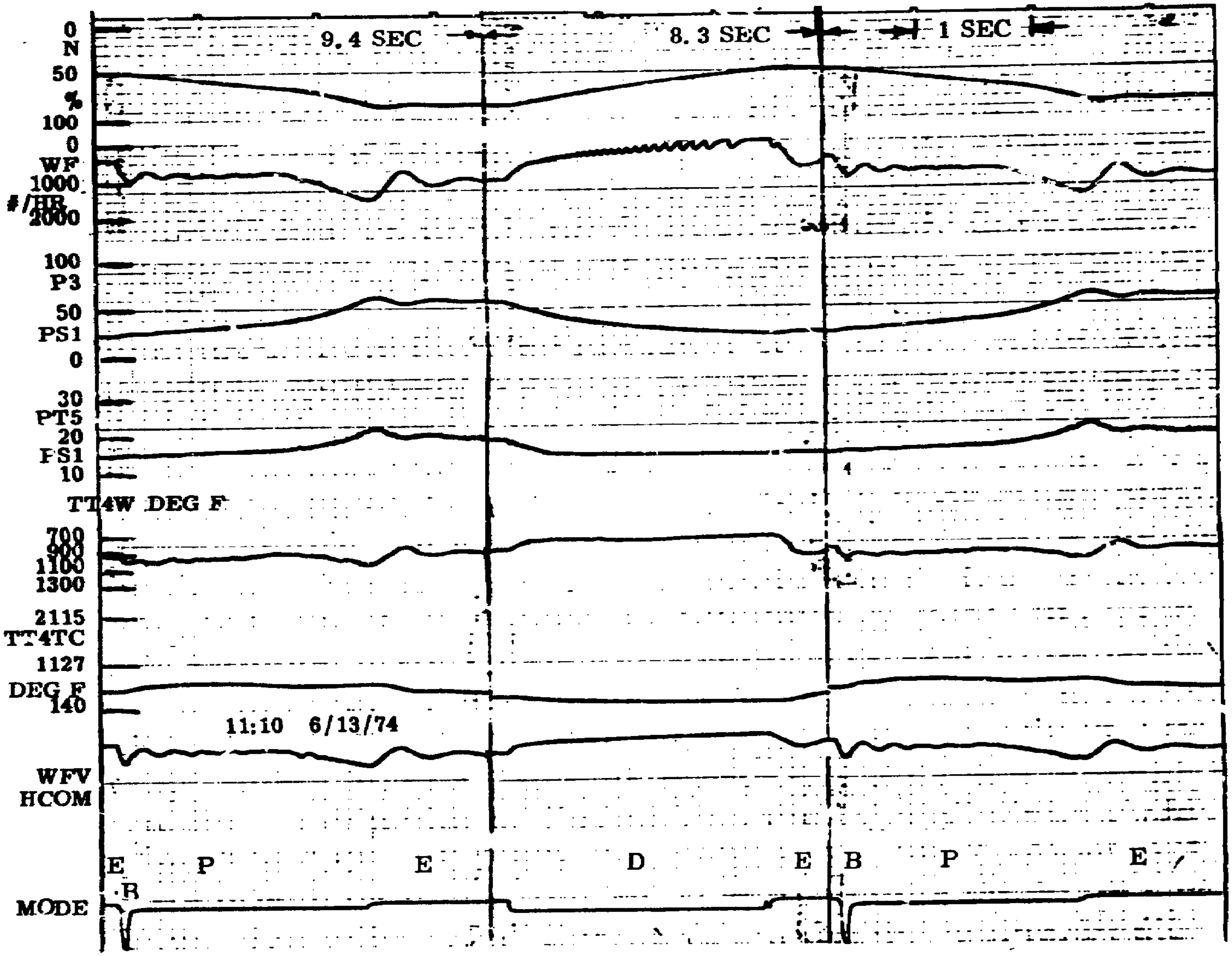

Figure 78. Speed-Pressure Bode Slam No. 3

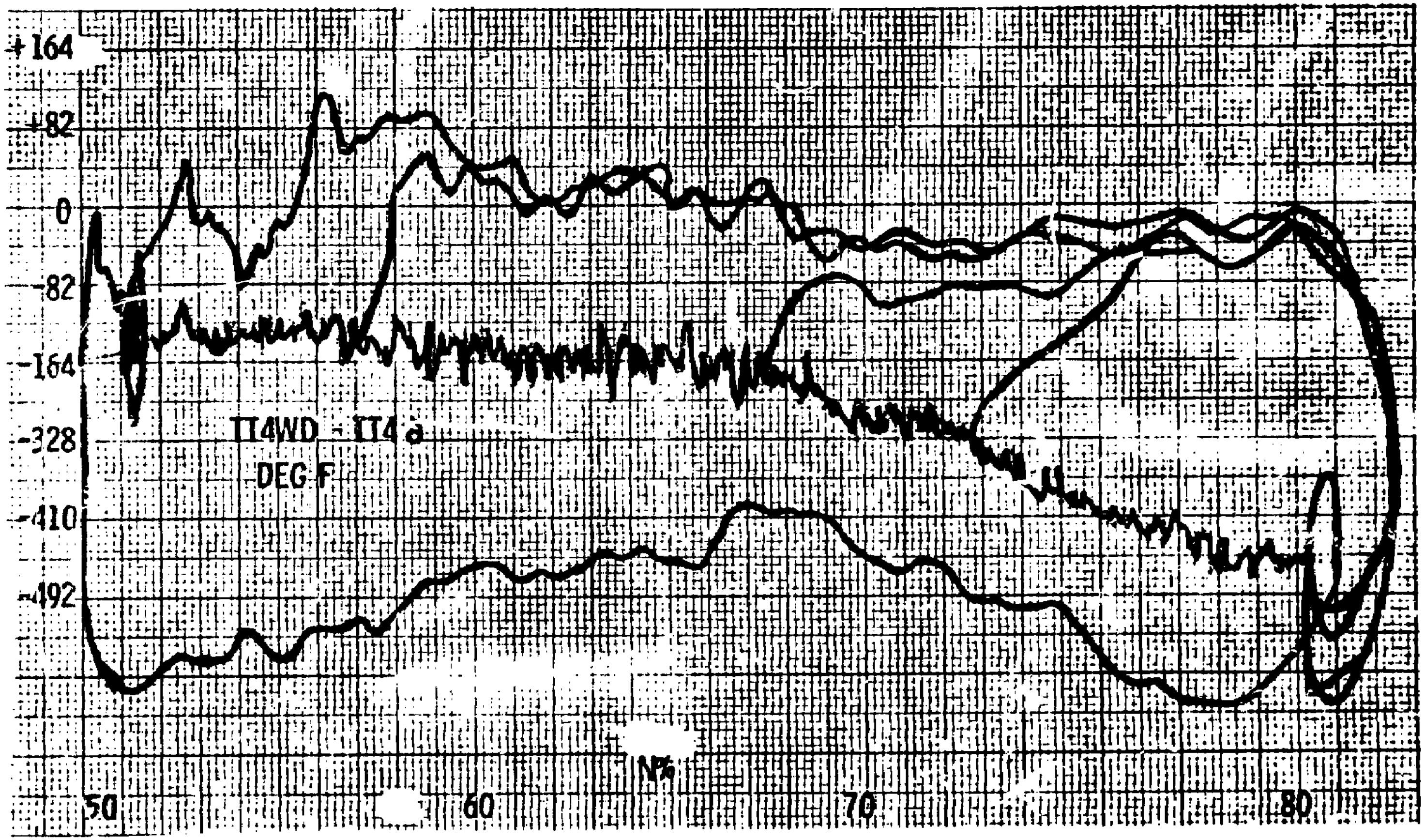

Figure 79. Speed-Temperature Plot

Mode Legend: D = Deceleration, E = Equilibrium, T = Temperature

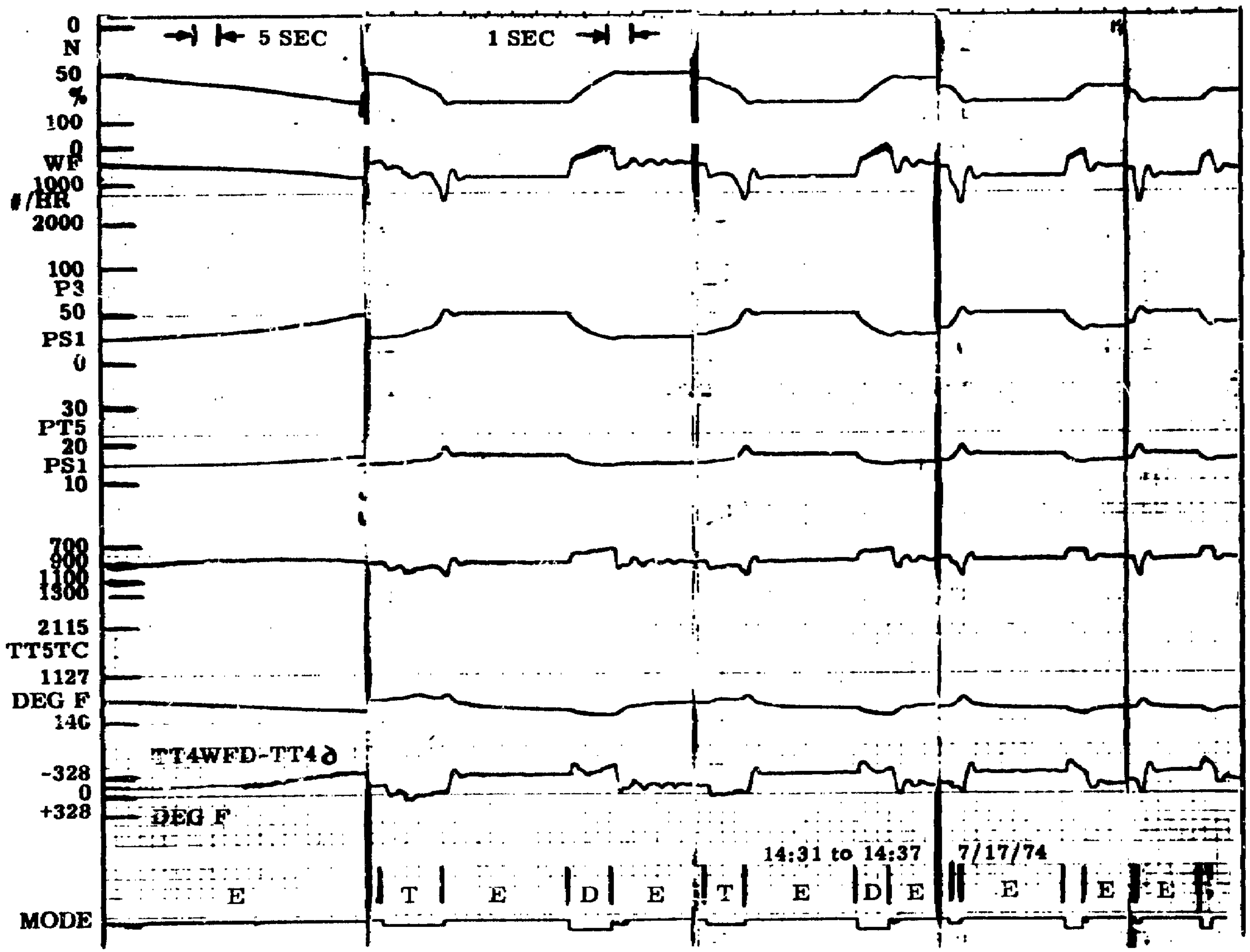

Figure 80. Speed-Temperature Control Trim and 52, 57, 68, and 73 to 82 Percent Speed

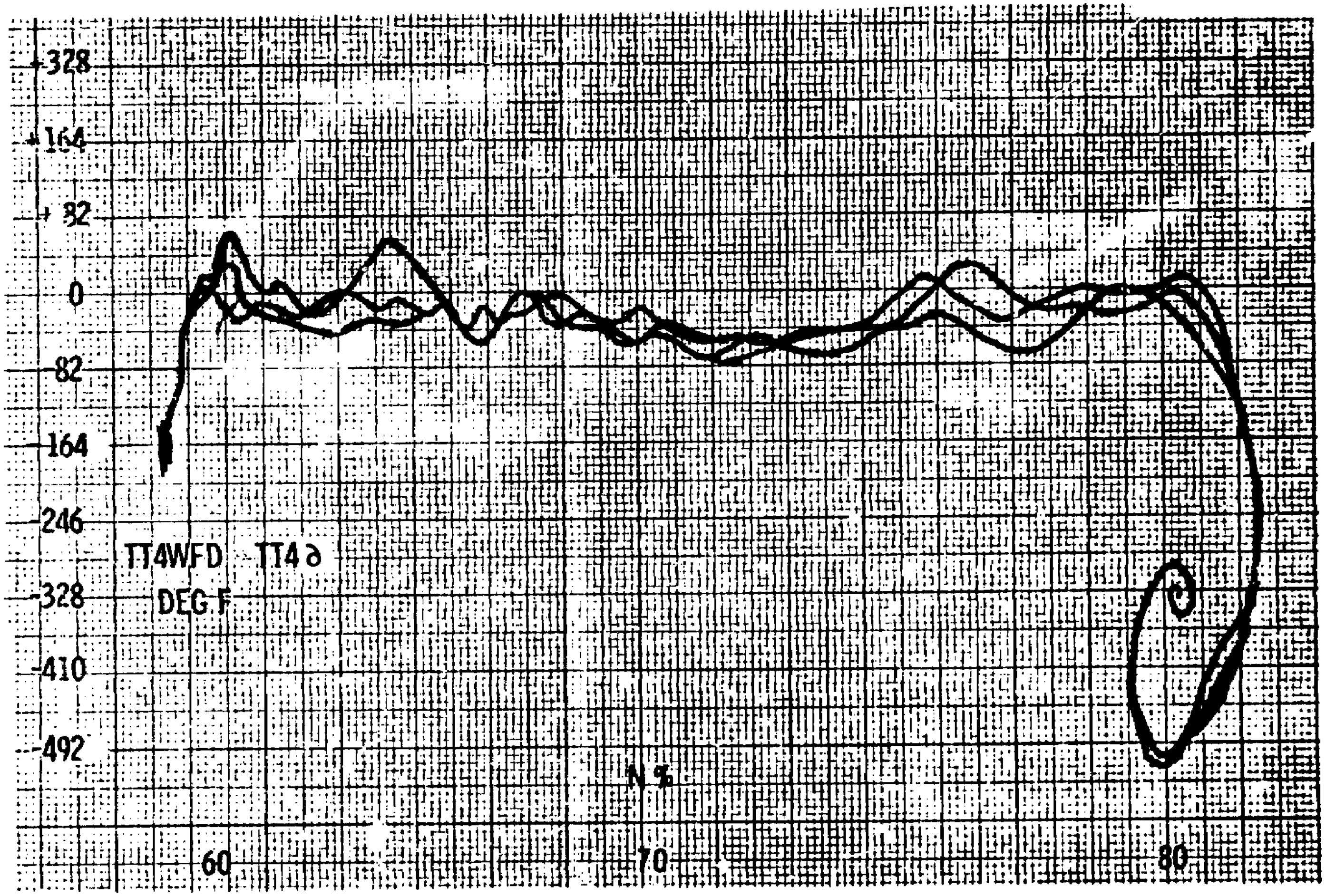

Figure 81. Speed-Temperature Plot - 3 of 57 to 84 Percent

Mode Legend: D = Deceleration, E = Equilibrium,
T = Temperature

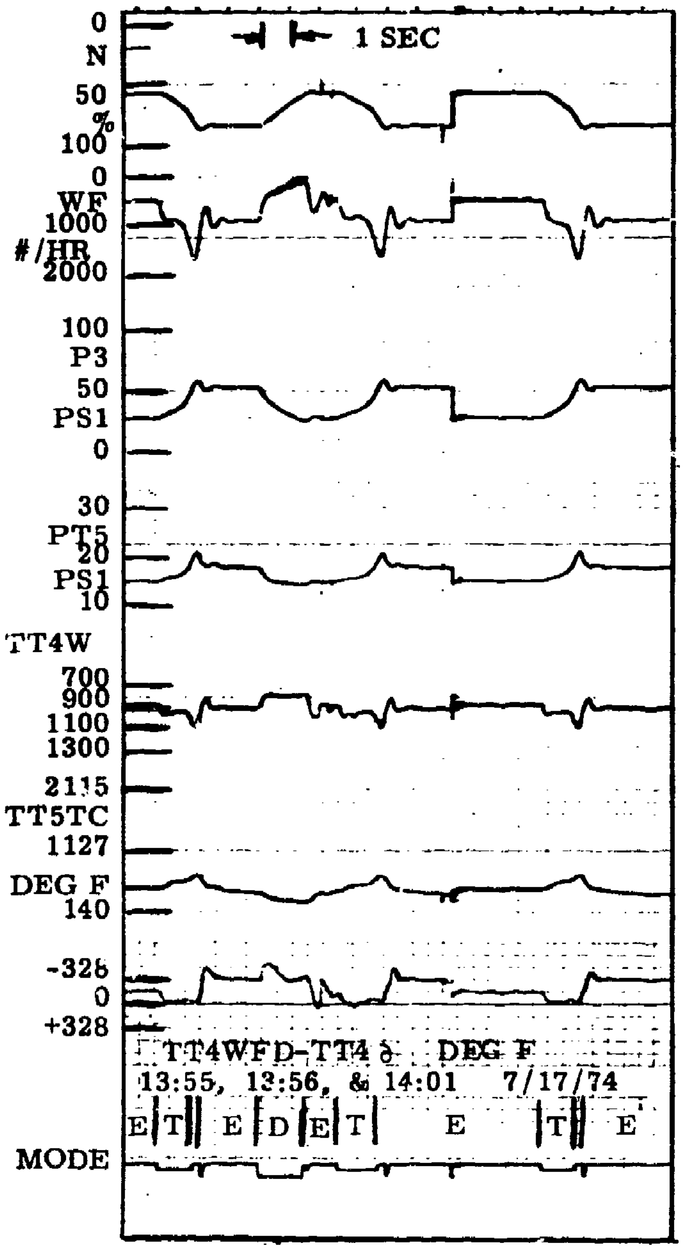

Figure 82. Speed-Temperature - 3 Repeats of 57 to 84 Percent Speed

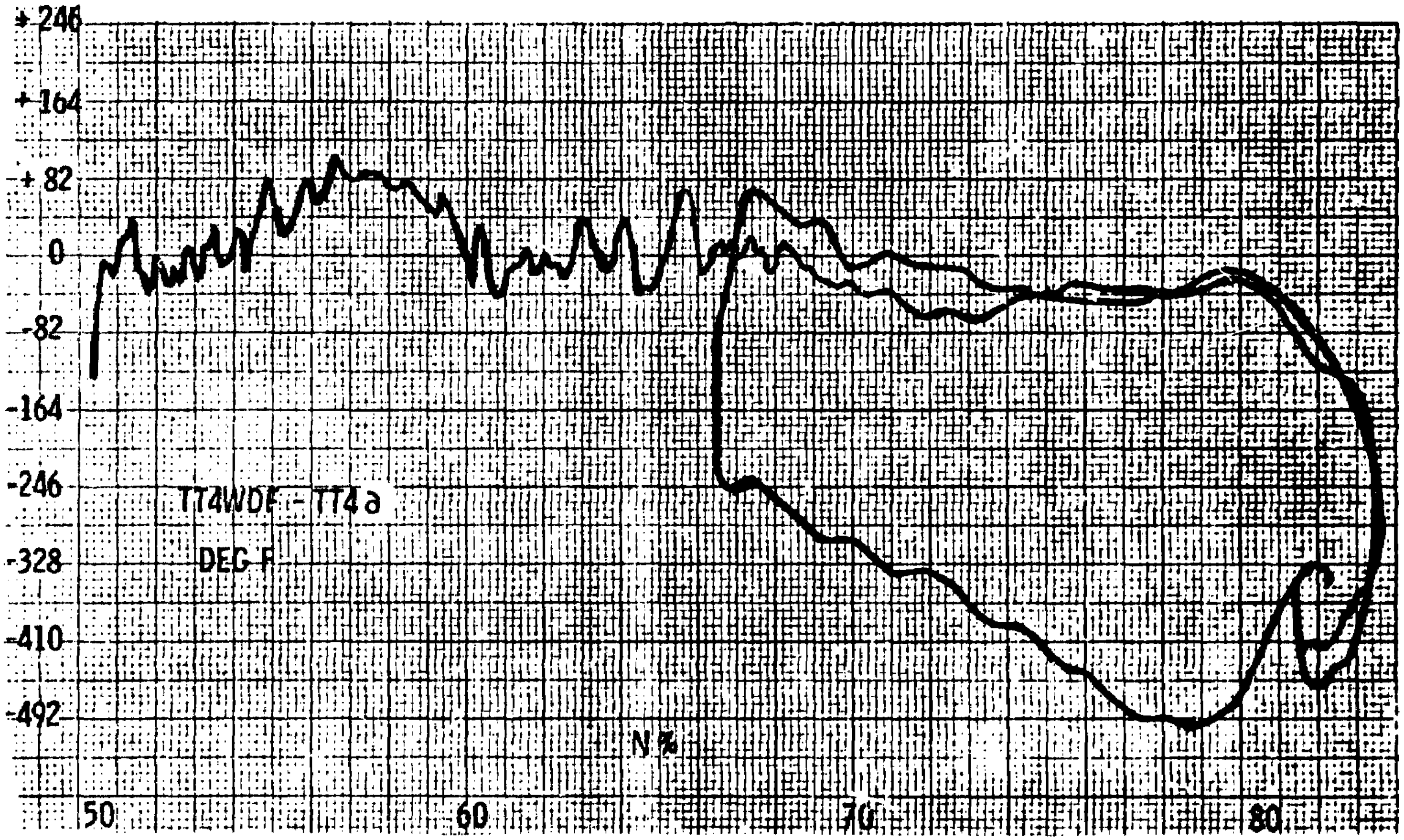

Figure 83. Speed-Temperature Bode Slam

Mode Legend: D = Deceleration, E = Equilibrium,
T = Temperature

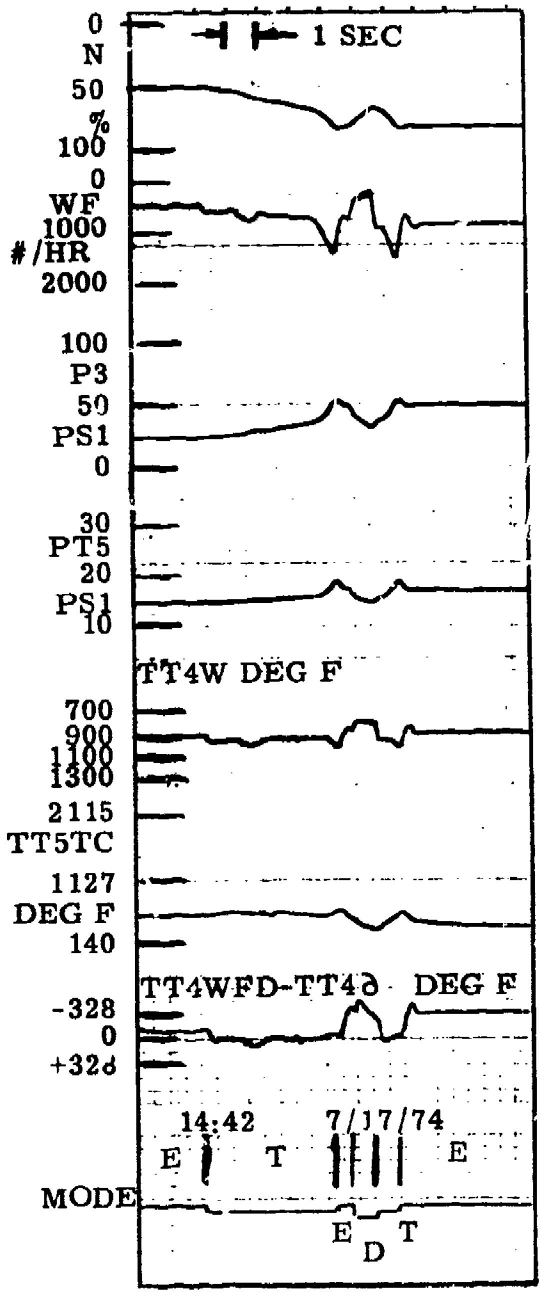

Figure 84. Speed-Temperature Bode Slam

Table 38. Design Objectives

Objective	Description
General	Design a good command controller for one flight condition (sea level static) that: • Provides good speed (N) stability • Provides good small-amplitude speed control • Demonstrates a good approximation to time-optimal control without: - Exceeding surge-stall constraints - Excesses in TT4 - Flameout
Perturbation	• Transient response: - Speed: 0.25 sec - Pressure: 0.25 sec for N ≤ 70% 0.10 sec for N ≥ 85% - Temperature: 0.10 sec • Stability margins (at the actuator and each sensor): - Greater than 6 db gain margin - Greater than 60 deg phase margin - Infinite phase margin above 30 rad/sec
Mode switching	• Smooth response transition between modes • Good approximation to time-optimal control
Miscellaneous	• IGV, BLD, and A8 to follow steady-state schedules • Digitally implemented (IBM 1800 with Bendix interface)

Table 39. Models for Linear State Control Synthesis

		1	2	3	4	5	6	7	8		
States											
Speed	$x' =$	N	TM	WF	A8	IGV	BLD	EN	P		
Pressure	$x' =$	N	TM	WF	A8	IGV	BLD	EP	P		
Temp	$x' =$	TM	WF	A8	IGV	BLD	ET	P	A8N		
Control	$u =$	U_F									
Noises	$\eta' =$	P	A8								
Responses											
Speed	$r' =$	N	$\boxed{EN}$	PT3	TT4	TM	TT5	PT5	$\boxed{\dot{WFV}}$	WFV	A8
		IGV	BLD	$\dot{N}-\dot{N}_M$	U_F						
Pressure	$r' =$	N	$\boxed{EP}$	PT3	TT4	TM	TT5	PT5	$\boxed{\dot{WFV}}$	WFV	A8
		IGV	BLD	$\boxed{\dot{PT3}-\dot{PT3M}}$	$\boxed{U_F}$						
Temp	$r' =$	P	$\boxed{ET}$	PT3	TT4	TM	TT5	PT5	$\boxed{\dot{WFV}}$	WFV	A8
		IGV	BLD	$\boxed{\dot{TT4}-\dot{TT4M}}$	$\boxed{U_F}$						

Table 40. Model for Linear Simplified Speed Control Synthesis

		1	2	3	4	5	6	7	8	9	10
States	$x' =$	N	TM	WF	A8	IGV	BLD	EN	P	A8N	$\frac{PT3S}{50}$
		$\frac{PT5S}{40}$	P3N	P5N	TD1	TD2	B2	B3	B4	$\frac{31U_F}{S+31}$[1]	$\frac{30X19}{S+30}$
Control	$u =$	U_F									
Noises	$\eta' =$	P	A8	PT3S	PT5S						
Responses	$r' =$	N	$\boxed{EN}$	PT3	TT4	TM	TT5	PT5	$\boxed{\dot{WFV}}$	WFV	A3
		IGV	BLD	$\boxed{\dot{N}-\dot{N}_M}$	$\boxed{U_F}$	$\dot{A8}$	$\dot{IGV}$	$\dot{BLD}$	PT3S	PT5S	
Measurement	$\tilde{m}' =$	$\boxed{N}$	TM	WF	A8	IGV	BLD	$\boxed{EN}$	$\boxed{P}$	A8N	PT3S
		PT5S	P3N	P5N	TD1	TD2	B2	B3	B4	X19	X20

Comment: [1] For optimization only; not for transient or frequency response

Table 41. Model for Linear Simplified Pressure Control Synthesis

		1	2	3	4	5	6	7	8	9	10
States	x' =	N	TM	WF	A8	IGV	BLD	$\widetilde{EP}$	P	A8N	$\frac{PT3S}{50}$
		$\frac{PT5S}{40}$	P3N	P5N	TD1	TD2	B2	B3	B4	$\frac{31X21}{S+31}$	$\frac{30X19}{S+30}$
		$\frac{10^6 U_F}{S+10^6}$									
Control	u =	U_F									
Noises	η' =	P	A8	PT3S	PT5S						
Responses	r' =	N	$\boxed{\widetilde{EP}}$	PT3	TT4	TM	TT5	PT5	$\boxed{\dot{WFV}}$	WFV	A8
		IGV	BLD	$\boxed{\dot{PT3}-\dot{PT3M}}$	$\boxed{UF}$	PT3S	PT5S				
Measurement	$\tilde{m}'$ =	N	TM	WF	A8	IGV	BLD	$\boxed{\widetilde{EP}}$	$\boxed{P}$	A8N	$\boxed{PT3S}$
		$\boxed{PT3S}$	P3N	P5N	TD1	TD2	B2	B3	P4	X19	X20
		X21									

Table 42. Model for Linear Simplified Temperature Control Synthesis

		1	2	3	4	5	6	7	8	9	10
States	x' =	TM	WFV	A8	IGV	BLD	$\tilde{ET}$	P	A8N	X9[1]	TT4WL
		TT4W	TW DUM	WN	$\frac{30X15}{S+30}$	$\frac{31U_F}{S+31}$[2]	$\frac{PT3S}{50}$	$\frac{PT5S}{40}$	TD1	TD2	B2
		B3	B4								
Control	u =	U_F									
Noises	η' =	P	A8	TT4WN							
Responses	r' =	P	$\boxed{\tilde{ET}}$	PT3	TT4	TM	TT5	PT5	$\boxed{\dot{WFV}}$	WFV	A8
		IGV	BLD	$\boxed{\dot{TT4}-\dot{TT4M}}$	$\boxed{U_F}$	X9	TT4W	X14	X15	P3S	X20
		U_F Fil	P5S	TT4 EST							
Measurement	$\tilde{m}'$ =	TM	WFV	A8	IGV	BLD	$\boxed{\tilde{ET}}$	$\boxed{PLA}$	A8N	X9	$\boxed{TT4\ EST}$
		TT4W	TW DUM	WN	X14	X15	$\boxed{PT3S}$	$\boxed{PT5S}$	TD1	TD2	B2
		B3	B4								

Comments: [1] X9 is not used

[2] For optimization only; not for transient or frequency response

Table 43. F Matrices - State Speed Control

100 PERCENT

1 1	-.29295E 01	1 2	.24975E 01	1 3	.13712E 05	1 4	.83393E 02	1 5	.30212E 04
1 6	.44729E 03	2 1	-.29815E-01	2 2	-.62000E 00	2 3	.90751E 03	2 5	.37842E 02
2 6	.75684E 02	3 3	-.62500E 02	4 4	-.30000E 01	4 8	-.14102E 04	5 5	-.50000E 01
5 8	-.34400E 01	6 6	-.20000E 01	6 8	-.24760E 01	7 1	-.53333E 01	7 8	.88000E 05
8 8	-.40000E 01								

85 PERCENT

1 1	-.18778E 01	1 2	.31032E 01	1 3	.24301E 05	1 4	.62386E 02	1 5	.59296E 02
1 6	-.13741E 04	2 1	-.35076E-01	2 2	-.60749E 00	2 3	.14898E 04	2 6	.26127E 02
3 3	-.62500E 02	4 4	-.30000E 01	4 8	-.14102E 04	5 5	-.50000E 01	5 8	-.33655E 02
6 6	-.20000E 01	6 8	-.10468E 02	7 1	-.53333E 01	7 8	.88000E 05	8 8	-.40000E 01

70 PERCENT

1 1	-.37430E 00	1 2	.21641E 01	1 3	.18900E 05	1 4	.22342E 02	1 5	.13152E 03
1 6	-.13169E 04	2 1	-.57336E-01	2 2	-.60688E 00	2 3	.23067E 04	2 4	-.11679E 00
2 5	-.92387E-04	[illegible]	-.37842E 02	3 3	-.62500E 02	4 4	-.30000E 01	5 5	-.50000E 01
6 6	-.20000E 01	7 1	-.53333E 01	7 8	.88000E 05	8 8	-.40000E 01		

50 PERCENT

1 1	-.14077E 00	1 2	.14663E 01	1 3	.96703E 04	1 4	.71490E 01	1 5	.14415E 03
1 6	.36740E 03	2 1	-.80270E-01	2 2	-.56930E 00	2 3	.41412E 04	2 4	-.11679E 00
2 5	.37842E 02	2 6	-.37842E 02	3 3	-.62500E 02	4 4	-.30000E 01	5 5	-.50000E 01
6 6	-.20000E 01	7 1	-.53333E 01	7 8	.88000E 05	8 8	-.40000E 01		

Table 44. G1 Matrices - State Speed and Pressure Control

3 1	.62500E 02

Table 45. G2 Matrices - State Speed and Pressure Control

4 2	.97980E 01	8 1	.28240E-01

Table 46. H Matrices - State Speed Control

100 PERCENT

1 1	.10000E 01	2 7	.10000E 01	3 1	.64891E-02	3 2	.19172E-02	3 3	.25687E 02
3 4	-.53317E-02	3 5	-.37752E 01	3 6	-.10377E 02	4 1	-.42773E-01	4 2	.11054E 00
4 3	.13019E 04	4 5	.54288E 02	4 6	.10858E 03	5 2	.10000E 01	6 1	-.48088E-01
6 2	-.13532E-01	6 3	.13136E 04	6 4	-.10006E 01	6 6	.61035E 02	7 1	.18262E-02
7 2	-.15283E-03	7 3	.13864E 02	7 4	-.76472E-01	7 5	-.16419E 01	7 6	-.35949E 01
8 3	-.62500E 02	9 3	.10000E 01	10 4	.10000E 01	11 5	.10000E 01	12 6	.10000E 01
13 1	.50705E 01	13 2	.24975E 01	13 3	.13712E 05	13 4	.83393E 02	13 5	.30212E 04
13 6	.44729E 03	13 7	-.30000E 01	13 8	-.88000E 05				

85 PERCENT

1 1	.10000E 01	2 7	.10000E 01	3 1	.76564E-02	3 2	.24081E-02	3 3	.31140E 02
3 4	-.48861E-02	3 5	-.27477E 00	3 6	-.23279E 01	4 1	-.47856E-01	4 2	.17118E 00
4 3	.20326E 04	4 6	.35645E 02	5 2	.10000E 01	6 1	-.69630E-01	6 2	-.40356E-01
6 3	.20895E 04	6 4	-.75347E 00	7 1	.12390E-02	7 2	-.24962E-03	7 3	.98456E 01
7 4	-.59098E-01	7 5	-.51570E-01	7 6	-.48776E 00	8 3	-.62500E 02	9 3	.10000E 01
10 4	.10000E 01	11 5	.10000E 01	12 6	.10000E 01	13 1	.61222E 01	13 2	.31032E 01
13 3	.24301E 05	13 4	.62386E 02	13 5	.59296E 02	13 6	-.13741E 04	13 7	-.30000E 01
13 8	-.88000E 05								

70 PERCENT

1 1	.10000E 01	2 7	.10000E 01	3 1	.58889E-02	3 2	.17882E-02	3 3	.23449E 02
3 4	-.60142E-02	3 5	-.78930E 00	3 6	-.45635E-03	4 1	-.71269E-01	4 2	.24565E 00
4 3	.28673E 04	4 4	-.14517E 00	4 5	.74506E-04	4 6	-.47038E 02	5 2	.10000E 01
6 1	-.11362E 00	6 2	-.21167E-01	6 3	.32741E 04	6 4	-.37674E 00	7 1	.67170E-03
7 2	-.17[illegible]94E-03	7 3	.60567E 01	7 4	-.25317E-01	7 5	-.11181E 00	7 6	.10211E 00
8 3	-.6[illegible]00E 02	9 3	.10000E 01	10 4	.10000E 01	11 5	.10000E 01	12 6	.10000E 01
13 1	.76257E 01	13 2	.21641E 01	13 3	.18900E 05	13 4	.22342E 02	13 5	.13152E 03
13 6	-.13169E 04	13 7	-.30000E 01	13 8	-.88000E 05				

50 PERCENT

1 1	.10000E 01	2 7	.10000E 01	3 1	.28703E-02	3 2	.97088E-03	3 3	.10332E 02
3 4	-.31521E-02	3 5	-.14397E 00	3 6	.60077E 00	4 1	-.76315E-01	4 2	.45876E 00
4 3	.39372E 04	4 4	-.11103E 00	4 5	.35977E 02	4 6	-.35377E 02	5 2	.10000E 01
6 1	-.14426E 00	6 2	.40889E-01	6 3	.60330E 04	6 4	-.18837E 00	6 6	-.61035E 02
7 1	.23025E-03	7 2	-.55615E-04	7 3	.32562E 01	7 4	-.84774E-02	7 5	-.28987E-01
7 6	.60305E-01	8 3	-.62500E 02	9 3	.10000E 01	10 4	.10000E 01	11 5	.10000E 01
12 6	.10000E 01	13 1	.78592E 01	13 2	.14663E 01	13 3	.96703E 04	13 4	.71490E 01
13 5	.14415E 03	13 6	.36740E 03	13 7	-.30000E 01	13 8	-.88000E 05		

Table 47. D Matrices - State Speed Control

8 1	.62500E 02	14 1	.10000E 01

Table 48. Speed Controller Quadratic Weights (Nonzero Values: Diagonal Elements Q_{ii})

r_i	i	100%	85%	70%	50%
EN	2	.30-4	.30-4	.30-4	.30-4
$\dot{W}FV$	8	.10+3	.10+3	.10+3	.20+2
$\dot{N}$ - $\dot{N}M$	13	.30-2	.10-2	.10-2	.10-2
UWF	14	.10+1	.10+1	.10+1	.10+1

Table 49. State Control Gain Matrices

Parameter	Operating Condition	1	2	3	4	5	6	7	8
Speed	100%	-.446-3	-.231-3	-.283+0	-.750-2	-.265+0	-.410-1	+.263-3	+.776+1
	85%	-.313-3	-.168-3	-.328+0	-.328-2	-.304-2	+.731+1	+.152-3	+.445+1
	70%	-.396-3	-.122-3	-.785-1	-.121-2	-.693-2	+.727-1	+.152-3	+.439+1
	50%	-.913-3	-.185-3	-.226+0	-.864-3	-.170-1	-.449-1	+.340-3	+.983+1
Pressure	100%	-.110-3	-.367-3	+.616+0	-.471-3	+.357-1	+.132+0	+.579-2	+.259+1
	85%	-.693-3	-.103-3	+.270+0	-.416-2	+.470-1	+.700-1	+.220-1	+.956+1
	70%	-.154-4	-.480-4	+.625+0	-.730-2	+.292-2	-.260-1	+.685-2	+.201+1
	50%	-.103-3	-.311-4	+.782+0	-.127-3	+.145-2	-.247-1	+.112-1	+.209+1
Temperature	100%	-.247-4	+.690+0	+.939-4	-.817-2	-.372-1	+.945-4	+.840-1	+.100-9
	85%	-.259-4	+.702+0	+.271-3	-.403-2	+.943-3	+.557-4	+.495-1	+.114-4
	70%	-.307-4	+.695+0	+.723-4	-.372-2	+.897-2	+.431-4	+.383-1	+.789-5
	50%	-.442-2	+.676+0	+.347-4	+.813-4	+.568-2	+.328-4	+.292-1	+.129-4

Table 50. Speed State Models Open-Loop Roots*

Association	100%	85%	70%	50%
N	-2.90	-1.79	+0.593	+0.445
TM	-0.653	-0.700	@0.828	@0.798
WFV	-62.5	-62.5	-62.5	-62.5
A	-3.0	-3.0	-3.0	-3.0
IGV	-5.0	-5.0	-5.0	-5.0
BLD	-2.0	-2.0	-2.0	-2.0
EN	---	---	---	---
P	-4.0	-4.0	-4.0	-4.0

Table 51. Speed State Controllers Closed-Loop Roots*

Association	No. 4(100%)	No. 7(85%)	No. 9(70%)	No. 11(50%)
N	-3.97	-4.01	-3.94	-3.97
TM	-0.785	-0.798	-0.871	-1.20
WFV	-74.9	-76.7	-59.5	-68.1
A8	-3.0	-3.0	-3.0	-3.0
IGV	-5.0	-5.0	-5.0	-5.0
BLDG	-2.0	-2.0	-2.0	-2.0
EN	-4.04	@0.999	-4.09	-4.05
P	-4.0	-4.0	-4.0	-4.0

*Real roots:
Tabular value = root value
Complex roots:
Tabular values = (+X.XXX, @ 0.YYY) = (frequency, damping ratio)

Table . Speed State Controllers RMS Response (P = 0.01 RMS; A8 = 4.0 Sq In. RMS)

Response	Response Component	100%		85%		70%		50%	
		ETA 1	ETA 2	ETA 1	ETA 2	ETA 1	ETA 2	ETA 1	ETA 2
N	r1	.1266+3	.2578+1	.1266+3	.1888+1	.1264+3	.8585+0	.1266+3	.2419+0
EN	r2	.1291+3	.3587+1	.1288+3	.2626+1	.1314+3	.1210+1	.1299+3	.3387+0
PT3	r3	.2296+1	.6146+0	.1688+1	.3228+0	.1036+1	.1292+0	.6814+0	.4095-1
TT4	r4	.7269+2	.3074+2	.5166+2	.2049+2	.8180+2	.1397+2	.2209+3	.1173+2
TM	r5	.2708+2	.1283+2	.1414+2	.8811+1	.1304+2	.6221+1	.4316+2	.5609+1
TT5	r6	.7405+2	.3431+2	.5233+2	.2330+2	.9323+2	.1605+2	.3344+3	.1650+2
PT5	r7	.1210+1	.6193+0	.5326+0	.3285+0	.1940+0	.1268+0	.1796+0	.4182-1
WḞV	r8	.1083+1	.3673+0	.6097+0	.1583+0	.6724+0	.6621-1	.1416+1	.4414-1
WFV	r9	.5849-1	.2312-1	.2675-1	.9758-2	.2834-1	.4449-1	.5514-1	.2611-2
A8	r10	.3072+1	.4000+1	.3072+1	.4000+1	.0000	.4000+1	.0000	.4000+1
IGV	r11	.5120-2	.0000	.5009-1	.0000	0000	.0000	.0000	.0000
BLD	r12	.7136-2	.0000	.3017-1	.0000	.0000	.0000	.0000	.0000
Ṅ - ṄM	r13	.2025+3	.6669+2	.2000+3	.4934+2	.2265+3	.2005+2	.2118+3	.5996+1
UWF	r14	.6101-1	.2386-1	.2648-1	.1908-1	.3032-1	.4573-2	.5962-1	.2705-2

Table 53. F Matrices - Simplified Speed Control

100 PERCENT

1 1	-.29295E 01	1 2	.24975E 01	1 3	.13712E 05	1 4	.83393E 02	1 5	.30212E 04
1 6	.44729E 03	2 1	-.29815E-01	2 2	-.62000E 00	2 3	.90751E 03	2 5	.37842E 02
2 6	.75684E 02	316	-.50400E 04	4 4	-.30000E 01	4 8	-.14102E 04	4 9	.10000E 01
5 5	-.50000E 01	5 8	-.34400E 01	5 9	.32784E-02	6 6	-.20000E 01	6 8	-.24760E 01
6 9	.20250E-02	7 1	-.53333E 01	7 8	.88000E 05	8 8	-.40000E 01	9 9	-.59909E 02
10 1	.64891E-02	10 2	.19172E-02	10 3	.25687E 02	10 4	-.53417E-02	10 5	-.37752E 01
10 6	-.10377E 02	1010	-.50000E 02	1012	.11190E 04	11 1	.18262E-02	11 2	-.15283E-03
11 3	.13864E 02	11 4	-.76472E-01	11 5	-.16419E 01	11 6	-.35949E 01	1111	-.40000E 02
1113	.14318E 03	1212	-.20000E 03	1313	-.62500E 02	1415	.10000E 01	1514	-.26667E 05
1515	-.20000E 03	1520	.10000E 01	16 3	.31333E 01	1616	-.50384E 02	1617	.18800E 04
1718	.10000E 02	1815	.23651E 04	1817	-.35462E 04	1818	-.30100E 03	1820	-.59127E 01
1919	-.31000E 02	2019	.30000E 02	2020	-.30000E 02				

85 PERCENT

1 1	-.18778E 01	1 2	.31032E 01	1 3	.24301E 05	1 4	.62383E 02	1 5	.59296E 02
1 6	-.13741E 04	2 1	-.35076E-01	2 2	-.60749E 00	2 3	.14898E 04	2 6	.26127E 02
316	-.50400E 04	4 4	-.30000E 01	4 8	-.14102E 04	4 9	.10000E 01	5 5	-.50000E 01
5 8	-.33655E 02	5 9	.32784E-02	6 6	-.20000E 01	6 8	-.10468E 02	6 9	.20250E-02
7 1	-.53333E 01	7 8	.88000E 05	8 8	-.40000E 01	9 9	-.59909E 02	10 1	.76564E-02
10 2	.24081E-02	10 3	.31140E 02	10 4	-.48861E-02	10 5	-.27477E 00	10 6	-.23279E 01
1010	-.50000E 02	1012	.11190E 04	11 1	.12390E-02	11 2	-.24962E-03	11 3	.98456E 01
11 4	-.59098E-01	11 5	-.51570E-01	11 6	-.48776E 00	1111	-.40000E 02	1113	.14318E 03
1212	-.20000E 03	1313	-.62500E 02	1415	.10000E 01	1514	-.26667E 05	1515	-.20000E 03
1520	.10000E 01	16 3	.31333E 01	1616	-.50384E 02	1617	.18800E 04	1718	.10000E 02
1815	.23651E 04	1817	-.35462E 04	1818	-.30100E 03	1820	-.59127E 01	1919	-.31000E 02
2019	.30000E 02	2020	-.30000E 02						

70 PERCENT

1 1	-.37430E 00	1 2	.21641E 01	1 3	.18900E 05	1 4	.22343E 02	1 5	.13152E 03
1 6	-.13169E 04	2 1	-.57336E-01	2 2	-.60688E 00	2 3	.23067E 04	2 4	-.11679E 00
2 5	-.92387E-04	2 6	-.37842E 02	316	-.50400E 04	4 4	-.30000E 01	4 9	.10000E 01
5 5	-.50000E 01	5 9	.32784E-02	6 6	-.20000E 01	6 9	.20250E-02	7 1	-.53333E 01
7 8	.88000E 05	8 8	-.40000E 01	9 9	-.59909E 02	10 1	.58889E-02	10 2	.17882E-02
10 3	.23449E 02	10 4	-.60142E-02	10 5	-.78930E 00	10 6	-.45635E-03	1010	-.50000E 02
1012	.11190E 04	11 1	.67170E-03	11 2	-.13894E-03	11 3	.60567E 01	11 4	-.25317E-01
11 5	-.11181E 00	11 6	.10211E 00	1111	-.40000E 02	1113	.14318E 03	1212	-.20000E 03
1313	-.62500E 02	1415	.10000E 01	1514	-.26667E 05	1515	-.20000E 03	1520	.10000E 01
16 3	.31333E 01	1616	-.50384E 02	1617	.18800E 04	1718	.10000E 02	1815	.23651E 04
1817	-.35462E 04	1818	-.30100E 03	1820	-.59127E 01	1919	-.31000E 02	2019	.30000E 02
2020	-.30000E 02								

50 PERCENT

1 1	-.14077E 00	1 2	.14663E 01	1 3	.96703E 04	1 4	.71490E 01	1 5	.14415E 03
1 6	.36740E 03	2 1	-.80270E-01	2 2	-.56930E 00	2 3	.41412E 04	2 4	-.11679E 00
2 5	.37842E 02	2 6	-.37842E 02	316	-.50400E 04	4 4	-.30000E 01	4 9	.10000E 01
5 5	-.50000E 01	5 9	.32784E-02	6 6	-.20000E 01	6 9	.20250E-02	7 1	-.53333E 01
7 8	.88000E 05	8 3	-.40000E 01	9 9	-.59909E 02	10 1	.28703E-02	10 2	.97088E-03
10 3	.10332E 02	10 4	-.31521E-02	10 5	-.14397E 00	10 6	.60077E 00	1010	-.50000E 02
1012	.11180E 04	11 1	.23025E-03	11 2	-.55615E-04	11 3	.32562E 01	11 4	-.84774E-02
11 5	-.28987E-01	11 6	.60305E-01	1111	-.40000E 02	1113	.14318E 03	1212	-.20000E 03
1313	-.62500E 02	1415	.10000E 01	1514	-.26667E 05	1515	-.20000E 03	1520	.10000E 01
16 3	.31333E 01	1616	-.50384E 02	1617	.18800E 04	1718	.10000E 02	1815	.23651E 04
1817	-.35462E 04	1818	-.30100E 03	1820	-.59127E 01	1919	-.31000E 02	2019	.30000E 02
2020	-.30000E 02								

Table 54. G1 Matrices Simplified Speed Control

191 .31000E 02

Table 55. G2 Matrices Simplified Speed Control

81 .28240E-01 92 .60150E 03 123 .20000E-01 134 .50705E 01

Table 56. H Matrices - Simplified Speed Control

100 PERCENT

1 1	.10000E 01	2 7	.10000E 01	3 1	.64891E-02	3 2	.19172E-02	3 3	.28687E 02
3 4	-.53417E-02	3 5	-.37752E 01	3 6	-.10377E 02	4 1	-.42777E-01	4 2	.11054E 00
4 3	.13019E 04	4 5	.54288E 02	4 6	.10858E 03	5 2	.10000E 01	6 1	-.48088E-01
6 2	-.13532E-01	6 3	.13136E 04	6 4	-.10006E 01	6 6	.61035E 02	7 1	.18262E-02
7 2	-.15283E-03	7 3	.13864E 02	7 4	-.76472E-01	7 5	-.16419E 01	7 6	-.35949E 01
816	-.50400E 04	9 3	.10000E 01	10 4	.10000E 01	11 5	.10000E 01	12 6	.10000E 01
13 1	.50705E 01	13 2	.24975E 01	13 3	.13712E 05	13 4	.83393E 02	13 5	.30212E 04
13 6	.44729E 03	13 7	-.30000E 01	13 8	-.88000E 05	15 4	-.30000E 01	15 8	-.14102E 04
15 9	.10000E 01	16 5	-.50000E 01	16 8	-.34400E 01	16 9	.32784E-02	17 6	-.20000E 01
17 8	-.24760E 01	17 9	.20250E-02	1810	.50000E 02	1911	.40000E 02		

85 PERCENT

1 1	.10000E 01	2 7	.10000E 01	3 1	.76564E-02	3 2	.24081E-02	3 3	.31140E 02
3 4	-.48861E-02	3 5	-.27477E 00	3 6	-.23273E 01	4 1	-.47856E-01	4 2	.17118E 00
4 3	.20326E 04	4 6	.35645E 02	5 2	.10000E 01	6 1	-.69630E-01	6 2	-.40356E-01
6 3	.20895E 04	6 4	-.75347E 00	7 1	.12390E-02	7 2	-.24962E-03	7 3	.98456E 01
7 4	-.59098E-01	7 5	-.51570E-01	7 6	-.48776E 00	816	-.50400E 04	9 3	.10000E 01
10 4	.10000E 01	11 5	.10000E 01	12 6	.10000E 01	13 1	.61222E 01	13 2	.31032E 01
13 3	.24301E 05	13 4	.62386E 02	13 5	.59296E 02	13 6	-.13741E 04	13 7	-.30000E 01
13 8	-.88000E 05	15 4	-.30000E 01	15 8	-.14102E 04	15 9	.10000E 01	16 5	-.50000E 01
16 8	-.33655E 02	16 9	.32784E-02	17 6	-.20000E 01	17 8	-.10468E 02	17 9	.20250E-02
1810	.50000E 02	1911	.40000E 02						

70 PERCENT

1 1	.10000E 01	2 7	.10000E 01	3 1	.58889E-02	3 2	.17882E-02	3 3	.23449E 02
3 4	-.60142E-02	3 5	-.78930E 00	3 6	-.45635E-03	4 1	-.71269E-01	4 2	.24565E 00
4 3	.28673E 04	4 4	-.14517E 00	4 5	.74506E-04	4 6	-.47038E 02	5 2	.10000E 01
6 1	-.11362E 00	6 2	-.21167E-01	6 3	.32741E 04	6 4	-.37674E 00	7 1	.67170E-03
7 2	-.13894E-03	7 3	.60567E 01	7 4	-.25317E-01	7 5	-.11181E 00	7 6	.10211E 00
816	-.50400E 04	9 3	.10000E 01	10 4	.10000E 01	11 5	.10000E 01	12 6	.10000E 01
13 1	.76257E 01	13 2	.21641E 01	13 3	.18900E 05	13 4	.22342E 02	13 5	.13152E 03
13 6	-.13169E 04	13 7	-.30000E 01	13 8	-.88000E 05	15 4	-.30000E 01	15 9	.10000E 01
16 5	-.50000E 01	16 9	.32784E-02	17 6	-.20000E 01	17 9	.20250E-02	1810	.50000E 02
1911	.40000E 02								

50 PERCENT

1 1	.10000E 01	2 7	.10000E 01	3 1	.28703E-02	3 2	.97088E-03	3 3	.10332E 02
3 4	-.31521E-02	3 5	-.14397E 00	3 6	.60077E 00	4 1	-.76315E-01	4 2	.45876E 00
4 3	.39372E 04	4 4	-.11103E 00	4 5	.35977E 02	4 6	-.35077E 02	5 2	.10000E 01
6 1	-.14426E 00	6 2	.40889E-01	6 3	.60330E 04	6 4	-.13537E 00	6 6	-.61035E 02
7 1	.23025E-03	7 2	-.55615E-04	7 3	.32562E 01	7 4	-.84774E-02	7 5	-.28987E-01
7 6	.60305E-01	816	-.50400E 04	9 3	.10000E 01	10 4	.10000E 01	11 5	.10000E 01
12 6	.10000E 01	13 1	.78592E 01	13 2	.14663E 01	13 3	.96700E 04	13 4	.71490E 01
13 5	.14415E 03	13 6	.36740E 03	13 7	-.30000E 01	13 8	-.88000E 05	15 4	-.30000E 01
15 9	.10000E 01	16 5	-.50000E 01	16 9	.32784E-02	17 6	-.20000E 01	17 9	.20250E-02
1810	.50000E 02	1911	.40000E 02						

Table 57. D Matrices - Simplified Speed Control

14 1 .10000E 01

Table 58. M Matrices - Simplified Speed Control

100 PERCENT

1 1	.10000E 01	2 2	.10000E 01	3 3	.10000E 01	4 1	.18262E-02	4 2	-.15283E-03
4 3	.13864E 02	4 4	-.76472E-01	4 5	-.16419E 01	4 6	-.35949E 01	5 5	.10000E 01
6 1	.64891E-02	6 2	.19172E-02	6 3	.25687E 02	6 4	-.53417E-02	6 5	-.37752E 01
6 6	-.10377E 02	7 7	.10000E 01	8 8	.10000E 01	9 9	.10000E 01	1010	.50000E 02
1111	.40000E 02	1212	.10000E 01	1313	.10000E 01	1414	.10000E 01	1515	.10000E 01
1616	.10000E 01	1717	.10000E 01	1818	.10000E 01	1919	.10000E 01	2020	.10000E 01

85 PERCENT

1 1	.10000E 01	2 2	.10000E 01	3 3	.10000E 01	4 1	.12390E-02	4 2	-.24962E-03
4 3	.98456E 01	4 4	-.59098E-01	4 5	-.51570E-01	4 6	-.48776E 00	5 5	.10000E 01
6 1	.76564E-02	6 2	.24081E-02	6 3	.31140E 02	6 4	-.48861E-02	6 5	-.27477E 00
6 6	-.23279E 01	7 7	.10000E 01	8 8	.10000E 01	9 9	.10000E 01	1010	.50000E 02
1111	.40000E 02	1212	.10000E 01	1313	.10000E 01	1414	.10000E 01	1515	.10000E 01
1616	.10000E 01	1717	.10000E 01	1818	.10000E 01	1919	.10000E 01	2020	.10000E 01

70 PERCENT

1 1	.10000E 01	2 2	.10000E 01	3 3	.10000E 01	4 1	.67170E-03	4 2	-.13894E-03
4 3	.60567E 01	4 4	-.25317E-01	4 5	-.11181E 00	4 6	.10211E 00	5 5	.10000E 01
6 1	.58889E-02	6 2	.17882E-02	6 3	.23449E 02	6 4	-.60142E-02	6 5	-.78930E 00
6 6	-.45635E-03	7 7	.10000E 01	8 8	.10000E 01	9 9	.10000E 01	1010	.50000E 02
1111	.40000E 02	1212	.10000E 01	1313	.10000E 01	1414	.10000E 01	1515	.10000E 01
1616	.10000E 01	1717	.10000E 01	1818	.10000E 01	1919	.10000E 01	2020	.10000E 01

50 PERCENT

1 1	.10000E 01	2 2	.10000E 01	3 3	.10000E 01	4 4	.10000E 01	5 5	.10000E 01
6 6	.10000E 01	7 7	.10000E 01	8 8	.10000E 01	9 9	.10000E 01	1010	.50000E 02
1111	.40000E 02	1212	.10000E 01	1313	.10000E 01	1414	.10000E 01	1515	.10000E 01
1616	.10000E 01	1717	.10000E 01	1818	.10000E 01	1919	.10000E 01	2020	.10000E 01

Table 59. Simplified Speed Control Closed-Loop Roots

Root Association	100%		85%		70%		50%	
	Frequency	Damping	Frequency	Damping	Frequency	Damping	Frequency	Damping
N	+11.18	.5161	+10.19	.5916	+8.917	+.7575	+7.753	+.8995
EN	-3.356		-2.835		-1.496		-1.895	
TM	-.7982		-.8049		-.7739		-.6326	
WF	125.4	.1977	+125.5	.1980	+125.5	+.1985	+125.5	+.1988
WF	162.9	.6076	+163.0	.6082	+163.0	+.6090	+163.1	+.6094
X19								
X20	-51.16		-49.82		-47.85		-46.67	
TD	+188.9	.7982	+188.8	.7983	188.7	+.7985	+188.7	+.7985
A8	-3.000		-3.000		-3.000		-3.000	
IGV	-5.000		-5.000		-5.000		-5.000	
BLD	-2.000		-2.000		-2.000		-2.000	
PT3S/50	-50.00		-50.00		-50.00		-50.00	
PT5S/40	-40.00		-40.00		-40.00		-40.00	
P	-4.0		-4.00		-4.000		-4.000	
A8W	-59.91		-59.91		-59.91		-59.91	
P3N	-200.0		-200.0		-200.0		-200.0	
P5N	-62.5		-62.5		-62.5		-62.5	

Table 60. Simplified Speed Control RMS Response

Response	100%		85%		70%		50%	
	ETA 1	ETA 2	ETA 1	ETA 2	ETA 1	ETA 2	ETA 1	ETA 2
N	.1219+3	.3534+2	.1239+3	.2741+2	.1284+3	.1278+2	.1319+4	.6261+1
EN	.1873+3	.5996+2	.1830+3	.5284+2	.1773+3	.3458+2	.1794+4	.1843+2
PT3	.2294+1	.7422+0	.1681+1	.3042+0	.1041+1	.8312-1	.6643+1	.2856-1
TT4	.7545+2	.3407+2	.5345+2	.2022+2	.8082+2	.1319+2	.2097+4	.1433+2
TM	.2704+2	.1390+2	.1419+2	.8581+1	.1343+2	.6079+1	.4621+3	.7635+1
TT5	.7721+2	.3734+2	.5473+2	.2286+2	.9209+2	.1482+2	.3165+4	.2023+2
PT5	.1233+1	.6301+0	.5446+0	.2917+0	.1926+0	.1114+0	.1694+1	.3924-1
$\dot{W}FV$	.5475+0	.1390+0	.2763+0	.4673-1	.2959+0	.1706-1	.5311+1	.1270-1
WFV	.6040-1	.2612-1	.2758-1	.9481-2	.2798-1	.3893-2	.5211+0	.3063-2
A8	.3072+1	.3999+1	.3072+1	.3999+1	.0000+0	.3999+1	.0000+0	.3999+1
IGV	.5120-2	.9999-2	.5009-1	.9999-2	.0000+0	.9999-2	.0000+0	.9999-2
BLD	.7136-2	.1000-1	.3017-1	.1000-1	.0000+0	.1000-1	.0000+0	.1000-1
$\dot{N}$ - $\dot{N}M$	6976+3	.3854+3	.6846+3	.2900+3	.6716+3	.1434+3	.6900+4	.7200+2
UF	.6674-1	.2690-1	.3113-1	.9721-2	.3201-1	.3971-2	.5915+0	.3117-2
$\dot{A}8$	.1064+2	.5362+2	.1064+2	.5362+2	.0000+0	.5362+2	.0000+0	.5362+2
$\dot{I}GV$	.2289-1	.1730+0	.2240+0	.1730+0	.0000+0	.1730+0	.0000+0	.1730+0
$\dot{B}LD$	.2018-1	.1094+0	.8533-1	.1094+0	.0000+0	.1094+0	.0000+0	.1094+0
PT3S	.2276+1	.7392+0	.1670+1	.3028+0	.1032+1	.8231-1	.6561+1	.2848-1
PT5S	.1217+1	.6253+0	.5390+0	.2879+0	.1883+0	.1095+0	.1651+1	.3864-1

*ETA 3 yields a PT3S response of 0.5 psi rms; ETA 2 yields a PT5S response of 0.2 psi rms.

Table 61. F Matrices - State Pressure Control

100 PERCENT

1 1 -.21273E 01	1 2 .22233E 01	1 3 .10283E 05	1 4 .88897E 02	1 5 .20208E 04
1 6 -.13432E 03	2 1 -.58483E-01	2 2 -.62000E 00	2 3 .88597E 03	2 5 .37842E 02
2 6 .11353E 03	3 3 -.62500E 02	4 4 -.30000E 01	4 8 -.14102E 04	5 5 -.50000E 01
5 8 -.34400E 01	6 6 -.20000E 01	6 8 -.24760E 01	7 1 -.10625E 00	7 2 -.20509E-01
7 3 -.27609E 03	7 4 .77557E-01	7 5 .55407E 02	7 6 .12632E 03	7 8 .34000E 04
8 8 -.40000E 01				

85 PERCENT

1 1 -.78927E 00	1 2 .20990E 01	1 3 .11319E 05	1 4 .11643E 03	1 5 .27402E 03
1 6 -.17600E 04	2 1 -.21585E 00	2 2 -.58668E 00	2 3 .16027E 04	2 4 -.11679E 00
2 5 .30552E 02	2 6 -.26127E 02	3 3 -.62500E 02	4 4 -.30000E 01	4 3 -.14102E 04
5 5 -.50000E 01	5 8 -.33655E 02	6 6 -.20000E 01	6 8 -.10468E 02	7 1 -.16373E 00
7 2 -.64384E-02	7 3 -.72461E 02	7 4 .11237E-01	7 5 .17228E 02	7 6 .16235E 01
7 8 .34000E 04	8 8 -.40000E 01			

70 PERCENT

1 1 .18223E 00	1 2 .19682E 01	1 3 .12933E 05	1 4 .40137E 02	1 5 .17702E 03
1 6 -.37655E 03	2 1 -.21132E 00	2 2 -.58421E 00	2 3 .23220E 04	2 4 -.11679E 00
2 5 .37842E 02	2 6 -.75684E 02	3 3 -.62500E 02	4 4 -.30000E 01	5 5 -.50000E 01
6 6 -.20000E 01	7 1 -.43939E-01	7 2 -.34612E-02	7 3 -.37358E 02	7 4 .11319E-01
7 5 .49149E 01	7 6 -.12913E 02	7 8 .88000E 03	8 8 -.40000E 01	

50 PERCENT

1 1 .53809E 00	1 2 .14508E 01	1 3 .48505E 04	1 4 .13708E 02	1 5 .96437E 02
1 6 .46436E 03	2 1 -.22476E 00	2 2 -.54284E 00	2 3 .42648E 04	2 4 -.35037E 00
2 5 -.18477E-03	2 6 -.75684E 02	3 3 -.62500E 02	4 4 -.30000E 01	5 5 -.50000E 01
6 6 -.20000E 01	7 1 -.17214E-01	7 2 -.25915E-02	7 3 -.22761E 02	7 4 .10548E-01
7 5 .12412E 01	7 6 -.45768E 01	7 8 .56000E 03	8 8 -.40000E 01	

Table 62. H Matrices - State Pressure Control

100 PERCENT

1 1 .10000E 01	2 7 .10000E 01	3 1 .79684E-02	3 2 .15382E-02	3 3 .20707E 02
3 4 -.58168E-02	3 5 -.41555E 01	3 6 -.94740E 01	4 1 -.83848E-01	4 2 .11110E 00
4 3 .12702E 04	4 4 -.81427E-06	4 5 .54234E 02	4 6 .16276E 03	5 2 .10000E 01
6 1 -.10173E 00	6 2 -.22170E-01	6 3 .13231E 04	6 4 -.66705E 00	6 5 .61035E 02
6 6 .12207E 03	7 1 .21738E-02	7 2 -.27403E-03	7 3 .11960E 02	7 4 -.79991E-01
7 5 -.12510E 01	7 6 -.31137E 01	8 3 -.62500E 02	9 3 .10000E 01	10 4 .10000E 01
11 5 .10000E 01	12 6 .10000E 01	13 1 .14233E 00	13 2 .47526E-01	13 3 -.79671E 03
13 4 .60948E 00	13 5 -.46172E 02	13 6 -.17143E 03	13 7 -.75000E 01	13 8 -.33540E 04

85 PERCENT

1 1 .10000E 01	2 7 .10000E 01	3 1 .12280E-01	3 2 .48288E-03	3 3 .54346E 01
3 4 -.84278E-03	3 5 -.12921E 01	3 6 -.12176E 00	4 1 -.29029E 00	4 2 .21102E 00
4 3 .21554E 04	4 4 -.15706E 00	4 5 .41087E 02	4 6 -.35136E 02	5 2 .10000E 01
6 1 -.35250E 00	6 2 .21499E-01	6 3 .24080E 04	6 4 -.13186E 01	6 5 .49278E 02
6 6 -.42140E 02	7 1 .28926E-02	7 2 -.47983E-03	7 3 .51329E 01	7 4 -.10672E 00
7 5 -.27966E 00	7 6 .26724E-01	8 3 -.62500E 02	9 3 .10000E 01	10 4 .10000E 01
11 5 .10000E 01	12 6 .10000E 01	13 1 .23580E 00	13 2 .35150E-01	13 3 -.91285E 02
13 4 .14154E 01	13 5 -.16002E 02	13 6 -.23817E 02	13 7 -.75000E 01	13 8 -.33541E 04

70 PERCENT

1 1 .10000E 01	2 7 .10000E 01	3 1 .82386E-02	3 2 .64898E-03	3 3 .70047E 01
3 4 -.21823E-02	3 5 -.92155E 00	3 6 .24212E 01	4 1 -.25316E 00	4 2 .30015E 00
4 3 .27816E 04	4 4 -.13991E 00	4 5 .45333E 02	4 6 -.90665E 02	5 2 .10000E 01
6 1 -.35934E 00	6 2 .23093E-01	6 3 .35111E 04	6 4 -.75347E 00	6 5 .61035E 02
6 6 -.12207E 03	7 1 .11009E-02	7 2 -.20302E-03	7 3 .40736E 01	7 4 -.39345E-01
7 5 -.11192E 00	7 6 .39236E 00	8 3 -.62500E 02	9 3 .10000E 01	10 4 .10000E 01
11 5 .10000E 01	12 6 .10000E 01	13 1 .67273E-01	13 2 .21028E-01	13 3 -.27370E 03
13 4 .31999E 00	13 5 -.12817E 01	13 6 .11376E 02	13 7 -.30000E 01	13 8 -.88000E 03

50 PERCENT

1 1 .10000E 01	2 7 .10000E 01	3 1 .32277E-02	3 2 .48590E-03	3 3 .42676E 01
3 4 -.20527E-02	3 5 -.23272E 00	3 6 .85815E 00	4 1 -.19291E 00	4 2 .53408E 00
4 3 .36588E 04	4 4 -.30072E 00	4 5 .29802E-03	4 6 -.64959E 02	5 2 .10000E 01
6 1 -.38101E 00	6 2 .79194E-01	6 3 .65809E 04	6 4 -.75347E 00	6 6 -.12207E 03
7 1 .33504E-03	7 2 -.12594E-03	7 3 .22742E 01	7 4 -.11186E-01	7 5 -.29494E-01
7 6 .10584E 00	8 3 -.62500E 02	9 3 .10000E 01	10 4 .10000E 01	11 5 .10000E 01
12 6 .10000E 01	13 1 .27449E-01	13 2 .83062E-02	13 3 -.20840E 03	13 4 .33812E-01
13 5 -.38689E 00	13 6 .66109E 01	13 7 -.30000E 01	13 8 -.56000E 03	

Table 63. D Matrices - State Pressure Control

100 PERCENT

8 1 .62500E 02	13 1 .12942E 04	14 1 .10000E 01

85 PERCENT

8 1 .62500E 02	13 1 .33966E 03	14 1 .10000E 01

70 PERCENT

8 1 .62500E 02	13 1 .43779E 03	14 1 .10000E 01

50 PERCENT

8 1 .62500E 02	13 1 .26672E 03	14 1 .10000E 01

Table 64. Pressure Controller Quadratic Weights (Nonzero Values: Diagonal Elements Q_{ii})

r_i	i	State	Simple
EP	2	.10-2	.10+1
$\dot{W}FV$	8	.10+0	.10+0
$\dot{P}T3$ - $\dot{P}T3M$	13	.10+1	.10+1
UWF	14	.10+1	.10+1

Table 65. State Control Gain Matrices

Parameter	Operating Condition	1	2	3	4	5	6	7	8
Speed	100%	-.446-3	-.231-3	-.283+0	-.750-2	-.265+0	-.410-1	+.263-3	+.776+1
	85%	-.313-3	-.168-3	-.328+0	-.328-2	-.304-2	+.731+1	+.152-3	+.445+1
	70%	-.396-3	-.122-3	-.785-1	-.121-2	-.693-2	+.727-1	+.152-3	+.439+1
	50%	-.913-3	-.183-3	-.226+0	-.364-3	-.170-1	-.449-1	+.340-3	+.983+1
Pressure	100%	-.110-3	-.367-3	+.616+0	-.471-3	+.357-1	+.132+0	+.579-2	+.259+1
	85%	-.693-3	-.103-3	+.270+0	-.416-2	+.470-1	+.70[illegible]-1	+.220-1	+.986+1
	70%	-.154-4	-.480-4	+.625+0	-.730-2	+.292-2	-.260-1	+.685-2	+.201+1
	50%	-.103-3	-.311-4	+.782+0	-.127-3	+.145-2	-.247-1	+.112-1	+.209+1
Temperature	100%	-.247-4	+.690+0	+.939-4	-.817-2	-.372-1	+.945-4	+.840-1	+.100-9
	85%	-.259-4	+.702+0	+.271-3	-.403-2	+.943-3	+.557-4	+.495-1	+.114-4
	70%	-.307-4	+.695+0	+.723-4	-.372-2	+.397-2	+.431-4	+.383-1	+.789-5
	50%	-.442-2	+.676+0	+.347-4	+.813-4	+.568-2	+.328-4	+.292-1	+.129-4

Table 66. Boundary State Models Open-Loop Roots*

Association	100%	85%	70%	50%
N	-2.04	+0.957	+0.556	+0.184
TM	-0.712	@0.719	@0.361	@0.013
WFV	-62.5	-62.5	-62.5	-62.5
A8	-3.0	-3.0	[illegible]	-3.0
IGV	-5.0	-5.0	-5.0	-5.0
BLD	-2.0	-2.0	-2.0	-2.0
P	-4.0	-4.0	-4.0	-4.0

Table 67. Pressure State Controllers Closed-Loop Roots*

Association	No. 203(100%)	No. 201(85%)	No. 17(70%)	No. 19(50%)
PT3	+10.0	-9.89	+4.00	+4.06
TM	-0.796	-0.894	-0.960	-1.86
WFV	-5.98	-26.1	-14.9	-3.69
A8	-3.0	-3.0	-3.0	-3.0
IGV	-5.0	-5.0	-5.0	-5.0
BLD	-2.0	-2.0	-2.0	-2.0
EP	@0.999	-10.1	@0.999	@0.998
P	-4.0	-4.0	-4.0	-4.0

*Real roots:
Tabular value = real value
Complex roots:
Tabular values = (+X.XXXX, @0.YYY) = (frequency, damping ratio)

Table 68. Pressure State Controllers RMS Response
(P = 0.01 RMS; A8 = 4.0 Sq. In. RMS)

Response	Response Component	100%		85%		70%		50%	
		ETA 1	ETA 2	ETA 1	ETA 2	ETA 1	ETA 2	ETA 1	ETA 2
N	r1	.1178+3	.4820+2	.1609+3	.1635+2	.1524+3	.1008+2	.2483+3	.1003+2
EP	r2	.2080+1	.1201-1	.2080+1	.1636-2	.1187+1	.6881-2	.7563+0	6683-2
PT3	r3	.2272+1	.9011-2	.2272+1	.1262-2	.1273+1	.5174-2	.8098+0	.5024-2
TT4	r4	.8053+2	.2642+2	.1779+3	.8398+2	.1270+3	.3387+2	.3727+3	.2616+2
TM	r5	.2629+2	.1326+2	.2604+2	.3678+2	.3174+2	.1655+2	.1298+3	.1615+2
TT5	r6	.8303+2	.2957+2	.1975+3	.9544+2	.1602+3	.4272+2	.6431+3	.4087+2
PT5	r7	.1223+1	.4036+0	.1069+1	.5466+0	.2276+0	.1847+0	.1972+0	.5490-1
$\dot{W}FV$	r8	.7197+0	.7351-1	.1938+1	.3341+0	.5342+0	.7487-1	.7566+0	.2195-1
WFV	r9	.6829-1	.1706-1	.8774-1	.3506-1	.4169-1	.1032-1	.9230-1	.5226-2
A8	r10	.3077+1	.4000+1	.3077+1	.4000+1	.0000	.4000+1	.0000	.4000+1
IGV	r11	.5128-2	.0000	.5017-1	.0000	.0000	.0000	.0000	.0000
BLD	r12	.7148-2	.0000	.3022-1	.0000	.0000	.0000	.0000	.0000
$\dot{P} - \dot{P}M$	r13	.1578-2	.5338-4	.1833-1	.1946-2	.4408-2	.4314-3	.1158-1	.1123-3
UFW	r14	.6923-1	.1710-1	.9306-1	.3546-1	.4256-1	.1039-1	.9309-1	.5238-2

Table 69. F Matrices - Simplified Pressure Control

100 PERCENT

1 1	-.21273E 01	1 2	.22233E 01	1 3	.10288E 05	1 4	.83997E 02	1 5	.20208E 04
1 6	-.13432E 03	2 1	-.58483E-01	2 2	-.62000E 00	2 3	.88597E 03	2 5	.37842E 02
2 6	.11353E 03	316	-.50400E 04	4 4	-.30000E 01	4 8	-.14102E 04	4 9	.10000E 01
5 5	-.50000E 01	5 8	-.34400E 01	5 9	.32784E-02	6 6	-.20000E 01	6 8	-.24760E 01
6 9	.20250E-02	7 8	.35332E 04	710	-.66665E 03	8 8	-.40000E 01	9 9	-.59909E 02
10 1	.79684E-02	10 2	.15382E-02	10 3	.20707E 02	10 4	-.58168E-02	10 5	-.41555E 01
10 6	-.94740E 01	1010	-.50000E 02	1012	.11180E 04	11 1	.21738E-02	11 2	-.27403E-03
11 3	.11960E 02	11 4	-.79991E-01	11 5	-.12510E 01	11 6	-.31137E 01	1111	-.40000E 02
1113	.14318E 03	1212	-.20000E 03	1313	-.62500E 02	1415	.10000E 01	1514	-.26667E 05
1515	-.20000E 03	1520	.10000E 01	16 3	.31333E 01	1616	-.50384E 02	1617	.18800E 04
1718	.10000E 02	1815	.23651E 04	1817	-.35462E 04	1818	-.30100E 03	1820	-.59127E 01
1919	-.31000E 02	1921	.31000E 02	2019	.30000E 02	2020	-.30000E 02	2121	-.10000E 07

85 PERCENT

1 1	-.78927E 00	1 2	.20990E 01	1 3	.11312E 05	1 4	.11643E 03	1 5	.27402E 03
1 6	-.17600E 04	2 1	-.21585E 00	2 2	-.58668E 00	2 3	.16027E 04	2 4	-.11679E 00
2 5	.30552E 02	2 6	-.26127E 02	316	-.50400E 04	4 4	-.30000E 01	4 8	-.14102E 04
4 9	.10000E 01	5 5	-.50000E 01	5 8	-.33655E 02	5 9	.32784E-02	6 6	-.20000E 01
6 8	-.10468E 02	6 9	.20250E-02	7 8	.34000E 04	710	-.66667E 03	8 8	-.40000E 01
9 9	-.59909E 02	10 1	.12280E-01	10 2	.48288E-03	10 3	.54346E 01	10 4	-.84278E-03
10 5	-.12921E 01	10 6	-.12176E 00	1010	-.50000E 02	1012	.11180E 04	11 1	.28926E-02
11 2	-.47983E-03	11 3	.51329E 01	11 4	-.10672E 00	11 5	-.27966E 00	11 6	.26724E-01
1111	-.40000E 02	1113	.14318E 03	1212	-.20000E 03	1313	-.62500E 02	1415	.10000E 01
1514	-.26667E 05	1515	-.20000E 03	1520	.10000E 01	16 3	.31333E 01	1616	-.50384E 02
1617	.18800E 04	1718	.10000E 02	1815	.23651E 04	1817	-.35462E 04	1818	-.30100E 03
1820	-.59127E 01	1919	-.31000E 02	1921	.31000E 02	2019	.30000E 02	2020	-.30000E 02
2121	-.10000E 07								

70 PERCENT

1 1	.18223E 00	1 2	.19682E 01	1 3	.12933E 05	1 4	.40137E 02	1 5	.17702E 03
1 6	-.37655E 03	2 1	-.21132E 00	2 2	-.58421E 00	2 3	.23220E 04	2 4	-.11679E 00
2 5	.37842E 02	2 6	-.75684E 02	316	-.50400E 04	4 4	-.30000E 01	4 9	.10000E 01
5 5	-.50000E 01	5 9	.32784E-02	6 6	-.20000E 01	6 9	.20250E-02	7 8	.88000E 03
710	-.26667E 03	8 8	-.40000E 01	9 9	-.59909E 02	10 1	.82386E-02	10 2	.64898E-03
10 3	.70047E 01	10 4	-.21223E-02	10 5	-.92155E 00	10 6	-.24212E 01	1010	-.50000E 02
1012	.11180E 04	11 1	.11009E-02	11 2	-.20303E-03	11 3	.40736E 01	11 4	-.39345E-01
11 5	-.11192E 00	11 6	.39236E 00	1111	-.40000E 02	1113	.14318E 03	1212	-.20000E 03
1313	-.62500E 02	1415	.10000E 01	1514	-.53333E 05	1515	-.40000E 03	1520	.10000E 01
16 3	.31333E 01	1616	-.50384E 02	1617	.18800E 04	1718	.10000E 02	1815	.47302E 04
1817	-.35462E 04	1818	-.30100E 03	1820	-.59127E 01	1919	-.12000E 02	1921	.12000E 02
2019	.30000E 02	2020	-.30000E 02	2121	-.10000E 07				

50 PERCENT

1 1	.53809E 00	1 2	.14508E 01	1 3	.68505E 04	1 4	.1[illegible]8E 02	1 5	.96437E 02
1 6	.46436E 03	2 1	-.22476E 00	2 2	-.54284E 00	2 3	.42628E 04	2 4	-.35037E 00
2 5	-.18477E-03	2 6	-.75684E 02	316	-.50400E 04	4 4	-.30000E 01	4 9	.10000E 01
5 5	-.50000E 01	5 9	.32784E-02	6 6	-.20000E 01	6 9	.20250E-02	7 8	.56000E 03
710	-.26667E 03	8 8	-.40000E 01	9 9	-.59909E 02	10 1	.32277E-02	10 2	.48590E-03
10 3	.42676E 01	10 4	-.20527E-02	10 5	-.23272E 00	10 6	.85815E 00	1010	-.50000E 02
1012	.11180E 04	11 1	.33504E-03	11 2	-.12594E-03	11 3	.22742E 01	11 4	-.12186E-01
11 5	-.29494E-01	11 6	.10584E 00	1111	-.40000E 02	1113	.14318E 03	1212	-.20000E 03
1313	-.62500E 02	1415	.10000E 01	1514	-.53333E 05	1515	-.40000E 03	1520	.10000E 01
16 3	.31333E 01	1616	-.50384E 02	1617	.18800E 04	1718	.10000E 02	1815	.47302E 04
1817	-.35462E 04	1818	-.30100E 03	1820	-.59127E 01	1919	-.30000E 02	1921	.30000E 02
2019	.15000E 02	2020	-.15000E 02	2121	-.10000E 08				

Table 70. G1 Matrices--Simplified Pressure Control

	100 Percent	
21	1	+.10000E+07
	85 Percent	
21	1	+.10000E+07
	70 Percent	
21	1	+.10000E+07
	50 Percent	
21	1	+.10000E+08

Table 71. G2 Matrices--Simplified Pressure Control

					100 Percent						
8	1	+.28284E-01	9	2	+.60150E+03	12	3	+.20000E-03	13	4	+.25000E-03
					85 Percent						
8	1	+.28284E-01	9	2	+.60150E+03	12	3	+.20000E-03	13	4	+.25000E-03
					70 Percent						
8	1	+.28284E-01	9	2	+.60150E+03	12	3	+.20000E-02	13	4	+.25000E-01
					50 Percent						
8	1	+.28284E-01	9	2	+.60150E+03	12	3	+.20000E-03	13	4	+.25000E-03

Table 72. H Matrices - Simplified Pressure Control

100 PERCENT

1 1	.10000E 01	2 7	.10000E 01	3 1	.79684E-02	3 2	.15382E-02	3 3	.20707E 02
3 4	-.58168E-02	3 5	-.41655E 01	3 6	-.94740E 01	4 1	-.83848E-01	4 2	.11110E 00
4 3	.12702E 04	4 4	-.81427E-06	4 5	.54254E 02	4 6	.16276E 03	5 2	.10000E 01
6 1	-.10173E 00	6 2	-.22170E-01	6 3	.13231E 04	6 4	-.66705E 00	6 5	.61035E 02
6 6	.12207E 03	7 1	.21738E-02	7 2	-.27403E-03	7 3	.11960E 02	7 4	-.79991E-01
7 5	-.12510E 01	7 6	-.31137E 01	816	-.50400E 04	9 3	.10000E 01	10 4	.10000E 01
11 5	.10000E 01	12 6	.10000E 01	13 1	.14233E 00	13 2	.47526E-01	13 3	.49748E 03
13 7	-.75000E 01	13 8	-.34872E 04	1316	-.10436E 06	1510	.50000E 02	1611	.40000E 02

85 PERCENT

1 1	.10000E 01	2 7	.10000E 01	3 1	.1228[illegible]E-01	3 2	.48288E-03	3 3	.54346E 01
3 4	-.84278E-03	3 5	-.12921E 01	3 6	-.12176E 00	4 1	-.29029E 00	4 2	.21102E 00
4 3	.21554E 04	4 4	-.15706E 00	4 5	.41087E 02	4 6	-.35136E 02	5 2	.10000E 01
6 1	-.35250E 00	6 2	.21499E-01	6 3	.24080E 04	6 4	-.13186E 01	6 5	.49278E 02
6 6	-.42140E 02	7 1	.28926E-02	7 2	-.47983E-03	7 3	.51329E 01	7 4	-.10672E 00
7 5	-.27966E 00	7 6	.26724E-01	816	-.50400E 04	9 3	.10000E 01	10 4	.10000E 01
11 5	.10000E 01	12 6	.10000E 01	13 1	.23580E 00	13 2	.35150E-01	13 3	.24838E 03
13 7	-.75000E 01	13 8	-.33514E 04	1316	-.27390E 05	1510	.50000E 02	1611	.40000E 02

70 PERCENT

1 1	.10000E 01	2 7	.10000E 01	3 1	.82386E-02	3 2	.64898E-03	3 3	.70047E 01
3 4	-.21223E-02	3 5	-.92155E 00	3 6	.24212E 01	4 1	-.25316E 00	4 2	.50015E 00
4 3	.27816E 04	4 4	-.13991E 00	4 5	.45333E 02	4 6	-.90665E 02	5 2	.10000E 01
6 1	-.35934E 00	6 2	.23093E-01	6 3	.35111E 04	6 4	-.75347E 00	6 5	.61035E 02
6 6	-.12207E 03	7 1	.11009E-02	7 2	-.20303E-03	7 3	.40736E 01	7 4	-.39345E-01
7 5	-.11192E 00	7 6	.39236E 00	816	-.50400E 04	9 3	.10000E 01	10 4	.10000E 01
11 5	.10000E 01	12 6	.10000E 01	13 1	.67273E-01	13 2	.21028E-01	13 3	.16409E 03
13 7	-.30000E 01	13 8	-.88000E 03	1316	-.35304E 05	1510	.50000E 02	1611	.40000E 02

50 PERCENT

1 1	.10000E 01	2 7	.10000E 01	3 1	.32277E-02	3 2	.48590E-03	3 3	-.42676E 01
3 4	-.20527E-02	3 5	-.23272E 00	3 6	.85815E 00	4 1	-.19291E 00	4 2	.53408E 00
4 3	.36588E 04	4 4	-.30072E 00	4 5	.29802E-03	4 6	-.64959E 02	5 2	.10000E 01
6 1	-.38101E 00	6 2	.79194E-01	6 3	.65809E 04	6 4	-.75347E 00	6 6	-.12207E 03
7 1	.[illegible]3504E-03	7 2	-.12594E-03	7 3	.22742E 01	7 4	-.12186E-01	7 5	-.29694E-01
7 6	.[illegible]0584E 00	816	-.50400E 04	9 3	.10000E 01	10 4	.10000E 01	11 5	.10000E 01
12 6	.10000E 01	13 1	.27449E-01	13 2	.83062E-02	13 3	.58323E 02	13 7	-.30000E 01
13 8	-.56000E 03	1316	-.21509E 05	1510	.50000E 02	1611	.40000E 02		

Table 73. D Matrices Simplified Pressure Control

141 .10000E-01

Table 74. M Matrices - Simplified Pressure Control

100 PERCENT

1 1	.10000E 01	2 2	.10000E 01	3 3	.10000E 01	4 4	.10000E 01	5 5	.10000E 01
6 6	.10000E 01	7 7	.10000E 01	8 8	.10000E 01	9 9	.10000E 01	1010	.50000E 02
1111	.40000E 02	1212	.10000E 01	1313	.10000E 01	1414	.10000E 01	1515	.10000E 01
1616	.10000E 01	1717	.10000E 01	1818	.10000E 01	1919	.10000E 01	2020	.10000E 01
2121	.10000E 01								

85 PERCENT

1 1	.10000E 01	2 2	.10000E 01	3 3	.10000E 01	4 4	.10000E 01	5 5	.10000E 01
6 6	.10000E 01	7 7	.10000E 01	8 8	.10000E 01	9 9	.10000E 01	1010	.50000E 02
1111	.40000E 02	1212	.10000E 01	1313	.10000E 01	1414	.10000E 01	1515	.10000E 01
1616	.10000E 01	1717	.10000E 01	1818	.10000E 01	1919	.10000E 01	2020	.10000E 01
2121	.10000E 01								

70 PERCENT

1 1	.10000E 01	2 2	.10000E 01	3 3	.10000E 01	4 4	.10000E 01	5 5	.10000E 01
6 6	.10000E 01	7 7	.10000E 01	8 8	.10000E 01	9 9	.10000E 01	1010	.50000E 02
1111	.40000E 02	1212	.10000E 01	1313	.10000E 01	1414	.10000E 01	1515	.10000E 01
1616	.10000E 01	1717	.10000E 01	1818	.10000E 01	1919	.10000E 01	2020	.10000E 01
2121	.10000E 01								

50 PERCENT

1 1	.10000E 01	2 2	.10000E 01	3 3	.10000E 01	4 4	.10000E 01	5 5	.10000E 01
6 6	.10000E 01	7 7	.10000E 01	8 8	.10000E 01	9 9	.10000E 01	1010	.50000E 02
1111	.40000E 02	1212	.10000E 01	1313	.10000E 01	1414	.10000E 01	1515	.10000E 01
1616	.10000E 01	1717	.10000E 01	1818	.10000E 01	1919	.10000E 01	2020	.10000E 01
2121	.10000E 01								

STOP 77777777

Table 75. Simplified Pressure Control Closed-Loop Roots

Root Association	100%		85%		70%		50%	
	Frequency	Damping	Frequency	Damping	Frequency	Damping	Frequency	Damping
N	+4.810	+.8673	-.9469		-3.585		+2.862	+.6283
$\tilde{E}P$			+11.90	.4223	-6.959		+17.71	.8271
TM	-.7987		-.3218		-.8359		-1.101	
WF	+125.4	+.1879	+125.4	+.1970	+125.6	+.1965	+125.7	+.1962
WF	+163.4	+.5901	+163.0	+.6062	186.5	+.7962	+186.3	+.7953
X19	+24.48	.6061	+41.18	+.9291	+11.49	+.6787		
X20	-29.85				-42.93		-32.30	
TD	+191.1	+.7964	+189.1	+.7980	+231.6	+.8650	+231.7	+.8649
PT3S/50								
PT5S/40	-92.01		-67.15		-66.85		-73.62	
A8	-3.000		-3.000		-3.000		-3.000	
IGV	-5.000		-5.000		-5.000		-5.000	
BLD	-2.000		-2.000		-2.000		-2.000	
X21	-.10+7		-.10+7		-.10+7		-.10+7	
P	-4.000		-4.000		-4.000		-4.000	
A8N	-59.91		-59.91		-59.91		-59.91	
P3N	-200.0		-200.0		-200.0		-200.0	
P5N	-62.5		-62.5		-62.50		-62.50	

Table 76. Simplified Pressure Controllers RMS Response

Response	100%				85%				70%				50%			
	ETA 1	ETA 2	ETA 3	ETA 4	ETA 1	ETA 2	ETA 3	ETA 4	ETA 1	ETA 2	ETA 3	ETA 4	ETA 1	ETA 2	ETA 3	ETA 4
N	.1317+3	.6113+2	.1749+0	.5991-1	.1606+3	.3769+2	.2655+0	.9585-1	.1554+3	.3976+2	.3006+0	.9804-1	.2537+3	.8154+1	.6873+0	.2599+0
$\tilde{EP}$	.3424+1	.8187-1	.4200-2	.2771-2	.3763+1	.1214+1	.5614-2	.7753-2	.1702+1	.6063+0	.2211-2	.1259-2	.1011+1	.5271-1	.2365-2	.1868-2
PT3	.2538+1	[illegible]	.3917-2	1500-2	.2534+1	.3330+0	.3668-2	.1298-2	.1304+1	.2826+0	.2716-2	.8965-3	.8300+0	.1441-1	[illegible]	.1165-2
TT4	.9435+2	.2493+2	.2050+0	.8139-1	.2283+3	.9765+2	.5541+0	.1907+0	.1403+3	.5043+2	.4911+0	.1701+0	.3882+3	.3410+2	.1997+1	.8165+0
TM	.2746+2	.1232+2	.1683-1	.5317-2	.2906+2	.3744+2	.3783-1	.1347-1	.3201+2	.1980+2	.5701-1	.1807-1	.1338+3	.1817+2	[illegible]	.1825+0
TT5	.9754+2	.2839+2	.2131+0	.8464-1	.2543+3	.1106+3	.6192+0	.2132+0	.1771+3	.6370+2	.6206+0	.2150+0	.6705+3	.5545+2	.3548+1	.1651+1
PT5	.1360+1	.3996+0	.2060-2	.8053-3	.1119+1	.5021+0	.1549-2	.5382-3	.2438+0	.1569+0	.7518-3	.2581-3	[illegible]	.5761-1	.1167-2	.4779-3
$\dot{W}FV$	.8406+0	.7488-1	.3787-2	.1350-2	.1440+1	.2756+0	.5391-2	.1597-2	.4258+0	.7673-1	.2639-2	.8394-3	.7422+0	.4204-1	.8583-2	.3132-2
WFV	.7920-1	.1643-1	.1632-3	.6461-4	.1100+0	.3999-1	.2560-3	.8812-4	.4668-1	.1468-1	.1721-3	.5977-4	.9630-1	.7458-2	.5293-3	.2168-3
A8	.3072+1	.3999+1	.0000+0	.0000+0	.3072+1	.3999+1	.0000+0	.0000+0	.0000+0	.3999+1	.0000+0	.0000+0	.0000+0	.3999+1	.0000+0	.0000+0
IGV	.5120-2	.9699-2	.0000+0	.0000+0	.5009-1	.9999-2	.0000+0	.0000+0	.0000+0	.9999-2	.0000+0	.0000+0	.0000+0	.9999-2	.0000+0	.0000+0
BLD	.7136-2	.1000-1	.0000+0	.0000+0	.3017-1	.1000-1	.0000+0	.0000+0	.0000+0	.1000-1	.0000+0	.0000+0	.0000+0	.1000-1	.0000+0	.0000+0
$\dot{P}T3 - \dot{P}T3M$	.2143+2	.1064+1	.8768-1	.4008-1	.2496+2	.5981+1	.5894-1	.6196-1	.5935+1	.1584+1	.2785-1	.1054-1	.3228+1	.3447+0	.4004-1	.1629-1
UF	.9094-1	.1681-1	.2773-3	.9793-4	.1336+0	.4204-1	.4084-3	.1229-3	.6359-1	.1632-1	.3636-3	.1099-3	.1153+0	.8162-2	.1035-2	.3638-3
PT3S	.2514+1	.3925-1	.6106-2	.1417-2	.2512+1	.3266+0	.6088-2	.1267-2	.1299+1	.2809+0	.5640-2	.8818-3	.8270+0	.1424-1	.5714-2	.1136-2
PT5S	.1338+1	.3936+0	.1874-2	.2201-2	.1100+1	.4954+0	.1444-2	.2105-2	.2401+0	.1538+0	.7163-3	.2000-2	.2014+0	.5677-1	.1101-2	.2082-3

Table 77. F Matrices - State Temperature Control

100 PERCENT

1 1 -.62000E 00	1 2 .88597E 03	1 4 .37842E 02	1 5 .11353E 03	2 2 -.62500E 02
3 3 -.30000E 01	3 8 .97980E 01	4 4 -.50000E 01	5 5 -.20000E 01	6 1 -.14813E 01
6 2 -.16936E 05	6 3 .10857E-04	6 4 -.72339E 03	6 5 -.21701E 04	6 7 .66665E 04
7 7 -.40000E 01	8 8 -.10000E 04			

85 PERCENT

1 1 -.58668E 00	1 2 .16027E 04	1 3 -.11679E 00	1 4 .30552E 02	1 5 -.20127E 02
2 2 -.62500E 02	3 3 -.30000E 01	3 8 .97980E 01	4 4 -.50000E 01	5 5 -.20000E 01
6 1 -.28136E 01	6 2 -.28739E 05	6 3 .20941E 01	6 4 -.54783E 03	6 5 .46848E 03
6 7 .66665E 04	7 7 -.40000E 01	8 8 -.10000E 04		

70 PERCENT

1 1 -.58421E 00	1 2 .23220E 04	1 3 -.11679E 00	1 4 .37842E 02	1 5 -.75684E 02
2 2 -.62500E 02	3 3 -.30000E 01	3 8 .97980E 01	4 4 -.50000E 01	5 5 -.20000E 01
6 1 -.40020E 01	6 2 -.37088E 05	6 3 .18655E 01	6 4 -.60444E 03	6 5 .12089E 04
6 7 .66665E 04	7 7 -.40000E 01	8 8 -.10000E 04		

50 PERCENT

1 1 -.54284E 00	1 2 .42628E 04	1 3 -.35037E 00	1 4 -.18477E-03	1 5 -.75684E 02
2 2 -.62500E 02	3 3 -.30000E 01	3 8 .97930E 01	4 4 -.50000E 01	5 5 -.20000E 01
6 1 -.71211E 01	6 2 -.48784E 05	6 3 .40096E 01	6 4 -.39736E-02	6 5 .86612E 03
6 7 .66665E 04	7 7 -.40000E 01	8 8 -.10000E 04		

Table 78. G1 Matrices - State Temperature Control

2 1 .62500E 02

Table 79. G2 Matrices - State Speed Control

7 1 .28284E-01   8 2 .10015E 04

Table 80. H Matrices - State Temperature Control

100 PERCENT

1 7 .10000E 01	2 6 .10000E 01	3 1 .15382E-02	3 2 .20707E 02	3 3 -.58168E-02
3 4 -.41555E 01	3 5 -.94740E 01	4 1 .11110E 00	4 2 .12702E 04	4 3 -.81427E-06
4 4 .54254E 02	4 5 .16276E 03	5 1 .10000E 01	6 1 -.22170E-01	6 2 .13231E 04
6 3 -.66705E 00	6 4 .61035E 02	6 5 .12207E 03	7 1 -.27403E-03	7 2 .11960E 02
7 3 -.79991E-01	7 4 -.12510E 01	7 5 -.31137E 01	8 2 -.62500E 02	9 2 .10000E 01
10 3 .10000E 01	11 4 .10000E 01	12 5 .10000E 01	13 1 .19667E 01	13 2 -.54748E 05
13 3 -.74538E 01	13 4 .64857E 03	13 5 .29536E 04	13 6 -.75000E 01	13 7 -.66666E 04
13 8 -.79782E-05				

85 PERCENT

1 7 .10000E 01	2 6 .10000E 01	3 1 .48288E-03	3 2 .54346E 01	3 3 -.84278E-03
3 4 -.12921E 01	3 5 -.12176E 00	4 1 .21102E 00	4 2 .21556E 04	4 3 -.15730E 00
4 4 .41087E 02	4 5 -.35136E 02	5 1 .10000E 01	6 1 .21499E-01	6 2 .24080E 04
6 3 -.13186E 01	6 4 .49278E 02	6 5 -.42140E 02	7 1 -.47981E-03	7 2 .51329E 01
7 3 -.10672E 00	7 4 -.27966E 00	7 5 .26724E-01	8 2 -.62500E 02	9 2 .10000E 01
10 3 .10000E 01	11 4 .10000E 01	12 5 .10000E 01	13 1 .34873E 01	13 2 -.34550E 05
13 3 -.36493E 02	13 4 .54321E 03	13 5 -.12705E 03	13 6 -.75000E 01	13 7 -.66668E 04
13 8 -.15389E 01				

70 PERCENT

1 7 .10000E 01	2 6 .10000E 01	3 1 .64898E-03	3 2 .70047E 01	3 3 -.81223E-02
3 4 -.92155E 00	3 5 .24212E 01	4 1 .30018E 00	4 2 .27816E 04	4 3 -.13391E 00
4 4 .45333E 02	4 5 -.90665E 02	5 1 .10000E 01	4 1 .23093E-01	6 2 .38111E 04
6 3 -.75347E 00	6 4 .61035E 02	6 5 -.12207E 03	7 1 -.20302E-03	7 2 .40736E 01
7 3 -.39345E-01	7 4 -.11192E 00	7 5 .39236E 00	8 2 -.62500E 02	9 2 .10000E 01
10 3 .10000E 01	11 4 .10000E 01	12 5 .10000E 01	13 1 .53294E 01	13 2 -.12080E 06
13 3 -.12575E 02	13 4 .64654E 03	13 5 -.15594E 04	13 6 -.75000E 01	13 7 -.66665E 04
13 8 -.13708E 01				

50 PERCENT

1 7 .10000E 01	2 6 .10000E 01	3 1 .48590E-03	3 2 .42676E 01	3 3 -.20527E-02
3 4 -.23272E 00	3 5 .85815E 00	4 1 .53408E 00	4 2 .36588E 04	4 3 -.30072E 00
4 4 .29802E-03	4 5 -.64959E 02	5 1 .10000E 01	6 1 .79194E-01	6 2 .65809E 04
6 3 -.75347E 00	6 5 -.12207E 03	7 1 -.12594E-03	7 2 .22742E 01	7 3 -.12186E-01
7 4 -.29494E-01	7 5 .10584E 00	8 2 -.62500E 02	9 2 .10000E 01	10 3 .10000E 01
11 4 .10000E 01	12 5 .10000E 01	13 1 .10112E 02	13 2 -.15454E 06	13 3 -.79438E 01
13 4 -.18599E 02	13 5 -.12993E 04	13 6 -.75000E 01	13 7 -.66665E 04	13 8 -.29465E 01

Table 81. D Matrices - State Temperature Control

100 PERCENT

8 1 .62500E 02	13 1 .79387E 05	14 1 .10000E 01

85 PERCENT

8 1 .62500E 02	13 1 .13471E 06	14 1 .10000E 01

70 PERCENT

8 1 .62500E 02	13 1 .17385E 06	14 1 .10000E 01

50 PERCENT

8 1 .62500E 02	13 1 .22867E 06	14 1 .10000E 01

Table 82. Temperature Controller Quadratic Weights (Nonzero Values: Diagonal Elements Q_{ii})

z_i	i	100%		85%		70%		50%	
		State	Simple	State	Simple	State	Simple	State	Simple
ET	2	.10-4	.10-4	.10-4	.10-4	.10-4	.10-4	.10-4	.10-4
WFV	8	.10-1	.10-1	.10-1	.10-1	.10-1	.10-1	.10-1	.10-1
$\dot{T} - \dot{T}$	13	.10+1	.10-5	.10+1	.10-5	.10+1	.10-5	.10+1	.10-5
UW	14	.10+1	.10-1	.10+1	.10+2	.10+1	.10+2	.10+1	.10+2

Table 83. State Control Gain Matrices

Parameter	Setting	1	2	3	4	5	6	7	8
Speed	100%	-.446-3	-.231-3	-.283+0	-.750-2	-.265+0	-.410-1	+.263-3	+.776+1
	85%	-.313-3	-.168-3	-.328+0	-.326-2	-.304-2	+.731+1	+.152-3	+.445+1
	70%	-.396-3	-.122-3	-.785-1	-.121-2	-.693-2	+.727-1	+.152-3	+.439+1
	50%	-.913-3	-.183-3	-.226+0	-.864-3	-.170-1	-.449-1	+.340-3	+.383+1
Pressure	100%	-.110-3	-.367-3	-.367-3	+.616+0	-.471-3	+.357-1	+.132+0	+.259+1
	85%	-.693-3	-.103-3	+.270+0	-.416-2	+.479-1	+.700-1	+.220-1	+.936+1
	70%	-.154-4	-.480-4	+.625+0	-.730-2	+.292-2	-.260-1	+.685-2	+.201+1
	50%	-.103-3	-.311-4	+.782+0	-.127-3	+.145-2	-.247-1	+.112-1	+.209+1
Temperature	100%	-.247-4	+.690+0	+.939-4	-.817-2	-.372-1	+.945-4	+.840-1	+.100-9
	85%	-.259-4	+.702+0	+.271-3	-.403-2	+.943-3	+.557-4	+.495-1	+.114-4
	70%	-.307-4	+.695+0	+.723-4	-.372-2	+.897-2	+.431-4	+.383-1	+.789-5
	50%	-.442-4	+.676+0	+.347-4	+.813-4	+.568-2	+.328-4	+.292-1	+.129-4

Table 84. Temperature State Controllers
Closed-Loop Roots*

Association	No. 67(100%)	No. 65(85%)	No. 57(70%)	No. 63(50%)
TM	-0.698	-0.745	-0.836	-1.17
WFV	+9.99	+9.99	+9.99	+9.99
A	-3.0	-3.0	-3.0	-3.0
IGV	-5.0	-5.0	-5.0	-5.0
BLD	-2.0	-2.0	-2.0	-2.0
ET	@0.906	@0.925	@0.942	@0.982
PLA	-4.0	-4.0	-4.0	-4.0
AN	-1000.	-1000.	-1000.	-1000.

*Real roots:
Tabular values = real values
Complex roots:
Tabular values = (+X.XXX, @ 0.YYY) = (frequency, damping ratios)

Table 85. Temperature State Controllers RMS Response
(P = 0.01 RMS; A8 = 4.0 Sq. In. RMS)

Response	Response Component	100%		85%		70%		50%	
		ETA 1	ETA 2	ETA 1	ETA 2	ETA 1	ETA 2	ETA 1	ETA 2
P	r1	.1000-1	.0000	.1000-1	.0000	.1000-1	.0000	.1000-1	.0000
ET	r2	.3830+1	.3313+1	.3539+1	.1531+2	.3657+1	.4620+1	.3941+1	.1219+1
PT3	r3	.7339-1	.1885-1	.1155-1	.9877-2	.1139-1	.5832-2	.5071-2	.6593-2
TT4	r4	.4515+1	.9108+0	.4597+1	.4288+1	.4562+1	.1284+1	.4483+1	.3327+0
TN	r5	.1925+1	.1485+0	.1984+1	.7272+0	.2079+1	.2416+0	.2366+1	.8317-1
TT5	r6	.4597+1	.2258+1	.4967+1	.4372+1	.5461+1	.1949+1	.7194+1	.7373+0
PT5	r7	.4150-1	.3151+0	.1026-1	.4200+0	.6157-2	.1556+0	.2402-2	.4790-1
$\dot{W}FV$	r8	.2623-1	.8916-2	.1582-1	.3097-1	.1212-1	.1307-1	.8970-2	.7820-1
WFV	r9	.3486-2	.7150-3	.2056-2	.2155-2	.1551-2	.5928-3	.1085-2	.3823-3
A8	r10	.0000	.4000+1	.0000	.4000+1	.0000	.4000+1	.0000	.4000+1
IGV	r11	.0000	.0000	.0000	.0000	.0000	.0000	.0000	.0000
BLD	r12	.0000	.0000	.0000	.0000	.0000	.0000	.0000	.0000
$\dot{T} - \dot{T}M$	r13	.6169-5	.6181-5	.2887-5	.1823-4	.1000-4	.1029-4	.9614-5	.0000
UFV	r14	.3512-2	.7291-3	.2072-2	.2212-2	.1563-2	.6285-3	.1094-3	.4805-3

Table 86. F Matrices - Simplified Pressure Control

100 PERCENT

1 1	-.62000E 00	1 2	.88597E 03	1 4	.37842E 02	1 5	.11353E 03	220	-.50400E 04
3 3	-.30000E 01	3 8	.10000E 01	4 4	-.50000E 01	4 8	.32784E-02	5 5	-.20000E 01
5 8	.20250E-02	6 7	.66665E 04	610	.88889E 01	611	-.22222E 02	7 7	-.40000E 01
8 8	-.59909E 02	9 9	-.10000E 07	1010	-.20833E 00	1011	.20833E 00	11 1	.33386E 01
11 2	.38170E 05	11 3	-.24469E-04	11 4	.16303E 04	11 5	.48909E 04	1112	.10000E 01
12 1	-.16665E 03	12 2	-.19053E 07	12 3	.12214E-02	12 4	-.81361E 05	12 5	-.24414E 06
1211	-.62500E 01	1212	-.50125E 02	1213	.10000E 01	1313	-.20000E 05	1414	-.30000E 02
1415	.30000E 02	15 9	.31000E 02	1515	-.31000E 02	16 1	.15382E-02	16 2	.20707E 02
16 3	-.58168E-02	16 4	-.41555E 01	16 5	-.94740E 01	1616	-.50000E 02	17 1	-.27403E-03
17 2	.11960E 02	17 3	-.79991E-01	17 4	-.12510E 01	17 5	-.31137E 01	1717	-.40000E 02
1819	.10000E 01	1914	.10000E 01	1918	-.26667E 03	1919	-.20000E 03	20 2	.31333E 01
2020	-.50384E 02	2021	.18800E 04	2122	.10000E 02	2214	-.59127E 01	2219	.23651E 04
2221	-.35462E 04	2222	-.30100E 03						

85 PERCENT

1 1	-.58668E 00	1 2	.16027E 04	1 3	-.11679E 00	1 4	.30552E 02	1 5	-.26127E 02
220	-.50400E 04	3 3	-.30000E 01	3 8	.10000E 01	4 4	-.50000E 01	4 8	.32784E-02
5 5	-.20000E 01	5 8	.20250E-02	6 7	.66665E 04	610	.10476E 02	611	-.23810E 02
7 7	-.40000E 01	8 8	-.59909E 02	9 9	-.20000E 03	1010	-.17857E 00	1011	.17857E 00
11 1	.59178E 01	11 2	.60446E 05	11 3	-.44046E 01	11 4	.11522E 04	11 5	-.98535E 03
1112	.10000E 01	12 1	-.29543E 03	12 2	-.30176E 07	12 3	.21988E 03	12 4	-.57522E 05
12 5	.49190E 05	1211	-.50000E 01	1212	-.50100E 02	1213	.10000E 01	1313	-.20000E 05
1414	-.30000E 02	1415	.30000E 02	1515	-.25000E 02	16 1	.48288E-03	16 2	.54346E 01
16 3	-.84278E-03	16 4	-.12921E 01	16 5	-.12176E 00	16 9	.11180E 04	1616	-.50000E 02
17 1	-.47983E-03	17 2	.51329E 01	17 3	-.10672E 00	17 4	-.27966E 00	17 5	.26724E-01
1717	-.40000E 02	1819	.10000E 01	1914	.10000E 01	1918	-.53333E 05	1919	-.40000E 03
20 2	.31333E 01	2020	-.50384E 02	2021	.18800E 04	2122	.10000E 02	2214	-.59127E 01
2219	.47302E 04	2221	-.35462E 04	2222	-.30100E 03				

70 PERCENT

1 1	-.58421E 00	1 2	.23220E 04	1 3	-.11679E 00	1 4	.37842E 02	1 5	-.75684E 02
220	-.50400E 04	3 3	-.30000E 01	3 8	.10000E 01	4 4	-.50000E 01	4 8	.32784E-02
5 5	-.20000E 01	5 8	.20250E-02	6 7	.66665E 04	610	.11823E 02	611	-.25157E 02
7 7	-.40000E 01	8 8	-.59909E 02	9 9	-.20000E 03	1010	-.11099E 00	1011	.11099E 00
11 1	.79623E 01	11 2	.73789E 05	11 3	-.371[illegible]5E 01	11 4	.12026E 04	11 5	-.24051E 04
1112	.10000E 01	12 1	-.39770E 03	12 2	-.36856E 07	12 3	.18538E 03	12 4	-.60066E 05
12 5	.12013E 06	1211	-.29412E 01	1212	-.50059E 02	1213	.10000E 01	1313	-.20000E 05
1414	-.30000E 02	1415	.30000E 02	1515	-.25000E 02	16 1	.64898E-03	16 2	.70047E 01
16 3	-.21223E-02	16 4	-.92155E 00	16 5	.24212E 01	16 9	.11180E 04	1616	-.50000E 02
17 1	-.20302E-03	17 2	.40736E 01	17 3	-.39345E-01	17 4	-.11192E 00	17 5	.39236E 00
1717	-.40000E 02	1819	.10000E 01	1914	.10000E 01	1918	-.53333E 05	1919	-.40000E 03
20 2	.31333E 01	2020	-.50384E 02	2021	.18800E 04	2122	.10000E 02	2214	-.59127E 01
2219	.47302E 04	2221	-.35462E 04	2222	-.30100E 03				

50 PERCENT

1 1	-.54284E 00	1 2	.42628E 04	1 3	-.35037E 00	1 4	-.18477E-03	1 5	-.75684E 02
220	-.50400E 04	3 3	-.30000E 01	3 8	.10000E 01	4 4	-.50000E 01	4 8	.32784E-02
5 5	-.20000E 01	5 8	.20250E-02	6 7	.66665E 04	610	.13333E 02	611	-.26667E 02
7 7	-.40000E 01	8 8	-.59909E 02	9 9	-.20000E 03	1010	-.66667E-01	1011	.66667E-01
11 1	.13361E 02	11 2	.91531E 05	11 3	-.75230E 01	11 4	.74555E-02	11 5	-.16251E 04
1112	.10000E 01	12 1	-.66760E 03	12 2	-.45735E 07	12 3	.3759[illegible]E 03	12 4	-.37253E 00
12 5	.81199E 05	1211	-.16667E 01	1212	-.50033E 02	1213	.10000E 01	1313	-.20000E 05
1414	-.30000E 02	1415	.30000E 02	1515	-.13333E 02	16 1	.48590E-03	16 2	.42676E 01
16 3	-.20527E-02	16 4	-.23272E 00	16 5	.85815E 00	16 9	.11180E 04	1616	-.50000E 02
17 1	-.12594E-03	17 2	.22742E 01	17 3	-.12186E-01	17 4	-.29494E-01	17 5	.10584E 00
1717	-.40000E 02	1619	.10000E 01	1914	.10000E 01	1918	-.53333E 05	1919	-.40000E 03
20 2	.31333E 01	2020	-.50384E 02	2021	.18800E 04	2122	.10000E 02	2214	-.59127E 01
2219	.47302E 04	2221	-.35462E 04	2222	-.30100E 03				

Table 87. G1 Matrices - Simplified Temperature Control

9 1	.10000E 07

Table 88. G2 Matrices-- Simplified Temperature Control

100 Percent

7	1 + .28284E + 00	8	2 + .60150E + 03	9	4 + .20000E - 03	13	3 + .50062E + 06

85 Percent

7	1 + .28284E + 00	8	2 + .60150E + 03	9	4 + .20000E - 03	13	3 + .44766E + 06

70 Percent

7	1 + .28284E + 00	8	2 + .60150E + 03	9	4 + .20000E - 03	13	3 + .34320E + 06

50 Percent

7	1 + .28284E + 00	8	2 + .60150E + 03	9	4 + .20000E - 03	13	3 + .25829E + 06

Table 89. H Matrices--Simplified Temperature Control

100 PERCENT

1 7	.10000E 01	2 6	.10000E 01	3 1	.15382E-02	3 2	.20707E 02	3 3	-.58168E-02
3 4	-.41555E 01	3 5	-.94740E 01	4 1	.11110E 00	4 2	.12702E 04	4 3	-.81427E-06
4 4	.54254E 02	4 5	.16276E 03	5 1	.10000E 01	6 1	-.22170E-01	6 2	.13231E 04
6 3	-.66705E 00	6 4	.61035E 02	6 5	.12207E 03	7 1	-.27403E-03	7 2	.11960E 02
7 3	-.79991E-01	7 4	-.12510E 01	7 5	-.31137E 01	8 20	-.50400E 04	9 1	.20000E-03
9 2	.10000E 01	10 3	.10000E 01	11 4	.10000E 01	12 5	.10000E 01	13 1	.21531E 01
13 2	.25502E 05	13 3	-.13843E-04	13 4	.81801E 03	13 5	.29423E 04	13 6	-.75000E 01
13 7	-.66665E 04	13 8	.50745E 00	13 20	-.64018E 07	15 9	.10000E 01	16 11	.10000E 01
17 14	.10000E 01	18 15	.10000E 01	19 16	.50000E 02	20 20	.10000E 01	21 14	-.59127E 01
21 19	.23651E 04	22 17	.40000E 02	23 10	-.66667E 00	23 11	.16667E 01		

85 PERCENT

1 7	.10000E 01	2 6	.10000E 01	3 1	.48288E-03	3 2	.54346E 01	3 3	-.84278E-03
3 4	-.12921E 01	3 5	-.12176E 00	4 1	.21102E 00	4 2	.21554E 04	4 3	-.15706E 00
4 4	.41087E 02	4 5	-.35136E 02	5 1	.10000E 01	6 1	.21499E-01	6 2	.24080E 04
6 3	-.13126E 01	6 4	.49278E 02	6 5	-.42140E 02	7 1	-.47983E-03	7 2	.51329E 01
7 3	-.10672E 00	7 4	-.27966E 00	7 5	.26724E-01	8 20	-.50400E 04	9 1	.20000E-03
9 2	.10000E 01	10 3	.10000E 01	11 4	.10000E 01	12 5	.10000E 01	13 1	.40966E 01
13 2	.43446E 05	13 3	-.26947E 01	13 4	.62275E 03	13 5	-.63796E 03	13 6	-.75000E 01
13 7	-.66665E 04	13 8	-.93511E-01	13 20	-.10863E 08	15 9	.10000E 01	16 11	.10000E 01
17 14	.10000E 01	18 15	.10000E 01	19 16	.50000E 02	20 20	.10000E 01	21 14	-.59127E 01
21 19	.47302E 04	22 17	.40000E 02	23 10	-.78571E 00	23 11	.17857E 01		

70 PERCENT

1 7	.10000E 01	2 6	.10000E 01	3 1	.64898E-03	3 2	.70047E 01	3 3	-.21223E-02
3 4	-.92155E 00	3 5	.24212E 01	4 1	.30015E 00	4 2	.27816E 04	4 3	-.13991E 00
4 4	.45333E 02	4 5	-.90665E 02	5 1	.10000E 01	6 1	.23093E-01	6 2	.35111E 04
6 3	-.75347E 00	6 4	.61035E 02	6 5	-.12207E 03	7 1	-.20302E-03	7 2	.40736E 01
7 3	-.39345E-01	7 4	-.11192E 00	7 5	.39236E 00	8 20	-.50400E 04	9 1	.20000E-03
9 2	.10000E 01	10 3	.10000E 01	11 4	.10000E 01	12 5	.10000E 01	13 1	.58276E 01
13 2	.56329E 05	13 3	-.24135E 01	13 4	.69135E 03	13 5	-.16547E 04	13 6	-.75000E 01
13 7	-.66665E 04	13 8	-.17489E 00	13 20	-.14019E 08	15 9	.10000E 01	16 11	.10000E 01
17 14	.10000E 01	18 15	.10000E 01	19 16	.50000E 02	20 20	.10000E 01	21 14	-.59127E 01
21 19	.47302E 04	22 17	.40000E 02	23 10	-.88679E 00	23 11	.18868E 01		

50 PERCENT

1 7	.10000E 01	2 6	.10000E 01	3 1	.48590E-03	3 2	.42676E 01	3 3	-.20527E-02
3 4	-.23272E 00	3 5	.85815E 00	4 1	.53408E 00	4 2	.36588E 04	4 3	-.30072E 00
4 4	.29802E-03	4 5	-.64959E 02	5 1	.10000E 01	6 1	.79194E-01	6 2	.65809E 04
6 3	-.75347E 00	6 5	-.12207E 03	7 1	-.12594E-03	7	.22742E 01	7 3	-.12186E-01
7 4	-.2[illegible]494E-01	7 5	.10584E 03	8 20	-.50400E 04	9 1	.20000E-03	9 2	.10000E 01
10 3	.10000E 01	11 4	.10000E 01	12 5	.10000E 01	13 1	.10392E 02	13 2	.75453E 05
13 3	-.52994E 01	13 4	.43716E-02	13 5	-.12097E 04	13 6	-.75000E 01	13 7	-.66665E 04
13 8	-.43226E 00	13 20	-.18440E 08	15 9	.10000E 01	16 11	.10000E 01	17 14	.10000E 01
18 15	.10000E 01	19 16	.50000E 02	20 20	.10000E 01	21 14	-.59127E 01	21 19	.47302E 04
22 17	.40000E 02	23 10	-.10000E 01	23 11	.20000E 01				

Table 90. D Matrices - Simplified Temperature Control

14 1 .10000E 01

Table 91. M Matrices - Simplified Temperature Control

100 PERCENT

1 1	.10000E 01	2 2	.10000E 01	3 3	.10000E 01	4 4	.10000E 01	5 5	.10000E 01
6 6	.10000E 01	7 7	.10000E 01	8 8	.10000E 01	9 9	.10000E 01	1010	-.66667E 00
1011	.16667E 01	1111	.10000E 01	1212	.10000E 01	1313	.10000E 01	1414	.10000E 01
1515	.10000E 01	1616	.50000E 02	1717	.40000E 02	1818	.10000E 01	1919	.10000E 01
2020	.10000E 01	2121	.10000E 01	2222	.10000E 01				

85 PERCENT

1 1	.10000E 01	2 2	.10000E 01	3 3	.10000E 01	4 4	.10000E 01	5 5	.10000E 01
6 6	.10000E 01	7 7	.10000E 01	8 8	.10000E 01	9 9	.10000E 01	1010	-.78571E 00
1011	.17857E 01	1111	.10000E 01	1212	.10000E 01	1313	.10000E 01	1414	.10000E 01
1515	.10000E 01	1616	.50000E 02	1717	.40000E 02	1818	.10000E 01	1919	.10000E 01
2020	.10000E 01	2121	.10000E 01	2222	.10000E 01				

70 PERCENT

1 1	.10000E 01	2 2	.10000E 01	3 3	.10000E 01	4 4	.10000E 01	5 5	.10000E 01
6 6	.10000E 01	7 7	.10000E 01	8 8	.10000E 01	9 9	.10000E 01	1010	-.88679E 00
1011	.18868E 01	1111	.10000E 01	1212	.10000E 01	1313	.10000E 01	1414	.10000E 01
1515	.10000E 01	1616	.50000E 02	1717	.40000E 02	1818	.10000E 01	1919	.10000E 01
2020	.10000E 01	2121	.10000E 01	2222	.10000E 01				

50 PERCENT

1 1	.10000E 01	2 2	.10000E 01	3 3	.10000E 01	4 4	.10000E 01	5 5	.10000E 01
6 6	.10000E 01	7 7	.10000E 01	8 8	.10000E 01	9 9	.10000E 01	1010	-.10000E 01
1011	.20000E 01	1111	.10000E 01	1212	.10000E 01	1313	.10000E 01	1414	.10000E 01
1515	.10000E 01	1616	.50000E 02	1717	.40000E 02	1818	.10000E 01	1919	.10000E 01
2020	.10000E 01	2121	.10000E 01	2222	.10000E 01				

Table 92. Simplified Temperature Control Closed-Loop Roots

Root Association	100% Frequency	100% Damping	85% Frequency	85% Damping	70% Frequency	70% Damping	50% Frequency	50% Damping
ẼT	-5.187		-5.254		-5.806		-3.410	
TM	-.7111		-.7738		-.8799		-1.386	
WF	+125.5	+.1950	+125.7	+.1954	+125.7	+.1946	+125.7	+.1937
WF	+163.1	+.6025	+185.9	+.7944	+186.6	+.7937	+185.2	+.7930
X14	+24.83	+.8790	20.68	.7164	+20.49	+.6742	18.78	.4752
X15								
TD	+189.5	+.7978	+231.9	+.8647	+232.0	+.8645	+232.2	+86.43
A8	-3.000		-3.000		-3.000		-.3000	
IGV	-5.000		-5.000		-5.000		-5.000	
BLD	-2.000		-2.000		-2.000		-2.000	
PT3S/50	-75.81		-75.63		-78.17		-78.92	
PT5S/40	-29.65		-40.12		-39.77		-39.97	
TT4WL	-.2089		-.1777		-.1112		-.06652	
TT4W	-50.00		-50.00		-50.00		-50.00	
TT4DUM	-.1250		-.1000		-.0588		-.03333	
X9	-.10+7		-.20+3		-.20+3		-.20+3	
P	-4.000		-4.000		-4.000		-4.000	
A8N	-59.91		-59.91		-59.91		-59.91	
W4N	-.20+5		-.20+5		-.20+5		-.20+5	

Table 93. Simplified Temperature Controllers RMS Response

Response	100%			85%				70%				50%			
	ETA1	ETA 2	ETA 3	ETA 1	ETA 2	ETA 3	ETA 4	ETA 1	ETA 2	ETA 3	ETA 4	ETA 1	ETA 2	ETA 3	ETA 4
P	.9999-1	.0000+0	.0000+0	.9999-1	.0000+0	.0000+0	.0000+0	.9999-1	.0000+0	.0000+0	.0000+0	.9999-1	.0000+0	.0000+0	.0000+0
ẼT	.6092+2	.2137+1	.4856+1	.6227+2	.7005+0	.2985+1	.9714-1	.6257+2	.2471+1	.1343+1	.5760+0	.6728+2	.4352+1	.1919+2	.2771+1
PT3	.7913+0	.1891+0	.2038-1	.1228+0	.1642-1	.3297-2	.1475-3	.1224+0	.1253-1	.3333-2	[illegible]	.5578-1	.3544-2	.1468-1	.1555+1
TT4	.4867+2	.1471+1	.1267+1	.4886+2	.2841+0	.1329+1	.5854-1	.4898+2	.9122+0	.1375+1	.4354+0	.4919+2	.1210+1	.1416+2	.1336+1
TM	.1949+2	.1049+0	.1130+1	.2014+2	.3350-1	.1205-1	.5054-2	.2119+2	.1454+0	.1292+1	.3956-1	.2455+2	.2820+0	.1380+2	.1759+0
TT5	.4968+2	.3249+1	.1183+1	.5296+2	.4704+1	.1255+1	.6531-1	.5896+2	.2868+1	.1313+1	.5485+0	.7982+2	.2682+1	.1389+2	.2388+1
PT5	.4485+0	.3807+0	.1062-1	.1097+0	.4262+0	.2150-2	.1390-3	.6698-1	.1535+0	.1265-2	.6359-3	.2680-1	.4719-1	.3005-2	.8240-3
WḞV	.3016+0	.1302-1	.9083-3	.1765+0	.1416-2	.6666-3	.5958-3	.1370+0	.2221-2	.6042-3	.3454-2	.1032+0	.2286-2	.3070-2	.7034-3
WFV	.3766-1	.1898-2	.9106-3	.2193-1	.2856-3	.5120-3	.2712-4	.6750-1	.4829-3	.3664-3	.1562-3	.1206-1	.4642-3	.1261-2	.3628-3
A8	.0000+0	.3999+1	.0000+0	.0000+0	.3999+1	.0000+0	.0000+0	.0000+0	.3999+1	.0000+0	.0000+0	.0000+0	.3999+1	.0000+0	.0000+0
IGV	.0000+0	.9999-2	.0000+0	.0000+0	.9999-2	.0000+0	.0000+0	.0000+0	.9999-2	.0000+0	.0000+0	.0000+0	.9999-2	.0000+0	.0000+0
BLD	.0000+0	.1000-1	.0000+0	.0000+0	.1000-1	.0000+0	.0000+0	.0000+0	.1000-1	.0000+0	.0000+0	.0000+0	.1000-1	.0000+0	.0000+0
TṪ4 - TṪ4M	.4002+3	.4057+2	.1113+2	.4132+3	.8673+1	.4801+1	.1646+1	.4182+3	.2425+2	.1791+2	.1214+2	.4608+2	.4378+2	.1442+3	.3496+2
UF	.4901-1	.1998-2	.9112-3	.2436-1	.2958-3	.5131-3	.4900-4	.1864-1	.4969-3	.3678-3	.2870-3	.1564-1	.5070-3	.1980-2	.8850-3
X9	.4069-1	.1998-2	.9112-3	.0000+0	.0000+0	.0000+0	.1000-4	.0000+0	.0000+0	.0000+0	.1000-4	.0000+0	.0000+0	.0000+0	.1000-3
TT4W	.2978+2	.8354+0	.2175+0	.2789+2	.1512+0	.1517+0	.3074-1	.2622+2	.4742+0	.9752-1	.2159+0	.2467+2	.5791+0	.8099+0	.6319+0
X14	.3753-1	.1893-2	.9102-3	.2165-1	.2852-3	.5118-3	.2649-4	.1668-1	.4822-3	.3662-3	.1525-3	.1201-1	.4635-3	.1960-2	.3561-3
X15	.3874-1	.1940-2	.9107-3	.2257-1	.2890-3	.5122-3	.3193-4	.1726-1	.4878-3	.3668-3	.1344-3	.1247-1	.4695-3	.1963-2	.4173-3
P3S	.7831+0	[illegible]	.2038-1	.1215+0	.1600-1	.3296-2	.5006-2	.1211+0	.1251-1	.3332-2	.5140-2	.5516-1	.3451-2	.1468-1	.4997-1
X20	.5984-4	.2584-5	.0000+0	.3502-4	.0000+0	.0000+0	.0000+0	.2720-4	.0000+0	.0000+0	.0000+0	.2048-4	.0000+0	.0000+0	.1395-5
UF	.2210+0	.1066-1	.4486-2	.1292+0	.1686-2	.3026-2	.1566-3	.9867-1	.2851-2	.2165-2	.9021-3	.7104-1	.2740-2	.1159-1	.2105-2
P5S	.4415+0	.3734+0	.1062-1	.1078+0	.4190+0	.2148-2	.1266-3	.6582-1	.1501+0	.1264-2	.5778-3	.2627-1	.4614-1	.3001-2	.7586-3
TT4EST	.4826+2	.1392+1	.3594+0	.4843+2	.2700+0	.2696+0	.5489-1	.4853+2	.8947+0	.1838+0	.4074+0	.4871+2	.1158+1	.1618+1	.1263+1

Table 94. Perturbation Gains

% N	k_N (lb/sec)/r p m	k_E N P T	k_{P3} (lb/sec)/psi	k_{PT5} (lb/sec)/psi	k_{TT4} (lb/sec)/(deg F)
50E	-.46718-3	+.58461-4	--	--	--
50P	--	+.45650-1	-.18636+0	+.15861+0	--
50T	--	+.11304-3	-.15966-2	+.12096-2	-.22757-3
70E	-.27436-3	+.53844-4	--	--	--
70P	--	+.20271-1	-.62334-1	-.44936-1	--
70T	--	+.14074-3	+.53354-1	-.20311-2	-.28462-3
85E	-.26479-3	+.12239-3	--	--	--
85P	--	+.15561-2	-.71783-1	+.51485-1	--
85T	--	+.16155-3	+.91896-2	-.74486-3	-.18812-3
100E	-.53363-3	+.31975-3	--	--	--
100P	--	+.12779-1	-.49166-1	+.43431-1	--
100T	--	+.23413-3	-.18094-1	+.13297-1	-.78669-5

Table 95. Speed Controller Gains, 50 Percent

ID	k_N	k_{EN}
15	-.75414-3	+.26419-3
18	-.46718-3	+.58461-4

Table 96. Wind Tunnel Test Summary

Item	Description
Results achieved:	**1) Speed setpoints to better than 0.1%N** **2) Good small-amplitude speed response** **3) Maximum PT3 surge-stall boundary excess 3.5 psi** **4) RMS ΔPT3 on boundary is approximately 30°F** **5) Maximum TT4 boundary excess 125°F** **6) Maximum time TT4 exceeds boundary plus 20°F is 0.3 sec** **7) RMS ΔTT4 on boundary is approximately 30°F at 0.5 psi**
Improvements achievable by:	1) Improving model accuracy 2) Revising speed-pressure logic to reduce overshoots by 50%

SECTION V
CONCLUSIONS

Results presented show that:

1) Synthesis of good command controllers by application of optimal control methodology is state of the art.

2) Optimal control methodology designs better command controllers than presently used methodology.

3) It is feasible to make the engine insensitive to disturbances while retaining good command control.

REFERENCES

1. Seldner, Kurt; Mihaloew, James R,; and Blaha, Ronald J., "Generalized Simulation Technique for Turbojet Engine System Analysis," Lewis Research Center, NASA TN D-6610, February 1972.

2. Den Hartog, J.P., Mechanical Vibrations, (pp. 334-336,) 2nd Edition, McGraw-Hill, 1940.

3. Webb, William S. and Reukauf, Paul J., "Development of a Turbine-Inlet Gas Temperature Measurement and Control System Using a Fluidic Temperature Sensor," AIAA Paper No. 73-1251, AIAA/SAE 9th Propulsion Conference, 5-7 November 1973.

4. VanDierondonck, A.J., "Design Method for Fully Augmented Systems for Variable Flight Conditions," U.S. Air Force Flight Dynamics Laboratory Technical Report AFFDL-TR-72-152, January 1972.

5. Tyler J.S., Jr., "The Characteristics of Model-Following Systems as Synthesized by Optimal Control," IEEE Transactions on Automatic Control, Vol. AC-9, No. 4, October 1964.

6. VanDierondonck, A.J.; Wynne, Capt. M.; and Kruczynski, Capt. L., "An Optimal Model-Following Flight Control System for Manual Control," 1972 JACC Paper 2-3.